

**A Thesis Submitted for the Degree of PhD at the University of Warwick**

**Permanent WRAP URL:**

<http://wrap.warwick.ac.uk/110305/>

**Copyright and reuse:**

This thesis is made available online and is protected by original copyright.

Please scroll down to view the document itself.

Please refer to the repository record for this item for information to help you to cite it.

Our policy information is available from the repository home page.

For more information, please contact the WRAP Team at: [wrap@warwick.ac.uk](mailto:wrap@warwick.ac.uk)

**Functional and structural studies of an Enterococcal  
Serine/Threonine kinase and its contribution to antibiotic  
resistance mechanisms**

by

**Christopher William Thoroughgood**

**A thesis submitted in partial fulfilment of the requirements for the degree  
of**

**Doctor of Philosophy**

**University of Warwick**

**MOAC DTC**

**April 2018**

# Contents

<b>Contents.....</b>	<b>2</b>
<b>List of Tables .....</b>	<b>7</b>
<b>List of Figures .....</b>	<b>9</b>
<b>Acknowledgments .....</b>	<b>14</b>
<b>Declaration.....</b>	<b>15</b>
<b>Abstract.....</b>	<b>16</b>
<b>Abbreviations.....</b>	<b>17</b>
<b>Chapter 1. Introduction .....</b>	<b>20</b>
<b>1.1. The Bacterial Cell Wall .....</b>	<b>20</b>
1.1.1. The role of Peptidoglycan .....	20
1.1.2. Peptidoglycan Structure .....	20
1.1.3. Peptidoglycan biosynthesis.....	22
1.1.4. Polymerisation of Peptidoglycan.....	27
1.1.5. Peptidoglycan hydrolases .....	28
1.1.6. Antibiotics that target the wall .....	29
<b>1.2. Background on Enterococci bacteria.....</b>	<b>31</b>
1.2.1. Characteristics and Physiology.....	31
1.2.2. Pathogenesis .....	32
1.2.3. Antimicrobial Therapy and Resistance .....	35
1.2.4. Antibiotics and antibiotic resistance in <i>Enterococcus</i> spp.....	35
<b>1.3. Bacterial Signalling.....</b>	<b>56</b>
1.3.1. Two-component systems.....	56
1.3.2. Eukaryotic like Ser/Thr Kinases/Phosphatases .....	70
1.3.3. Convergence of Eukaryotic-like Ser/Thr kinases and two-component systems .....	76
1.3.4. Convergence of the <i>E. faecalis</i> eSTK, IreK and the vancomycin resistance TCS, VanS .....	77
<b>1.4. Project Aims and Outline .....</b>	<b>81</b>
<b>Chapter 2. Materials and Methods.....</b>	<b>82</b>
<b>2.1. Materials .....</b>	<b>82</b>

2.1.1. Bacterial Strains.....	82
2.1.2. Media.....	82
2.1.3. Buffers and solutions.....	82
2.1.4. Vectors for Cloning, Complementation and Protein Expression .....	82
2.1.5. Oligonucleotides and Synthetic DNA.....	95
<b>2.2. Methods in Molecular Biology.....</b>	<b>95</b>
2.2.1. Preparation of Competent cells .....	95
2.2.2. Polymerase Chain Reaction .....	96
2.2.3. Agarose Gel Electrophoresis .....	96
2.2.4. Transformation of Electrocompetent cells .....	96
2.2.5. Preparation of Plasmid DNA .....	97
2.2.6. Purification of amplified DNA .....	97
2.2.7. Restriction Digestion .....	97
2.2.8. Restriction Cloning Ligation .....	98
2.2.9. Plasmid Mutagenesis.....	98
2.2.10. Gibson Cloning .....	98
2.2.11. Construct Validation .....	98
<b>2.3. Methods in Microbiology.....</b>	<b>99</b>
2.3.1. Genetically modifying <i>E. faecalis</i> chromosome .....	99
2.3.2. MIC Determination.....	99
2.3.3. Real Time Quantitative PCR analysis of transcripts.....	101
2.3.4. Fluorescence Microscopy .....	102
<b>2.4. Protein Expression and Purification.....</b>	<b>103</b>
2.4.1. Expression of unlabelled proteins .....	103
2.4.2. Expression of labelled proteins .....	103
2.4.3. Preparation of cell lysates.....	104
2.4.4. Protein Purification .....	104
2.4.5. SDS-PAGE analysis .....	105
2.4.6. Western Blots.....	106
2.4.7. Protein Quantification .....	107
<b>2.5. Peptidoglycan Purification and Hydrolysis.....</b>	<b>107</b>
2.5.1. Growth of Bacteria .....	107
2.5.2. Peptidoglycan Extraction .....	107
2.5.3. Peptidoglycan Hydrolysis.....	108

<b>2.6. Biophysical Techniques.....</b>	<b>108</b>
2.6.1. Circular Dichroism .....	108
2.6.2. Size Exclusion Chromatography-Multiple Angle Laser Light Scattering .....	109
2.6.3. Size Exclusion Chromatography-Small Angle X-Ray Scattering.....	109
2.6.4. Surface Plasmon Resonance (SPR) .....	110
2.6.5. Microscale thermophoresis .....	110
2.6.7. Analytical Ultracentrifugation.....	111
2.6.8. Mass Spectrometry .....	111
2.6.9. Nuclear Magnetic Resonance .....	112
<b>Chapter 3. Phenotypic characterisation of IreK in <i>E. faecalis</i> .....</b>	<b>115</b>
<b>3.1. Introduction .....</b>	<b>115</b>
<b>3.2. <i>E. faecalis</i> isogenic series to study antibiotic resistance mechanisms .....</b>	<b>115</b>
3.2.1. Construction of the OG1RF <i>ΔireK</i> and Tn1549 isogenic series .....	116
3.2.2. Construction of the JH2-2 <i>ΔireK</i> isogenic series.....	119
3.2.3. Construction of <i>ΔireP</i> strains in OG1RF.....	119
<b>3.3 Tn1549 is required for enhanced cephalosporin resistance and <i>ireK</i> is essential for both intrinsic and enhanced cephalosporin resistance in OG1RF strains.....</b>	<b>120</b>
<b>3.4. Tn1549 is not required for enhanced cephalosporin resistance in JH2-2 strains ...</b>	<b>124</b>
<b>3.5. The linkage between cephalosporin resistance and the Tn1549 structural genes is not at the transcriptional level. ....</b>	<b>125</b>
<b>3.6. Identifying possible substrates of VanS<sub>B</sub> .....</b>	<b>128</b>
<b>3.7. Cephalosporin sensitivity in <i>E. faecalis</i> can be established by a chemical genetic approach .....</b>	<b>130</b>
3.7.1. Staurosporine and Cefotaxime work synergistically to restore cephalosporin sensitivity .....	130
3.7.2. Staurosporine and <i>ΔireK</i> confer similar phenotype .....	131
3.7.3. Enhanced cephalosporin resistant is observed in other VanB type genotypes and species and can be restored using staurosporine .....	132
3.7.4. Other potential eSTK kinase inhibitors.....	133
<b>3.8. Exploring the contribution of each IreK domain on enhanced cefotaxime resistance. ....</b>	<b>136</b>
3.8.1. Background into the inducible complementation system.....	136
3.8.2. Increasing anhydrotetracycline can tune <i>ireK</i> expression.....	138
3.8.3. Complementation experiments of various IreK constructs.....	140

<b>3.9.</b>	<b>Localisation of IreK in inducible complementation experiments .....</b>	<b>144</b>
3.9.1.	Identification of valid fluorescent fusion constructs.....	144
3.9.2.	Optimising concentration of conditions for localisation experiments.....	145
3.9.3.	Localisation of GFP-IreK(FL) in OG1RF strains.....	147
3.9.4.	Localisation of GFP-IreK ( $\Delta kinase$ ), GFP-IreK ( $\Delta K41R$ ) and GFP-IreK ( $\Delta PASTA$ ). .....	148
3.9.5.	Localisation of different PASTA truncations in IreK .....	149
3.9.6.	Localisation of different PASTA substitutions in IreK.....	151
<b>3.10.</b>	<b>Conclusions and future direction .....</b>	<b>152</b>
<b>Chapter 4.</b>	<b>Biophysical analysis of IreK Domains .....</b>	<b>155</b>
<b>4.1.</b>	<b>Introduction.....</b>	<b>155</b>
<b>4.2.</b>	<b>Initial characterisation of each protein construct .....</b>	<b>156</b>
4.2.1.	SDS-PAGE and SEC-MALS analysis .....	156
4.2.2.	Determining the fold of each protein construct by CD .....	161
4.2.3.	Determining the melting temperature ( $T_M$ ) of each protein construct by CD.....	164
<b>4.3.</b>	<b>Studying oligomerisation of IreK domains using AUC .....</b>	<b>168</b>
<b>4.4.</b>	<b>Confirming MW by determining experimental MW by mass spectrometry and summary of oligomerisation .....</b>	<b>172</b>
<b>4.5.</b>	<b>Identification of Ligands that bind to IreK PASTA domains.....</b>	<b>174</b>
<b>4.6.</b>	<b>Surface Plasmon Resonance .....</b>	<b>176</b>
4.6.1.	Introduction to SPR .....	176
4.6.2.	pH Scouting and immobilisation of the extracellular PASTA domain .....	179
4.6.3.	Identification of a suitable regeneration solution.....	181
4.6.4.	Issues with the TEV-cleaved PASTA 1 to 5 construct .....	182
4.6.5.	Screening potential analytes against <i>E. faecalis</i> PASTA domains 1 to 5.....	184
<b>4.7.</b>	<b>Microscale Thermophoresis (MST) .....</b>	<b>195</b>
<b>4.8</b>	<b>Conclusions and Future Directions.....</b>	<b>200</b>
<b>Chapter 5.</b>	<b>Towards structural studies of IreK PASTA domains .....</b>	<b>203</b>
<b>5.1.</b>	<b>Introduction.....</b>	<b>203</b>
<b>5.2.</b>	<b>Small angle X-ray scattering.....</b>	<b>203</b>
5.2.1.	Introduction .....	203
5.2.2.	Initial characterisation of PASTA constructs .....	204
<b>5.3.</b>	<b>Identifying a suitable PASTA construct for NMR studies.....</b>	<b>206</b>
5.3.1.	Initial characterisation of PASTA domains 4 to 5 .....	207
5.3.2.	AUC characterisation of the terminal PASTA domains.....	208

5.3.3. CD characterisation of PASTA domains 4 to 5 .....	209
5.3.4. SAXS characterisation of the terminal PASTA domains 4 to 5 .....	210
<b>5.3. Nuclear magnetic resonance.....</b>	<b>212</b>
5.3.1. Introduction .....	212
5.3.2. The Heteronuclear Single Quantum Coherence (HSQC) experiment.....	212
<b>5.3. Ligand binding studies using NMR .....</b>	<b>219</b>
<b>5.4. Backbone assignment .....</b>	<b>225</b>
5.4.1. 3D HSQC TOCSY Experiments.....	226
5.4.2 Backbone assignment using triple resonance (CHN) 3D NMR.....	229
5.4.3. Examples of Backbone assignment of PASTA 4 to 5 .....	232
<b>5.5. <i>Ab initio</i> modelling .....</b>	<b>235</b>
<b>5.6. Conclusions and future directions .....</b>	<b>237</b>
<b>Chapter 6.    General Discussions and Conclusions.....</b>	<b>240</b>
6.1. Impact of Tn1549 acquisition and enhanced cephalosporin resistance .....	240
6.2. Characterisation of phosphorylation targets .....	241
6.3. Further characterisation of IreK domains .....	242
6.4. Structural and Functional Properties of PASTA domains .....	243
6.5. Final Conclusion .....	245
<b>Chapter 7.    Bibliography.....</b>	<b>246</b>
<b>Chapter 8.    Appendix.....</b>	<b>293</b>
8.1. DNA gBlock Sequences .....	293
8.2. MIC of Enterococcal isogenic series and CSLI controls for each antibiotic .....	298
8.4. Extended AUC data .....	302
8.5. Mass Spectrometry.....	307
8.6. Nanotemper MST controls.....	315

# List of Tables

Table 1.1 - Summary of PG branching in key Gram-positive bacteria. ....	25
Table 1.2 - Summary of Class A and Class B PBPs in key Gram-positive bacteria. ....	27
Table 1.3 - List of both clinically used cell wall antibiotics and antibiotics in clinical trials. ....	30
Table 1.4 - Types and distribution of glycopeptide resistance in <i>Enterococcus</i> spp.. ....	44
Table 1.5 - Commonly conserved amino acids residues located in the H box within the DHP domain of a prokaryotic HKs. ....	59
Table 1.6 - Summary and evaluation of the TCS distributed and identified in two <i>E. faecalis</i> strains including V538 and OG1RF .....	63
Table 2.1 - Experimental Strains used for <i>E. coli</i> and <i>Enterococcus</i> spp. experiments. ....	83
Table 2.2: Media used for culturing bacteria in this study. ....	84
Table 2.3: Buffers used for protein purification, storage and assays. ....	85
Table 2.4: Plasmids used for recombinant protein expression in <i>E. coli</i> .....	86
Table 2.5: Plasmids used for mutagenesis in <i>E. faecalis</i> strains. ....	87
Table 2.6: Plasmids used for complementation in <i>E. faecalis</i> .....	88
Table 2.7: Plasmids used for complementation with N-terminal GFP fusions in <i>E. faecalis</i> . ....	90
Table 2.8: Primers used for sequencing and analytical PCR. ....	93
Table 2.9: Primers used in the design of plasmids used for expression of recombinant protein. ....	93
Table 2.10: Primers used for the design of plasmids used or mutagenesis in <i>E. faecalis</i> .....	93
Table 2.11: Primers used fluorescence and complementation plasmids.....	94
Table 2.12: gBlock Identifiers and description .....	95
Table 2.13: Primers used for qPCR experiments. ....	102
Table 2.14: Pulse Programmes and basic parameters used in NMR experiments. ....	113
Table 2.15: Overview of lyophilized ligand aliquots for incremental titration experiments for chemical shift perturbation experiments with <sup>15</sup> N-PASTA 4 to 5. ....	114
Table 3.1: Summary of <i>E. faecalis</i> isogenic experimental strains and the associated genotype used in the study. ....	120
Table 3.2: Tn1549 causing VanB type resistance causes enhanced cephalosporin resistance: MIC OG1RF WT/Tn1549 with cephalosporin's and vancomycin.....	121
Table 3.7: Comparison of isogenic strains of <i>E. faecalis</i> OG1RF and the effect of staurosporine .....	131

Table 3.10: Complementation of different <i>ireK</i> constructs in the complementation plasmid under 20 ng mL <sup>-1</sup> anhydrotetracycline in Iso-sensitest media .....	141
Table 3.11: MIC determination of OG1RF Tn1549, OG1RF::Tn1549 $\Delta$ <i>ireK</i> in comparison to OG1RF::Tn1549 $\Delta$ <i>ireK</i> TetH-gfp- <i>ireK</i> (FL) with different concentration of anhydrotetracycline in BHI broth .....	146
Table 4.1: The estimated MW from each species as determined by AUC by the c(s) analysis of the KD .....	170
Table 4.2: The estimated MW from each species as determined by AUC by the c(s) analysis of each PASTA domain truncation .....	171
Table 4.3: Summary of the MW of each construct and estimates their oligomeric states by a range of biophysical techniques including Mass Spectrometry, SEC-MALS and AUC (Absorbance and Interference).....	173
Table 4.4: Measurement of hydrolysis activity the hydrolase AtIA (amidase) from <i>S. aureus</i> against the PG from three different Gram-positive species .....	176
Table 4.5: Summary of ligands tested using MST against PASTA 1 to 5 .....	198
Table 5.1: Parameters from analysed SAXS data using SCATTER (Bioisis) of each PASTA truncation.....	206
Table 5.2: Species estimated molecular weights from the c(s) analysis of each PASTA domain truncation.....	209
Table 5.3: Parameters from analysed SAXS data using SCATTER of each terminal PASTA truncation.....	211
Table 8.1: gBlock sequences .....	293
Table 8.2: MIC of OG1RF isogenic series with CSLI control strains .....	298
Table 8.3: GSK protein kinase inhibitor set 1 .....	299
Table 8.4: GSK protein kinase inhibitor set 2 .....	299
Table 8.5: GSK protein kinase inhibitor set 3 .....	300
Table 8.6: Species estimated molecular weights from the c(s) analysis of IreP.....	303
Table 8.7: Species estimated molecular weights from the c(s) analysis of Vans <sub>B</sub> .....	304

# List of Figures

Figure 1.1 - Bacterial cell wall architecture. ....	21
Figure 1.2 - The cytoplasmic and membrane associated steps in PG biosynthesis. ....	22
Figure 1.3 - Summary of PG polymerisation and the cell wall antibiotics that can inhibit the process .....	26
Figure 1.4 - Classification of the major types of proteins involved in PG transpeptidation in <i>Enterococcus</i> spp. ....	28
Figure 1.5 - Summary of PG hydrolase classes and the cleavage sites for each hydrolase. ....	29
Figure 1.6 – Mode of action of vancomycin and the effect of antibiotic resistance .....	42
Figure 1.7 - Structure, composition and architecture of the vancomycin resistance clusters vanA-N .....	43
Figure 1.8 – The role Tn1549 in vancomycin resistance .....	47
Figure 1.9: Schematic of the canonical architecture and different types of the 17 HKs found in the <i>E. faecalis</i> V538 genome .....	64
Figure 1.10 - CLUSTALW sequence alignment of the protein sequences of VanS <sub>A</sub> and VanS <sub>B</sub> ..	68
Figure 1.11 - The chemical structures of vancomycin, teicoplanin and moenomycin.....	69
Figure 1.12 – Schematic highlighting the eSTK in <i>E. faecalis</i> , IreK and the architecture and distribution of PASTA domains from other Gram-positive bacteria.....	71
Figure 1.13: IreK <sub>KD</sub> autophosphorylates and phosphorylates the VanS <sub>KD</sub> and not VanR of the VanB type Tn1549 cassette.....	78
Figure 1.14: IreK <sub>KD</sub> from both <i>E. faecalis</i> (A) and <i>E. faecium</i> (B) phosphorylates VanS <sub>KD</sub> from the Tn1549 cassette at position T223 .....	79
Figure 1.15: The cognate phosphatase of IreK, IreP dephosphorylates IreK and its substrate VanS .....	79
Figure 1.16: Staurosporine inhibits IreK <sub>KD</sub> <i>in vitro</i> .....	80
Figure 3.1: Schematic of inserting the <i>ireK</i> gene back into an OG1RF::Tn1549 strain using the pGhost9 plasmid.....	118
Figure 3.2: 16S ribosome gene transcription profile via qPCR experiments in various OG1RF strains under different experimental conditions .....	126
Figure 3.3: Inducing transcriptional expression of the Tn1549 structural genes on OG1RF::Tn1549 and OG1RF::Tn1549 $\Delta$ <i>ireK</i> strains.....	127
Figure 3.4: Developing model for the role of Tn1549 in cephalosporin resistance.....	127

Figure 3.5: The Tn1549 cassette, IreK and the DdcSR/DdcY TCS are essential for enhanced cephalosporin resistance .....	129
Figure 3.6: Schematic for possible TCS crosstalk leading to enhanced cephalosporin resistance .....	129
Figure 3.7: Amino acid alignment of the eSTK IreK from <i>E. faecalis</i> and CDK2 from <i>Homo sapiens</i> .....	130
Figure 3.8: Growth curves of OG1RF isogenic strains without (Blue) and with (Red) 50 $\mu$ M staurosporine in MHII broth .....	132
Figure 3.9: Structural comparison of eukaryotic kinase inhibitors that are potential prokaryotic eSTK inhibitors.....	135
Figure 3.10: TetH Plasmid map highlighting the key features of the plasmid .....	137
Figure 3.11: A tetracycline inducible system for tuneable expression of a gene of interest... 137	137
Figure 3.12: Testing the effect of anhydrotetracycline complementation using E-test strips. 139	139
Figure 3.13: Expression of GFP fused IreK constructs.....	147
Figure 3.14: Localization of GFP and GFP-IreK constructs in OG1RF $\Delta$ ireK .....	148
Figure 3.15: Localization of GFP-IreK constructs with domain mutations in the OG1RF $\Delta$ ireK strains.....	149
Figure 3.16: Localization of GFP-IreK constructs in the OG1RF $\Delta$ ireK strains with PASTA truncations .....	150
Figure 3.17: Localization of GFP-IreK constructs in the OG1RF $\Delta$ ireK strains with PASTA substitutions .....	152
Figure 4.1: IreK domain constructs for recombinant protein expression .....	156
Figure 4.2: Recombinantly expressed IreK Kinase domains analysed SDS-PAGE for purity and SEC-MALS for oligomerisation .....	158
Figure 4.3: Recombinantly expressed IreK PASTA domains analysed SDS-PAGE for purity and SEC-MALS for oligomerisation .....	159
Figure 4.4: Overview of SEC-MALS data obtained for each PASTA construct.....	160
Figure 4.5: Schematic showing a CD profile of $\alpha$ -helix, $\beta$ -sheet and random coil spectra expected when predominately formed of that secondary structure feature .....	161
Figure 4.6: CD spectra of each KD of IreK.....	162
Figure 4.7: CD spectra of each PASTA construct of IreK from <i>E. faecalis</i> .....	163
Figure 4.8: Secondary structure percentage distribution determined by CD .....	164
Figure 4.9: CD T <sub>M</sub> of IreK KD following 222 nm.....	165
Figure 4.10: CD T <sub>M</sub> of IreK of PASTA constructs from <i>E. faecalis</i> following 222 nm .....	166

Figure 4.11: CD T <sub>M</sub> spectra of each PASTA construct of IreK .....	167
Figure 4.12: Native-PAGE gel of Kinase domains from <i>Enterococcus</i> spp.....	169
Figure 4.13: Schematic of hydrolases and location of cleavage for <i>E. faecalis</i> binding studies .....	174
Figure 4.14: SDS-PAGE of recombinant hydrolases used in this study .....	175
Figure 4.15: Schematic view of SPR assay .....	177
Figure 4.16: Pre-concentration pH scouting.....	180
Figure 4.17: Immobilisation of PASTA 1 to 5 (TEV).....	181
Figure 4.18: Immobilisation of PASTA 1 to 5 (His).....	181
Figure 4.19: Sensogram profile of candidate regeneration solutions using PASTA 1 to 5 (HIS) constructs .....	183
Figure 4.20: Identification of PG motifs recognised by the PASTA domains using <i>E. faecalis</i> PG .....	186
Figure 4.21: Identification of PG motifs recognised by the PASTA domains using <i>S. aureus</i> PG .....	187
Figure 4.22: Binding activity of PASTA domains 1 to 5 with sugar polysaccharides. ....	188
Figure 4.23: Binding of PG glycan monomers extracellular PASTA domains of <i>E. faecalis</i> IreK .....	189
Figure 4.24: Binding of cephalosporin antibiotic to the extracellular PASTA domains of <i>E. faecalis</i> IreK .....	190
Figure 4.25: Binding of aminoglycoside antibiotic to the extracellular PASTA domains of <i>E. faecalis</i> IreK .....	192
Figure 4.26: Binding of glycopeptide antibiotics to the extracellular PASTA domains of <i>E. faecalis</i> IreK .....	194
Figure 4.27: Dose-response curves of MST analysis.....	199
Figure 4.28: Possible models for IreK oligomerisation .....	201
Figure 5.1: SEC-SAXS analysis of PASTA domains from <i>E. faecalis</i> IreK .....	204
Figure 5.2: Schematic demonstrating the different protein characteristics from processed SAXS data using the dimensionless Kratky plot .....	205
Figure 5.3: Sequence alignment of the individual PASTA domains from <i>E. faecalis</i> Irek OG1RF .....	207
Figure 5.4: SDS and SEC-MALS analysis of purified Terminal PASTA domains from <i>E. faecalis</i> IreK .....	208
Figure 5.5: Temperature melts of IreK terminal PASTA domains following CD at 222 nm .....	210

Figure 5.6: SAXS analysis of the terminal PASTA domains from <i>E. faecalis</i> IreK. (A) Log <sub>10</sub> ....	211
Figure 5.7: Schematic showing correlations for <sup>1</sup> H- <sup>15</sup> N HSQC experiments .....	213
Figure 5.8: 1D NMR of 1.2 mM PASTA 4 to 5 constructs .....	214
Figure 5.9: Buffer optimisation for NMR studies of PASTA 4 to 5 .....	216
Figure 5.10: Temperature optimisation for NMR studies of PASTA 4 to 5 .....	218
Figure 5.11: PASTA domains 4 and 5 bind to vancomycin.....	220
Figure 5.12: Local overview of PASTA domains 4 and 5 binding to vancomycin .....	222
Figure 5.13: 16 mM vancomycin causes PASTA 4 to 5 to aggregate in these experimental conditions.....	223
Figure 5.14: PASTA domains 4 and 5 also bind to vancomycin in pH 6.5 sodium phosphate .	224
Figure 5.15: The effect of exchange rate on NMR peak shapes.....	225
Figure 5.16: HSQC- TOCSY strips corresponding to the residues that observed chemical shifts in the presence of 8 mM vancomycin .....	228
Figure 5.17: Correlation for triple resonance experiments .....	231
Figure 5.18: CBCACONH and CBCANH experimental example of the backbone assignment of 1 mM PASTA 4 to 5 IreK from <i>E. faecalis</i> . .....	232
Figure 5.19: HNCA and HNCOCA experimental example of the backbone assignment of PASTA 4 to 5 IreK from <i>E. faecalis</i> . Includes the HNCA (Pink) and HNCOCA (Brown) pair.....	233
Figure 5.20: HNCO and HNCACO experimental example of the backbone assignment of PASTA 4 to 5 IreK from <i>E. faecalis</i> .....	233
Figure 5.21: Amino acid sequence of PASTA domains 4 to 5 from IreK <i>E. faecalis</i> and progress of backbone assignment.....	234
Figure 5.22: Regions of possible site of ligand interaction .....	235
Figure 5.23: Schematic demonstrating the process of obtaining a dummy atom model of the PASTA 4 to 5 domains from <i>E. faecalis</i> IreK .....	236
Figure 5.24: Dummy atom model of PASTA domains 4 to 5 from IreK <i>E. faecalis</i> .....	237
Figure 5.25: Comparison of ligand binding locations on PASTA domains.....	238
Figure 5.26: Towards dynamic hybrid modelling .....	239
Figure 8.1: Sedimentation coefficient distributions of Kinase and Phosphatase domains used in this study .....	302
Figure 8.2: Sedimentation coefficient distributions of PASTA domains from <i>E. faecalis</i> IreK used in this study .....	305
Figure 8.3: Sedimentation coefficient distributions of the terminal PASTA domains from <i>E. faecalis</i> IreK used in this study.....	306

Figure 8.4: ESI-MS of <i>E. faecalis</i> KD .....	307
Figure 8.5: Highlighted ESI-MS of <i>E. faecalis</i> KD to show post translational modifications....	308
Figure 8.6: Highlighted ESI-MS of <i>E. faecium</i> .....	309
Figure 8.7: Highlighted ESI-MS of PASTA 1 to 5 (His).....	310
Figure 8.8: Highlighted ESI-MS of PASTA 1 to 5 (TEV) .....	311
Figure 8.9: Highlighted ESI-MS of PASTA 1 to 4 (TEV) .....	312
Figure 8.10: Highlighted ESI-MS of PASTA 1 to 3 (TEV) .....	313
Figure 8.11: Highlighted ESI-MS of PASTA 1 to 2 (TEV) .....	314
Figure 8.12: Nanotemper experiment controls with ligand that produced a $K_D$ .....	315
Figure 8.13: Nanotemper experiment controls with PG glycan monomers.....	316
Figure 8.14: Nanotemper experiments with PG pentapeptide stem.....	317
Figure 8.15: Nanotemper experiment controls with GlcNAc polymers .....	318
Figure 8.16: Nanotemper experiment controls with PG peptide stem (Dipeptide).....	319
Figure 8.17: Nanotemper experiment controls with PG peptide stem (Unamidated Tripeptide). .....	320
Figure 8.18: Nanotemper experiment controls with PG peptide stem (Unamidated MurNAc Tripeptide).....	321
Figure 8.19: Nanotemper experiment controls with PG peptide stem (Amidated Tripeptide) .....	322

## Acknowledgments

I would like to thank my supervisors Prof. David Roper and Dr. Ann Dixon for their guidance, support and patience during my PhD and allowing me to freely explore ideas and new techniques and share the same enthusiasm. I would also like to thank Dr. Johnathan Dworkin and his lab for allowing me to spend some time his lab and allowing me to integrate into the group easily. Thanks also goes to Dr. Stephane Mesnage and Dr. David Scott for great advice throughout my thesis in matter microbiological and biophysical respectively.

Particular thanks go to individuals who have helped me feed my passion for learning new techniques. This includes Dr. Adrian Lloyd for his help with the Mass Spec experiments and also his expertise and inspirational advice, Dr. Mussa Quareshy for advice on SPR studies, Michael Lockhart for help on SAXS analysis, Gemma Harris for help with AUC and SEC-MALS analysis, Dr. Muhammad Hasan for encouragement and help with NMR analysis and John Moat for training in techniques in microbiology. Further thanks go to Sarah Bennet and WISB for allowing me to use their facilities as an external user.

Thanks also goes to past and current C10 members for making the lab such a great place to work. In particular Julie, Anita, Nicola, Cathy, Anna, Kathryn, Ricky and Katie for their advice and friendship in and out of the lab. Thanks also goes to Christine for being great support.

I would like to thank many members for MOAC including Alison, Nikola, Hugo and Naomi for giving me the opportunity to come to Warwick and providing constant support throughout my MSc and PhD.

Special thanks goes to my family in particular to Marikka for continuous support and sharing an understanding during the whole PhD process. I would like to thank my parents Julie and Pete and siblings Josie and Jack for support and understanding over the years.

## Declaration

I hereby declare that I personally have carried out the work submitted in this thesis under the supervision of Prof. David Roper (School of Life Sciences) and Dr. Ann Dixon (The Department of Chemistry) at the University of Warwick and Dr. Jonathan Dworkin at the Department of Microbiology and Immunology, The University of Columbia, USA. Where work has been contributed to by other individuals, it is specifically stated in the text.

No part of this work has previously been submitted to be considered for a degree or qualification. All sources of information are specifically acknowledged in the form of references.

## Abstract

The emergence of vancomycin-resistant enterococci (VRE) since the 1980s has turned this Gram-positive bacterium into a serious and growing clinical challenge. Enterococci have acquired resistance to a number of different antibiotics and are intrinsically resistant to cephalosporin  $\beta$ -lactam drugs. As a result, they are now placed in the World Health Organisation list of priority pathogens for which new antibiotics are urgently needed. An important risk factor for the emergence of VRE is treatment with cephalosporins, suggesting a connection between the origins of resistance between these two different types of antibiotics, the mechanistic basis for which was unknown.

In this study I demonstrate that cephalosporin resistance is significantly enhanced in the well characterized *E. faecalis* OG1RF strain containing the Tn1549 transposon conferring the VanB type vancomycin resistance. Cephalosporin resistance is shown to be enhanced to the presence of the Tn1549 transposon and a single, chromosomally encoded Serine/Threonine (ST) kinase gene called *ireK*. Complementation experiments and fluorescence microscopy with a range of biophysical techniques to characterise the protein. Deletion of the gene results in cephalosporin sensitivity. Moreover, this phenotype can be chemically simulated by treatment of *E. faecalis* with inhibitors of cytoplasmic ST kinases such as staurosporine, demonstrating a requirement for ST kinase activity for cephalosporin resistance. This also demonstrates a therapeutic potential for targeting ST kinases in Gram-positive pathogens with small molecule inhibitors to restore cephalosporin sensitivity which may have clear translational significance. IreK was identified as a key protein involved in enhanced cephalosporin resistance and led to examination of its extracellular and intracellular domains to understand its signal transduction mechanisms and its linkage to resistance. The extracellular domain of IreK was essential for cellular location. Further biophysical experiments identified ligands for the extracellular domains include sugar motifs such as the glycan backbone of peptidoglycans and sugar containing antibiotics. This has led to a new functional model for ST kinases in enterococci.

## Abbreviations

1D	One-dimensional
2D	Two-dimensional
3D	Three-dimensional
Å	Angstrom
ADP	Adenosine 5'-diphosphate
ATP	Adenosine 5'-Triphosphate
AUC	Analytical ultracentrifugation
BHI	Brain heart infusion
bp	Base pair
C-terminus	Carboxy-terminus
CD	Circular Dichroism
CV	Column Volume
Da	Dalton
DMSO	Dimethyl sulfoxide
DNA	Deoxyribonucleic acid
EDC	1-Ethyl-3-(3-dimethylaminopropyl)carbodiimide
EDTA	Ethylenediaminetetraacetic acid
ESI-MS	Electrospray Ionisation-Mass Spectrometry
eSTK	eukaryotic-like Serine/Threonine kinase
eSTP	eukaryotic-like Serine/Threonine phosphatase
FL	Full Length
GFP	Green fluorescent Protein
GlcNAc	N-acetylglucosamine
HCL	Hydrochloric acid
HEPES	4-(2-hydroxyethyl)-1-piperazineethanesulfonic acid
HK	Histidine Kinase
HMW	High molecular weight
HP	High Performance

HSQC	Heteronuclear single quantum coherence
IE	Infective Endocarditis
IMAC	Immobilised Metal Affinity Chromatography
IPTG	Isopropyl $\beta$ -D-1-thiogalactopyranoside
IR	Infrared
$K_a$	Association constant
Kb	Kilo base
$K_d$	Dissociation constant
$K_D$	Equilibrium dissociation constant
KD	kinase domain
KDa	Kilo Dalton
LB	Lysogeny Broth
LMW	Low molecular weight
mEGFP	monomeric enhanced green fluorescent protein
MGT	Monofunctional glycosyltransferase
MHII	Muller Hinton (cation adjusted)
MIC	Minimal Inhibitory Concentration
MSRA	Methicillin Resistant Staphylococcus aureus
MST	Microscale Thermophoresis
MurNAc	N-acetylmuramic acid
Mw	Molecular Weight
N-terminus	Amino-terminal
NADPH	Nicotinamide adenine dinucleotide phosphate
NHS	N-hydroxysuccinimide
NMR	Nuclear magnetic resonance
NOE	Nuclear Overhauser Effect
NOESY	Nuclear Overhauser Effect spectroscopy
$^{\circ}\text{C}$	Degrees Celsius
$\text{OD}_{600\text{nm}}$	Optical density at 600nm
PAGE	polyacrylamide gel electrophoresis
PASTA	Penicillin binding protein and serine/threonine kinase associated

PBP	Penicillin Binding Protein
PBS	Phosphate buffered saline
PCR	Polymerase chain reactions
PDB	Protein Data Bank
PEP	phosphoenol- pyruvate
PG	Peptidoglycan
pH	$\text{Log}_{10}[\text{H}^+]$
pI	Isoelectric point
qPCR	quantitative Polymerase chain reaction
Rg	radius of gyration
RNA	Ribonucleic acid
RPM	Rotations per minute
RR	Response regulator
SAXS	Small angle x-ray scattering
SDS	Sodium dodecyl sulphate
SEC-MALS	Size exclusion chromatography-multiple angle light scattering
Spp.	Species
SPR	Surface plasmon resonance
TCS	Two component systems
TEMED	Tetramethylethylenediamine
TEV	Tobacco Etch Virus
TM	Transmembrane
$T_M$	Melting Temperature
TM	transmembrane domain
TOCSY	Total Correlated spectroscopy
UDP	Uridindiphosphate
UTI	Urinary tract infection
VRE	Vancomycin Resistant Enterococcus
WHO	World health organisation
WT	Wild type

# Chapter 1. Introduction

## 1.1. The Bacterial Cell Wall

### 1.1.1. The role of Peptidoglycan

Peptidoglycan (PG) is essential for bacterial survival and inhibition of its biosynthesis can result in cell lysis. PG is a macromolecular polymer that forms a semi-rigid exoskeleton that surrounds the bacterial cytoplasmic membrane. Its role is to endure the cellular turgor pressure by stretching as the cytoplasm grows and is strong enough to prevent cellular rupture (Vollmer *et al.*, 2008a; Bugg, 1999; Young, 2010). It can contribute to the cellular shape of bacteria through its close association with cell growth and division (Vollmer *et al.*, 2008b). PG also provides a non-structural role as a scaffold to anchor extracellular structures such as lipoproteins in Gram-negative bacteria and teichoic acids in Gram-positive bacteria. The proteins that associate with PG on the bacterial cell surface in Gram-positives are involved in adhesion, invasion, and resistance to phagocytic killing and are therefore important in pathogenicity (Navaare and Schneevind, 1999).

### 1.1.2. Peptidoglycan Structure

#### 1.1.2.1. The Gram-negative bacterial cell envelope

The Gram-negative cell envelope is comprised of an outer membrane, a thin layer of PG, and an inner cytoplasmic membrane. The outer membrane outer leaflet is composed of glycolipid lipopolysaccharides, and the inner leaflet contains phospholipids. The outer-membrane acts as a semi-permeable surface and prevents molecules that result in lysis, including cell wall antibiotics and lysozyme from entering the cell (Silhavy *et al.*, 2010) (**Figure 1.1, Left**). The PG layer in Gram-negatives is relatively thin in comparison to Gram-positives. Crosslinking in Gram-negatives also differs and is mostly achieved through direct cross-linking between adjacent peptide stems, compared to Gram-positives where more significant variation occurs in the third position of the peptide stem resulting in side-chain branching (Vollmer, 2008b). Due to the PG layer in Gram-negative being thin, advanced mechanisms have evolved to evade destruction by

the antibiotic that targets the cell wall by interfering with its polymerization such as  $\beta$ -lactamases that target  $\beta$ -lactam antibiotics (Zeng and Lin, 2013).

### 1.1.2.2. The Gram-positive bacterial cell wall

The Gram-positive cell wall include the inner membrane and a thick PG layer (**Figure 1.1, Right**). An additional S-layer external to the PG layer is also present in some Gram-positive species. The cell walls are thick, with 20-50 interconnected layers of PG resulting in a sizeable macromolecular structure (Young, 2010). Although the PG is the primary component of the Gram-positive cell wall, this structure is supplemented by secondary cell wall glycopolymers that can alter the rigidity and biological characteristics of the wall. These include teichoic acid (a linear polymer of glycerol or ribitol connected by phosphate groups) and lipoteichoic acids (where fatty acid substitutions anchor teichoic acid to the plasma membrane). The role of these secondary components protects the cells from various chemicals and enzymes such as antimicrobial compounds and also decreases host immune defences to allow survival in hostile environments (Kohler *et al.*, 2009; Rajagopal *et al.*, 2016). They may also play a role in recognition by internal and external proteins (Steen *et al.*, 2003).

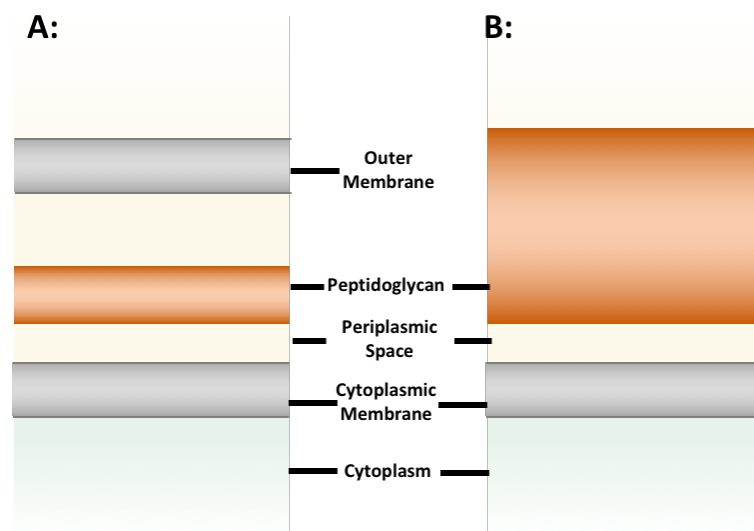


**Figure 1.1 - Bacterial cell wall architecture.** Major features are highlighted in schematic form of both Gram-negatives (A) and Gram-positives (B). Both cell walls contain a PG layer which is thick in Gram-positive bacteria (20-50 layers) and thin in Gram negatives (1-3 layers).

### 1.1.3. Peptidoglycan biosynthesis

PG biosynthesis is a complex polymerization process with the precursors of PG are synthesized in the cytoplasm and in the inner membrane of the cell, and the polymerization occurring at the extracellular region. PG synthesis begins in the cytoplasm, where multiple enzymatic steps are necessary to assemble a disaccharide-peptide precursor attached to a lipid carrier molecule. This can be summarised in three main reactions including the formation of UDP-MurNac from UDP-GlcNac, the assembly of the peptide stem leading to UDP-MurNac-pentapeptide and the membrane steps in the accumulation of lipid I and lipid II (**Figure 1.2**) (Barreteau *et al.*, 2008).

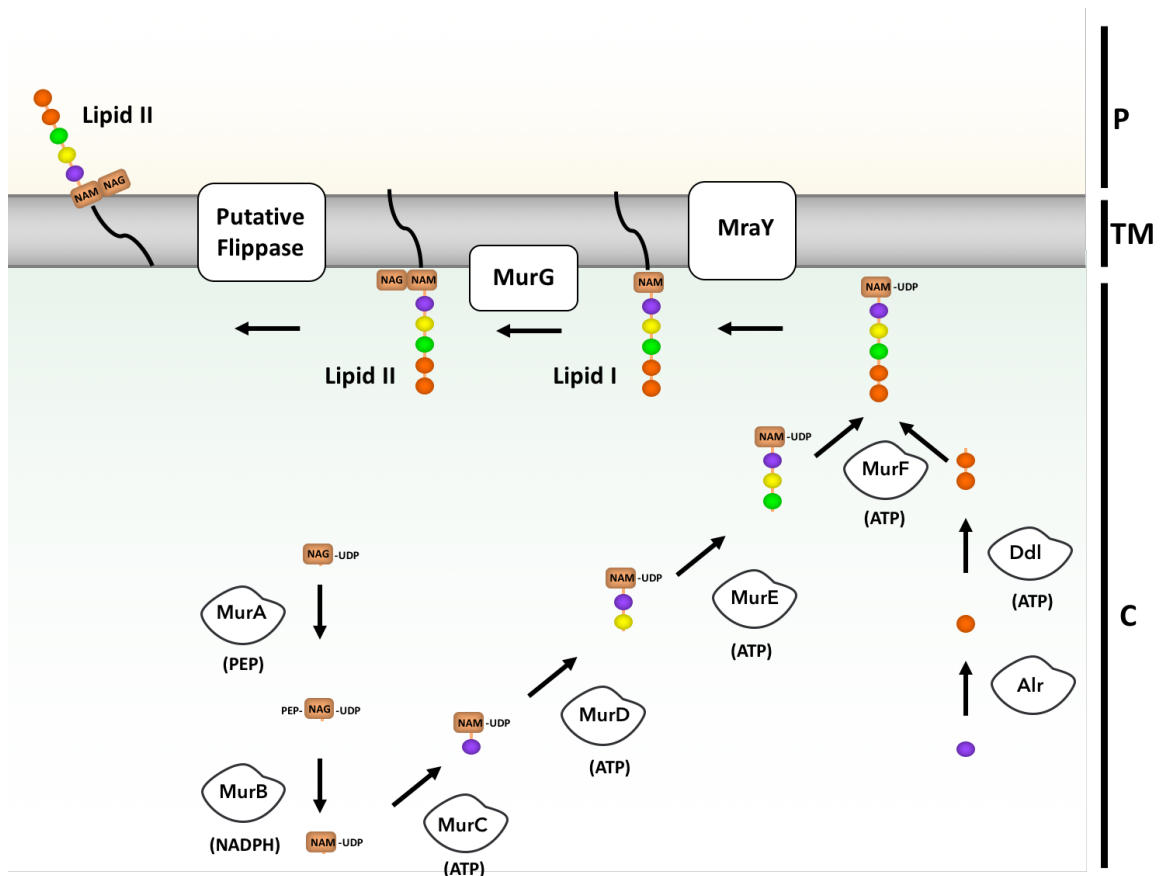


**Figure 1.2 - The cytoplasmic and membrane associated steps in PG biosynthesis.** NAM = MurNac, NAG = GlcNac, P = periplasm, TM = Transmembrane and C = Cytoplasm. UDP-GlcNac is converted to UDP-MurNac by MurA and MurB. MurC-MurF sequentially add L-Ala, D-Glu, L-Lys (or meso- DAP) and D-Ala-D-Ala to UDP-MurNac. MraY transfers UDP-MurNac-pentapeptide to the undecaprenyl lipid carrier and MurG adds a final GlcNac to form Lipid II. Lipid II is flipped to the extracellular space by a flippase.

UDP-GlcNAc is the first precursor molecule in the PG biosynthesis pathway and is derived from fructose-6-phosphate. UDP-MurNAc is formed from UDP-GlcNAc and requires two enzymes. MurA catalyses the first step of this transformation by transferring the enolpyruvate moiety of the phosphoenolpyruvate (PEP) to the 3'hydroxyl of UDP-GlcNAc with the release of the organic phosphate (Pi). The resulting product, UDP-GlcNAc-enol-pyruvate, undergoes a reduction catalysed by MurB using NADPH and a solvent derived proton and results in UDP-MurNAc. In *E. faecalis*, there are two MurA proteins that have been identified, denoted MurAA and MurAB, with MurAA (and not MurAB) being associated with the intrinsic cephalosporin resistance of the organism (Vesic and Kristich, 2012).

The second step in PG biosynthesis is the stepwise assembly of the peptide stem, carried out sequentially by a group of enzymes known as the Mur ligases including MurC, MurD, MurE and MurF. The Mur ligases have the same reaction mechanisms and catalyse the formation of an amide or a peptide bond with simultaneous formation of ADP and Pi from ATP. A divalent cation, Mg<sup>2+</sup> or Mn<sup>2+</sup> is essential for the reaction. The ligase MurC incorporates the first amino acid into the peptide stem. In most bacterial species, this is L-Ala, but other amino acids including Gly or L-Ser have also been observed at this position (Schleifer & Kandler, 1972). The MurD ligase is responsible for the incorporation the second amino acid into the peptide stem. In all species, this amino acid is D-Glu, but chemical modifications can occur at a later step resulting in either D-Ile for most Gram-negative bacteria or D-Ile for most Gram-positive bacteria in the second position. The ligase MurE catalyses addition of the third amino acid into the peptide stem. The amino acid substrate is a di-amino acid and is usually either meso-A2pm in most Gram-negative bacteria, *Mycobacteria* spp. and *Bacilli* spp., or L-Lys in most Gram-positive bacteria (Ruane *et al.*, 2013). In certain species of bacteria, other di-amino acids and mono-amino acids are used as substrates. The specificity of the MurE ligase for its substrate is specific (Strancar *et al.*, 2007).

The terminal amino acid residues in the peptide stem reside in the fourth and fifth positions and are incorporated as a dipeptide, usually as D-Ala-D-Ala. Ddl is the enzyme responsible for the synthesis of the D-Ala-D-Ala dipeptide, and MurF is the ligase responsible for the incorporation of the substrate into the peptide stem. The D-Ala residue in the fourth position is present all species to date, but variation can occur in the

5th position. D-Lac or D-Ser occurring in the terminating fifth position is often associated with bacteria that utilize intrinsic or acquired vancomycin resistance mechanisms. These changes in the fifth position can result in a reduced affinity of antibiotics like vancomycin from binding to PG precursors and allowing the continuation of PG maturation (Healy *et al.*, 2000).

The membrane associated step begins with the transfer of the phosphor-MurNAc-pentapeptide moiety from the cytoplasmic precursor to the membrane receptor undecaprenol phosphate (C55~P). This transfer is catalysed by the transferase enzyme *MraY* to yield Lipid I (undecaprenyl-pyrophosphoryl-MurNAc-pentapeptide). *MurG* then catalyses the transfer of the GlcNAc moiety from UDP-GlcNAc to lipid I, yielding lipid II (undecaprenyl-pyrophosphoryl-MurNAc-pentapeptide-GlcNAc). Once amassed, the lipid II is translocated through the cell membrane by a yet unidentified mechanism although candidates have been proposed and are of current debate (Al-Dabbagh *et al.*, 2008). Recent evidence suggests that *MurJ* is the protein responsible for translocation of lipid II across the membrane although other candidates have included *FtsW* (Bolla *et al.*, 2018; Leclercq *et al.*, 2017; Mohammadi *et al.*, 2011). On the periplasmic side of the cytoplasmic membrane, membrane-associated transglycosylases and transpeptidases attach the PG monomers to the nascent growing sacculus, forming rigid glycan chains and crosslinking adjacent stem peptides, respectively.

Variations in the PG peptide stem including amidation, hydroxylation, acetylation, attachment of amino acids or other groups, and attachment of proteins occur after the action of the Mur ligases, often at the level of lipid II. These modifications occur essentially at positions 2 and 3 although most of the enzymes for these modifications are still unknown. Most chemical and structural variation in PG is due to the different cross-linking patterns that can occur. These variations are as a result not only the position in the peptide stem the cross-linking occurs but also the chemical composition of the cross-link itself. 3-4 cross-linking between peptide stems is the primary form of cross-linking in most bacteria (except coryneform bacteria where 2-4 cross-linking occurs). The cross-linkage extends from the amino group of the side-chain of the residue at position 3 of one peptide subunit (acyl acceptor) to the carboxyl group of D-Ala at position 4 of another (acyl donor). A direct cross-link (most bacteria, *Mycobacteria* or *Bacilli*) or a branched bridge (most Gram-positive bacteria) is used to link peptide stems. Various amino acids

can be encountered during branching at varying lengths, with some examples listed in **Table 1.1** along with the enzymes involved. Gly and L-amino acids are activated as aminoacyl-tRNAs and transferred to the precursors by a family of non-ribosomal peptide bond-forming enzymes called Fem transferases (Lavollay *et al.*, 2008). By contrast, D-Amino acids are activated as acyl phosphates by proteins belonging to the ATP-grasp family, which is composed of highly diverse enzymes that catalyse the ATP-dependent ligation of a carboxyl group to an amino or imino nitrogen, hydroxyl oxygen or thiol sulphur (Galperin and Koonin, 1997).

**Table 1.1 - Summary of PG branching in key Gram-positive bacteria** (adapted from Vollmer *et al.*, 2008).

Species	Branching Type	Enzyme	Family	Reference
<i>E. faecalis</i>	L-Ala-L-Ala	BppA1, BppA2	Fem Transferase	Bouhss <i>et al.</i> , 2002
<i>E. faecium</i>	D-Asx	Asl <sub>fm</sub>	ATP-grasp	Bellais <i>et al.</i> , 2006
<i>S. aureus</i>	(Gly) <sub>5</sub>	FmhB, FemA, FemB	Fem Transferase	Schneider <i>et al.</i> , 2004
<i>S. pneumoniae</i>	L-Ala-L-Ala or L-Ala L-Ser	MurM, MurN	Fem Transferase	Fiser <i>et al.</i> , 2003; Lloyd <i>et al.</i> , 2008

D-Ala at position 4 is not the only possible acyl donor: the carboxyl group of the amino acid at position 3 can also play this role. This gives rise to the appearance of 3–3 cross-links, which were initially discovered in Mycobacteria where their formation is catalysed by penicillin-insensitive L,D-transpeptidases (Mainardi *et al.*, 2005). Such mechanisms have now been identified in bacteria including pathogens such as *M. tuberculosis*, *E. coli* and *E. faecium*.

PG metabolism is a dynamic process which coordinates with the dynamic process of cellular growth and division. Old PG is actively hydrolysed and removed, and new cell wall material is incorporated into actively growing cells. Gram-negative bacteria have also evolved sophisticated PG recycling mechanisms which have not clearly demonstrated in Gram-positives (Reith and Mayer, 2011). PG hydrolases are a class of enzymes that associate with the removal of existing PG by digesting PG at a particular motif in the cell wall to help incorporate new precursors. New PG is incorporated into existing PG by a PG synthetase (also known as a Penicillin-binding protein; PBP). These enzymes can catalyse

the polymerization of glycol strands (transglycosylation) and the cross-links between peptide stems (transpeptidation) (**Figure 1.3**). PBPs are broadly classified into two classes; the high molecular weight Class A and Class B PBPs and the low molecular weight Class C PBPs. The functions of each PBP can vary from transglycosylation, transpeptidation, carboxypeptidation, and endopeptidation. Class A PBPs are multi-modular and usually bifunctional enzymes with both a transglycosylase and D,D-transpeptidase domain. Class B PBPs are monofunctional enzymes containing D,D-transpeptidase domain (**Figure 1.4**). The activity of the Class C PBPs is often associated with cell operation, PG maturation, and recycling (Sauvage *et al.*, 2008). **Table 1.2** highlights the key PBPs in various Gram-positive bacteria.

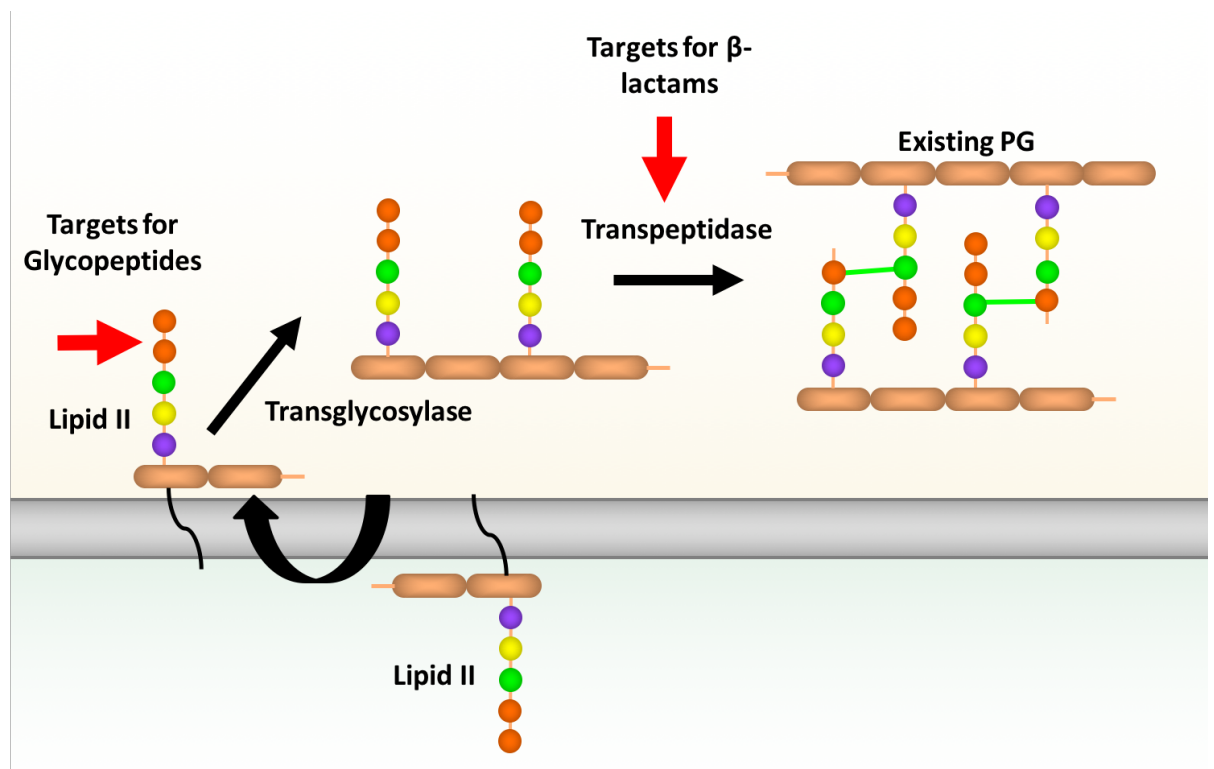


**Figure 1.3 - Summary of PG polymerisation and the cell wall antibiotics that can inhibit the process.** Following the translocation of Lipid II to the side of the cytoplasmic membrane, the GlcNAc /MurNAc disaccharides of lipid II are polymerised into glycan chains by transglycosylases. Transpeptidases form cross-links between newly synthesised PG and existing PG via the pentapeptide stems to give structural rigidity. The lipid carrier

is translocated back across the cytoplasmic membrane either before or after dephosphorylation.

**Table 1.2 - Summary of Class A and Class B PBPs in key Gram-positive bacteria.** MWs are in brackets in kDa adapted from Arbeloa *et al.*, (2004).

Species	Class A			Class B		
	A3	A4	A5	B1	B4	B5
<i>E. faecalis</i>	<i>ponA</i> (85.4)	<i>pbpF</i> (79.5)	<i>pbpZ</i> (88.5)	<i>pbp5</i> (74.0)	<i>pbpB</i> (81.7)	<i>pbpA</i> (77.9)
<i>E. faecium</i>	<i>ponA</i> (86.6)	<i>pbpF</i> (86.6)	<i>pbpZ</i> (86.7)	<i>pbp5</i> (73.7)	<i>pbpB</i> (81.0)	<i>pbpA</i> (78.9)
<i>S. aureus</i>	<i>pbp2</i> (79.3)	-	-	<i>pbp2a*</i> (76.3)	<i>pbp1</i> (82.7)	<i>pbp3</i> (77.2)
<i>S. pneumoniae</i>	<i>pbp1a</i> (79.8)	<i>pbp2a</i> (80.8)	<i>pbp1b</i> (89.5)	-	<i>pbp2x</i> (82.3)	<i>pbp2b</i> (73.9)

\*Note that Pbp2a is an acquired resistance mechanism that results in MSRA

#### 1.1.4. Polymerisation of Peptidoglycan

The formation of 3-3 crosslinks is catalysed by the L,D-transpeptidases and is thought to be a bypass mechanism for the 4-3 cross-linking pathway that is a target by the  $\beta$ -lactam antibiotics (Mainardi *et al.*, 2008). L,D-transpeptidases cleave the remaining D-ala moiety of the peptide stem and transfers the bond energy to the side chain of another meso-diaminopimelic in an adjacent peptide chain. The first enzyme found to possess L,D transpeptidase activity was isolated from an *E. faecium* mutant strain that acquired high-level resistance to ampicillin by producing exclusively 3-3 cross-linked PG (Mainardi *et al.*, 2000). Genes encoding L,D-transpeptidases have been identified in the genomes of Gram-positive and Gram-negative bacteria alike (Magnet *et al.*, 2007). Although L,D-transpeptidases and PBPs perform similar reactions, they are structurally unrelated to one another. D,D-transpeptidases have a serine residue for their catalytic activity and use a pentapeptide stem as the acyl donor substrate (Goffin *et al.*, 2002). L,D-transpeptidases contain an active site cysteine and recognize tetrapeptide stems as the donor substrates (**Figure 1.4**) (Lecoq *et al.*, 2012).

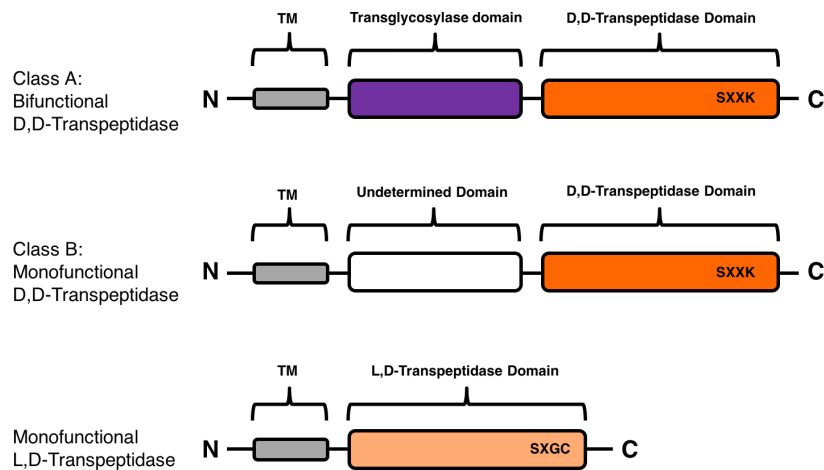


**Figure 1.4 - Classification of the major types of proteins involved in PG transpeptidation in *Enterococcus* spp.** Classifications identified on the left hand side and domain topology for each class is shown where TM: transmembrane, N: amino-terminus, C: carboxyl-terminus, Catalytic sequence motifs for each type identified (SXXK for D,D-transpeptidation and SXGC for L,D-transpeptidation).

Other variations can occur in PG between different species. Classically, the glycan strands are composed of alternating MurNAc and GlcNAc residues linked by a  $\beta$ -1,4 glycosidic bond. Many organisms display glycan modifications such as deacetylation of MurNAc/GlcNAc residues and N-glycosylation, O-acetylation or phosphorylation of MurNAc residues (Vollmer, 2008b).

### 1.1.5. Peptidoglycan hydrolases

As previously mentioned, PG hydrolases are a class of enzymes responsible for cleaving PG at particular motif in the cell wall to help incorporate new precursors ensuing the maintenance of overall cell wall PG turnover. There are three main classes of bacterial PG hydrolases that include the glycosidase, which cleave the glycan backbone, the amidases, that cleave the side-chain peptides and the peptidases, which includes the endopeptidases and carboxypeptidases that can cleave within the peptide side chain. **Figure 1.5** highlights the classes of hydrolases and the location of their hydrolase activity in the PG (Vollmer *et al.*, 2008a; Ghuysen *et al.*, 1966). Glycosidases are classified into two groups; the N-acetylglucosaminidases which hydrolyses GlcNAc residues and N-acetylmuramidases which hydrolyse the  $\beta$ -1-4 glycosidic bond between the MurNAc and GlcNAc residues from the glycan strands (Vollmer *et al.*, 2008a).

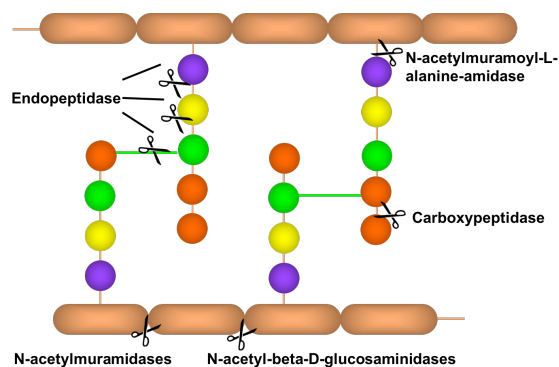


**Figure 1.5 - Summary of PG hydrolase classes and the cleavage sites for each hydrolase.**

PG terminases have been described recently and have a similar function to that of hydrolases. MltG is a terminase first described in *E. coli* and has been associated with determining and regulating the length of the glycan strand in PG. The activity of the MltG terminase results in a terminating anhydro-MurNAc residue of oligomeric glycan chains. MltG-like proteins have been identified in 70% of sequenced bacteria including *E. faecalis*. Species that lack MltG includes coccal species or those that lack a cell wall (Yunck *et al.*, 2016).

### 1.1.6. Antibiotics that target the wall

Cell wall antibiotics are a class of antibacterial that interfere with the synthesis and maintenance of PG. They mainly include the  $\beta$ -lactam and glycopeptide classes alongside a few other independent antibiotics including Fosfomycin, Bacitracin, D-cycloserine, Colistin, Polymyxin B and Daptomycin (Bugg and Walsh, 1992).

The function and role of each antibiotic including those associated with the cell wall are discussed further in relation to targeting *Enterococcus* spp. and associated resistance but a summary of clinically used antibiotics are summarised in **Table 1.3** and highlights the most critical antibiotics as highlighted by the World Health Organization (WHO) list of essential medicines (WHO, 2017). The list highlights the most essential drugs in modern medicine and enables the assistance in the development of tools for antibiotic stewardship at local, national and global levels to reduce antimicrobial resistance in both adults and children. The number of antibiotics that fall under the WHO essential medicines and those prioritized for reservation highlights the importance of these antibiotics in modern medicine.

**Table 1.3 - List of both clinically used cell wall antibiotics and antibiotics in clinical trials.** Antibiotics in the WHO essential medicines listed are included and include Group 1 Access (**Bold**), Group 2 Watch (Underline) and Group 3 Reserve (**Red Bold**) (WHO, 2017).

Class	Sub-Class	Generation	Name
B-lactam	Penicillin's	$\beta$ -lactamase sensitive	<b>Benzylpenicillin, Benzathine benzylpenicillin, Procaine benzylpenicillin, Phenoxymethylpenicillin</b>
		$\beta$ -lactamase resistant	<b>Cloxacillin, Dicloxacillin, Oxacillin, methicillin</b>
		Aminopenicillins	<b>Ampicillin, Amoxicillin, Pivampicillin, Bacampicillin, Flucloxacillin</b>
		Carboxypenicillins	Ticarcillin, Temocillin
		Ureidopenicillins	Piperacillin,
	Penems		<u>Faropenem</u>
	Carbapenems		Ertapenem, Doripenem, <u>Imipenem, Meropenem,</u>
	Cephalosporin's	1 <sup>st</sup> Generation	<b>Cefazolin, Cefalexin, Cefadroxil</b>
		2 <sup>nd</sup> Generation	Cefaclor, Cefotetan, Cefoxitin, Cefprozil, Cefuroxime, Cefuroxime axetil
		<u>3<sup>rd</sup> Generation</u>	<u><b>Cefixime, Ceftriaxone, Ceftazidime, Cefdinir, Cefotaxime, Ceftibuten, Cefditoren</b></u>
		<b>4<sup>th</sup> Generation</b>	<b>Cefepime</b>
		<b>5<sup>th</sup> Generation</b>	<b>Ceftaroline, Ceftobiprole</b>
Monobactams	-	<b>Aztreonam</b>	
B-lactam inhibitors	-	Avibactam, Clavam	
Glycopeptides	-	-	<u><b>Vancomycin, Teicoplanin, Oritavancin, Ramoplanin, Telavancin</b></u>
Intracellular Targets	-	-	<b>Fosfomycin, D-Cycloserine, Bacitracin</b>
Other Targets	-	-	<b>Polymixin B, Colistin, Daptomycin</b>

## 1.2. Background on Enterococci bacteria

### 1.2.1. Characteristics and Physiology

The genus *Enterococcus* belongs to the low GC branch of Gram-positive bacteria belonging to the phylum Firmicutes and members of the lactic acid bacteria group (Klare *et al.*, 2001). Before 1984, *Enterococcus* spp. were classified with the *Streptococcus* spp. but were found later to be distinctly different to streptococci (Schleifer and Kilpper-Balz, 1984). The *Enterococcus* genus is placed in the Enterococcaceae family along with genus *Bavariicoccus*, *Catelliococcus*, *Melissococcus*, *Pilibacter*, *Tetragenococcus* and *Vagococcus* (Ludwig *et al.*, 2009). The genus contains 54 species and includes species that reside in the gastrointestinal (GI) tracts of humans and animals forming part of the healthy flora (Mundt, 1963a; Parte *et al.*, 2013). Species can also be isolated from the guts of insects (Martin and Mundt, 1972), various environments including plants (Mundt, 1963b), sewage (Kenner *et al.*, 1961) and water (Ator and Starzyk, 1976).

*Enterococcus* spp. can endure a broad pH and temperatures as well as hypotonic and hypertonic conditions which plays an important feature in their broad distribution. They typically have an optimum growth temperature of 35°C and a growth range from 10 to 45°C (Sherman, 1937; Sherman, 1938; Byappanahalli *et al.*, 2012). Enterococci colonise a small proportion of the gut consortium, (1 % of the adult microflora) (Finegold *et al.*, 1983; Sghir *et al.*, 2000). Little is known about the primary mechanisms used by enterococci to colonize GI tracts of either healthy individuals or hospitalized patients. The exposure of hospitalized patients to antibiotics results in significant modifications of the gut microbiota, which facilitate colonization of the GI tract by drug-resistant enterococci (Donskey *et al.*, 2000; Ubeda *et al.*, 2010).

The main morphological characteristics of all enterococci include their spherical or ovoid shape and their arrangement in either pairs or chains with single cells having a diameter of around 1 µm (Domig *et al.*, 2003). Physiologically, enterococci are non-spore forming facultative anaerobes and obligatory fermentative chemoorganotrophs (Facklam, 1973).

As a reflection of their highly evolved role as members of a consortium in an extremely competitive environment, enterococci have reduced genomes that range from

2.3 Mb to 3.9 Mb across species sequenced thus far (Van Schaik *et al.*, 2010; Dubin and Pamer, 2014). Gene mobility and exchange have allowed *Enterococcus* spp. to prominently rise as a nosocomial pathogen. The *E. faecalis* strain OG1X is a fully susceptible, well characterized and studied strain. It contained no mobile elements and no acquired DNA when its genome was sequenced (Bourgogne *et al.*, 2008). This contrasts sharply with the genome of *E. faecalis* V583 which confers vancomycin resistance, in which approximately 25% of its genome consists of acquired DNA (Polidori *et al.*, 2011; Kristich *et al.*, 2014). The selective pressure in a clinical setting and the presence of antibiotics in the environment have resulted in clinical isolates that have gained an array of resistant mechanisms through the acquisition and exchange of DNA elements.

### **1.2.2. Pathogenesis**

*Enterococcus* spp. are a leading cause of infective endocarditis, bacteraemia, and urinary tract infections (UTIs) and have been emerging as leading causes of multidrug-resistant hospital-acquired infections in the 1970s and 1980s (Huycke *et al.*, 1998; Jett *et al.*, 1994). They now rank among leading causes of hospital-acquired infections of the bloodstream, urinary tract, surgical wounds, and other sites (Hidron *et al.*, 2008; Tacconelli *et al.*, 2017). Both *E. faecalis* and *E. faecium* are identified as being the causative agents of over 90% of *Enterococcus* spp. related nosocomial infections and recently identified as high priority and placed at the top of the list of Gram-positive bacteria that are on the WHO priority list of antibiotic-resistant bacteria (Tacconelli *et al.*, 2017). Infections affect immunocompromised patients, children and the elderly. Infections by *Enterococcus* spp. are therefore associated with haemato-oncological, paediatric and intensive care units. The growing number of infections caused by *Enterococcus* spp. is also linked to a growing population, especially in industrialized countries. Some members of the microbiota, including commensal *Enterococcus* spp. can act as opportunistic pathogens and translocate across the mucosal barrier to cause systemic infection in immune-compromised hosts (Berg, 1996; Donskey *et al.*, 2004). More commonly, however, infection results from the colonization, overgrowth, and translocation of hospital-adapted antibiotic-resistant strains with enhanced

pathogenicity. *Enterococcus* spp. can cause a variety of infections that are summarised below.

#### **1.2.2.1. Infective Endocarditis**

Infective endocarditis (IE) is causes inflammation of the endocardium in both native and prosthetic heart valves (Fitzsimmons *et al.*, 2010). *E. faecalis* causes 97% of IE infection out of those from the *Enterococcus* spp. (Baddour *et al.*, 2015). Colonization of the heart valves is thought to occur during transient bacteraemia where microorganisms adhere via cell surface receptors which are formed over areas of injured endothelial tissue. Endothelial cells respond to bacterial cell binding and internalization through tissue factor activity and cytokine production which attracts monocytes from the blood leading to enlargement of the endocardial vegetation which is poorly responsive to antimicrobial therapy. Disruption of these lesions through sheer force via blood flow or endothelial cells lysis can result in fragments of the lesions (septic emboli) travelling to remote areas of the body with sometimes fatal effects (Prendergast, 2006).

Factors that coincide with IE include poor dental hygiene, long-term haemodialysis and diabetes mellitus with human immunodeficiency virus (HIV) also increasing the risk of IE (Mylonakis and Calderwood, 2001). Infections from *Enterococcus* spp. are associated with high mortality rates including IE. Mortality rates are as high as 20-40 % in those patients with infections from *Enterococcus* spp. and has broadly remained unchanged in the past 30 years (Miro *et al.*, 2013).

Treatment of IE is often difficult as the organism must first be isolated and identified (Lang, 2008). In patients who have become acutely ill, empirical therapy will be given until the organism has been identified. Once antibiotic susceptibility tests have been carried out on the isolate, an appropriate antibiotic therapy regime can be initiated (Elliott *et al.*, 2004). Different regimes have been developed with the use of aminoglycosides as a standard for IE infections caused by *Enterococcus* spp. but a rise in resistance has led to new therapies being explored. This includes double  $\beta$ -lactam therapies including ampicillin and ceftriaxone but comes a great risk as they both target the bacterial cell wall (Beganovic *et al.*, 2018).

#### **1.2.2.2. Bacteraemia**

Bacteraemia is the presence of bacteria in the blood. 10% of all blood stream infections are caused by *Enterococcus* spp. The occurrence of bacteraemia by *Enterococcus* spp. is often the consequence of a primary infection. Common sources include the urinary tract from catheters, infections of the bile tract or an intra-abdominal infection (Murray, 1990; Soule and Climo, 2016). Due to the ability for *Enterococcus* spp. to harbour different resistant mechanisms, mortality is often higher in patients with bacteraemia from these strains. The mortality associated with VRE bacteraemia is 20-46% (Salgado and Farr, 2003). Intensive care unit (ICU) patients are one of the most susceptible groups to be affected by infection from *Enterococcus* spp. due to the severity of illness and constant exposure to multiple antibiotic regimes (Zhu *et al.*, 2009). A recent study demonstrated that recurrent bacteraemia from *E. faecium* was from different strains using genome-based analysis. This was likely due to cross transmission in a hospital environment (Raven *et al.*, 2018).

#### **1.2.2.3. Urinary tract infections**

Urinary tract infections (UTIs) are one of the most common bacterial infections caused by both Gram-positive and Gram-negative bacteria effecting 150 million people worldwide every year. (Stamm and Norrby, 2001). *E. coli* is the most frequently reported pathogen causing 70-95 % of upper and lower UTIs (Foxman, 2010; Chakupurakal *et al.*, 2010). The urinary tract is usually a sterile environment, but this can be disturbed by a variety of factors. These include cystitis, having a prior UTI, sexual activity, pregnancy, vaginal infections, diabetes, obesity and genetic susceptibility (Foxman, 2010). UTIs account for the most common type of bacterial infection in women, with around half of them experiencing at least one infection in their lifetime (Nicolle, 2012). Factors that make *Enterococcus* spp. successful UTI pathogens include the presence of adherence factors Esp (adhesin), Ace (adhesin) and Ebp (Pili), which aid in biofilm formation (Flores-Mireles *et al.*, 2015).

#### **1.2.2.4. Meningitis**

Meningitis caused by *Enterococcus* spp. is rare and uncommon, but patients who suffer will have an underlying disease such as diabetes mellitus or renal failure (Laguna *et al.*, 2009). Recently it was reported that Enterococcal meningitis was identified in a 70

year old male without any predisposing factors and highlights the significance of Enterococcal infections arising from a community setting (Dhanalakshmi *et al.*, 2015).

### **1.2.3. Antimicrobial Therapy and Resistance**

During antimicrobial chemotherapy, treatment aims to achieve a drug concentration above the minimum inhibitory concentration (MIC) for the organism concerned; the concentration of antimicrobial agent at which growth is sufficiently inhibited (Andrews, 2001; Baddour *et al.*, 2005). Therapeutic treatment depends on the susceptibility profile of the microorganism to avoid the emergence of antimicrobial resistance. For antibiotic susceptible enterococci, glycopeptide antibiotics are bactericidal at clinically achievable concentrations, but the emergence of VRE strains has led to the use of these antibiotics being limited to combination therapies when required (Landman and Quale, 1997; Elliott *et al.*, 2004; Baddour *et al.*, 2005). Combinations of glycopeptides and aminoglycosides or ampicillin and ceftriaxone are the main arsenal used to treat enterococcal infections. Hospital outbreaks of vancomycin-resistant enterococci (VRE) have been associated with haematology, renal surgery and intensive care units where patients are severely immunocompromised (Timmers *et al.*, 2002; Kawalec *et al.*, 2007; Beganovic *et al.*, 2018).

Difficulties in treating *Enterococcal* spp. infections has resulted in proposals for new therapies including the use of Niclosamide, a drug commonly used for tape work infections as it has been shown to have potent antibacterial properties against VRE strains (Mohammad *et al.*, 2018). The evolution of antibiotics used to treat *E. faecalis* bloodstream infections and infective endocarditis has recently been evaluated and highlights how rapid in antibiotic regimes change to treat Enterococcal spp. infections (Beganovic *et al.*, 2018).

### **1.2.4. Antibiotics and antibiotic resistance in *Enterococcus* spp.**

The discovery of penicillin by Alexander Fleming (1929) led to the global introduction of antimicrobials to treat bacterial infections and has been considered one of the most significant developments in medicine. A large number of new classes of antibiotics emerged between 1940-1960 and kept bacterial infections at a low level (Walsh and Wright, 2005). Due to the success of these antimicrobials, the pharmaceutical

industry has been investing less in such therapeutics leading to a period of nearly 40 years in which no new antimicrobials have been introduced (von Nussbaum *et al.*, 2006). Due to the lack of new antibiotic classes and the overuse of existing drugs, there is an increasing prevalence of antimicrobial resistance globally.

Antimicrobial resistance is a significant threat to modern society, and a current concern leading to the commission of the O'Neill report (2015). This report estimates that by 2050, 10 million people will die annually, overtaking cancer death rates and a worldwide economic burden of \$100 trillion. Besides the ability to adapt to a wide range of environmental and physiological stresses, *Enterococcus* spp. possess a broad spectrum of natural antibiotic resistance mechanisms (Murray., 1990; Klare *et al.*, 2003; Arias and Murray 2008). The treatment of infections from *Enterococcus* spp. has become an enormous challenge for clinicians due to the ability of these organisms to develop resistance to the standard drug choices, namely ampicillin, vancomycin and aminoglycosides (Arias and Murray, 2012). *Enterococcus* spp. are intrinsically resistant to a large number of penicillin's, all classes of cephalosporins (except for the 5th generation cephalosporin, ceftobiprole in *E. faecalis*) and monobactams to name a few (Arias *et al.*, 2010; Kristich *et al.*, 2014). Antibiotics that target *Enterococcus* spp. and their associated resistance mechanisms is discussed below.

#### **1.2.4.1. Types of antimicrobial resistance**

Isolated or multiple genes can be involved in antimicrobial resistance. These genes can involve several different targets and have access to a variety of different protection pathways via different mechanisms (Martinez and Baquero, 2000). The mechanism for antimicrobial resistance can occur through inherent or intrinsic mechanisms within the organism, horizontal acquisition of resistance genes either carried by plasmids or transposons that results in the recombination of foreign DNA into the organism's chromosome or by mutations that can occur in different chromosomal loci (Davies and Wright, 1997).

Intrinsic resistance is the innate ability of a bacterial species to resist activity to a particular antimicrobial molecule through its inherent structural and functional mechanisms. This results in a particular tolerance of a specific antimicrobial or class. An example of this which will form a predominant focus of this thesis is intrinsic resistance

to cephalosporin in *Enterococcus* spp. Although extensive research has been performed, the overall mechanism is not fully understood in either *E. faecalis* or *E. faecium* (Djoric and Kristich, 2017).

The selective pressure of the antibiotic can result in acquired resistance by spontaneous mutations, which may be point mutations, deletions or insertions within the bacterial genome (Normark and Normark, 2002). In the absence of an antimicrobial agent, chromosomal mutations for resistance to antibiotics often have an adverse effect on the fitness of the organism (Levin *et al.*, 2000). The acquisition of genes associated with antibiotic resistance will produce a general metabolic burden, and it is thought that in the absence of selection, the resistant organisms would be outcompeted by the susceptible ones. If that were always true, discontinuation of antibiotic use would render the disappearance of resistant microorganisms. Several studies have shown that, once resistance emerges, the recovery of a fully susceptible population even in the absence of antibiotics is not easy (Hernando-Amado *et al.*, 2017). Factors that can influence the rate of mutation in an organism in the presence of an antibiotic include the antibiotic concentration, physiological conditions and bacterial stress (Foster., 1993; Kohler *et al.*, 1997; Shapiro, 1997). An example of this type of resistance includes linezolid resistance in Enterococci. Linezolid inhibits protein synthesis by interacting with the 23S ribosomal RNA. The resistance mechanism involves a point mutation G2576U in the genes encoding the 23S ribosomal RNA and results in the interaction of Linezolid to interact with the 23S ribosomal RNA and continuation of protein synthesis (Zurenko *et al.*, 1996; Prystowsky *et al.*, 2001).

Eukaryotic organisms have evolved principally through the modification of the genetic information that already exists. The genetic diversity in bacteria has been a result of the acquisition of genes from other distantly related organisms. This is achieved through horizontal gene transfer where DNA can be introduced or deleted from the chromosome and can result in a different bacterial genotype and phenotype (Ochman *et al.*, 2000). Antimicrobial resistance caused by horizontal gene transfer can occur through genes in bacteriophages, plasmids, naked DNA and transposon elements (Levy and Marshall, 2004). This occurs through either transduction, conjugation or transformation (Alekhshun and Levy, 2007). Conjugation is the direct transfer of DNA between two bacterial cells in a mating process. Transduction requires a DNA carrier (bacteriophage)

to transfer genetic material into another bacterium, and transformation involves the uptake of DNA from the environment. Transposons are known to carry resistance elements and include those that are involved in Glycopeptide resistance throughout the *Enterococcus* spp. including Tn1546, Tn1547 and Tn1549 (Aleksun and Levy, 2007).

There are many types of antibiotic resistance in *Enterococcus* spp. to different classes of antibiotics including to the aminoglycosides, rifampicin, quinolones and linezolid (Llano-Sotelo *et al.*, 2002; Vakulenko and Mobashery., 2003; Telenti *et al.*, 1993; Oyamada *et al.*, 2006; Werner *et al.*, 2010; Prystowsky *et al.*, 2001; Pai *et al.*, 2002; Ruggero *et al.*, 2003; Seedat *et al.*, 2006). As the primary focus of this project is on the cell wall in *Enterococcus* spp. and associated antibiotic resistance, only those antibiotics that affect the cell wall will be discussed.

#### **1.2.4.2. Daptomycin and Resistance in *Enterococcus* spp.**

Daptomycin is a lipopeptide antibiotic derived from *Streptomyces roseosporus* used to treat Gram-positive infections (Carpenter and Chambers, 2004). It has a unique mechanism of action compared to other antibiotics by disrupting multiple aspects of bacterial membrane function. It is only active against Gram-positive bacteria as it is unable to penetrate the outer membrane of Gram-negative bacteria (Miller *et al.*, 2016). Daptomycin inserts into the cell membrane in a phosphatidylglycerol-dependent fashion and aggregates. The effect of aggregation in the membrane alters the curvature of the membrane resulting in holes that allow ions to leak. This causes rapid depolarization of ions (especially potassium) with an associated ion dissipation of the ion concentration gradient. This results in a loss of membrane potential leading to inhibition of protein DNA and RNA synthesis, resulting in bacterial cell death. Large molecules are not released from the cytoplasm (Tally *et al.*, 1999; Tally and DeBruin, 2000).

Daptomycin has been used to treat severe VRE infections, especially when a lack of other treatment options are available. Daptomycin resistance has been reported in cases where VRE infections are being treated. Little is known about the mechanism of resistance, but an essential event for the activity of daptomycin is a calcium-mediated interaction with the cell membrane, a property that daptomycin shares with related cationic antimicrobial peptides. The charge in the bacterial surface also appears to play an essential role in the interaction of daptomycin with the cell membrane, and it has been

postulated that a more positively charged cell envelope “repels” the cationic daptomycin from the cell membrane, contributing to the development of resistance (Jones *et al.*, 2008).

A significant factor in the cell-envelope charge is the phospholipid composition of the inner and outer cell-membrane leaflets, such as the negatively charged phospholipid cardiolipin and the positively charged amino derivatives of phosphatidylglycerol. In some *S. aureus* isolates, reduced susceptibility to daptomycin has been attributed to a decrease in the negative surface charge of the cell membrane as a result of modifications in phospholipid content. This is mainly through increased synthesis and translocation (“flipping”) of the positively charged lysyl-phosphatidylglycerol from the inner to the outer leaflet of the cell membrane (Zhang *et al.*, 2014). It has also been shown that lysyl-phosphatidylglycerol attenuates membrane perturbations caused by cationic antimicrobial peptides. It has been shown that resistance to daptomycin in VRE strains is associated with the cell envelope and biophysical properties of the cell membrane. The genes responsible for such changes include *liaF* and *gdpD*, and both are required for full expression of the resistant phenotype. LiaFSR is a three-component system which is known to adapt the cell envelope to antibiotics and antimicrobial peptides in some Gram-positive bacteria. This system is well characterized in *B. subtilis*, *S. mutans*, and *Pneumococcal* spp. The system is activated in the presence of antibiotics that disrupt the cell wall membrane and PG synthesis through alterations of Lipid-II metabolism (PG precursor). In daptomycin resistant *Enterococcus* spp., activation of the LiaFSR system occurs through mutations in *liaF* or other components of the LiaFSR system (which might be selected through exposure to antibiotics that alter lipid-II metabolism). It is thought that activation of the system may influence cell-envelope homeostasis by affecting the transcription of several genes that can help mitigate the damage caused by the antibiotic. A subsequent alteration in the cell membrane occurs through changes in enzymes involved in phospholipid metabolism leading to critical and compensatory changes in the composition or distribution of phospholipids in the cell membrane. *GdpD* has been shown to be important in glycerol metabolism, hydrolysing several cell-membrane glycerophosphodiesterases that affect phospholipid metabolism (Schwan *et al.*, 2003).

#### 1.2.4.3. Glycopeptides and Resistance in *Enterococcus* spp.

Glycopeptides are a class of antibiotics that consist of a peptide ring to which several sugars are covalently linked. They are produced by actinomycetes and have a large complex structure that prevents the penetration through the outer membrane of Gram-negative bacteria limiting their therapeutic use only to treat infections with Gram-positive bacteria. However recently it has been demonstrated that cold stress makes Gram-negatives such as *E. coli* more susceptible to glycopeptide antibiotics and can alter the outer membrane integrity (Stokes *et al.*, 2016).

Two naturally produced antibiotics have historically been used in antimicrobial treatment, vancomycin and teicoplanin. Four glycopeptide derivatives have also been developed including ramoplanin, dalbavancin, telavancin, oritavancin and are promising candidate drugs that are partially active against multi-resistant bacteria and VRE (Zhanet *et al.*, 2010). The primary target of glycopeptides is the C-terminal D-Alanyl-D-Alanine terminus of the peptide side chain of lipid II (**Figure 1.6, left**). Due to steric hindrance, cell wall synthesis enzymes like transglycosylases, transpeptidases and, D,D-carboxypeptidases cannot access their target and, cell wall synthesis stops (Batchelor *et al.*, 2010).

The emergence of vancomycin resistance took the clinical community by surprise in the late 1980s. *Enterococcus* spp. have acquired vancomycin resistance mechanisms and corresponding strains have been isolated from clinical samples from patients in the USA and Europe including the *E. faecium* strain BM4147 from France conferring VanA resistance and the *E. faecalis* strain V583 from the USA conferring VanB resistance (Leclercq *et al.*, 1988; Leclercq *et al.*, 1989; Sahm *et al.*, 1989; Evers *et al.*, 1996). The structure, localization and functional interplay of the resistance determinants arranged in specific transposable elements in *Enterococcus* spp. have been identified in multiple strains with nine types of vancomycin resistance throughout the *Enterococcus* spp. These share a related mechanism of resistance and a similar resistance gene cluster composition but show significant genotypic and phenotypic differences (**Figure 1.7** and **Table 1.4**). VanA is the most prevalent type of vancomycin resistance followed by VanB resistance. The primary clinically relevant reservoir of *vanA* and *vanB* elements is in *E. faecium* but has been observed in other enterococcal species (Zirakzadeh and Patel,

2005; Werner *et al.*, 2008). Phylogenetic analysis of the genes associated with vancomycin resistance has shown that the sequence clusters appeared in ancient strains of Actinobacteria. These also appear to have similarities to that of modern strains and functional studies have suggested that ancient strains also exhibited genuine antibiotic resistance mechanisms to vancomycin (D'Costa *et al.*, 2011). Vancomycin-resistant *Enterococcus* spp. are also resistant to other antibiotics and host defences and have evolved to colonize the GI tract. Some strains have also been shown to colonize the bloodstream and have evolved antibiotic tolerance in an immunocompromised host achieving this by activating the stringent response as a result of a mutation in *relA* (Van Tyne and Gilmore, 2017).

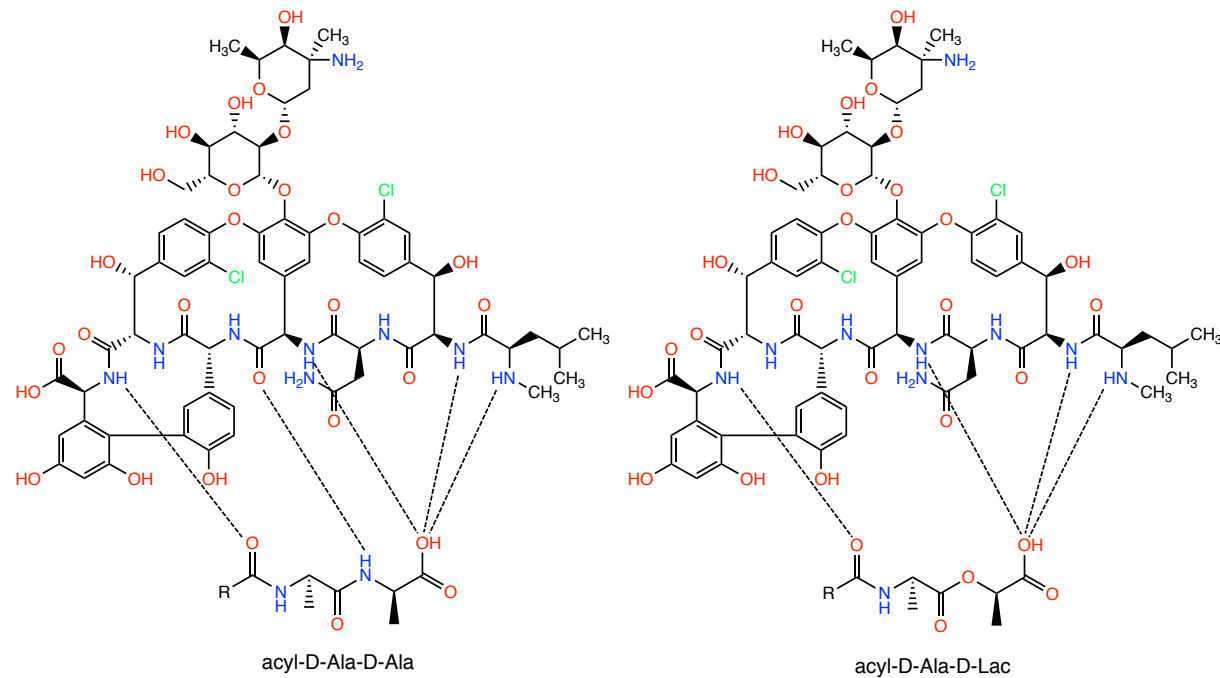


**Figure 1.6 – Mode of action of vancomycin and the effect of antibiotic resistance.** Schematic of (Left) vancomycin forming five hydrogen bonds between the N-acetyl-D-Ala-D-Ala of lipid II and (Right) the loss of a critical hydrogen bond caused by the vancomycin resistance mechanisms leading to a N-acetyl-D-Ala-D-Lac lipid II. This causes a 1000-fold reduction in the affinity of vancomycin to lipid II and inhibition of the transglycosylation and transpeptidation steps (adapted from Bugg *et al.*, 1991).

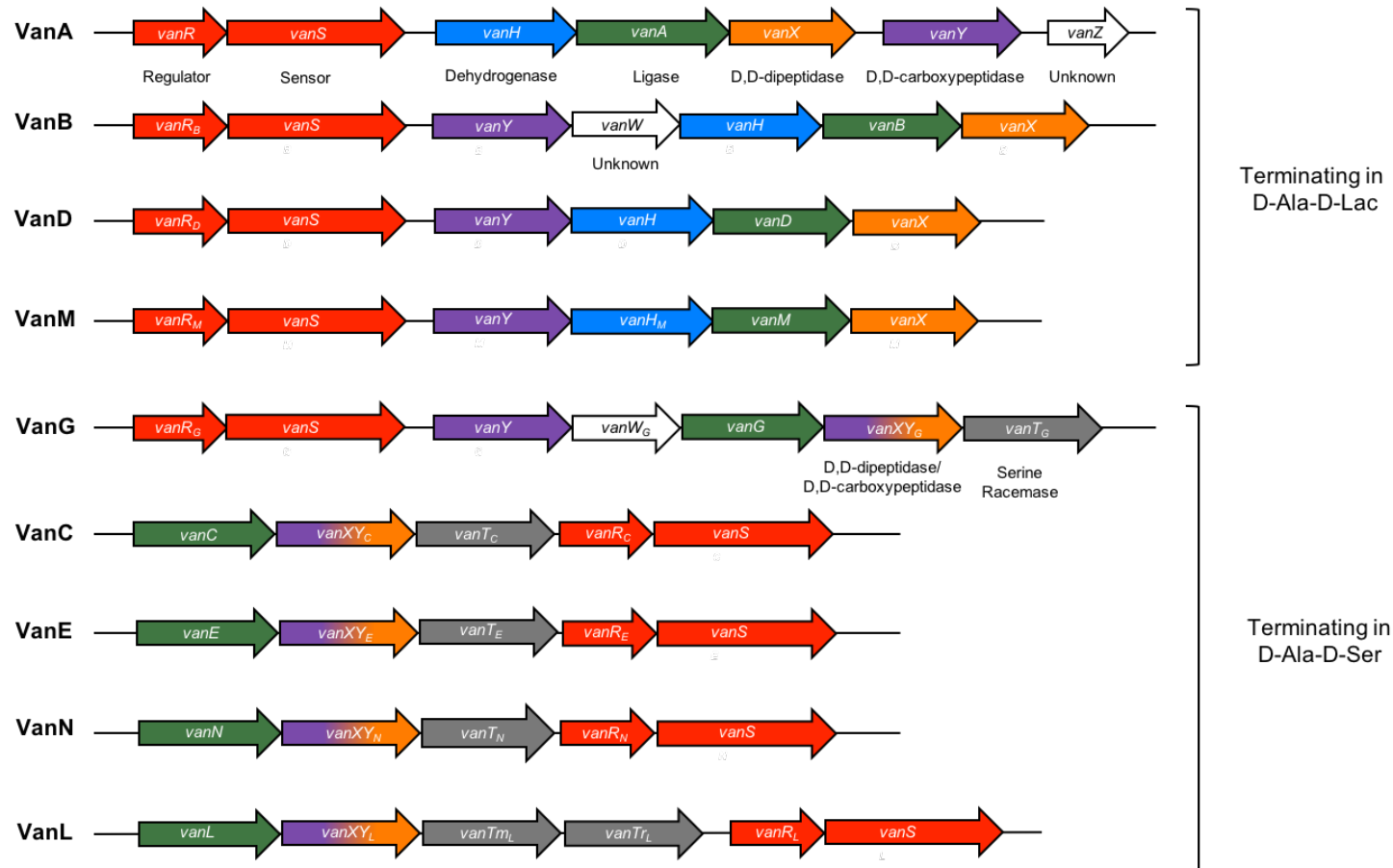


**Figure 1.7 - Structure, composition and architecture of the vancomycin resistance clusters vanA-N.** Two-component systems encoding Sensor Kinase (VanS) and Response Regulator (VanR) are coloured in Red, dehydrogenase (VanH) in Blue, ligase (VanA-N) in green, D,D-dipeptidase (VanX) in Orange, D,D-carboxypeptidase (VanY) in purple, Serine Racemase (VanT) in grey, bifunctional D,D-dipeptidase/ D,D-carboxypeptidase (VanXY) in gradient purple and orange and those of unknown function highlighted in white (VanZ and VanW) (adapted from Werner, 2008).

**Table 1.4 - Types and distribution of glycopeptide resistance in *Enterococcus* spp.** Summary of the different Van phenotypes that are present across the *Enterococcus* spp. and different characteristics between each phenotype. These include the species associated with the phenotype, the level of glycopeptide resistance, its specificity to different glycopeptides, the location of the *van* genes, mode of transcription activation and the modifications in PG that can occur (adapted from Werner, 2008).

Resistance phenotype	Microorganisms	Level of resistance	Glycopeptide Sensitivity	Location of Genes	Transcription of Genes	C-terminal modification	Reference
VanA	<i>E. faecalis</i> <i>E. faecium</i>	High	Vancomycin Resistant Teicoplanin Resistant	Plasmid Chromosome	Inducible	D-Ala-D-Lac	Arthur and Quintiliani, 2001; Healy <i>et al.</i> , 2000
VanB	<i>E. faecalis</i> <i>E. faecium</i>	Variable	Vancomycin Resistant Teicoplanin Sensitive	Plasmid Chromosome	Inducible	D-Ala-D-Lac	Courvalin, 2006; Arthur <i>et al.</i> , 1996; Arthur and Quintiliani, 2001
VanC	<i>E. gallinarum</i> <i>E. casseliflavus</i> <i>E. flavescens</i>	Intrinsic, low level resistance	Vancomycin Resistant Teicoplanin Sensitive	Chromosome	Constitutive	D-Ala-D-Ser	Depardieu <i>et al.</i> , 2004;
VanD	<i>E. faecalis</i> <i>E. faecium</i>	Moderate	Vancomycin Resistant Teicoplanin Resistant	Chromosome	Constitutive	D-Ala-D-Lac	Perichon <i>et al.</i> , 1997; Ostrowsky <i>et al.</i> , 1999
VanE	<i>E. faecalis</i>	Low	Vancomycin Resistant Teicoplanin Sensitive	Chromosome	Inducible	D-Ala-D-Ser	Fines <i>et al.</i> , 1999; Patino <i>et al.</i> , 2002
VanG	<i>E. faecalis</i> <i>E. faecium</i>	Low	Vancomycin Resistant Teicoplanin Sensitive	Chromosome	Inducible	D-Ala-D-Ser	McKessar <i>et al.</i> , 2000; Depardieu <i>et al.</i> , 2003
VanL	<i>E. faecalis</i>	Low	Vancomycin Resistant Teicoplanin Sensitive	Chromosome	Inducible	D-Ala-D-Ser	Boyd <i>et al.</i> , 2008
VanM	<i>E. faecium</i>	Variable	Vancomycin Resistant Teicoplanin Sensitive	Plasmid Chromosome	Inducible	D-Ala-D-Lac	Xu <i>et al.</i> , 2010
VanN	<i>E. faecium</i>	Low	Vancomycin Resistant Teicoplanin Sensitive	Plasmid	Constitutive	D-Ala-D-Ser	Nomura <i>et al.</i> , 2012; Lebreton <i>et al.</i> , 2011

#### **1.2.4.3.1 VanA type resistance in *Enterococcus* spp.**

The *vanA* gene is an integrated part of *Tn1546* transposon which is usually located on transferable plasmids (Werner *et al.*, 2008). The *vanA* gene cluster contains nine genes which are arranged in a transposon structure (Arthur *et al.*, 1993). It is flanked by two incomplete inverted repeats and possesses two coding sequences. The entire element is 10,981 bp and designated *Tn1546*, belonging to transposons of the *Tn3*-family which also encode a  $\beta$ -lactamase (*bla*), the *Tn3* transposase (*tnpA*) and the *Tn3* resolvase (*tnpR*) for successful transposon integration.

Expression of VanA type vancomycin resistance in enterococci is through an inducible transcription mechanism. The mechanism for detecting the presence of the effect of vancomycin is still unknown, but the sensor kinase (VanS) of the regulator two-component system is activated by autophosphorylation when changes in the extracellular environment have been detected, and the corresponding phosphate moiety is transferred to a cytoplasmic response regulator (VanR). Phosphorylated VanR functions as a transcriptional activator binding at two promoters in the VanA resistance gene cluster leading to the expression of two transcripts of genes that are arranged in an operon structure (Arthur *et al.*, 1997). This includes the *vanRS* genes and the gene cluster *vanHAXYZ*. The proteins VanH, VanA and VanX possess essential functions for the expression of glycopeptide resistance whereas VanY encodes a D,D-carboxypeptidase contributing to elevated resistance levels and a VanZ protein of unknown function but contributing by an unknown mechanism to low-level teicoplanin resistance (Arthur and Quintiliani, 2001). The resulting enzymes of the VanA gene cluster provide an alternative pathway for synthesizing cell wall precursors ending in D-Alanyl-D-Lactate (D-Ala-D-Lac). This results in a 1000-fold reduction in vancomycin binding (**Figure 1.6, Right**) (Bugg *et al.*, 1991; Arthur and Quintiliani, 2001).

#### **1.2.4.3.2 VanB type resistance in *Enterococcus* spp.**

The typical VanB phenotype is characterized by inducible and variable levels of vancomycin but is susceptible to teicoplanin. The *vanB* gene can be divided into three different allele types (*van B1-3*) with *vanB-2* the most prevalent type worldwide. The *vanB* alleles are part of *Tn1547*, *Tn1549* or *Tn5382* transposons which are mainly chromosomally located and less frequently, on plasmids (Zheng *et al.*, 2009; Hegstad *et*

*al.*, 2010; Bjorkeng *et al.*, 2011). They are derivatives of the *Tn196* transposon family associated with tetracycline resistance and can be separated into three functional regions: (i) the right end, implicated in the excision-integration process; (ii) the central part, in which the *vanB2* operon replaces the *tet(M)* gene; and (iii) the left extremity, in which eight of the 18 ORFs could be implicated in the conjugative transfer (Garnier *et al.*, 2000). The *vanB* gene cluster resembles the core structure of the *vanA* gene cluster, but in a different arrangement (**Figure 1.7**). Genes of related composition and function are arranged similarly, an equivalent to *vanZ* is lacking, but an additional gene *vanW* of unknown function occurs. The TCS genes (*vanR<sub>B</sub>* and *VanS<sub>B</sub>*) are distant to their *vanA* gene cluster *Tn1546* counterparts and regulation of gene expression is different. This may be the reason why it is only resistant to vancomycin, but not teicoplanin (**Figure 1.8**). The entire transposon backbone of *vanB* gene clusters is different to the *vanA* gene cluster. The *vanB* gene clusters are either flanked by certain IS elements or an integral part of more extensive mobile and/or conjugative elements (Carias *et al.*, 1998; Dahl and Sundsfjord, 2003; Launay *et al.*, 2006; Lopez *et al.*, 2009). The conjugative transposon *Tn1549* is widely prevalent among VanB type *Enterococcus* spp. and *Clostridium* spp. (Launay *et al.*, 2006; Tsvetkova *et al.*, 2010).

Teicoplanin does not induce VanB type resistance, but constitutively resistant mutants can occur following antimicrobial therapy through a point mutation in the VanS kinase domain or extracellular loop (Baptista *et al.*, 1999; Kawalec *et al.*, 2001; San Millan *et al.*, 2009). Accordingly, teicoplanin treatment is not recommended for eradicating VanB VRE infections despite a correspondingly suggestive diagnostic result.

A recent study evaluating the VRE isolates from hospitals in Poland concluded that, although the initially VanA represented the primary phenotype in Poland, after 2006, there has been an increasing number of cases with VanB type isolates in *Enterococcus* spp. since the first VanB type isolate was reported in Poland in 1999 (Sadowy *et al.*, 2018). Although VanA also appears to be the predominant phenotype in *Enterococcus* spp. in the USA and the rest of Europe, the VanB phenotype constitutes 80% of the VRE isolates in Australia, and there is an increasing number of VanB isolates in Germany (Bender *et al.*, 2016; Deshpande *et al.*, 2007).

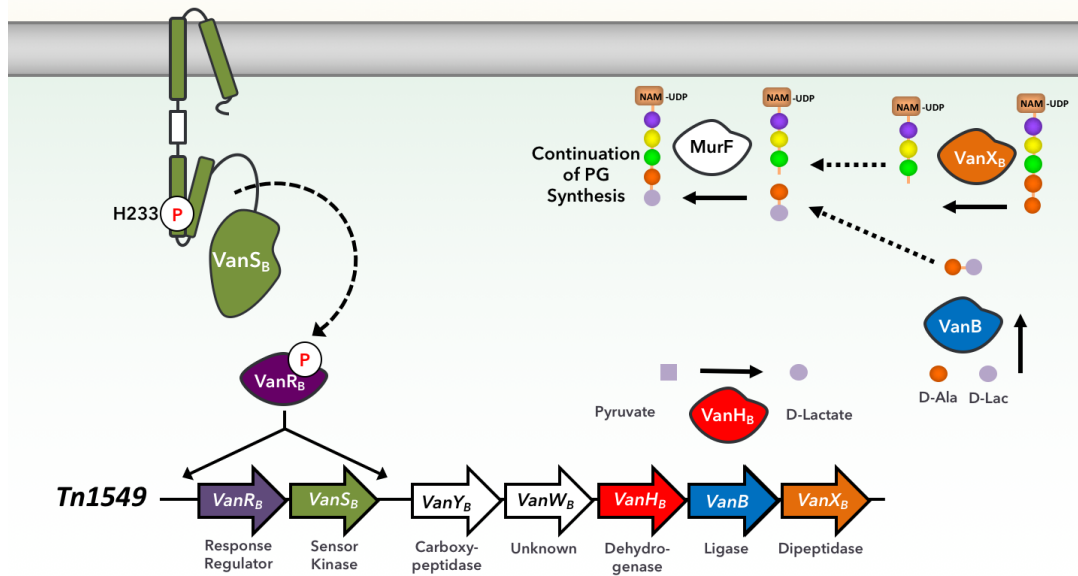


**Figure 1.8 – The role Tn1549 in vancomycin resistance.** Schematic of the TCS signalling cascade of VanS<sub>B</sub> and VanR<sub>B</sub> and the gene targets they upregulate. These include genes that change the biosynthesis pathway of PG such that D-Ala is no longer the fifth position and terminating amino acid in the peptide stem of Lipid II, but instead D-Lac. The three genes that are essential for VanB-type vancomycin resistance include VanH<sub>B</sub>, VanB and VanX.

#### 1.2.4.3.3 VanC type resistance in *Enterococcus* spp.

*E. gallinarum* and *E. casseliflavus* possess intrinsic resistance to vancomycin at a low level. The corresponding *vanC* ligase gene possesses minor sequence diversity resulting in the subtypes *vanC-1* and *vanC-2* respectively (Panesso *et al.*, 2005). VanC type resistance is mediated via a modified D-Ala-D-Ser moiety which is shared by the VanE, VanG, VanL, and VanN gene clusters that also has a low level of resistance (Arias *et al.*, 2000). All these resistance types require the activity of a serine racemase converting L-Ser into D-Ser. The *vanC* gene cluster was first described in *E. gallinarum* (Arias *et al.*, 1999). It contains a ligase gene *vanC-1*, a combined bifunctional D-Ala-D-Ala dipeptidase/carboxypeptidase *vanXY* gene, a *vanT* racemase gene and two genes encoding a sensor HK and RR TCS (*vanR<sub>C</sub>* and *VanS<sub>C</sub>*) (Reynolds *et al.*, 1999; Reynolds and Courvalin 2005). Due to the different VanC resistance mechanism, a *vanH* equivalent is not required and is missing. Initially, it was thought that VanC type resistance was always constitutively expressed as a species-specific property, but in *E. casseliflavus*, an inducible

resistance phenotype is detected several hours after induction (Dutta and Reynolds, 2002). *E. gallinarum* isolates expressing an inducible and constitutive phenotype have been identified with mutational changes in the amino acid sequences of the corresponding sensor HKs VanS correlating to constitutive and inducible strains (Panesso *et al.*, 2005).

#### **1.2.4.3.4. VanD type resistance in *Enterococcus* spp.**

The primary organization of the *vanD* operons, which are located exclusively on the chromosome, is similar to that of the *vanA* and *vanB* clusters (**Figure 1.7**) (Casadewall and Courvalin 1999; Boyd *et al.*, 2000; Depardieu *et al.*, 2003; Depardieu *et al.*, 2004; Boyd *et al.*, 2004). Genes equivalent to *vanZ* or *vanW* are absent. VanD type strains have negligible VanX activity, an enzyme that usually shuts down synthesis of vancomycin-susceptible, housekeeping cell wall precursors. This otherwise physiological drawback is compensated by an inactivated D-Ala-D-Ala ligase host enzyme, preventing synthesis of vancomycin-susceptible precursors ending in D-Ala-D-Ala. However, *vanD* expression and corresponding essential cell wall precursor synthesis would still request induction by glycopeptides. Consequently, all investigated VanD type *E. faecalis*, *E. faecium* and *E. avium* strains show a constitutive resistance phenotype resulting from different mutations in the VanS or VanR. Another unusual feature of VanD type strains is their only slightly diminished susceptibility to teicoplanin which cannot be explained by already known DNA sequence diversities. Due to different strategies in establishing those complex and highly regulated networks independently and via different routes five different *vanD* cluster types had arranged and had been characterized (Boyd *et al.*, 2000; Depardieu *et al.*, 2004).

Different VanD type enterococci present a number of different combinations of mutations with the most significant amount of mutations occurring in VanS suggesting an independent development and convergent evolution (Depardieu *et al.*, 2009). These various modifications also led to a wide range of resistance phenotypes with low to high-level vancomycin-resistant strains. Remarkably, a VanD strain *E. faecium* BM4656 had a wildtype Ddl enzyme being the only VanD strain with a functional D-Ala-D-Ala ligase. In this strain, also enzymes VanX and VanY were active mainly for shutting down synthesis

of glycopeptide-susceptible cell wall precursors in a background of an active host Ddl enzyme for mediating vancomycin resistance (Depardieu *et al.*, 2009).

#### **1.2.4.3.5. VanE type resistance in *Enterococcus* spp.**

Isolates representing a VanE resistance type were described in a few *E. faecalis* strains from Northern America and Australia (Fines *et al.*, 1999; Patino *et al.*, 2002; Boyd *et al.*, 2002; Patino *et al.*, 2004). The VanE resistance cluster resembles structures of the VanC-1 cluster naturally occurring in *E. gallinarum* and also shows highest similarities with the corresponding proteins. Therefore, resistance is mediated by producing D-Ala-D-Ser-terminated cell wall precursors. VanE type vancomycin resistance requires a VanT racemase converting L-Ser into D-Ser (Fines *et al.*, 1999; Patino *et al.*, 2002). It remains teicoplanin- susceptible and show moderate to low levels of inducible vancomycin resistance. Despite this phenotype, sequence determination suggested a putative non-functional VanS protein indicating cross-talk between the VanR response regulator and other functional membrane- located kinase activators. All five consecutive genes of the vanE gene cluster were co-transcribed from a single promoter (Patino *et al.*, 2004).

#### **1.2.4.3.6. VanG type resistance in *Enterococcus* spp.**

*E. faecalis* possessing a VanG cluster were low-level vancomycin-resistant and teicoplanin susceptible (McKessar *et al.*, 2000; Depardieu *et al.*, 2003; Boyd *et al.*, 2006). Resistance is mediated via inducible synthesis of D-Ala-D-Ser-terminated cell wall precursors. Only a few isolates have been described, and *vanG* gene clusters identified allow differentiation into two subtypes. The chromosomal *vanG* cluster consists of seven genes which according to its order and gene composition appear to be reassembled from different Van operons. The *vanY* gene is present, but a frame-shift mutation resulting in premature termination of the encoded protein accounted for the lack of disaccharide-tetrapeptide precursors in the cytoplasm (Depardieu *et al.*, 2003). VanG type resistance was successfully transferred in vitro and acquisition of the VanG cluster was associated with a transfer of a 240 Kb chromosomal fragment flanked by imperfect inverted repeats (Depardieu *et al.*, 2003). Crystallisation and X-ray analysis of the VanG D-Ala-D-Ser ligase in complex with ADP has been recently described (Weber *et al.*, 2009). Recently, the first strain of *E. faecium* harbouring the VanG cluster resistance mechanisms was isolated and shares a similar profile to the *E. faecalis* strain (Sassi *et al.*, 2018).

#### **1.2.4.3.7. VanL type resistance in *Enterococcus* spp.**

An *E. faecalis* isolate from Canada expressed low levels of vancomycin resistance and was denoted VanL (Boyd *et al.*, 2008). The *vanL* gene mediates D-Ala-D-Ser ligation and, the cluster was similar in organization to the *vanC* operon, but the VanT serine racemase was encoded by two separate genes including *vanTm* (membrane binding) and *vanTr* (racemase). The two genes resemble the two functional domains of the otherwise combined *vanT* type racemase (Boyd *et al.*, 2008).

#### **1.2.4.3.8. VanM type resistance in *Enterococcus* spp.**

The *vanM* genotype was identified in seven Chinese VRE isolates showing resistance to both vancomycin and teicoplanin from a single hospital (Xu *et al.*, 2010). The translated sequence of the ligase VanM showed high sequence similarity to the VanA but, the *vanM* gene cluster shows a gene arrangement similar to *vanB* and *vanD* with the D,D-carboxypeptidase gene *vanY* preceding the ligase gene. VanM type resistance is transferable by conjugation *in vitro* and plasmid located.

#### **1.2.4.3.9. VanN type resistance in *Enterococcus* spp.**

The VanN genotype was first described in *E. faecium* UCN71 isolated from blood culture. It shows resistance to vancomycin but is sensitive to teicoplanin (Lebreton *et al.*, 2011). It follows the same cultural architecture to VanC and VanE and also resulting in D-Ala-D-Ser terminating pentapeptides. The VanN ligase shares 65% identity with the VanL ligase. Five VanN type vancomycin-resistant *E. faecium* strains have been further identified and isolated from a sample of domestic chicken meat in Japan (Nomura *et al.*, 2012) and more recently found to be in a plasmid form isolated from *E. faecium* strain from a 51-year male in Canada (Boyd *et al.*, 2015).

#### **1.2.4.3.10. Other Gram-positive species with *van* gene clusters**

The occurrence of the Van operon had been reported in different non-enterococcal, human intestinal colonizers including *Clostridium* spp., *Ruminococcus* spp. and others (Patel 2000; Stinear *et al.*, 2001; Domingo *et al.*, 2005; Ballard *et al.*, 2005;

Domingo *et al.*, 2007). One of these isolates was investigated as a new naturally occurring vancomycin resistant species, *Ruminococcus gauvreauii* and possessed a *vanD* gene cluster (Domingo *et al.*, 2007). In strains of *Clostridium symbiosum* an entire *vanB2* type Tn1549 cluster was identified which was transferable *in vitro* and *in vivo* in the digestive tract of mice highlighting the critical role that commensal, intestinal, non-enterococcal hosts may play by acting as a reservoir for resistance elements by acquiring, preserving and distributing the vancomycin resistance genes to nosocomial pathogens (Launay *et al.*, 2006). The corresponding conjugative transposon Tn1549 encodes all necessary functions for a successful transfer of the element across species and genus barriers also demonstrating its potential to transfer VanB type vancomycin resistance from *Enterococcus* spp. to other critical nosocomial pathogens like *Staphylococcus* spp., *C. difficile* and others (Tsvetkova *et al.*, 2010). Conjugative transposons like Tn5397/Tn916 (and also Tn1549) are easily exchanged between members of different bacterial species and genera and are identified in a wide range of different, Gram-positive bacterial species capable of self-transfer and mobilisation of other, genetic elements (Roberts *et al.*, 2001; Jasni *et al.*, 2010; Roberts and Mullany, 2011).

Certain soil bacteria produce glycopeptide antibiotics including vancomycin (*Amycolatopsis orientalis*) and teicoplanin (*Actinoplanes teichomyceticus*) as secondary metabolites. They prevent themselves from sensitivity against their own products by intrinsic resistance mechanisms similar but not identical to acquired resistance types in *Enterococcus* spp. (Marshall *et al.*, 1997; Marshall *et al.*, 1998; Patel, 2000). It was speculated that resistance in *Enterococcus* spp. originated from corresponding glycopeptide producers (Marshall *et al.*, 1998; Patel 2000); however, comparably weak amino acid and nucleotide similarities among key genes and proteins involved in the resistance mechanism and the comparably high % GC of the VanRS regulatory system in the glycopeptide producers *Streptomyces toyocaensis* and *A. orientalis* suggested that a possible exchange between glycopeptide producers and nosocomial pathogens having acquired resistance properties did not happen recently (Courvalin, 2005).

#### **1.2.4.3.11. Vancomycin resistance in *S. aureus***

Vancomycin was once the antibiotic of choice for treating MRSA infected patients. Insusceptibility to vancomycin associated with treatment failure is insofar a matter of

serious concern. Various microbiological changes could lead to reduced susceptibility against vancomycin including increased cell wall thickness, activated cell wall synthesis and reduced autolysis. The former changes are based on a modified host gene expression of determinants involved in cell wall synthesis leading to a so-called “trapping effect” where more unlinked cell wall precursors are present being able to bind (more) vancomycin (“to trap” the drug) (Cui *et al.*, 2005; Werner *et al.*, 2008; Nannini *et al.*, 2010). The vancomycin intermediate-resistant phenotype (VISA) could be expressed homogeneously and, VISA phenotypes are not associated with the *van* gene acquisition.

Early *in vitro* studies demonstrated the capability of a transfer of the enterococcal VanA type resistance into non-virulent and virulent methicillin-resistant *S. aureus* (MRSA) rendering descendants as vancomycin and oxacillin resistant (Noble *et al.*, 1992). The first clinical *vanA* mediated high-level vancomycin-resistant MRSA (VRSA) was isolated from a dialysis patient in Michigan, USA (Weigel *et al.*, 2003; Chang *et al.*, 2003). Since then, multiple cases have been described (Sievert *et al.*, 2008; Finks *et al.*, 2007; Nannini *et al.*, 2010). The USA VRSA isolates showed high-level vancomycin resistance of >32 mg L<sup>-1</sup>. All US patients affected by VRSA infections had a history of several underlying conditions, and accordingly, all of them were treated extensively with antibiotics including vancomycin and most of them were co-colonized with VRE, respectively. Typing of corresponding strains, their resistance plasmids and corresponding *Tn1546* like VanA clusters revealed that the isolates were unique and had evolved separately.

From the first case-patient an MRSA strain, a VanA type *E. faecalis* and a VanA type MRSA were isolated which allowed constructing a scenario where the MRSA received the *vanA* type resistance from the resistant co-colonising *E. faecalis*. This has been confirmed by molecular analysis of the corresponding VanA type plasmids from related VRSA and MRSA isolates (Weigel *et al.*, 2003; Clark *et al.*, 2005; Zhu *et al.*, 2008). The VRSA isolate contained a 58 Kb conjugative plasmid pLW1043, the MRSA contained a 47 Kb pAM829 plasmid, and the VRE two plasmids of 45 and 95 Kb pLW1043 was fully sequenced and revealed a *Tn1546*-like VanA cluster integrated between the *blaZ* ( $\beta$ -lactamase) and the *aacA-aphD* (gentamicin resistance) regions. It showed a mosaic-like structure, but the backbone was similar to staphylococcal type pSK1 plasmids and different from typical enterococcal plasmids suggesting acquisition of the VanA cluster

by a resident staphylococcal-type plasmid indicating a critical concern for the dissemination of VRSA clinical isolates (Kwong *et al.*, 2008).

#### **1.2.4.4. $\beta$ -lactam antibiotics and resistance in *Enterococcus* spp.**

Antibiotics in the  $\beta$ -lactam family target PBPs preventing crosslinking of PG by transpeptidation which results in the termination of cell wall synthesis. *Enterococcus* spp. can exhibit intrinsic resistance to a number of  $\beta$ -lactam antibiotics, but this varies among the different classes of  $\beta$ -lactams and between enterococcal species. This spectrum of antibiotic resistance is reflected in the utility of these drugs for treatment. (Kristich 1.2.4.3.10., 2014).

The intrinsic resistance of *Enterococcus* spp. to  $\beta$ -lactams involves the production of the low-affinity class B PBP, Pbp5, an orthologue of the acquired PBP2a (MecA) in MSRA strains (See **Table 1.2**) (Arbeloa *et al.*, 2004). Pbp5 is capable of carrying out PG synthesis in the presence of  $\beta$ -lactam antibiotics in comparison to the other PBPs that are still sensitive and inactivated (Arbeloa, *et al.*, 2004; Rice *et al.*, 2005). Pbp5 is therefore a required component for intrinsic  $\beta$ -lactam resistance in *Enterococcus* spp. (Kristich *et al.*, 2014).

##### **1.2.4.4.1. Ampicillin Resistance**

Modifications in transpeptidase domain of Pbp5 has resulted in increase of ampicillin resistance where 5% of the gene (*pbp5*) can be altered in *E. faecium* strains in a hospital environment (Garnier *et al.*, 2000). The sequence difference is not the only factor contributing to ampicillin resistance in *E. faecium* strains including the overproduction of Pbp5 (Fontana *et al.*, 1994). The region upstream of Pbp5 has also been associated with ampicillin resistance. An 87 bp upstream of *pbp5* in the open reading frame was associated with increased *pbp5* levels and increased ampicillin resistance (Liggozzi *et al.*, 1993). *E. faecium* strains can be divided into two main clades including the clade A1 and A2 (hospital associated) and clade B (community associated) and that both these clades differ in ampicillin susceptibility. This has been attributed to two different allele forms of the *pbp5* gene whose sequences differ. These major clade rearrangements of *pbp5* have been attributed to insertions, deletions and single nucleotide

polymorphisms that are associated with the varying ampicillin resistance levels due to *pbp5* (Montealegre *et al.*, 2017).

#### 1.2.4.4.2. Cephalosporin Resistance

*Enterococcus* spp. are intrinsically resistant to most cephalosporin's. Chromosomal determinants encode this in the core genome of these organisms, but its molecular basis remains to be identified. In *E. faecalis*, PBP5, a TCS (CroRS), a eukaryotic like serine/threonine kinases (eSTK), IreK, and one of the first enzymes involved in the synthesis of PG precursors, MurAA have been associated with intrinsic resistance in *E. faecalis*. The role of these determinants has been best studied in *E. faecalis*, and it appears likely that similar mechanisms are present in *E. faecium* (Sacco *et al.*, 2014).

Genetic studies have demonstrated that Pbp5 has an essential role in intrinsic cephalosporin resistance in *E. faecalis* and *E. faecium* strains isogenic strains (Arbeloa, *et al.*, 2004; Rice *et al.*, 2005). Strains that lack *pbp5* results in cephalosporin and ampicillin sensitivity. The deletion mutants also exhibit a decrease in resistance to the non-cephalosporin  $\beta$ -lactam including ampicillin. As Pbp5 is a class B PBP, and contains a TP domain, but lacks a TG domain which is necessary for cell wall biosynthesis to continue. During cephalosporin therapy, Pbp5 is the only functional PBP, therefore there has been a lot of interest in identifying a possible mechanism of TG activity in Enterococcal strains under cephalosporin therapy as Pbp5 must work with an alternative TG. *S. aureus* contains a monofunctional TG (MGT) but no examples have yet been identified in *Enterococcus* spp. (Kristich, 2014; Rice *et al.*, 2005). Recently it has been shown that FtsW has transglycosylase activity which is not inhibited by moenomycin and therefore may constitute this missing GTase activity in *Enterococcus* spp. however this has not been proven yet (Meeske *et al.*, 2016).

Systematic inactivation of the 17 two-component systems in the *E. faecalis* strain V583 TCSs demonstrated that a CroRS deletion rendered *E. faecalis* susceptible to cephalosporin's, but not to other antibiotics (Hancock and Perego, 2004; Kristich, 2014). This is consistent with studies in another strain of *E. faecalis*, where the deletion of the genes encoding the CroRS TCS resulted in a loss of resistance to ceftriaxone (Comenge *et al.*, 2003) A similar phenotype was also observed in *E. faecium* with the deletion of the CroRS TCS resulting in susceptibility to cephalosporin's (Kellogg *et al.*, 2017). CroR been

has shown to act directly as a promoter for the gene *salB* (Muller *et al.*, 2006) and likewise *SalB* has been shown to be essential for intrinsic cephalosporin resistance in the *E. faecalis* strain JH2-2 (Djoric and Kristich, 2017).

A second signal transduction protein (IreK) is required for cephalosporin resistance in *E. faecalis* (Kristich *et al.*, 2007). IreK is a eukaryotic-like Serine/Threonine kinase that contains an extracellular domain containing five penicillin-binding protein and serine/threonine kinases associated (PASTA) repeats. In the same operon as IreK is its cognitive Eukaryotic like Serine/Threonine phosphatase (eSTP) (IreP) and is thought to regulate the phosphorylation of IreK and its targets substrates. Deletion strains of IreK in the strain OG1RF has resulted in cephalosporin sensitivity and, deletion of IreP has caused hyper-resistance to cephalosporin's. This highlights the key responsibility of IreP in regulating IreK activity (Kristich *et al.*, 2007; Kristich *et al.*, 2014; Yeats *et al.*, 2002).

## 1.3. Bacterial Signalling

Bacteria are required to sense, respond and adapt to a wide range of environments to survive. They have evolved a series of mechanisms to probe variations in the extracellular environment that may be beneficial or detrimental to the survival of the organism. Extracellular signals are commonly relayed into the cells through reversible protein phosphorylation via protein kinases and phosphatases to result in modulation of their target activities. In this context, the TCSs are the best described prokaryotic signalling cascades which use a histidine kinase (HK) to detect extracellular environmental signals and are commonly found in both Gram-positive and Gram-negative bacteria (Hoch and Silhavy, 1995). TCSs were thought to be the only way in which bacteria could sense their extracellular environments, but recently eukaryotic-like serine/threonine kinases (eSTKs) and eukaryotic-like serine/threonine phosphatases (eSTPs) have been found to play an essential role in prokaryotic environmental adaptation. Unlike their TCS counterparts, eSTKs and eSTPs are present at far fewer numbers per bacterial genome (Pereira *et al.*, 2011). The VanS/VanR TCS and the IreK/IreP eSTK system is important for both vancomycin resistance and cephalosporin resistance respectively in *E. faecalis*, the architecture, genotypic and phenotypic roles of both signalling cascades will be discussed. Studies highlighting the convergence of both signalling cascades will also be reviewed to emphasize the importance of these two signalling systems and how highly evolved they have become for prokaryotic survival.

### 1.3.1. Two-component systems

TCSs are considered to be one of the key and most common mechanisms in signal transduction in bacteria. Although they are abundant in most bacteria, they also can occur in yeast, fungi, archaea and some plants to regulate physiological and molecular processes, by sensing and responding to a specific signal (Gao and Stock, 2009). A bacterium can have tens to hundreds of these systems which have been implicated in mediating the response to a wide range of signals and stimuli including nutrients, cellular redox state, changes in osmolality, quorum signals and antibiotics (Bhate *et al.*, 2015). Their basic architecture is formed from a membrane-bound HK which detects changes in its extracellular environment resulting in autophosphorylation of a particular His residue

within the cytoplasmic portion of the protein. The HK can then trans-phosphorylate a RR on an aspartate residue which acts as a transcription factor to upregulate a cellular response. These phosphorylation events are often labile, and a phosphatase is not usually required, but HKs can also exhibit phosphatase activity (Goulian., 2010; Dworkin., 2015; Stock *et al.*, 2000). Well characterized TCSs included those that are involved in bacterial chemotaxis (Falke *et al.*, 1997), sporulation of *Bacillus subtilis* (Hoch, 1993) and multicellular development in *Myxococcus xanthus* (Kaplan and Plamann, 1996).

#### **1.3.1.1. TCS Sensor Histidine Kinases**

HKs are multi-domain proteins and, the architecture of HKs is often complex and diverse. Although these proteins are prevalent in most bacteria and are important to study and many high-resolution structures have been solved of individual or grouped domains from these proteins, a full-length structure has yet to be solved (Bhate *et al.*, 2015). HKs are active in the form of a dimer, which is controlled by the interaction of the dimerization domains of each monomer HK subunit. Dimerization of the transmembrane protein is also essential for its autophosphorylation and phosphorelay signal transduction to its RR (Taylor *et al.*, 1981; Nikaido, 2003).

A canonical HK model consists of an extracellular sensory domain, TM domain, and an intracellular kinase domain. The extracellular sensor domains are the most diverse domain of HKs to recognize the different ligands to upregulate a cellular response (Cheung and Hendrickson, 2010; Mascher *et al.*, 2006). Although most sensor domains bind directly to the ligand, the binding interface can vary, for example, some HK sensors detect the state of a secondary protein that binds the ligand such as the sensor domain of LuxQ which interacts with LuxP and binds directly to AI-2 an autoinducer involved in light production in *Vibrio harveyi* (Neiditch *et al.*, 2006). Despite the differences and diversity in the extracellular sensory domain, all are involved in sensing a stimulus that results in a conformational change that can propagate through the receptor and TM domains (Bhate *et al.*, 2015).

The TM domain is represented by an antiparallel pair of TM helix domains separate the extracellular sensor domain. The TM domain in many HKs form a four-helical bundle in the membrane with two TM helices being represented from each monomer. There are no crystal structures of a HK TM domain, but structures exist, but only acquired and solved in the monomeric form (Maslennikov *et al.*, 2010). The TM domain for PhoQ

has shown through site-directed mutagenesis, disulphide crosslinking and molecular dynamics that a polar residue forms a small water pocket in the TM helix and is critical for the signal transduction (Goldberg *et al.*, 2010; Lemmin *et al.*, 2013).

A variety of different signal-transducing elements can connect the extracellular domain and TM domain to the intracellular kinase domain. The first intercellular domain that is involved in signal transduction from the TM helix can vary and are predominately represented by either HAMP or PAS domains that reside in the cytoplasm just below the TM domain. These domains often reside below the TM domain and are present in either combination or tandem repeats. These types of transducing domains are generic and can be found in other bacterial and eukaryotic protein systems (Bhate *et al.*, 2015). HAMP domains are formed of four parallel helical bundles with two helices deriving from a single monomer. A conserved Gly residue marks the end of the first HAMP helix, and a conserved glutamate marks the beginning of the second HAMP helix. The PAS domains contain a mixed  $\alpha/\beta$  structure containing a central anti-parallel five-stranded  $\beta$ -sheet surrounded by several helices. The central  $\beta$ -sheet is curved, and the two faces make contacts that are critical in signalling. The inner surface is responsible for binding cofactors or ligands while the outer surface forms contacts between dimers or with flanking output helices. The architecture of a PAS domain allows ligand binding to alter the packing and dynamics of flanking  $\alpha$ -helices that transmit the signal. These domains can function as linkers and as periplasmic linkers and are the sensor transducing domains for multiple HKs in *B. subtilis* (Chang *et al.*, 2010; Cheung and Hendrickson, 2010).

The second intracellular domain is the dimerization and histidine phosphotransfer (DHp) domain. This is the site of the three catalytic reactions including (i) His phosphorylation, (ii) phosphotransfer to the RR, and (iii) phosphatase reaction for bifunctional HKs. The DHp forms a homodimeric anti-parallel four-helical bundle with two helices connected by a hairpin loop. The catalytic His is located a few turns down the bundle on the solvent-exposed side of helix 1 and is the start of a stretch of seven conserved amino acids known as the H box (**Table 1.5**). Residue 2 serves to act as a hydrogen bond acceptor via the side chains for Asp or Glu, and residue 4 is involved with interactions of the acidic phosphoryl groups of the Lys and Arg residues during phosphotransfer. Residues 5 and 6 form a locus involved in helix bending that allows the

N-terminal end of helix 1 to form multiple conformations during catalysis. The bottom of the DHp bundle hosts the binding interface for the RR and is connected to the catalytic domain through a flexible loop which is variable in size and sequence, fitting its role in providing a sequence-specific interaction for recognising its cognate RR (Capra and Laub, 2012; Podgornaia *et al.*, 2013; Bhate *et al.*, 2015).

**Table 1.5 - Commonly conserved amino acids residues located in the H box within the DHp domain of a prokaryotic HKs.**

Residue	1	2	3	4	5	6	7
AA sequence	H	D/E	L/I	K/R	T/N	P	L

The third and final intracellular domain from the TM helix is the catalytic domain (CA) and is the ATP binding domain containing a highly conserved  $\alpha/\beta$  sandwich with three helices packed against five anti-parallel  $\beta$  strands. These are distinct from any known Ser/Thr kinases (Dutta & Inouye, 2000). The CA domain stands as a monomer when all of the other domains have been removed (Dutta *et al.*, 1999). The nucleotide binds between two helices and is held by a loop known as the ATP lid which can adopt different positions upon ATP binding giving it an open or closed state upon binding to ATP. In the absence of ATP, this loop is partially disordered in crystal structures. Even in the presence of ATP, the lid shows flexibility, allowing ATP to bind and interact with the DHp domain for phosphotransfer. The ATP-lid also enables the CA domain to adopt multiple positions relative to the DHp domain, to function as a kinase, phosphotransferase or phosphatase in response to external stimuli. Conserved nucleotide binding sequences exist and comprise of the N, G1, G2, and F boxes (Kim and Forst, 2001). The F and G2 box resides in a highly mobile central loop containing the Phe residue that is located near the ATP binding cleft and extends away from the rest of the molecule. The G2 box forms the ATP lid that closes over the bound nucleotide. N, G1 and G2 motifs in solved structures make specific contacts with  $Mg^{2+}$  ions, phosphate oxygens and adenine moiety of the bound nucleotide (West and Stock, 2001).

### 1.3.1.2. TCS Response Regulators

Response regulators (RR) are the second component of the TCS and are more straightforward in structure than HK. They are mobile, cytoplasmic proteins that are composed of two primary domains; a receiver domain (REC) and an effector domain. A prototypical RR has an N-terminal receiver domain that participates in catalysis of phosphoryl transfer by accepting a phosphoryl group from its cognate HK onto a conserved aspartate residue. Phosphorylation of the receiver domain changes its conformation and causes activation of its C-terminal effector domain in a phosphorylation-dependent manner (Wang, 2012). The effector domain is variable in sequence due to its variability in different DNA sequence targets and elicits the output of the signalling event, allowing for a diverse array of output functions. The majority of RRs are transcription regulators with their effector domains acting as DNA-binding regions (Gao and Stock, 2009).

The REC domain acts as a phosphorylation-induced switch and is a binary logical element either appearing in a phosphorylated or unphosphorylated state, although this is not always the case as TCSs are not restricted to on/off outputs and can be influenced through crosstalk. Phosphorylation in the REC domain occurs at a conserved Asp residue, generating a high-energy acyl-phosphate. It is thought that the acyl phosphate provides the energy to drive a conformational change in the REC domain (Gao and Stock, 2009). The REC domain has enzymatic activity, catalysing phosphotransfer and dephosphorylation. Phosphotransfer from HK to RR involves a complex of the two, where both proteins contribute to the active site. The catalytic activity of the RR is exemplified by its ability to autophosphorylate at the Asp residue using small-molecule phosphodonors such as acetyl phosphate too. However, the rate of phosphotransfer is much slower than that of the cognate HK (Lukat *et al.*, 1992). The REC domain has an  $\alpha/\beta$ -fold, alternating  $\beta$ -strands and  $\alpha$ -helices in the primary structure fold into a central five-stranded parallel  $\beta$ -sheet surrounded by two  $\alpha$ -helices on one side and three on the other. Three runs of four consecutive hydrophobic residues correspond to the three central  $\beta$ -sheet in the core of the REC domain. Conserved active site residues are located at the C-terminal ends of these three  $\beta$ -strands (1, 3 and 5).  $\alpha 1$  is involved in binding to the DHp domain of HK and is likely to play an essential role in the specificity of HK-RR pair (Casino *et al.*, 2009). In addition to the Asp site of phosphorylation on the  $\beta 3$  strand, the

active site contains two Asp/Glu residues on the  $\beta$ 1 strand, that coordinate a  $Mg^{2+}$  ion (Gao and Stock, 2009).

The effector domains are diverse in sequence and structure, in order to provide a variety of output responses. They can be characterised by a small number of structural families, named after highly characterised members. These include the OmpR/PhoB 'winged-helix' domain and the four-helix NarL/FixJ 'helix-turn-helix' domain. The C-terminal DNA-binding domain of the NarL/FixJ subfamily is a compact bundle of 4  $\alpha$ -helices (Maris *et al.*, 2005). In the inactive form, the REC and effector domains interact, masking the DNA-recognition helix (Maris *et al.*, 2002). In the active phosphorylated state, the RRs dimerise and the DNA recognition helix ( $\alpha$ 9) from both monomers inserts into the major groove of DNA, leading to transcription.

#### **1.3.1.3. Two Component Systems in *Enterococcus* spp.**

Many TCS have been identified between *E. faecalis* strains and describe those that are both HK and RR pairs. These have been classified according to previous literature and also using P2CS TCS database (Barakat *et al.*, 2009; Hancock and Perego, 2002; Hancock and Perego, 2004). In some strains, orphan RRs are apparent, but in the strain OG1RF there are 16 intrinsic TCS with known HK and RR pairs, and in the V538 strain there are 16 intrinsic and 1 acquired TCS pairs. The TCS can be organised and group according to the conservation of amino acids surrounding the His in the H-Box (Fabret and Hoch, 1998) but a some TCS HKs in *E. faecalis* does not fit into this current classification. **Table 1.6** summarises the grouping of TCS according to V538 and OG1RF and **Figure 1.9** highlights the canonical architecture of these classes of the HKs in *E. faecalis*. All HKs in *E. faecalis* TCS localize to the membrane and have a TM domain except HK17. The majority of these HKs have been expressed and purified in a HK extensive study in *E. faecalis* and their phosphorylation activities further characterized (Ma *et al.*, 2008). The majority of TCS found in *E. faecalis* share strong sequence homology with other TCS from different species, but it has been suggested that a small subset is specific to *Enterococcus* spp. The Van cassettes are all orthologues of the VanS and VanR TCS that is transferred through horizontal gene transfer and is present in other species too. The majority of TCS in *Enterococcus* spp. are yet to be functionally characterized in the genus, but some orthologues do exist and are highlighted in **Table 1.6** where the TCS name for that species

is used to describe that in *Enterococcus* spp. The TCS in *Enterococcus* spp. that have been characterized and will be discussed include CroS/R, VicS/VicR, FsrAS/R and VanS/VanR.

The CroSR TCS has been shown to be essential for cephalosporin resistance in a study where RRs were individually knocked out from the vancomycin-resistant strain V538. Without the presence of CroR, intrinsically resistant *Enterococcus* spp. had become sensitive to cephalosporin's (Hancock and Perego, 2004). It has recently been demonstrated that a CroR knockout can interfere with the expression of other gene products including *salB* (a potential PG hydrolase), *lytM* (PG hydrolase), *metC* (PG hydrolase), *alr* (alanine racemase) and *pbp5* ( $\beta$ -lactam resistant PBP) (Muller *et al.*, 2018). Specific to cephalosporin resistance, CroR has been shown to act directly as a promoter for the gene *salB* (Muller *et al.*, 2006) and likewise *SalB* has been shown to be essential for intrinsic cephalosporin resistance in the *E. faecalis* strain JH2-2 (Djoric and Kristich, 2017). The gene *pbp5* encodes a class B PBP in *Enterococcus* spp. and is known to be sensitive to resistant cephalosporin's (Kristich *et al.*, 2011; Arbeloa *et al.*, 2004).

The VicS/R TCS has been partially functionally and structurally characterised in *E. faecalis*. A VicR has been shown to be essential as a knockout could not be created in a RR study in *E. faecalis* V538 (Hancock and Perego., 2004). The structure of VicR from *E. faecalis* has been solved and, the DNA target for the promoter has been predicted (Trinh *et al.*, 2007). The orthologue of VicR in *B. subtilis* WalR from the Walk/R TCS has also been shown to be essential for the organism and has been associated with PG synthesis (Libby *et al.*, 2015).

The FsrAS/R TCS in *E. faecalis* is a virulence regulator and is involved in the mediation of biofilm formation (Del Papa and Perego, 2011). The VanS/R TCS associated with vancomycin resistance is the most characterized system in *Enterococcus* spp. even though it is an acquired mechanism.

**Table 1.6 - Summary and evaluation of the TCS distributed and identified in two *E. faecalis* strains including V538 and OG1RF (Adapted from Hancock and Perego, 2002).**

HK #	TCS	HK Group	V538	OG1RF	Comments
1	YesM/N	<b>Group I Kinases</b>	Yes	Yes	<ul style="list-style-type: none"> <li>• Not functional characterised in <i>Enterococcus</i> spp.</li> <li>• Orthologue in <i>B. subtilis</i></li> </ul>
2	LytS/R		Yes	Yes	<ul style="list-style-type: none"> <li>• Not functional characterised in <i>Enterococcus</i> spp.</li> <li>• Orthologue in <i>S. aureus</i></li> </ul>
3	VraS/R	<b>Group II Kinase</b>	Yes	Yes	<ul style="list-style-type: none"> <li>• Not functional characterised in <i>Enterococcus</i> spp.</li> <li>• Orthologue in <i>S. aureus</i></li> </ul>
4	PhoP/R	<b>Group III Kinase</b>	Yes	Yes	<ul style="list-style-type: none"> <li>• Functionally characterised in <i>Enterococcus</i> spp.</li> </ul>
5	CroS/R		Yes	Yes	<ul style="list-style-type: none"> <li>• Functional characterised in <i>E. faecalis</i></li> </ul>
6	YclK/J		Yes	Yes	<ul style="list-style-type: none"> <li>• Not functional characterised in <i>Enterococcus</i> spp.</li> <li>• Orthologues in <i>B. subtilis</i></li> </ul>
7	VicS/R		Yes	Yes	<ul style="list-style-type: none"> <li>• Characterised in <i>E. faecalis</i></li> <li>• Orthologue in <i>B. subtilis</i></li> </ul>
8	VncS/R	<b>Group III Kinase</b>	Yes	Yes	<ul style="list-style-type: none"> <li>• Not functional characterised in <i>Enterococcus</i> spp.</li> <li>• Orthologue in <i>S. pneumoniae</i></li> </ul>
9	Unknown		Yes	Yes	<ul style="list-style-type: none"> <li>• Not functional Characterised in <i>Enterococcus</i> spp.</li> </ul>
10	LicS/R		Yes	Yes	<ul style="list-style-type: none"> <li>• Characterised in <i>Enterococcus</i> spp.</li> </ul>
11	VanS/R		Yes	No	<ul style="list-style-type: none"> <li>• Well characterised in <i>Enterococcus</i> spp.</li> </ul>
12	KdpD/E		Yes	Yes	<ul style="list-style-type: none"> <li>• Not functional Characterised in <i>Enterococcus</i> spp.</li> <li>• Multiple Orthologues</li> </ul>
13	Unknown	<b>Group IV Kinase</b>	Yes	Yes	<ul style="list-style-type: none"> <li>• Not functional characterised in <i>Enterococcus</i> spp.</li> <li>• No known orthologues</li> </ul>
14	Unknown		Yes	Yes	<ul style="list-style-type: none"> <li>• Not functional characterised in <i>Enterococcus</i> spp.</li> <li>• No known orthologues</li> </ul>
15	FsrAS/R	<b>Group Arg Kinase</b>	Yes	Yes	<ul style="list-style-type: none"> <li>• Characterised in <i>Enterococcus</i> spp.</li> </ul>
16	Unknown	N/A	Yes	Yes	<ul style="list-style-type: none"> <li>• Not functional characterised in <i>Enterococcus</i> spp.</li> <li>• No known orthologues</li> </ul>
17	Unknown	N/A	Yes	Yes	<ul style="list-style-type: none"> <li>• Not functional characterised in <i>Enterococcus</i> spp.</li> <li>• No known orthologues</li> </ul>

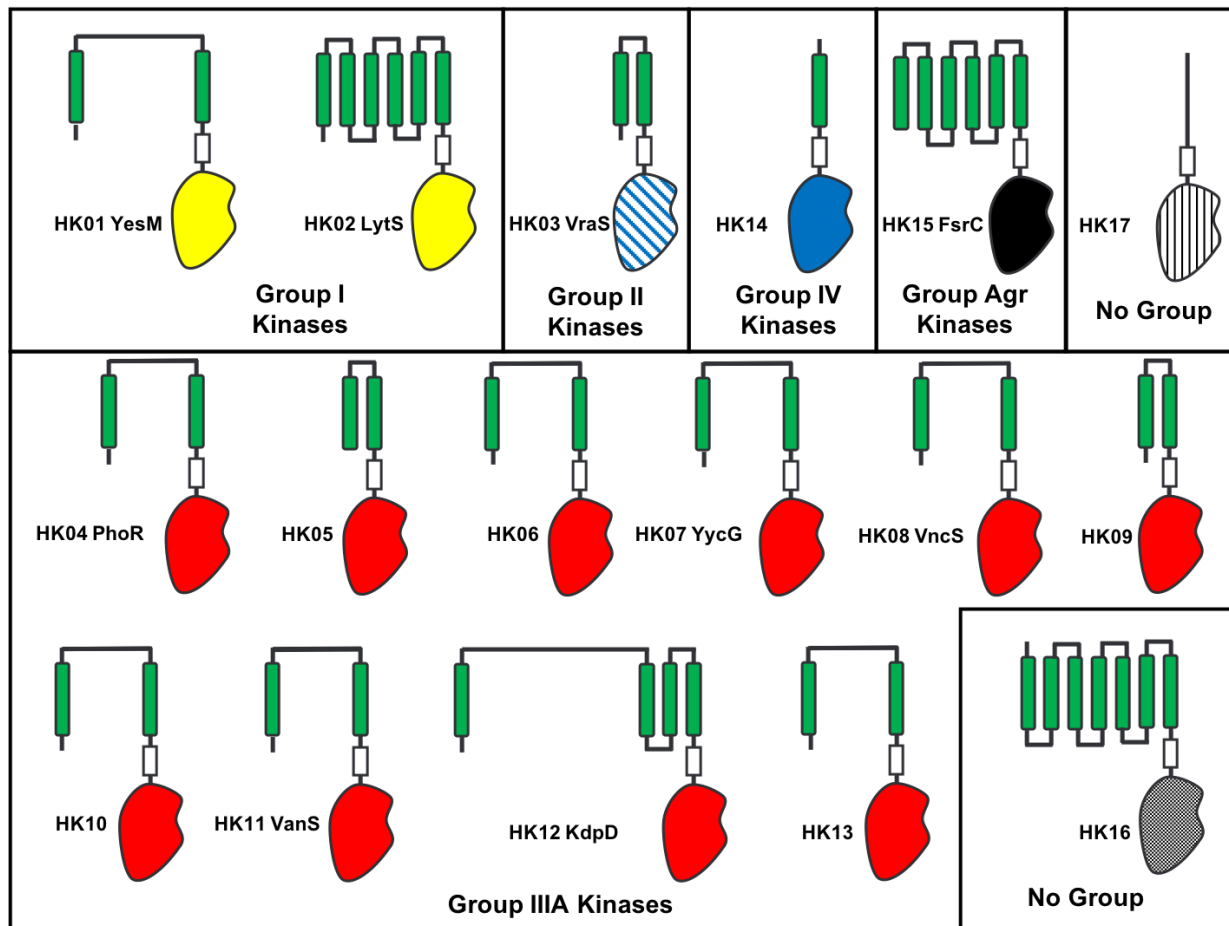


**Figure 1.9: Schematic of the canonical architecture and different types of the 17 HKs found in the *E. faecalis* V538 genome.** They are classified by the homology of the residue surrounding the conserved phosphorylated His in the catalytic domain according to the classification by Fabret and Hoch., (1998) and are grouped and coloured accordingly. Green rectangles highlight the TM domains and white boxes highlight the possible HAMP/PAS/GAF domains. VanS<sub>B</sub> is categorised as a Group IIIA TCS kinase.

Adapted from Hancock and from Perego (2002).

#### 1.3.1.4. TCS and vancomycin resistant in *Enterococcus* spp.

The mechanism of vancomycin resistance is well described in the literature and the architecture and function of the HK VanS and RR VanR from VanA and VanB systems will be discussed respectively. The VanS/R TCS is a part of the vancomycin resistance gene cassette that can be seen in many different Enterococcal spp. that have either acquired the gene cassette or forms an intrinsic part of the genome. High-level vancomycin-resistance is associated with acquired resistance through plasmid and transposon mechanism, as exemplified by the VanA and VanB type resistance. A remarkable effect of this system is that the genes are only expressed in the presence of the drug which includes either vancomycin and teicoplanin for VanA resistance or just vancomycin for VanB. In contrast to many other antibiotic mechanisms, in strains of *E. faecalis* and *E. faecium* containing the Tn1549 cassette conferring VanB type resistance, it has been shown that the acquisition of the vancomycin resistance cassette had no fitness cost to the host in the absence of induction, but upon induction of vancomycin, the host not only had reduced fitness but was also severely impaired its ability to colonize and disseminate in mice (Foucault *et al.*, 2010). The effect that the HK and RR in the TCS of the VanS/R system have on cellular fitness is essential in the ability for the system to work efficiently via an inducible system. Therefore, it is necessary for the sensor HK to efficiently detect the presence of glycopeptides to upregulate an efficient cellular response and the genes to be down-regulated when there is no vancomycin present (Foucault *et al.*, 2010).

VanS<sub>B</sub> catalyses both autophosphorylation and rapid phosphotransfer to VanR<sub>B</sub> (Wright *et al.*, 1993). VanS<sub>B</sub> causes a 6-fold increase in VanR<sub>B</sub>~P dephosphorylation and acts as a VanR<sub>B</sub> specific phosphatase (Depardieu *et al.*, 2003). The cytoplasmic domain of VanS can also autophosphorylate and catalyse both the phosphorylation and dephosphorylation of VanR *in vitro* (Hutchings *et al.*, 2006). Therefore, like other TCS, VanS is a bifunctional protein that can switch between kinase and phosphatase activity. In *Enterococcal* spp., VanR<sub>B</sub> is converted from a monomer to a dimer upon phosphorylation (Depardieu *et al.*, 2005). In the deletion of *vanS* in enterococci, there is up-regulation of expression in the vancomycin resistance genes, suggesting VanS negatively regulates VanR function in the absence of vancomycin. Therefore, VanR~P is generated in a VanS~P independent manner and VanS acts as a VanR~P phosphatase in

the absence of a glycopeptide inducer in which it maintains a basal expression of the *van* resistance genes (Arthur *et al.*, 1997).

Strains that constitutively upregulate the vancomycin-resistant genes have been isolated from VanB type strains. It had been identified that a T237K amino acid substitution in a H Box of VanSB leads to constitutive activation and has been demonstrated to be required for phosphatase activity (Baptista *et al.*, 1997; Willett and Kirby, 2012). An 18 bp nucleotide deletion removing six amino acids (402-407) in VanSB was identified in a mutant strain with constitutive vancomycin resistance. This deletion occurs in the G2 motif which is a part of the ATP binding domain and is important in modulating the phosphatase activity. This deletion has been observed previously and was observed *in vitro* as well as *in vivo*. Therefore, this type of mutation may occur relatively frequently under the increased selection pressure of the antibiotic (Depardieu *et al.*, 2003).

The mechanisms of how VanR/S senses glycopeptide antibiotics is still unclear, and there are many theories regarding whether the glycopeptide is a direct ligand for VanSB or if VanSB measures the presence of vancomycin indirectly through the interaction with cell wall intermediates that accumulate or degrade upon antibiotic treatment (Hong *et al.*, 2008). A third mechanism has been proposed that input from another sensory system is responsible for detecting cell wall fragments (Boudreau *et al.*, 2012). A signalling system that responds to cell wall fragments in *E. faecalis* has been identified as an eSTK denoted IreK (Kristich *et al.*, 2007). As previously mentioned, the VanB type cluster confers resistance to vancomycin but not to teicoplanin. Previous resistant mutants have been isolated conferring VanB type resistance due to amino acid substitutions in the sensor HK. Two amino acid substitutions include S-232Y and T-237M in the H Box in four strains and are thought to be an indirect effect of teicoplanin resistance and causes impairment of vanRB phosphorylation. Amino acid substitutions in the glycopeptide sensor domain of VanSB led to a gain in function when induced by teicoplanin. The two substitutions were A-30G and D-114Y and located in the extracellular loop (**Figure 1.10**). Other mutations that have been identified in the sensor domain of this protein include A-167S. This suggests that this is the region that the glycopeptides could interact with the VanS<sub>B</sub> protein (Reynolds *et al.*, 1989 and Baptista *et al.*, 1999). This supports the idea that VanS<sub>B</sub> detects the presence of vancomycin

directly as these strains were resistant to vancomycin and teicoplanin but not moenomycin which has a different mode of action. VanA type strains are resistant to moenomycin as well as vancomycin and teicoplanin (**Figure 1.11**) (Handwerger and Kolokathis, 1990). Glycopeptides and moenomycin inhibit transglycosylation but through different mechanisms and are structurally unrelated compounds. This indicates that VanS<sub>A</sub> is unlikely to involve direct interaction of the drugs and that VanS<sub>A</sub> and VanS<sub>B</sub> may detect the presence of glycopeptides through different mechanisms. This is supported by the fact that there is no sequence homology in the sensor domain VanS<sub>A</sub> and VanS<sub>B</sub> (**Figure 1.10**) (Baptista *et al.*, 1996; Evers and Courvalin, 1996). Vancomycin has been shown to bind directly to the sensor domain of VanS from *Streptomyces coelicolor* using a vancomycin photoprobe. This organism does not produce any glycopeptide antibiotics but does show resistance to vancomycin but is still sensitive to teicoplanin and therefore associated with the VanB phenotype (Koteva *et al.*, 2010).

```

VanSA MVIKLNKNDYDKLERKLYMYIVAIVVVAIVFVLYIRSMIRGKLG---DWILSILENKYDLNHLDMAMKLYQYS-- 71
VanSB MERKGIKIKVFSYTIIVLLLVGVATLFAQQFVSYFRAMEAQQTVKSYQPLVELIQNSDRLDMQEVAGLFHYNNQ 76
* * * .: * : * : .: .: * ** * : * : * : .: .: .: .: .: .: * . * : .: * : * :
VanSA -----IRNN-----IDIFIYVAIVISILILCR 93
VanSB SFEFYIEDKEGSVLYATPNADTSNSVRPDLFVYVVRHDDNISIVAQSKAGVGLLYQGLTIRGIVMIAIMVFSLLCA 152
* .: .: .: .: .: .: .: .: .: .: .: .: .: .: .: .: .: .: .: .: .: .: .: .: .: .: .: .: .:
VanSA VMLS-----KFAKYFDEIN-TGIDVLIQNEKQIELSAEMDVMEQKLNLTLEKREQDAK---LAEQRKNDVV 159
VanSB IYFARQMTTPIKALAD[SANKMANLKEVPPPLERKDELGALAHDMHSMYIRLKETIARLEDEIAREHELEETQRYFF 228
.: .: .: .: .: .: .: .: .: .: .: .: .: .: .: .: .: .: .: .: .: .: .: .: .: .: .: .: .:
VanSA MYLAHDIKTPLTSIIGYLS-LLDEAPDMPVDQKAKYVHITLTKAYRLEQLIDEFFEITRYNLQTITLTKTHIDLY 234
VanSB AAASH[ELKTPIAAVSVLLEGMLENIGDY--KDHSKYLRECIKMMDRQGKTISEILELVS[NDGRIVPIAEPLDIGR 302
.: .: .: .: .: .: .: .: .: .: .: .: .: .: .: .: .: .: .: .: .: .: .: .: .: .: .: .: .:
VanSA MLVQMTDEFYPQLSAHGKQAVIHAPEDLTVSGDPDK[LARVFNNILKNA]AAAYSEDNSIIDITAGLSGDVVSIEFKNT 310
VanSB TVAELLPDFQTLAEANNQRFVTDIPAGQIVLSDPRL[LQKALSNVILNA]VQNTPOGGEVRIWSEPGAKEYRL[SVLNM 378
.: .: .: .: .: .: .: .: .: .: .: .: .: .: .: .: .: .: .: .: .: .: .: .: .: .: .: .: .:
VanSA GS-IPKDKLAAIFEKFYRLDNARSSDTGGAGLGLAIAKEIIVQHGGQIYAESNDNYTFRVELPAMPDLVDKRRS 384
VanSB GVHIDDTALS[KLFI]FYRIDQARSRKS[GRSGLGLA]IVQKTLDAMSLQYALENTSDGVLFWLDLPPTSTL----- 447
* * . * : * ** * : * : * : * : * : .: .: .: .: .: .: .: .: .: .: .: .: .: .: .: .: .: .:

```

**Figure 1.10 - CLUSTALW sequence alignment of the protein sequences of VanS<sub>A</sub> and VanS<sub>B</sub>.** Sensor domain in green. Membrane spanning regions in red. G2 box shown in blue. N motif highlighted in yellow. G1 motif highlighted in light blue. F motif highlighted in pink. The key conserved phosphorylated His residue in green. The mutations causing teicoplanin resistance in the sensor domain are boxed in Blue. The phosphorylated Thr residue (T223) associated only with VanS<sub>B</sub> is boxed. "\*" amino acids are identical in all sequences in the alignment, ":" show where conserved amino acids substitutions have been observed and "." show where semi-conserved amino acids substitutions have been observed.

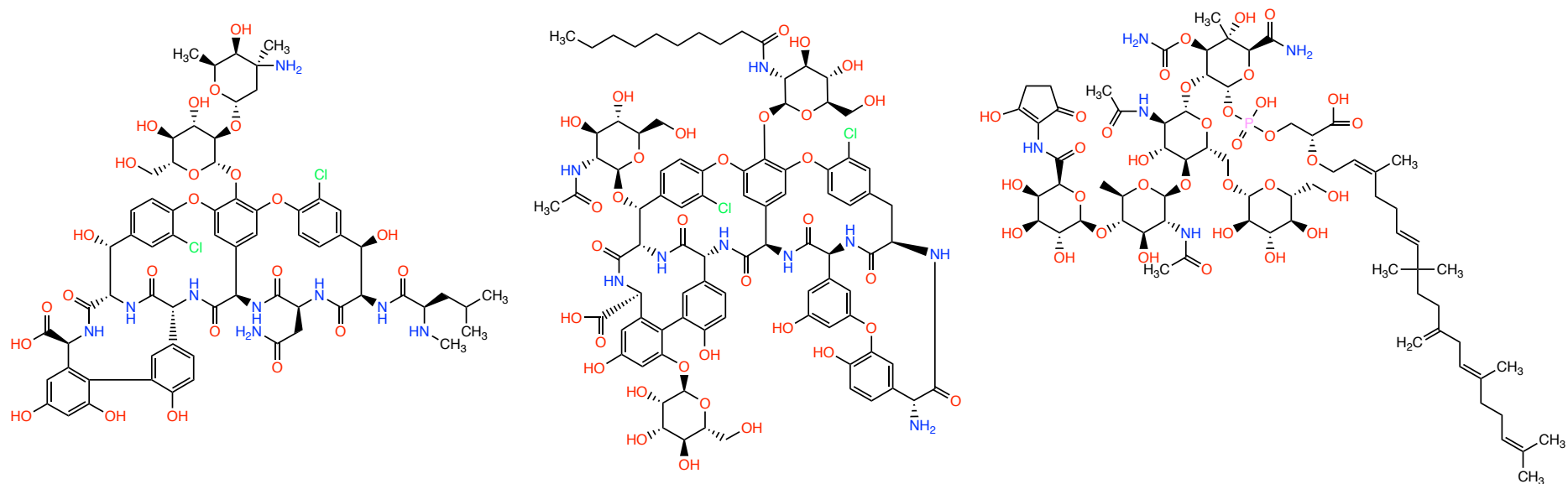


**Figure 1.11 - The chemical structures of vancomycin, teicoplanin and moenomycin.** Vancomycin (Left), teicoplanin (Centre) and moenomycin (Right), that can trigger resistance mechanisms for glycopeptide resistances depending on the type of Van resistance. Vancomycin, teicoplanin and moenomycin are inducers of VanA type resistance and only vancomycin is an inducer for normal VanB type resistance, unless specific mutations are introduced on the extracellular loop of the VanS<sub>B</sub> protein where teicoplanin can become an inducer for VanB type resistance.

### 1.3.2. Eukaryotic like Ser/Thr Kinases/Phosphatases

The main family of Ser/Thr/Tyr protein kinases was initially described and highlighted in eukaryotic organisms (Hanks *et al.*, 1988) It was initially believed that these kinases do not exist in bacteria, but extensive genome sequencing revealed their existence in many bacteria, even though Ser/Thr/Tyr protein kinases were described in *E. coli* in 1969 (Kuo and Greengard, 1969). A Ser/Thr kinase was identified in the social bacteria *Myxococcus xanthus*, with significant sequence homology to that of Eukaryotic kinases and denoted eukaryotic-like Ser/Thr kinases (eSTKs) (Munoz –Dorado *et al.*, 1991; Pereira *et al.*, 2011). Since the age of whole-genome sequencing, many bacteria were identified to contain an eSTK (Kannan *et al.*, 2007).

The ability for bacteria to detect changes in their extracellular environment and adapt accordingly was once thought to be a predominant function of the TCSs. Recently whole genome sequencing has also revealed that many bacteria contain eSTKs with signalling domains (Bakal and Davies, 2000; Pereira *et al.*, 2011). These eSTKs share strong homology to that of the Hanks type eSTK but are structurally and functionally different to other Ser/Thr kinases in bacteria (Hanks and Hunter, 1995; Stancik *et al.*, 2018). These kinases are present in all Gram-positive bacteria and have a cognate eukaryotic-like Ser/Thr phosphatase (eSTP) that is present in the same operon and is transcriptionally coupled. Unlike their TCS counterparts, eSTKs and eSTPs are also present at far fewer numbers per bacterial genome with one cognate pair found only in Gram-positive species. eSTKs are also pleiotropic in nature and phosphorylate a number of substrates that are crucial for cellular functions, including TCS HKs that often have only one RR partner (Pereira *et al.*, 2011).

eSTKs and eSTPs in Gram-positive bacteria are associated with many cellular functions including cell division, dormancy, antibiotic resistance, virulence and the control of transcription and translation mechanisms. Whilst the deletion of these kinase genes is not generally associated with essentiality, the eSTK in *M. tuberculosis*, PknB appears to have an essential role (Fernandez *et al.*, 2006, Kang *et al.*, 2005, Sasseti *et al.*, 2003).

### 1.3.2.1. Eukaryotic like Ser/Thr Kinases

The eSTK PknB from *M. tuberculosis* was the first eSTK structure that was solved via X-ray crystallography and shown to have strong structural and mechanical similarity to that of the mouse cyclic AMP-dependent protein kinase (PKA) (Akamine *et al.*, 2002; Ortiz-Lombardia *et al.*, 2003; Young *et al.*, 2003). Both PKA and PknB share a high degree of conservation in the intracellular kinase domain, but receptor eSTK in bacteria have an additional extracellular domain linked through a TM helix (Krupa and Srinivasan, 2005). The extracellular domain associated with eSTK in Gram-positive bacteria is the variable PASTA (penicillin-binding protein and Ser/Thr kinase-associated) domain (Yeats *et al.*, 2002).

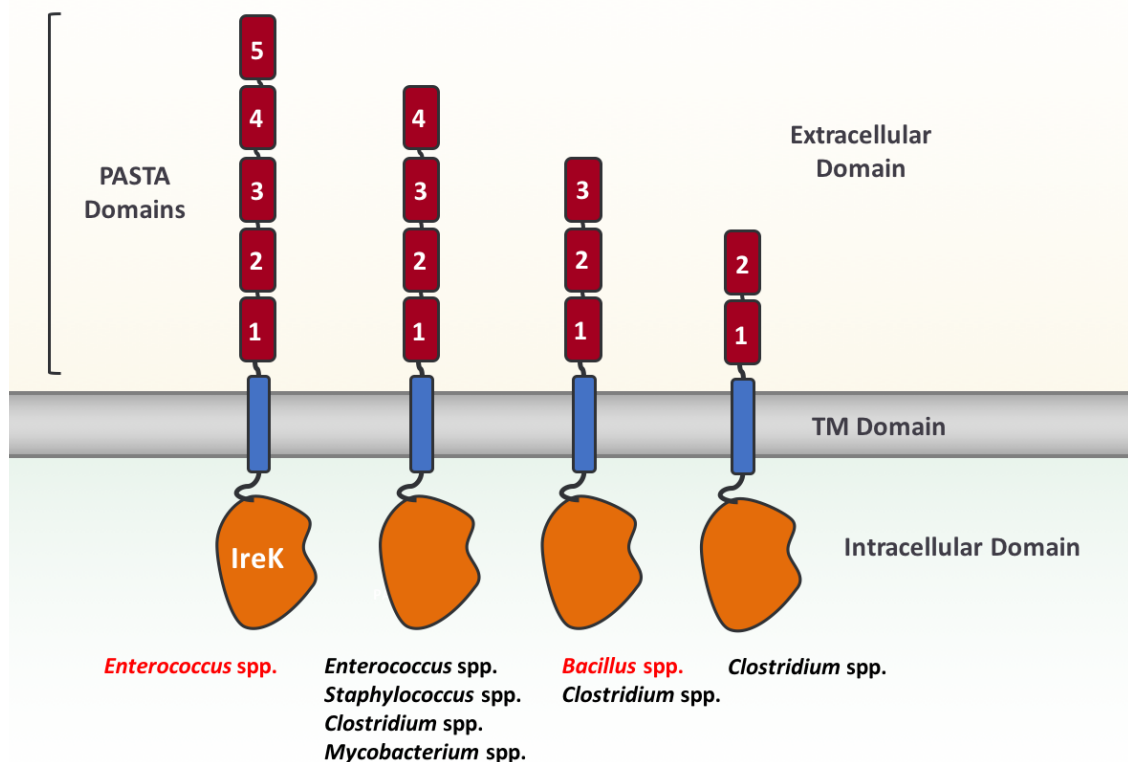


Figure 1.12 – Schematic highlighting the eSTK in *E. faecalis*, IreK and the architecture and distribution of PASTA domains from other Gram-positive bacteria.

PASTA domains were first described in Pbp2X from *S. pneumonia* and including a structure with the  $\beta$ -lactam antibiotic cefuroxime interacting with one of the PASTA

repeats (Yeats *et al.*, 2002; Gordon *et al.*, 2000). Cefuroxime bound to the PASTA domain is structurally analogous to that of unlinked PG, so it was proposed that these PASTA repeats can also bind PG. The architecture of these types of eSTK receptor proteins in Gram-positive have been highlighted and determined using the SMART database and shows how each of the PASTA domains vary in number between different Gram-positive bacteria not only on a genus level but also on a species level (**Figure 1.12**) (Letunic *et al.*, 2014). Structural studies of the PASTA domains from the eSTK PknB from *M. tuberculosis* and PknB from *S. aureus* has revealed that the PASTA domains extend into the extracellular space in a linear arrangement. It has been proposed that the autophosphorylation activity of the intracellular kinase is increased upon dimerization of the kinase domain mediated via a ligand-induced dimerization of the PASTA domains that propagates into the intracellular kinase domain (Barthe *et al.*, 2010). PknB crystallized as a dimer, indicating interactions between the opposite or “back” sides of the N- terminal lobes of two catalytic domains (Wehenkel *et al.*, 2006). The dimerization interface is conserved amongst Gram-positive receptor eSTK homologues.

It has been shown that a PASTA containing kinase (PrkC) in *B. subtilis* was responsible for detecting PG derived muropeptides (Shah *et al.*, 2008). It has also been shown that there is a direct interaction of PG with PASTA repeats or PrkC using biophysical techniques (Squeglia *et al.*, 2011). This includes the PASTA domain of PrkC interacting with muropeptides at the meso-A2pm moiety in the third position in the pentapeptide stem with the Arg500 residue within the terminal PASTA domain using NMR (Squegila *et al.*, 2011). Other supporting data includes homologs of PrkC also demonstrates that these PASTA domains interact with PG with great specificity. It was also demonstrated that the PASTA domains in PrkC are essential in stationary phase growth and not in the exponential (Libby *et al.*, 2015).

Biochemical evidence has recently shown that the PASTA domains from PrkC in *S. aureus* interact with Lipid II (Hardt *et al.*, 2017). *M. tuberculosis* has many different modifications in its cell wall and PG containing a 1,6-anhydro-MurNAc and longer glycan chains exhibit a higher binding potency to PASTA domains and that the fourth residue in the peptide stem of PG was crucial for protein recognition (Wang *et al.*, 2017). Previous experiments also studying PG interactions on PknB from *M. tuberculosis* used Surface Plasmon Resonance (SPR) and demonstrated that the second and third positions of the

peptide stem were important for binding to PASTA and also the presence of the sugar moieties (Mir *et al.*, 2011). As there is high diversity in the modular structures and sequences found among the C-terminal sensory PASTA domains of eSTKs, different homologues may bind to different ligands for species-specific signalling. This is further exemplified by the fact that if PG is the ligand of these domains, there is already so much variability that can occur in PG between species.

Recently, the four PASTA domains in StkP, the eSTK from *S. pneumoniae* have been characterized. It concluded that the first three PASTA membrane proximal domains had interchangeable modules and were required for StkP kinase activity. They also have a role in controlling and maintain the thickness of the PG cell wall with the removal of each PASTA domain resulting in a thinner cell wall. The fourth membrane distal PASTA domain had an alternative function in contrast to the other three PASTA domains and was found to have a unique motif that was critical in the final stages of cellular division and thought to interact with the cell wall hydrolase LytB (Zucchini *et al.*, 2018).

Although the extracellular PASTA domains and the intracellular kinase domain from eSTK in Gram-positive bacteria are well studied, the linker TM domains are not. The effect of homodimerization of PrkC in *B. subtilis* has been studied and showing not only was the extracellular domain capable of promoting dimerization, but the TM domain was also important in promoting dimerization (Madec *et al.*, 2002).

### **1.3.2.2. Eukaryotic-like Ser/Thr Phosphatases in Gram-positive bacteria**

The ability for an organism to reverse the phosphorylation event of kinases occurs is essential in controlling signal cascades and maintaining cell fitness in both Eukaryotic and Prokaryotic organisms. Unlike TCS HKs where the phosphorylated His residue is labile, phosphorylation of Ser, Thr and Tyr residues are not and require a cognate phosphatase to quench the signalling cascade (Dworkin, 2015). As it has been mentioned previously, eSTKs are involved in many cellular functions such as cell division and cell wall synthesis. Deletions of eSTPs have been shown to alter normal cell division and growth in bacteria. Recently it was demonstrated that MapZ, a membrane protein required for cell division in *S. pneumoniae* by identifying the division sites and positioning the Z-ring at the mid-cell undergoes phosphorylation by StkP (Garcia *et al.*, 2016).

### 1.3.2.3. IreK and IreP in *Enterococcus* spp.

It has been known for many years that *E. faecalis* are naturally resistant to the class of  $\beta$ -lactams, the cephalosporin's, but the molecular basis to the resistance is not well understood. The eSTK from *E. faecalis*, IreK has been shown to be an essential protein involved in intrinsic cephalosporin resistance. Like other eSTKs, IreK is a signal transduction protein and exhibits a bipartite domain architecture (**Figure 1.12**). This includes the eSTK signalling domain through a putative TM segment and an extracellular domain comprised of PASTA domains (Kristich *et al.*, 2007). Initial identification of Ser/Thr kinase domains in *E. faecalis* was identified by analysing the *E. faecalis* V583 genome where a homolog of the *B. subtilis* PrkC was identified. Phenotypic studies of its function showing that this protein was critical in intrinsic cephalosporin resistance led to its name IreK (Intrinsic resistance in *Enterococcus* kinase). The role of PASTA domains in IreK is not well understood, but it has been proposed that like other Gram-positive bacteria, that they bind to PG which suggests IreK could serve as a transmembrane receptor kinase that senses damage or perturbation of PG and that it initiates a signalling circuit to restore cell wall integrity (Squeglia *et al.*, 2011). IreK differs to most other Gram-positive sensor eSTKs by having the most number of PASTA domains in *E. faecalis* with five in total (**Figure 1.12**). Its *B. subtilis* homologue PrkC responds to fragments of PG by growing cells as a signal to exit dormancy (Shah *et al.*, 2008).

*E. faecalis* IreK and its homologs in other low-GC Gram-positive bacteria are encoded immediately adjacent to a gene that encodes a PP2C-type protein phosphatase (called IreP in *E. faecalis*). IreP can dephosphorylate both IreK and substrates of IreK *in vitro*, and analysis of deletion mutants lacking IreP indicate that this activity is important *in vivo*. IreP mutants exhibit substantial hyper-resistance to cephalosporin's, a finding which is consistent with hyper-activation of the IreK kinase (Kristich *et al.*, 2007). Furthermore, mutants that lack IreP exhibit a significant reduction in fitness in the absence of cephalosporin's compared to wild-type. *E. faecalis*, which indicates that uncontrolled activation of cephalosporin resistance mechanisms imparts a significant fitness cost to the cell. The complex regulatory circuitry controlling intrinsic cephalosporin resistance in *E. faecalis* may, therefore, stem from the fitness cost that is associated with expression of this phenotype.

One known substrate of IreK is a protein of unknown function IreB but is widespread across low GC Gram-positive bacteria. IreB has an adverse effect on cephalosporin resistance and is a substrate for both IreK and IreP. Mutations on the phosphorylated Thr residues by IreK on IreB led to impaired cephalosporin resistance (Hall *et al.*, 2013). There is an NMR structure of IreB that has revealed that it forms a dimer *in vitro*. Mutations at the dimer interface impaired IreB function and showed that dimerization is functionally essential for IreB (Hall *et al.*, 2017).

The *E. faecalis* IreK homologue in *E. faecium* StkP has also been linked to cephalosporin resistance and that the activity of Pbp5 which has a low affinity to cephalosporin's allowing PG polymerization resume is controlled by kinase activity of StkP and the IreP homologue in *E. faecium* StpA (Desbonnet *et al.*, 2016). The structure of StkP differs to that of other Gram-positive eSTKs and has an associated C-terminal tail formed predominantly of Ser residues. Mutations of this type result in a truncation that have caused an increase in StkP activity and are thought to occur in constitutive activation of the intracellular kinase portion and an increase in cephalosporin resistance. StkP and StpA have also been linked to alterations in PG biosynthesis. The loss of StpA activity that regulates StkP phosphorylation events leads to the production of DdcY, a D,D-carboxypeptidase under the control of a TCS including the sensor HK DdcS and RR DdcR. The upregulation of DdcY leads to the production of tetrapeptide PG and provide a substrate for L,D-transpeptidases to bypass the mostly  $\beta$ -lactam sensitive PBPs (Sacco *et al.*, 2014).

### 1.3.3. Convergence of Eukaryotic-like Ser/Thr kinases and two-component systems

It has previously been determined that crosstalk can occur between different TCSs in different organisms raising the question of their once though specificity between the HK and the RR. Studies of the PhoR-PhoB and the VanS-VanR TCSs have been particularly useful in highlighting the mechanisms used by cells to prevent cross-talk. The PhoR-PhoB TCS is endogenous to *E. coli* and allows the organism to sense and respond to changes in phosphate availability. The VanS-VanR TCS regulates the expression of genes conferring vancomycin resistance in enterococci and other Gram-positive bacteria but can be expressed and studied in *E. coli*. Cross-talk from the kinase VanS to the response regulator PhoB can occur in *E. coli*, but only in the absence of PhoR. Similarly, the kinase PhoR can cross-talk to the response regulator VanR, but just in the absence of VanS. In each case, the cross-talk is likely a consequence of eliminating the phosphatase activity normally provided by the other histidine kinase, which is bifunctional (Fisher *et al.*, 1995). HKs and RRs each derive from paralogue gene families that share significant sequence and structural similarities; therefore, it is possible that cross-talk to occur in the same organism. It is essential for cross-talk between pathways to be kept to a minimum to ensure the organism can elicit the specific cellular response in the presence of a stimulus.

It has also been demonstrated that the phosphatase activity of the sensory HK is vital in controlling and preventing RR cross-talk. In a study looking at the WalkR TCS in *S. pneumoniae*, it had been shown that Walk had a similar amino acid sequence to that of five other HKs and that there was low-level crosstalk between three of the HKs and WalR (Wayne *et al.*, 2012).

There are many similar and highly related signalling proteins in individual bacteria; therefore, it has been suggested that cells may take advantage of these signalling proteins by integrating signals or diversifying responses to enhance their ability to process information (Laub and Goulain, 2007). It has recently come to light that TCSs and eSTKs do not function in isolation but rather can converge to upregulate the same process. An advantage of this mechanism is that phosphohistidine and phosphoapartyl modifications are more labile compared to phosphothreonine and phosphoserine modifications which are more stable. Therefore, the convergence of these two signalling pathways could lead to kinetic regulation of the same pathway (Pereira *et al.*, 2011).

eSTKs have been shown to directly phosphorylate the TCS HKs including the HK DegS in *B. subtilis* showing direct phosphorylation by the eSTK PrkC (Jers *et al.*, 2011). The majority of observed phosphorylation events observed between eSTKs and TCSs is between eSTKs and RR. The TCS WalKR is essential in *B. subtilis* and is involved in both PG biosynthesis and degradation. The RR WalR has been identified as a phosphorylation target of PrkC at position Thr101 immediately adjacent to the dimerization interface of the RR and thought to influence dimerization and the DNA binding (Libby *et al.*, 2015).

#### **1.3.4. Convergence of the *E. faecalis* eSTK, IreK and the vancomycin resistance TCS, VanS**

In a previous study, a number of eSTKs in a range of Gram-positive bacteria and demonstrated cross talk between these eSTKs and TCSs (Goss, 2013). The study included PrkC from *B. subtilis* and its interaction with WalKR TCS (Libby *et al.*, 2015), PknB from *S. aureus* and its interactions with PhoPR TCS and IreK from *E. faecalis* and its interaction with the VanSR<sub>B</sub>.

##### **1.3.4.1. IreK phosphorylates VanS<sub>B</sub> *in vitro***

It has been initially demonstrated that T101 on WalR is phosphorylated by the eSTK PrkC in *B. subtilis* (Libby *et al.*, 2015; Goss, 2013). When comparing the sequence homology of WalR from *B. subtilis* to that of other TCS from other species, there was a conserved T101 residing in the sequence of VanR<sub>B</sub>. It was therefore hypothesised that T101 may be the site of phosphorylation by IreK on VanR<sub>B</sub> and contribute to the signal transduction cascade involved in vancomycin resistance. Initial experiments used recombinant expressed and affinity purified, full-length response regulator VanR, and the corresponding KD VanS (VanS<sub>BKD</sub>) and kinase domain of IreK (IreK<sub>KD</sub>). The hypothesis was explored in a classical radioactive phosphoryl-transferase assay. IreK<sub>KD</sub> was incubated with  $\gamma^{32}\text{P}$  labelled ATP and analysed by SDS-PAGE confirming autophosphorylation of IreK (**Figure 1.13.A**). Using autophosphorylated IreK<sub>KD</sub> which had been desalted to remove excess  $\gamma^{32}\text{P}$  labelled ATP, the protein was then further incubated with VanR and VanS<sub>KD</sub> proteins in separate experiments. This analysis revealed no distinct phosphoryl transfer reaction between IreK<sub>KD</sub> and VanR but between IreK<sub>KD</sub> and VanS<sub>KD</sub> (**Figure 1.13.B** and **Figure 1.13.C** respectively).

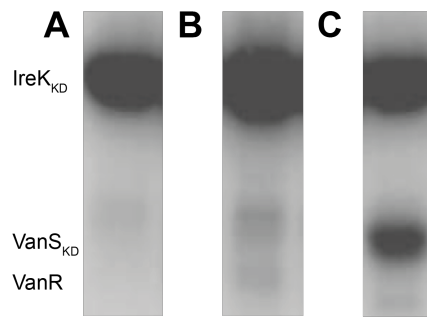


**Figure 1.13: IreK<sub>KD</sub> autophosphorylates and phosphorylates the VanS<sub>KD</sub> and not VanR of the VanB type Tn1549 cassette.** The *in vitro* kinase assay included (A) 4μM IreK<sub>KD</sub>, (B) 4μM IreK<sub>KD</sub> and 4μM VanR and (C) 4μM IreK<sub>KD</sub> and 4μM VanS<sub>KD</sub>. Samples were boiled at 95°C to ensure I was not observing phosphohistidine autophosphorylation. Gels were visualized by autoradiography (Goss, 2013).

As there was robust transphosphorylation, the *in vitro* phosphorylated VanS<sub>KD</sub> was analysed by mass spectrometry to identify the residues on VanS that underwent transphosphorylation by IreK<sub>KD</sub>. This analysis revealed multiple phosphopeptides with phosphorylation of VanS at residue T223, S243 and T244. A series of point mutants of VanS<sub>KD</sub> were produced by site directed mutagenesis of T233, S243 and T242 and reanalysed by phosphotransfer from autophosphorylated IreK<sub>KD</sub>. This showed that the single amino acid substitutions of S243 and T242 had no effect on phosphoryl transfer from IreK to VanS but the substitution of T233A abolished the effect. This analysis was extended to the corresponding IreK from *Enterococcus faecium* and the same phosphorylation pattern was found (**Figure 1.14.A and Figure 1.14.B** respectively). From the biochemical dissection, it can be concluded that IreK<sub>KD</sub> specifically phosphorylates VanS<sub>KD</sub> at T233 *in vitro*. This is in a location that is distinct from that used by VanS in its autophosphorylation reaction (H164) in the widely described TCS signalling cascade associated with vancomycin resistance (Bhate *et al.*, 2015; Fisher *et al.*, 1995).

IreP, the cognate phosphatase of IreK is normally associated with the physiological balance of IreK autophosphorylation (Kristich *et al.*, 2011). Given the observed transfer of phosphate from IreK<sub>KD</sub> to VanS<sub>KD</sub> as reported above, the interaction of IreP with autophosphorylated IreK<sub>KD</sub> and phosphorylated VanS<sub>KD</sub> on T223 (as a result of IreK<sub>KD</sub> phosphorylation) was investigated. IreK was incubated with  $\gamma^{32}\text{P}$  labelled ATP and VanS<sub>KD</sub> prior to addition of IreP. Following an hour incubation with IreK, we analysed the phosphorylation state of VanS and IreK by autoradiography. In this analysis the

majority of both VanS and IreK had been dephosphorylated by IreP (**Figure 1.15.A** and **Figure 1.15.B** respectively). Furthermore, there appears to be a shift in migration of the IreK sample in the SDS-PAGE analysis following dephosphorylation consistent with previous observations of IreK behaviour (Kristich *et al.*, 2011). This demonstrates that IreK and VanS<sub>B</sub> are substrates for IreP.

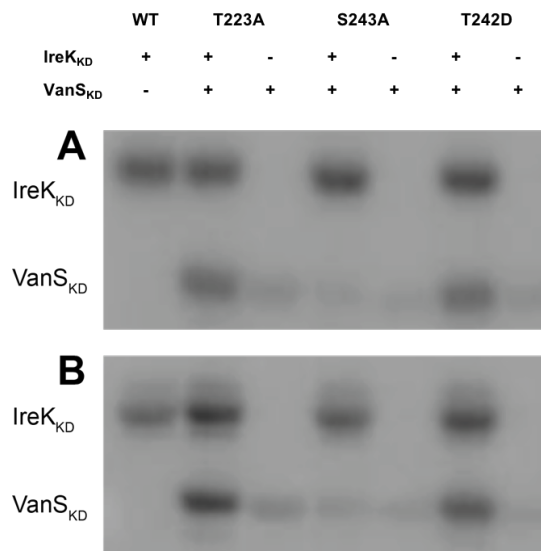


**Figure 1.14: IreK<sub>KD</sub> from both *E. faecalis* (A) and *E. faecium* (B) phosphorylates VanS<sub>KD</sub> from the Tn1549 cassette at position T223.** The *in vitro* kinase assay included 2  $\mu$ M *E. faecalis* or *E. faecium* IreK<sub>KD</sub> with 2  $\mu$ M of various VanS<sub>KD</sub> mutant proteins to verify the site of phosphorylation. Samples were boiled at 95°C to ensure I was not observing phosphohistidine autophosphorylation. Gels were visualized by autoradiography (Goss, 2013).

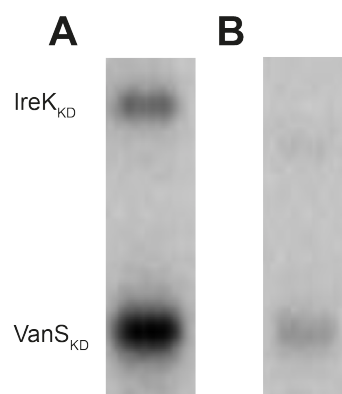


**Figure 1.15: The cognate phosphatase of IreK, IreP dephosphorylates IreK and its substrate VanS.** The *in vitro* kinase assay included (A) 1  $\mu$ M IreK<sub>KD</sub> which autophosphorylates and phosphorylates 3  $\mu$ M VanS<sub>KD</sub>. Experiments were performed for 30 minutes at 37°C. (B) 1  $\mu$ M IreK<sub>KD</sub> is incubated with 3  $\mu$ M VanS<sub>KD</sub> where transphosphorylation is observed. 2 $\mu$ M IreP was added and allowed to incubate for 1 hour at 37°C. (Goss, 2013).

#### 1.3.4.2. Staurosporine inhibits the effect of IreK phosphorylation *in vitro*

Many eukaryotic STKs are inhibited by staurosporine and that this effect may be extended to bacterial eSTKs as well (Lawrie *et al.*, 1997). Staurosporine is an indolocarbazole compound and is known to have a range of biological activities as a result of its ability to bind to the ATP site of protein kinases and has been tested in an anticancer drug context. To test the hypothesis that staurosporine might also elicit an effect on IreK, the effect of increasing staurosporine concentration on IreK kinase domain autophosphorylation was also assessed. Purified IreK<sub>KD</sub> was incubated with a range of staurosporine concentrations in the presence of ATP, prior to analysis by SDS-PAGE and autoradiography. This showed that with increasing staurosporine concentration, IreK<sub>KD</sub> autophosphorylation was reduced (**Figure 1.16**).

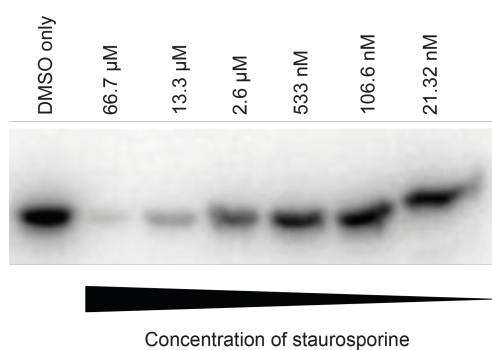


**Figure 1.16: Staurosporine inhibits IreK<sub>KD</sub> *in vitro*.** The *in vitro* kinase experiment included increasing concentration of staurosporine inhibits autophosphorylation of IreK<sub>KD</sub>. The amount of staurosporine is indicated above the lanes. DMSO was used as a negative control. Staurosporine was added prior to addition of radioactive ATP and reactions were allowed to incubate for 30 minutes at 37°C (Goss, 2013).

#### 1.3.4.3. Initial genetic attempts to understand the effects IreK on Van<sub>B</sub> resistance

Initial attempts to create a  $\Delta ireK$  mutant strain in JH2-2 and JH2-2 Tn1549 were unsuccessful and it was concluded that *ireK* might be essential in the genetic background of that strain. It has been demonstrated previously that *ireK* can be deleted in an OG1RF strain (Kristich *et al.*, 2007). Since an OG1RF  $\Delta ireK$  strain had been created, both OG1RF and OG1RF  $\Delta ireK$  were kindly provided by Christopher Kristich and the Tn1549 cassette was conjugated into both strains by Dr. Courvalin and Dr. Depardieu (Institute Pasteur). Unfortunately, only a single transfer event was obtained into the OG1RF  $\Delta ireK$  strain but none was obtained into OG1RF.

## 1.4. Project Aims and Outline

The development of multi-drug resistance by pathogenic bacteria is an urgent clinical issue. A key mechanism underlying the acquisition of multi-drug resistance is cross-protection by one resistance mechanism for another antibiotic. The pathogen *Enterococcus faecalis* becomes resistant to the glycopeptide vancomycin when the bacterium acquires the Tn1549 transposon which encodes proteins that remodel the peptidoglycan. *Enterococcus* spp. that are resistant to vancomycin and has recently placed on the WHO priority list of antibiotic-resistant Gram-positive bacteria (Tacconelli *et al.*, 2017). The so-called VRE strains are thought to emerge in clinical settings following treatment with vancomycin. However, extensive epidemiological evidence, obtained over the past two decades, indicates that an important risk factor in VRE emergence is treatment with the  $\beta$ -lactam cephalosporins, suggesting a connection between the resistance to these two different classes of compounds. However, a mechanistic basis for this connection has been unclear. This project is aimed at investigating this question with the ultimate goal of identifying strategies that prevent this cross-resistance.

IreK from *E. faecalis* and homologues in other *Enterococcus* spp. has already been shown to be essential for cephalosporin resistance (Kristich *et al.*, 2007). Preliminary data from my collaborators suggests that there is an interaction between IreK and the VanS<sub>B</sub> kinase. This thesis aims to:

- (1) In considering the role of the Tn1549 cassette in relation to cephalosporin resistance, is cephalosporin resistance mediated by the Vancomycin resistance genes? If not, what other genes may be implicated in this mechanism?
- (2) Can the kinase activity of IreK be inhibited by well-defined eukaryotic kinase inhibitors to restore antibiotic susceptibility?
- (3) How does IreK function, what are its ligands and what is its cellular localisation? What extracellular ligands are implicated in binding to the PASTA domains of IreK? What influence do the PASTA domains have on cellular location?
- (4) Does the additional PASTA domain found in *Enterococcus faecalis* IreK have significance for ligand binding and overall structure?

## Chapter 2. Materials and Methods

### 2.1. Materials

#### 2.1.1. Bacterial Strains

Bacterial strains used in this study are listed in **Table 2.1**. *E. coli* Top10 and NEB5 were used for cloning and BL21 (DE3) cells were used for the expression of recombinant proteins and *E. faecalis* JH2-2 and OG1RF strains were used for the preparation of PG, mutagenesis and fluorescent microscopy experiments. Antibiotic susceptibility testing was performed on multiple clinical and standard isolates listed in **Table 2.1**. All bacterial strains were stored in cryogenic tubes supplemented with 20% glycerol in a -80°C freezer.

#### 2.1.2. Media

The composition of *E. coli* and *E. faecalis* culture media are described in **Table 2.2**. Selective media was supplemented with either 100 µg mL<sup>-1</sup> Ampicillin (Amp) and either 30 µg mL<sup>-1</sup> or 200 µg mL<sup>-1</sup> Erythromycin (Erm). For media containing agar, antibiotics were added at 50°C and poured into sterile Petri dishes. Selective agar plates were composed of the required broth, to which 15 g of bacto-agar was added in 1 L of media and autoclaved.

#### 2.1.3. Buffers and solutions

All chemicals obtained were of analytical grade unless otherwise stated. Companies and vendors are referenced with specific chemicals. MilliQ pure water was used to make all buffers. A summary of protein buffers used for the purification, storage and assays of recombinant proteins are summarised in **Table 2.3**. Buffers were sterilised with a 0.2 µm filter and stored at 4°C for up to 1 month.

#### 2.1.4. Vectors for Cloning, Complementation and Protein Expression

Vectors used for cloning, mutagenesis, expression of recombinant protein and complementation are described in **Table 2.5**, **Table 2.6** and **Table 2.7**.

**Table 2.1 - Experimental Strains used for *E. coli* and *Enterococcus spp.* experiments.** Relevant characteristics and sources of each strain are included.

Strain	Relevant Characteristics	Reference
<b>Experimental <i>E. coli</i></b>		
Top10	$\Delta(ara-leu)$ 7697 <i>araD139 fhuA</i> $\Delta lacX74$ <i>galK16 galE15 e14-</i> $\phi 80dlacZ\Delta M15$ <i>recA1 relA1</i>	Grant <i>et al.</i> , (1990)
NEB5	<i>endA1 nupG rpsL</i> (Str <sup>R</sup> ) <i>rph spoT1</i> $\Delta(mrr-hsdRMS-mcrBC)$ F' <i>proA<sup>+</sup>B<sup>+</sup> lac<sup>R</sup> <math>\Delta(lacZ)M15</math> zzf::Tn10</i> (Tet <sup>R</sup> ) / <i>fhuA2<math>\Delta</math>(argF-lacZ)U169 phoA glnV44</i>	NEB
BL21(DE3)	$\Phi 80\Delta(lacZ)M15$ <i>gyrA96 recA1 relA1 endA1 thi-1 hsdR17</i> F- <i>ompT hsdSB(rB<sup>-</sup>, mB<sup>-</sup>) gal dcm</i> (DE3)	Stratagene; Studier and Moffatt (1986)
<b>Experimental <i>E. faecalis</i></b>		
JH2-2	Fus <sup>R</sup> , Rif <sup>R</sup> , JH2 spontaneous mutant	Jacob and Hobbs (1974)
JH2-2 Tn1549	Van <sup>R</sup> , vanB (Tn1549)	Launay <i>et al.</i> , 2006
OG1RF	Rif <sup>R</sup> , Fus <sup>R</sup> , OG1 isolate from human oral cavity	Dunny <i>et al.</i> , (1978)
OG1RF:: <i>ΔireK</i>	Rif <sup>R</sup> , Fus <sup>R</sup> , ireK,	Kristich <i>et al.</i> , 2007
OG1RF Tn1549	Rif <sup>R</sup> , Fus <sup>R</sup> , Van <sup>R</sup> , vanB (Tn1549)	This Study
OG1RF <i>ΔireK</i> ::Tn1549	Rif <sup>R</sup> , Fus <sup>R</sup> , Van <sup>R</sup> , vanB (Tn1549), <i>ΔireK</i>	Goss, 2013
<b>Clinical and Control Strains</b>		
<i>E. faecalis</i> ATCC 51299	Van <sup>R</sup> , vanB2 (Tn1542) <i>ant(6)-I aac(6') aph(2''')</i>	ATCC
<i>E. faecium</i> ATCC 700221	Van <sup>R</sup> , vanA (Tn1549)	ATCC
<i>E. faecium</i> BM4525	Van <sup>R</sup> , vanB (Tn1549)	Depardieu <i>et al.</i> , 2003
<i>E. faecalis</i> ATCC 29212	CSLI Control Strain	ATCC
<i>E. coli</i> ATCC 25922	CSLI Control Strain	ATCC
<i>K. pneumoniae</i> ATCC 700603	CSLI Control Strain	ATCC

**Table 2.2: Media used for culturing bacteria in this study.**

<b>Name</b>	<b>Composition</b>	<b>Reference</b>
<b>Standard Media</b>		
LB Broth	10 g Tryptone, 5 g Sodium Chloride, 5 g Yeast Extract, prepared to 1 L in water and autoclaved	N/A
SOC	20 g Tryptone, 0.5 g Sodium Chloride, 5 g Yeast Extract, 0.2 g Potassium Chloride, 3.6 g Glucose and 1 g Magnesium Chloride and made up to 1 L with double-distilled water and autoclaved	Hanahan (1983)
BHI	Manufacturer's Instructions (Oxoid CM1135)	N/A
<b>Media for Expression of Isotopically labelled proteins</b>		
5x M9 Salts	32 g Sodium Phosphate Dibasic, 6 g Potassium Phosphate Monobasic, 2.5 g Sodium chloride made up to 500 mL with double distilled water and autoclave	Adapted from (Cai <i>et al.</i> , 1998)
Minimal Media	200 mL 5x M9 Salts, 2 mL 1 M Magnesium Sulphate, 100 µL Calcium Chloride	Adapted from (Cai <i>et al.</i> , 1998)
<b>Media for antibiotic susceptibility</b>		
Muller Hinton II Broth	See Manufacturer's Instructions (BD L007475)	N/A
Isosensitest Broth	See Manufacturer's Instructions (Oxoid CM0471)	N/A
<b>Media for E. faecalis competent cells</b>		
5x M17 broth	5.0 g Pancreatic Digest of Casein, 5.0 g Soy Peptone, 5.0 g Beef Extract, 2.5 g Yeast Extract, 0.5 g Ascorbic Acid, 0.25 g Magnesium Sulphate and 10.0 g Disodium-glycerophosphate and was prepared to 200 mL in water and autoclaved	Terzaghi and Sandine (1975)
M17Glu	1x M17 Broth and sterile 0.5% Glucose	Shepard and Gilmore (1995)
SGM17	1x M17 Broth, sterile 0.5 M Sucrose, sterile 2% Glycine and sterile 10% Glycerol pH 7.0	Shepard and Gilmore (1995)
SM17MC	1x M17 Broth, sterile 0.5 M Sucrose, sterile 10 mM Magnesium Chloride and sterile 10 mM Calcium Chloride pH 7.0	Shepard and Gilmore (1995)
Suc-Gly	Sucrose 0,5M, and 10% Glycerol, pH 7.0	Shepard and Gilmore (1995)

**Table 2.3: Buffers used for protein purification, storage and assays.**

<b>Name</b>	<b>Composition</b>
<b>Buffers used for competent cells</b>	
TFB1	30 mM potassium acetate, 10 mM CaCl <sub>2</sub> , 50 mM MnCl <sub>2</sub> , 100 mM RbCl and 15% glycerol
TFB2	10 mM MOPS, pH 6.5, 75 mM CaCl <sub>2</sub> , 10 mM RbCl and 15% glycerol
<b>General Buffers</b>	
TAE	40 mM Tris acetate, 1 mM EDTA
<b>Purification of recombinant IreK domain proteins</b>	
Buffer A	20 mM Sodium Phosphate, 500 mM Sodium Chloride, 10 mM Imidazole and 10% Glycerol, pH 7.4
Buffer B	20 mM Sodium Phosphate, 500 mM Sodium Chloride, 200 mM Imidazole and 10% Glycerol, pH 7.4
Gel Filtration Buffer	20 mM Sodium Phosphate, pH 7.4
<b>Purification of Recombinant TEV protease</b>	
Buffer A	100 mM Tris, 20 mM Imidazole, 500 mM Sodium Chloride, 10 mM Magnesium Chloride pH 8.0
Buffer B	100 mM Tris, 500 mM Imidazole, 500 mM Sodium Chloride, 10 mM Magnesium Chloride pH 8.0
Dialysis Buffer	10 mM Tris, pH 8.0, 300 mM NaCl, 1 mM TCEP, 10 % glycerol
<b>Purification of Recombinant Atl Amidase</b>	
Buffer A	10 mM Tris pH 8.0, 20 mM Imidazole, 500 mM Sodium Chloride
Buffer B	10 mM Tris pH 8.0, 500 mM Imidazole, 500 mM Sodium Chloride
Gel Filtration Buffer	10 mM TrisHCl pH 7.0 and 1 mM Calcium Chloride
<b>Buffers used in Biophysical Experiments</b>	
NMR Buffer	20 mM Sodium Acetate pH 4.5
CD and AUC Buffer	10 mM Sodium Phosphate pH 7.4
SEC-MALS and SEC SAXS Buffer	10 mM HEPES pH 7.4 and 150 mM Sodium Chloride
SPR Running Buffer	10 mM HEPES pH 7.4, 150 mM Sodium Chloride 0.005% (v/v) Tween-20
SPR Regeneration Buffer	6M Guanidine Hydrochloride
MST Buffer	Phosphate Buffered Saline, 0.05% Tween

**Table 2.4: Plasmids used for recombinant protein expression in *E. coli*.**

Plasmid	Features	Content	Cloning (Type and Features)	Source and Primers	Reference	Vector
pAT816	T7-6x His-VanSB KD (Amp <sub>R</sub> )	<i>E. faecalis</i> Tn1549 VanS <sub>B</sub> KD	N/A	N/A	Depardieu <i>et al.</i> , 2003	pET28/16
pLG226	T7-6x His-IreK KD (Amp <sub>R</sub> )	<i>E. faecalis</i> IreK Soluble KD	N/A	N/A	Goss, 2013	pET Duet
pLG234	T7-6x His-IreK KD (Amp <sub>R</sub> )	<i>E. faecium</i> IreK Soluble KD	N/A	N/A	Goss, 2013	pET Duet
pLG370	T7-IreP-6x His (Amp <sub>R</sub> )	<i>E. faecalis</i> IreP FL	N/A	N/A	Goss, 2013	pET Duet
pCWT001	T7-Strep-HRV3C-IreK FL-Thrombin-10His (Amp <sub>R</sub> )	<i>E. faecalis</i> IreK FL	Synthetic, codon optimised for <i>E. coli</i> expression, <i>NcoI</i> and <i>XhoI</i>	GenScript	This Study	pET52b
pCWT002	trc-TEV-6x His-IreK PASTA 1,2,3,4 and 5 ED (Amp <sub>R</sub> )	<i>E. faecalis</i> IreK PASTA 1, 2, 3, 4 and 5 ED	Restriction Cloning, <i>NcoI</i> and <i>HindIII</i>	pCWT001, CWT001/CWT002	This Study	pProEX HTa
pCWT003	trc-TEV-6x His-IreK PASTA 1,2,3 and 4 ED (Amp <sub>R</sub> )	<i>E. faecalis</i> IreK PASTA 1, 2, 3 and 4 ED	Restriction Cloning, <i>NcoI</i> and <i>HindIII</i>	pCWT001, CWT001/CWT003	This Study	pProEX HTa
pCWT004	trc-TEV-6x His-IreK PASTA 1,2 and 3 ED (Amp <sub>R</sub> )	<i>E. faecalis</i> IreK PASTA 1, 2 and 3 ED	Restriction Cloning, <i>NcoI</i> and <i>HindIII</i>	pCWT001, CWT001/CWT004	This Study	pProEX HTa
pCWT005	trc-TEV-6x His-IreK PASTA 1 and 2 ED (Amp <sub>R</sub> )	<i>E. faecalis</i> IreK PASTA 1 and 2 ED	Restriction Cloning, <i>NcoI</i> and <i>HindIII</i>	pCWT001, CWT001/CWT005	This Study	pProEX HTa
pCWT006	trc-TEV-6x His-IreK PASTA 4 and 5 ED (Amp <sub>R</sub> )	<i>E. faecalis</i> IreK KD IreK PASTA 4 and 5 ED	Restriction Cloning, <i>NcoI</i> and <i>HindIII</i>	pCWT001, CWT006/CWT002	This Study	pProEX HTa
pCWT007	trc-TEV-HIS-IreK PASTA 4 and 5 (C-terminal truncation) ED (Amp <sub>R</sub> )	<i>E. faecalis</i> IreK PASTA 4 and 5 (C-terminal truncation) ED	Restriction Cloning, <i>NcoI</i> and <i>HindIII</i>	pCWT001, CWT006/CWT007	This Study	pProEX HTa
pSR002	T7-AtIA-6x His (Amp <sub>R</sub> )	<i>B. subtilis</i> AtIA catalytic domain	N/A	N/A	Hayhurst <i>et al.</i> , 2008	pET21a
pEF1473_21	T7-EnpA-6x His (Amp <sub>R</sub> )	<i>E. faecalis</i> EnpA Endopeptidase	N/A	N/A	De Roca <i>et al.</i> , 2010	pET2818
pRK793	tac-MBP-6x His-Tev (Amp <sub>R</sub> )	Tobacco etch virus protease	N/A	N/A	Kapust <i>et al.</i> , 2001	pMal-C2

**Table 2.5: Plasmids used for mutagenesis in *E. faecalis* strains.**

Plasmid	Features	Content	Cloning (Type and Features)	Source and Primers	Reference	Vector
pCWT020	<i>ireK</i> insertion FL construct (Erm <sub>R</sub> )	500 bp upstream and downstream flanking and including <i>ireK</i> merged leaving first 13 codons and last 6 codons	Gibson (NEBuilder)	Assembly OG1RF (CWT020/CWT021), pGhost9 (CWT022/CWT023)	This Study	pGhost9
pCWT021	<i>ireK</i> deletion FL construct (Erm <sub>R</sub> )	500 bp upstream and downstream flanking <i>ireK</i> merged leaving first 13 codons and last 6 codons	Overlap Extension PCR and Gibson (NEBuilder)	Assembly gCWT012, pGhost9 (CWT022/CWT023)	This Study	pGhost9
pCWT022	<i>ireP</i> Deletion FL construct (Erm <sub>R</sub> )	500 bp upstream and downstream flanking <i>ireP</i> leaving first 10 codons and last 10 codons.	Overlap Extension PCR and Gibson (NEBuilder)	Assembly gCWT013, pGhost9 (CWT022/CWT023)	This Study	pGhost9

**Table 2.6: Plasmids used for complementation in *E. faecalis*.**

Plasmid	Features	Content	Cloning (Type and Features)	Source and Primers	Reference	Vector
pCWT050	TetP-IreK FL (Erm <sub>R</sub> )	<i>E. faecalis</i> IreK FL WT	Gibson Assembly (NEBuilder)	OG1RF (CWT050/CWT051), TetH (CWT052/CWT053)	This Study	TetH (Unpublished)
pCWT051	TetP-IreK with a 15 aa C terminal truncation (Erm <sub>R</sub> )	<i>E. faecalis</i> IreK minus PASTA 5	Q5 Site-Directed Mutagenesis - Deletion	Mutagenesis of pCWT050 (CWT054/CWT055)	This Study	TetH (Unpublished)
pCWT052	TetP-IreK minus PASTA 5 (Erm <sub>R</sub> )	<i>E. faecalis</i> IreK minus PASTA 5	Q5 Site-Directed Mutagenesis - Deletion	Mutagenesis of pCWT050 (CWT054/CWT056)	This Study	TetH (Unpublished)
pCWT053	TetP-IreK minus PASTA 4 and 5 (Erm <sub>R</sub> )	<i>E. faecalis</i> IreK minus PASTA 4 and 5	Q5 Site-Directed Mutagenesis - Deletion	Mutagenesis of pCWT050 (CWT054/CWT057)	This Study	TetH (Unpublished)
pCWT054	TetP-IreK minus PASTA 3, 4 and 5 (Erm <sub>R</sub> )	<i>E. faecalis</i> IreK minus PASTA 3, 4 and 5	Q5 Site-Directed Mutagenesis - Deletion	Mutagenesis of pCWT050 (CWT054/CWT058)	This Study	TetH (Unpublished)
pCWT055	TetP-IreK minus PASTA 2, 3, 4 and 5 (Erm <sub>R</sub> )	<i>E. faecalis</i> IreK minus PASTA 2, 3, 4 and 5	Q5 Site-Directed Mutagenesis - Deletion	Mutagenesis of pCWT050 (CWT054/CWT059)	This Study	TetH (Unpublished)
pCWT056	TetP-IreK minus PASTA 1, 2, 3, 4 and 5 (Erm <sub>R</sub> )	<i>E. faecalis</i> IreK minus PASTA 1, 2, 3, 4 and 5	Q5 Site-Directed Mutagenesis - Deletion	Mutagenesis of pCWT050 (CWT054/CWT060)	This Study	TetH (Unpublished)
pCWT057	TetP-IreK minus PASTA 1, 2 and 3 (Erm <sub>R</sub> )	<i>E. faecalis</i> IreK minus PASTA 1, 2, 3	Q5 Site-Directed Mutagenesis - Deletion	Mutagenesis of pCWT050 (CWT060/CWT061)	This Study	TetH (Unpublished)

pCWT058	TetP-IreK minus PASTA 1, 2 and 3 and C terminal truncation (Erm <sub>R</sub> )	<i>E. faecalis</i> IreK minus PASTA 1, 2 and 3 with a 15 aa C terminal truncation	Q5	Site-Directed Mutagenesis - Deletion	Mutagenesis of (CWT060/CWT061)	pCWT051	This Study	TetH (Unpublished)
pCWT062	TetP-IreK $\Delta K41R$ (Erm <sub>R</sub> )	<i>E. faecalis</i> IreK with a substitution $\Delta K41R$ )	Q5	Site-Directed Mutagenesis - Deletion	Mutagenesis of (CWT071/CWT072)	pCWT050	This Study	TetH (Unpublished)
pCWT063	TetP-IreK minus KD (Erm <sub>R</sub> )	<i>E. faecalis</i> IreK minus KD	Q5	Site-Directed Mutagenesis - Deletion	Mutagenesis of (CWT073/CWT074)	pCWT050	This Study	TetH (Unpublished)
pCWT064	TetP-IreK KD and TM with <i>S. aureus</i> PASTA ED (Erm <sub>R</sub> )	<i>E. faecalis</i> IreK KD and TM with <i>S. aureus</i> PASTA ED	Gibson	Assembly (NEBuilder)	pCWT050 (CWT075/CWT076), gCWT001 (CWT077/CWT078)		This Study	TetH (Unpublished)
pCWT065	TetP-IreK KD and TM with <i>B. subtilis</i> PASTA ED (Erm <sub>R</sub> )	<i>E. faecalis</i> IreK KD and TM with <i>B. subtilis</i> PASTA ED	Gibson	Assembly (NEBuilder)	pCWT050 (CWT075/CWT076), gCWT002 (CWT079/CWT080)		This Study	TetH (Unpublished)
pCWT066	TetP-IreK KD and TM with <i>S. Pyrogenes</i> PASTA ED (Erm <sub>R</sub> )	<i>E. faecalis</i> IreK KD and TM with <i>S. Pyrogenes</i> PASTA ED	Gibson	Assembly (NEBuilder)	pCWT050 (CWT075/CWT076), gCWT003 (CWT081/CWT082)		This Study	TetH (Unpublished)
pCWT067	TetP-IreK KD and TM with <i>L. monocytis</i> PASTA ED (Erm <sub>R</sub> )	<i>E. faecalis</i> IreK KD and TM with <i>L. monocytis</i> PASTA ED	Gibson	Assembly (NEBuilder)	pCWT050 (CWT075/CWT076), gCWT004 (CWT083/CWT084)		This Study	TetH (Unpublished)
pCWT068	TetP-IreK KD and TM with <i>S. coielocor</i> PASTA ED (Erm <sub>R</sub> )	<i>E. faecalis</i> IreK KD and TM with <i>S. coielocor</i> PASTA ED	Gibson	Assembly (NEBuilder)	pCWT050 (CWT075/CWT076), gCWT005 (CWT085/CWT086)		This Study	TetH (Unpublished)
pCWT069	TetP-IreK KD and TM with <i>M. tuberculosis</i> PASTA ED (Erm <sub>R</sub> )	<i>E. faecalis</i> IreK KD and TM with <i>M. tuberculosis</i> PASTA ED	Gibson	Assembly (NEBuilder)	pCWT050 (CWT075/CWT076), gCWT006 (CWT087/CWT088)		This Study	TetH (Unpublished)
pCWT070	TetP-IreK KD and TM with <i>B. sphaericus</i> PASTA ED (Erm <sub>R</sub> )	<i>E. faecalis</i> IreK KD and TM with <i>B. sphaericus</i> PASTA ED	Gibson	Assembly (NEBuilder)	pCWT083 (CWT075/CWT076), gCWT010 (CWT089/CWT090)		This Study	TetH (Unpublished)

**Table 2.7: Plasmids used for complementation with N-terminal GFP fusions in *E. faecalis*.**

Plasmid	Features	Content	Cloning (Type and Features)	Source and Primers	Reference	Vector
pCWT080	TetP-mEGFP-TEV linker-IreK FL (Erm <sub>R</sub> )	<i>E. faecalis</i> IreK FL WT with N-terminal mEGFP	Gibson Assembly (NEBuilder)	pCWT050 (CWT090/CWT091), gCWT001	This Study	TetH (Unpublished)
pCWT081	TetP-mTFP-TEV linker-IreK FL (Erm <sub>R</sub> )	<i>E. faecalis</i> IreK FL WT with N-terminal mTFP	Gibson Assembly (NEBuilder)	pCWT050 (CWT090/CWT091), gCWT002	This Study	TetH (Unpublished)
pCWT082	TetP-mCherryP-TEV linker-IreK FL (Erm <sub>R</sub> )	<i>E. faecalis</i> IreK FL WT with N-terminal mCherry	Gibson Assembly (NEBuilder)	pCWT050 (CWT090/CWT091), gCWT003	This Study	TetH (Unpublished)
pCWT083	TetP-mEGFP-TEV linker-IreK FL (Erm <sub>R</sub> )	<i>E. faecalis</i> IreK FL WT with N-terminal codon optimised mEGFP	Gibson Assembly (NEBuilder)	pCWT050 (CWT090/CWT091), gCWT004	This Study	TetH (Unpublished)
pCWT084	TetP-IreK with a 10 aa C terminal truncation (Erm <sub>R</sub> )	<i>E. faecalis</i> IreK minus PASTA 5	Q5 Site-Directed Mutagenesis - Deletion	Mutagenesis of (CWT054/CWT055)	pCWT083 This Study	TetH (Unpublished)
pCWT085	TetP-IreK minus PASTA 5 (Erm <sub>R</sub> )	<i>E. faecalis</i> IreK minus PASTA 5	Q5 Site-Directed Mutagenesis - Deletion	Mutagenesis of (CWT054/CWT056)	pCWT083 This Study	TetH (Unpublished)
pCWT086	TetP-IreK minus PASTA 4 and 5 (Erm <sub>R</sub> )	<i>E. faecalis</i> IreK minus PASTA 4 and 5	Q5 Site-Directed Mutagenesis - Deletion	Mutagenesis of (CWT054/CWT057)	pCWT083 This Study	TetH (Unpublished)
pCWT087	TetP-IreK minus PASTA 3, 4 and 5 (Erm <sub>R</sub> )	<i>E. faecalis</i> IreK minus PASTA 3, 4 and 5	Q5 Site-Directed Mutagenesis - Deletion	Mutagenesis of (CWT054/CWT058)	pCWT083 This Study	TetH (Unpublished)

pCWT088	TetP-IreK minus PASTA 2, 3, 4 and 5 (Erm <sub>R</sub> )	<i>E. faecalis</i> IreK minus PASTA 2, 3, 4 and 5	Q5	Site-Directed Mutagenesis - Deletion	Mutagenesis of (CWT054/CWT059)	pCWT083	This Study	TetH (Unpublished)
pCWT089	TetP-IreK minus PASTA 1, 2, 3, 4 and 5 (Erm <sub>R</sub> )	<i>E. faecalis</i> IreK minus PASTA 1, 2, 3, 4 and 5	Q5	Site-Directed Mutagenesis - Deletion	Mutagenesis of (CWT054/CWT060)	pCWT083	This Study	TetH (Unpublished)
pCWT090	TetP-IreK minus PASTA 1, 2 and 3 (Erm <sub>R</sub> )	<i>E. faecalis</i> IreK minus PASTA 1, 2, 3	Q5	Site-Directed Mutagenesis - Deletion	Mutagenesis of (CWT060/CWT061)	pCWT083	This Study	TetH (Unpublished)
pCWT091	TetP-IreK minus PASTA 1, 2 and 3 and C terminal truncation (Erm <sub>R</sub> )	<i>E. faecalis</i> IreK minus PASTA 1, 2 and 3 with a 10 aa C terminal truncation	Q5	Site-Directed Mutagenesis - Deletion	Mutagenesis of (CWT060/CWT061)	pCWT083	This Study	TetH (Unpublished)
pCWT092	TetP-mEGFP (Erm <sub>R</sub> )	Codon optimised mEGFP	Q5	Site-Directed Mutagenesis - Deletion	Mutagenesis of (CWT060/CWT061)	pCWT083	This Study	TetH (Unpublished)
pCWT095	TetP-IreK_K41R (Erm <sub>R</sub> )	<i>E. faecalis</i> IreK with a substitution (K41R)	Q5	Site-Directed Mutagenesis - Deletion	Mutagenesis of (CWT071/CWT072)	pCWT083	This Study	TetH (Unpublished)
pCWT096	TetP-IreK minus KD (Erm <sub>R</sub> )	<i>E. faecalis</i> IreK minus KD	Q5	Site-Directed Mutagenesis - Deletion	Mutagenesis of (CWT73/CWT091)	pCWT083	This Study	TetH (Unpublished)
pCWT097	TetP-IreK KD and TM with <i>S. aureus</i> PASTA ED (Erm <sub>R</sub> )	<i>E. faecalis</i> IreK KD and TM with <i>S. aureus</i> PASTA ED	Gibson	Assembly (NEBuilder)	pCWT083 (CWT075/CWT076), gCWT005 (CWT077/CWT078)		This Study	TetH (Unpublished)

pCWT098	TetP-IreK KD and TM with <i>B. subtilis</i> PASTA ED (Erm <sub>R</sub> )	<i>E. faecalis</i> IreK KD and TM with <i>B. subtilis</i> PASTA ED	Gibson Assembly (NEBuilder)	pCWT083 (CWT075/CWT076), gCWT006 (CWT079/CWT080)	This Study	TetH (Unpublished)
pCWT099	TetP-IreK KD and TM with <i>S. Pyrogenes</i> PASTA ED (Erm <sub>R</sub> )	<i>E. faecalis</i> IreK KD and TM with <i>S. Pyrogenes</i> PASTA ED	Gibson Assembly (NEBuilder)	pCWT083 (CWT075/CWT076), gCWT007 (CWT081/CWT082)	This Study	TetH (Unpublished)
pCWT100	TetP-IreK KD and TM with <i>L. monocytis</i> PASTA ED (Erm <sub>R</sub> )	<i>E. faecalis</i> IreK KD and TM with <i>L. monocytis</i> PASTA ED	Gibson Assembly (NEBuilder)	pCWT083 (CWT075/CWT076), gCWT008 (CWT083/CWT084)	This Study	TetH (Unpublished)
pCWT101	TetP-IreK KD and TM with <i>S. coielocor</i> PASTA ED (Erm <sub>R</sub> )	<i>E. faecalis</i> IreK KD and TM with <i>S. coielocor</i> PASTA ED	Gibson Assembly (NEBuilder)	pCWT083 (CWT075/CWT076), gCWT009 (CWT085/CWT086)	This Study	TetH (Unpublished)
pCWT102	TetP-IreK KD and TM with <i>M. tuberculosis</i> PASTA ED (Erm <sub>R</sub> )	<i>E. faecalis</i> IreK KD and TM with <i>M. tuberculosis</i> PASTA ED	Gibson Assembly (NEBuilder)	pCWT083 (CWT075/CWT076), gCWT010 (CWT087/CWT088)	This Study	TetH (Unpublished)
pCWT103	TetP-IreK KD and TM with <i>B. sphaericus</i> PASTA ED (Erm <sub>R</sub> )	<i>E. faecalis</i> IreK KD and TM with <i>B. sphaericus</i> PASTA ED	Gibson Assembly (NEBuilder)	pCWT083 (CWT075/CWT076), gCWT010 (CWT089/CWT090)	This Study	TetH (Unpublished)

**Table 2.8: Primers used for sequencing and analytical PCR.**

Primer Identifier	5'-3' Sequence
pGhost Up	GTCACGACGTTGTAAAACGACGG
pGhost Down	CTAGCGGACTCTAGAGGATCCCA
pProEx Up	AGCGGATAACAATTTACACAGGA
pProEx Down	CGCCAGGTTTTCCAGTCACGAC
TetH Up	CTGGACTTCATGAAAACTAAAAAAATAT
TetH Down	TAAAACTTATAGGATCTGGTGCGCC
T7 Up	TAATACGACTCACTATAGGGG
T7 Down	GCTAGTTATTGCTCAGCGG

**Table 2.9: Primers used in the design of plasmids used for expression of recombinant protein.**

Restriction sites are in *italics and underlined*.

Primer Identifier	5'-3' Sequence
CWT001	GAT <u><i>CCATGGG</i></u> CGGTAAAGATGTGGAAGTCCGGAC
CWT002	CGT <u><i>AAGCTT</i></u> TATTAGTTGCTGGTAGATGATTCCGCTGGTGGTGCT
CWT003	CCCA <u><i>AAGCTT</i></u> TATTATTTGAGACATGCAGGGTAATCGTGTC
CWT004	CCCA <u><i>AAGCTT</i></u> TATTATTTGAGACGTACAGCGTAACCTGACC
CWT005	CCCA <u><i>AAGCTT</i></u> TATTATTCGCTCACGGTCAGCGTGACTTTATC
CWT006	GAT <u><i>CCATGGG</i></u> GCTCGGATAAAGTACCCTGAGCGAC
CWT007	CCCA <u><i>AAGCTT</i></u> TTTGCTATCGTTCGCTTTGCTGTAGTAGA

**Table 2.10: Primers used for the design of plasmids used for mutagenesis in *E. faecalis*.**

Primer Identifier	5'-3' Sequence
CWT020	ACTCATGACAACCACACCTAGATCCACAT
CWT021	GAAAAAATTTATGAACGCGGACAATCGAAA
CWT022	TTGATATCGAATTCCTGCAG
CWT023	GGTACCAATTCGCCCTATAG
CWT032	TGGTTAATTCAGCAATTCAAAAGGAAAAT
CWT033	CAAATTAACGAAAAATTTGGCGAAACCAT

**Table 2.11: Primers used fluorescence and complementation plasmids.**

Primer Identifier	5'-3' Sequence
CWT050	ACAGATCTGAGCTCAAGGAGGAGACTGACCATGATAGAAATCGGCAAGAAG
CWT051	TCTTTAGTGATGATGGTGATGGTGATGGTGTTAATTACTCGTACTACTTTCACTAG
CWT052	CACCATCACCATCACCATC
CWT053	GGTCAGTCTCCTCCTTGAG
CWT054	TAACACCATCACCATCACCATCACTA
CWT055	GCCAGCGGATGGGCTAGTTC
CWT056	TTTGCTGACATAAAGTAATC
CWT057	TTTACTTACATATAACGTCAC
CWT058	TTCACTGACCGTTAAAGAG
CWT059	CAATGAAATATATAGTAAC
CWT060	CGACATTGCAAAGGCTAAG
CWT061	GGTAGCGACAAAGTGACAC
CWT062	CTCGGCATGGACGAGCTGTACAAG
CWT063	GATGGTGATGGTGATGGTGTTA
CWT071	CGTTGCAGTAGCCGTCTTGCCTTTG
CWT072	TCTCGGTCTAAAATTAATCG
CWT073	GGTGGTAAAGACGTTGAAGT
CWT074	ACTGGTCAGTGTGGTGGT
CWT075	CCGACATTGCAAAGGCTAAG
CWT076	TAACACCATCACCATCACC
CWT077	GGTGGCTTAGCCTTTGCAATGTCGGGGTAATAAATACGAAGAGACACC
CWT078	AGTGATGATGGTGATGGTGATGGTGTTATTATACATCATCATAGCTGACTTC
CWT079	GGTGGCTTAGCCTTTGCAATGTCGGATGCCTAAGGATGTCAAATAAC
CWT080	AGTGATGATGGTGATGGTGATGGTGGTAATAATCATCTTTCCGATACTCAATG
CWT081	TGGTGATGGTGATGGTGTTAAGGAGTCTGAGCGGTGGTTTTC
CWT082	GCTTAGCCTTTGCAATGTCGAAGCCAACATCAGTCAAGGTTCC
CWT084	TGGTGATGGTGATGGTGTTAATTCGGATATGGCACCGTTCC
CWT083	GCTTAGCCTTTGCAATGTCGTCACCAGATGAGGTAGCTG
CWT085	TGGTGATGGTGATGGTGTTAATCGCCGAAGCCCGGCAA
CWT086	GCTTAGCCTTTGCAATGTCGGGAAATGACAAGTCCCTGTCCC
CWT087	TGGTGATGGTGATGGTGTTACTGCCCAAAGCGTAGGGTAATTATC
CWT088	GCTTAGCCTTTGCAATGTCGATCACCCGAGATGTACAAGTC
CWT089	TGGTGATGGTGATGGTGTTAGTTTACATCATCGTAACTGAAC
CWT090	GCTTAGCCTTTGCAATGTCGAGTCCTAAAAAGATAGCTG

**Table 2.12: gBlock Identifiers and description.** Sequences are displayed in **Chapter 8: Appendix 8.1**

gBlock Identifier	5'-3' Sequence
gCWT001	mEGFP
gCWT002	Codon Optimised for <i>E. faecalis</i> mCherry
gCWT003	Codon Optimised for <i>E. faecalis</i> mTFP
gCWT004	Codon Optimised for <i>E. faecalis</i> mEGFP
gCWT005	<i>S. aureus</i> Extracellular PASTA domains
gCWT006	<i>B. subtilis</i> Extracellular PASTA domains
gCWT007	<i>S. pyogenes</i> Extracellular PASTA domains
gCWT008	<i>L. monocytis</i> Extracellular PASTA domains
gCWT009	<i>S. coelicolor</i> Extracellular PASTA domains
gCWT010	<i>M. tuberculosis</i> Extracellular PASTA domains
gCWT011	<i>B. sphaericus</i> Extracellular PASTA domains
gCWT012	500 bp up and down stream of <i>ireK</i> flanking the first 13 codons and last 6 codons
gCWT013	500 bp up and down stream of <i>ireP</i> flanking the first 6 codons and last 6 codons

### 2.1.5. Oligonucleotides and Synthetic DNA

Oligonucleotides were designed against the appropriate gene or plasmid targets with relevant restriction enzyme or mutation sites included and ordered from Integrated DNA Technologies (IDT) or Sigma Aldrich for primers larger than 50 bp. A list of primers is summarised in **Table 2.8**, **Table 2.9**, **Table 2.10** and **Table 2.11** and categorised to their applications. Synthetic DNA was ordered from IDT (gBlocks) and was codon optimised where appropriate and summarised in **Table 2.12**.

## 2.2. Methods in Molecular Biology

### 2.2.1. Preparation of Competent cells

BL21 (DE3), TOP10 and NEB5 chemically competent cells were prepared according to an adapted version Hanahan (1985). A single colony from an LB plate was inoculated in 2.5 mL LB broth and incubated overnight at 37°C and 180 RPM. The entire culture was used to inoculate 250 mL of LB medium containing 20 mM MgSO<sub>4</sub>. The cells were grown

in a 1 L flask until  $A_{600}$  reached between 0.4 and 0.6. The cells were pelleted by centrifugation at  $4,500 \times g$  for 5 minutes at  $4^{\circ}\text{C}$ . The supernatant was discarded, and the cell pellet was gently re-suspended in 40 mL TFB1 buffer and incubated on ice for 5 minutes. The cells were pelleted by centrifugation at  $4,500 \times g$  for 5 minutes at  $4^{\circ}\text{C}$ . The cells were re-suspended in 4 mL TFB2 and incubated on ice for 60 minutes and aliquoted into 200  $\mu\text{L}$  volumes in 1.5 mL microcentrifuge tubes and stored at  $-80^{\circ}\text{C}$ .

### **2.2.2. Polymerase Chain Reaction**

The composition of a standard PCR mix was followed using manufacturers protocol. Either Q5 or Phusion polymerase (NEB) was used. Occasionally DMSO was added to disrupt secondary structure formation. Manually designed primers were synthesised by IDT. PCRs were performed on an SureCycler 8800 Thermal cycler following recommendations using the online BaseChanger tool (NEB) or NEBuilder tool (NEB).

### **2.2.3. Agarose Gel Electrophoresis**

0.8 % (w/v) agarose gels were prepared in TAE buffer **Table 2.3** supplemented with ethidium bromide. DNA was mixed with 6x DNA loading dye (NEB) according to manufacturer's instructions and loaded onto the gel. Separation was achieved following the application of 100 V for 1 hour. DNA was visualised using a UV transilluminator.

### **2.2.4. Transformation of Electrocompetent cells**

#### **2.2.4.1. Transformation in *E. coli***

Transformation of chemically competent cells were performed on *E. coli* BL21 (DE3), TOP10 and NEB5 cells. Cryo-preserved competent cells were thawed on ice, mixed with 5 - 50 ng of plasmid DNA and incubated on ice for 30 minutes. Cells were then heat-shocked by incubation at  $42^{\circ}\text{C}$  for 30 seconds. Following incubation on ice for 5 minutes, pre-warmed SOC was added to a final volume 10 times the original cell suspension volume. Prior to plating on selective LB agar, cells were incubated at  $37^{\circ}\text{C}$  at 180 RPM for an hour.

#### **2.2.4.2. Transformation in *E. faecalis***

Transformation of electrocompetent cells were performed on various strains of *E. faecalis* cells. Cryo-preserved competent cells, plasmid DNA and the electroporation

cuvettes were chilled on ice. Competent cells were gently mixed with 100 ng - 1 µg of plasmid DNA. The mixture was transferred to the 2 mm electroporation cuvette and performed at 25 V, 200 Ohms and 2.4 kV. 1 mL of cold SM17MC was immediately added to the cells which were stored on ice for 5 minutes. Prior to plating on selective BHI agar, cells were incubated at 28°C without agitation for 3 hours.

#### **2.2.5. Preparation of Plasmid DNA**

A single colony of freshly transformed Top10 or NEB5 *E. coli* cells were grown overnight in LB medium at 28°C for pGhost9 plasmids or 37°C for other plasmids at 180 RPM. Plasmid DNA was isolated using GeneJET plasmid MiniPrep kit (ThermoFisher) according to manufacturer's instructions. DNA concentration was determined by measuring the absorbance on a nanodrop (ThermoFisher). The purity of DNA was estimated using A260/A280 and samples with a ratio between 1.6 and 2.0 were stored at -20°C.

#### **2.2.6. Purification of amplified DNA**

Purification of DNA after PCR was conducted using Gel purification kit (QIAGEN). Briefly, 40 µL of DNA with 6x Loading buffer was loaded onto a 0.8% agarose gel. The band was visualised on a UV transilluminator and extracted using a scalpel. Purification of the DNA from the gel was conducted following manufactures protocol.

#### **2.2.7. Restriction Digestion**

Reaction digests of PCR products and plasmids were performed using *NcoI* and *HindIII* from New England Biolabs (NEB). Reactions were conducted according to manufactures protocol. Reaction mixtures were typically 1000 ng with 10 - 20 units of each restriction enzyme and reaction buffer in 50 µL reaction volume. Reactions were incubated at 37°C between 4 hours to overnight. Digested plasmid DNA was incubated with recombinant shrimp alkaline phosphatase (rSAP) for a further 30 minutes at 37°C to prevent self-ligation. Enzymes were inactivated at 65°C for 10 minutes. Digested DNA was separated using a gel extraction kit (QIAGEN) and re-quantified using a nanodrop (ThermoFisher). DpnI was occasionally added to PCRs prior to ligation to ensure any template plasmid DNA was removed. Reactions were incubated at 37°C for 60 minutes before inactivation at 80°C for 20 minutes.

### **2.2.8. Restriction Cloning Ligation**

Ligation mixtures composed approximately 50 ng of linearized vector with 150 ng of digested insert DNA, 20 units of T4 DNA ligase (NEB) and the supplied reaction buffer to 20  $\mu$ L. Ligation reactions were incubated at 16°C overnight. 10  $\mu$ L of each reaction was then used to transform 100  $\mu$ L of competent TOP10 or NEB5 cells.

### **2.2.9. Plasmid Mutagenesis**

Plasmid mutagenesis including insertion, deletions and substitutions were carried out using the Q5 mutagenesis kit (NEB) according to the manufacturer's instructions. The kit is advantageous as it allows amplified material to be added directly to a unique Kinase, Ligase and DpnI enzyme mix for ligation at room temperature and the removal of template DNA.

### **2.2.10. Gibson Cloning**

Multiple DNA fragments were cloned together with Gibson assembly (Gibson *et al.*, 2009). The NEBuilder cloning kit (NEB) was used and experiments conducted following manufacturer's instructions. Briefly, the aim of Gibson assembly is to fuse two or more different sequences of DNA together. To achieve this, both DNA fragments must be modified to contain complimentary overlapping ends. The primers were designed so that PCR of fragment A will result in an end product containing at the 3' end of the 20 bases of fragment B. The PCR of the two fragments thus creates a 20 bp region of overlap between the two genes.

### **2.2.11. Construct Validation**

Plasmid DNA constructs or genetic mutants was verified by Sanger sequencing. 5  $\mu$ L of 80 - 100 ng DNA with 5  $\mu$ L of 10  $\mu$ M primer (GATC-Biotech).

## 2.3. Methods in Microbiology

### 2.3.1. Genetically modifying *E. faecalis* chromosome

Insertion and deletions of genes was carried out by allelic exchange using the pGhost9 system (Maguin *et al.*, 1992). Briefly, for gene deletions, two chromosomal fragments flanking roughly 500 bp upstream and downstream of the gene of interest in the chromosomal DNA were designed *in silico* and fused together and a gBlock ordered (Table 2.12) for both *IreK* and *IreP*. This fragment was fused together with the pGhost9 vector via Gibson assembly. For reinsertion of *ireK* back into mutant OG1RF strains, a fragment encompassing 500 bp upstream and downstream of *ireK* and *ireK* itself was amplified and also used with the pGhost9 vector via Gibson assembly. The resulting plasmid ligations were transformed in *E. coli* NEB 5 $\alpha$  cells and incubated at 28°C and selected on Erm 200 plates. Colonies were selected inoculated in a 10 mL culture for mini-prep at 28°C. Potential positive constructs were identified and confirmed by sequencing. The plasmids were then electroporated into electrocompetent OG1RF cells and selected at the permissive temperature (28°C) on BHI plates with erythromycin. Single colonies were selected and grown overnight in BHI broth at 28°C without shaking before diluting (1:100) to the non-permissive temperature 42°C in the presence of erythromycin to select for single-crossover integrant. Plasmid excitation by a second recombination event was stimulated by growing integrant at 28°C without erythromycin. Overnight cultures were passaged at least 5 times and then plated on BHI plates with and without erythromycin at 42°C to confirm successful transformation. Successful targeted mutations were confirmed via PCR and sequencing of the PCR product.

### 2.3.2. MIC Determination

Minimum inhibitory concentrations (MICs) are defined as the lowest concentration of antimicrobial that will inhibit the visible growth of a micro-organism after overnight incubation. The range of antibiotic concentrations used for determining MICs is universally accepted to be in doubling dilution steps. All testing was undertaken according to CSLI standards or adapted when stated. The MIC defined here is 95% inhibition.

### **2.3.2.1. Preparation of inoculum**

Direct colony suspension was used to prepare MIC determination tests. This method is suited to fastidious organisms such as *E. faecalis*. Colonies are taken directly from the plate into sterile distilled water. The suspension should match the density of the 0.5 McFarland standard. Suspensions should contain between  $10^7$  and  $10^8$  cfu mL<sup>-1</sup> depending on genus. For the agar dilution method, further dilution of suspension in sterile distilled water before inoculation was required 1:10 for *Enterococcus* spp. and CSLI control strains. For broth microdilution methods, a final inoculum of  $5 \times 10^5$  cfu mL<sup>-1</sup> is required and therefore suspensions equivalent to a 0.5 McFarland standard should be diluted 1:100 in broth medium used for preparing the antibiotic dilutions.

### **2.3.2.2. Agar M.I.C. Evaluator method**

Strains were isolated on Iso-Sensitest agar. The MICs of various antibiotics were determined by the method of M.I.C. Evaluation after 24 hours of incubation. High level antibiotic resistance is confirmed after 48 hours. The system (Oxoid) comprises a predefined and continuous concentration gradient with 30 graduations of antimicrobial agent over a range of 256 - 0.015 µg mL<sup>-1</sup>. When applied to inoculated agar plates and incubated at 37°C in an aerobic atmosphere, creates an ellipse of microbial inhibition. The MIC is determined where the ellipse of inhibition intersects the strip and the MIC corresponds to the graduation at the intersection with the strip.

### **2.3.2.3. Broth microdilution method**

Antibiotic ranges are prepared one step higher than the final dilution range required. For microdilution experiments, the equivalent broth media was used to that in the E-test method. A 96 well sterile microtiter tray with appropriate antibiotics was labelled with triplicates at each concentration. Stock solutions of antibiotic were prepared according to manufactures instructions. Further dilutions were prepared in the chosen media for the experiment. 100 µL of antibiotic was added to each well at twice the concentration for the MIC. This was further diluted to the correct concentration by adding 100 µL of test organism in media. Inoculated and uninoculated wells of antibiotic-free broth were included to determine the adequacy of the broth to support the growth of the organism and check of sterility.

### 2.3.3. Real Time Quantitative PCR analysis of transcripts

500  $\mu$ L of an overnight culture of *E. faecalis* was used to inoculate 50 mL BHI broth. Cells were incubated at 37°C with shaking until OD<sub>600</sub> 0.6 was reached. Cells were divided into 10 mL fractions and incubated with and without antibiotics for 30 minutes at 37°C with agitation. Cells were centrifuged (10,000 RPM; 10 minutes) and the supernatant was decanted into waste. *E. faecalis* cultures were stabilized with 300  $\mu$ L TRIzol reagent (amicon) stored at -80°C for at least one night. Cells were lysed via mechanical disruption by adding 0.2 g of 0.1 mm silica beads (BioSpec) and agitated using the FastPrep homogeniser (MP Biomed) with 4 cycles of 40 seconds homogenization at 6.0 m/sec with 300 seconds rest in-between.

Lysates were centrifuged (10,000 RMP, 10 minutes) and the supernatant collected. RNA was extracted using the Direct-zol RNA MiniPrep according to manufacturer's instructions (Zymo Research) with on column DNase treatment. RNA was quantified using the Nanodrop (ThermoFisher) and 500 ng of DNase treated RNA was used as a template in the High-capacity cDNA reverse transcription kit using random hexamer primers according to manufacturer's instructions (Applied Biosystems). qPCR primers were designed using Primer3Plus online qPCR primer tool. All products are between 70-150 bp with an annealing temperature of 60°C. 2 primer sets were ordered for each locus in order to identify primers with high efficiency and low presence of primer dimers. RT-qPCR was performed in 10  $\mu$ L reaction volumes of 1X Perfecta SYBR-Green (Quanta) using 2.5  $\mu$ L of a 1:200 dilution of cDNA as input. A final concentration of primers (0.1 M) was used for all experiments. RT-PCR was performed on a Bio-Rad CFX384 Touch Real-Time PCR detection system with cycle parameters of: 95°C 3 min followed by 35 cycles of 95°C 10 seconds, 60°C 30 seconds. Technical triplicates were used and averaged to generate C<sub>t</sub> values. Minus reverse transcriptase controls were performed to ensure efficient DNase treatment. Melting curves were also generated to confirm specific PCR products. Water controls were also used to check for primer dimers. Data was analysed using  $\Delta\Delta C_t$  normalizing to 16S rRNA.

**Table 2.13: Primers used for qPCR experiments.**

Primer Identifier	5'-3' Sequence	Target	Primer Direction	Size (bp)
CWT150	AGCAACGCGAAGAACCTTAC	16s	F	92
CWT151	ATGCACCACCTGTCACTTTG	16s	R	
CWT152	GCTAAAGCGGAAGCAGAAAC	VanY	F	135
CWT153	GCTGTTTTTCATCCCAGCCATC	VanY	R	
CWT154	GGCTGCGATATTCAAAGCTC	VanB	F	119
CWT155	TCCGGCTTGTCACCTTTATC	VanB	R	
CWT156	AAAATCCGCATCTTGAATGG	VanR	F	147
CWT157	TGGGCATGAACTTCTACGTG	VanR	R	
CWT158	CAGGGCTGTCATCATCAGAA	VanR	F	87
CWT159	ATTATGCTGCCCGGTATGAA	VanR	R	
CWT160	AGCAGAACGTCAGGGAGAAG	DdcR	F	117
CWT161	TCCCTTAAACGGCCAATATG	DdcR	R	
CWT162	TGGCCGTTTAAGGGAAAAAT	DdcR	F	77
CWT163	TATACCCCACTCCCAAACA	DdcR	R	
CWT164	CCATGATTGATCGCCTTCTT	DdcY	F	124
CWT165	TATTGTGGGCATGGCTGTTA	DdcY	R	
CWT166	ATCGTTACTTTGCGCATTT	DdcY	F	112
CWT167	GGATTCAGCGAACAAGAAGC	DdcY	R	

#### 2.3.4. Fluorescence Microscopy

*E. faecalis* cells were prepared for microscopy by inoculating 1:100 overnight culture into 50 mL fresh BHI media containing 20 ng  $\mu\text{L}^{-1}$  anhydrotetracycline. Cells were incubated at 37°C with shaking until  $A_{600}$  0.6 was reached. For visualization of membranes, the membrane dye FM4-64 (100 mg  $\text{mL}^{-1}$  stock; Molecular Probes) was added to cells at a final concentration of 10  $\mu\text{g mL}^{-1}$  prior to mounting the cells on agarose-coated slides (Gene frame – ThermoFisher). The pellet was resuspended in 10  $\mu\text{L}$  phosphate-buffered saline and added to a poly-L-lysine-pre-treated coverslip. All microscopy was performed on a Nikon Eclipse 90i with a 100 $\times$  objective using phase contrast and fluorescence images and captured by using a Hamamatsu Orca-ER camera using Nikon Elements BR software.

## 2.4. Protein Expression and Purification

### 2.4.1. Expression of unlabelled proteins

Recombinant proteins were over expressed in BL21 (DE3) *E. coli* strains that were suitable for protein expression using Isopropyl-D-1-thiogalactopyranoside (IPTG) induction. A single colony expressing the recombinant gene of interest was picked for a small-scale pre-culture in 5 mL LB broth containing Amp and incubated overnight (37°C at 180 RPM).

For large scale expression, 10 mL of the overnight small-scale pre-culture was used to inoculate 1 L of LB broth containing and incubated (37°C at 180 RPM) until an OD<sub>600nm</sub> of 0.7-1.0 was reached. IPTG was added to each 1 L culture to a final concentration of 1 mM and incubated (22°C at 180 rpm for 3 hours). Cells were harvested by centrifugation (10,000 x g for 10 minutes) (Beckman Coulter - Avanti J-20 XPI). The supernatant was discarded, and the cell pellets were collected in a falcon tube and stored at -80°C.

### 2.4.2. Expression of labelled proteins

PASTA 4 to 5 with (pCWT006) were over expressed in BL21 (DE3) *E. coli* strains using IPTG induction. A single colony expressing the recombinant gene of interest was picked for a small-scale pre-culture in 100 mL LB broth containing Amp and incubated overnight (37°C at 180 RPM). For large scale expression, 10 mL of the overnight small-scale pre-culture was used to inoculate 2 x 1 L of LB broth containing 1 mL Amp and incubated (37°C at 180 RPM) until an OD<sub>600nm</sub> 0.6 was reached. The 2 L cultures were harvested by centrifugation (10,000 x g for 10 minutes, 4°C) (Beckman Coulter - Avanti J-20 XPI). To obtain high yield of the labelled protein, the cell condensation method was used (Sivashanmugam *et al.*, 2009). The supernatant was discarded, and cells washed and resuspended in 200 mL M9 salts. Cells were centrifuged again (10,000 x g for 10 minutes, 4°C) (Beckman Coulter - Avanti J-20 XPI). The supernatant was discarded and resuspended in 500 mL M9 media wither supplemented with 1 g <sup>15</sup>N Ammonium chloride and 0.5 g <sup>13</sup>C Glucose. Both cultures were pooled together and continued to incubate at 25°C and 180 RPM for 1 hour to equilibrate. After 1 hour, cells were induced with 1 mM IPTG and allowed to express overnight. Cells were harvested by centrifugation (10,000 x

g for 10 minutes) (Beckman Coulter - Avanti J-20 XPI). The supernatant was discarded, and the cell pellets were collected in a falcon tube and stored at -80°C.

### **2.4.3. Preparation of cell lysates**

In preparation of cell lysates, frozen cell pellets were left to thaw. Buffer A was added to the to 30 mL in a falcon tube and a protease inhibitor tablet (ThermoFisher - 88666F) was added. The cells were sonicated on ice (20 seconds at 70%, x 5) using an ultra-sonicator (Bandelin Sonoplus) and then centrifuged (45 minutes at 50,000 x g) (Beckman Coulter - Avanti J-20 XPI) to remove the cell debris and produce a clear lysate and then stored on ice for immobilised metal ion affinity chromatography (IMAC).

### **2.4.4. Protein Purification**

The basic methods describing the main purification techniques used in this study are summarised below.

#### **2.4.4.1. Affinity Chromatography**

Proteins with a poly-histidine (x6) affinity tag were purified by immobilised metal affinity chromatography (IMAC) using pre-packed HiTrap HP Nickel column (GE Healthcare) at room temperature unless stated otherwise. Columns are washed with 10 column volumes (CV) sterile water and equilibrated with a further 10 CV with Buffer A (Binding and equilibration buffer; see **Table 2.3**). Protein supernatant are loaded directly onto the column using a peristaltic pump. Columns were washed further with 10 CV Buffer A to remove un-bound protein. Columns were attached to an AKTA and protein was eluted using a gradient with Buffer B. 5 mL fractions were collected and protein elution was monitored by absorbance at 280 nm and occasionally also at 230 nm. Columns were washed with 10 CV of buffer containing 1 M imidazole, 10 CV sterile water and 10 CV 20% ethanol and stored at 4°C. Columns were stripped, cleaned and recharged between different protein preparations following manufacturer protocols.

#### **2.4.4.2. Size exclusion Chromatography**

For highly concentrated proteins and large volumes, preparative size exclusion chromatography was used. Proteins were separated by size using wither a Superdex 200 (16/60), Superdex 200 (26/60) or Superdex 75 (16/60) on an AKTA Pure system at RT.

Columns were equilibrated with 1.5 CV of the required buffer and samples loaded on via a super-loop. Elution was with 1 CV buffer at 1 mL min<sup>-1</sup> and 5 mL fractions were collected. Protein elution was monitored at 280 nm and occasionally 230 nm. For analytical studies, size exclusion chromatography was performed using a Superdex 200 increase 10/300 GL column (GE Healthcare). Pre-equilibrated columns were initially subjected to calibration using a LMW and HMW calibration kit (GE Healthcare) in the chosen buffer to allow for molecular weight determination. 100 µL of protein was loaded onto the column using an injection loop and elution was at 0.5 mL min<sup>-1</sup>.

#### **2.4.4.3. Buffer Exchange and concentration**

Buffer exchange was either initially through size exclusion chromatography, or with a VivaSpin centrifugal concentrator (Sartorius) with a molecular weight cut off either 5 or 10 kDa unless otherwise stated. Concentrators were centrifuged at 4°C at 3,000 x *g* in a bench-top centrifuge (Eppendorf Centrifuge 5810R) and if buffer exchange was required, refilled with exchange buffer until a sufficient dilution factor was reached. Protein solutions were concentrated until the required volume was achieved and subsequently quantified.

#### **2.4.4.4. Protein Purification of TEV protease**

To remove the poly-histidine tag of recombinant proteins, TEV protease was prepared and used. Buffers used are listed in **Table 2.3**. Cell pellets of TEV were re-suspended in Buffer A on ice and passed through the cell disruptor three times (10,000 psi). The lysate was centrifuged at 14,000 RPM for 45 minutes. The supernatant was collected and loaded onto a 5 mL HiTrap HP Nickel column (GE Healthcare) pre-equilibrated with Buffer A using a peristaltic pump at 5 mL min<sup>-1</sup>. The column was loaded onto an AKTA and a gradient was performed from Buffer A to Buffer B from 0 to 100% respectively over 30 minutes at 2 mL min<sup>-1</sup>. Fractions were analysed on a 12% SDS-PAGE gel and fractions were pooled for dialysis overnight in dialysis buffer overnight at 4°C. The protein concentration was measured using nanodrop at 8 mg mL<sup>-1</sup> and stored at -80°C.

#### **2.4.5. SDS-PAGE analysis**

Proteins were separated and visualised under denaturing conditions by SDS- Poly-acrylamide Electrophoresis (SDS-PAGE) with Tris-glycine buffer with either a 12 or 15 %

acrylamide gels. Gels were prepared and run on the Mini- PROTEAN tetra system (BIORAD). 4.2 mL of the separating gel (1.75 mL distilled water, 2.5 mL 1.5 M Tris-HCl pH 8.8, 100  $\mu$ L 10% SDS, 4.0 mL 30% acrylamide (Geneflow - 12-0066), 30  $\mu$ L 10% ammonium persulfate (APS) (fresh), 30  $\mu$ L tetram-ethylethylenediamine (TEMED) (Sigma Life Sciences - t9281) was added and overlaid with 100% ethanol whilst it set to remove the meniscus. The stacking gel (6.1 mL distilled water, 2.5 mL 0.5 M Tris-HCl pH 6.8, 100  $\mu$ L 10% SDS, 1.3 mL 30% Acrylamide (Geneflow - 12-0066), 40  $\mu$ L 10% ammonium persulfate (fresh), 40  $\mu$ L TEMED (Sigma-T9281) was then added to the gel once the ethanol was removed and the comb was added. Protein samples for analysis were prepared in sample buffer (12% 1 M Tris- HCl pH 6.8, 20% glycerol, 0.4% SDS, 1% bromophenol blue, 10%  $\beta$ -mercaptoethanol). The protein samples and 10  $\mu$ L of low molecular weight calibration ladder (Phosphorylase b, Bovine Serum Albumin, Ovalbumin, Carbonic anhydrase, Trypsin Inhibitor,  $\beta$  - Lactalbumin) (GE Healthcare - 17-0446-01) were heat denatured in a heat block (80°C for 10 minutes). The cast gel was loaded onto the electrophoresis unit Mini-PROTEAN tetra system (BIORAD) and 15  $\mu$ L of each sample was loaded into the respective well and gels were run in electrode buffer (25 mM Tris, 0.192 M Glycine, 0.1 % SDS, pH 8.3) for 45 minutes at 180 V. Development of SDS-PAGE gels were stained overnight with instant blue (Expedeon - ISB1L) then washed with water. Gels were imaged GelBox (Syngene) with a short-pass filter. Precast gels were occasionally used for analysis using either Criterion TGX Stain-Free gels, 4-20% gradient gels (BIORAD) or Mini-PROTEAN TGX Stain-Free gels, 4-20% (BIORAD).

#### **2.4.6. Western Blots**

*E. faecalis* cells were cultures in BHI broth containing 20 ng  $\mu$ L<sup>-1</sup> anhydrotetracycline at 37°C with agitation until OD<sub>600nm</sub> = 0.6. After centrifugation (5000 *x g*, 10 min, 4°C) pellets were resuspended in SDS loading buffer and cells were then lysed by sonication. 20  $\mu$ L of crude cell extract was analysed by SDS-PAGE and transferred to a polyvinylidene difluoride (PVDF) membrane using a BioRad Mini Transfer Blot. The Western membrane was blotted in 20% milk powder in PBS buffer for 1 hour. The blot was washed for 3 x 5 minutes in PBS. Detection of GFP fusions was performed with an anti-GFP-HRP goat polyclonal antibody (ThermoFisher – GF28R) (1/2000 in 10 mL PBS-tween) and left to incubate overnight. The blot was washed for 3 x 5 minutes in PBS. After

a further 1hour wash, blots were imaged by HRP chemiluminescence. Briefly a 1:1 ratio of the ECL substrate (BioRad) was mixed to a final volume of 10 mL. The mixed ECL substrate was added to the membrane for 5 minutes. After, excess ECL substrate was removed from the membrane and the membrane was placed in between two sheets of acetate. The membrane was imaged on a digital imager (Image Quant, GE).

#### **2.4.7. Protein Quantification**

To determine protein concentrations the Nanodrop ND-1000 Spectrophotometer (Nanodrop Technologies) was used. Each purified protein construct was determined measuring the protein absorbance at 280 nm and the specific molecular weight and molar extinction coefficients of each protein construct.

## **2.5. Peptidoglycan Purification and Hydrolysis**

### **2.5.1. Growth of Bacteria**

A single colony of *E. faecalis* JH2-2 was added to one litre of BHI and left overnight at RT without shaking. The following day, the growth phase of bacteria was recorded to ensure it was in the exponential phase at OD<sub>600</sub> of 0.7. Cultures were harvested by centrifugation (10,000 x g for 10 minutes, RT) (Beckman Coulter - Avanti J-20 XPI). Pellets were harvested and resuspended in 25 mL saline buffer and frozen in liquid nitrogen.

### **2.5.2. Peptidoglycan Extraction**

PG was extracted from *E. faecalis* cells using boiling SDS. Briefly, the cells pellet was boiled with 15 mL of 8% SDS at 100°C for 30 minutes with a magnetic stirrer and allowed to cool overnight. The PG was washed five times by centrifugation (12,000 x g for 10 min at 20°C) with 20 mL water. The PG was serially treated overnight first at 37°C with Pronase (200 µg mL<sup>-1</sup>) in 1 mL Tris-HCL (10 mM, pH 7.4) and then with trypsin (200 µg mL<sup>-1</sup>) in 1 mL phosphate buffer (20 mM, pH 7.8). The volume was adjusted to 15 mL with MilliQ water and treated again with 8% SDS at 100°C for 30 minutes and left to cool overnight. The PG was washed five times by centrifugation (12,000 x g for 10 min at 20°C) with 20 mL water. The PG was lyophilised and resuspended in MilliQ water at 20 mg mL<sup>-1</sup>. The PG was then treated with hydrofluoric acid (48%) at 5 mg mL<sup>-1</sup> for 48 hours at 4°C to remove PG bound secondary polymers. The pellet was then washed extensively as

described previously at least 5 times with centrifugation. The PG was lyophilised and resuspended in MilliQ water at 20 mg mL<sup>-1</sup>.

### 2.5.3. Peptidoglycan Hydrolysis

PG sacculi were digested with well-characterised enzymes that display distinct PG cleavage specificity. *S. aureus* PG fragments were a kind gift from Dr. Stephane Mesnage (University of Sheffield) and were prepared and purified as described in Mesnage *et al.*, (2014). For *E. faecalis* sacculi, the following enzymes were used for PG cleavage including Mutanolysin, a muramidase (Sigma – M9901); the amidase domain from *S. aureus* AtlA autolysin and EnpA, an endopeptidase recombinantly expressed and purified from *E. faecalis*. Both AtlA and EnpA was expressed and purified accordingly and is previously described (Hayhurst *et al.*, 2008; De Roca *et al.*, 2010). 1 mg of PG was digested in a final volume of 250 µL. Specific buffers and enzyme amounts were as follows: mutanolysin, 50 unit's phosphate buffer (pH 6.5) and AtlA amidase, 75 µg in phosphate buffer (pH 7.5) containing CaCl<sub>2</sub>. Double digestion with AtlA then Mutanolysin was also in 20 mM phosphate buffer (pH 7.5) containing CaCl<sub>2</sub> with a heat denaturation step in between (100°C 30 mins) and then the pH adjusted (pH 6.0) before the addition of mutanolysin, 50 units. Double digestion of Mutanolysin was also in 20 mM phosphate buffer (pH 6.5) then EnpA with an adjusted pH (pH 7.5) was performed with a heat denaturation step in between (100°C, 30 mins) and centrifugation (22,000 *x g*) to obtain the soluble fragments. Each hydrolysis step was for 16 hours overnight at 37°C After centrifugation for 20 min at 22,000 *x g*, two-fold serial dilutions of the digestion mixtures in PBS were used to test the interaction of PG fragments with the PASTA domains from *E. faecalis*.

## 2.6. Biophysical Techniques

### 2.6.1. Circular Dichroism

Recombinant proteins were diluted into 10 mM Sodium Phosphate to a final concentration of 50 µM. 200 µL of protein was loaded into a quartz cuvette with a path-length of 0.1 mm. Proteins were initially characterised at 25°C from 300 - 180 nm using 2 nm bandwidth, 1 sec response time, 0.2 nm data pitch and 100 nm min<sup>-1</sup> scanning speed on a Jasco J810 CD spectrophotometer. The High Tension (HT) was monitored in parallel to the spectra to ensure the salt content in the samples did not interfere with CD analysis.

Temperature melts ( $T_M$ ) were performed on proteins from 20°C to 100°C. Data was processed using Dichroweb (Whitmore and Wallace, 2004) and Prism (GraphPad). The reported  $T_M$  is the inflection point of the sigmoidal curve and is calculated using the Boltzmann sigmoid equation below:

$$y = Min + \frac{Max - Min}{1 + \exp\left(\frac{T_M - x}{slope}\right)}$$

The Boltzmann sigmoid equation is characterised by a plateau  $Max$  (Top) and  $Min$  (Bottom) with a  $T_M$  where the  $X$  value is exactly between top and bottom of the plateau. The slope indicates the range in which the temperature transition occurs.

### 2.6.2. Size Exclusion Chromatography-Multiple Angle Laser Light Scattering

SEC-MALS experiments were performed using either a Superdex 200 HR10/30 increase or Superdex 75 10/30 increase column (GE Healthcare) on a AKTA HPLC system at the Research Complex Harwell, Didcot. 100  $\mu\text{L}$  of 1  $\text{mg mL}^{-1}$  protein samples were loaded onto the size exclusion column and eluted at 0.75  $\text{mL min}^{-1}$  with 1 CV (24 ml) of an appropriate running buffer. Protein elution was monitored using a Wyatt Technologies Dawn HELEOS- II light-scattering detector and an Optilab REX refractive index monitor. Recorded data were analysed using Astra 5.0 software (Wyatt Technologies).

### 2.6.3. Size Exclusion Chromatography-Small Angle X-Ray Scattering

SAXS data were collected on beamline BM29 from the European Synchrotron Radiation Facility in Grenoble (France) using the in-line Shimadzu size exclusion chromatography system with a Superdex 200 increase (3.2/300) (GE Healthcare) to separate potential oligomers and contaminants at low concentration at 0.75  $\text{mL min}^{-1}$ . Protein samples were previously dialysed, and column were equilibrated in 50 mM HEPES, 150 NaCl pH 7.4. 900 frames of 2 sec each was recovered over the course of each run. For each sample, frames were normalised to the intensity of the transmitted beam before being merged. The buffer was subtracted from the scattering using SCATTER. The radius of gyration ( $R_g$ ), forward scattering intensity ( $I(90)$ ), maximum particle dimension ( $D_{max}$ ) and distance distribution function ( $P(R)$ ) was evaluated using the same software. The sample was positioned at 2.86m from a Pilatus detector, at a wavelength of 0.99 nm. To determine *ab initio* models, 3D envelopes were determined using the ATSAS package

and DAMMIF programme to generate a compact bead model fitting the experimental data to minimize discrepancy (Svergun, 1999). Dummy atom models from repeated calculations were superimposed and compared using the program DAMAVER (Volkov and Svergun, 2003).

#### **2.6.4. Surface Plasmon Resonance (SPR)**

PASTA proteins with the 6x His-Tag were immobilised on a CM5 sensor chip using amine coupling at a flow rate of 10  $\mu\text{L min}^{-1}$ . Briefly, the carboxymethylated dextran surface was activated by injecting 40  $\mu\text{L}$  of a solution containing 0.2M 1-ethyl-3-(3-(dimethylamino)propyl)carbodiimide hydrochloride (EDC; Sigma) and 0.05 M N-hydroxysuccinimide (NHS; Sigma). Covalent immobilization of PASTA proteins was carried out using 70  $\mu\text{L}$  of a protein solution diluted in 10 mM sodium acetate (pH 4.5). The reaction was quenched with 40  $\mu\text{L}$  of 1 M ethanolamine-HCl (pH 8.5).

SPR experiments were performed on a BIACORE T200 instrument with research grade CM5 sensor chips at a temperature of 25°C. The running buffer was HEPES-buffered saline (HBS-P; 10 mM HEPES (pH 7.4), 150mM NaCl, 0.005% (v/v) Tween-20). If not otherwise indicated, the flow rate was 10  $\mu\text{L min}^{-1}$ . The sample compartment temperature was kept at 5°C. The chip was regenerated using a 1-min pulse of 6 M guanidine hydrochloride followed by an injection of 30  $\mu\text{L}$  of HBS-P buffer. Various immobilization densities and flow rates were tested to test optimal steady-state analysis conditions.

#### **2.6.5. Microscale thermophoresis**

The dissociation constant between the PASTA domains and a short list of different ligands from the previous SPR experiments was determined by Monolith NT.115 (NanoTemper Technologies, Germany). Protein was labelled with red (MO-L008 NT-647) using Monolith NT Protein Labelling Kit Red-NHS (Nano Temper Technologies, Germany) according to the manufacturers protocol. The label was covalently linked to the protein at the x6 His site. Unlabelled ligands were serially diluted by two-fold scheme in HBS-P supplemented with 0.05% Tween-20. A total of 5  $\mu\text{L}$  labelled PASTA proteins (200 nM) and 5  $\mu\text{L}$  ligand titrations were mixed and incubated at room temperature for 1 h before loaded into standard capillaries (NanoTemper Technologies, Germany).

### **2.6.7. Analytical Ultracentrifugation**

AUC experiments were performed at the Research complex at Harwell, Didcot. For, characterisation of the protein samples, SV scans were recorded for a two-fold protein dilution series, starting from 1 mg mL<sup>-1</sup>, unless otherwise stated. All experiments were performed at 50,000 RPM, using a Beckman XL-I analytical ultracentrifuge with an An-50Ti rotor. Data were recorded using the absorbance (at 280 nm) and interference optical detection systems. The density and viscosity of the buffer was measured experimentally using a DMA 5000M densitometer equipped with a Lovis 200ME viscometer module. Data and interpretation was analysed with the help of Gemma Harris. The partial specific volume for the protein constructs were calculated using Sednterp from the amino acid sequences. Data were processed using SEDFIT, fitting to the c(s) model.

### **2.6.8. Mass Spectrometry**

Electrospray ionisation mass spectrometry (ESI-MS) was conducted with assistance from Dr. Adrian Lloyd. Protein samples were buffer exchanged into 10 mM ammonium acetate and concentrated to a final concentration of 5 µM. Protein samples were mixed with an equal volume of 99.8 % (v/v) acetonitrile and 0.2 % (v/v) formic acid.

Samples (0.2 mL) were dispensed into glass vials and were then loaded into the 96 well sample rack of a Waters M-class sample manager interspersed with blank vials containing 50% (v/v) acetonitrile and 0.1% formic acid. The sample manager was held at 10°C and was interfaced with a Waters M-class solvent manager and a Waters Synapt G2-Si time of flight mass spectrometer equipped with an electrospray source.

The synapt G2-Si was set up to run in positive ion and resolution modes, with a capillary voltage of 2.5 kV, a sampling cone voltage of 30 V and a source temperature of 80°C. Desolvation gas (N<sub>2</sub>) was applied at 300 L h<sup>-1</sup>. Data was collected in continuum mode at a scan rate over the desired m/z range of one per second with a total cycle time of 1.014 seconds. Calibration of the instrument was carried out using 32 sodium iodide clusters in the m/z range 300-5000 (smallest m/z cluster = 322.809 to largest m/z cluster, 4967.415). All 32 clusters were matched with reference values and the RMS residual of the resulting calibration was. 0.3 ppm.

Samples were delivered to the mass spectrometer by injection of 5  $\mu\text{L}$  sample into a solvent stream delivered at a flow rate of 30  $\mu\text{L min}^{-1}$  by the M-class solvent manager. The solvent stream was composed of a 1:1 mixture of 0.1 % (v/v) formic acid in water and 0.1% (v/v) formic acid in acetonitrile. For sample analysis the Synapt G2-Si was set to scan between 300 and 2500  $m/z$  in one second scans and data was accumulated over 9 minutes.

The total ion chromatograms resulting from these analysis were combined to generate mass spectra, where typically only the first 2 minutes of the chromatogram contained the ionising species of interest. Data was then interrogated using the Maximum Entropy algorithm to resolve the protein mass spectra to the simplest interpretation of the data on a mass scale. This algorithm regenerates a mock mass spectrum based upon its interpretation of the raw mass spectrum. We confirmed the quality of the Maximum Entropy interpretation of our raw data by superimposition of mock and raw data.

### **2.6.9. Nuclear Magnetic Resonance**

All NMR experiments were carried out at 25°C unless otherwise stated on a 700 MHz Bruker Avance spectrometer fitted with a cryoprobe running in triple resonance mode for  $^1\text{H}/^{15}\text{N}/^{13}\text{C}$  NMR experiments. All samples were analysed in 3 mm NMR tubes and spectra recorded on Bruker instruments were referenced to residual water on the DSS scales (Wishart *et al.*, 1995). All samples contained 10%  $\text{D}_2\text{O}$  so that the spectrometer field was locked on to the resonance position of deuterium during acquisition. The basic parameters of all NMR experiments used throughout this work are listed in **Table 2.14**.

#### **2.6.8.1. 1D Experiments**

1D proton spectra were acquired using the zgpgw5 pulse programme using WATERGATE methods for water suppression (Liu *et al.*, 1998). Spectra were acquired using 32k complex data points and 32 co-added scans. The acquisition time was 1.67 secs and the spectral window was 20 ppm. The data was Fourier transformed using zero-filling to 32k and processed using a squared sine window function.

### 2.6.8.2. 2D Experiments

2D  $^1\text{H}$ - $^{15}\text{N}$  HSQC spectra were acquired over a wide range of conditions and parameters to ensure the best resolution in the shortest time which is important for later titration experiments (Kay *et al.*, 1992). The data were Fourier transformed using a zerofilling on 4k in  $F_2$  and 2k in  $F_1$ . Processing was done using Gaussian multiplication (GM) window function with a line broadening of -10 Hz in both dimensions. Additionally, a polynomial baselines correction was used in  $F_2$  and a linear prediction was used in  $F_1$ .

### 2.6.8.3. 3D Experiments

The triple resonance ( $^1\text{H}$ - $^{13}\text{C}$ - $^{15}\text{N}$ ) experiments included CBCA(CO)NH (Grzesiek and Bax, 1992), CBCANH (Wittekind and Mueller, 1993), HNCA (Kay *et al.*, 1990), HN(CO)CA (Bax and Ikura, 1991), HNCO (Kay *et al.*, 1990),  $^{15}\text{N}$ -TOCSY-HSQC (Marion *et al.*, 1989b) and  $^{15}\text{N}$ -NOSEY-HSQC (Marion *et al.*, 1989a). Processing was done by Fourier transforming using Gaussian multiplication (GM) window function and using a line broadening of -10 Hz in all dimensions. Baseline correction was done in  $F_1$  and linear prediction was used in dimensions  $F_2$  and  $F_3$ .

**Table 2.14: Pulse Programmes and basic parameters used in NMR experiments.**

Experiment	Pulse Programme	Scans	Number of Points			Spectral Width (ppm)		
			$^1\text{H}$	$^{15}\text{N}$	$^{13}\text{C}$	$^1\text{H}$	$^{15}\text{N}$	$^{13}\text{C}$
HSQC	hsqcf3gpph19	32	2048	128	-	14	50	-
HNCA	hncagpwg3d	16	2048	40	90	14	32	32
HN(CO)CA	hncocagpwg3d	16	2048	40	90	14	32	32
HNCO	hncogpwg3d	16	2048	40	80	14	32	22
HN(CA)CO	hncacogpwg3d	16	2048	40	65	14	32	22
HNCACB	hncacbpgwg3d	32	2048	40	110	14	32	75
HN(CO)CACB	cbcaconhpgwg3d	32	2048	40	100	14	32	75

Experiment	Pulse Programme	Scans	Number of Points			Spectral Width (ppm)		
			$^1\text{H}$	$^{15}\text{N}$	$^{15}\text{N}$	$^1\text{H}$	$^1\text{H}$	$^1\text{H}$
$^{15}\text{N}$ -HSQC-TOCSY	dipsihsqcf3gpsi3d	56	2048	40	90	14	40	14

Experiment	Pulse Programme	Scans	Number of Points			Spectral Width (ppm)		
			$^1\text{H}$	$^{15}\text{N}$	$^{15}\text{N}$	$^1\text{H}$	$^{15}\text{N}$	$^1\text{H}$
$^{15}\text{N}$ -HSQC-NOSEY	noesyhsqcfpf3gpsi3d	40	2048	40	90	14	40	14

#### 2.6.8.4. NMR Titration Experiments

HSQC spectra were used to monitor interactions between vancomycin and the terminal PASTA domains 4-5 from IreK. Eight aliquots of vancomycin were prepared with a total amount of ligand corresponding to 0.125, 0.25, 0.5, 1, 2, 4, 8 and 16 mM in 200  $\mu$ L and the aliquots were lyophilized in 1.5 mL microcentrifuge tubes (**Table 2.15**).

**Table 2.15: Overview of lyophilized ligand aliquots for incremental titration experiments for chemical shift perturbation experiments with  $^{15}$ N-PASTA 4 to 5.**

	Ref.	Exp. 1	Exp. 2	Exp. 3	Exp. 4	Exp. 5	Exp. 6	Exp. 7
<b>Protein Conc.</b>	1 mM	1 mM	1 mM	1 mM	1 mM	1 mM	1 mM	1 mM
<b>Ligand Increment</b>	-	0.125 mM	0.25 mM	0.5 mM	1 mM	2 mM	4 mM	8 mM
<b>Ligand Conc.</b>	0 mM	0.25 mM	0.5 mM	1 mM	2 mM	4 mM	8 mM	16 mM

After HSQC acquisition of the reference sample containing only protein, the ligand concentration was increased stepwise by transferring the protein sample to the microcentrifuge tube with the denoted amount of vancomycin prior to acquisition of the next HSQC spectrum. The pH and temperature were maintained throughout experiments. Saturation was not achieved as protein samples began to aggregate at 16 mM and impaired the HSQC resolution. A total of eight spectra were acquired by repeating this procedure totalling in one reference spectrum and seven titration experiments. The protein was equilibrated inside the NMR spectrometer for 15 minutes at 25°C before starting the NMR spectra acquisition. Once the HSQC spectrum was obtained, the sample was removed from the spectrometer and transferred to the first microcentrifuge containing the lyophilized ligand and vortexed and centrifuged (5000 x RCF, 1 min, RT) and transferred to the previously used NMR tube and re-equilibrated in the NMR spectrometer as described. This process was repeated for each ligand.

#### 2.6.8.5. Data Processing

Spectra were processed using Topspin 4.0.2 and analysed using CCPN Analysis Assign (Fogh *et al.*, 2002; Vranken *et al.*, 2005).

# Chapter 3. Phenotypic characterisation of IreK in *E. faecalis*

## 3.1. Introduction

Our collaborators in the Dworkin group at Columbia University (New York) demonstrated that there is an *in vitro* interaction between IreK and VanS<sub>B</sub>. The IreK<sub>KD</sub> domain phosphorylated VanS<sub>KD</sub> on position T223 and that the cognate phosphatase of IreK (IreP), dephosphorylates IreK and the associated substrate VanS<sub>B</sub>. Early experiments tried to obtain an *E. faecalis* isogenic series to compare the effect of both IreK and the Tn1549 cassette but were unsuccessful in obtaining the full strain series. The aim of this chapter is to build on the work that has already been conducted in the Dworkin group by complementing the *in vitro* biochemical experiments to gain a further understanding on the effects of IreK in antibiotic resistance.

An isogenic series of mutants to study the effect of IreK and Tn1549 in antibiotic resistance was constructed to study their effect in antibiotic resistance. Other experiments include methods to understand the role of staurosporine and other inhibitors on IreK *in vivo* and also the relationship between the intracellular KD and extracellular PASTA domains of IreK and its overall roles in the capacity of antibiotic resistance in *E. faecalis*.

## 3.2. *E. faecalis* isogenic series to study antibiotic resistance mechanisms

To understand the consequences for VanB resistance mechanisms of IreK, a set of isogenic strains were constructed to study the potential effects *in vivo*. An isogenic series was generated in a suitable parental strain of *E. faecalis*. Analysis between OG1RF and V583 conferring VanB type resistance has demonstrated that OG1RF is clonally distinct from V583 (Nallapareddy *et al.*, 2005). Although OG1RF does confer rifampicin and fusidic acid resistance, up to one quarter of the DNA from V583 has derived from mobile elements which confers multiple antibiotic resistance determinants, and therefore makes it a difficult strain to create mutants and study antibiotic resistance and

therefore is unsuitable to use in this study (Sahm *et al.*, 1989). OG1 strains and derivatives have also been successfully used in animal models to characterise virulence of *E. faecalis* including peritonitis in a mouse model (Singh *et al.*, 1998), endophthalmitis in a rabbit model (Mylonakis *et al.*, 2002), endocarditis in a rat model (Singh *et al.*, 2005) and UTIs in a mouse model (Singh *et al.*, 2007). OG1RF has also been shown to be as virulent as V583 in the model *Caenorhabditis elegans* (Sifri *et al.*, 2001). For this reason, OG1RF was chosen as a model strain for the construction of the isogenic series. Additional advantages of OG1RF as a strain to create an isogenic series are that it does not carry any plasmids, it is readily transformable by electroporation and it is not resistant to any other antibiotics other than rifampicin and fusidic acid and these resistances were selected in the OG1 derivative to provide strain markers (Oliver *et al.*, 1977). The lack of resistance to common antibiotics facilitates the selection of plasmids, transposons and allelic replacement markers into the strain (Bourgogne *et al.*, 2008). JH2-2 is another laboratory strain of *E. faecalis* that is well characterised and in a previous study has successfully had the Tn1549 transposon conferring VanB type resistance transfer into the strain and therefore enables another platform for an isogenic series to study the interaction between IreK and the Tn1549 cassette (Quintiliani and Courvalin, 1994).

### **3.2.1. Construction of the OG1RF $\Delta$ ireK and Tn1549 isogenic series**

The principle strains used in this study include OG1RF, a common lab strain of *E. faecalis*, OG1RF  $\Delta$ ireK, a kind gift from Christopher Kristich and OG1RF::Tn1549  $\Delta$ ireK is a strain created for a previous study (Goss, 2013) where Tn1549 was conjugated into *E. faecalis*, OG1RF  $\Delta$ ireK. Unfortunately, in that study Tn1549 could not be conjugated successfully into OG1RF WT strain after many attempts. To ensure we had the full isogenic strain library, we took an inverse approach. We reinserted *ireK* back into the OG1RF::Tn1549  $\Delta$ ireK strain. We used the pGhost9 system (Maguin *et al.*, 1996) to make the genetic insertion of *ireK* back into the OG1RF::Tn1549  $\Delta$ ireK.

The pGhost9 system is an efficient insertional mutagenesis method by associating the insertion sequence ISS1 (transposable bacterial sequences) with the thermosensitive replicon pGhost. This mutagenic tool, named pGhost9::ISS1, can be used even in poorly transformable strains, and has been reported to be transformed in a number of *Enterococcus*, *Lactobacillus*, *Lactococcus*, and *Streptococcus* species. High frequency

transposition using pGhost9::*ISS1* allows efficient gene inactivation and direct cloning of DNA surrounding the insertion. Excision of the plasmid replicon by a temperature shift, gives rise to a stable mutant strain, which doesn't contain any antibiotic resistant markers. This is achieved when pGhost9::*ISS1* is transformed at a permissive temperature, and transposition is selected for at a higher non-permissive temperature. This temperature increase causes the replicative transposition of the *ISS1* sequences to insert into the chromosome and leads to the integration of the plasmid vector. Transposition is therefore revealed by selection for antibiotic-resistant clones able to grow at a temperature restrictive for plasmid replication.

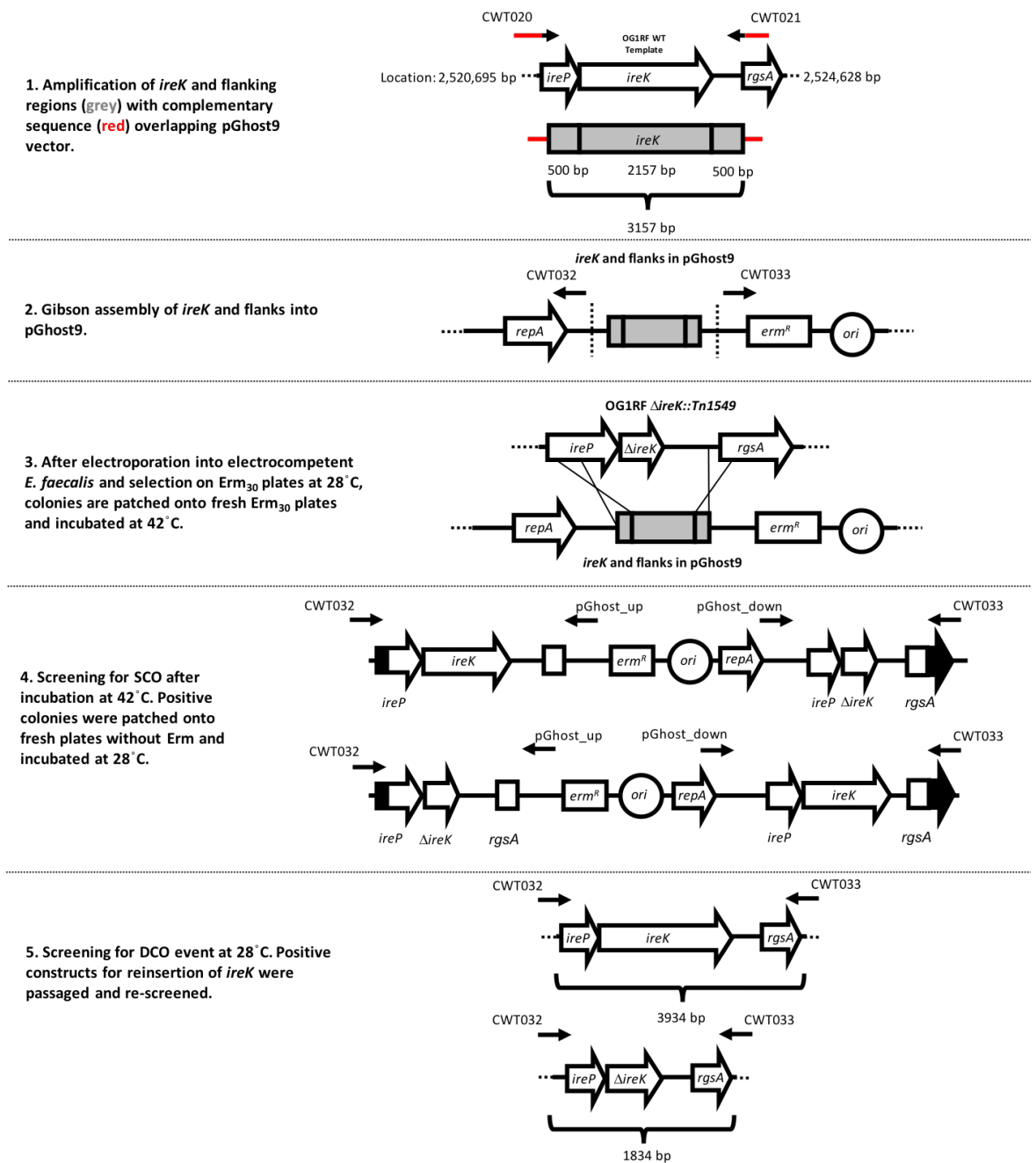


**Figure 3.1: Schematic of inserting the *ireK* gene back into an OG1RF::Tn1549 strain using the pGhost9 plasmid.** This strategy resulted in scarless insertion of *ireK* gene from the OG1RF::Tn1549  $\Delta ireK$  strain via homologous recombination. The erythromycin cassette allowed for selection of single cross over events (SCO). Passing positive SCO without erythromycin allowed for selection of double cross over events (DSO). Positive constructs were PCR amplified and sequence to confirm insertion.

The schematic for the insertion is depicted in **Figure 3.1**. Using OG1RF WT as a template, *ireK* and sequences immediately 500 bp upstream and downstream of *ireK* were amplified and inserted into the temperature-sensitive pGhost9 plasmid through

Gibson assembly. After transformation into *E. faecalis* the plasmid is propagated at the permissive temperature (28°C) with antibiotic selection. It is shifted to the non-permissive temperature (42°C) in the presence of antibiotic selection to stimulate single crossover events to occur. After selecting for single crossover events, the cultures are further shifted back to the permissive temperature in absence of selection and screened for double crossover events by passaging into BHI (at least 5 times) and screened on both BHI only and BHI Erm<sub>30</sub> plates. Double cross over events were confirmed when no colonies are present on the BHI Erm plates but are present on the BHI only plates. The strain was screened via PCR using primers that flank the gene of interest to confirm the successful insertion of *ireK* to form an OG1RF::Tn1549  $\Delta ireK$  strain. A summary of strains is in **Table 3.1**.

### **3.2.2. Construction of the JH2-2 $\Delta ireK$ isogenic series**

Although other groups had tried to create a  $\Delta ireK$  deletion strain in both JH2-2 and JH2-2::Tn1549, it was attempted again in this study to try and obtain another isogenic series to compare the effects *ireK* and Tn1549 on the OG1RF isogenic series. The pGhost9 system was used again and a plasmid construct containing 500 bp upstream and downstream flanking *ireK* and inserted into the temperature sensitive pGhost9 plasmid (pCWT021). Unfortunately, neither single or double crossover events were observed.

### **3.2.3. Construction of $\Delta ireP$ strains in OG1RF**

Deletion of *ireP* in OG1RF and OG1RF::Tn1549 was attempted to understand the effects of the cognate phosphatase in a Tn1549 background. The pGhost9 system was used and a plasmid construct containing 500 bp upstream and downstream flanking *ireP* was inserted into the temperature sensitive pGhost9 plasmid (pCWT022). Although a single and double crossover event was observed and selected in the OG1RF WT strain which has previously been observed (Kristich *et al.*, 2011), after several attempts, a  $\Delta ireP$  strain was not observed in the single and double crossover events.

**Table 3.1: Summary of *E. faecalis* isogenic experimental strains and the associated genotype used in the study.**

OG1RF	JH2-2
Wild Type	Wild Type
<i>ΔireK</i>	-
Tn1549 ( <i>vanB</i> )	Tn1549 ( <i>vanB</i> )
Tn1549 <i>ΔireK</i> ( <i>vanB</i> )	-

### **3.3 Tn1549 is required for enhanced cephalosporin resistance and *ireK* is essential for both intrinsic and enhanced cephalosporin resistance in OG1RF strains**

The effect of the presence of the Tn1549, VanB resistance genes was probed by measuring the MIC of these strains in the presence of a range of cephalosporin antibiotics (Table 3.2). There was a significant difference in MIC when comparing OG1RF Wild-type (WT), *ΔireK* and derivatives containing the Tn1549 resistance cassette. The MIC of vancomycin in OG1RF increases 16-fold, from 4 to 64 μg mL<sup>-1</sup> in the presence of the Tn1549 cassette. There was no change in MIC in the presence of teicoplanin which is to be expected as Tn1549 cassette conferring VanB type resistance is reported to be resistant to vancomycin but not teicoplanin (Garnier *et al.*, 2000).

When challenged by cephalosporin antibiotics, the intrinsic resistance of the OG1RF strains containing the Tn1549 cassette increases significantly compared to WT OG1RF. Whilst vancomycin enhanced cephalosporin susceptibility has been seen in the past, this is the first time to our knowledge that the presence of the Tn1549 cassette upon enhanced cephalosporin resistance in *E. faecalis* has been observed in the absence of vancomycin (Kristich *et al.*, 2007; Kristich *et al.*, 2011). The addition of the Tn1549 cassette causes a remarkable 128-fold increase in cefotaxime resistance in comparison to the OG1RF WT strain.

**Table 3.2: Tn1549 causing VanB type resistance causes enhanced cephalosporin resistance: MIC OG1RF WT/Tn1549 with cephalosporin's and vancomycin.** *E. faecalis*  $\Delta ireK$  strains in both WT and Tn1549 strains removes intrinsic and enhanced cephalosporin resistance respectively. Experiments were in accordance to CSLI protocols and performed in duplicates. MIC reported in  $\mu\text{g mL}^{-1}$ . \*Note Teicoplanin is not an approved antibiotic in the USA, therefore there are no appropriate controls to compare the MIC ranges.

Antibiotic	Class	Sub-Class	MIC ( $\mu\text{g mL}^{-1}$ )			
			WT	Tn1549	$\Delta ireK$	Tn1549 $\Delta ireK$
Vancomycin	Glycopeptide	-	4	64	1	32
Teicoplanin*	Glycopeptide	-	0.5	0.5	0.125	0.0625
Cephalexin	$\beta$ -lactam	Cephalosporin (1 <sup>st</sup> Generation)	32	128	16	32
Ceftriaxone	$\beta$ -lactam	Cephalosporin (3 <sup>rd</sup> Generation)	16	256	0.5	8
Cefotaxime	$\beta$ -lactam	Cephalosporin (3 <sup>rd</sup> Generation)	2	256	0.0625	1
Cefepime	$\beta$ -lactam	Cephalosporin (4 <sup>th</sup> Generation)	8	32	2	8
Ceftobiprole	$\beta$ -lactam	Cephalosporin (5 <sup>th</sup> Generation)	0.03125	>0.00781	0.03125	0.03125

An  $\Delta ireK$  mutation was introduced into strains of OG1RF WT and Tn1549. Of note, the MIC for vancomycin in the  $\Delta ireK$  mutants is 4-fold lower than the wild type suggesting a direct interaction between IreK and some element of the Tn1549 resistance gene cassette (**Table 3.2**). Remarkably in the OG1RF  $\Delta ireK$  strain, the overall level of resistance to all cephalosporin's decreases to a level below that of the WT strain. Deletion of *ireK* results in a significant reduction of both intrinsic resistance as demonstrated previously (Kristich *et al.*, 2007; Kristich *et al.*, 2011) and enhanced cephalosporin resistance in *E. faecalis*. This effect is represented across all cephalosporin generations from 1<sup>st</sup> to 4<sup>th</sup>, but not in the case of ceftobiprole, a 5<sup>th</sup> generation cephalosporin drug recently approved to treat hospital-acquired pneumonia (Bogdanovich *et al.*, 2005). These results suggest a direct causal linkage between IreK function and enhanced cephalosporin resistance, caused by an unknown component of the Tn1549 transposon responsible for vancomycin resistance, independent of vancomycin induction. To investigate the effect of *ireK* and

Tn1549 on antibiotic sensitivity on the OG1RF isogenic series, other drugs were tested including other cell wall antibiotics and other classes of antibiotics. Generally, the differences observed are not on the same scale to that of cephalosporin including small variations when ampicillin, meropenem, D-cycloserine, kanamycin, rifampicin and linezolid are used.

In all four isogenic strains, ampicillin sensitivity is observed which is consistent with the use of ampicillin as a clinical therapeutic in *E. faecalis* treatments (Beganovic *et al.*, 2018). Although there is slight difference in MIC, the organisms still considered to be sensitive to ampicillin and that *ireK* strains in both the WT and Tn1549 as little effect. Little difference was also observed with meropenem, an antibiotic that is has been shown to be sensitive in a number of *E. faecalis* strains (Edwards *et al.*, 1995).

**Table 3.3: MIC determination of the OG1RF isogenic series to determine the effect of the Tn1549 cassette and *ireK* on other cell wall antibiotics.** Experiments were in accordance to CSLI protocols and performed in duplicates. MIC reported in  $\mu\text{g mL}^{-1}$ .

Antibiotic	Class	Sub-Class	MIC ( $\mu\text{g mL}^{-1}$ )			
			WT	Tn1549	$\Delta ireK$	Tn1549 $\Delta ireK$
Ampicillin	$\beta$ -lactam	-	0.0313	0.0625	0.0156	0.0156
Meropenem	$\beta$ -lactam	Carbapenem	1	2	0.5	2
Fosfomycin	MurA Inhibitor	Intracellular Specific Target	16	128	16	64
D-Cyclo serine	Ddl	Intracellular Specific Target	128	128	64	64
Bacitracin	Lipid II	-	128	128	16	128
Daptomycin	Membrane	-	64	32	8	16

Of interest is the increase in fosfomycin from 16 to 128  $\mu\text{g mL}^{-1}$  in a OG1RF WT and Tn1549 strain respectively. Fosfomycin targets MurA, a protein involved in the PG biosynthesis pathway. There are two homologs of MurA in *E. faecalis* denoted MurAA and MurAB. It has previously been determined that both proteins have distinct role in *E.*

*faecalis* physiology and that the MurAA homologue is involved in enhanced intrinsic cephalosporin resistance (Kristich *et al.*, 2011). The enhanced fosfomycin resistance shown in **Table 3.3** suggests that the Tn1549 cassette may have a role in the downstream PG biosynthesis pathway.

Although there was little difference in the MICs between bacitracin and daptomycin with the introduction of the Tn1549 cassette, in the OG1RF WT strain and OG1RF  $\Delta ireK$  strain there was a decrease in MIC of both antibiotics with the deletion of *ireK*. Daptomycin interacts directly with the membrane and causes curvature, therefore as IreK is a membrane protein with a large extracellular domain, IreK in an OG1RF WT strain may be able to elicit a cellular response to overcome the effects of Daptomycin. OG1RF  $\Delta ireK$  resulted in a 4-fold decrease in MIC in comparison to WT and 2-fold decrease when comparing a OG1RF Tn1549 and OG1RF::Tn1549  $\Delta ireK$  strain. Bacitracin targets C<sub>55</sub>-isoprenyl pyrophosphate which is involved in PG biosynthesis and only in a  $\Delta ireK$  strain is a difference in MIC observed in all strains. In comparison to OG1RF WT strain, there is a 4-fold change in MIC.

**Table 3.4** evaluates antibiotics that are not cell wall antibiotics. There is no difference in MIC between each strain and these antibiotics apart from a small shift in MIC in a  $\Delta ireK$  strain against kanamycin. Kanamycin resistance is reported in many *E. faecalis* strains due to the presence of the *aph(3')-IIIa* gene which confers high level resistance of kanamycin (Woegerbauer *et al.*, 2014). As previously mentioned OG1RF and derivatives of the OG1X strains are resistance to rifampicin and fusidic acid to provide strain markers. All strains show resistance greater than 256  $\mu\text{g mL}^{-1}$ , therefore the variation between each strain cannot be evaluated due to higher concentration not being tested (Oliver *et al.*, 1977). Each strain also showed sensitivity to linezolid and no difference in MIC. Linezolid is a protein synthesis inhibitor and like ampicillin, is also regularly used in the treatment of *Enterococcal* spp. infections (Beganovic *et al.*, 2018).

**Table 3.4: MIC determination of the OG1RF isogenic series to determine the effect of the Tn1549 cassette and *ireK* resistance to other classes of antibiotics.** Experiments were in accordance to CSLI protocols and performed in duplicates. MIC reported in  $\mu\text{g mL}^{-1}$ .

Antibiotic	Class	Sub-Class	MIC ( $\mu\text{g mL}^{-1}$ )			
			WT	Tn1549	$\Delta ireK$	Tn1549 $\Delta ireK$
Kanamycin	Protein Synthesis	Aminoglycoside	256	256	128	256
Linezolid	Protein Synthesis	Inhibition Inhibitor	2	2	2	2
Rifampicin	RNA Synthesis	RNA Polymerase	<256	<256	<256	<256

Although there are differences in the MIC of different antibiotics between the four strains of OG1RF *E. faecalis* with different antibiotics, the changes in MIC with the largest variations comes intrinsically from the cephalosporin's with smaller differences in variation from other cell wall antibiotics including Bacitracin and Daptomycin. The effect of Tn1549 and *ireK* on enhanced cephalosporin resistance forms the main focus of the subsequent experiments to explore the phenotype further.

### 3.4. Tn1549 is not required for enhanced cephalosporin resistance in JH2-2 strains

Although an isogenic series of JH2-2 with an  $\Delta ireK$  mutation in both the WT and Tn1549 backgrounds could not be generated, the hypothesis of enhance cephalosporin resistance was tested by comparing the JH2-2 WT and Tn1549 strains (**Table 3.5**). There is a clear difference in MIC between the WT and Tn1549 strains (1 to 128  $\mu\text{g mL}^{-1}$  respectively) exhibiting a 128-fold difference in comparison to 16-fold difference when comparing the OG1RF WT and Tn1549 backgrounds. Unlike the OG1RF isogenic series, JH2-2 strains with the Tn1549 cassette does not exhibit enhanced cephalosporin resistance in comparison to WT. A factor that may contribute to this observation may include that JH2-2 is original clinical isolate that was derived from a patient undergoing antibiotic therapy. Although there is no acquired resistance mechanism in JH2-2, others virulent mechanism in the chromosomal genome may contribute to the high cephalosporin resistance independent of the Tn1549 cassette (Jacob and Hobbs, 1974). Another factor may include the location of conjugation of the Tn1549 cassette in both

strains and if such conjugation events disrupted essential genes involved in resistance to cell wall antibiotics resistance.

**Table 3.5: MIC of JH2-2 WT/Tn1549 with cephalosporin's and vancomycin.** Experiments were in accordance to CSLI protocols and performed in duplicates. MIC reported in  $\mu\text{g mL}^{-1}$ .

Antibiotic	Class	Sub-Class	MIC ( $\mu\text{g mL}^{-1}$ )	
			WT	Tn1549
Vancomycin	Glycopeptide	-	1	128
Ceftriaxone	$\beta$ -lactam	Cephalosporin (3 <sup>rd</sup> Generation)	2048	2048
Cefotaxime	$\beta$ -lactam	Cephalosporin (3 <sup>rd</sup> Generation)	2048	2048
Ceftazidime	$\beta$ -lactam	Cephalosporin (3 <sup>rd</sup> Generation)	<2048	<2048

### 3.5. The linkage between cephalosporin resistance and the Tn1549 structural genes is not at the transcriptional level.

To investigate the possible linkage between enhanced cephalosporin resistance and the presence of the Tn1549 cassette at a transcriptional level, qPCR analysis of the expression of representative genes from the Tn1549 cassette was performed. In this experiment, the transcriptional levels of *vanY* and *vanB*, whose expression is controlled by the same promoter were monitored when a *E. faecalis* OG1RF::Tn1549 cultures was challenged by either vancomycin ( $2 \mu\text{g mL}^{-1}$ ) or a representative cephalosporin antibiotic; cefotaxime ( $64 \mu\text{g mL}^{-1}$ ) (See **Figure 3.3.A**). Cefotaxime was chosen as its level of resistance is enhanced by over 8-fold ( $2$  to  $256 \mu\text{g mL}^{-1}$ ) compared of the OG1RF parental strain and thus provides a strong reporter system for comparison of both cephalosporin and vancomycin resistance.

The 16S ribosome gene was used as the control housekeeping gene and experiments were normalized to samples that were not induced with antibiotics (**Figure 3.3**). Initial control experiments included comparison of the 16S ribosome gene under each experimental condition (uninduced, with vancomycin and with cephalosporin) for each strain (OG1RF WT, Tn1549 and Tn1549  $\Delta ireK$ ). qPCR experiments to compare

contamination of cDNA and gDNA were also included in experiments without reverse transcriptase.

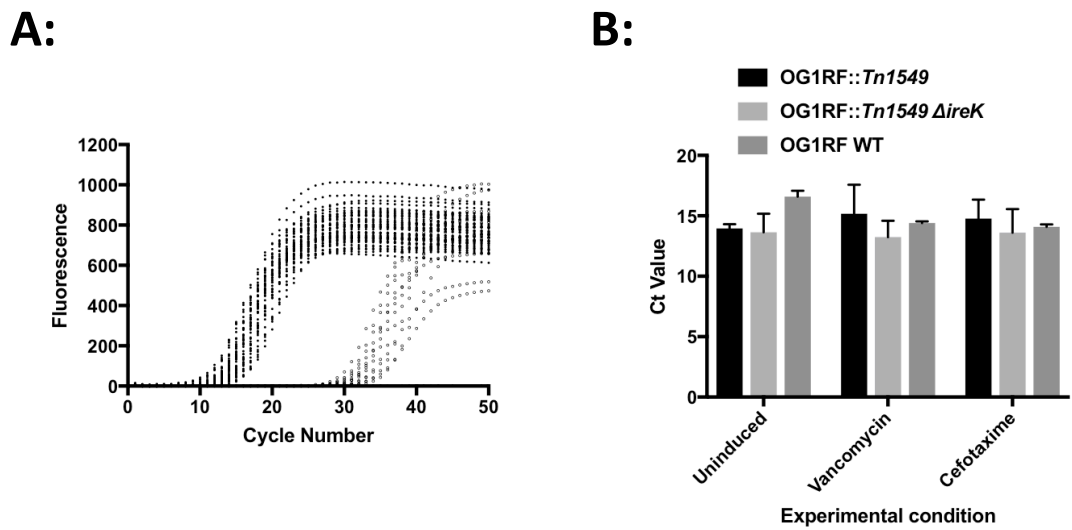
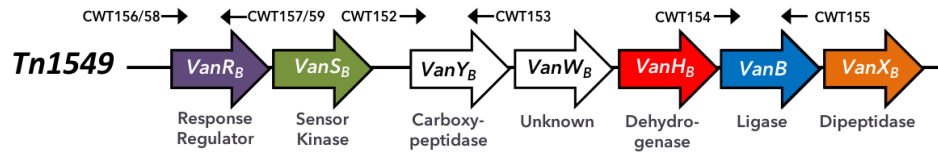


**Figure 3.2: 16S ribosome gene transcription profile via qPCR experiments in various OG1RF strains under different experimental conditions.** A: Real time amplification plot of 16S ribosomal gene after generation of cDNA with reverse transcriptase (filled circles – positive control) and without reverse transcriptase (open circles – negative control). This shows that amplification of the 16S ribosome gene is from amplification of cDNA and not contaminating genomic DNA B: Comparison of cycle threshold (Ct) values for each strain and experimental condition in technical triplicate and experimental duplicate. Error bars show standard deviation between experimental replicates.

To compare the effect of the Tn1549 structural genes primers for *vanY* and *vanB* were designed and to also evaluate the effect of the TCS genes, primers for *vanR* were also designed (**Figure 3.3**). In cells challenged by a sub-inhibitory amount of vancomycin, a strong induction of expression of both *vanY* and *vanB* is observed as expected given the inducible nature of Tn1549 vancomycin resistance. Interestingly there is expression of VanR in both the uninduced and cefotaxime experiment but not to the same scale as vancomycin. When challenged with a sub-inhibitory concentration of cefotaxime, no apparent induction of the *vanR*, *vanY* or *vanB* in the OG1RF::Tn1549 strain was detected. There is no apparent transcriptional enhancement of the Tn1549 vancomycin resistance structural genes in the presence of cefotaxime. Interestingly, there is no noticeable difference in expression of the *van* genes when comparing the OG1RF::Tn1549 and OG1RF::Tn1549 ΔireK strains. **Figure 3.4** summarises the qPCR results demonstrating that the Tn1549 structural genes are not induced in the presence of cephalosporin's.

**A:**



**B:**

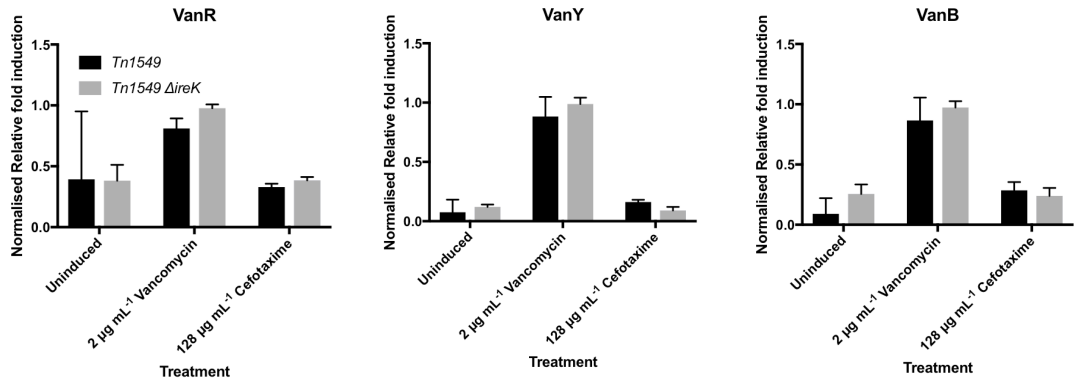
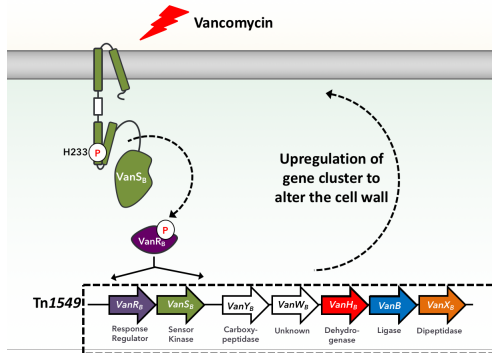


**Figure 3.3: Inducing transcriptional expression of the *Tn1549* structural genes on OG1RF::*Tn1549* and OG1RF::*Tn1549* *ΔireK* strains.** (A) Representation of the *Tn1549* cassette and genes associated with vancomycin resistance and regions for qPCR primers. (B) Normalised relative fold induction for each experimental condition and gene target in biological duplicate and technical triplicates. Error bars show standard deviation between biological replicates.

**A:**



**B:**

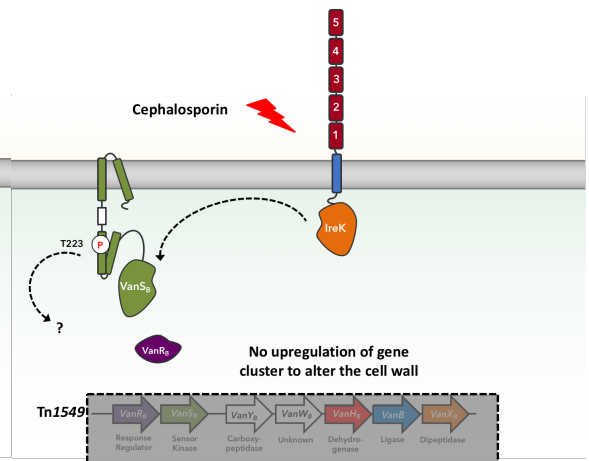


**Figure 3.4: Developing model for the role of *Tn1549* in cephalosporin resistance.** (A) In response to vancomycin, the VanS<sub>B</sub> HK phosphorylates the VanR<sub>B</sub> RR which activates the transcription of the *van* genes to modify the cell wall to increase their resistance to vancomycin. (B) Cephalosporin stimulates expression of genes that likely modify peptidoglycan to increase resistance to cephalosporins. This enhanced resistance requires VanS<sub>B</sub> and IreK which phosphorylates VanS<sub>B</sub> but does not trigger the upregulation of the *van* genes.

### 3.6. Identifying possible substrates of VanS<sub>B</sub>

As previously demonstrated, IreK has been shown *in vitro* to interact and phosphorylate the T223 residue on VanS<sub>B</sub>. Likewise, it has been demonstrated that in OG1RF with the Tn1549 cassette, enhanced cephalosporin is exhibited, but this phenotype is not demonstrated in JH2-2. The enhanced cephalosporin resistance in OG1RF Tn1549 is lost in an OG1RF Tn1549  $\Delta ireK$  strain. Cross talk between eSTKs and TCS has been shown previously and was discussed earlier. To identify potential targets of VanS T223 phosphorylation, the TCS of OG1RF and JH2-2 were compared. Of the 16 TCSs identified in OG1RF all but two were identified in JH2-2 draft genome sequence. These include TCS associated with RR10 and RR12 of the V538 and OG1RF genome. RR10 is involved in stress response and the upregulation of virulence factors (Hancock and Perego, 2002). RR12 is a homologue of the *E. faecium* RR DdcR which has been implicated in reprogramming of the cell wall by upregulating the protein DdcY, a homologue of VanY to generate a population of tetrapeptide lipid II substrates for Ldt<sub>fm</sub> for 3-3 PG crosslinking (D,D-transpeptidase) instead of 3-4 protein crosslinking (L,D-transpeptidase) (Sacco *et al.*, 2014). Although the counterpart DdcY is located in OG1RF, it is not present in the draft genome of JH2-2. To understand the potential effects of IreK phosphorylation of position T223 in the context of DdcY and its associated TCS, qPCR primers were designed to target *ddcR* and *ddcY* transcriptional upregulation in the conditions and strains described previously. **Figure 3.5** highlights the difference between each strain and each experimental condition and were calculated using the  $\Delta\Delta ct$  value with respect to the uninduced sample and the 16S ribosome housekeeping gene.

In both the vancomycin and the cefotaxime experiments there is an upregulation in the transcription of *ddcR* and *ddcY* in the OG1RF::Tn1549 strain. In the OG1RF::Tn1549  $\Delta ireK$  strain there is no comparable expression of the *ddcR* and *ddcY* transcripts with regards to the OG1RF::Tn1549 strain but is comparable to the OG1RF WT strain where the Tn1549 cassette is not present. From these early experiments it can be suggested that the Tn1549 cassette, the *ireK* gene and the DdcSR TCS upregulating DdcY are important components of enhanced cephalosporin resistance in the OG1RF isogenic series (**Figure 3.6**). This also highlights a reason why the JH2-2 isogenic series did not exhibit enhanced cephalosporin resistance due to the lack of a full DdcSR TCS and DdcY.

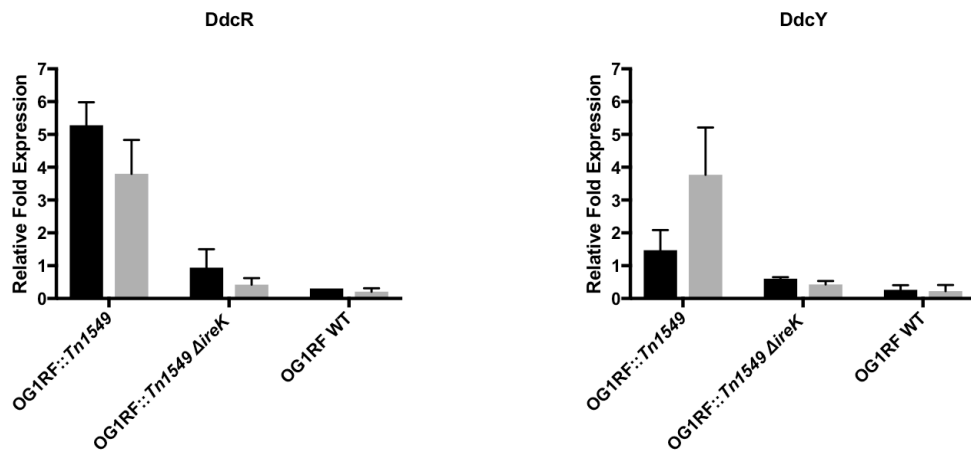


**Figure 3.5: The Tn1549 cassette, IreK and the DdcSR/DdcY TCS are essential for enhanced cephalosporin resistance.** Relative fold expression determined by  $\Delta\Delta ct$  values against 16S ribosome housekeeping gene and uninduced sample. Experimental conditions include  $2 \mu\text{g mL}^{-1}$  vancomycin and  $128 \mu\text{g mL}^{-1}$  cefotaxime at  $37^\circ\text{C}$ . Each experimental condition and gene target in biological duplicate and technical triplicates. Error bars show standard deviation between biological replicates.

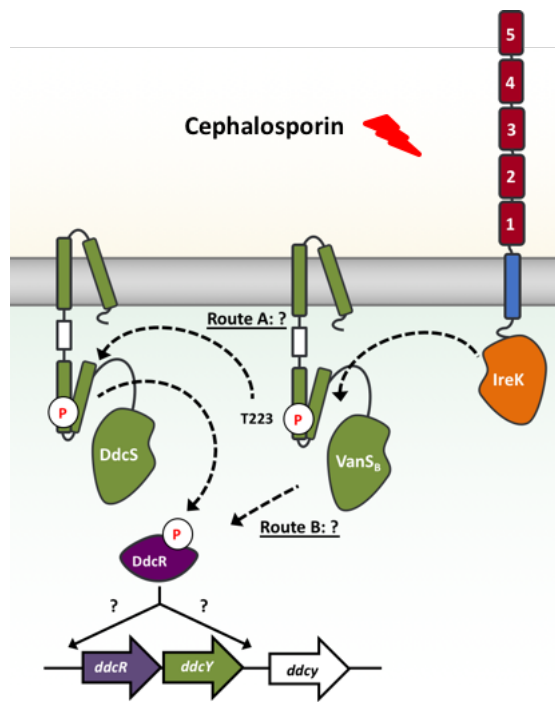


**Figure 3.6: Schematic for possible TCS crosstalk leading to enhanced cephalosporin resistance.** IreK phosphorylates VanS<sub>B</sub> on residue Thr 223 and cross phosphorylation could either phosphorylate the DdcS protein for subsequent DdcR phosphorylation (Route A) or VanS<sub>B</sub> directly phosphorylates DdcR for upregulation of DdcY which is a carboxypeptidase and alters the overall PG architecture. Sites for the DdcR promoter are yet to be identified, but like other TCS it is expected to be before the RR (*ddcR*) and substrate targets (*ddcY*).



of strain backgrounds include *ΔireK* strains. In the WT OG1RF strain and its *ΔireK* variant that MIC for Cefotaxime was slightly reduced in the presence of staurosporine, however in the OG1RF::Tn1549 background there was a marked decrease of 256-fold in the presence of 50 μM staurosporine. This effect abolished the resistance to cefotaxime and returned it to essentially WT levels (**Table 3.7**).

**Table 3.3: Comparison of isogenic strains of *E. faecalis* OG1RF and the effect of staurosporine.**

Experiments were in accordance to CSLI protocols and performed in duplicates. MIC reported are in comparison to cefotaxime (μg mL<sup>-1</sup>)

Conc. Staurosporine	MIC (μg mL <sup>-1</sup> )			
	<i>E. faecalis</i> OG1RF WT	<i>E. faecalis</i> OG1RF <i>ΔireK</i>	<i>E. faecalis</i> OG1RF Tn1549	<i>E. faecalis</i> OG1RF Tn1549 <i>ΔireK</i>
0 μM	2	0.0625	256	1
50 μM	0.125	0.03125	1	0.5

### 3.7.2. Staurosporine and *ΔireK* confer similar phenotype

To further explore the effect of staurosporine, each OG1RF strain was incubated in a growth curve experiment with and without staurosporine (**Figure 3.8**). In each strain, the presence of staurosporine caused a decrease in the overall OD in comparison to WT strains but staurosporine did not prevent cell growth. When comparing OG1RF with staurosporine and OG1RF *ΔireK* strains it appears that staurosporine is targeting *ireK* as the growth profiles are similar between each experiment. Likewise, a similar trend can be observed between OG1RF::Tn1549 with staurosporine and OG1RF::Tn1549 *ΔireK* without but not to the same effect. This might be due to factors of the Tn1549 cassette that are not well described in the stationary phase.

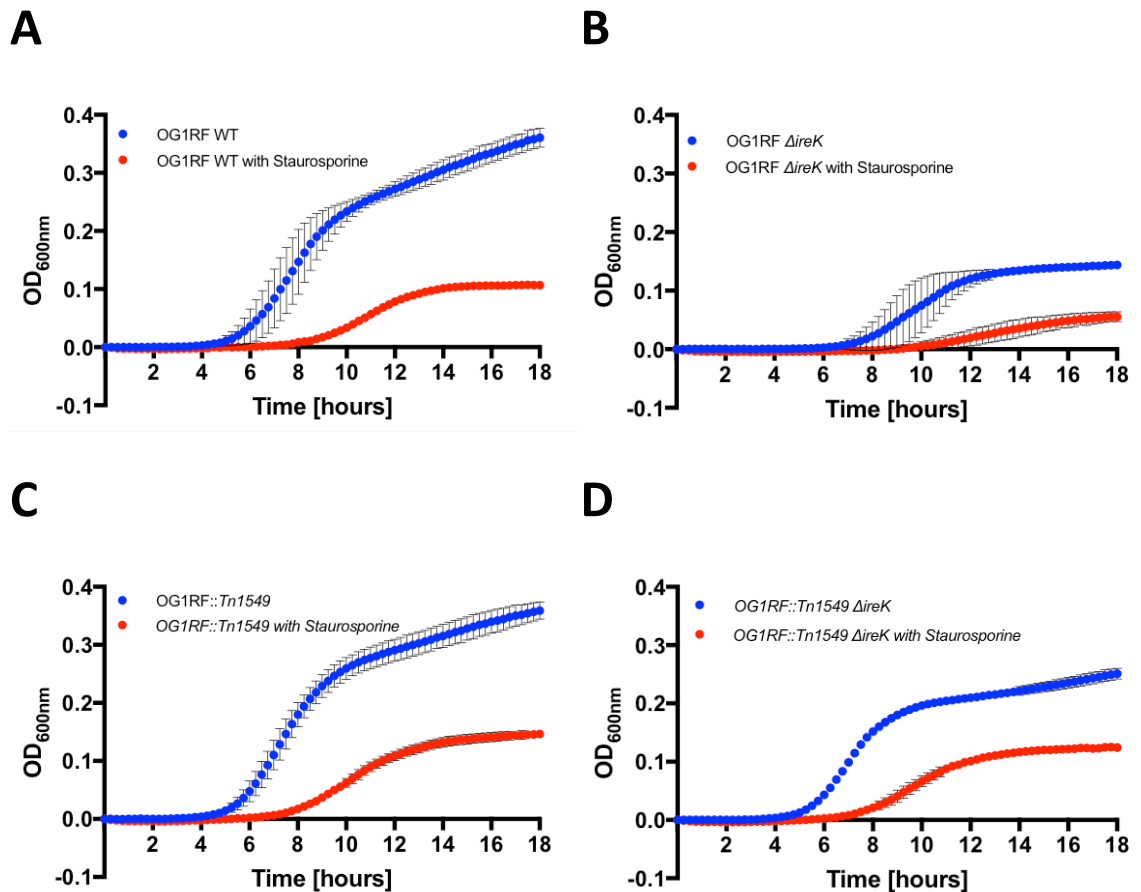


**Figure 3.8: Growth curves of OG1RF isogenic strains without (Blue) and with (Red) 50 µM staurosporine in MHII broth. (A) OG1RF WT, (B) OG1RF  $\Delta ireK$  (C) OG1RF::Tn1549 and (D) OG1RF::Tn1549  $\Delta ireK$ . Samples were incubated at 37°C and OD was recorded every 15 minutes with brief shaking before each read. Experiments were performed in duplicates with the mean represented by individual data points and standard deviation error bars.**

### 3.7.3. Enhanced cephalosporin resistant is observed in other VanB type genotypes and species and can be restored using staurosporine

This analysis was extended to a range of other vancomycin resistant *E. faecalis* and *E. faecium* strains. The two genotypes of greatest clinical importance are *vanA* (resistant to vancomycin and teicoplanin) and *vanB* (resistant to vancomycin only), with three alleles of the *vanB* ligase gene (*vanB1*, *vanB2*, and *vanB3*) (Ballard *et al.*, 2005). Both the *vanA* and the *vanB* operons are associated with transposons, and the transfer of resistance among enterococci appears to be mediated via acquisition of these elements. Although the *vanA* operon is located on the transposon, Tn1546, three transposons have been described that contain the *vanB* operon: Tn1547, Tn5382, and Tn1549 (Ballard *et*

*al.*, 2005). To demonstrate the effect that IreK has on enhanced cephalosporin across acquired vancomycin strains, the effect using cefotaxime resistance in the presence of staurosporine against VanA strains of *E. faecium* (Tn1546) and VanB strains of both *E. faecalis* and *E. faecium* including that of the *vanB1* allele (Tn1547) and the *vanB2* allele (Tn1549) was compared (Table 3.7). In all strains tested, staurosporine restored the sensitivity of otherwise intrinsically and acquired resistant enterococcal strains to cefotaxime.

**Table 3.7: Comparison of multiple *Enterococcus* spp. strains with acquired Van resistance cassettes and the effect of staurosporine in each strain.** Experiments were in accordance to CSLI protocols and performed in duplicates. MIC reported are in comparison to cefotaxime ( $\mu\text{g mL}^{-1}$ ). The *vanA* strain tested is highlighted in grey.

Conc. Staurosporine	MIC ( $\mu\text{g mL}^{-1}$ )				
	<i>E. faecalis</i> OG1RF Tn1549 ( <i>vanB1</i> )	<i>E. faecalis</i> JH2-2 Tn1549 ( <i>vanB1</i> )	<i>E. faecium</i> BM4525 Tn1549 ( <i>vanB1</i> )	<i>E. faecalis</i> ATCC 51299 Tn15482 ( <i>vanB2</i> )	<i>E. faecium</i> ATCC 700221 Tn1546 ( <i>vanA</i> )
0 $\mu\text{M}$	256	1024	1024	1024	2048
50 $\mu\text{M}$	1	1	4	0.125	2048

#### 3.7.4. Other potential eSTK kinase inhibitors

Although staurosporine has been demonstrated here and elsewhere as an inhibitor of eSTKs in most Gram-positive bacteria, it probably has little therapeutic potential due to its promiscuity to eukaryotic kinases. In a previous study looking at the eSTK in *Listeria monocytis*, a kinase screen has revealed a potential new inhibitor structurally different to staurosporine called AZD5438, (a CDK inhibitor) and showed to act synergistically with  $\beta$ -lactam antibiotics against *L. monocytis* (Pensinger *et al.*, 2014) (Figure 3.9). In this study I observed that AZD5438 is an inhibitor of IreK in OG1RF Tn1549 strains and works synergistically with the  $\beta$ -lactam cephalosporin, cefotaxime (Table 3.8). Although staurosporine appears to have a stronger effect, AZD538 is a synthetic compound and not a natural product like staurosporine.

**Table 3.8: Comparison of non-staurosporine kinase inhibitors in the presence of increasing concentrations of cefotaxime ( $\mu\text{g mL}^{-1}$ ).** Tested on OG1RF *Tn1549* with kinase inhibitors diluted in 5-fold dilutions from 50  $\mu\text{M}$ . Experiments were in accordance to CSLI protocols and performed in duplicates.

Concentration of Compound	MIC ( $\mu\text{g mL}^{-1}$ ) OG1RF <i>Tn1549</i>		
	AZD5438	UCN01	Staurosporine
0 $\mu\text{M}$	256	256	256
0.4 $\mu\text{M}$	256	256	256
2 $\mu\text{M}$	256	256	124
10 $\mu\text{M}$	16	256	8
50 $\mu\text{M}$	2	256	1

As staurosporine has been a successful eukaryotic kinase inhibitor *in vitro* and has also gone through phase I and II clinical trials, many derivatives of staurosporine have been isolate or synthesised. For example, UCN-01, a staurosporine derivative was also tested. However, there was no difference in MIC against cefotaxime in the presence of UCN-01 at any concentration. The single difference between staurosporine and UCN-01 is the presence of a single hydroxyl group suggesting a structure-activity relationship (SAR) between these compounds (**Figure 3.9**). Although not tested in this context UCN-01 may target IreK but there might be pharmacokinetics problems targeting IreK *in vivo*.

Other inhibitors that were also explored included a GSK published kinase inhibitor set (Knapp *et al.*, 2013; Bramson *et al.*, 2001; Stevens *et al.*, 2008; Tang *et al.*, 2003). This list includes 376 compounds in the hope to better identify new targets for these inhibitors. 30 of the 376 compounds were selected as they were strong inhibitors of CDK2 which has already been demonstrated to have strong homology to IreK (**Figure 3.7**). The structures and identity of each compound are highlighted in (**Chapter 8: Appendix 8.2**). In an experiment similar to that demonstrated in **Table 3.8**, 0  $\mu\text{M}$ , 0.4  $\mu\text{M}$  and 4  $\mu\text{M}$  was incubated with increasing concentrations of cefotaxime. No difference in MIC was observed with the two concentrations of each inhibitor. Like UCN-01, these inhibitors may target IreK but there might be pharmacokinetics problems targeting IreK *in vivo*.

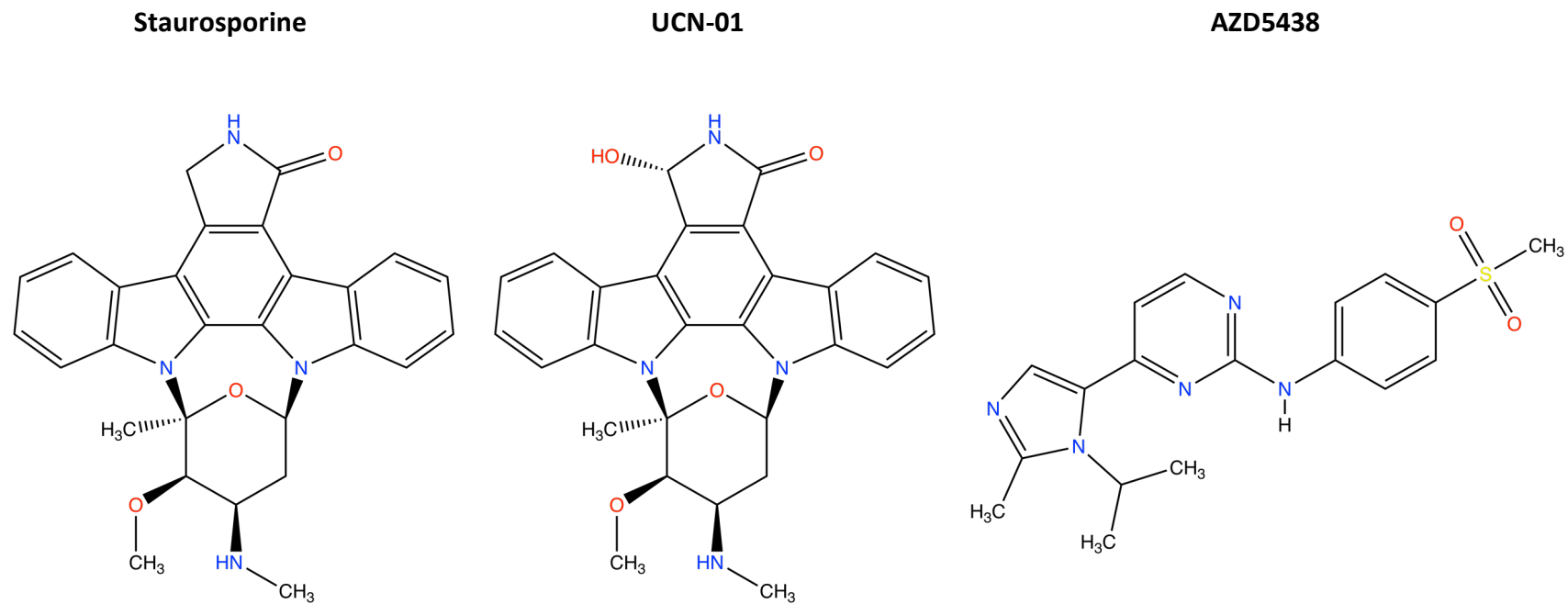


**Figure 3.9: Structural comparison of eukaryotic kinase inhibitors that are potential prokaryotic eSTK inhibitors. Left: Staurosporine, Centre: UCN-01 and Right: AZD548.**

## 3.8. Exploring the contribution of each IreK domain on enhanced cefotaxime resistance

To understand the role of IreK in enhanced cephalosporin resistance, a series of complementation experiments with different mutations and truncations made in the IreK gene. Complementation experiments are advantageous over creating chromosomal mutants as creating chromosomal mutants is often time consuming and the creation of a mutant, truncation or chimera is not guaranteed.

### 3.8.1. Background into the inducible complementation system

The complementation experiments used in this study were performed in the Plasmid TetH a kind gift from Stephane Mesnage. The plasmid is selective ( $Erm_{30}$ ) and can be readily transformed into electrocompetent *E. faecalis* cells. The plasmid enables tuneable expression of a gene of interest in a tetracycline inducible system (**Figure 3.10**). Tetracycline inducible systems offer advantages over other inducible systems such as metal ions as it is not confounded by secondary effects when anhydrotetracycline is used. Anhydrotetracycline binds the tetracycline repressor (TetR) 35-fold more strongly than tetracycline (Gossen and Bujard, 1993; Degenkolb *et al.*, 1991). Anhydrotetracycline also binds poorly to the 30S ribosomal subunit compared to tetracycline so therefore shows very poor antibiotic activity (Rasmussen *et al.*, 1991).

The TetH plasmid can be described as a Tetracycline “on” system where TetR induction is activated in the presence of anhydrotetracycline and binds to the tetracycline operator (*tetO*). In contrast, the tetracycline “off” system works when the presence of anhydrotetracycline causes reduced expression of the gene of interest by binding TetR. The Tet “on” functions by amino acid point mutations in the TetR that led to resilience in the presence of tetracycline for induction rather than repression (Gossen *et al.*, 1995). The *tetO* is a 19-nucleotide promoter sequence upstream of the gene of interest and is recognised by TetR. Without the anhydrotetracycline, TetR is unable to bind to the *tetO* (**Figure 3.11.A**). Binding of anhydrotetracycline by TetR enables the protein to bind *tetO* and enable expression of the gene of interest (**Figure 3.11.B**). The system is inducible and enables tight regulation of the gene of interest.

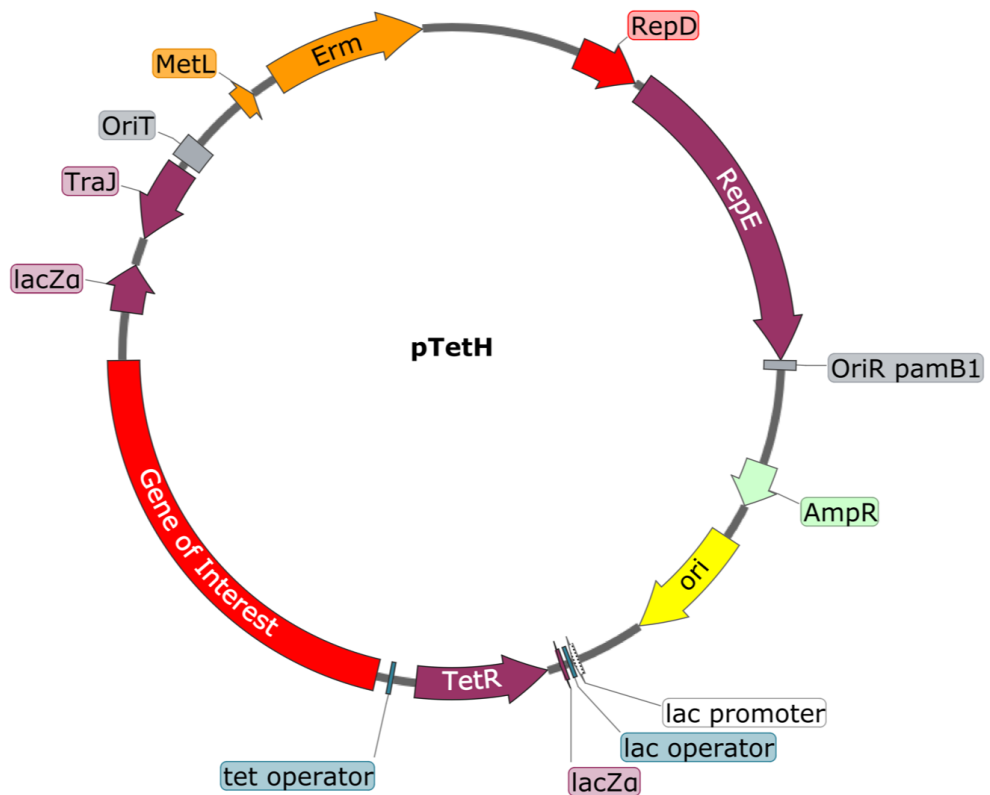
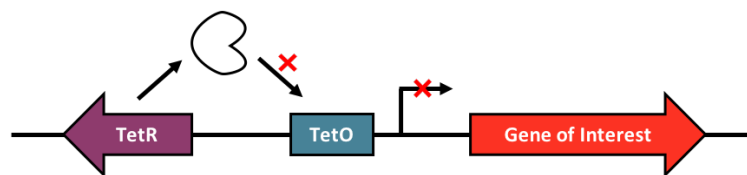


**Figure 3.10: TetH Plasmid map highlighting the key features of the plasmid.** The gene of interest is cloned via Gibson assembly into the region highlighted in red. This plasmid was a kind gift from Dr. Stephane Mesnage, The University of Sheffield.

**A:**



**B:**

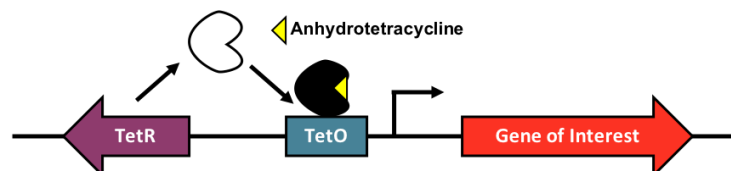


**Figure 3.11: A tetracycline inducible system for tuneable expression of a gene of interest. (A)** No anhydrotetracycline present results no transcription of the gene of interest as TetR cannot bind the *tetO*. **(B)** In the presence of anhydrotetracycline transcription of the gene of interest is permitted as TetR is activate when bound to anhydrotetracycline and can bind to *tetO* (Gossen *et al.*, 1995).

### 3.8.2. Increasing anhydrotetracycline can tune *ireK* expression

Iso-sensitest was used instead of Muller Hinton II as complementation was not achieved in Muller Hinton II. Iso-sensitest is another media used frequently in testing antibiotic susceptibility and is often employed to overcome issues in MHII (Koeth *et al.*, 2000).

#### 3.8.2.1. Testing complementation using E-test strips

To initially screen the enhanced cephalosporin phenotypes of the TetH-*ireK* plasmid in an OG1RF::Tn1549  $\Delta ireK$  strains, the bacteria were plated onto Iso-sensitest agar plates following EUCAST protocols (**Figure 3.12**). The plates contained different concentrations of anhydrotetracycline and were tested using a ceftazidime E-test strip. The OG1RF::Tn1549 and OG1RF::Tn1549  $\Delta ireK$  strains shows a clear phenotype which is comparable to previous observations (256 and 8  $\mu\text{g mL}^{-1}$  ceftazidime respectively). Increasing concentrations of anhydrotetracycline shows an increase in ceftazidime resistance. These results using the E-test strips demonstrate that anhydrotetracycline can successfully induce the complementation of *ireK* to demonstrate enhanced cephalosporin resistance similar to a OG1RF::Tn1549 strain.

The limitations of this methods include the range of the ceftazidime E-test strip from 0.05 to 256  $\mu\text{g mL}^{-1}$  which could be out of range of the MIC needed to be detected. Likewise, previous MIC determination have been undertaken in broth and are more directly comparable. Also, Macro colonies can be observed in some of the experiments with high concentrations of anhydrotetracycline and therefore makes interpretation of the true MIC difficult as reported by the manufacture of the E-test strips and the clinical standards agency (Oxoid and EUCAST respectively).

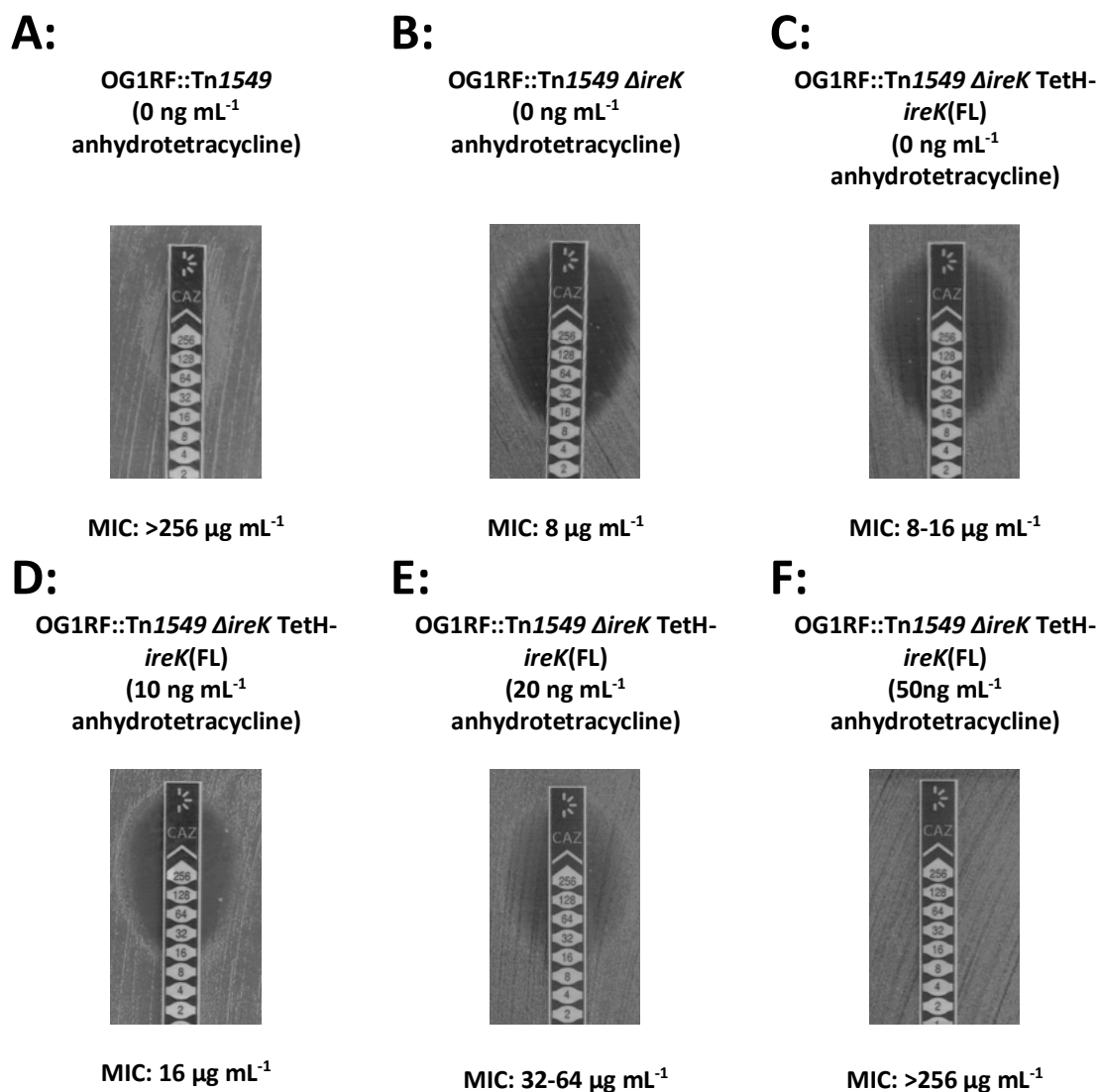


**Figure 3.12: Testing the effect of anhydrotetracycline complementation using E-test strips.** MIC determination of OG1RF Tn1549, OG1RF::Tn1549  $\Delta$ ireK in comparison to OG1RF::Tn1549  $\Delta$ ireK TetH-ireK(FL) with different concentration of anhydrotetracycline following EUCAST protocol for MIC determination using EUCAST with E-test strips. (A) OG1RF Tn1549, (B) OG1RF::Tn1549  $\Delta$ ireK, (C) OG1RF::Tn1549  $\Delta$ ireK-TetH-ireK(FL) (0 ng mL<sup>-1</sup>), (D) OG1RF::Tn1549  $\Delta$ ireK-TetH-ireK(FL) (10 ng mL<sup>-1</sup>), (E) OG1RF::Tn1549  $\Delta$ ireK-TetH-ireK(FL) (20 ng mL<sup>-1</sup>), (F) OG1RF::Tn1549  $\Delta$ ireK-TetH-ireK(FL) (50 ng mL<sup>-1</sup>). Experiments were performed in duplicates with MIC ranges displayed under each figure.

To confirm the effect of the MIC phenotype from the E-test strips on Iso-sensitest agar and improve experimental conditions, different concentrations of anhydrotetracycline with either cefotaxime or ceftazidime was measured though microdilution series in Iso-sensitest broth. Initial experiments indicated that a much

lower concentration of anhydrotetracycline was required to complement *ireK* back to WT levels (Data not shown). The concentrations of anhydrotetracycline were adjusted accordingly and MIC using the TetH-*ireK* construct (CWT050) in OG1RF::Tn1549  $\Delta$ *ireK* were compared to OG1RF isogenic strains in a Tn1549 background (Table 3.9). In presence of both antibiotics, in the absence of anhydrotetracycline an MIC is achieved that is higher when compared to the OG1RF::Tn1549  $\Delta$ *ireK* and indicated leaky expression. In the presence of both antibiotics full complementation is achieved at a concentration of 20 ng mL<sup>-1</sup> and in the case of cefotaxime, goes beyond WT MIC levels of cefotaxime. This initially shows that IreK has a tuneable effect on enhanced cephalosporin resistance. The results from these experiments allows other mutants of *ireK* to be measured at the assumed WT levels of IreK expression with 20 ng mL<sup>-1</sup>.

**Table 3.9: MIC determination of OG1RF Tn1549, OG1RF::Tn1549  $\Delta$ *ireK* in comparison to OG1RF::Tn1549  $\Delta$ *ireK* TetH-*ireK*(FL) with different concentrations of anhydrotetracycline in Iso-sensitest broth.** Samples were incubated at 37°C without shaking and without Erm<sub>30</sub> present. Includes OG1RF Tn1549, OG1RF::Tn1549 and OG1RF::Tn1549  $\Delta$ *ireK*-TetH-*ireK*(FL) at different concentrations anhydrotetracycline ranging from 0-25 ng mL<sup>-1</sup>. Experiments were performed in duplicates with MIC ranges reported for either cefotaxime or ceftazidime in  $\mu$ g mL<sup>-1</sup>

MIC Cefotaxime ( $\mu$ g mL <sup>-1</sup> )					
Concentration of anhydrotetracycline	0 ng mL <sup>-1</sup>	5 ng mL <sup>-1</sup>	10 ng mL <sup>-1</sup>	20 ng mL <sup>-1</sup>	25 ng mL <sup>-1</sup>
OG1RF Tn1549	512	512	512	512	512
OG1RF::Tn1549 $\Delta$ <i>ireK</i>	8	8	8	8	8
OG1RF::Tn1549 $\Delta$ <i>ireK</i> TetH- <i>ireK</i> (FL)	256	512	512	512	1024
MIC Ceftazidime ( $\mu$ g mL <sup>-1</sup> )					
Concentration of anhydrotetracycline	0 ng mL <sup>-1</sup>	5 ng mL <sup>-1</sup>	10 ng mL <sup>-1</sup>	20 ng mL <sup>-1</sup>	25 ng mL <sup>-1</sup>
OG1RF Tn1549	2048	2048	2048	2048	2048
OG1RF::Tn1549 $\Delta$ <i>ireK</i>	32	32	32	32	32
OG1RF::Tn1549 $\Delta$ <i>ireK</i> TetH- <i>ireK</i> (FL)	128	1024	1024	2048	2048

### 3.8.3. Complementation experiments of various IreK constructs

To test the contribution of either the kinase or PASTA domains of IreK in *E. faecalis*, various mutants and constructs were designed and synthesised using the TetH-

*ireK*(FL) plasmid (pCWT050) as the backbone vector. These constructs were electroporated into OG1RF::Tn1549  $\Delta$ *ireK* strains and selected on Erm<sub>30</sub> plates. To gain an understanding into the contribution of each domain, the enhanced cephalosporin resistance was phenotypically tested for each construct and compared to OG1RF::Tn1549, OG1RF::Tn1549  $\Delta$ *ireK* and Tn1549  $\Delta$ *ireK* TetH-*ireK*(FL) (Table 3.10). Each complementation strain was induced with 20 ng mL<sup>-1</sup> anhydrotetracycline. Ceftazidime was used to test each of the different constructs as it had the strongest MIC that was in a detectable range and was thought to give the largest difference if any between each construct using the micro-dilution MIC method.

**Table 3.4: Complementation of different *ireK* constructs in the complementation plasmid under 20 ng mL<sup>-1</sup> anhydrotetracycline in Iso-sensitest media.** (Experiments performed in duplicates). Green – KD, Blue – TM, Red – *E. faecalis* PASTA, Yellow - Substituted PASTA.

Schematic of Construct	Construct Description (OG1RF)	MIC Ceftazidime ( $\mu$ g mL <sup>-1</sup> )
	Tn1549	2048
	Tn1549 $\Delta$ <i>ireK</i>	32
	Tn1549 $\Delta$ <i>ireK</i> TetH- <i>ireK</i> (FL)	2048
	Tn1549 $\Delta$ <i>ireK</i> TetH- <i>ireK</i> (No Pasta)	128
	Tn1549 $\Delta$ <i>ireK</i> TetH- <i>ireK</i> (K41R)	32
	Tn1549 $\Delta$ <i>ireK</i> TetH- <i>ireK</i> (No Kinase)	32
	Tn1549 $\Delta$ <i>ireK</i> TetH- <i>ireK</i> (PASTA 1-5 minus peptide)	2048
	Tn1549 $\Delta$ <i>ireK</i> TetH- <i>ireK</i> (PASTA 1-4)	2048
	Tn1549 $\Delta$ <i>ireK</i> TetH- <i>ireK</i> (PASTA 1-3)	2048
	Tn1549 $\Delta$ <i>ireK</i> TetH- <i>ireK</i> (PASTA 1-2)	1024
	Tn1549 $\Delta$ <i>ireK</i> TetH- <i>ireK</i> (PASTA 1)	1024
	Tn1549 $\Delta$ <i>ireK</i> TetH- <i>ireK</i> (PASTA 4-5)	2048
	Tn1549 $\Delta$ <i>ireK</i> TetH- <i>ireK</i> ( <i>S. aureus</i> PASTA)	1024
	Tn1549 $\Delta$ <i>ireK</i> TetH- <i>ireK</i> ( <i>B. subtilis</i> PASTA)	512

When testing each of the TetH inducible constructs containing either a different mutant or truncation, the most significant differences were apparent when a whole domain was truncated (Kinase (KD) or PASTA). The truncation of the KD showed a large decrease in MIC that mirrored Tn1549 *DireK* levels at 32  $\mu\text{g mL}^{-1}$ . This illustrates the role of the kinase in phosphorylating other protein targets to cause enhanced cephalosporin resistance. Of particular note in **Table 3.10** is the K41R mutation in the FL IreK construct. Initial characterisation of the eSTK in *B. subtilis* revealed that a mutation of residue K40 to K40R removed the enzymatic activity of the protein (Madec *et al.*, 2002). This residue was constructed following alignment of the *B. subtilis* study and the K40 residue was aligned and homologous to the IreK amino acid sequence (K41). This mutation was also constructed in the Tn1549 *DireK TetH-ireK* (FL) and demonstrated how critical this amino acid residue is on enzymatic activity as it caused the FL protein to become inactive in the enhanced cephalosporin phenotype experiment.

Removal of all the PASTA domains (Tn1549 *DireK TetH-ireK* (No Pasta)) resulted in a sharp decrease in MIC from 2048 to 128  $\mu\text{g mL}^{-1}$  when compared directly with OG1RF::Tn1549 and Tn1549 *DireK TetH-ireK* (FL). Although the removal of all the PASTA domains does not result in a Tn1549 *DireK* MIC phenotype (32  $\mu\text{g mL}^{-1}$  ceftazidime), this may be attributed to the ability of the kinase domain to self oligomerize independently of the PASTA domains and that the role of the PASTA domains is to concentrate the kinase domain of the protein in a particular location in the *E. faecalis* cell. In a study comparing the role of the IreK homologue in *S. aureus* PknB, two virulent strains were compared, including COL and USA300 (Tamber *et al.*, 2010). Interestingly COL had a point mutation on the gene for PknB that resulted in a stop codon being introduced resulting in the truncation of the PASTA domains. When comparing the antibiotic resistance between both strains, it was suggested that the kinase alone was sufficient for antibiotic resistance.

Truncation of each individual PASTA domain resulted in a phenotype that was similar to OG1RF::Tn1549 MIC levels to ceftazidime (1024-2048  $\mu\text{g mL}^{-1}$ ) and that a single PASTA domain (Tn1549 *DireK TetH-ireK* (PASTA 1)) was sufficient to complement to WT levels. Therefore, the number of PASTA domains present in *E. faecalis* is not directly linked to the enhanced cephalosporin resistance observed in this study and indicated that they may have a separate role. A recent paper has suggested that the PASTA domains

may act as a “molecular ruler” and monitor the thickness of the PG in growing cells. This was demonstrated in *S. pneumoniae* and the removal of each PASTA domain resulted in a decrease in PG thickness (Zucchini *et al.*, 2018). It has also been recently demonstrated that in *E. faecalis* OG1 WT strains with various PASTA chromosomal truncations, that there is not much of a change in MIC against ceftriaxone with each truncation and is consistent with the phenotype observed here (Labbe and Kristich, 2017). In a previous study looking at the IreK homologue in *E. faecium*, a long C-terminal S/T terminal peptide is present and was suggested to interfere with PASTA oligomerisation (Desbonnet *et al.*, 2016). This motif is also present in *E. faecalis* but is much shorter. A truncation of this Ser/Thr terminal peptide was also constructed in IreK but showed no difference in MIC.

To explore the role of PASTA domains in the context of enhanced cephalosporin resistance further, the PASTA domains from *E. faecalis* were substituted with either the PASTA domains from *S. aureus* PrkC (containing 4 PASTA domains) or *B. subtilis* PrkC (containing 3 PASTA domains). Although the *S. aureus* PASTA domains did not show a large difference in MIC compared to *E. faecalis* IreK PASTA domains ( $1024 \mu\text{g mL}^{-1}$ ), there was a modest difference between the *B. subtilis* PASTA domains in IreK ( $512 \mu\text{g mL}^{-1}$ ). It has been suggested and shown in a different study that PASTA domains can bind PG directly and upregulate a cellular response when changes in the extracellular environment are detected (Shah *et al.*, 2008). The major difference between *E. faecalis* and *S. aureus* is the PG cross linking stem (L-ala<sub>2</sub> and G<sub>5</sub> respectively) and the major difference between *E. faecalis* and *B. subtilis* is amidation in the second position, the 3<sup>rd</sup> position in the pentapeptide stem (Lys and Dap respectively) and therefore no crosslinking stem is present in *B. subtilis*.

There are also modifications of the glycan strands that can occur between each species including *N*-deacetylation (*B. subtilis*) and *O*-acetylation of the MurNAc residue (*E. faecalis* and *S. aureus*) (Vollmer, 2008). Therefore, the difference in MIC observed in this experiment with the PASTA domains substitutions might be due to the variation in the PG between each species.

### 3.9. Localisation of IreK in inducible complementation experiments

As discussed previously, the largest difference in enhanced cephalosporin resistance with regards to the PASTA domains comes from the removal of all PASTA domains in comparison to the full length IreK (MIC 2048 to 128  $\mu\text{g mL}^{-1}$  ceftazidime respectively). A single PASTA domain was enough to almost follow a phenotype of a FL IreK construct. It has been established in *M. tuberculosis* and *S. pneumonia* that PASTA repeats are required for cellular division and localisation to the mid-cell (Mir *et al.*, 2011; Giefing *et al.*, 2010). As *E. faecalis* has the most PASTA domains of any known eSTK in Gram-positive bacteria, the localisation of IreK was explored. To decipher the role of the PASTA repeats in localisation, the PASTA repeats were deleted, or substituted from other bacterial species. The role of the kinase in localisation was also explored. The TetH vector construct used previously was also used for testing localisation of IreK.

#### 3.9.1. Identification of valid fluorescent fusion constructs

To ensure that the addition of a fluorescent protein fusion did not impact on the overall function of IreK, the fluorescent protein had to have minimal oligomeric activity. Homologues of IreK are active oligomers and it was important that the activity was not contributed or impeded by the addition of the fluorescent protein (Barthe *et al.*, 2010). A recent study quantitatively characterised the brightness, photo stability, pH stability and oligomeric properties of 40 fluorescent proteins (Cranfill *et al.*, 2016). Enhanced GFP was the fluorescent protein of choice as it is frequently used in localisation studies and has been described as the gold standard of fluorescent proteins. Most fluorescent proteins are oligomeric in their natural environment so to ensure that such interactions didn't interfere with the results of the subsequent experiments, a A206K point mutation in the GFP domain was generated which has been shown to be mostly monomeric (98.1%) compared to WT GFP (76.5%) (Cranfill *et al.*, 2016). In another experiment, codon optimised fluorescent mTFP and mCherry for microscopy experiments has been specifically designed in *Enterococcus* spp. and were also fusions that were fused to IreK (Vickerman *et al.*, 2015).

### 3.9.2. Optimising concentration of conditions for localisation experiments

Although in localisation experiments, the effect of antibiotics was not tested, the effect of antibiotics was used to determine the right concentration of anhydrotetracycline to use as an inducer of *ireK* expression. As antibiotic susceptibility was not being tested in the context of localisation, BHI media was used instead of Iso-sensitest media. As ceftazidime has a high MIC in the complementation experiments (2048 and 32  $\mu\text{g mL}^{-1}$  respectively) and BHI is a rich media, cefotaxime was chosen as it still had a relatively large range in MIC between Tn1549 and Tn1549  $\Delta ireK$  when tested in MHII (2 and 256  $\mu\text{g mL}^{-1}$  respectively). Initial optimisation included testing the GFP fusion to full length *ireK* in TetH to map a phenotype that aligned with OG1RF::Tn1549. mEGFP, mCherry and mTFP all showed an antibiotic susceptibility phenotype that matched the phenotype of OG1RF::Tn1549  $\Delta ireK$  (1  $\mu\text{g mL}^{-1}$ ) with increasing concentrations of anhydrotetracycline. One concern was that the mEGFP construct used was not codon optimised. To overcome this issue, a codon optimised mEGFP gene was constructed using *E. faecalis* specific codon specificity.

**Table 3.11.** highlights all the constructs used to test the efficiency in the codon optimised mEGFP construct and at 20 ng mL<sup>-1</sup> anhydrotetracycline can complement to OG1RF::Tn1549 levels (512 ng mL<sup>-1</sup>). Other key mutants and truncations show previously to have a large phenotype difference and shows a similar trend in MIC profile. Like the complementation experiments describes previously, 20 ng mL<sup>-1</sup> anhydrotetracycline was sufficient to complement *ireK* to WT levels with the GFP fusion with a different media (BHI) and different antibiotic (Cefotaxime) and was used for all localisation experiments that are described.

**Table 3.5: MIC determination of OG1RF Tn1549, OG1RF::Tn1549 *ΔireK* in comparison to OG1RF::Tn1549 *ΔireK* TetH-gfp-*ireK*(FL) with different concentration of anhydrotetracycline in BHI broth.** Samples were incubated at 37°C without shaking and without Erm<sub>30</sub> present. Includes OG1RF Tn1549, OG1RF::Tn1549 and OG1RF::Tn1549 *ΔireK*-TetH-*ireK*(FL) at different concentrations anhydrotetracycline ranging from 0-25 ng mL<sup>-1</sup>. Experiments were performed in duplicate with MIC reported for either cefotaxime or cefotaxime in μg mL<sup>-1</sup>.

Concentration of anhydrotetracycline	MIC Cefotaxime (μg mL <sup>-1</sup> )				
	0 ng mL <sup>-1</sup>	5 ng mL <sup>-1</sup>	10 ng mL <sup>-1</sup>	20 ng mL <sup>-1</sup>	25 ng mL <sup>-1</sup>
<b>OG1RF Tn1549</b> 	512	512	512	512	512
<b>OG1RF::Tn1549 <i>ΔireK</i></b> 	1	1	1	1	1
<b>OG1RF::Tn1549 <i>ΔireK</i> TetH-gfp</b> 	1	1	1	1	1
<b>OG1RF::Tn1549 <i>ΔireK</i> TetH-gfp-<i>ireK</i>(FL)</b> 	1	2	64	512	512-1024
<b>OG1RF::Tn1549 <i>ΔireK</i> TetH-gfp-<i>ireK</i> (No Pasta)</b> 	1	1	2	128	256
<b>OG1RF::Tn1549 <i>ΔireK</i> TetH- gfp -<i>ireK</i> (K40A)</b> 	1	1	1	1	1
<b>OG1RF::Tn1549 <i>ΔireK</i> TetH- gfp -<i>ireK</i> (No Kinase)</b> 	1	1	1	1	1

Before testing the localisation of each construct, the TetH-*gfp-ireK* FL construct in OG1RF::Tn1549 *ΔireK* was incubated with 20 ng mL<sup>-1</sup> anhydrotetracycline in BHI, without Erm<sub>30</sub> with shaking at 37°C until and OD<sub>600nm</sub> 0.6 was reached. Samples were harvested and whole cells were extracted, lysed and loaded onto an SDS-PAGE gel and western blot performed. Blots were incubated with anti-GFP antibody and screened to ensure no protein degradation had occurred with the addition of the mEGFP fusion which was confirmed (**Figure 3.13**).

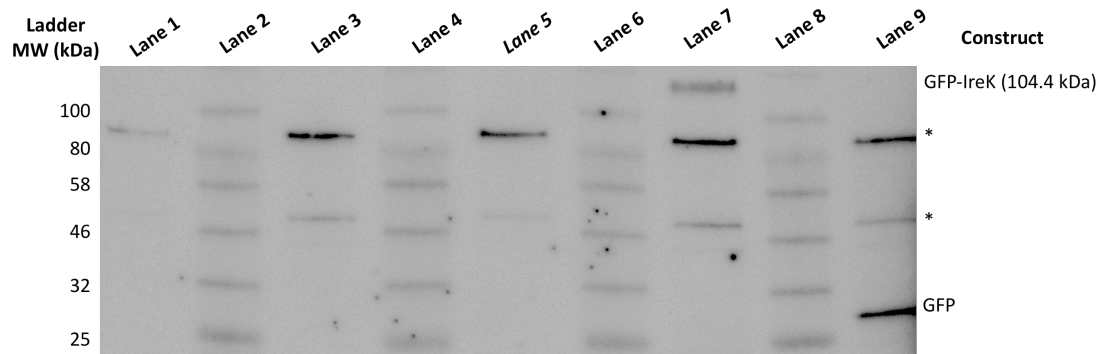


**Figure 3.13: Expression of GFP fused IreK constructs.** Expression of GFP-fused IreK via using complementation. Each construct was grown in BHI media with or without the presence of  $20 \text{ ng } \mu\text{L}^{-1}$  anhydrotetracycline to  $\text{OD}_{600}$  0.6 before harvesting and lysing for processing. Ladders are represented in Lanes 2, 4, 6 and 8 with MW represented on the left-hand side. Lane 1: *E. faecalis* OG1RF WT cells. Lane 3: OG1RF  $\Delta ireK$  cells. Lane 5: OG1RF  $\Delta ireK$  with pCWT080 complementation plasmid expressing GFP-IreK with no anhydrotetracycline. Lane 7: OG1RF  $\Delta ireK$  with pCWT080 complementation plasmid expressing GFP-IreK with  $20 \text{ ng } \mu\text{L}^{-1}$  anhydrotetracycline. Lane 9: OG1RF  $\Delta ireK$  with pCWT092 complementation plasmid expressing GFP only with  $20 \text{ ng } \mu\text{L}^{-1}$  anhydrotetracycline. Non-specific binding of antibodies is highlighted by \*. Expected MW of IreK only is 77.4 kDa.

### 3.9.3. Localisation of GFP-IreK(FL) in OG1RF strains

To establish experimental conditions that were to be replicated with each construct and strain, OG1RF delta *ireK* and OG1RF::Tn1549  $\Delta ireK$  strains were both transformed with TetH-*gfp-ireK* (FL) and TetH-*gfp* optimised and tested for localisation. Homogeneity between each cell for localisation was achieved 100 mL BHI inoculated with a 1:100 overnight culture that had been selected in the presence of  $\text{Erm}_{30}$  but no longer contained the selective antibiotic in a 250 mL conical flask, with shaking at  $37^\circ\text{C}$ . Cells were incubated for 10 minutes with the FM 4-64 which stains the membrane of the cells. **Figure 3.14** highlights the difference observed between each construct and each strain.

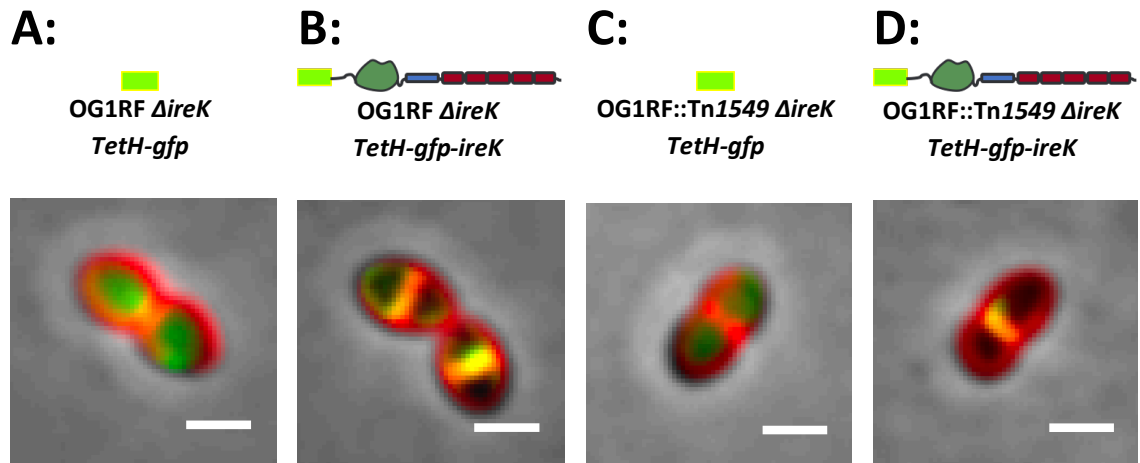


**Figure 3.14: Localization of GFP and GFP-IreK constructs in OG1RF  $\Delta ireK$ .** Images displayed are overlaid Phase contrast, GFP fluorescent signal (Green) and FM 4-64 dye (Red). Localisation of GFP constructs to the membrane (Yellow). Scale bar, 1  $\mu m$ .

IreK localised to the septum of the dividing cells whereas GFP alone is distributed throughout the cytoplasm (**Figure 3.14**). GFP-IreK(FL) also localises to the division site in addition to membrane localisation. This observation has been observed in the homologous protein StkP in *S. pneumoniae* (Zucchini *et al.*, 2018). As organisms like *E. faecalis* lack the protein MreB involved in peripheral growth and cell elongation in rod shaped bacteria, it is thought that PG synthesis occurs mainly at the septum. It has previously been determined in *S. pneumoniae* that the homologue of IreK, StkP is responsible for PG synthesis and controls septum progression and closure (Beilharz *et al.*, 2012). Therefore, localisation of IreK to the septum is in accordance of previously determined observations. As there was little difference in localisation observed between each strain of the FL GFP-IreK fusion, subsequent experiments were performed in OG1RF  $\Delta ireK$  strains.

#### 3.9.4. Localisation of GFP-IreK ( $\Delta kinase$ ), GFP-IreK ( $\Delta K41R$ ) and GFP-IreK ( $\Delta PASTA$ )

In the previous complementation study, the largest difference in phenotype with regards to MIC came from whole protein truncations from either the kinase to PASTA domains or a single amino acid substitution (K41R) in the kinase domain. To compare this phenotype with regards to localisation, these constructs were transformed into OG1RF  $\Delta ireK$  strains with a GFP fusion.

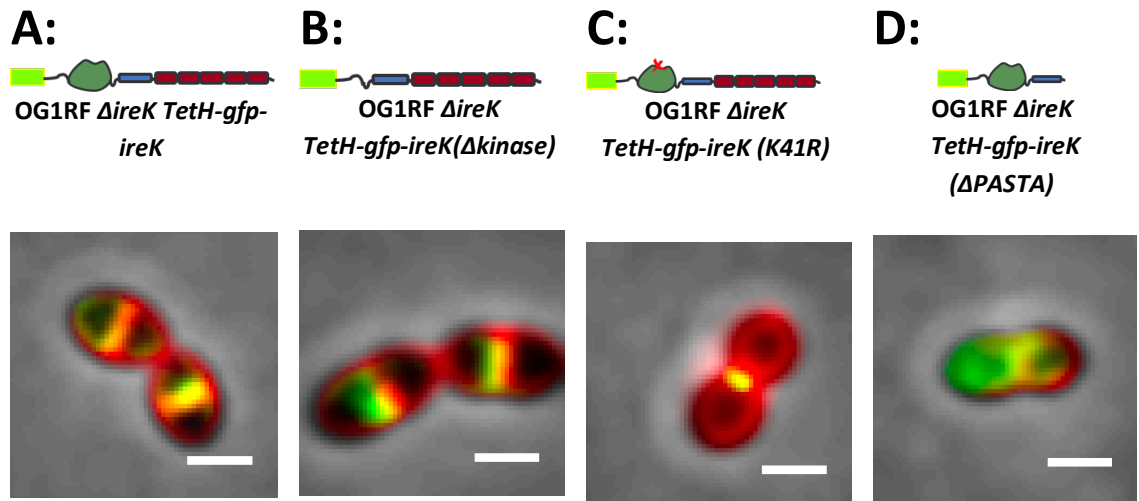


**Figure 3.15: Localization of GFP-IreK constructs with domain mutations in the OG1RF  $\Delta ireK$  strains.** Images displayed are overlaid Phase contrast, GFP fluorescent signal (Green) and FM 4-64 dye (Red). Localisation of GFP constructs to the membrane (Yellow). Scale bar, 1  $\mu$ m. **A** is replicated from **Figure 3.14.B.** for direct comparison.

When comparing each of the images in **Figure 3.15**, it is clear that the largest difference in localisation comes from the construct where no PASTA is present in which there is weak localisation and disruption of the GFP around the Periphery of the dividing cell but still maintains localised to the membrane. A similar localisation profile is observed in a recent study of StkP in *S. pneumoniae* with the removal of all the PASTA domains from the construct (Zucchin *et al.*, 2018). In comparison, the construct where no kinase is present or the single K41R amino acid substitution, localisation is still observed even though these constructs are not functionally active.

These localisation experiments are in contrast to the complementation experiment where the largest observable difference was with the truncation of the kinase domains. This experiment highlights the key role of each domain of the protein. The kinase domains are essential in upregulating the cellular response to cephalosporin and enhanced cephalosporin resistance, and the PASTA domains are essential for protein localisation to the septum.

### 3.9.5. Localisation of different PASTA truncations in IreK

When testing the effect of the removal of each PASTA domain in the complementation experiment, it was determined that the presence of at least one PASTA domain was sufficient to effectively upregulate cephalosporin resistance. To investigate

if the presence of an increasing number of PASTA domains is linked to stronger septal localisation, PASTA domains were truncated iteratively, and localisation measured. The final two PASTA domains (PASTA 4 and 5) were also individually tested. It is established that the absence of PASTA domains causes weak localisation and **Figure 3.16** evaluates the contribution of each PASTA domain in the context of cellular localisation.

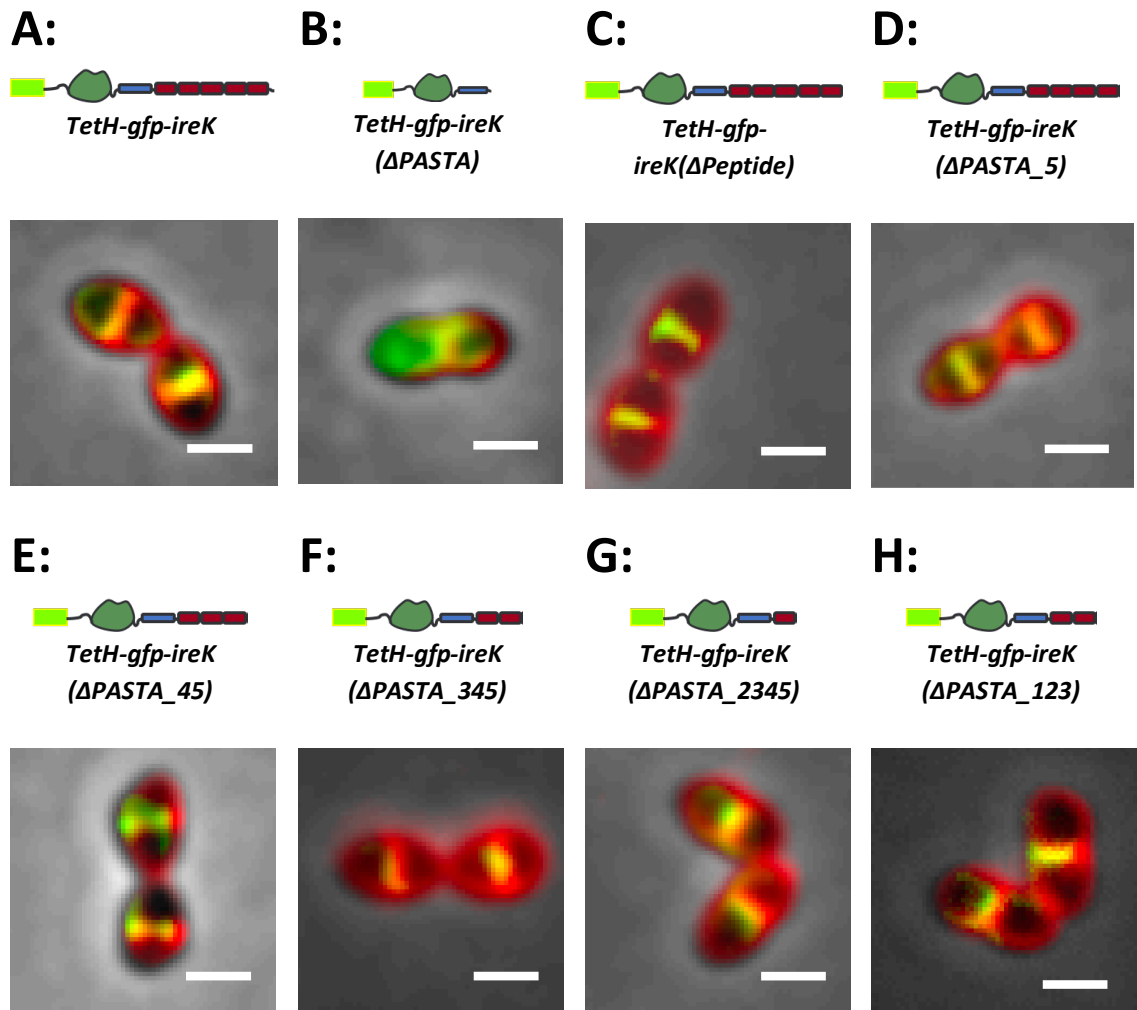


**Figure 3.16: Localization of GFP-IreK constructs in the OG1RF  $\Delta ireK$  strains with PASTA truncations.** Images displayed are overlaid Phase contrast, GFP fluorescent signal (Green) and FM 4-64 dye (Red). Localisation of GFP constructs to the membrane (Yellow). Scale bar, 1  $\mu$ m. A is replicated from Figure 3.14.B. and B is replicated from Figure 3.15.D for direct comparison.

When comparing the contribution of each PASTA domains truncation with respect to localisation, it is clear that one PASTA domain is sufficient for protein localisation of

IreK to the septum of growing and dividing *E. faecalis*. From a qualitative perspective, there is no difference in localisation between any of the PASTA domain truncations in comparison to the full removal PASTA domains (**Figure 3.16.B**) and appears to have a phenotype similar to that of the FL IreK protein (**Figure 3.16.A**). These results are comparable to the complementation experiment where there was little difference between the MIC of each PASTA truncation with respect to ceftazidime. Therefore, this further supports the hypothesis that the number of PASTA domains in an eSTK has a different role which has been suggested to act as a “molecular ruler” for measuring PG thickness in an organism, although in this study it is clear that at least one PASTA domains is required for both enhanced cephalosporin resistance and localisation to the septum (Zucchini *et al.*, 2018).

### **3.9.6. Localisation of different PASTA substitutions in IreK**

In the previous complementation the main difference in MIC associated with the PASTA domains was with an IreK construct that contained the three PASTA domains derived from the *B. subtilis* eSTK (PrkC). The MIC to ceftazidime in the presence of the four PASTA domains from *S. aureus* PrkC had an MIC similar to that of *E. faecalis*. To test if there is a correlation between the MIC experiments and the localisation experiments, GFP fusion to IreK to the PASTA fusions from *S. aureus* and *B. subtilis* were constructed and tested and compared to FL IreK constructs and IreK- $\Delta$ PASTA constructs (**Figure 3.17**).

When comparing each of the substituted PASTA domains qualitatively, it is clear that the majority of the constructs localise strongly to the septum apart from the construct that contains the *B. subtilis* PASTA domains where localisation is still to the membrane and is evenly distributed around the cell.

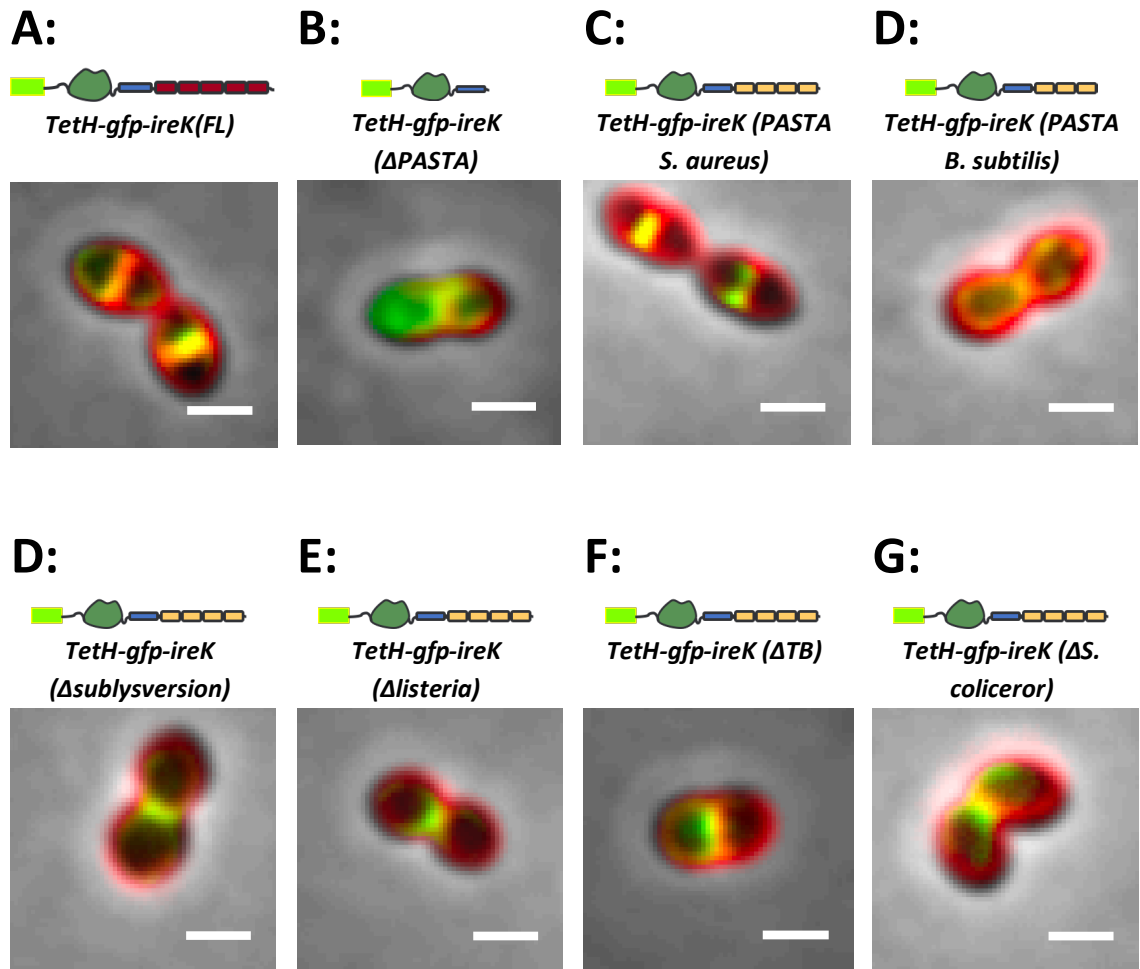


**Figure 3.17: Localization of GFP-IreK constructs in the OG1RF  $\Delta ireK$  strains with PASTA substitutions.** Images displayed are overlaid Phase contrast, GFP fluorescent signal (Green) and FM 4-64 dye (Red). Localisation of GFP constructs to the membrane (Yellow). Scale bar, 1  $\mu\text{m}$ . A is replicated from **Figure 3.14.B** and B is replicated from **Figure 3.15.D** for direct comparison.

### 3.10. Conclusions and future direction

There is a difference in phenotype between the OG1RF isogenic series and the Tn1549 isogenic strains where the OG1RF strains exhibit enhanced cephalosporin resistance with respect to the WT strain and the Tn1549 strains, JH2-2 strains do not. Staurosporine synergistic MIC experiments with cefotaxime managed to demonstrate that in both OG1RF and JH2-2 strains, cephalosporin sensitivity is restored with or without the addition of the Tn1549 cassette. One factor that might contribute to the JH2-2 strains not exhibiting enhanced cephalosporin resistance is due to the lack of a full DdcS/R TCS

and associated DdcY protein in JH2-2 strains that is present in OG1RF strains. qPCR experiments showed that *ddcR* and *ddcY* transcripts are upregulated in an OG1RF::Tn1549 background in the presence of both vancomycin and cefotaxime individually and the phenotype is removed when *irek* is deleted or in a WT strains. As described in the introduction, DdcY has been shown in *E. faecium* to be a major factor in reprogramming PG cell wall to bypass  $\beta$ -lactam PBPs by generating tetrapeptide substrates for LDT<sub>fm</sub> (Sacco *et al.*, 2014). This mechanism might also explain the contribution of enhance cephalosporin resistance in *E. faecalis* OG1RF::Tn1549.

To ensure the Tn1549 cassette has not inserted into an area in the genome which could contribute to the differences between the OG1RF and JH2-2 phenotype, sequencing of the strains OG1RF WT, OG1RF::Tn1549, JH2-2 WT and JH2-2::Tn1549 is required. When comparing the TCSs in OG1RF and JH2-2, the JH2-2 genome is only a draft sequence with the contigs not assembled. At the time of submission, the four strains were sent for sequencing at Microbe NG.

To complement the qPCR experiments which show transcriptional differences at a local level, RNA sequencing will give wide coverage of transcription at a global level. This will support the RT-PCR data and highlight other genes that might enhance cephalosporin resistance in a Tn1549. Recent studies have managed to successfully gain an insight into antibiotic resistance in different pathogenic bacteria. This includes a study where RNA sequencing was performed on 135 clinical *P. aeruginosa* isolates and identified a variety of transcription variations associated with resistance to different classes of antibiotics (Khaledi *et al.*, 2016). The combination of RNA-sequencing and *Tn*-sequencing also identified key fitness determinants in a vancomycin resistance *E. faecium* strain and concluded that 27.8% of the genes are differentially expressed in growth medium or human serum and most of the genes were associated with carbohydrate metabolism when grown in human serum (Zhang *et al.*, 2017). RNA-sequencing could therefore provide a global evaluation of transcription variation in a Tn1549 *E. faecalis* strain to evaluate its overall effect on cephalosporin resistance.

The work from this study suggests that the DdcRS TCS and DdcY proteins are important in the observed enhanced cephalosporin resistance phenotype in the OG1RF::Tn1549 strain from the qPCR. The lack of enhanced cephalosporin resistance in JH2-2 strains due to the DdcRS TCS not being observed. Mutation experiments of the

DdcRS TCS can help identify if there is a direct link with DdcY with enhanced cephalosporin resistance. Previous experiments identified that IreK phosphorylates VanS<sub>B</sub> at position T223 *in vitro*. The same experiments could be transferred into a system to test whether IreK can directly phosphorylate DdcS or DdcR or whether the phosphorylation of VanS<sub>B</sub> is essential for the signal transduction cascade. As mentioned previously, DdcY has been determined to be a homologue of VanY which is a carboxypeptidase that forms tetrapeptide substrates for 3-3 crosslinking. To test if this is the case, uninduced cells or those that contain sub-inhibitory levels of vancomycin or cefotaxime can be grown harvested and the PG extracted and purified to look at the PG profile in the different experimental conditions. Recent advancement has been achieved to use automated systems to analyse PG structure through enzymatic digestion, followed by separation by reverse phase HPLC and collection of individual peaks for MALDI-TOF and tandem mass spectrometry where PG structural and chemical modifications can be automatically assigned (Bern *et al.*, 2017). Therefore, mass spectrometry analysis of whole cell wall PG from *E. faecalis* strains under different antibiotic treatment could provide a suitable system for analysing the PG structure in these experimental conditions.

## Chapter 4. Biophysical analysis of IreK Domains

### 4.1. Introduction

The experiments summarised in **Chapter 3** demonstrate that cephalosporin resistance in *E. faecalis* is enhanced by the presence of the Tn1549 cassette. In *E. faecalis* strains with intrinsic resistance to cephalosporin and enhanced cephalosporin resistance with the Tn1549 cassette, a deletion of the *irek* gene resulted in susceptible strains of *E. faecalis*. Likewise, the addition of staurosporine, a known ST kinase inhibitor, managed to result in inhibition of the KD of IreK and presents a comparable phenotype to an *irek* deletion. Complementation and localisation studies provide insight into the role of IreK with an association to cephalosporin resistance and managed to identify that the PASTA domains are essential for localisation to the septum. This study showed that one PASTA domain is required and that the kinase is still partially functional but distributed around the growing cell and not the septum.

To support the results from **Chapter 3**, the protein domains from IreK have been recombinantly expressed and purified for a range of biophysical studies to gain further insight into the physical properties of IreK. Previous data on eSTKs in *M. tuberculosis* PknB suggested a model of ligand-dependent eSTK autophosphorylation. In this model, dimerization of the extracellular PASTA domains is in response to ligand binding and leads to activation via trans-phosphorylation of the cytoplasmic domain (Barthe *et al.*, 2010). After initial protein domain characterisation including qualitative SDS-PAGE gels, mass spectrometry of samples to establish and compare experimental MW to theoretical MW, and CD analysis at a range of temperatures, the data in this Chapter aim to highlight the oligomeric states of the kinase and PASTA domains using size exclusion chromatography-multiple angle light scattering (SEC-MALS) and analytical ultracentrifugation (AUC).

At present there is a lack of clarity on the nature and identity of ligands that associate with the PASTA domains between species, with a component of PG being the most likely associated ligand. I have screened the binding properties of PASTA domains 1 to 5 against enzymatically cleaved *E. faecalis* native PG, highly purified and well characterised PG mimetic compounds and a range of different antibiotics. These

potential ligand candidates were then tested using microscale thermophoresis to remove any possibility of a false positive being detected from SPR through non-specific binding.

## 4.2. Initial characterisation of each protein construct

The KD from *E. faecalis* and *E. faecium* IreK (pLG226 and pLG234 respectively) were previously cloned into pET Duet, and the constructs were used in this study. The PASTA domain constructs were cloned from the *E. faecalis* IreK plasmid (codon-optimised) (pCWT001) into pProEX with an N-terminal histidine tag followed by a TEV cleavage site. PASTA constructs were cloned into the *NcoI* and *HindIII* sites and allowed only three residual amino acids not associated with the PASTA constructs to remain (G-A-M) following TEV cleavage. All proteins were purified using IMAC purification on a nickel column and gel filtration on either a Superdex 75 or Superdex 200 column (depending on the size of the protein) as described in **Chapter 2.4** of the Materials and Methods. Final constructs are illustrated in **Figure 4.1**.

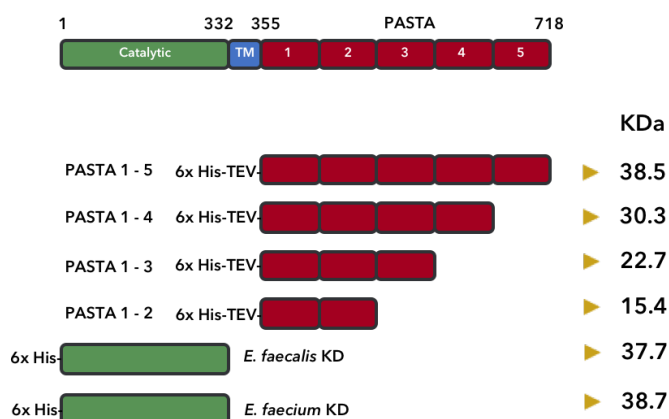


**Figure 4.1: IreK domain constructs for recombinant protein expression.** Schematic of protein constructs used in this study including the IreK PASTA domains in *E. faecalis* or the IreK KD domains from both *E. faecalis* and *E. faecium*. Size of constructs are represented post TEV cleavage (kDa).

### 4.2.1. SDS-PAGE and SEC-MALS analysis

The overall purity and oligomeric states of the various domains of IreK were evaluated in the absence of ligands using SDS-PAGE and SEC-MALS analyses. These results are summarised in **Figure 4.2** for KD constructs and **Figure 4.3** for PASTA constructs. From inspection of the SDS-PAGE gels for each protein domain after IMAC and gel filtration, it

is clear that each protein domain has been produced at high purity (**Figure 4.2** and **Figure 4.3**). The pure proteins were also subjected to SEC-MALS analysis. SEC-MALS is an advantageous technique as it allows you to separate out protein species (oligomeric or protein containments from purification) using an analytical gel filtration column while gaining individual measurement properties of that species. MALS analysis of a sample allows multiple angles to be measured simultaneously where the scattering intensity can be directly related to the solution molecular mass of the sample (Philo, 2009; Some, 2013).

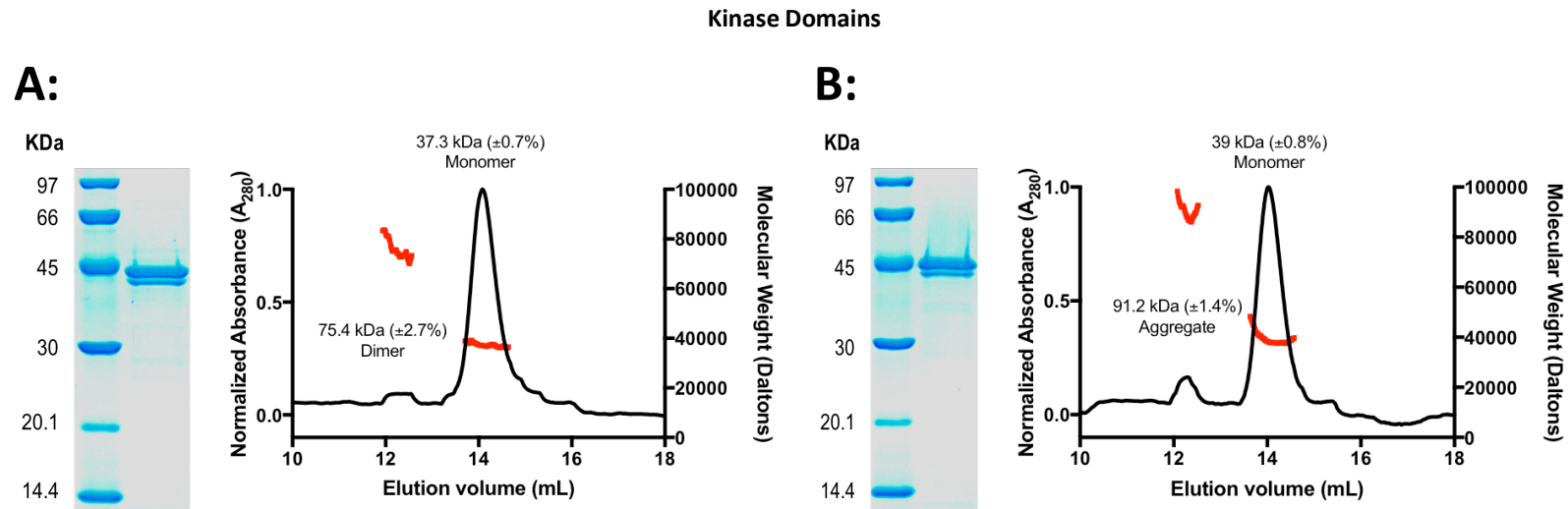
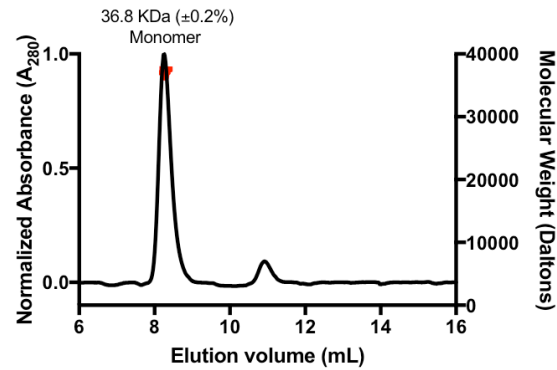
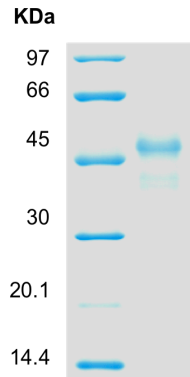


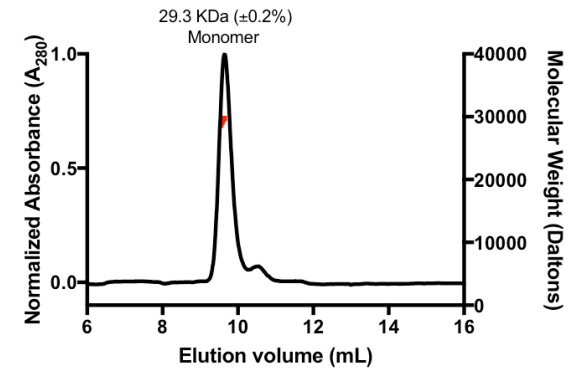
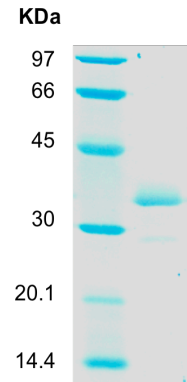
**Figure 4.2: Recombinantly expressed IreK Kinase domains analysed SDS-PAGE for purity and SEC-MALS for oligomerisation.** Analysis of purified IreK kinase domains from *E. faecalis* (A) or *E. faecium* (B) by SDS-PAGE (Left) or oligomerisation by SEC-MALS (Right). Elution profiles of kinase domains were examined by SEC-MALS on a Superdex 200 increase (10/300) at a flow rate of 0.75 ml min<sup>-1</sup>. Absorbance at A<sub>280</sub> for each chromatogram was normalised. MALS data are presented in Red with predicted molecular weight above each peak.

PASTA Domains

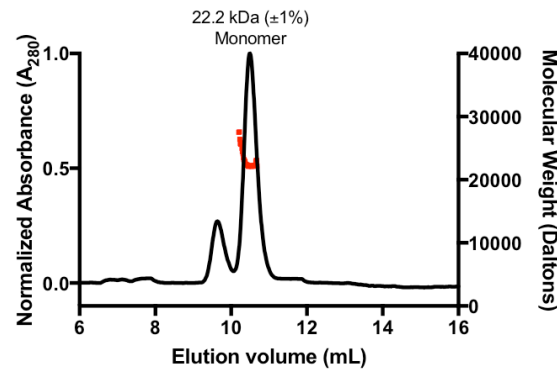
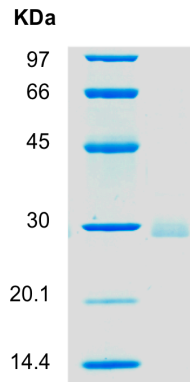
**A:**



**B:**



**C:**



**D:**

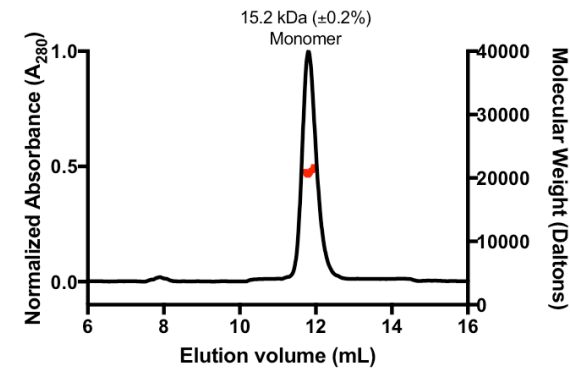
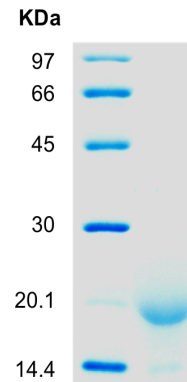


**Figure 4.3: Recombinantly expressed IreK PASTA domains analysed SDS-PAGE for purity and SEC-MALS for oligomerisation.** Analysis of purified PASTA domains from *E. faecalis* including (A) PASTA 1-5, (B) PASTA 1-4, (C) PASTA 1-3 and (D) PASTA 1-2 by SDS-PAGE (Left) or SEC-MALS (Right). Elution profiles of PASTA domains were examined by SEC-MALS on a Superdex 75 increase (10/300) at a flow rate of  $0.75 \text{ ml min}^{-1}$ . Absorbance at  $A_{280}$  for each chromatogram was normalised. MALS data are presented in Red with predicted molecular weight above each peak.

From the analysis of the SEC-MALS data of the kinase domains from *E. faecalis* and *E. faecium*, it is clear that the primary species is the monomeric form of the kinase from both species. In both experiments, another oligomeric species is present and is predicted to be a dimer for the *E. faecalis* kinase construct and a high molecular weight aggregate for the *E. faecium* kinase construct.

For each of the PASTA domain constructs initially measured by SEC-MALS, each construct is predominately monomeric. A small molecular weight contaminant is present in the PASTA 1 to 5 construct and a small low MW shoulder is present for the PASTA 1 to 4 construct. There is a high molecular weight component present in the PASTA 1 to 3 construct, but when compared to **Figure 4.4** with an overlay each of the four PASTA constructs analysed, it appears that the high molecular weight contamination may have come from residual protein left in the sample loading loop from PASTA 1 to 4. The SEC-MALS analysis for sample 1-2 shows a single species. The experimental molecular weight of each construct from SEC-MALS is compared later in this chapter with the theoretical molecular weight and other experimental molecular weights from other techniques.

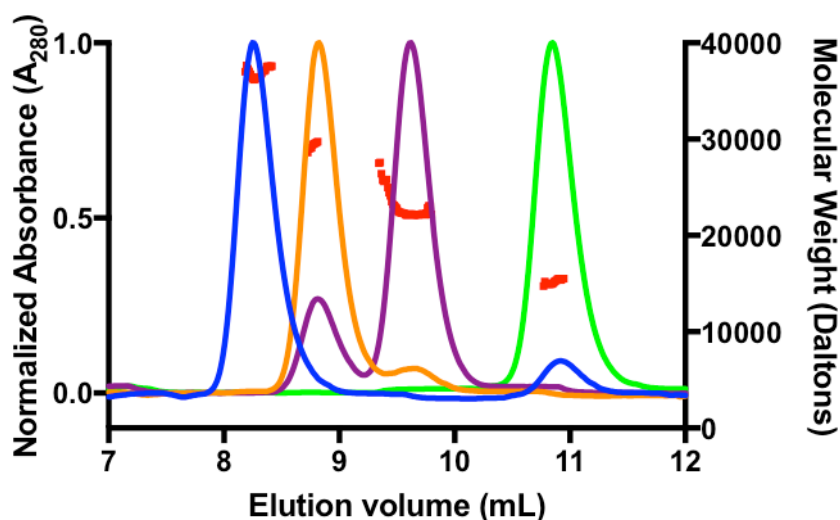


**Figure 4.4: Overview of SEC-MALS data obtained for each PASTA construct.** Chromatograms of each PASTA construct shown in PASTA 1-5 (Blue), PASTA 1-4 (Orange), PASTA 1-3 (Purple) and PASTA 1-2 (Green). MALS data are presented in Red.

#### 4.2.2. Determining the fold of each protein construct by CD

After analysis of each construct by SDS-PAGE and SEC-MALS, the secondary structure composition was measured using CD to gauge whether the proteins were well-folded after being recombinantly expressed. CD is often used as a quality control check after recombinant protein production and gives early estimates of secondary structure and folding properties of the protein. **Figure 4.5** highlights the structural features that can be identified using CD using when formed predominantly of that structural feature.

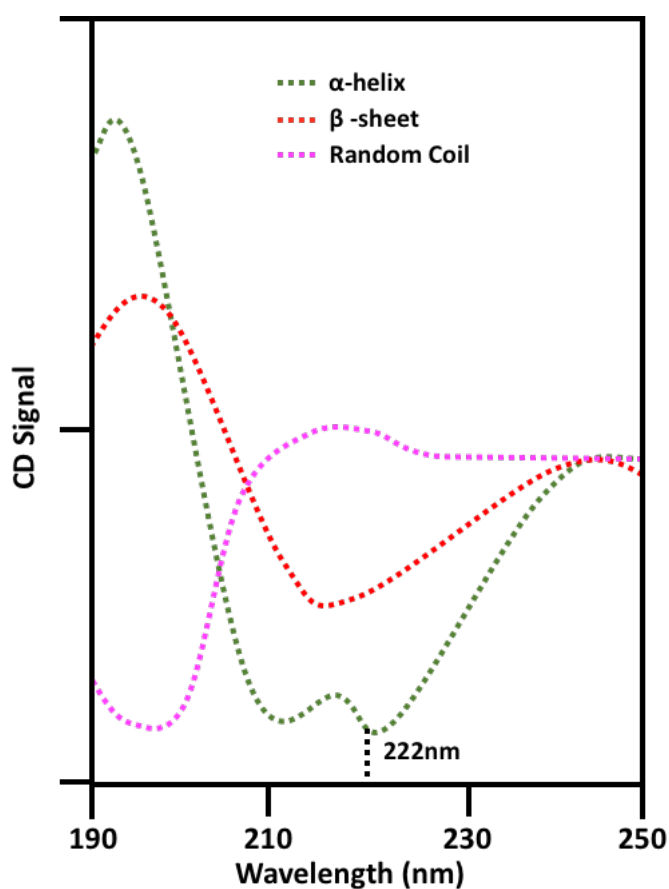


**Figure 4.5:** Schematic showing a CD profile of  $\alpha$ -helix,  $\beta$ -sheet and random coil spectra expected when predominately formed of that secondary structure feature. Most proteins will be a mixture of all three of these structural features but measuring 222 nm is often used to monitor changes in  $\alpha$ -helix content in different buffers or temperatures.

Although CD allows rapid quantification of protein structure on a global scale, it does not give residue specific information like other structural techniques including cryo-EM, X-ray crystallography and NMR (Greenfield, 2006). **Figure 4.6** and **Figure 4.7** show processed CD data for either the KD or PASTA domains, respectively, and the associated predicted secondary structure composition as estimated from fitting of the data using DichroWeb (**Figure 4.8**) (Whitmore and Wallace, 2004).

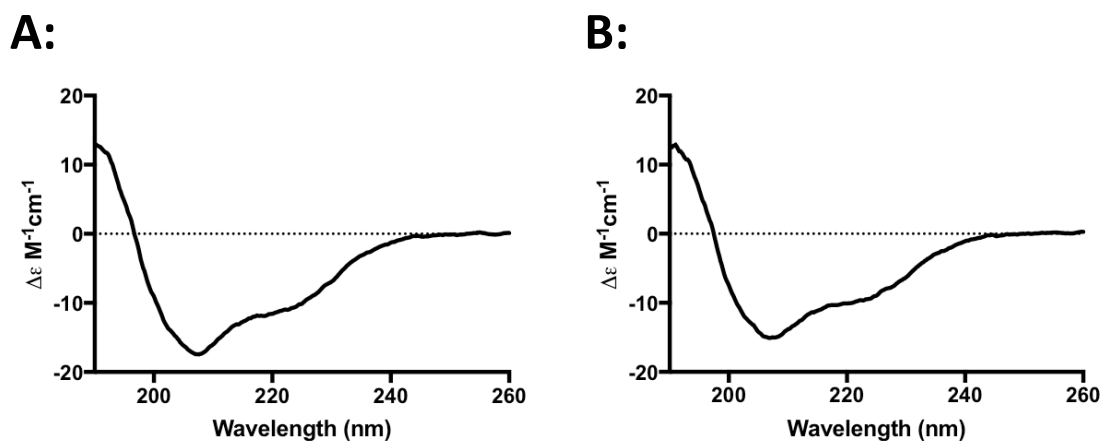


**Figure 4.6:** CD spectra of each KD of IreK. (A) KD from *E. faecalis* and (B) KD from *E. faecium* at 0.2 mg mL<sup>-1</sup> in 10 mM Sodium Phosphate, pH 7.4 buffer at 25°C.

Inspection of the CD spectra of KD from both *E. faecalis* and *E. faecium* IreK in **Figure 4.6** suggests a significant amount of helical content due to the presence of negative maxima at 208 and 222 nm. This is confirmed when using DichroWeb to estimate the secondary structure composition. **Figure 4.8A** shows that the domains are highly helical, with 70% and 75%  $\alpha$ -helix for *E. faecalis* and *E. faecium* respectively. The  $\beta$ -sheet content is estimated as 12% and 11% for *E. faecalis* and *E. faecium* respectively. When comparing these estimations with structures obtained from homologous proteins including *S. aureus* (PDB: 4EQM, 34% and 17%  $\alpha$ -helix and  $\beta$ -sheet respectively (Rakette *et al.*, 2002)) and *M. tuberculosis* (PDB: 1O6Y, 35% and 19%  $\alpha$ -helix and  $\beta$ -sheets respectively (Ortiz-Lombardia *et al.*, 2013)), the percentage of  $\alpha$ -helix is observed in the *E. faecalis* and *E. faecium* IreK KD is more than double, but still shows that the  $\alpha$ -helix is the most dominant secondary structure in the protein.

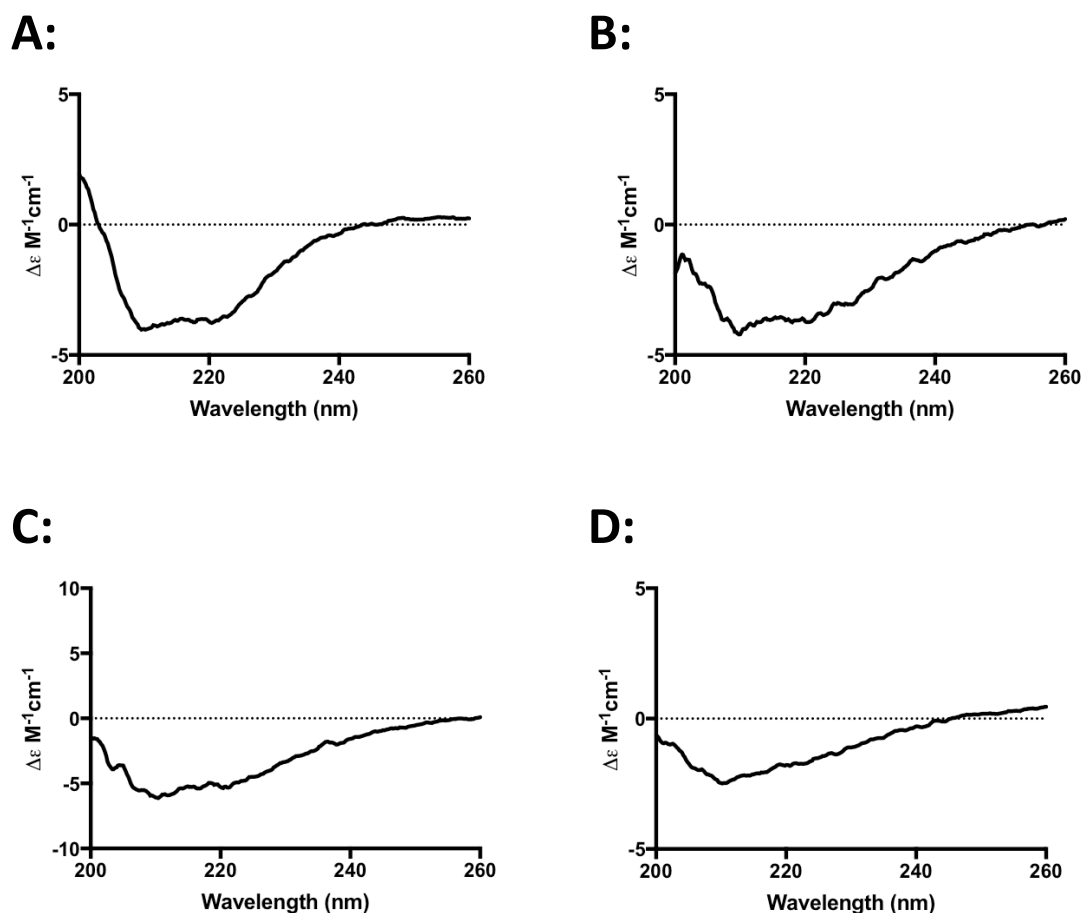


**Figure 4.7:** CD spectra of each PASTA construct of IreK from *E. faecalis*. (A) PASTA 1 to 5, (B) PASTA 1 to 4, (C) PASTA 1 to 3 and (D) PASTA 1 to 2 at 0.2 mg mL<sup>-1</sup> in 10 mM Sodium Phosphate, pH 7.4 buffer at 25°C.

The CD spectra of each of the PASTA domains (FL and truncations) from IreK *E. faecalis* are shown in **Figure 4.7**. The estimated secondary structure composition is highlighted in **Figure 4.8.B** for each construct and shows a decrease in secondary structure (and an increase in disorder) from PASTA 1 to 5 to PASTA 1 to 2. The estimated secondary structure composition of PASTA 1 to 5 (16% and 41 %  $\alpha$ -helix and  $\beta$ -sheet, respectively) agrees well with the known structures of *S. aureus* PASTA domains (PDB: 3M9G, 13% and 33%  $\alpha$ -helix and  $\beta$ -sheet respectively (Paracuellos *et al.*, 2010)) and *M. tuberculosis* PASTA domains (PDB: 2KUI, 16% and 30%  $\alpha$ -helix and  $\beta$ -sheet respectively (Barthe *et al.*, 2010), and it is apparent that PASTA domains are predominately  $\beta$ -sheet in secondary structure.

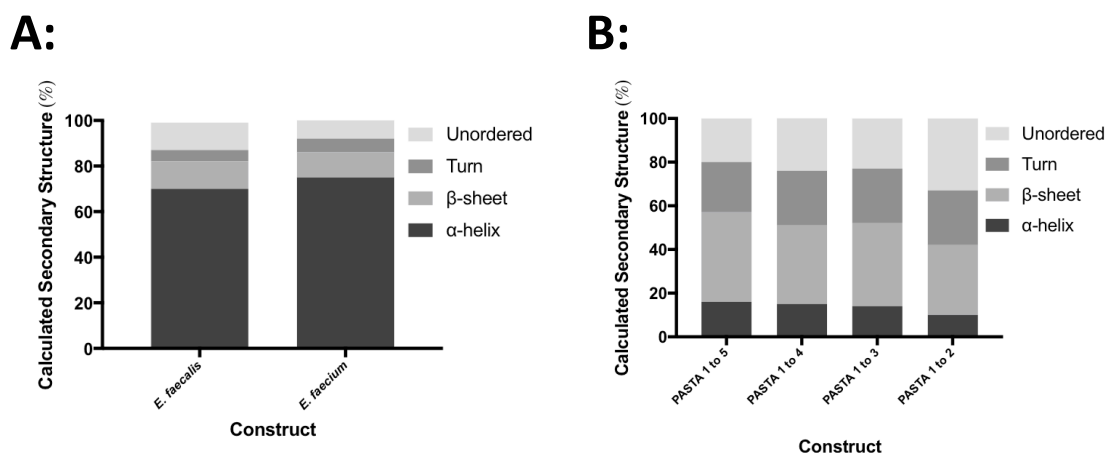


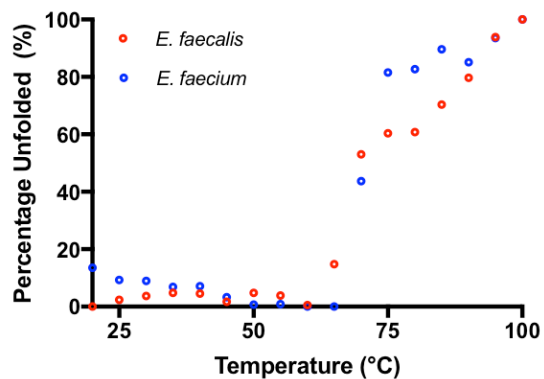
**Figure 4.8: Secondary structure percentage distribution determined by CD.** KD (A) and PASTA domains (B) according to DichroWeb determined by using the CDSSTR method with Reference set 3 (kinases) and Reference set 4 (PASTA) for data fitting.

#### 4.2.3. Determining the melting temperature ( $T_M$ ) of each protein construct by CD

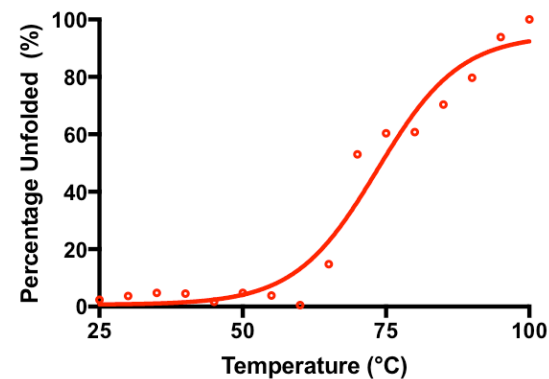
The  $T_M$  is determined by the midpoint of the unfolding transition from secondary structure components in proteins (Greenfield, 2006). As CD monitors secondary structure in a protein, heat can be applied at incremental temperatures to study how proteins lose these highly ordered structures. To assess the stability of each IreK construct and confirm that each domain is well-folded, melting temperatures ( $T_M$ ) were performed between 25-100°C for kinase domains in 5°C increments or between 20-100°C for PASTA domains in 1°C increments (**Figure 4.9** and **Figure 4.10** respectively).

The IreK kinase domains from *E. faecalis* and *E. faecium* have a high and similar melting temperature, confirming that the recombinantly expressed and purified protein is well-folded. When comparing the PASTA domains from *E. faecalis* and the incremental truncations, it is clear that the melting temperature decreases upon each truncation after PASTA 1 to 4. PASTA 1 to 5 and PASTA 1 to 4 have a high  $T_M$ , but there is a decrease in  $T_M$  associated with PASTA 1 to 3 and a very low  $T_M$  observed for PASTA 1 to 2. To confirm that the PASTA domains were not unfolded after purification and after thawing from storage in -80°C, the  $T_M$  was monitored across the whole CD spectrum (**Figure 4.11**).

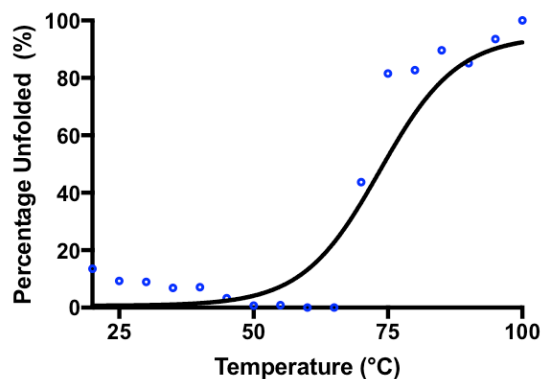
**A:**



**B:**



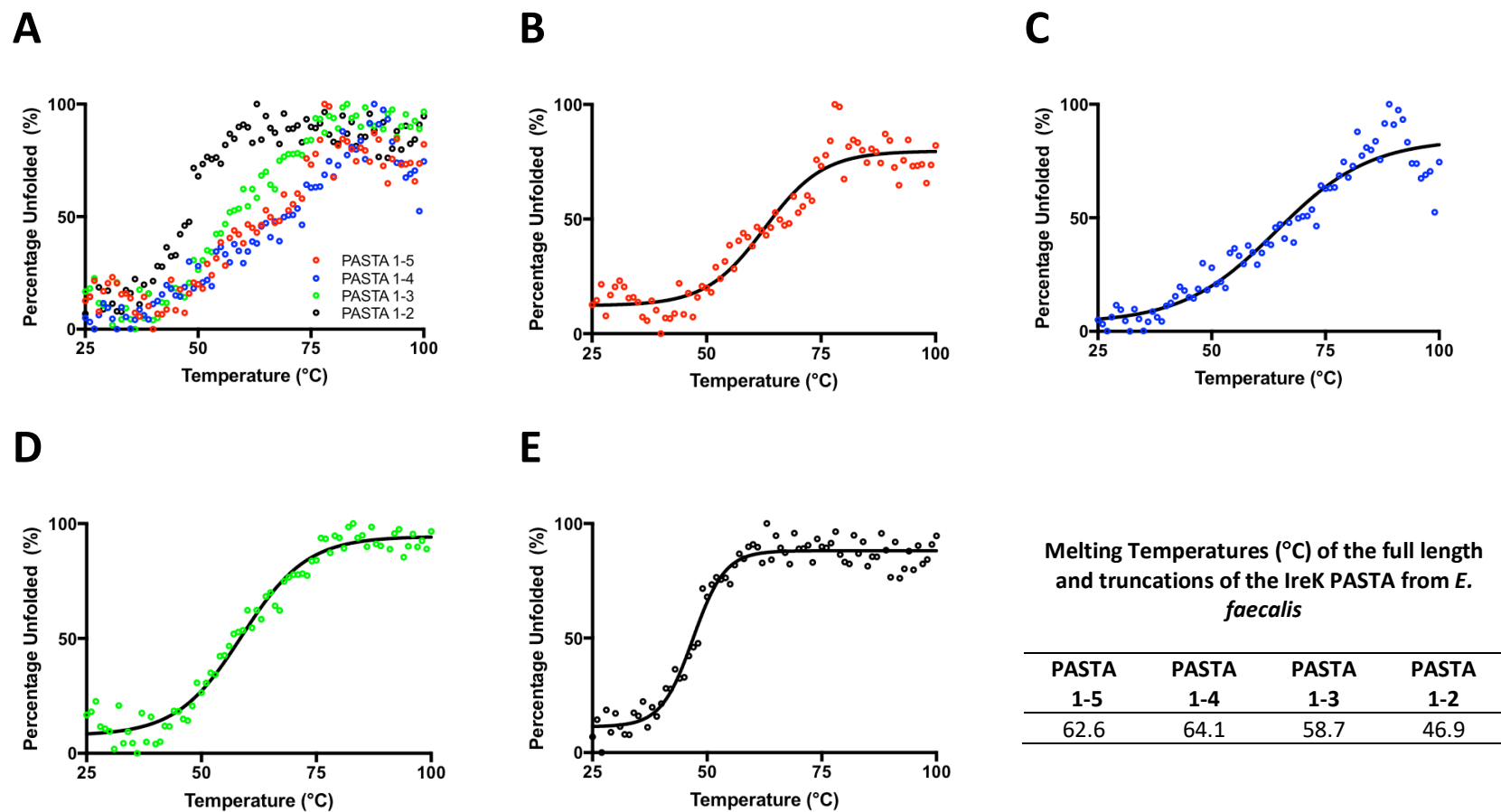
**C:**



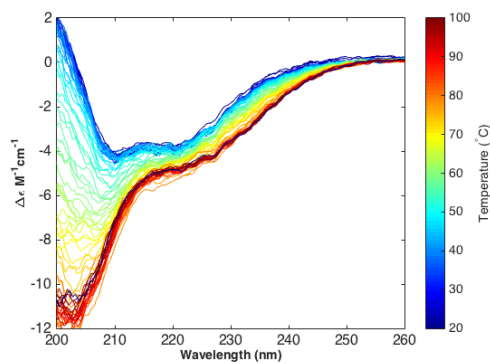
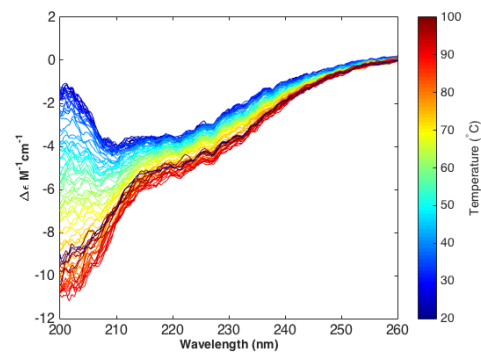
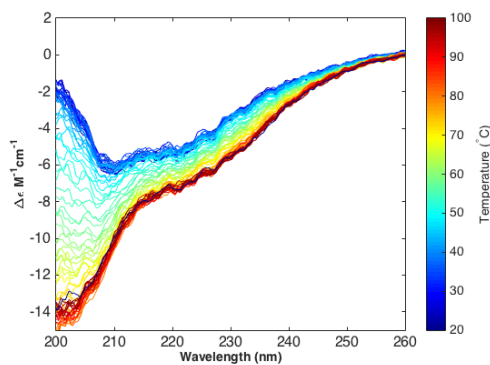
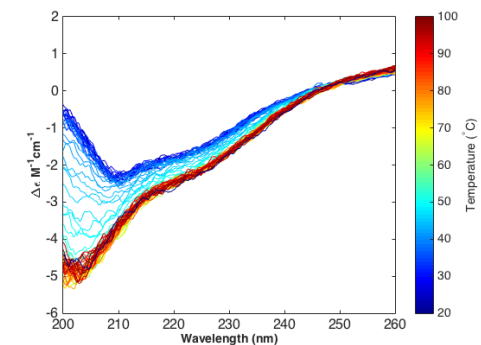
Melting Temperatures (°C) of IreK KD from *E. faecalis* and *E. faecium*

<i>E. faecalis</i>	<i>E. faecium</i>
73.5	70.6

**Figure 4.9: CD  $T_M$  of IreK KD following 222 nm.** Protein constructs at 0.2 mg mL<sup>-1</sup> in 10 mM Sodium Phosphate, pH 7.4 buffer were incubated at incremental temperatures from 20 to 100°C with CD spectra collected at each temperature point. Including (A) overlay plot of kinase constructs, (B) IreK *E. faecalis*, (C) IreK *E. faecium*, with the Boltzmann sigmoid fit (Solid Black line). Insert: table of  $T_M$  of each construct as determined by the Boltzmann sigmoid equation



**Figure 4.10:** CD  $T_M$  of IreK of PASTA constructs from *E. faecalis* following 222 nm. Protein constructs at 0.2 mg mL<sup>-1</sup> in 10 mM Sodium Phosphate, pH 7.4 buffer were incubated at incremental temperatures from 20 to 100°C with CD spectra collected at each temperature point. Including (A) overlay plot of PASTA constructs, (B) PASTA 1 to 5, (C) PASTA 1 to 4, (D) PASTA 1 to 3 and (E) PASTA 1 to 2 with the Boltzman sigmoid fit (Solid Black line). Insert: table of  $T_M$  of each construct as determined by the Boltzmann sigmoid equation.

**A:****B:****C:****D:**

**Figure 4.11: CD  $T_M$  spectra of each PASTA construct of IreK.** Protein constructs at  $0.2 \text{ mg mL}^{-1}$  in 10 mM Sodium Phosphate, pH 7.4 buffer were incubated at incremental temperatures from 20 to  $100^\circ\text{C}$  with CD spectra collected at each temperature point Includes (A) PASTA 1 to 5, (B) PASTA 1 to 4, (C) PASTA 1 to 3 and (D) PASTA 1 to 2 at  $0.2 \text{ mg mL}^{-1}$  following a  $T_M$  melt from 20 to  $100^\circ\text{C}$ .

### 4.3. Studying oligomerisation of IreK domains using AUC

Analytic ultracentrifugation (AUC) is a well-established technique and is readily used to study oligomerisation of proteins (Uttinger *et al.*, 2017). It has many advantages over other techniques such as SEC-MALS as biomolecules are free in solution, no immobilisation is acquired, and it can measure homo- and hetero-interactions and stoichiometry. It is known that sedimentation of macromolecules correlates with a concentration effect and the transport properties of macromolecules are related to their spatial distribution (Brown and Schuck, 2006). A major benefit of AUC is its ability to study weak interactions as even the weakest interaction can still cause a change in sedimentation and diffusion behaviour in concentrated systems (Solovyova *et al.*, 2001).

To further explore the oligomerisation previously observed by SEC-MALS (**Figure 4.2 to 4.4**) sedimentation velocity AUC experiments were used to study the kinase domains and PASTA domains (**Table 4.1** and **Table 4.2**). The sedimentation coefficient distributions for the absorbance and interference data are shown in **Appendix 8.4**. In each table the characteristics in the MW calculated for a species in the  $c(s)$  (sedimentation coefficient) analysis which is dependent on the frictional ratio parameter ( $f/f_0$ ). The frictional ratio is fit globally during the analysis, thus when there is more than one species present the calculated  $f/f_0$  is an average value for all of the species present. MWs calculated using this average  $f/f_0$  will not give the true MW values for each individual species. Both the absorbance at 280 nm ( $A_{280nm}$ ) and interference data were used. The interference optics are more sensitive than the absorbance optics, which is good for low concentration samples, but has the drawback that they will also detect differences between the sample and reference buffers, which can affect the analysis. The greater sensitivity means they will also detect contaminants that are not visible in the absorbance data, meaning the presence of contaminants will have a greater effect on the accuracy of the interference data than on the absorbance data.

The kinase domain constructs do not exhibit any thermodynamic or hydrodynamic non-ideality, and there is clearly a self-association equilibrium (**Table 4.1**). When comparing the absorbance data, the predominant species is monomeric, but there is also a dimer and a possible trimer/tetramer. The interference data also reveals the presence of a low MW contaminant in both samples.

To complement the AUC data, and clarify the oligomeric state of each species present in samples of the KD, a native-PAGE gel was run for the IreK kinase domains from *E. faecalis* and *E. faecium* (**Figure 4.12**). It is clear from the native-PAGE gel there are at least 4 oligomeric species present in the kinase domain. Although interpretation of which species type is difficult as a marker was not used, in comparison to the AUC data and the SEC-MALS data, it can be assumed that the bottom band is a monomer and the one following is a dimer with two higher order oligomers being visible. It is clear in these experiments that the KD can self-associate independent of the PASTA domains, and if dimerization is required for autophosphorylation, the PASTA domains might have different role from that of promoting oligomerization.



**Figure 4.12: Native-PAGE gel of Kinase domains from *Enterococcus* spp.** 40  $\mu$ g of either the KD of IreK from *E. faecalis* (Left) and *E. faecium* (Right) was loaded onto a 4-20% acrylamide gradient Native-PAGE gel for inspection of oligomerization.

When comparing the PASTA domain constructs (**Table 4.2**), no concentration dependence was noted for the sedimentation co-efficient of any of the PASTA constructs, suggesting no self-association or non-ideal behaviour, over this concentration range. The predominant species present in all of these samples appears to be a monomer (note the dependence of the MW on the best-fit  $f/f_0$ ). The interference data also reveals the presence of a low MW contaminant in PASTA 1- 3 and 1-4.

Although previous models have hypothesised that eSTKs oligomerize upon binding of a ligand to the PASTA domains (Barthe *et al.*, 2010), the AUC and SEC-MALS data show no propensity for self-association of these domains, even at high concentrations. Therefore, a ligand must be essential to support the model, or a different mechanism of action is necessary for oligomerisation of eSTKs and activation of the kinase domains.

**Table 4.1: The estimated MW from each species as determined by AUC by the c(s) analysis of the KD.** For each sample concentration the signal-weighted sedimentation co-efficient and the estimated MW of each species is shown, together with the best-fit frictional ratio for the distribution. \* Average values of two unresolved species. Sedimentation coefficients are displayed in **Appendix 8.4**.

Theoretical MW Monomer (kDa)	Detection method	Concentration (mg mL <sup>-1</sup> )	Identified Species								f/f <sub>0</sub>
			Peak 1		Peak 2		Peak 3		Peak 4		
			MW (kDa)	Sed. Co (S)	MW (kDa)	Sed. Co (S)	MW (kDa)	Sed. Co (S)	MW (kDa)	Sed. Co (S)	
<b>Kinase (<i>E. faecalis</i>)</b>											
40.1	Absorbance	1.0	-	-	42.3	2.21	87.0	3.57	167*	5.51*	1.84
		0.5	-	-	46.7	2.25	120*	4.24*	-	-	1.93
		0.25	-	-	44.1	2.31	115*	4.38*	-	-	1.81
	Interference	1.0	7.9	0.81	40.6	2.41	75.5	3.64	117.0	4.86	1.64
		0.5	8.1	0.88	37.0	2.42	70.1	3.70	115.0	5.17	1.54
		0.25	8.1	0.94	33.6	2.43	66.4	3.83	99.8*	5.03*	1.43
<b>Kinase (<i>E. faecium</i>)</b>											
41.1	Absorbance	1.0	-	-	43.2	2.20	91.9	3.65	162	5.32	1.87
		0.5	-	-	42.1	2.25	127.0*	4.70*	-	-	1.81
		0.25	-	-	45.9	2.29	136.0*	4.71*	-	-	1.88
	Interference	1.0	6.5	0.73	39.3	2.41	77.1	3.78	128	5.29	1.61
		0.5	7.2	0.84	35.5	2.41	66.0	3.65	116	5.33	1.50
		0.25	8.7	0.94	36.6	2.45	78.4	4.08	140*	6.01*	1.51

**Table 4.2: The estimated MW from each species as determined by AUC by the c(s) analysis of each PASTA domain truncation.** Each sample concentration the signal-weighted sedimentation co-efficient and the estimated MW of each species is shown, together with the best-fit frictional ratio for the distribution. Sedimentation coefficients are displayed in **Appendix 8.4**.

Theoretical MW Monomer (kDa)	Detection method	Concentration (mg mL <sup>-1</sup> )	Identified Species				f/f <sub>0</sub>
			Peak 1		Peak 2		
			MW (kDa)	Sed. Co (S)	MW (kDa)	Sed. Co (S)	
<b>PASTA 1-2</b>							
15.4	Absorbance	1.0	17.1	1.58	-	-	1.47
		0.5	16.8	1.59	-	-	1.44
		0.25	16.5	1.59	-	-	1.42
	Interference	1.0	17.0	1.57	-	-	1.48
		0.5	17.2	1.57	-	-	1.49
		0.25	17.2	1.58	-	-	1.48
<b>PASTA 1-3</b>							
22.7	Absorbance	1.0	-	-	25.8	1.66	1.86
		0.5	-	-	31.9	1.68	2.11
		0.25	-	-	31.3	1.65	2.13
	Interference	1.0	9.3	0.93	25.9	1.84	1.68
		0.5	8.4	0.90	24.7	1.84	1.62
		0.25	-	-	27.2	1.87	1.71
<b>PASTA 1-4</b>							
30.3	Absorbance	1.0	-	-	34.1	1.77	2.09
		0.5	-	-	37.3	1.79	2.19
		0.25	-	-	51.9	1.79	2.73
	Interference	1.0	7.0	0.71	31.7	1.96	1.80
		0.5	8.4	0.84	30.5	1.98	1.73
		0.25	-	-	31.4	1.99	1.76
<b>PASTA 1-5</b>							
38.4	Absorbance	1.0	41.2	2.18	-	-	1.96
		0.5	39.0	2.21	-	-	1.87
		0.25	40.8	2.21	-	-	1.93
	Interference	1.0	42.0	2.14	-	-	1.79
		0.5	44.4	2.14	-	-	1.82
		0.25	40.4	2.17	-	-	1.73

#### 4.4. Confirming MW by determining experimental MW by mass spectrometry and summary of oligomerisation

As there was some ambiguity between oligomerisation states of the different constructs with different analytic techniques, mass spectrometry was used to validate the size of the protein constructs. **Table 4.3** summarizes the MW obtained by mass spectrometry for each construct (spectra of each construct can be found in **Appendix 8.5**), and well as the oligomeric states obtained from AUC and SEC-MALS. It is clear that the mass spectrometry results are in good accordance to the theoretical molecular weight.

Interestingly, the experimental KD MWs from both constructs are not comparable to the theoretical mass. Difference mass abundances are present and correspond to a mass difference that confers multiple phosphorylated residues (~80 Da) and indicated that the protein is autophosphorylated and that there is also non-specific phosphorylation. There also appears to be other post translational modifications present. Mass spec of the PASTA 1 to 5 with N-terminal His construct (non-TEV cleaved) (PASTA 1 to 5 (His)) was also conducted as this construct was used in subsequent ligand binding experiments. Interestingly, the TEV cleaved PASTA 1 to 5 (PASTA 1 to 5 (TEV)) protein showed decreasing mass abundances that correspond to an approximate decreasing PASTA domain suggesting degradation over a long period of time. (See **Appendix 8.5 - Figure 8.8**).

The SEC-MALS data predict a single monomeric species for the PASTA domains, but two oligomeric species for the KD of *E. faecalis* and *E. faecium* (i.e. monomeric forms in both constructs and/or dimers or aggregates for the second oligomeric species). Generally, AUC data showed agreed with the theoretical MW when using the interference data to compare MW in both the kinase and PASTA domains. The absorbance data overestimates the MW of each construct and made it difficult to determine high order oligomeric states in the kinase domains. In conclusion, when comparing the oligomeric states of the kinase and PASTA domains, the PASTA domains only appear as a single monomeric state and the kinase domain can form multiple oligomeric states.

**Table 4.3: Summary of the MW of each construct and estimates their oligomeric states by a range of biophysical techniques including Mass Spectrometry, SEC-MALS and AUC (Absorbance and Interference). \* Multiple posttranslational modifications are observed.**

Construct	Theoretical (MW)	Mass Spectrometry		SEC-MALS		AUC Absorbance		AUC Interference	
	kDa	kDa	Error	kDa	Oligomeric State	kDa	Oligomeric State	kDa	Oligomeric State
<b>IreK KD</b>									
<i>E. faecalis</i>	37726.78	38706.3008*	0.0506	37.30	Monomer	44.37	Monomer	37.07	Monomer
		38626.2500*	0.0781	75.4	Dimer	107.3	Aggregate	70.67	Dimer
		38546.2148*	0.1823			167	Aggregate	110.6	Trimer
		38466.1289*	0.0911						
		38386.1992*	0.5078						
<i>E. faecium</i>	38691.98	39008.3086	0.1678	39.00	Monomer	43.73	Monomer	37.13	Monomer
		38928.2266*	0.1143	91.20	Aggregate	118.3	Aggregate	73.83	Dimer
		38848.1836*	0.2358			162	Aggregate	128	Trimer
		38768.2734*	0.3516						
<b>IreK PASTA domains from <i>E. faecalis</i></b>									
<b>PASTA 1 to 5</b>	38465.35	38464.8516	0.0391	36.80	Monomer	40.33	Monomer	42.23	Monomer
<b>PASTA 1 to 5 (His)</b>	41301.53	41301.6758	0.0318	ND	ND	ND	ND	ND	ND
<b>PASTA 1 to 4</b>	30294.67	30293.9219	0.0340	29.30	Monomer	41.1	Monomer	31.2	Monomer
<b>PASTA 1 to 3</b>	22693.30	22692.8203	0.0434	22.20	Monomer	29.67	Monomer	25.93	Monomer
<b>PASTA 1 to 2</b>	15403.22	15403.0957	0.0485	15.20	Monomer	16.8	Monomer	17.13	Monomer

## 4.5. Identification of Ligands that bind to IreK PASTA domains

PG is a highly complex matrix with wide structural variation. To initially test the binding of PASTA to PG, a chemi-enzymatic approach was adopted to obtain more chemically defined PG fragments. This approach has been initially used to assess the binding of *S. aureus* PG to LysM domains (Mesnage *et al.*, 2014). This approach is one that can be transferred to initially study PG interactions with the PASTA domains from *E. faecalis*.

*E. faecalis* JH2-2 was grown until an  $OD_{600nm} = 0.6$  was reached. Cells were harvested, and the PG purified as described in **Section 2.6** of the Material and Methods. Purified *E. faecalis* PG was then used as a substrate for various hydrolase enzymes to yield different PG profiles. Mutanolysin is a commercially available hydrolase (Sigma-M9901) and was used according to manufactures instructions. EnpA is a homologue of lysostaphin and is an endopeptidase. EnpA was recombinantly expressed and purified and its hydrolase activity has been tested previously (De Roca *et al.*, 2010). Full activity from EnpA requires pre-digestion of the PG with mutanolysin first. Recombinantly expressed hydrolases including EnpA and AtIA were purified according to previous studies (**Figure 4.13.A** and **Figure 4.13.B** respectively) (**Figure 4.14**) (De Rocca *et al.*, 2010; Hayhurst *et al.*, 2008).

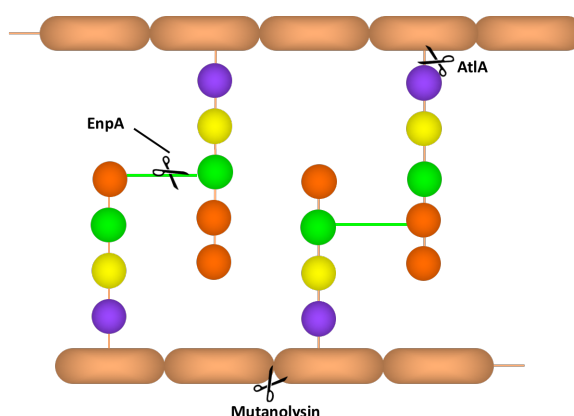


**Figure 4.13: Schematic of hydrolases and location of cleavage for *E. faecalis* binding studies.** Scissors highlights the location of the hydrolases used in this study for ligand binding characterisation. Includes the amidase AtIA, Endopeptidase EnpA and the 1-4 N-acetylmuramyl-N-acetylglucosamine mutanolysin.

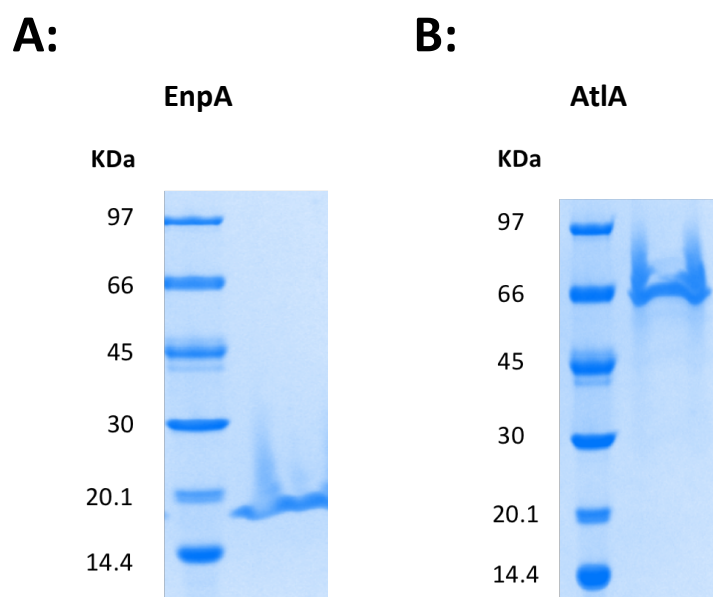


**Figure 4.14: SDS-PAGE of recombinant hydrolases used in this study.** Proteins purified by IMAC and GF including (A) Recombinantly expressed EnpA and (B) Recombinantly expressed AtIA.

The AtIA enzyme is isolated from *S. aureus*. Its hydrolase domains have been recombinantly purified and tested before using *S. aureus* PG (Mesnage *et al.*, 2014). To initially test the activity of the AtIA amidase against PG from other species, the activity of the purified amidase enzyme AtIA, at different concentration of the amidase AtIA in buffer (25 mM Tris (pH 7.5), 50 mM NaCl, 0.1 mM CaCl<sub>2</sub>), the enzyme was mixed with 75 µg PG that was labelled with [<sup>14</sup>C] GlcNAC in 15 µL (Roughly 50,000 cpm). Reactions were incubated at 37°C overnight then 400 µL H<sub>2</sub>O added where 200 µL was counted (Total scintillation count). Then 3.8 mL scintillation cocktail (Lablogic) was added to the remaining 200 µL digested PG and 225 µL was taken and centrifuged. The soluble fraction was harvested then counted to monitor PG hydrolysis (soluble scintillation count). Results of the amidase activity across three Gram-positive species are highlighted in **Table 4.4**.

From analysis of the radiolabelled PG hydrolysis from different Gram-positive species at different concentrations of enzyme, it appears that hydrolase activity is inhibited at high enzyme concentrations. For subsequent digestion of PG for the chemi-enzymatic SPR study, 1 mg of PG was digested with 175 µg amidase in 300 µL overnight. To ensure full hydrolysis, samples were boiled for 10 minutes to denature and precipitate the protein. After centrifugation samples were hydrolysed further under the same amidase. Samples were stored in buffer at -20°C.

**Table 4.4: Measurement of hydrolysis activity the hydrolase AtIA (amidase) from *S. aureus* against the PG from three different Gram-positive species.** The AtIA enzyme was shipped and experiments performed by Dr. Stephane Mesnage on radio-labelled PG (University of Sheffield). Activity of the AtIA amidase was determined by measuring the percentage of hydrolysis. This was determined by measuring the total scintillation count (soluble and insoluble PG) and the soluble scintillation count (digested PG caused by amidase).

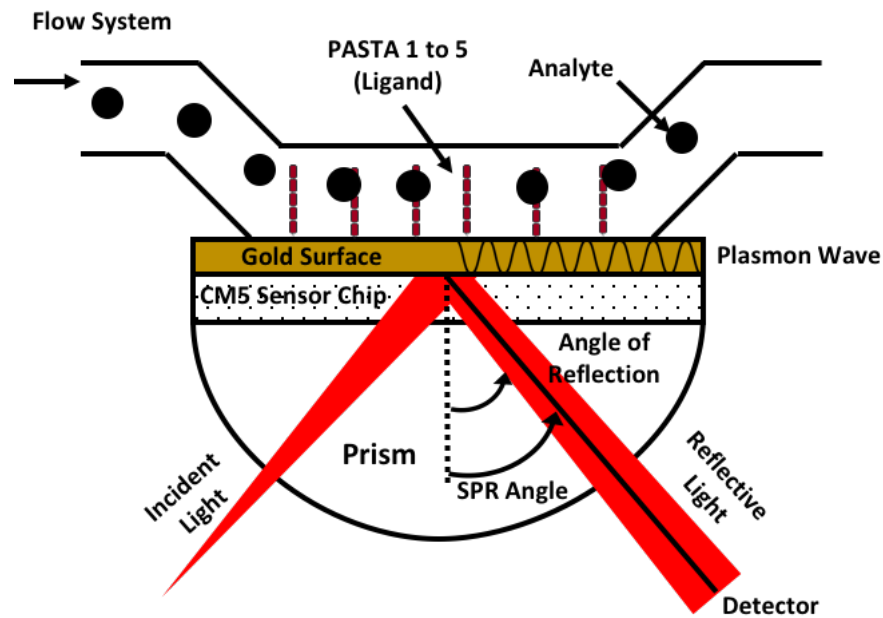
Species	Concentration of AtIA ( $\mu\text{g}$ ) in 15 $\mu\text{L}$	Total scintillation count	Soluble scintillation count	% of Hydrolysis
<i>E. faecalis</i> JH2-2	67.5	17303	13648	78.9
	22.5	16990	15535	91.4
	7.5	17577	16561	94.2
	2.5	17452	17555	95.5
<i>S. aureus</i> COL	67.5	7232	6531	90.3
	22.5	7585	6645	87.6
	7.5	7396	7517	101.6
	2.5	7546	7615	100.9
<i>B. subtilis</i>	67.5	12122	10305	78.9
	22.5	12226	12333	91.4
	7.5	12868	12534	94.2
	2.5	12101	11918	95.4

## 4.6. Surface Plasmon Resonance

### 4.6.1. Introduction to SPR

Surface plasmon resonance (SPR) is an optical biophysical technique used to measure molecular interactions. It is a label-free technique where radioisotope or fluorophore labelling is avoided, but the ligand is immobilised to the sensor surface. Interactions are measured from total internal reflection generated from an incident light source that passes and reflects back through a prism. The photons interact with a gold surface where some of the energy is converted to surface plasmons. The plasmons create an electrical field that extends wither side of the chip and produces an evanescent wave and can measure perturbations 300 nm from the gold surface. Changes in solution adsorption or viscosity can influence the refractive index and implicate the SPR angle. Therefore, binding of biomolecules to the sensor surface results in the change in refractive index and is measured as a change in resonance angle. (Figure 4.15.A) (Schasfoort, 2017).

**A:**



**B:**

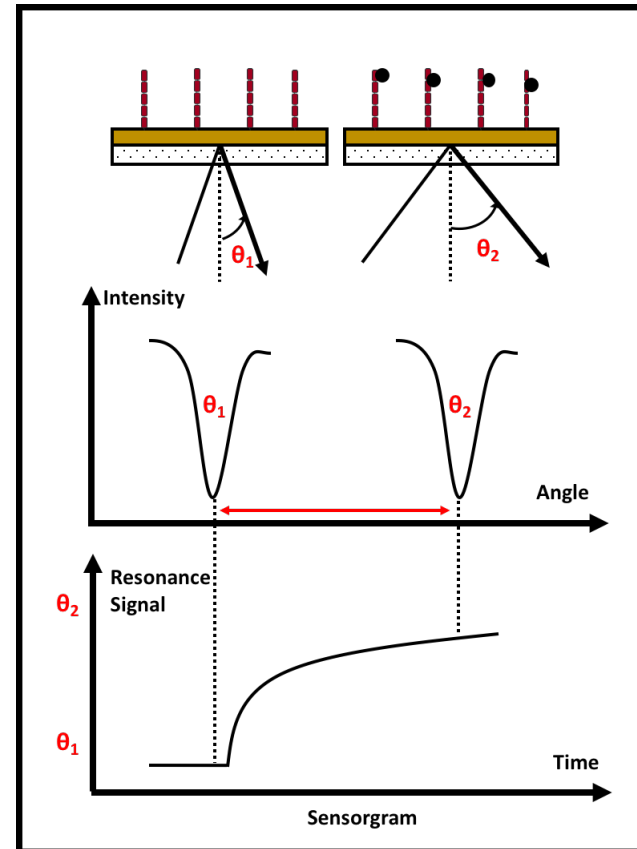


**Figure 4.15: Schematic view of SPR assay.** The CM5 sensor chip and PASTA 1 to 5 (ligand) are included as examples. **(A)** Schematic view of SPR Detector. The incident polarised light is coupled by a glass prism on the CM5 chip coated with a thin gold layer that is integrated with the flow cell channel for continuous buffer flow. **(B)** Schematic of reflective light comparing unbound and bound ligands with analytes to produce a typical SPR sensorgram (Adapted from Skankaran and Miura (2007)).

In a typical SPR experiment, the ligand is immobilised onto the sensor surface. Its binding partner (the analyte) is injected in aqueous buffer solution through the flow cell under continuous flow. Interactions between biomolecules leads to an increase in the mass at the SPR interface, changing the observable SPR angle in real time yielding a binding curve (sensorgram) (**Figure 4.15.B**). Sensorgrams are presented in response units (RUs). Analytes are also subjected to a blank channel to ensure any contributions with the analyte and the sensor surface chip are subtracted from the experimental data.

The immobilization of either one of the binding partners onto the chip surface as ligand can be achieved by a number of different immobilisation methods using a BIACORE system. There are three main ways to attach biomolecules to a surface including covalently, affinity-tag or capture partner immobilization. Generally covalent immobilisation involves the biomolecule covalently immobilising to the dextran matrix on the sensor surface and often provides a very stable attachment of the ligand to the sensor surface. Amide coupling covalently links the ligand to the surface through primary amine surface residues or nucleophilic groups forming an amide bond. Thiol coupling exploits thiol-disulphide exchange between thiol groups and active disulphides that have been introduced to either the ligand or matrix surface. Aldehyde coupling uses the reaction between hydrazine or carbohydrazine groups introduced on the surface or aldehyde groups obtained by oxidation in the ligand.

Biotin capture requires the ligand to have a biotinylated linker group to bind to a streptavidin-coated surface where the biotin-streptavidin interaction is one of the strongest non-covalent interactions (Green, 1975) lending itself well to SPR immobilization. His-capture works for proteins with a poly-Histidine tag to co-ordinate with a  $\text{Ni}^{2+}$  cation. Antibody capture relies on firstly capturing an antibody protein onto the surface via any of the previous techniques and then subsequently capturing the ligand containing the complimentary antibody epitope.

The chip surface containing the immobilised ligand requires regeneration to ensure multiple analytes at different concentrations can be screened. Regeneration is the involves removing the bound analyte from the surface after the analysis cycle without damaging the ligand in preparation for a new cycle. The regeneration solution should not also degrade the sensor surface so as to cause the immobilized ligand to detach.

To test the binding of a sub set of ligands to the extracellular PASTA domains, a CM5 chip was used to which the protein was immobilised by amide coupling as it is often recommended as a starting chip for testing initial immobilisation. Its general properties include, high capacity capture and support of a wide range of immobilisation levels which is advantageous when studying small molecules.

#### **4.6.2. pH Scouting and immobilisation of the extracellular PASTA domain**

Amine coupling is based on amide bond formation between a carboxylic acid group on the chip and a primary amine on the ligand surface. In order to drive the formation of an amide bond, the OH of the carboxylic acid group must be activated into a better leaving group. This is achieved by conversion of the OH into a reactive succinimide ester group via EDC (1-Ethyl-3-(3-dimethylaminopropyl)carbodiimide) and then NHS (N-hydroxysuccinimide) additions to yield a stabilized but highly reactive NHS ester. Once activated, a ligand in favourable buffer conditions will be conjugated to the carboxylic acid group and immobilized. Any remaining activated esters are reacted with ethanolamine. Amide coupling can result random orientation of the ligand to the dextran surface and may block potential binding sites.

When immobilising the ligand using amide coupling, the surface chemistry needs to be considered. Above pH 3.5, the dextran matrix is negatively charged and will concentrate positively charged ligands through electrostatic attractive forces. This process requires the pH of the buffer to be between 3.5 and the isoelectric point (pI) of the ligand to maintain a cationic protein surface on the latter. In order to maximize ligand capture, a “pH scouting” protocol is used to identify the pH for maximum ligand attraction prior to activating the surface for covalent ligand capture where 10 mM sodium acetate buffers in 0.5 pH unit increments is used (i.e. pH 4, 4.5, 5 and 5.5).

Binding of PASTA domains to various ligands was studied using SPR. Recombinant PASTA proteins made of the full extracellular modules (PASTA 1 to 5) that were immobilized on a sensor chip with the poly-his(x6) tag with TEV cleavage site (PASTA 1 to 5 (His)), or with TEV Cleaved protein (PASTA 1 to 5 (TEV)). Before immobilisation of the PASTA constructs onto the sensor surface chip, pH scouting was performed (**Figure 4.16**). Conditions for pH scouting included 180 seconds contact time and a flow rate of 5  $\mu\text{L min}^{-1}$ . Only the constructs that were diluted in pH 5 and 5.5 showed association with the

sensor surface with the TEV cleaved PASTA, whereas all diluted PASTA constructs without TEV cleavage showed association to the surface chip and also showed weak dissociation and required a regeneration step to clean the surface. A pH of 5.5 did not show the highest response unit in comparison to the other adjusted pH, but it did reach saturation and also had the highest response after injection of the protein stopped. Although pre-concentration is more efficient at high pH values, the amine coupling chemistry requires uncharged amino groups, immobilisation it is more efficient at a higher pH. Therefore, for both constructs, immobilisation was performed in pH 5.5 sodium acetate.

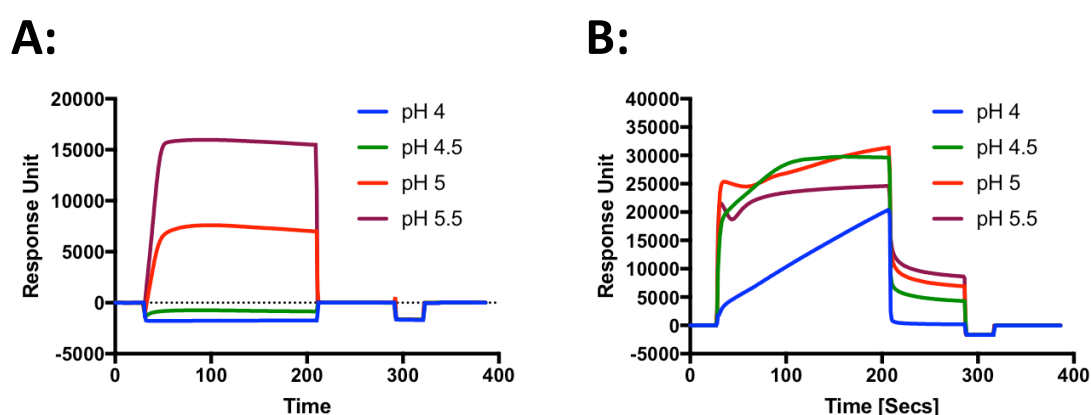


**Figure 4.16: Pre-concentration pH scouting.** Each PASTA 1 to 5 construct was diluted to a final concentration of  $0.02 \text{ mg mL}^{-1}$  in 10 mM sodium acetate at either pH 4, 4.5, 5 or 5.5. The affinity for the CM5 sensor surface for each construct was assessed (A) PASTA 1 to 5 (His) and (B) PASTA 1 to 5 (TEV) in each of the buffer conditions at a flow rate of  $5 \mu\text{L min}^{-1}$  on a BIACORE T200.

After pH scouting, the two PASTA 1 to 5 constructs were immobilised onto the CM5 surface chip using amide coupling with the ligand diluted in  $0.02 \text{ mg mL}^{-1}$  and pH 5.5 for the constructs PASTA 1 to 5 (His) and PASTA 1 to 5 (TEV). Conditions included 420 secs contact time and a flow rate of  $10 \mu\text{L min}^{-1}$ . **Figure 4.17** highlights the immobilisation profile for PASTA 1 to 5 (TEV) giving a final response of 725 RU and **Figure 4.18** highlights the immobilisation of the PASTA 1 to 5 (His) giving a final response of 6347 RU. Immobilisation in other experiments in these conditions were performed on the PASTA 1 to 5 construct (His) (7750 RU and 4536 RU).

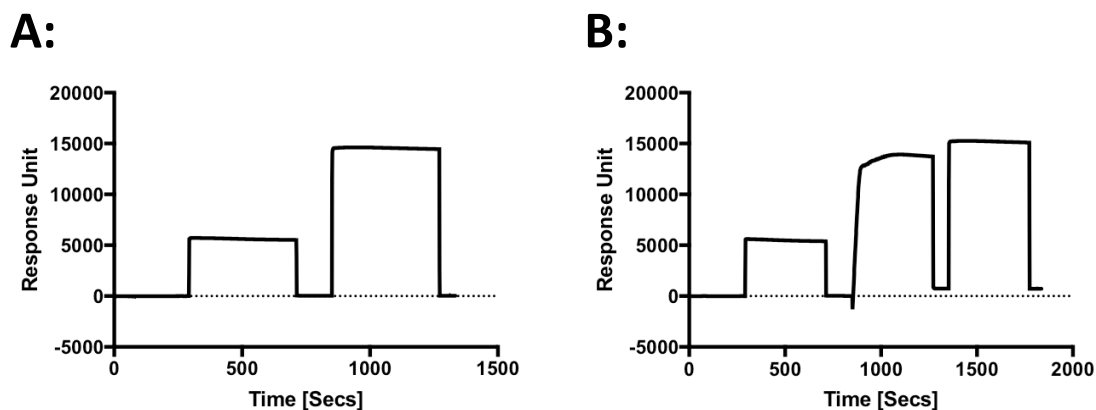


**Figure 4.17: Immobilisation of PASTA 1 to 5 (TEV).** PASTA 1 to 5 (TEV) was diluted to a final concentration of  $0.02 \text{ mg mL}^{-1}$  in 10 mM sodium acetate, pH 5.5 and immobilised on a CM5 sensor surface chip on a BIACORE T200 at a flow rate of  $10 \mu\text{L min}^{-1}$ . Sensogram demonstrate immobilisation by amide coupling of (A) blank flow cell and (B) PASTA 1 to 5 (TEV).

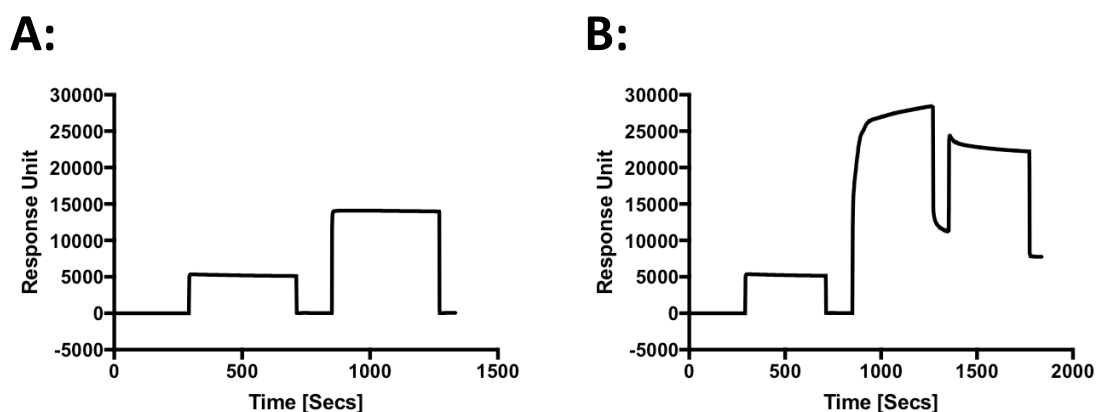


**Figure 4.18: Immobilisation of PASTA 1 to 5 (His).** PASTA 1 to 5 (HIS) was diluted to a final concentration of  $0.02 \text{ mg mL}^{-1}$  in 10 mM sodium acetate, pH 5.5 and immobilised on a CM5 sensor surface chip on a BIACORE T200 at a flow rate of  $10 \mu\text{L min}^{-1}$ . Sensogram demonstrate immobilisation by amide coupling of (A) blank flow cell and (B) PASTA 1 to 5 (HIS).

#### 4.6.3. Identification of a suitable regeneration solution

Prior to full titration experiments, a suitable regeneration solution was required for subsequent high-throughput analysis. Binding was analysed using analyte mixtures prepared from PG sacculi hydrolysed by enzymes displaying distinct cleavage specificities. Initial binding was observed by the amidase treated *E. faecalis* PG construct and provided a suitable control to look into suitable regeneration solutions. Although binding was not

observed for the TEV cleaved construct, binding was observed for the non-TEV cleaved construct. Ligand regeneration using 10 mM NaOH caused a decrease in RU of the immobilised protein (**Figure 4.19.A**) and regeneration using 5 M NaCl did not allow the regeneration step to reach base line (**Figure 4.19.B**). In a previous study where the extracellular domains of LysM from the *E. faecalis* protein AtIA were studied, 6M guanidine hydrochloride was efficient to regenerate the immobilised construct on the sensor surface chip (Mesnage *et al.*, 2014). **Figure 4.19.C** shows that guanidine hydrochloride is efficient in removing the analyte from the immobilised ligand and that the baseline is restored after regeneration. All subsequent binding experiments were performed in triplicates to ensure there was no irreversible damage to the immobilised ligand.

#### **4.6.4. Issues with the TEV-cleaved PASTA 1 to 5 construct**

After initial scouting for a suitable regeneration solution using PASTA 1 to 5 (His), the immobilised TEV cleaved PASTA construct was screened against the analytes used to study PASTA 1 to 5 (TEV). Unfortunately, no binding was observed. Initial observation of the immobilisation of PASTA 1 to 5 (TEV) shows very weak immobilisation to the sensor surface chip (**Figure 4.17**). The pIs of the cleaved and non-cleaved PASTA 1 to 5 domains are close to one another (4.78 and 4.89, respectively). Although there is no conclusive explanation for the difference in immobilisation between the two constructs, it is possible that the addition of the His-tag and TEV cleavage site gives the protein slightly more charge and more propensity to interact with the sensor surface chip. For all subsequent studies, the non-TEV cleaved PASTA constructs were used to study interactions with potential analytes.

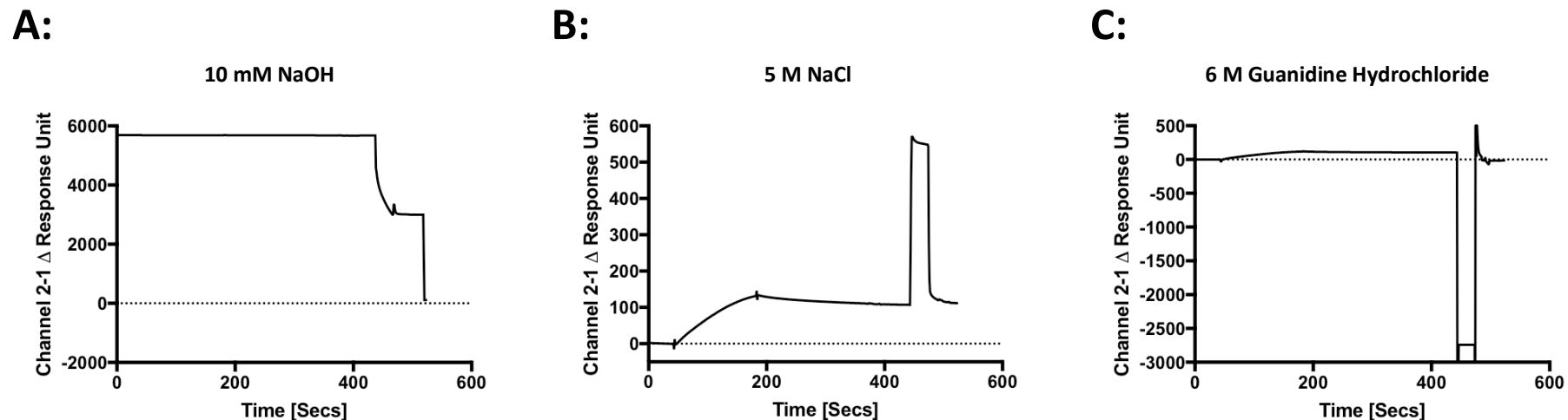


**Figure 4.19: Sensogram profile of candidate regeneration solutions using PASTA 1 to 5 (HIS) constructs.** Immobilised PASTA 1 to 5 (HIS) construct on a CM5 surface chip was subjected to regeneration scouting to optimise conditions for testing multiple analytes and concentrations on the same ligand on the same sensor surface. Running conditions included  $10 \mu\text{L min}^{-1}$  and initial runs were tested with just SPR running buffer to ensure a steady baseline. (A) The first regeneration step using 10 mM NaOH caused a sharp decrease and removed immobilised protein from the sensor surface. Data not normalised to baseline. (B) After 1 injection of  $10 \mu\text{g mL}$  *E. faecalis* digested PG with amidase, regeneration with NaCl did not restore the sensogram to baseline and indicates NaCl was inefficient at removing the analyte from the ligand. (C) After 1 injection of  $10 \mu\text{g mL}$  *E. faecalis* digested PG with amidase, regeneration with 6M guanidine hydrochloride did restore the sensogram to baseline and indicates 6M guanidine hydrochloride was efficient in removing the analyte from the ligand.

#### 4.6.5. Screening potential analytes against *E. faecalis* PASTA domains 1 to 5

It was previously determined in **Chapter 3** that the PASTA domains in IreK localise the protein to the septum of growing cells where PG polymerisation and cell division occur. As this is the site of high PG activity, including transpeptidation and transglycosylation, it is also the location of antibiotic targets that target PBPs. The subsequent experiments aimed to characterise potential interactions between PASTA domains and PG derivatives and antibiotics.

##### 4.6.5.1. Binding of Heterogeneous PG derivatives to *E. faecalis* PASTA domains 1 to 5

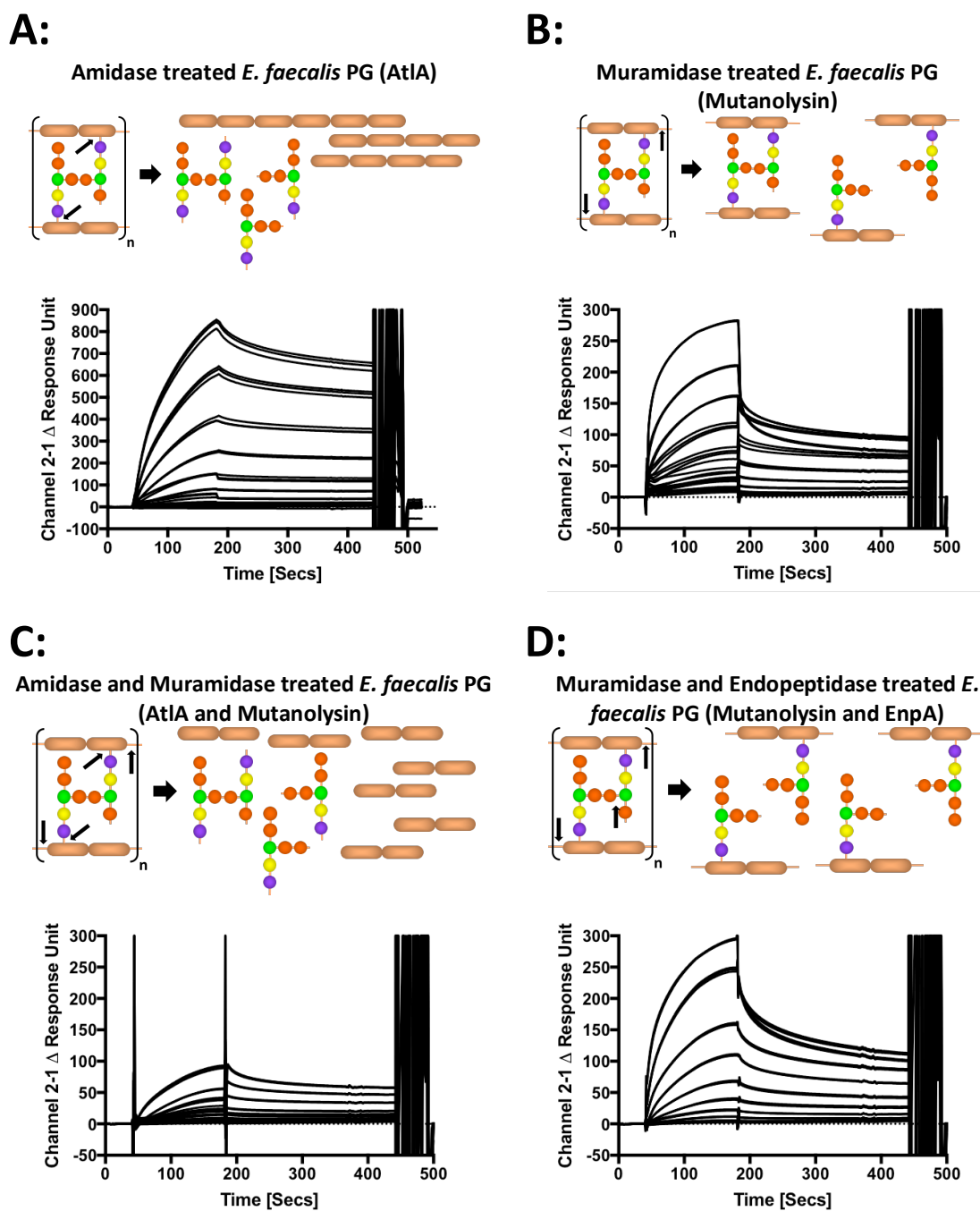
To determine the impact of PG motifs on binding to PASTA, hydrolysed PG fragments were generated and have been shown to bind using this method to the *E. faecalis* LysB domains using SPR (Mesnage *et al.*, 2014). Dose-dependent binding was observed with soluble PG hydrolysed fragments from *E. faecalis* using amidase, muramidase or endopeptidase digestion. Fragments treated with amidase showed an apparent higher binding affinity compared to those treated with muramidase or muramidase and endopeptidase, but binding was still observed in the presence of other PG hydrolases (**Figure 4.20**).

Interestingly, there was little difference in binding when comparing the muramidase treated PG products and the muramidase and endopeptidase treated products (**Figure 4.20.B** and **Figure 4.20.D** respectively). The greatest difference in binding was in comparison to the amidase treated PG with heterogeneous populations of glycan strands and peptide stems and that endopeptidase treatment followed my muramidase treatment giving heterogeneous populations of peptide stems and shorter glycan strands (**Figure 4.20.A** and **Figure 4.20.C** respectively). This indicates that longer glycan strands provide a more favourable ligand for binding of PASTA domains than shorted glycan strands.

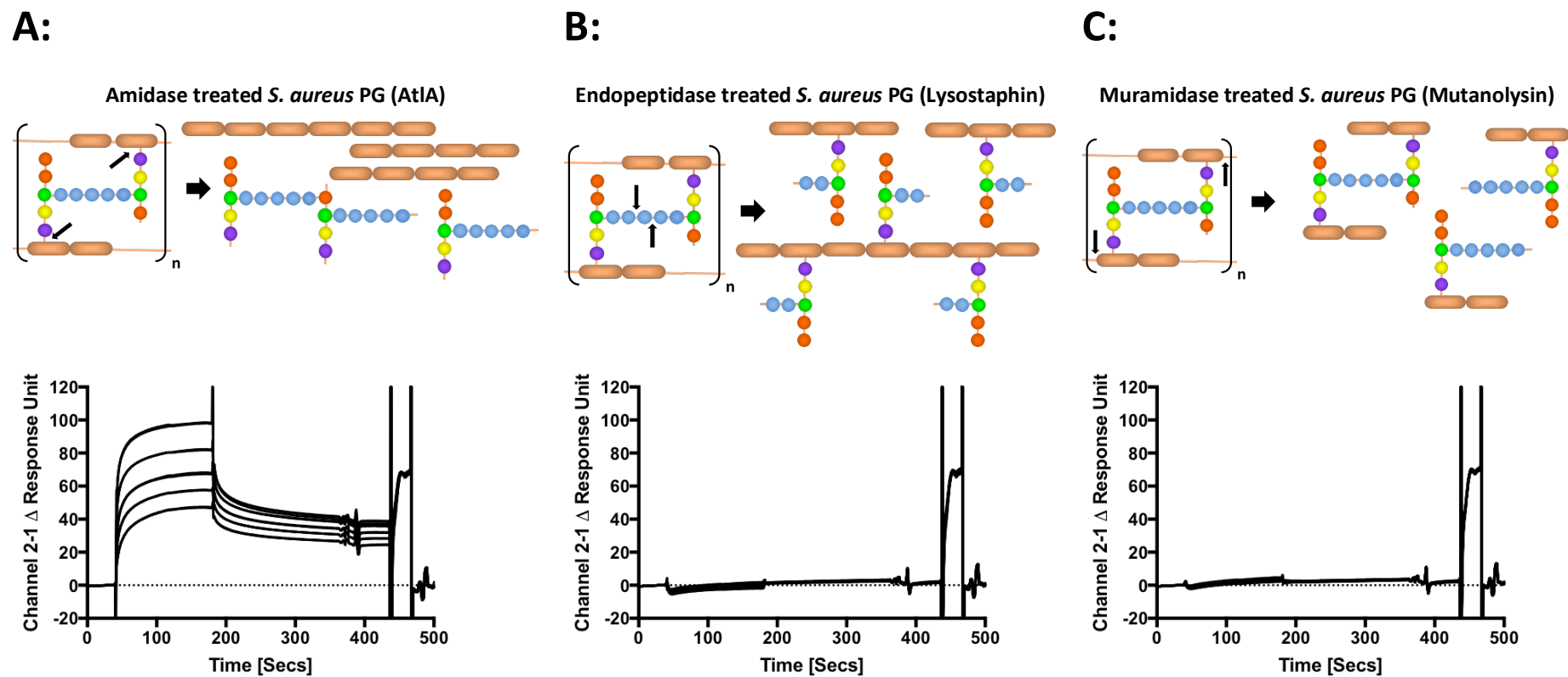
To complement the experiments studying the hydrolysis of PG from *E. faecalis*, **Figure 4.21** illustrates the dose dependency of *S. aureus* PG against *E. faecalis* extracellular PASTA domains. Interestingly, the only experiment to demonstrate ligand binding is that of *S. aureus* PG that has been digested with amidase to give a heterogeneous population of long glycan strands and peptide stems. The other

experiments showing endopeptidase treatment of muramidase treatment did not show any dose dependent response. This indicates that the oligomeric glycan strand is the main ligand for the PASTA domains of *E. faecalis* from both *E. faecalis* and *S. aureus* amidase treated PG and that the pentapeptide bridge in *E. faecalis* (Ala-Ala) is also important since binding is also observed when the glycan strands are hydrolysed with mutanolysin. Binding is not observed in *S. aureus* PG treated with mutanolysin and indicates that the *S. aureus* PG bridge (Gly<sub>5</sub>) is not important for PASTA interactions.

To study the effect of glycan motifs binding to PASTA domains from *E. faecalis*, whole cell PG and natural polymeric derivatives with different sugar chains were tested in an SPR experiment. Insoluble PG was used with a GlcNAc-MurNAc glycan backbone, chitin presented a comparable poly-GlcNAc ligand, cellulose as an alternative linear polysaccharide containing multiple glucose motifs and xylan containing xylose as its polysaccharide sub-unit (**Figure 4.22**). The *E. faecalis* PG showed the highest binding activity and also showed a dose dependent response with a two-fold serial dilution of the ligands. The other polysaccharide substrates showed either weak (chitin and xylan) or no binding of cellulose. These experiments indicate that at least the GlcNAc and MurNAc motifs are required for binding to the PASTA domains.



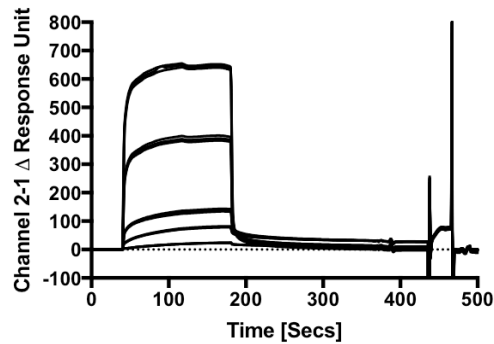
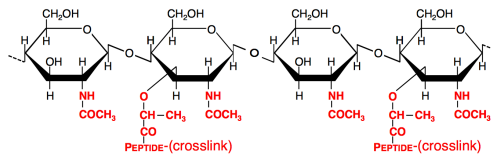
**Figure 4.20: Identification of PG motifs recognised by the PASTA domains using *E. faecalis* PG.** Experiments performed on Immobilised PASTA 1 to 5 (HIS) construct on a CM5 surface chip at a flow rate of  $10 \mu\text{L min}^{-1}$ . This chemi-enzymatic approach provides a heterogeneous population of *E. faecalis* PG that have been specifically cleaved by certain cell wall hydrolases. These include (A) The AtIA amidase, (B) The mutanolysin muramidase, (C), Amidase and Muramidase treatment with AtIA and Mutaolysin respectively and (D) Muramidase and Endopeptidase treatment with Mutanolysin and EnpA respectively. All were performed in a titration series including 100, 50, 25, 12.5 and  $6.25 \mu\text{g mL}^{-1}$  of each hydrolysed PG product. Schematics of a typical digestion profile is also highlighted above each respective sensogram. Each concentration was performed in triplicates.



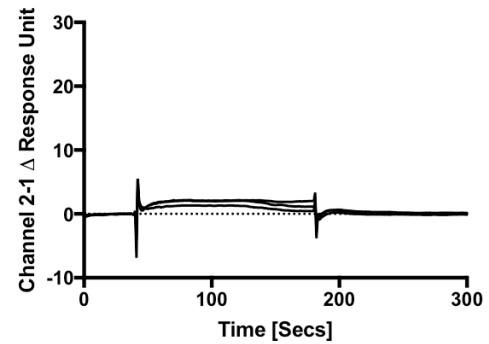
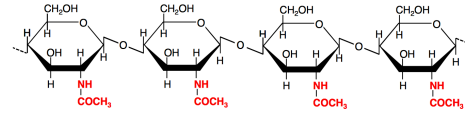
**Figure 4.21: Identification of PG motifs recognised by the PASTA domains using *S. aureus* PG** (Kind gift from Stephane Mesnage, The University of Sheffield). Experiments performed on Immobilised PASTA 1 to 5 (HIS) construct on a CM5 surface chip at a flow rate of  $10 \mu\text{L min}^{-1}$ . This chemo-enzymatic approach provides a heterogeneous population of *S. aureus* PG that have been specifically cleaved by certain cell wall hydrolases. These include (A) The AtIA amidase, (B), The mutanolysin muramidase and (C) Endopeptidase treatment lysostaphin. All were performed in a titration series including  $100, 50, 25, 12.5$  and  $6.25 \mu\text{g mL}^{-1}$  of each hydrolysed PG product. Schematics of a typical digestion profile is also highlighted above each respective sensogram. Each concentration was performed in triplicates.

**A:****Peptidoglycan**

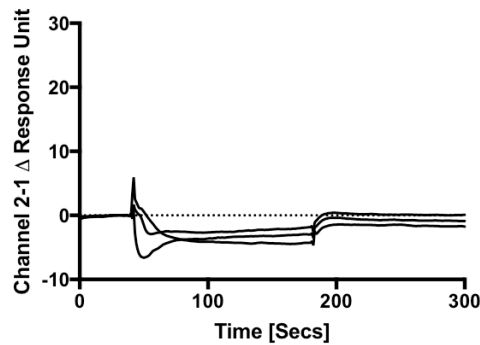
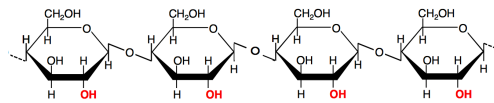
B-1,4-GlcNAc-MurNAc-peptide polymer

**B:****Chitin**

B-1,4-GlcNAc polymer

**C:****Cellulose**

B-1,4-Glucose polymer

**D:****Xylan**

B-1,4-xylose polymer

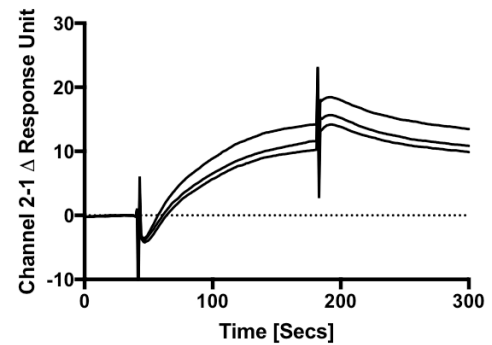
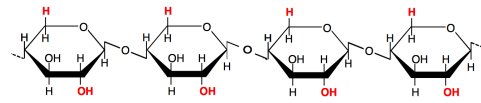


**Figure 4.22: Binding activity of PASTA domains 1 to 5 with sugar polysaccharides.** Experiments performed on Immobilised PASTA 1 to 5 (HIS) construct on a CM5 surface chip at a flow rate of  $10 \mu\text{L min}^{-1}$ . Includes (A) whole cell PG with an increasing titration ( $10, 50, 100, 500, 1000 \mu\text{g mL}^{-1}$ ), (B) Chitin at  $1000 \mu\text{g mL}^{-1}$ , (C) Cellulose at  $1000 \mu\text{g mL}^{-1}$ , and (D) Xylan at  $1000 \mu\text{g mL}^{-1}$  including schematics of structures of each polysaccharide used where differences are highlighted in Red. Each binding experiment of polysaccharide was performed in triplicate.

### 5.3.6.2 Binding of PASTA 1 to 5 to pure PG motifs

In a previous *in vivo* model studying the effect of the eSTK in PrkC in *B. subtilis*, it was shown that *B. subtilis* spores could germinate in the presence of DAP-type but not Lys-type cell wall muropeptides (Shah *et al.*, 2008). The extracellular PASTA domains of PrkC were further explored in a ligand binding study using STD NMR and had showed that the PASTA domains for PrkC in *B. subtilis* interacted directly with the DAP moiety of a muropeptide and interact directly with an arginine residue in the C-terminal PASTA domain. Mutation of this residue completely suppressed muropeptide binding and gave the first indication into the sensing mechanism of the PASTA domains in PrkC (Squeglia *et al.*, 2011). Although in these experiments the binding of muropeptides was not tested, they were tested in MST experiments described later. It was clear from earlier experiments that the glycan chains may be implicated in the binding of PASTA 1 to 5 of IreK in *E. faecalis* unlike muropeptides shown previously. In **Figure 4.23**, the monomeric units of the glycan chain of PG were tested individually at a high concentration (2 mM) in triplicates. From the preliminary analysis of these two ligands, it appears that MurNAc binds slightly higher than GlcNAc but the initial binding activity of either is not high even at 2 mM concentration.

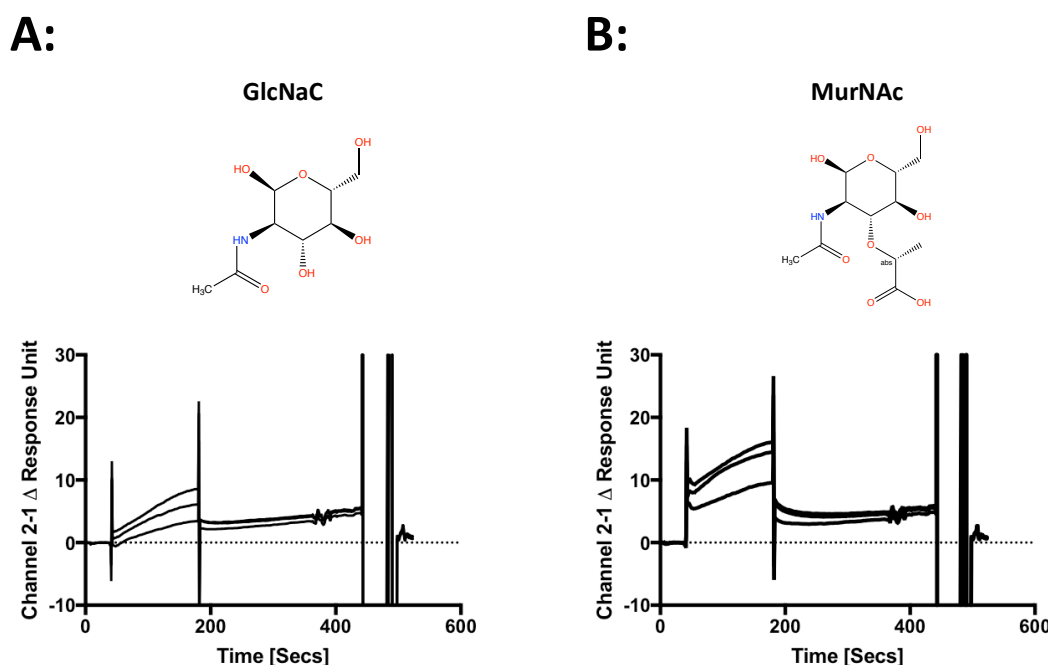


**Figure 4.23: Binding of PG glycan monomers extracellular PASTA domains of *E. faecalis* IreK.**

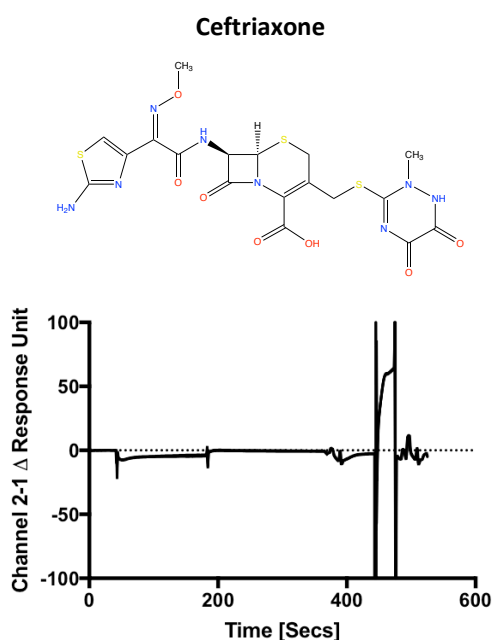
Experiments performed on Immobilised PASTA 1 to 5 (HIS) construct on a CM5 surface chip at a flow rate of  $10 \mu\text{L min}^{-1}$ . Includes (A) GlcNAc and (B) MurNAc at 2 mM in triplicates.

### 5.3.6.3. Binding of PASTA 1 to 5 to $\beta$ -lactam antibiotics

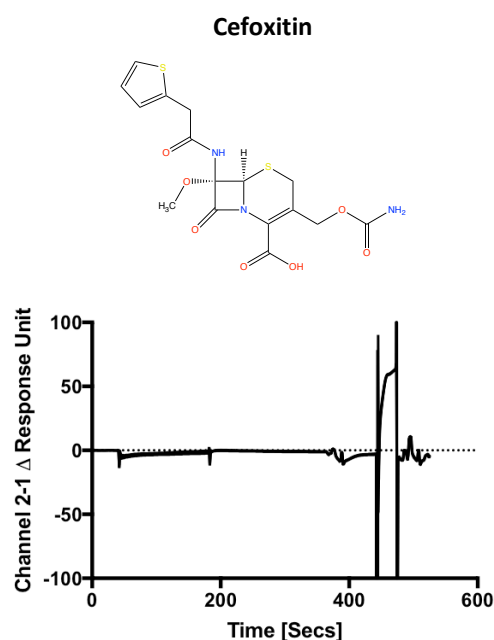
PASTA domains are not only found on eSTKs but can also be found on some PBPs such as PBP2x in *S. pneumoniae*. Previous experiments have demonstrated that Bocillin FL (a fluorescent penicillin) was essential in the binding to the PASTA domains, and that the binding also provided stability to PBP2x (Schweizer *et al.*, 2014). Consistent with the role of PASTA domains in PBPs binding  $\beta$ -lactams, the X-ray structure of an acylated PBP2x crystallised was solved in the presence of a high concentration ( $14 \text{ mg mL}^{-1}$ ) of cefuroxime with two molecules bound. One was covalently bound to the active site serine and the second was non-covalently positioned between the TP and the first PASTA domain (Gordon *et al.*, 2000).

**Figure 4.24** shows an SPR experiment studying the interactions between two  $\beta$ -lactams of the cephalosporin class ceftriaxone and cefoxitin. In **Chapter 3**, it was highlighted that IreK was essential in intrinsic and enhanced cephalosporin resistance in *E. faecalis*. The SPR experiment where 2 mM of each antibiotic was tested against PASTA 1 to 5 found that there is no interaction.

**A:**



**B:**

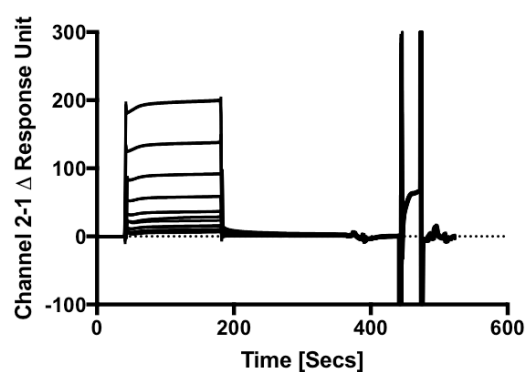
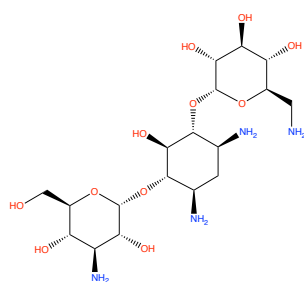
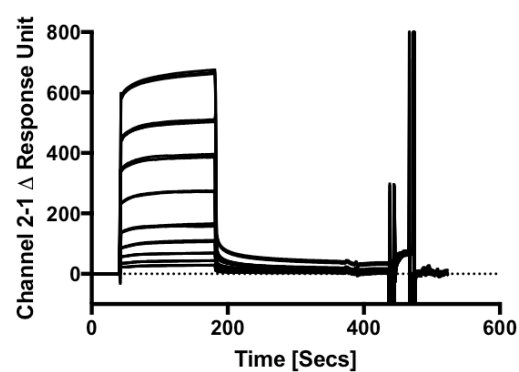
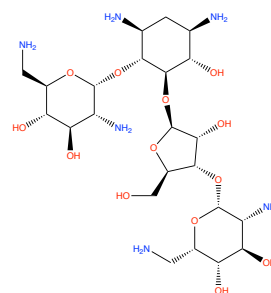
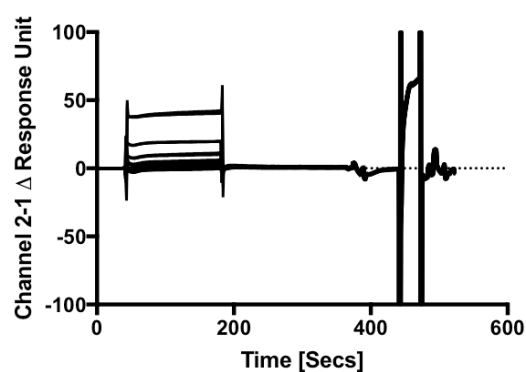
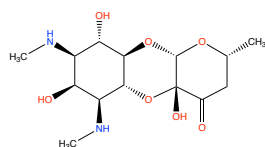
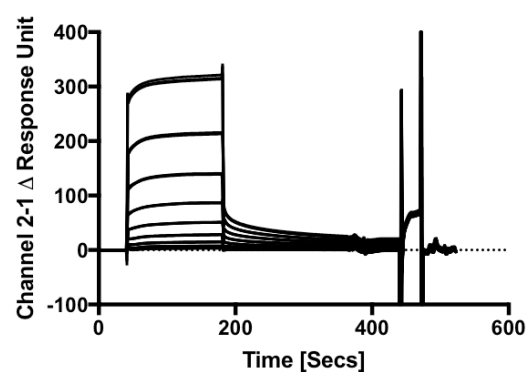
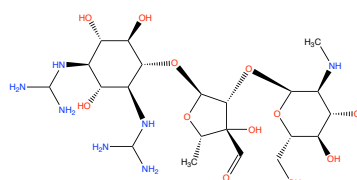


**Figure 4.24: Binding of cephalosporin antibiotic to the extracellular PASTA domains of *E. faecalis* IreK.** Experiments performed on Immobilised PASTA 1 to 5 (HIS) construct on a CM5 surface chip at a flow rate of  $10 \mu\text{L min}^{-1}$ . Includes structures of each cephalosporin and SPR sensorgrams showing a dose dependence response. Antibiotics were 2-fold serially diluted from 2 mM.

#### 5.3.6.4. Binding of PASTA 1 to 5 to aminoglycoside antibiotics

Previous research has highlighted that aminoglycosides have little effect on IreK homologues in other species including PknB in *S. aureus* (Tamber *et al.*, 2010). In this study in **Chapter 3**, it is also highlighted that there is little difference in the MIC when comparing gene deletions of *ireK*. A small subset of aminoglycosides was tested against the PASTA domain 1 to 5 from *E. faecalis* IreK including kanamycin, neomycin, spectinomycin and streptomycin (**Figure 4.25**).

Interestingly, although there is little difference in the MICs that have been observed when studying eSTKs in Gram-positives and aminoglycosides, there appears to be a dose dependent response with increasing concentrations of each aminoglycoside. It was previously described in this chapter that the PASTA domains may potentially have an interaction with the glycan chains of the heterogeneous PG samples. In comparison to the glycan backbone of PG, an important feature of aminoglycosides is the presence of an amino-modified glycoside. This chemical property might suggest why there is an interaction between the aminoglycosides and the PASTA domains from IreK.

**A:****Kanamycin****B:****Neomycin****C:****Spectinomycin****D:****Streptomycin****Figure 4.25: Binding of aminoglycoside antibiotic to the extracellular PASTA domains of *E. faecalis* IreK.**

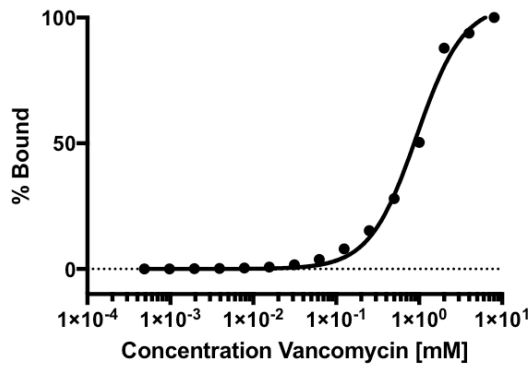
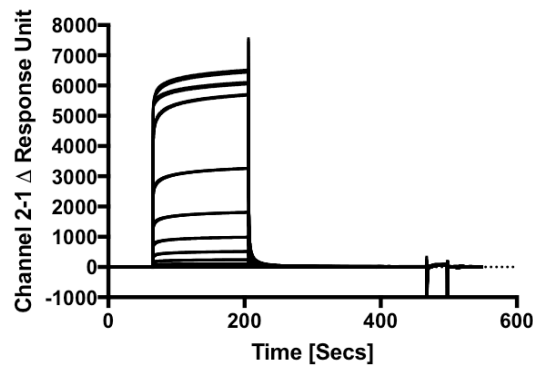
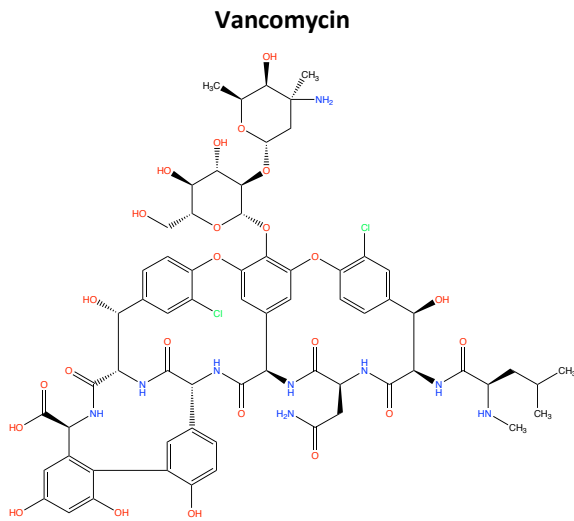
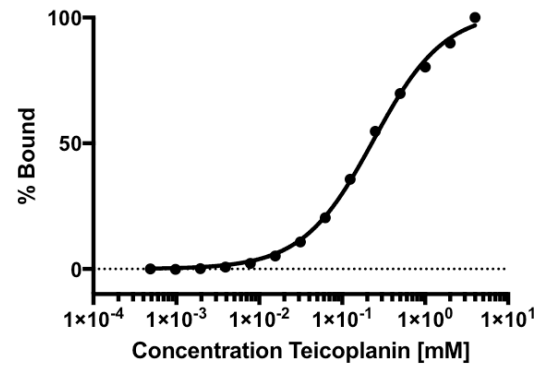
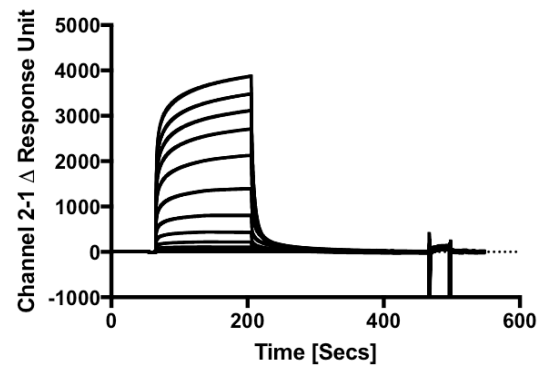
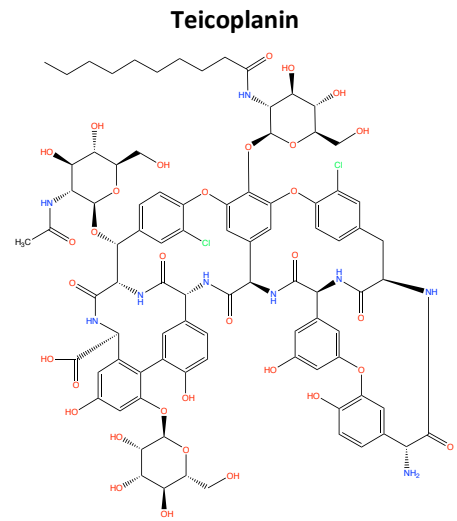
Experiments performed on Immobilised PASTA 1 to 5 (HIS) construct on a CM5 surface chip at a flow rate of  $10 \mu\text{L min}^{-1}$ . Includes structures of each aminoglycoside and SPR sensorgrams showing a dose dependence response. Antibiotics were 2-fold serially diluted from 2 mM.

### 5.3.6.5. Binding of PASTA 1 to 5 to glycopeptide antibiotics

In **Chapter 3** it has highlighted that although the Tn1549 resistance cassette conferring *vanB* type resistance and its interaction with IreK was essential for enhanced cephalosporin resistance, it appeared that IreK was only important to vancomycin tolerance (not resistance) as there was only a small difference in MIC. Like the aminoglycosides, glycopeptides such as vancomycin have not been shown to have a direct impact on strains when comparing WT and mutation strains of eSTKs including *S. aureus* and *L. monocytis* indicating that any interaction with eSTKS is not associated with resistant mechanisms (Tamber *et al.*, 2010; Pensinger *et al.*, 2014).

Similar to the aminoglycoside sensorgrams in **Figure 4.25**, the glycopeptides vancomycin and teicoplanin also appear to be ligands for the PASTA domains of IreK from *E. faecalis* as shown in **Figure 4.26**, it is clear that vancomycin and teicoplanin bind to the PASTA domains in a dose dependent manner as determined by the SPR sensorgrams, and unlike the aminoglycosides, binding reached saturation for both antibiotics. Therefore, the steady state binding kinetics were determined for both antibiotics. This included vancomycin  $K_D$  at  $929 \mu\text{M} \pm 41 \mu\text{M}$  and teicoplanin  $K_D$  at  $238 \mu\text{M} \pm 8.6 \mu\text{M}$ . Although these ligands show a low binding affinity to the IreK PASTA domains, they do provide a reference point for future experiments using other techniques. Along with the aminoglycosides, the glycopeptides may not be the true ligands for the PASTA domains, but may provide further evidence that the PASTA domains are detecting sugar like molecules such as the glycan chain of PG. It is clear when determining the  $K_D$  using SPR of these two analytes, that teicoplanin binds more readily to the PASTA domains than vancomycin.

Although SPR has many advantages over other binding techniques due to its ability to calculate not only the dissociation equilibrium constant ( $K_D$ ), but also the association rate constant ( $k_a$ ) and dissociation rate constant ( $k_d$ ). As most ligands that have bound efficiently have been heterogeneous in the study, only a dose dependent response can be reported. When studying the glycopeptides, a  $K_D$  could be determined from the steady state binding kinetics, but the binding constants  $k_a$  and  $k_d$  were difficult to determine as they were approaching the limits of the instrument.

**A:****B:**

**Figure 4.26: Binding of glycopeptide antibiotics to the extracellular PASTA domains of *E. faecalis* IreK.** Experiments performed on Immobilised PASTA 1 to 5 (HIS) construct on a CM5 surface chip at a flow rate of  $10 \mu\text{L min}^{-1}$ . Includes structures of each glycopeptide and SPR sensorgrams showing a dose dependence response. Binding curves of steady state saturation are also included and performed in triplicate. Antibiotics were 2-fold serially diluted from 8 mM for vancomycin or 4 mM for teicoplanin.

## 4.7. Microscale Thermophoresis (MST)

MST is a relatively new technology for studying the interaction between biomolecules. It measures the diffusion of molecules in a temperature gradient produced by IR irradiation. There are currently two methods, the first is a label free method that uses the inherent fluorescence of tryptophan residues in proteins, and the second requires the use of fluorescent labels that are covalently linked to the protein via lysine, cysteine or polyhistidine. Due to the PASTA domains in *E. faecalis* containing few aromatic amino acids and no tryptophan's, fluorescent labelling techniques were used.

To ensure that the fluorescent label would not interfere with the binding of different ligands to the PASTA domains, the His-label kit was used. In both the label free and labelling methods, an infrared (IR) laser was used to induce the temperature gradient and a detector that can measure and quantify the movement of the fluorescent molecules. MST has offered many advantages over SPR and NMR as it only requires a relatively small volume of ligand and receptors in a final volume of 10  $\mu$ L in each capillary. Another major advantage includes that proteins and ligands are free in solution when using MST and not immobilised to a surface. As some of the ligands used in this study are very expensive and available in only small quantities, MST proved an excellent technique not only to validate ligands from other experiments, but to establish binding affinities for expensive ligands. These ligands included pure PG peptides that are synthesised and a polymeric PG glycan.

Labelling of the PASTA 1 to 5 domains was achieved with the fluorescent labels that targets the 6x poly His-tag. To ensure samples were not aggregating with the addition of the tag, initial experiments included that there was homogeneity between different capillaries of the same labelled protein and that there was no difference in the diffusion of the samples when a temperature gradient was applied (**See Appendix 8.6**). It can be concluded that homogeneity was best achieved with the labelled PASTA 1 to 5 protein when the protein was diluted to a final concentration of 50 nM in PBS-Tween.

Initial experiments using MST determined the binding affinities of vancomycin and teicoplanin. This initial experiment would not only set up initial parameters for identifying ligands with higher  $K_D$  than vancomycin and teicoplanin and their  $K_D$  were in the mM and high  $\mu$ M range respectively, it would also validate they are true ligands and

not false positives. **Table 4.5** highlights all the ligands screened against PASTA 1 to 5 using MST including vancomycin and teicoplanin. Although the  $K_D$  between each technique is different using either SPR and MST for vancomycin and teicoplanin, (Vancomycin: SPR ( $K_D = 929 \mu\text{M}$ ) and MST ( $K_D = 2.1 \text{ mM}$ ) and Teicoplanin: SPR ( $K_D = 238 \mu\text{M}$ ) and MST ( $K_D = 930 \mu\text{M}$ )), both techniques estimate the  $K_D$  of vancomycin to be higher than that of teicoplanin. The binding curves for both vancomycin and teicoplanin are highlighted in **Figure 4.27.A** and **Figure 4.27.B** respectively.

After confirming that teicoplanin and vancomycin are ligands for the PASTA domains by MST and SPR, a series of PG derivatives were screened that could not be screened using SPR because of the availability including derivatives of the glycan strand and the peptide stem. Before a binding profile was determined for each ligand, an experiment was set up to compare the differences of the highest concentration of ligand with a sample that had no ligand. If the response altitude is large enough, experiments can then proceed to characterise the binding affinities between the two biomolecules. Unfortunately, all the experiments where derivatives of the peptide stem were tested, the response altitude was not large enough to conclude binding (**Table 4.5; See Appendix 8.6**). Although binding has been observed in *M. tuberculosis* and *B. subtilis* of the peptide stems to their respective PASTA domains, these organisms do not contain a crosslinking bridge in the 3<sup>rd</sup> position of the peptide stem like *E. faecalis* (Ala-Ala) (Squeglia *et al.*, 2011; Mir *et al.*, 2011). Unfortunately, a suitable ligand was not available to test in these circumstances that looked at the pentapeptide stem with a Ala-Ala-bridge and may be a suitable ligand candidate for the PASTA domains.

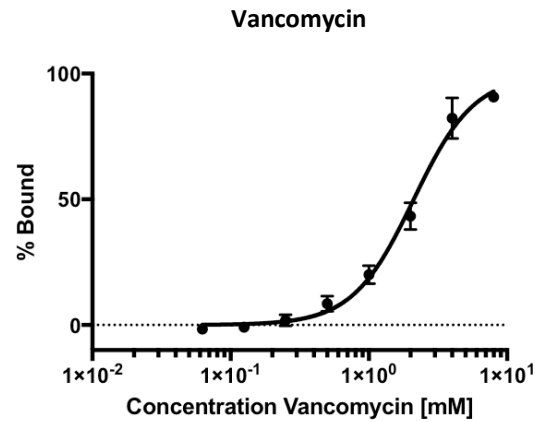
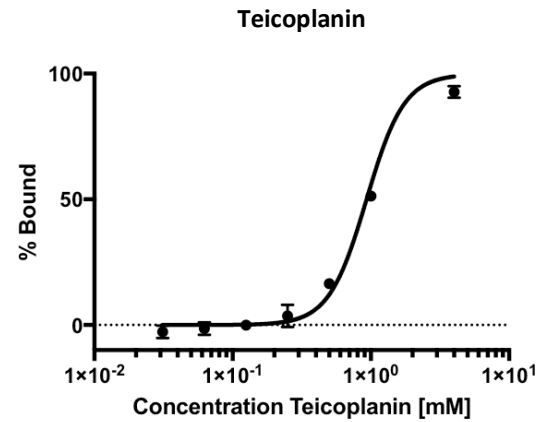
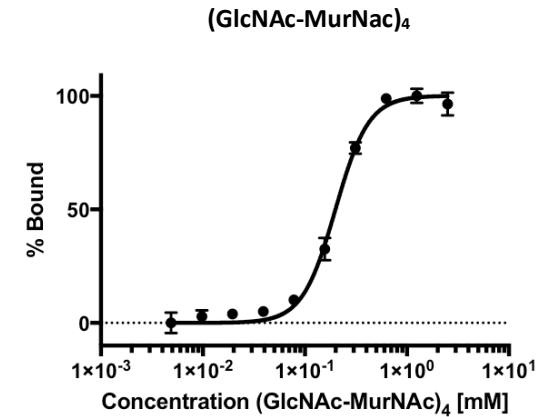
In the SPR study, amidase treated PG from *E. faecalis* showed strong interactions with the PASTA 1 to 5 domains of *E. faecalis*. Dr. Stephane Mesnage (University of Sheffield) provided pure (GlcNAc-MurNAc)<sub>4</sub> to test binding of the PASTA domains using MST (**Figure 4.27.C** and **Table 4.5**). The  $K_D$  is  $199.7 \pm 5.7 \mu\text{M}$  and shows the strongest binding out of the three ligands where a  $K_D$  was determined. In a comparison study, chitotose (GlcNAc)<sub>8</sub> was screened and although binding was observed, saturation could not be reached to determine a  $K_D$  **Table 4.5**.

A recent study studying the interactions of PknB in *M. tuberculosis* with synthetic PG fragments identified that mucopeptides containing a 1,6-anhydro-MurNAc and longer glycan chains exhibit high binding affinity and identified that the binding stoichiometry of

PASTA to ligand was 1:1 (Wang *et al.*, 2017). This data supports the results in this study includes the heterogeneous PG samples from *S. aureus* and *E. faecalis* that had been treated amidase to give long glycan chains and also the pure synthetic (GlcNAc-MurNAc)<sub>4</sub> substrate used in the MST study, although a 1,6-anhydro-MurNAc was not tested.

**Table 4.5: Summary of ligands tested using MST against PASTA 1 to 5.**  $K_D$  values of the IreK PASTA domains 1 to 5 with PG substrates and cell wall antibiotics obtained from fitting the data from at least 3 independent MST experiments in a 1:2 dilution series. Ligands with a small response amplitude with the highest ligand concentration are reported, but  $K_D$  values not determined. Experiments were obtained at room temperature. The response amplitude is the fluorescence intensity shift between bound and unbound state. Replicates increased to 4 for ligands with a low response amplitude.

Analyte	Ligand	$K_D$ [ $\mu$ M]	Response Amplitude [counts]	# of Replicates	SE of Regression	Reduced $\chi^2$	Signal to Noise
IreK: PASTA Domains 1 to 5	Vancomycin	2102 $\pm$ 159.8	24.11	3	0.88	2.23	36.15
	Teicoplanin	930 $\pm$ 41.75	63	3	0.98	3.2	20.6
	(GlcNAc-MurNAc) <sub>4</sub>	199 $\pm$ 5.7	30.93	3	0.76	1.71	49.88
	(GlcNAc) <sub>2</sub>	ND	0.40	4	ND	ND	2.20
	(GlcNAc) <sub>8</sub>	ND	ND	4	ND	ND	ND
	MurNAc	ND	0.20	4	ND	ND	1.20
	MurNAc-L-Ala-D-isoGlu	ND	0.40	4	ND	ND	0.90
	MurNAc-L-Ala-L-isoGlu	ND	0.30	4	ND	ND	0.90
	D-isoGlu-DAP	ND	0.90	4	ND	ND	1.30
	D-isoGlu-Lys	ND	2.20	4	ND	ND	20.20
	MurNAc-L-Ala-D-isoGlu-mDAP	ND	0.7	4	ND	ND	1.8
	MurNAc-L-Ala-D-isoGlu-Lys	ND	0.5	4	ND	ND	1.8
	L-Ala-D-isoGlu-mDAP	ND	0.7	4	ND	ND	1
	L-Ala-D-isoGlu-Lys	ND	1.1	4	ND	ND	6.2
	L-Ala-D-isoGlu-Lys-D-Ala-D-Ala	ND	0.2	4	ND	ND	0.9

**A:****B:****C:**

**Figure 4.27: Dose-response curves of MST analysis.** Experiments performed on PASTA 1 to 5 labelled with the Monolith His-Tag Labeling Kit RED-tris-NTA following manufacturers protocol and conducted on a Monolith NT.115. Includes IreK PASTA domains 1 to 5 with (A) Vancomycin  $K_D = 2.102 \text{ mM} \pm 0.160 \text{ mM}$ , (B) Teicoplanin  $K_D = 930.2 \text{ } \mu\text{M} \pm 41.75 \text{ } \mu\text{M}$  and (C) (GlcNAc-MurNAc)<sub>4</sub>  $K_D = 199 \text{ } \mu\text{M} \pm 5.7 \text{ } \mu\text{M}$  (% bound, 3 repeats).

## 4.8 Conclusions and Future Directions

The previous model for oligomerisation of the eSTKs kinase domains is based on ligand-induced dimerization in analogous eukaryotic systems. The evidence for this situation in bacterial S/T kinases is not well established however (Manuse *et al.*, 2016). Greenstein *et al.*, 2007, described an *in-vitro* experiment demonstrating the dimerization of *M. tuberculosis* PknD KD dimerization was required for PknD autophosphorylation. Thus, based upon a model of eukaryotic S/T kinase dimerization and *in-vitro* observation of PknD dimerization in *M. tuberculosis*, one might expect to see evidence for dimer activation of IreK and by extension homologs in other species.

When the structure of the PASTA domains from *M. tuberculosis* was determined, a model for ligand induced dimerization via the PASTA domains was proposed (Barthe *et al.*, 2010) (**Figure 4.28.A**). This study has tried to use a range of *in vivo* microbiology and *in vitro* biophysical techniques to explore the role of eSTKs in Gram-positive bacteria using *E. faecalis* IreK as a model protein. From the experiments in **Chapter 3**, it can be concluded via the complementation experiments that the kinase domain could function independently from the PASTA domains as the MIC of cefotaxime did not reach  $\Delta$ *IreK* levels. Therefore, the kinase domains could dimerise and autophosphorylate by themselves. The fluorescent microscopy experiments indicated that the PASTA domains are essential in localisation to the septum of growing *E. faecalis* cells. The *in vitro* biophysical experiments described in this Chapter demonstrate that the polymeric glycan backbone of PG is an important potential ligand for the PASTA domains of *E. faecalis*. As PG is polymerised at the site of cell division at the septum, a possible alternative model might include the PASTA domains not dimerising in the presence of a ligand but interacting with the PG at the septum in a symmetrical manner such that IreK is concentrated at the septum and kinase autophosphorylation can readily happen. The location of IreK at the site of PG polymerisation also enables the PASTA domains to detect the local effects of certain antibiotics (e.g. cephalosporins) indirectly, since a lack of transpeptidase crosslinking leads to an increase in the amount of uncrosslinked MurNac-GlcNAc glycan strands. Thus, the PASTA domains are able to detect disruptions in the surrounding PG. This in turn upregulates a cellular response through the IreK signal transduction mechanism (**Figure 4.28.A**).

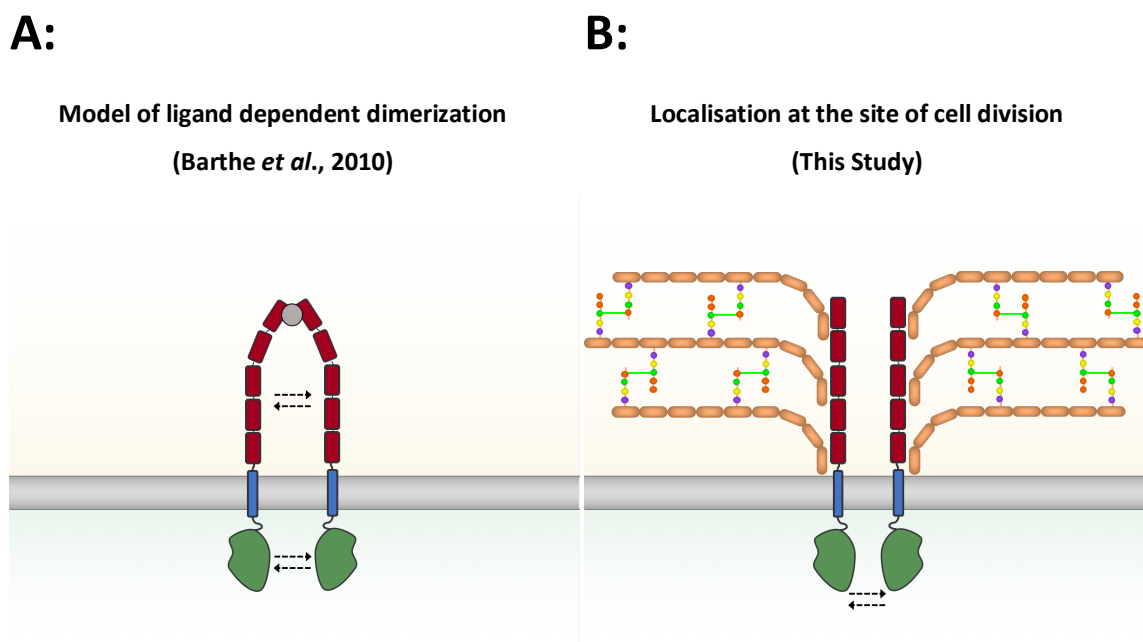


**Figure 4.28: Possible models for IreK oligomerisation.** Comparison of the models proposed for the function of eSTKs in bacteria using *E. faecalis* IreK as an example. **A:** highlights the model for oligomerisation of eSTKs in Gram-positive bacteria via a ligand. **B:** highlights an alternative model in which the PAST domains interact with the glycan backbone of PG as demonstrate in this chapter (Chapter 5). Chapter 4 also highlighted that IreK from *E. faecalis* localises at the site of cell division, a region where newly synthesised PG is actively being incorporated into existing PG. Arrows point to sites of oligomerisation determined by each model.

In *B. subtilis* it has been shown that spores will exit dormancy in the presence of DAP containing mucopeptides and removal of the PASTA domains from PrkC prevented germination (Shah *et al.*, 2008). Likewise, with PknB in *M. tuberculosis*, the  $K_D$  of several mucopeptides have been determined using SPR (Mir *et al.*, 2011). In experiments in this study where mucopeptides were tested against PASTA 1 to 5 in *E. faecalis* using MST, the signal was not strong enough for determining the  $K_D$ .

The model for ligand-dependent dimerization is also a possibility in particular in the organisms such as PknB from *M. tuberculosis* and PrkC from *B. subtilis*. Although dimerization through the PASTA domains was not observed with *E. faecalis* IreK under the range of biophysical techniques used, these experiments were conducted without the presence of a potential ligand.

When comparing *E. faecalis* with *M. tuberculosis* and *B. subtilis*, these organisms are distantly related and have many features that may contribute to a different model for

eSTK kinase dimerization. *M. tuberculosis* is a part of the Actinobacteria phylum and has a bacterial cell wall much different to that of Gram-positive bacteria, and *B. subtilis* is a part of the Bacilli class in the Firmicutes phylum and Bacillales order and has DAP in the 3rd position of the pentapeptide stem. Other Gram-positive such as *E. faecalis* are in the Firmicutes phylum and Baccili class but are in the Lactobacillales order, and most have Lys in the 3rd position of the pentapeptide stem and also have a crosslinking bridge that both *M. tuberculosis* and *B. subtilis* do not have. Therefore, the PASTA domains of these organisms might have evolved accordingly to enable them to detect the changes in their PG environment.

# Chapter 5. Towards structural studies of IreK PASTA domains

## 5.1. Introduction

In this chapter, small-angle X-Ray scattering (SAXS) and nuclear magnetic resonance (NMR) techniques have been used to study the structure and interactions of the PASTA domains. The major advantage of NMR and SAXS over other structural techniques such as X-Ray crystallography and cryo-electron microscopy is that experiments are carried out in aqueous solution and can allow different conditions to be studied readily, including buffer type and pH which are factors that are important when considering structure-function relationships (Montelione *et al.*, 2000). Although significant progress has been made to study large proteins, the main limitation of solution NMR is that structural assignment is not possible above 30 kDa.

## 5.2. Small angle X-ray scattering

### 5.2.1. Introduction

Small angle X-ray scattering is considered to be an additional and complimentary structural and biophysical technique used to measure proteins in solution and does not have the size limitations of NMR nor the conformational restriction of X-ray crystallography. Although SAXS models do not have the same resolution achieved by X-ray crystallography or NMR, SAXS data analysis allows the ternary and quaternary structures from overall size and shape to be identified. X-rays irradiate the sample, then every atom inside the sample scatters the incident radiation into all directions and gives background radiation that is almost constant at small angles. Clusters of atoms inside the sample will produce additional scattering as the atoms have a different density and are in the size range of the X-ray wavelength. Measuring the angle dependent distribution of the scattered radiation allows the average particle size to be determined (Kikhney and Svergun, 2015).

As the PASTA domains from *E. faecalis* IreK are multi-modular, it is likely that these structures will exhibit inter-domain flexibility and will complicate or prevent

crystallisation for X-ray crystallography. Flexibility of proteins is also important for function, therefore characterisation of these PASTA domains by crystallography may be unsuitable as it requires the sample to be in a single dominant state (Wen *et al.*, 2014). To confirm the flexibility of PASTA domains, small angle X-ray scattering (SAXS) was used.

### 5.2.2. Initial characterisation of PASTA constructs

Proteins were analysed at the ESRF (Grenoble) and processed and analysed using SCATTER as described in the **Material and Methods**. **Figure 5.1** highlights the scattering data collected including the scattering intensity (**Figure 5.1.A**) and dimensionless Kratky plot (**Figure 5.1.B**) of the IreK PASTA domain truncations. The scattering intensity is proportional to the concentration and confirms that all proteins analysed were roughly the same concentration. The Kratky plot allows disordered states in proteins to be identified and to distinguish them from globular proteins. The profile allows the visualisation of particular features of the scattering profile to be represented and allows identification of the folding state and flexibility (Uversky and Dunker, 2010).

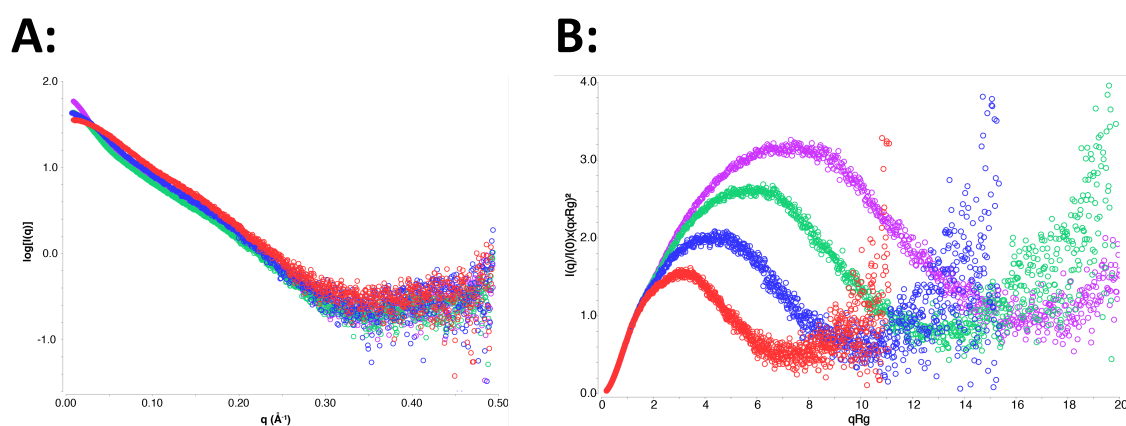


**Figure 5.1: SEC-SAXS analysis of PASTA domains from *E. faecalis* IreK.** (A) Log<sub>10</sub> Intensity plot and (B) dimensionless Kratky plot. 1 mg ml<sup>-1</sup> of purified protein was used in the SEC-SAXS experiment including PASTA 1 to 2 (Red), PASTA 1 to 3 (Blue), PASTA 1 to 4 (Green) and PASTA 1 to 5 (Pink). Data was processed including subtraction from the buffer blank and analysed using SCATTER (Bioisis).

The dimensionless Kratky plot for a folded globular protein will show a compact bell-shaped curve, and deviations from this suggests protein flexibility or unfolding (Receveur-Brechot and Durand, 2012; Durand *et al.*, 2010). Unfolded proteins will often present a hyperbolic plateau (**Figure 5.2**). In **Figure 5.1.B**, each of the PASTA constructs

show a bell-shaped curve with PASTA 1 to 2 (Red) being the most compact and the addition of each PASTA domain amplifying the flexibility. Therefore, structural characterisation of the full-length PASTA domains using X-ray crystallography is likely to be unsuitable.

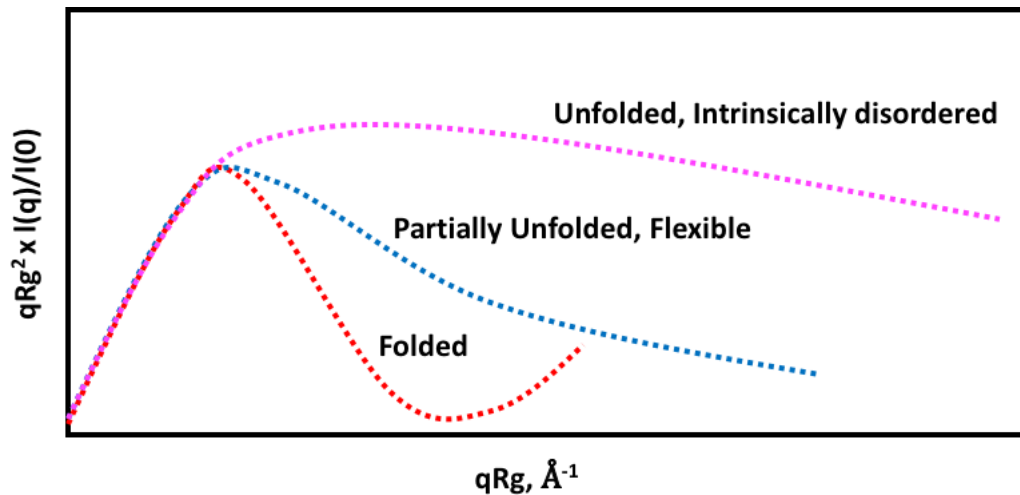


**Figure 5.2: Schematic demonstrating the different protein characteristics from processed SAXS data using the dimensionless Kratky plot.** Figures are based on experimental data obtained from Burger *et al.*, (2016). Red: folded protein in a compact curve, Blue: Partially unfolded or flexible and Magenta: Unfolded or intrinsically disordered.

Several characteristic parameters can also be obtained directly from experimental scattering patterns including molecular weight and radius of gyration ( $R_g$ ). These parameters are useful for quantitatively characterising the flexibility of proteins.  $R_g$  provides a measure of the overall size of the macromolecule. The  $R_g$  is the root-mean-squared distance to the centre of density in the molecule weighted by the scattering density length. The  $R_g$  is smaller for proteins with a compact shape compared to extended proteins. A Guinier fit is used to provide a linear fit to determine the  $R_g$  and the intercept gives the forward scattering  $I(0)$  which is proportional to the molecular weight and the concentration of the protein. The predicted MW is determined for each protein but is lower than that of the theoretical MW and the experimental MW previously determined (Kikheney and Svergun, 2015). **Table 5.1** highlights some of the parameters determined, and the  $R_g$  increases as the number of PASTA domains increase also providing evidence of protein flexibility.

**Table 5.1: Parameters from analysed SAXS data using SCATTER (Bioisis) of each PASTA truncation.** The parameters determined including  $R_g$  (radius of gyration) show that the addition of each PASTA construct increases the overall protein flexibility.

	I(0)	$R_g$	Volume	Predicted MW (kDa)	Expected MW (kDa)
<b>PASTA 1 to 5</b>	6.3 +-0.16	53.67+- 1.26	52	35	38.2
<b>PASTA 1 to 4</b>	4.5+-0.14	41.24+- 0.34	40	26	30.3
<b>PASTA 1 to 3</b>	4.3 +-0.08	31.31+- 0.35	31.7	18.2	22.7
<b>PASTA 1 to 2</b>	3.6 +-0.05	22.82+- 0.17	22.7	13.4	15.4

As mentioned previously, NMR is a useful structural technique for studying dynamic proteins but is often limited by the size. Therefore, a smaller PASTA construct would be required. Hybrid approaches in structural biology by combining different structural techniques can provide great structural insight than can a single individual technique. The combination of high-resolution structural methods such as NMR, providing atomic scale structural and dynamics information, with lower resolution methods such as SAXS that yield nanometer scale structure, is a powerful approach for the study of biomacromolecules in near native environments. In particular, NMR and SAXS are considered the most appropriate tools for the study of highly dynamic and flexible systems, which for both modern electron microscopy (EM) and X-ray crystallography remain problematic (Mertens and Svergun, 2017). High resolution structural information from the PASTA domain truncations using NMR and global characterisation of the full PASTA set from IreK may allow a system to be developed to study the dynamics of these flexible domains.

### 5.3. Identifying a suitable PASTA construct for NMR studies

NMR is particularly valuable for analysing protein structures outside the scope of X-Ray crystallography, unfortunately, the full length extracellular PASTA domains from IreK are outside the size limitations for standard NMR studies. Suitable truncations of the PASTA domains are therefore required to perform subsequent NMR studies. When

comparing the alignment of the individual PASTA domains in **Figure 5.3.**, it is clear that PASTA 5 has the most unique sequence as well as a C-terminal extension.

```

PASTA2    GTEKIEMADYTNESYESAVALKKLGFSEDQITTKKEYSDSVSTDNIIKQKPAAGKKVDPKKDKVTLTVSE-----
PASTA3    GPEAVTLPSYAGYSYTNNAVNALQGLGISESQITRVDQASDTVEPGLVITQDPAPGGTVTPKNGQVTLVYSK-----
PASTA4    GSDKVTLSDYSGISYDNAVSRILALGIPESQIKRVDEESDKVEKDTVISQEPASGTAVDPKNDTITLHVSK-----
PASTA1    GGKDVEVPDVTNETKVDASQALQSAGLKVDSET-KKIPDDKIEEGKVVKTDPEAKSSVK-KGRSVTLYISS-----
PASTA5    GSDSVTVPDISGYSPKAAEDSINNAGLKINEQG-LSGSG---DGQVVERTSPSAGSKVK-KGDSVTVYYSKANDSKSTTESSTSN
          * . . : . . : . : * . : * : . . . . . : . * * * : * : * .

```

**Figure 5.3: Sequence alignment of the individual PASTA domains from *E. faecalis* Irek OG1RF.** Domains are organised by phylogenetic disruption aligned using Clustal Omega. "\*" amino acids are identical in all sequences in the alignment, ":" show where conserved amino acids substitutions have been observed and "." show where semi-conserved amino acids substitutions have been observed.

### 5.3.1. Initial characterisation of PASTA domains 4 to 5

To understand the dynamics between PASTA domains, a recombinant protein with at least two PASTA domains is required. From initial CD experiments highlighted in **Chapter 3**, PASTA 1 to 2 may be unsuitable for NMR studies as it has a low  $T_M$  which suggests that it is the least stable of all constructs investigated and thus unsuitable for long experimental times during NMR acquisition. Instead of the initial two PASTA domains, (PASTA 1 to 2), the terminal two PASTA domains were recombinantly expressed and purified with and without the 10 AA C-terminal extension (PASTA 4 to 5). **Figure 5.4** highlights the purity of both constructs by SDS-PAGE analysis and the oligomeric state by SEC-MALS. The C-terminal extension has been hypothesised in *E. faecium* to be involved in oligomerisation dynamics in IreK in *E. faecium* (Sacco *et al.*, 2014). Initial SEC-MALS analysis shows that both constructs appear to be monomeric although construct PASTA 4 to 5 appears to have a tailing shoulder.

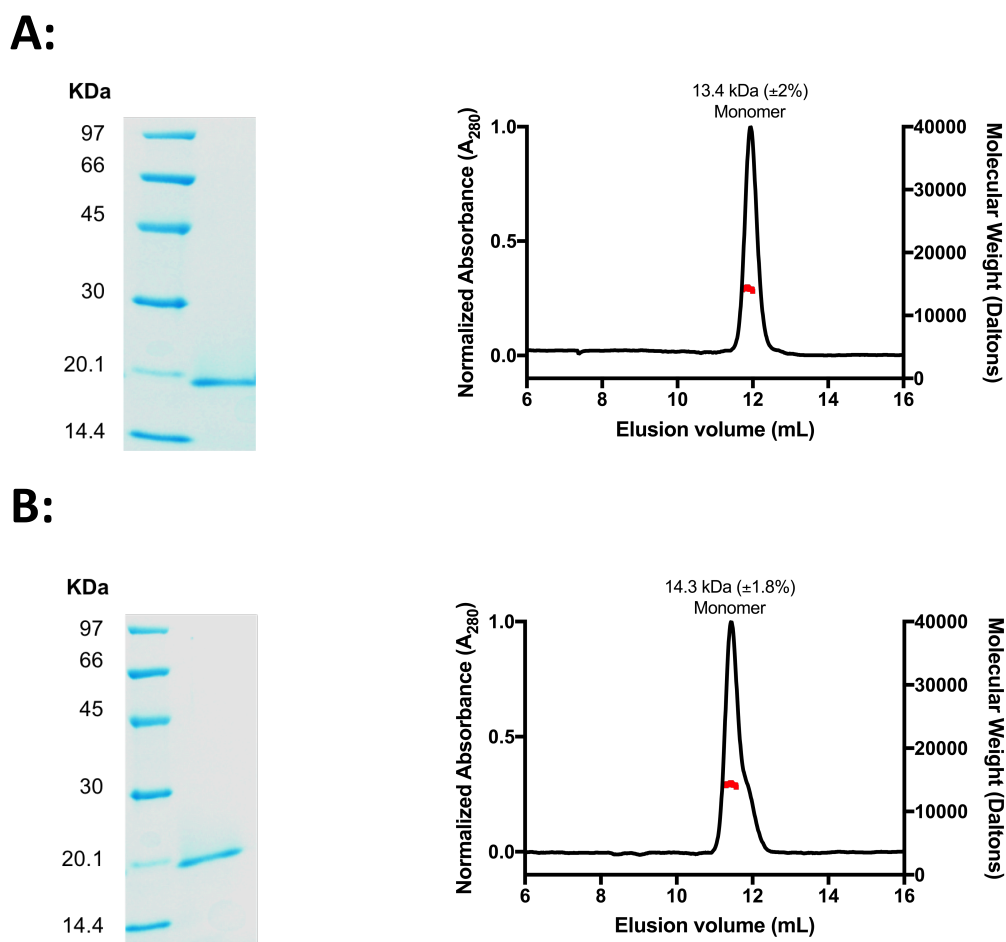


**Figure 5.4: SDS and SEC-MALS analysis of purified Terminal PASTA domains from *E. faecalis* IreK.**

Includes (A) PASTA 4 to 5 with C-terminal truncation or (B) PASTA 4 to 5 without C-terminal truncation by SDS-PAGE (Left) or SEC-MALS (Right). Elution profiles of the PASTA domains were examined by SEC-MALS on a Superdex 75 increase (10/300). Absorbance at  $A_{280}$  for each chromatogram was normalised. MALS data are presented in Red with predicted molecular weight above each peak.

### 5.3.2. AUC characterisation of the terminal PASTA domains

To confirm these observations, AUC was also performed on both constructs and confirmed that the C-Terminal extension is not involved in oligomerisation and that they are both monomeric, as a single oligomeric species was observed around the MW of the protein (**Table 5.2**).

**Table 5.2: Species estimated molecular weights from the c(s) analysis of each PASTA domain truncation.** For each sample concentration the signal-weighted sedimentation co-efficient and the estimated molecular weight of each species is shown, together with the best-fit frictional ratio for the distribution.

Monomer MW (kDa)	Detection method	Concentration (mg mL <sup>-1</sup> )	Peak		f/f <sub>0</sub>
			MW (kDa)	Sed. Co (S)	
<b>PASTA 4-5 (Full Length)</b>					
16.0	Absorbance	0.75	19.4	1.33	2.01
		0.5	20.2	1.37	2.02
		0.25	18.1	1.37	1.87
	Interference	0.75	16.1	1.50	1.58
		0.5	18.3	1.55	1.66
		0.25	15.1	1.51	1.50
<b>PASTA 4-5 (C-Terminal Truncation (10 aa))</b>					
14.6	Absorbance	0.75	18.0	1.33	1.88
		0.5	17.9	1.36	1.84
		0.25	18.6	1.40	1.82
	Interference	0.75	15.9	1.49	1.55
		0.5	15.5	1.49	1.52
		0.25	15.6	1.53	1.51

### 5.3.3. CD characterisation of PASTA domains 4 to 5

As the C-terminal extension does not appear to have an effect on oligomerisation, the full-length PASTA 4 to 5 was tested for overall stability using a  $T_M$  by CD. As mentioned previously, the  $T_M$  for PASTA 1 to 2 was very low, and it is important for NMR studies that the protein is stable and can withstand long incubations at temperatures greater than storage conditions. **Figure 5.5** highlights  $T_M$  of PASTA 4-5 and compares it to the  $T_M$  of PASTA 1 to 5 (**Figure 4.10**). Interestingly, unlike PASTA 1 to 2 where the  $T_M$  was lower than that of PASTA 1 to 5, PASTA 4 to 5 is actually higher than that of PASTA 1 to 5 (12.5°C difference) and is therefore a stable candidate protein for isotopic labelling and NMR studies. The increased stability of their terminal PASTA domains as determined by the CD  $T_M$  might indicate that the role of the terminal PASTA proteins is different to that of the PASTA domains closer to the cell membrane and be related to the overall function of the protein.

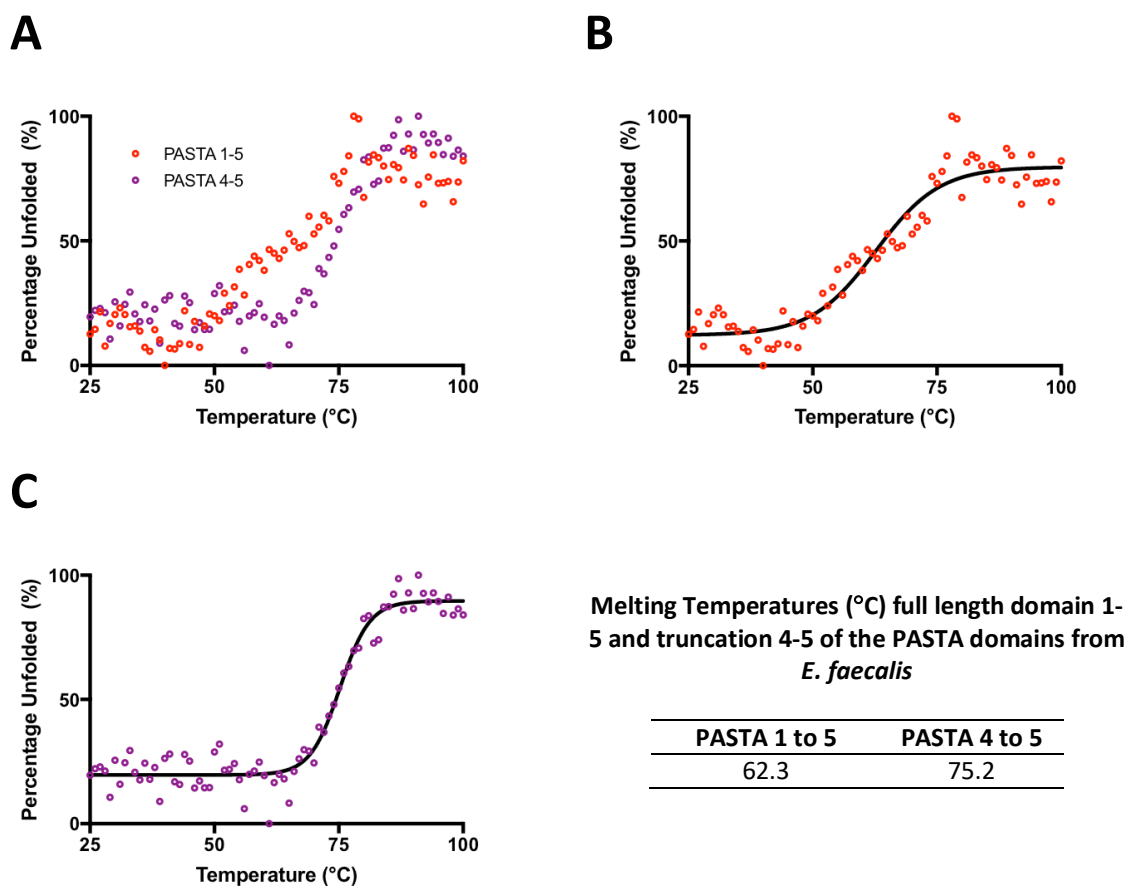


**Figure 5.5: Temperature melts of IreK terminal PASTA domains following CD at 222 nm.** Protein constructs at  $0.2 \text{ mg mL}^{-1}$  in 10 mM Sodium Phosphate, pH 7.4 buffer were incubated at incremental temperatures from 20 to  $100^\circ\text{C}$  with CD spectra collected at each temperature point. Includes (A) overlay plot of PASTA constructs, (B) PASTA 1 to 5 and (C) PASTA 4 to 5 without C-terminal truncations, with the Boltzmann sigmoid fit (Solid Black line). Insert table displays  $T_M$  of each construct as determined by the Boltzmann sigmoid equation.

#### 5.3.4. SAXS characterisation of the terminal PASTA domains 4 to 5

To determine the flexibility of the PASTA 4 to 5 construct, SAXS was also performed on these constructs to obtain data that can later be used to produce an *Ab initio* model of the constructs. **Figure 5.6** shows the analysed SAXS data from the PASTA 4 to 5 constructs. Generally, the two constructs overlay each other, in particular when comparing them in the normalised Kratky plot (**Figure 5.6.B**), but there is an increase in protein flexibility in the PASTA 4 to 5 construct containing the 10 aa C-terminal extension. The C-terminal peptide is likely to generate disorder at the terminus of the protein.

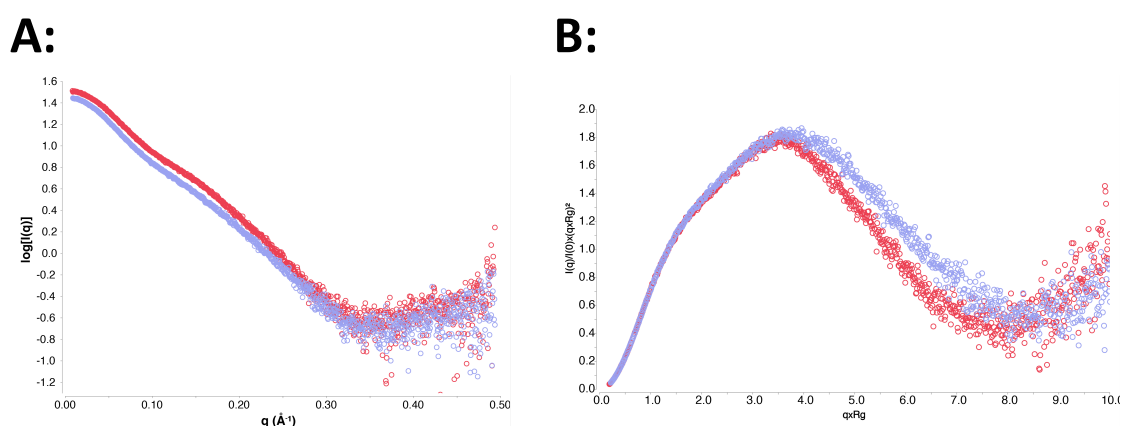


**Figure 5.6: SAXS analysis of the terminal PASTA domains from *E. faecalis* IreK.** (A) Log<sub>10</sub> Intensity plot and (B) dimensionless Kratky plot including PASTA 4 to 5 (Purple) and PASTA 4 to 5 with 10 aa truncation (Red). Data was processed including subtraction from the buffer blank and analysed using SCATTER (Bioisis).

**Table 5.3.** highlights the parameters obtained from the processed SAXS data from the PASTA 4 to 5 constructs. The  $R_g$  also confirms that the presence of the C-terminal peptide causes a degree of protein flexibility or disorder in this region of the protein. Although the MW is not predicted to be correct, the predicted MW decreased with the truncation of the 10 aa C-terminal peptide, as expected.

**Table 5.3: Parameters from analysed SAXS data using SCATTER of each terminal PASTA truncation.** The parameters determined including  $R_g$  (radius of gyration). The presence of the 10 aa on the C-terminus of the PASTA domains does increase the overall flexibility of the protein.

	I(0)	$R_g$	Volume	Predicted MW (kDa)	Expected MW (kDa)
<b>PASTA 4 to 5</b>	2.8	25.11	22	15	16
<b>PASTA 4 to 5 (10 aa truncation)</b>	3.2	23.41	20	13	15

## 5.3. Nuclear magnetic resonance

### 5.3.1. Introduction

PASTA 4 to 5 was identified as suitable for studying the overall effects of the PASTA domains by NMR due to its biophysical properties. For ligand binding studies, PASTA 4 to 5 was a suitable candidate as PASTA 4 shared similar sequence homology to that of PASTA domains 1 to 3. This also enabled characterisation of PASTA domains that has lowered sequence homology to the other PASTA domains (**Figure 5.3**). This construct was stable over a long period of time as determined by CD and presented inter-domain flexibility as determined by SAXS. PASTA 4 to 5 also behaves like the other PASTA domains in terms of its oligomerisation (primarily monomeric) and bioinformatics comparison between individual PASTA domains from *E. faecalis* IreK. The PASTA 4 to 5 construct was isotopically labelled for initial ligand binding experiments and structural characterisation.

### 5.3.2. The Heteronuclear Single Quantum Coherence (HSQC) experiment

The HSQC is one of the most important and frequently used experiments in biomolecular NMR and is usually a prerequisite experiment used to assess the characteristics of the protein before further NMR experiments are performed. The HSQC provides a 'fingerprint' of the labelled protein due to the NH functional groups of amino acids (except prolines) in the protein backbone.

The HSQC involves the transfer of the magnetisation on the proton to the  $^{15}\text{N}$  through an INEPT (Insensitive nuclei enhanced by polarisation transfer) step, which uses J-coupling for the polarisation transfer. After a time delay ( $t_1$ ) the magnetization is transferred back to the proton for detection (**Figure 5.7**). In a 2D HSQC experiment, a series of experiments with an increasing incremental  $t_1$  time delay are acquired. The proton signal is directly measured in each experiment and the chemical shift of the  $^{15}\text{N}$  is recorded in the indirect dimension. The HSQC was used to test standard conditions including optimisation of pH and temperature of the protein sample. All experiments were conducted on a 700 MHz spectrometer as detailed in **Chapter 2: Material and Methods**.

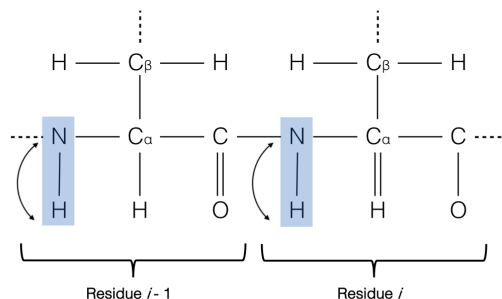


**Figure 5.7: Schematic showing correlations for  $^1\text{H}$ - $^{15}\text{N}$  HSQC experiments.** Magnetisation is transferred through J-coupling from the hydrogen attached to the  $^{15}\text{N}$  nuclei and the chemical shift is evolved on the  $^{15}\text{N}$  and the magnetisation is transferred back to the hydrogen for detection.

Before the initial HSQC experiments were performed, short 1D proton experiments of the PASTA 4-5 terminal domains were acquired. 1D  $^1\text{H}$  data allows the different chemical structures present in the sample to be distinguished through chemical shifts of each nucleus in the sample precessing at a different frequency resulting in separation of the signals in the NMR spectrum. Evaluation of the chemical shifts of a protein sample in a 1D- $^1\text{H}$  spectrum is useful as it can also give information on the extent of protein folding in the sample due to the dispersion of the chemical shift peaks. A well dispersed spectrum indicated that the nuclei are in many different environments, suggesting the presence of elements of secondary structure and tertiary folding. **Figure 5.8** demonstrates that, although the protein shows evidence of folding by excellent chemical shift dispersion, there are many overlapping peaks due to the size of the protein and, as expected, the protein is too large to interpret the 1D data. For this reason, 2D and 3D heteronuclear ( $^{15}\text{N}$  and  $^{13}\text{C}$ ) experiments were utilised.

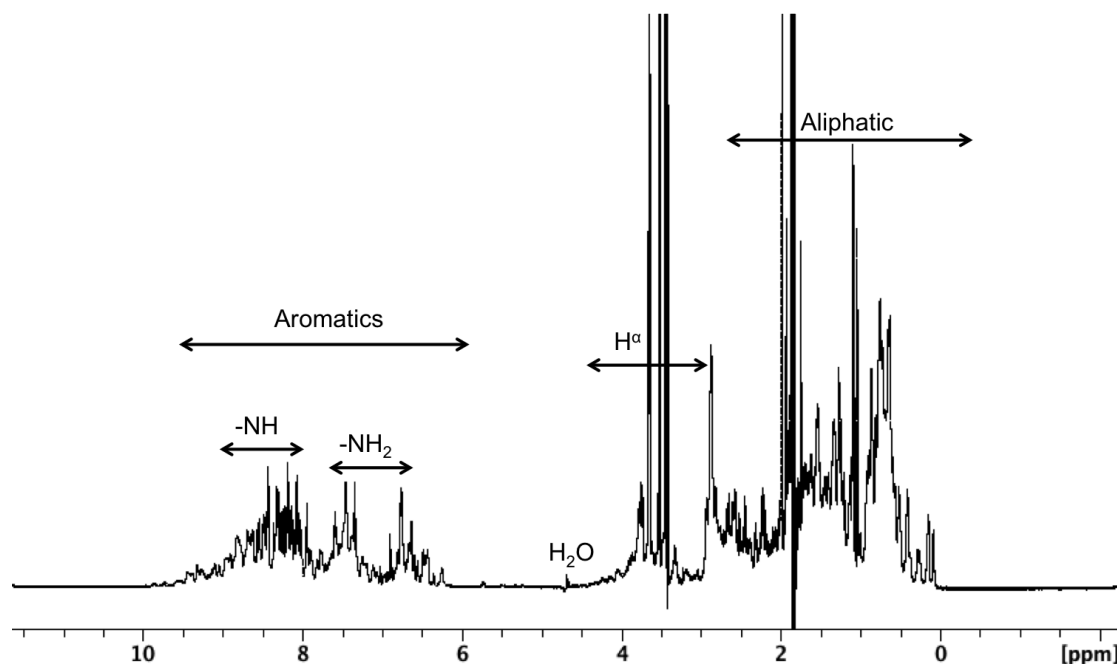


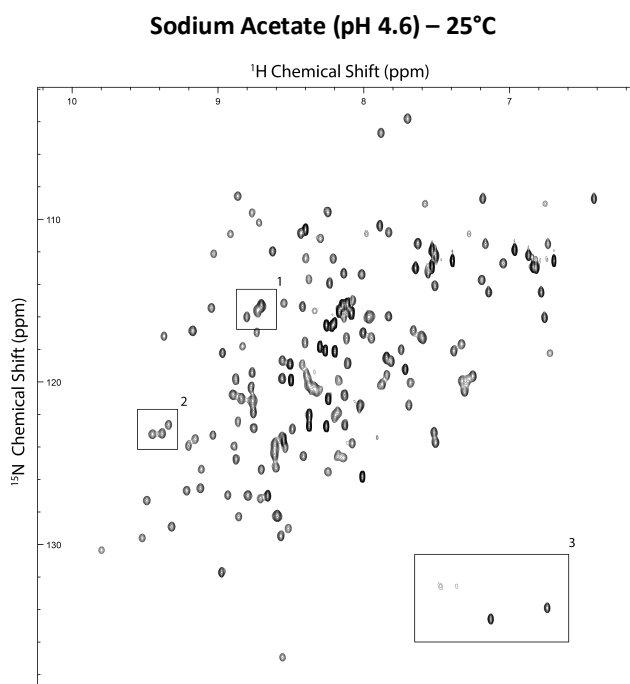
**Figure 5.8: 1D NMR of 1.2 mM PASTA 4 to 5 constructs.** Experiments were performed in a Bruker 700 MHz NMR spectrometer. Indicates protein folding due to the presence of sharp and narrow peaks with good chemical shift dispersion in 10 mM Sodium Acetate, pH 4.6 at 25°C.

### 5.2.2.1 Optimisation of protein samples for NMR experiments

Acquisition of data for the PASTA domains from *M tuberculosis* PknB was previously performed in sodium acetate at a low pH (4.6). Initial experiments for IreK PASTA 4 to 5 were also performed in sodium acetate pH 4.6, and the <sup>1</sup>H-<sup>15</sup>N HSQC spectrum of PASTA 4 to 5 shows well dispersed resonances between 6 to 10 ppm in the <sup>1</sup>H dimension (**Figure 5.9.A**) at 25°C. Certain amino acid resonances are readily identified, including Gly in the top region (<115 ppm <sup>15</sup>N ) of the spectrum and side chain peaks from Asn and Gln where two parallel peaks are present in the same <sup>15</sup>N dimension but different <sup>1</sup>H dimension. There are areas of peak overlap in the center of the spectrum that may prove difficult for assignment. From this spectrum 176 peaks were observed, whereas the theoretical number of HSCQ peaks calculated from the IreK PASTA 4 to 5 sequence is 148. This number is calculated by taking the total number of residues and subtracting the number of Pro residues in the sequence, then adding on any NH-bearing side chains. There is a total of 6 Pro residues in the peptide sequence and 7 Asn and 4 Gln residues bearing NH-side chains. There is a total of 155 aa in the sequence for PASTA 4 to 5.

To investigate the impact of solution pH on the quality of the NMR spectrum, the sample was buffer exchanged into sodium phosphate pH 6.5 and the resulting HSQC is shown in **Figure 5.9.B**. Although there is good dispersion of resonances over the 6 to 10 ppm region in the  $^1\text{H}$  dimension, there are slight differences when comparing the samples in sodium acetate, pH 4.6 (**Figure 5.9.A**) and sodium phosphate (**Figure 5.9.B**) highlighted by boxes. Box 1 highlights a region of overlap in both buffer systems but is more resolved in the presence of sodium acetate, pH 4.6. There is a loss of a peak in box 2 in the presence of sodium phosphate pH 6.5, and in box 3 there is a loss of 4 peaks in the sodium phosphate sample in the 140 to 130 ppm region of  $^{15}\text{N}$  chemical shift. It is known that protein samples in the low pH region can give good quality spectra due to slow NH exchanges which is evident when comparing PASTA 4 to 5 in the presence of sodium acetate pH 4.6 and sodium phosphate pH 6.5. Further experiments were performed in sodium acetate pH 4.6 unless otherwise stated.

**A:**



**B:**

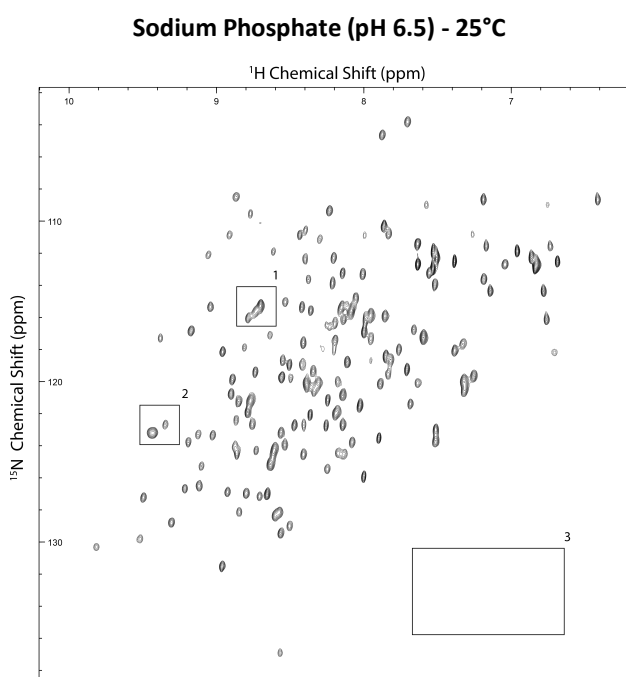


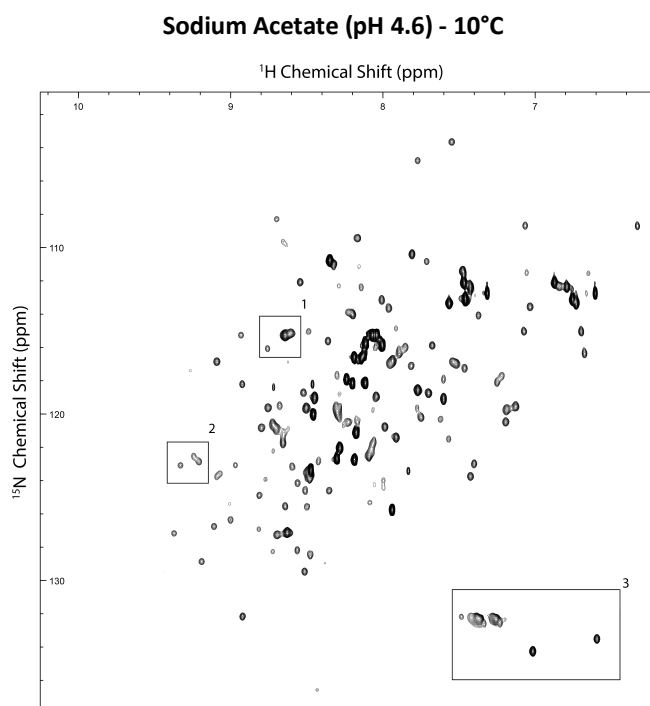
**Figure 5.9: Buffer optimisation for NMR studies of PASTA 4 to 5.** Experiments were performed in a Bruker 700 MHz NMR spectrometer. A  $^1\text{H}$ - $^{15}\text{N}$  HSQC spectrum of uniformly labelled 1 mM  $^{15}\text{N}$ -PASTA 4 to 5 in (A) 10 mM sodium acetate pH 4.6 and (B) 10 mM sodium phosphate pH 6.5 on a Bruker 700 MHz spectrometer at 25°C. Major regions of broadness and differences between the spectra are highlighted in a black box.

To continue the optimisation of the PASTA 4 to 5 IreK construct, HSQC experiments were performed over a range of different temperatures including 10°C, 25°C (RT) and 37°C. Previous characterisation of PASTA domains from *M. tuberculosis* PknB was performed at 10°C (Barthe *et al.*, 2010). Using the same box regions described previously, when comparing PASTA 4 to 5 at 25°C (**Figure 5.9.A**) and PASTA 4 to 5 at 10°C (**Figure 5.10.A**) it is clear that there is a loss in resolution of the resonances in these regions and overall in the spectrum at a lower temperature. Globally, there are variable peak intensities at 10°C

When comparing PASTA 4 to 5 at 25°C (**Figure 5.9.A**) and PASTA 4 to 5 at 37°C (**Figure 5.10.A**) there is little difference when comparing the overall resolution for the whole spectrum, but there is some peak overlap in Box 1 and Box 2 and loss of 2 peaks in Box 3 at 37°C compared to 25°C.

As previous ligand binding experiments were performed at 25°C using other methods, and good resolution was achieved at 25°C in these NMR optimisation experiments, future NMR experiments including chemical shift perturbation experiments for ligand binding studies and 3D experiments for structure characterisation were carried out at 25°C.

**A:**



**B:**

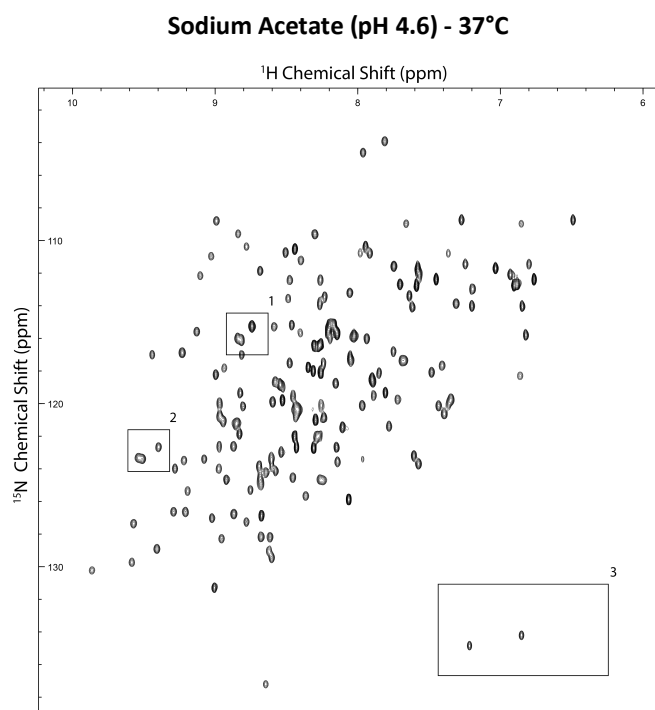


**Figure 5.10: Temperature optimisation for NMR studies of PASTA 4 to 5.** Experiments were performed in a Bruker 700 MHz NMR spectrometer. A  $^1\text{H}$ - $^{15}\text{N}$  HSQC spectrum of uniformly labelled  $^{15}\text{N}$ -PASTA 4 to 5 in 10 mM sodium acetate pH 4.6 at (A) 10°C and (B) 37°C on a Bruker 700 MHz spectrometer. Major regions of broadness and differences in comparison of each spectra are highlighted in a black box.

### 5.3. Ligand binding studies using NMR

Chemical shift perturbation experiments were used to determine the binding affinity of the PASTA 4 to 5 protein from *E. faecalis* to vancomycin. Chemical shift perturbations in NMR studies provide a powerful and useful technique by not only determining the ligand binding affinity, but also following changes in the chemical environments of residues within the protein to determine the exact location of the binding site. The chemical shifts are very sensitive to structural changes that can occur and can be measured very accurately. Therefore, all of the genuine binding interactions will produce chemical shift perturbations. To determine the location of a bound ligand in the protein,  $^{15}\text{N}$  HSQC spectra of PASTA 4 to 5 were acquired with increasing ligand concentration. This enables the changes in chemical shift of all peaks to be determined and enables the specific amino acids in the protein that directly interact with the ligand to be determined (Williamson., 2013).

The aim here was to use the chemical shift perturbations to provide important validation that the ligands that bound to PASTA 4 to 5 according to both the SPR and MST experiments were not false positives. Vancomycin was used as a control molecule as it yielded a dose dependent response and measurable binding affinity using both SPR and MST experiments, and it is relatively inexpensive. Therefore, chemical shift perturbation NMR experiments can remove the premise of false positives from other biophysical experiments.

**Figure 5.11** highlights the chemical shift perturbations observed in a sample of 1 mM  $^1\text{H}$ - $^{15}\text{N}$  labelled PASTA 4 to 5 in the absence and presence of 8 mM vancomycin. Although there is not a global change in chemical shifts when comparing the overall resonances in the spectrum, there are local chemical shift changes observed which suggest direct binding to a region in the PASTA 4 to 5 construct. Boxes in **Figure 5.11** highlight regions where chemical shift perturbations are observed and include a region where 2 amino acid side chain resonances (Box 3) also display chemical shift perturbations, indicating that 2 Gln or Asn residues are affected by the binding of vancomycin.

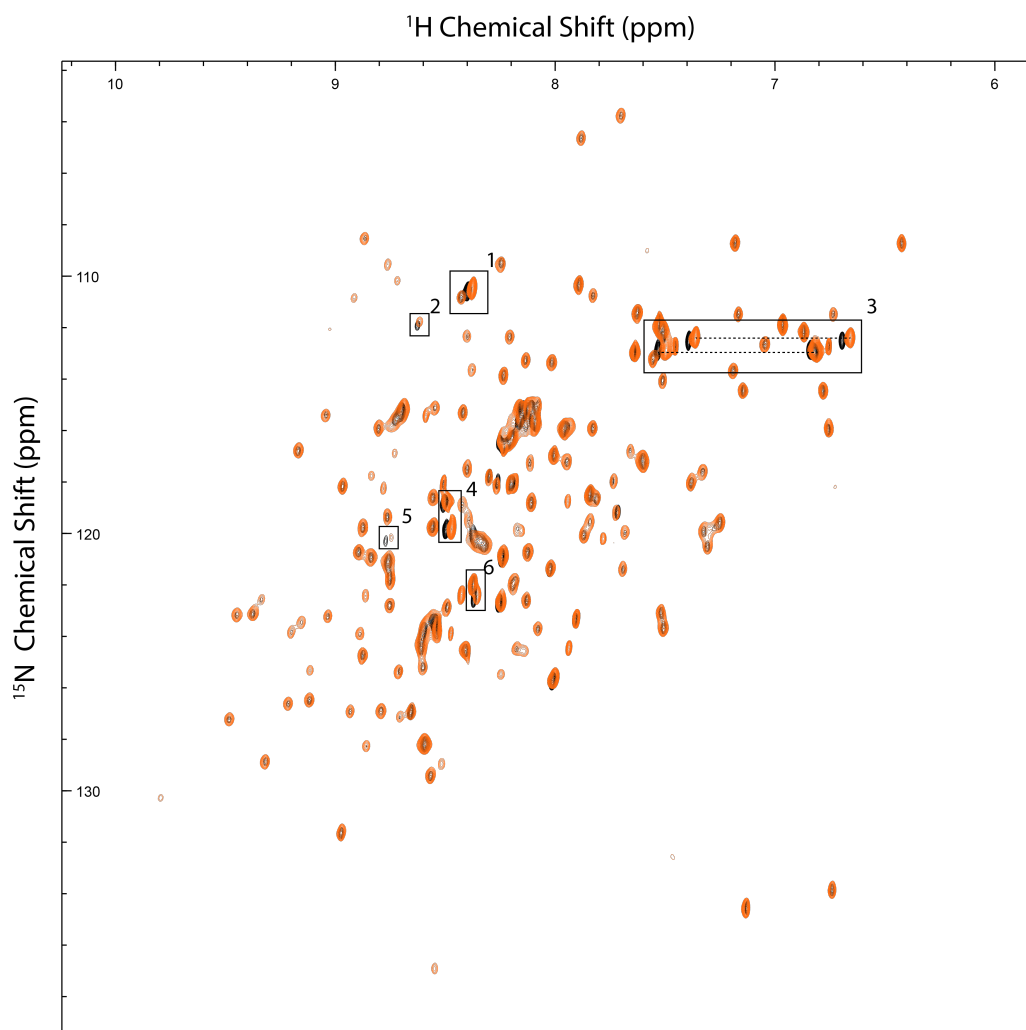
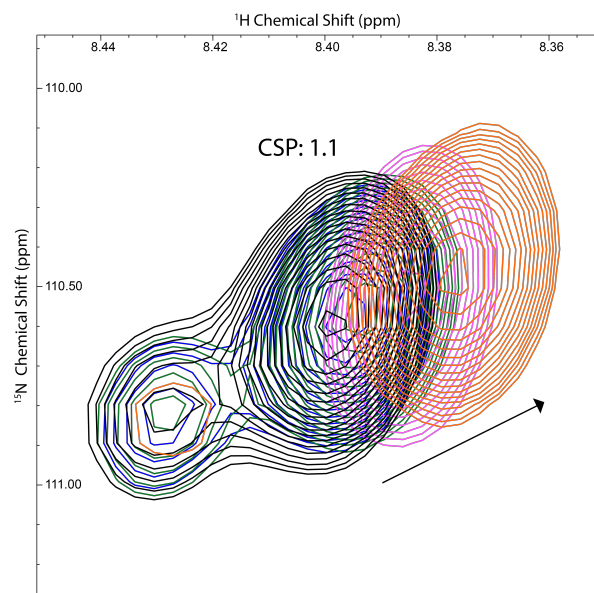


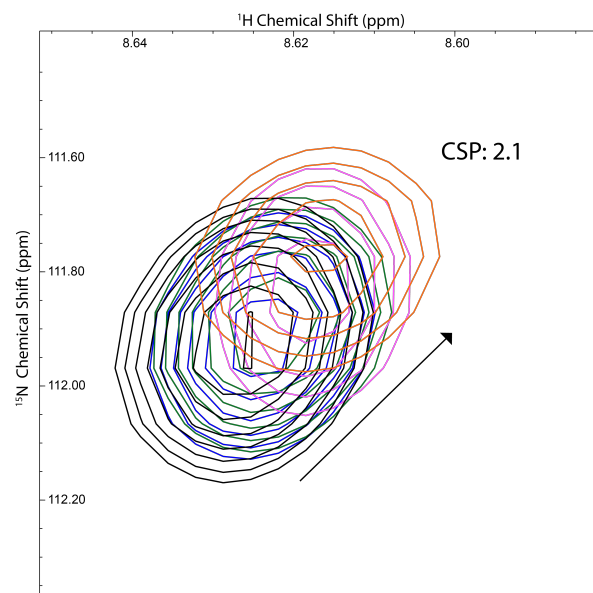
**Figure 5.11: PASTA domains 4 and 5 bind to vancomycin.** Experiments were performed in a Bruker 700 MHz NMR spectrometer. Overlaid  $^1\text{H}$ – $^{15}\text{N}$  HSQC spectra of 1 mM PASTA 4 to 5 (Black) and 1 mM PASTA 4 to 5 with 8 mM vancomycin (Orange) in 10 mM sodium acetate pH 4.6. Chemical shift perturbations are observed only for some peak and key peaks are highlighted by boxes. Dashed lines represent side chain peaks from either Asn or Gln residues. Six other resonances display chemical shift perturbations.

**Figure 5.11** highlights each of the individual boxed regions shown in **Figure 5.10**, where experiments were performed with increasing concentrations of vancomycin. Where chemical shift perturbations were observed in **Figure 5.10**, **Figure 5.11** demonstrates that each of the resonances in these regions are affected by an increasing concentration of vancomycin. Experiments were performed with 0.25 – 8 mM vancomycin, with spectra acquired upon a 2-fold increase in concentration in the titration series. The pH was monitored at each titration point to ensure any chemical shift changes are not simply a result of changes in pH.

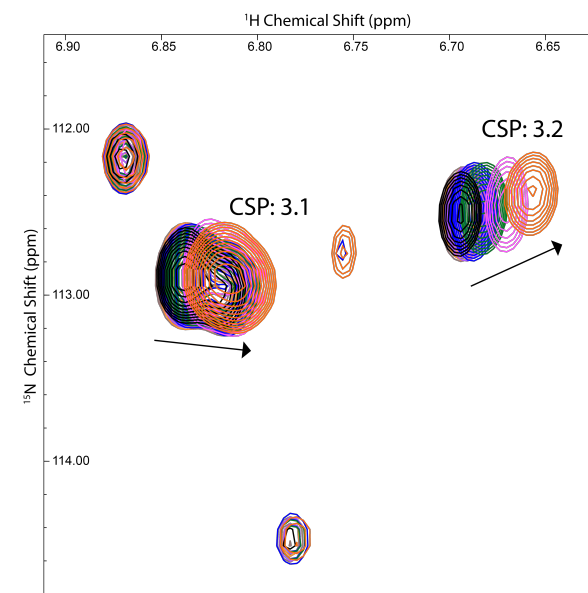
**A:**

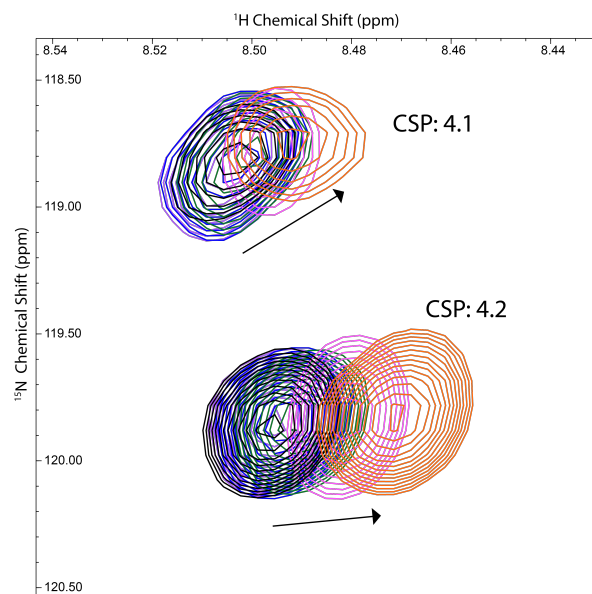
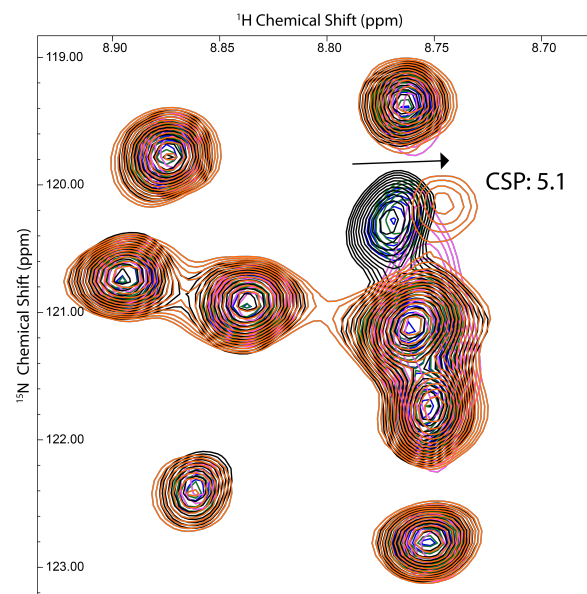
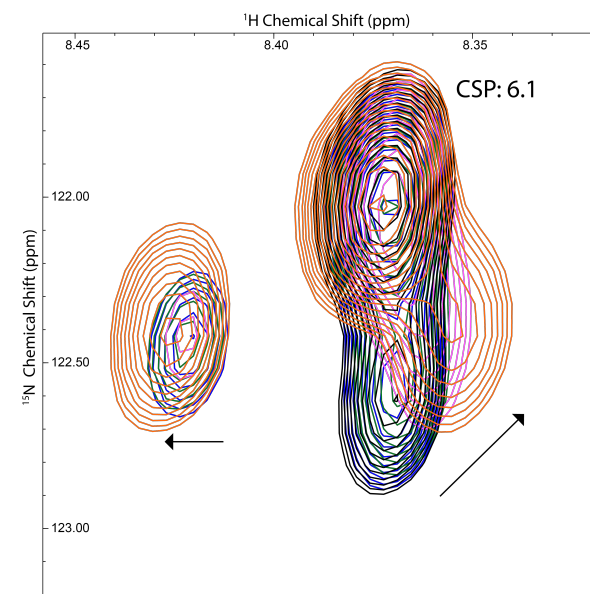


**B:**



**C:**



**D:****E:****F:**

**Figure 5.12: Local overview of PASTA domains 4 and 5 binding to vancomycin.** Experiments were performed in a Bruker 700 MHz NMR spectrometer. Overlaid spectra of 1 mM PASTA 4 to 5 (Black) with 0 mM vancomycin and increasing concentrations of vancomycin 0.25 mM (Grey), 0.5 mM (Purple) 1 mM (Blue), 2 mM (Green), 4 mM (Pink) and 8 mM vancomycin (Orange) in 10 mM sodium acetate pH 4.6. Chemical shift perturbations are initially assigned by the boxed regions described in **Figure 5.11**.

Although chemical shift perturbations were observed in the titration experiments highlighted in **Figure 5.12**, saturation of vancomycin binding to PASTA domains 4 and 5 was not achieved. **Figure 5.13** highlights that, at high vancomycin concentrations of up to 16 mM, spectral lines were significantly broadened across the spectrum. After acquisition and removal of the sample from the spectrometer, protein aggregation was visible. This broadening and precipitation suggest aggregation of the PASTA 4 to 5 protein at high vancomycin concentration, preventing saturation of binding and calculation binding kinetics (and a value for  $K_D$ ) using NMR.

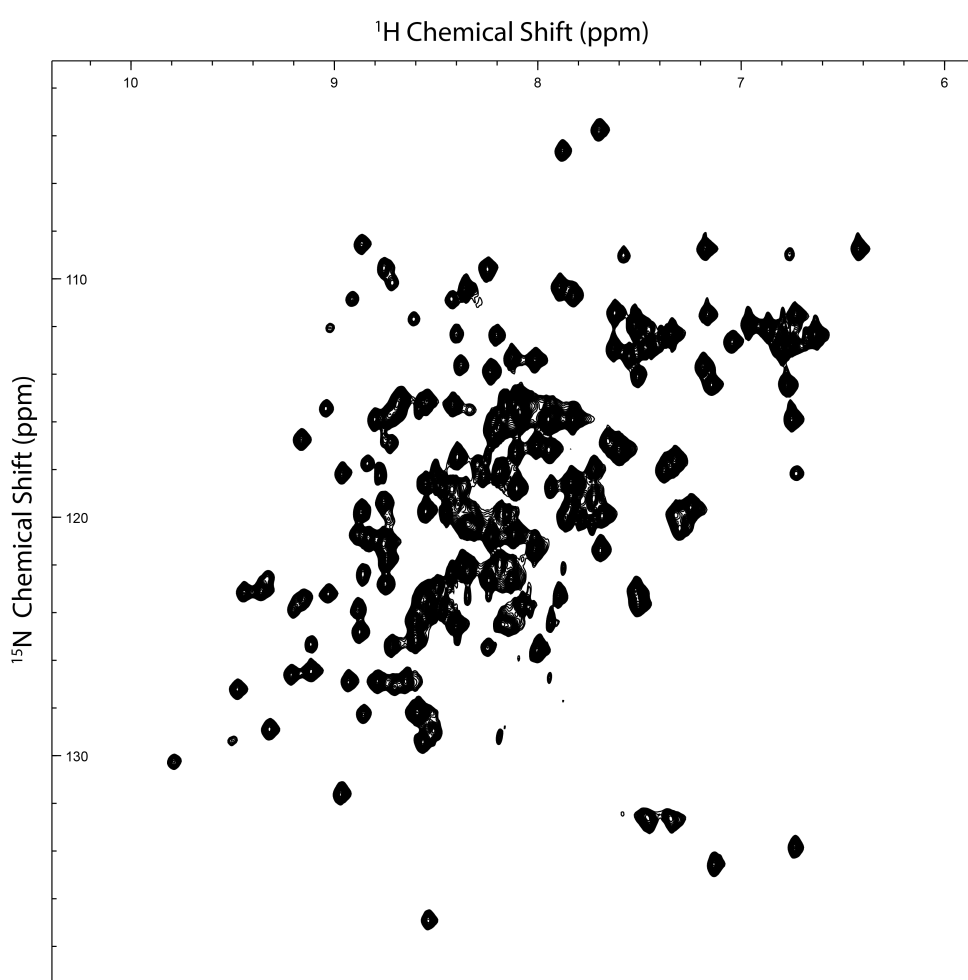


**Figure 5.13: 16 mM vancomycin causes PASTA 4 to 5 to aggregate in these experimental conditions.** Experiments were performed in a Bruker 700 MHz NMR spectrometer. 1 mM PASTA 4 to 5 (Black) with 16 mM vancomycin in 10 mM sodium acetate pH 4.6. Peak broadness is observed across each of the resonances in the presence of 16 mM vancomycin. Visual inspection after acquisition indicated protein precipitation.

To ensure that the binding of vancomycin in low pH buffer was not adversely impacting binding (SPR and MST experiments were performed at pH 7.5), a chemical shift perturbation experiment was performed in sodium phosphate pH 6.5 with 1 mM PASTA 4 to 5 in the absence and presence of 8 mM vancomycin (**Figure 5.14**).

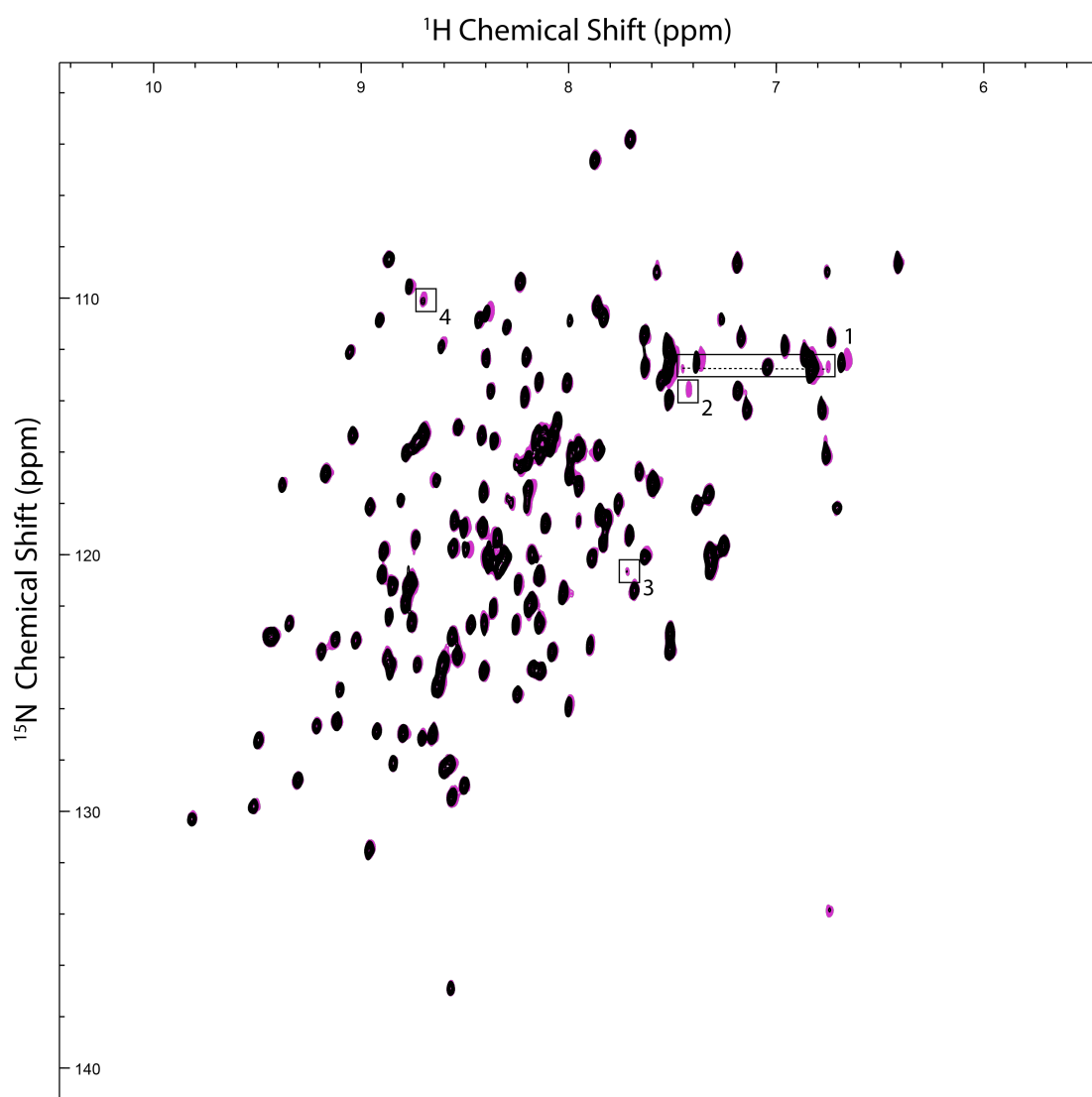


**Figure 5.14: PASTA domains 4 and 5 also bind to vancomycin in pH 6.5 sodium phosphate.** Experiments were performed in a Bruker 700 MHz NMR spectrometer. Overlaid spectra of 1 mM PASTA 4 to 5 (Black) and 1 mM PASTA 4 to 5 with 8 mM vancomycin (Pink) in 10 mM sodium phosphate pH 6.5. Chemical shift perturbations are observed only for some peaks and key peaks are highlighted by boxes. Dashed lines represent side chain peaks from either Asn or Gln residues.

Generally, the same chemical shift perturbations are observed at pH 4.5 (**Figure 5.11 and Figure 5.12**), but two new regions demonstrate additional chemical shift

changes after addition of 8 mM vancomycin (Box 1 and Box 2, **Figure 5.14**). Box 1 resembles the addition of side chain peaks from either a Gln or Aln residue. Box 2 contains a unique peak that is only present in the 8 mM vancomycin sample. When using NMR chemical shift perturbations to determine the protein ligand interactions, two different exchange rates can occur. When the exchange rate is fast on the NMR chemical shift timescale ( $K_{off}$  is significantly greater than the difference in ppm of chemical shifts between free and bound protein), they move smoothly through the spectrum. The frequency in the signal of any titration point is the weighted average of free and bound shifts (**Figure 5.15, left**). When the exchange rate is slow on the chemical shift timescale ( $K_{off}$  is significantly slower than the difference in ppm of chemical shifts between free and bound protein), a free signal will disappear and appear somewhere else in the spectrum (**Figure 5.15, right**) (Williamson, 2013).

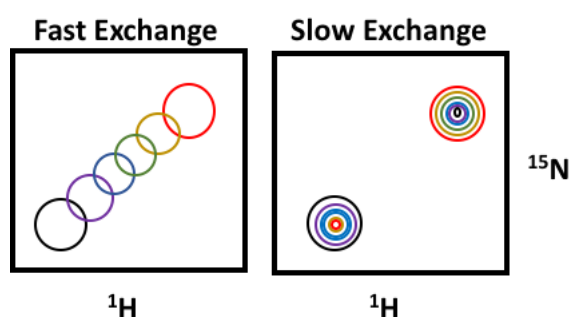


**Figure 5.15: The effect of exchange rate on NMR peak shapes.** (Left) Fast exchange: a gradual transition from unbound to bound. Slow exchange: the peak representing the unbound state reduces in intensity as the peak from bound state increases in intensity. Figure adapted from Williamson (2013).

Box 3 and 4 in **Figure 5.14** show increased signal intensity of peaks that may be explained by the slow exchange rate. It is unclear if Box 2, which contains the additional resonance, is described by fast or slow exchange chemical shifts as there is not another resonance on the HSQC spectrum that is missing an overlapping resonance.

## 5.4. Backbone assignment

Previous experiments have shown that certain resonances exhibit chemical shift changes in the presence of vancomycin. Although vancomycin at the highest concentration measurable in these experiments did not yield a  $K_d$ , the resonances that

displayed a chemical shift change prompts further examination of what amino acids these resonances represent. As teicoplanin or (GlcNAc-MurNAc)<sub>4</sub> could not be used in this NMR study because of the expense of the ligand, by identifying the amino acids in the HSQC that exhibit a chemical shift perturbation in the presence of vancomycin, constructs could be generated that contain a point mutation for further experiments using other techniques like MST that require a significantly smaller ligand concentration. The  $K_d$  can then be compared across the different mutants to the WT protein to determine if vancomycin, teicoplanin and GlcNAc-MurNAc)<sub>4</sub> are binding to the same residues.

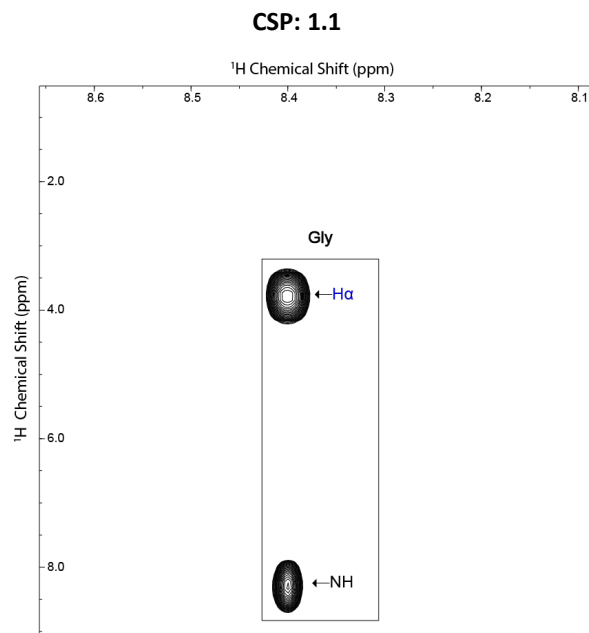
#### 5.4.1. 3D HSQC TOCSY Experiments

HSQC-TOCSY (Total correlation spectroscopy) is a useful experiment that can help aid assignment of amino acid types from an HSQC spectrum. An isotropic mixing step transfers the magnetisation between <sup>1</sup>H spins and then is transferred back to the neighbouring <sup>15</sup>N and back to <sup>1</sup>H for detection. In a spectrum, a strip can be identified where the side chain hydrogen residues of that amino acid can be identified.

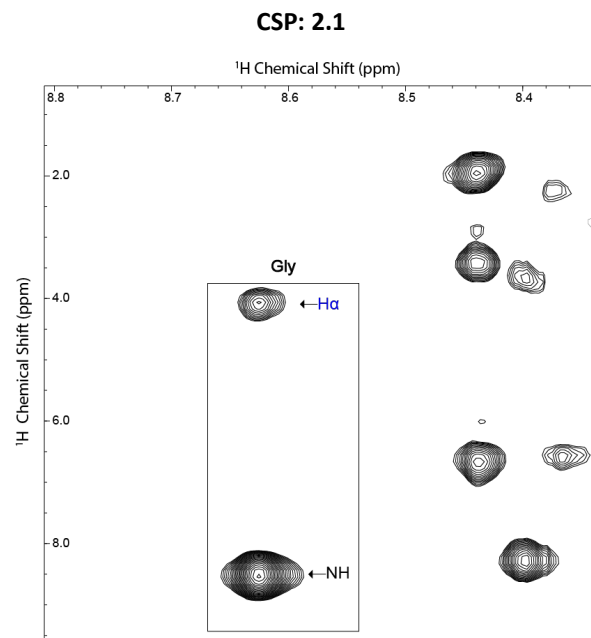
**Figure 5.16** illustrates strips in the HSQC-NOESY experiment that correspond to the resonances that exhibited chemical shift perturbations in **Figures 5.11** and **5.12** (CSP 1.1, 1.2, 2.1, 4.1, 4.2, 5.1 and 6.1). Amino acid types were determined by comparing a particular amino acid's <sup>1</sup>H chemical shifts to published values for each amino acid in a disordered peptide sequence (GGXA) (Richarz and Wuthich, 1978). Two amino acid types have been estimated using HSQC TOCSY including Gly (CSP: 1.1) and Ser (CSP5.1). One residue has been estimated to be either a Gln or Glu residue, but the proton chemical shifts are similar (CSP: 2.2 and CSP: 6.1). The two other peaks display proton chemical shifts that are similar to several other amino acid types and could not be determined.

To further characterise the other amino acid types, further 3D experiments with <sup>13</sup>C,<sup>15</sup>N labelled protein was required for 3D experiments that help identify these amino acid types and also identify where in the protein sequence they occur. The HSQC TOCSY experiments will be used with further 3D experiments to confirm amino acid types being identified in the backbone assignment.

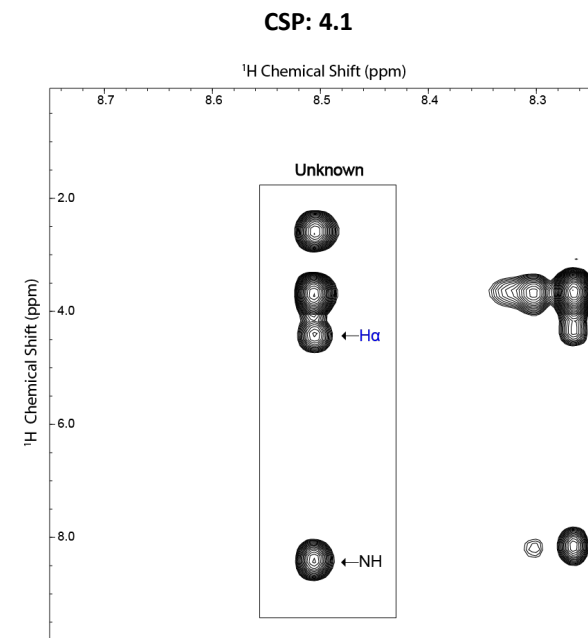
**A:**

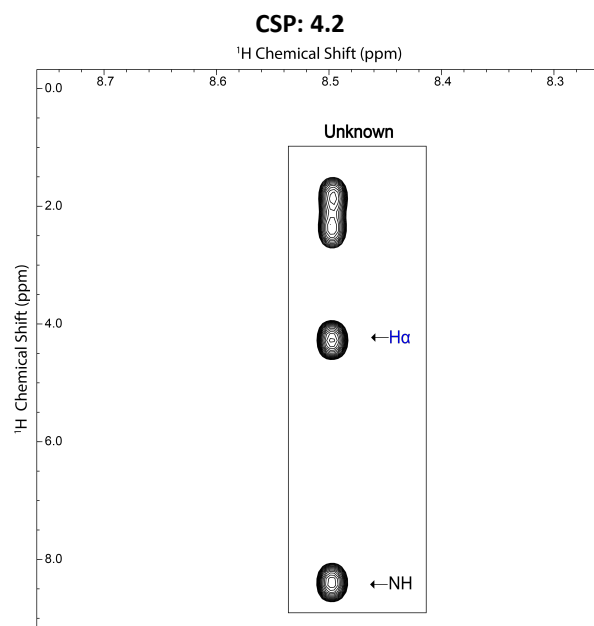
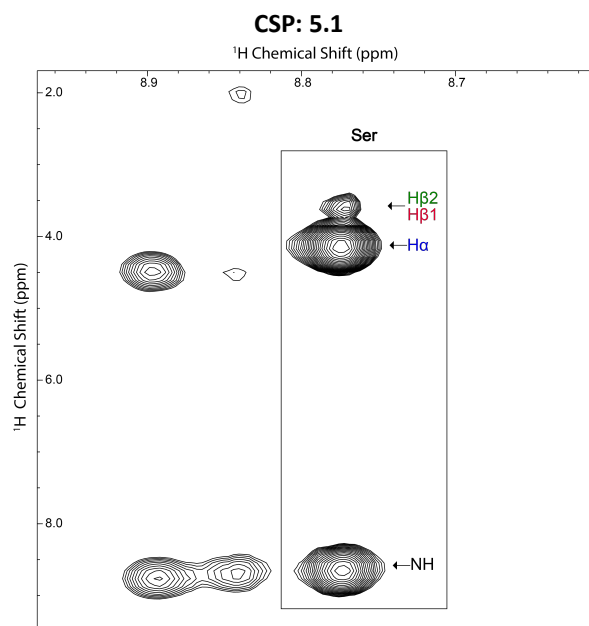
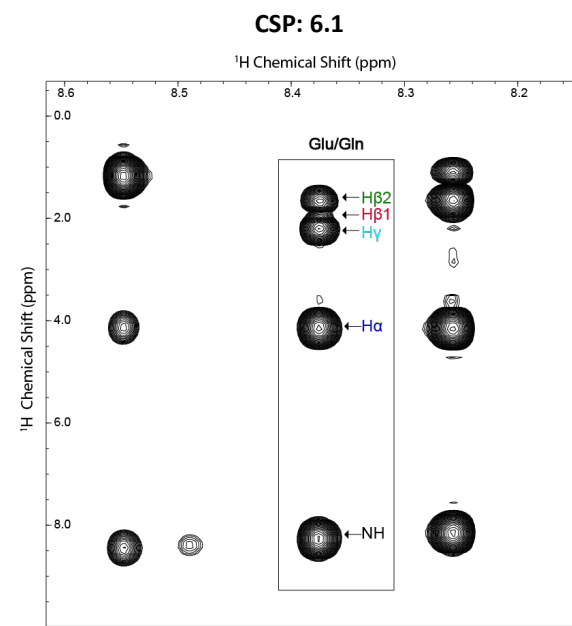


**B:**



**C:**



**D:****E:****F:**

**Figure 5.16: HSQC- TOCSY strips corresponding to the residues that observed chemical shifts in the presence of 8 mM vancomycin. Experiments were performed in a Bruker 700 MHz NMR spectrometer. Corresponding residues are boxed and when determined protons assigned.**

## 5.4.2 Backbone assignment using triple resonance (CHN) 3D NMR

To assign each peak in the HSQC spectrum, in order to determine the amino acid information for future chemical shift perturbation experiments, triple resonance 3D experiments were used to sequentially assign the protein backbone. Higher dimensional experiments have lower sensitivity, and some 3D experiments are less sensitive than others, so it is essential to ensure the initial acquisition parameters are optimised. 3D experiments for backbone assignment utilise the same proton and nitrogen dimensions as observed in the HSQC, with an additional dimension of carbon chemical shift. By correlating each dimension, the CA (alpha carbon), CB (beta carbon), and CO (carbonyl carbon) can be identified within the same residue (i) and the preceding residue (i-1) of a protein sequence. The known protein sequence can then be used to follow the connectivity between 3D experiments to assign the HSQC spectrum. Certain amino acid types can also be determined using these triple labelled proteins in 3D experiments such as Gly residues, that do not contain a CB atom, and help validate an assignment. The 3D experiments will be described to highlight how they are used in the backbone assignment.

### 5.4.2.1. CBCACONH and CBCANH

The CBCACONH and CBCANH 3D experiments form a complementary pair, and the data in both correlate the chemical shifts of the backbone N, the NH, and the CA and CB atoms. In the CBCACONH experiment, magnetisation is transferred from the  $CB_{i-1}$  and  $CA_{i-1}$  respectively and transferred to the  $CO_{i-1}$  and then the  $NH_i$ . This experiment will usually produce two  $^{13}C$  peaks at each N-H correlation, corresponding to the CA and CB from the preceding residue (i-1). It can confirm if the residue follows a Gly residue as a  $CB_{i-1}$  resonance would not be present (**Figure 5.17.A Top**).

In the CBCANH experiment, magnetisation is transferred from the  $NH_i$  to the CA and CB of both residues i and i-1, resulting in four assignable resonances. The  $CA_i$  and  $CB_i$  will exhibit greater resonance intensity over the  $CA_{i-1}$  and  $CB_{i-1}$ . Differentiating between CA and CB residues is easy due to CA resonances being positive and CB resonances being negative (**Figure 5.17.A Bottom**). The CBCACONH and CBCANH experiments can be used in conjunction for the identification of CA and CB I and i-1 resonances.

#### 5.4.2.2. HNCA and HNCOCA

The HNCA and HNCOCA experiment pair correlate the chemical shifts of the backbone N, the NH, and the CA atoms for sequential backbone assignment. In the HNCA experiment, magnetisation is transferred from the NH to the CA and CA<sub>i-1</sub> atoms and produces two CA resonances at each N-H correlation. The CA<sub>i</sub> resonances are more intense than the CA<sub>i-1</sub> due to the coupling between the N<sub>i</sub>-CA<sub>i</sub> being greater than the CA<sub>i</sub>-N<sub>i-1</sub> (Figure 5.17.B Top).

In the HNCOCA experiment, magnetisation is transferred through the CO<sub>i-1</sub> and produces only a single resonance belonging to the CA<sub>i-1</sub> atom. The resonance correlates to the backbone NH<sub>i</sub> and allows assignment of the CA atom (Figure 5.17.B Bottom). In conjunction with the HNCA experiment, the CA peaks that overlap in both experiments correspond to the CA<sub>i-1</sub> and the single resonance in the HNCA corresponds to the CA<sub>i</sub>.

#### 5.4.2.3. HNCO and HNCACO

The HNCO and HNCOA experiment pairs displays resonances of the CO groups in the protein. In the HNCO experiment, magnetisation is transferred through the NH<sub>i</sub> to the preceding CO<sub>i-1</sub> via J-coupling. J-coupling occurs where there is an indirect interaction between two nuclear spins. The interactions are mediated via electrons participating in the bonds connecting the nuclei. This residue therefore produces a single resonance correspond to the CO<sub>i-1</sub> atom (Figure 5.17.C Top). This experiment is the most sensitive of the 3D experiments and is used to validate backbone assignment of the HSQC spectrum.

In the HNCACO experiment, the magnetisation is transferred through the CA<sub>i</sub> and CA<sub>i-1</sub> to both the CO<sub>i</sub> and CO<sub>i-1</sub>. As there is stronger coupling between the N<sub>i</sub> and CA<sub>i</sub> compared to the N<sub>i-1</sub> and CA<sub>i-1</sub> atoms, the CO<sub>i</sub> residue is generally more intense (Figure 5.17.C Bottom). In conjunction with the HNCO experiment, the CO<sub>i</sub> and CO<sub>i-1</sub> resonances can be identified for validation of the backbone assignment.

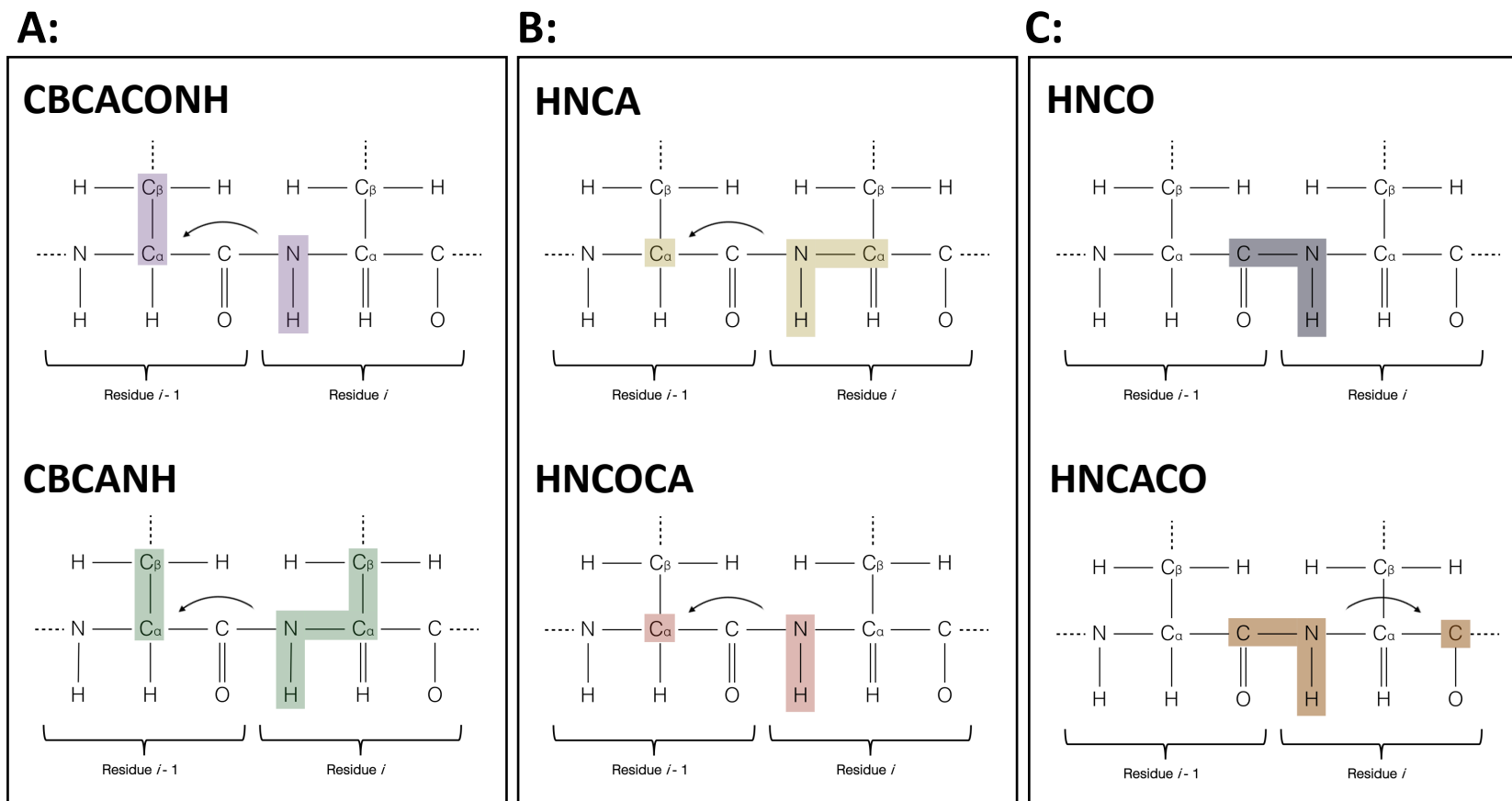


**Figure 5.17: Correlation for triple resonance experiments.** (A) CBCACONH and CBCANH: During CBCACONH, the residue ( $i$ ) is correlated with  $C\alpha$  and  $C\beta$  of the preceding residue ( $i-1$ ) whereas in CBCANH the residue ( $i$ ) is correlated with  $C\alpha$  and  $C\beta$  of the same residue as well as the previous residue. (B) HNCA and HNCOCA: HNCA correlates the residue ( $i$ ) with the  $C\alpha$  of the same residue as well as the previous residue ( $i-1$ ) whereas HNCOCA correlates the residue ( $i$ ) with  $C\alpha$  of the previous residue ( $i-1$ ). (C) HNCO and HNCACO: HNCO correlates residue ( $i$ ) with the CO of the preceding residue whereas HNCACO provides the same correlation in addition correlating it the CO of the current residue.

### 5.4.3. Examples of Backbone assignment of PASTA 4 to 5

CBCACONH and CBCANH, HNCA and HNCOCA and the HNCO and HNCACO pairs were used to assign the back-bone of the PASTA 4 to 5 domains from *E. faecalis* IreK. An example of each experiment in the assignment of PASTA 4 to 5 domain is illustrated below (Figure 5.18, Figure 5.19 and Figure 5.20).

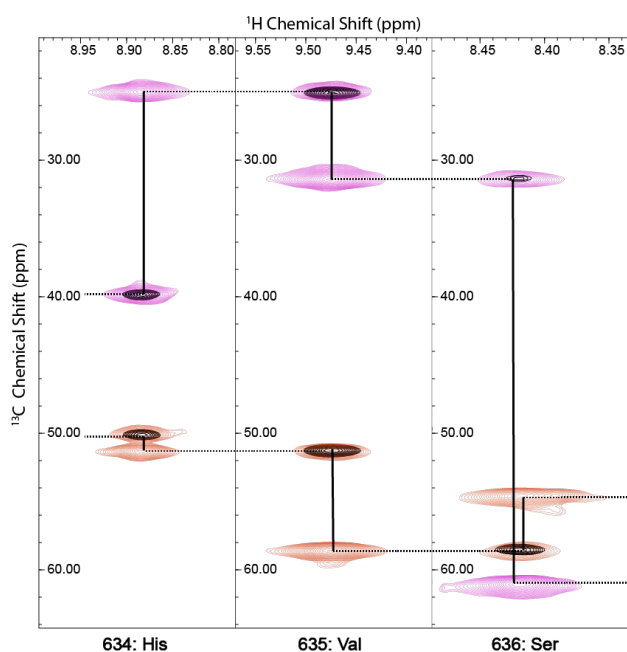


**Figure 5.18: CBCACONH and CBCANH experimental example of the backbone assignment of 1 mM PASTA 4 to 5 IreK from *E. faecalis*.** Includes the CBCACONH (Black) and CBCANH pair (Red: CA positive; Pink: CB negative).

The CBCACONH and CBCANH experiment illustrates the assignment of the CA and CB atoms. It also highlights the easy identification of Ser and Thr residues where the CB atom appears below the CA atom in the spectrum (Figure 5.18).

The HNCA and HNCOCA experiment illustrates the backbone assignment of the CA atoms and confirms and validates assignments made in the CBCACONH and CBCANH (Figure 5.19). The HNCO and HNCOCA experiment pairs illustrates the backbone assignment of the CO atoms (Figure 5.20). The acquisition and processing of the data from the HNCO experiment generally result in well resolved resonances, the HNCOCA experiment resulted in distorted resonances that can be seen in Figure 5.20 (Red peaks). This made the initial assignment of the protein backbone difficult.

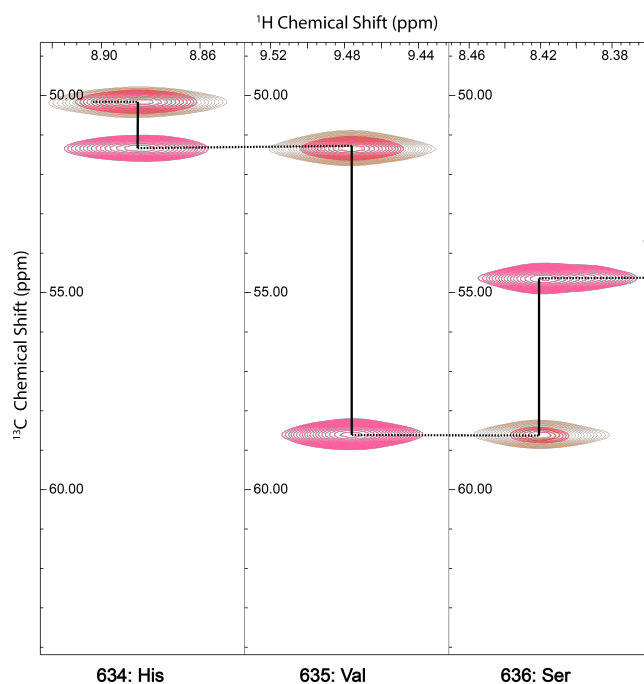


Figure 5.19: HNCA and HNCOCA experimental example of the backbone assignment of PASTA 4 to 5 IreK from *E. faecalis*. Includes the HNCA (Pink) and HNCOCA (Brown) pair.

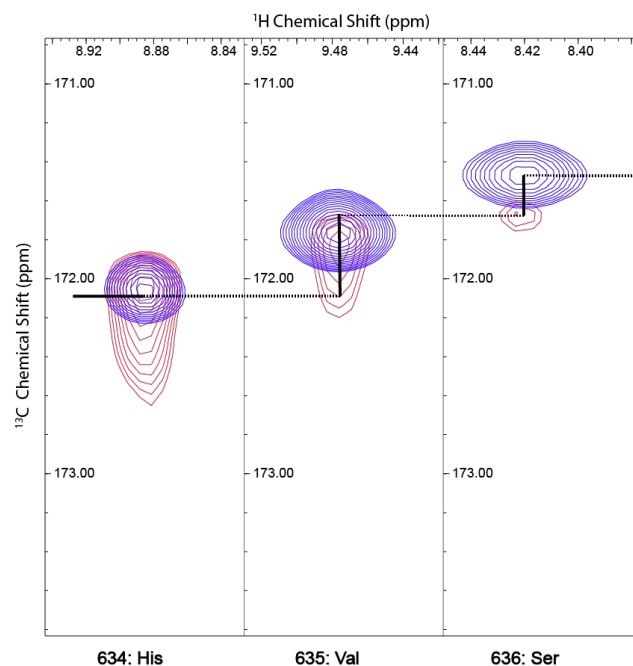


Figure 5.20: HNCO and HNCACO experimental example of the backbone assignment of PASTA 4 to 5 IreK from *E. faecalis*. Includes the HNCO (Blue) and HNCACO (Red) pair.

Figure 5.21 illustrates the sequence of PASTA 4 to 5 from IreK *E. faecalis* and highlights the residues that have been assigned during the backbone assignment. In the

3D experiments, many of the residues were overlapped which made interpretation of the preceding or proceeding residue in the sequence chain difficult. There is also a large number of possible serine or threonine residues that contributed to the ambiguity in the backbone assignment.

**PASTA 4** GAMGSDK**V**TL**S**DYSGISYDNAVSRLLIA**L**GIPESQIKRVDEESDKVEKDTVISQEPASGT**A**VD**P****K**ND**T****I****L****H****V****S****K**  
**PASTA 5** **G****S****D****S****V****T****V****P****D****I****S****G****Y****S****P****K****A****E****D****S****I****N****N****A****G****L****K****I****N****E****Q****G****L****S****G****S****G****D****G****Q****V****V****E****R****T****S****P****S****A****G****S****K****V****K****G****D****S****V****T****V****Y****S****K****A****N****D****S****K****S****T****T****S****E****S****S****T****S****N**

**Figure 5.21: Amino acid sequence of PASTA domains 4 to 5 from IreK *E. faecalis* and progress of backbone assignment.** Black letters and underline indicates the residual amino acids from post-TEV cleavage not associated to the native PASTA domains. Proline residues are highlighted in black bold. The backbone assignment of PASTA residues is highlighted in green. The backbone assignment of the two amino acids that display a chemical shift perturbation in the presence of vancomycin is highlighted in green and underlined.

From the backbone assignment two of the peaks involved in the chemical shift perturbation against vancomycin were identified including **CSP2.1** (Gly) and **CSP4.2** (Leu) from **Figures 5.11, 12 and 16**. **Figure 5.22** highlights the location of these residues (bold and underlined) and compares them to the PASTA sequences of *M. tuberculosis* and *S. aureus*. These homologous residues were then mapped onto the corresponding structures of the PASTA domains that had been determined for these species and shows an unordered region flanked between an alpha helix and beta sheet and in *M. tuberculosis* maps onto the end of an alpha helix. The unordered loop is larger in the *S. aureus* PASTA domain compared to the *M. tuberculosis* structures and might explain the binding properties of these PASTA domains from different species binding to different ligands. It is worth considering that the PASTA domains from *M. tuberculosis* was determined using NMR and offer more of a dynamic representation of the PASTA structure. Full backbone assignment will confirm the other residues that showed chemical shift perturbations and confirm if these residues also reside in the same site as the Leu and Gly residue highlighted in **Figure 5.22.C**.

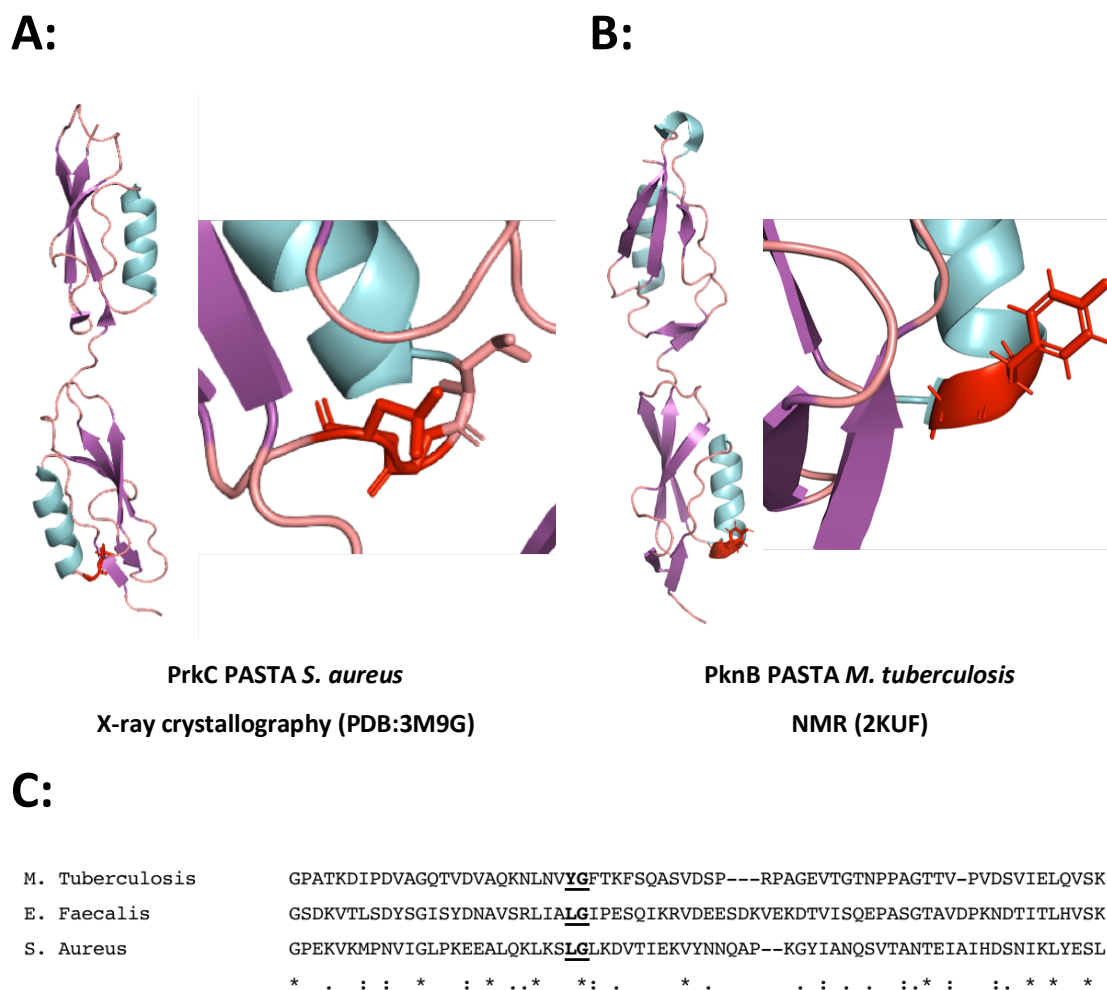


**Figure 5.22: Regions of possible site of ligand interaction.** (A) PASTA domains *S. aureus* (PDB: 3M9G) and (B) *M. tuberculosis* (PDB: 2KUF) identify possible regions of ligand interaction. Highlighted in Red is the region of possible ligand binding. (C) Sequence homology of PASTA 3 from *M. tuberculosis*, PASTA 4 from *E. faecalis* and PASTA 2 from *S. aureus* with possible binding site highlighted in Bold.

## 5.5. *Ab initio* modelling

Using the SAXS data generated for PASTA domains 4 to 5 from *E. faecalis* IreK, a dummy atom model was generated to understand the shape of the protein to aid structural studies and dynamics in future NMR experiments (Figure 5.23). To obtain the model,  $d_{\max}$  (the maximum vector) was determined  $P(r)$  (distance distribution function) of  $\sim 83.5$  Å.  $d_{\max}$  calculates the protein radius where it is large enough to contain an entire molecule but small enough to exclude neighbouring molecules. These parameters were used with the experimental SAXS data to generate dummy atom models.

**Figure 5.23** highlights the programmes used to generate the dummy atom models for PASTA domains 4 to 5. DAMMIF was used to generate dummy atom models to look at the overall shape determination of PASTA domains 4 to 5 from *E. faecalis*. In dummy atom modelling, a particle is represented as a collection of a large number of densely packed beads inside a search volume. Each bead belongs either to the particle or to the solvent. DAMMIF constructs a compact interconnected model yielding a scattering pattern that fits the experimental data (Franke and Svergun, 2009). 17 *Ab initio* models were generated using the DAMMIF programme. Each model was processed to find those that are the most similar and superimpose and average the selections. DAMSEL was used to select models and identify and remove outliers. A normalised spatial discrepancy (NSD) value where NSD is > 1 implies that models are similar. From the 17 models, only 1 was discarded and an NSD value  $0.889 \pm 0.083$ . DAMSUP (Dummy atom model superposition) is used to align the set of models to a reference model. The models are then averaged using two methods. The first is DAMAVER which created a bead density probability within the search volume and DAMFILT that generates the averaged model created from a DAMAVER model where low occupancy and loosely connected dummy atoms are present.



**Figure 5.23: Schematic demonstrating the process of obtaining a dummy atom model of the PASTA 4 to 5 domains from *E. faecalis* IreK.** Data was analysed SEC-SAXS data acquired on PASTA 4 to 5 and processes using SCATTER (Bioisis) with the built in ATSAS programme (EMBL) .

Visualisation of the DAMAVER and DAMFILT output (**Figure 5.24.A** and **Figure 5.24.B**, respectively). Representation for the PASTA 4 to 5 PASTA domains suggests that the PASTA domains from *E. faecalis* IreK in solution are elongated, which is similar to observations made of *M. tuberculosis* PknB PASTA domains NMR and SAXS experiments (Barthe *et al.*, 2010).

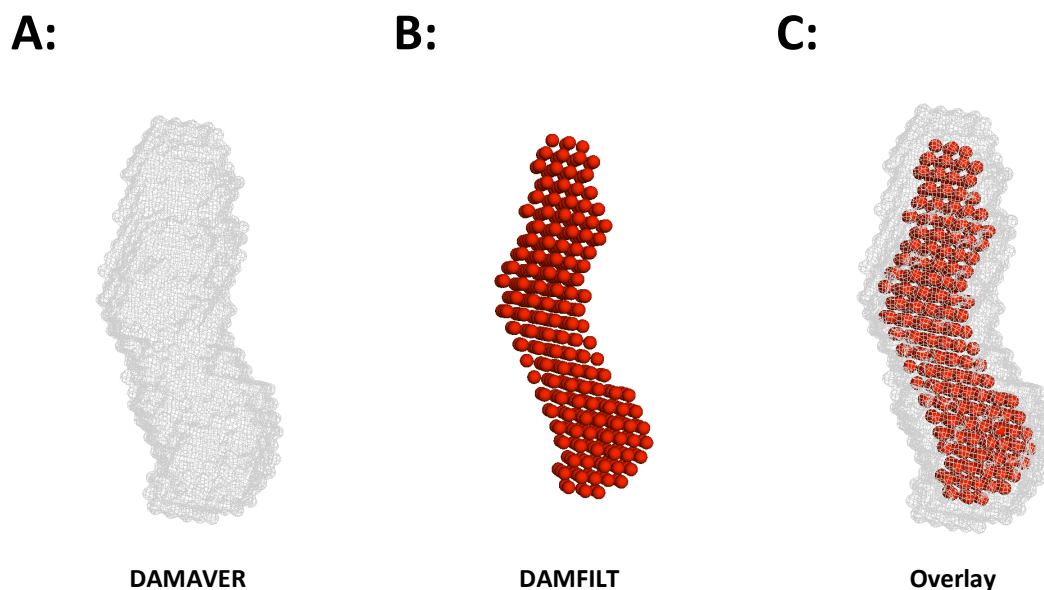


**Figure 5.24: Dummy atom model of PASTA domains 4 to 5 from IreK *E. faecalis*.** Dummy atom models were determined using DAMAVER (A) based on the bead density probability of the search volume and DAMFILT which generates the averaged model created from a DAMAVER model where low occupancy and loosely connected dummy atoms are present. The overlay of both models is represented by (C).

## 5.6. Conclusions and future directions

In this Chapter, confirmation of direct ligand binding using vancomycin as an example ligand was observed in chemical shift perturbation experiments in NMR. A platform has been established where the terminal PASTA domains 4 to 5 from IreK *E. faecalis* can be used to understand dynamics between neighbouring PASTA domains in future structural studies.

Although a full backbone assignment was not achieved in the time frame of this study due to difficulties differentiating between resonances in the 3D experiments, partial assignment was achievable. Future NMR experiments may include longer acquisition time of the HNCACO experiment and also an HSQC of the terminal PASTA domains without the C-terminal peptide sequence. This region is Ser and Thr rich and the protein already has a large number of Ser and Thr residue in the protein sequence (28 residues (18.1%) and 11 residues (7.1%) respectively). An HSQC experiment without the C-terminal peptide will help aid in the identification and differentiation of other Ser and Thr residues in the protein back bone assignment. On completion of the backbone

assignment, further experiments are required including H(CCO)NH, (H)C(CO)NH and HCCH TOCSY NOSEY experiments to assign the protein side chains.

From the partial backbone assignment, some of the chemical shift perturbation residues were identified. They were associated in a region that has not secondary structure elements. In a previous experiment looking at ligands interaction with PrkC from *B. subtilis* using STD NMR, it was established that R500 in the protein was essential for binding to the DAP moiety of the PG tripeptide mimetic. **Figure 5.25** demonstrates that this conserved Arg residue is not present in any of the *E. faecalis* PASTA domains and instead either has a Pro residue (PASTA 1, 5 or 3) which would not be detected in a chemical shift perturbation experiment or Ala (PASTA 2) or Ser (PASTA 4). The observed site for vancomycin binding appears to be in a different location to that proposed of *B. subtilis* PrkC. Only the terminal PASTA domains 4 to 5 were examined in NMR experiments and it was not determined with there was a direct interaction between any of the other PASTA domains. A possibility to why saturation was not achieved in the chemical shift perturbation experiments is that there may be a number of sites vancomycin binds too between the PASTA domains that was measured in MST and SPR experiments where the full-length PASTA 1 to 5 domains was used.

```

B. subtilis - PASTA3  GPEDITLRDLKTYSKEAASGYLEDNGLKLV---KEAYSDDVPEGQVVKQKPAAGTAVKPGNE-VEVTFSL-----
E. Faecalis - PASTA5  GSDSVTVPDISGYSPKAAEDSINNAGLKINEQGL----SGSGDGQVVERTSPSAGSKVK-KGDSVTVYYSKANDSKSTTSSESSTSN
E. Faecalis - PASTA1  GGKDVEVPDVTNETKVDASQALQSAGLKVDSET-KKIPDDKIEEGKVVKTDPEAKSSVK-KGRSVTLTYISS
E. Faecalis - PASTA2  GTEKIEMADYTNESYESAVEALKKLGFSQITTKKEYSDSVTDNIIKQKPAAGKKVDPKDKVTLTVSE
E. Faecalis - PASTA3  GPEAVTLPSYAGYSYTNVAVNALAQLGISESQITRVDQASDTPVEPGLVITQDPAPGGTTPKNGQVTLVYSK
E. Faecalis - PASTA4  GSDKVTLSDYSGISYDNAVSRLLIAGLIPESQIKRVDEESDKVEKDTVISQEPASGTAVDPKNDTITLHVSK
* . : : . : * : * : . . : .* * : : *

```

**Figure 5.25: Comparison of ligand binding locations on PASTA domains.** Sequence alignment of the individual PASTA domains from *E. faecalis* and the terminal PASTA domain from *B. subtilis* (PASTA domain 3) with the key R500 residue associated with ligand binding highlighted in red. "\*" amino acids are identical in all sequences in the alignment, ":" show where conserved amino acids substitutions have been observed and "." show where semi-conserved amino acids substitutions have been observed.

Of the three ligands where a  $K_D$  was determined in Chapter 4 (vancomycin, teicoplanin and (GlcNAc-MurNAc)<sub>4</sub>), vancomycin which had the highest  $K_D$  of the three ligands was used in this NMR study due to the expense of the other two ligands. As chemical shift perturbations were observed in a region of the PASTA domains and the amino acids identified from the partial backbone assignment, further mutagenesis

experiments of these residue may be used to help validate the contribution of this residues involved in ligand binding. These mutant constructs can then be sued in an MST experiment against the other ligands where a  $K_D$  was determined in the full-length PASTA 1 to 5 constructs and compared to the WT construct. This would also confirm that all three ligands are SAXS binding to the same site or if they target different regions in the protein.

One of the main goals of this study was to establish the global dynamics that can occur between PASTA domains. SAXS experiments demonstrated that the addition of the PASTA domains resulted in increased flexibility of the protein and that the PASTA domains generally represent and elongated shape. Although an NMR structure of PASTA domains 4 to 5 was not obtained in the time frame of this study, future experiment would include the combination of the NMR structure with the SAXS data obtained to be used in hybrid modelling (**Figure 5.26**). This would give valuable data that could help gain further insight into the dynamic properties of these proteins that techniques such as X-ray crystallography cannot elucidate.

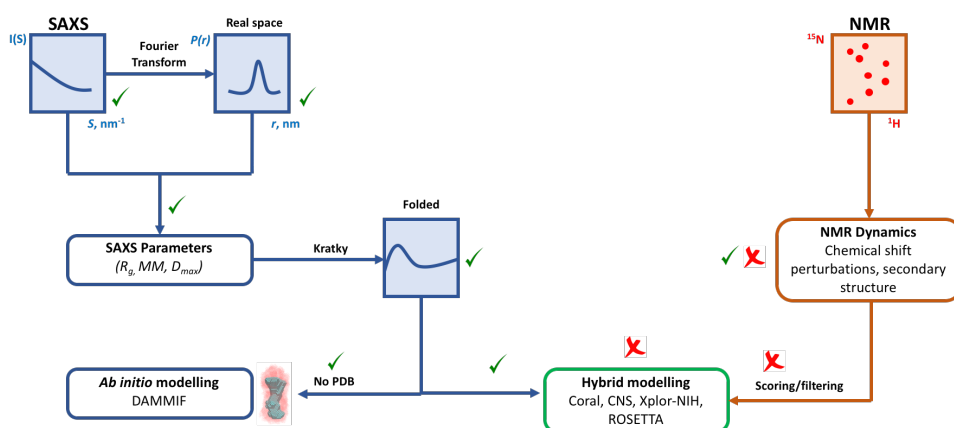


**Figure 5.26: Towards dynamic hybrid modelling.** Schematic adapted from Mertens and Svergun (2017) illustrating hybrid methods for determining dynamics of NMR structure of PASTA 4 to 5 and SAXS models of multiple PASTA constructs that can be mapped to the NMR data. Tick and crosses highlights completed experiments and areas where further experiments are required respectively.

Other experiments may include saturation transfer diffusion(STD) NMR where the chemical shift of the ligand is assigned (eg. vancomycin) and increasing concentration of the protein is added to saturate the chemical shift signals from the ligand in a 1D spectrum. It is an alternative technique that is useful for monitoring weak ligand binding (mM -  $\mu$ M) (Venkitakrishnan *et al.*, 2012). Regions where the protein is interacting with the ligand can be identified for epitope mapping.

## Chapter 6. General Discussions and Conclusions

### 6.1. Impact of Tn1549 acquisition and enhanced cephalosporin resistance

It is well established that Enterococcus species are intrinsically resistant to cephalosporin antibiotics (Kristich *et al.*, 2007). Although the Tn1549 cassette was originally thought solely associated with acquired vancomycin resistance (Healy *et al.* 2000), in a novel and unexpected finding, I demonstrate in this study that *E. faecalis* has a phenotype of enhanced resistance to cephalosporins in the presence of the Tn1549 cassette and that the two are linked via the serine-threonine kinase, IreK and the two-component system, VanS.

One consequence of this finding is the impact this linkage may have upon the widespread usage of cephalosporins in clinical practice. Cephalosporin's are used to treat a variety of infections including skin, UTI and respiratory tract infections commonly caused by Gram-positive and Gram-negative bacteria (Barry and Klasner, 2009). Both *E. faecalis* and *E. faecium* can cause a number of infections as highlighted in **Chapter 1** including UTIs, bacteraemia and infective endocarditis. In patients under cephalosporin therapy therefore, a cause of concern would be a clinical treatment environment where cephalosporin treatment is used to eradicate systemic bacterial species but as a consequence, VRE can proliferate and cause further infection as a consequence of their enhanced cephalosporin resistance. It has already been noted in the literature that there are a number of risk factors for VRE infection which include this scenario:

*“In addition to prior exposure to vancomycin, treatment with cephalosporins or antimicrobial drugs with significant activity against anaerobic bacteria (e.g. metronidazole, clindamycin, imipenem) is associated with increased risk for colonization or infection with VRE”*

(Shepard and Gilmore 2002)

A study of the acquisition of VRE in patients, found a correlation between higher rates of VRE infection and the use of 3<sup>rd</sup> generation cephalosporin's and vancomycin

(Fridkin *et al.*, 2001). The reduction in the use of vancomycin alone had previously failed to reduce the rate of VRE in patients and it had been suggested that the reduction of the use of cephalosporins was more important in reducing rates of VRE colonisation (Morris *et al.*, 1995; Quale *et al.*, 1996). The selection pressure for VRE infection was from the use of cephalosporin, not the use of vancomycin and we now have a molecular level explanation for this observation.

In this study, I demonstrated that IreK; an eSTK in *E. faecalis*, is involved in intrinsic cephalosporin resistance and also involved in the enhance acquired resistance mechanism of cephalosporin resistance as a consequence of the presence of the Tn1549 vancomycin resistance transposon. Deletion of *ireK* in a Tn1549 strain, restores susceptibility to cephalosporin's. This study went further to characterise potential inhibitors of the IreK kinase domain and has identified that the eukaryotic kinase inhibitor staurosporine was effective in also causing cephalosporin sensitivity thus establishing the role of IreK at a genetic and chemical level. This experiment was extended into a variety of different vanB phenotypic resistant strains and that cefotaxime sensitivity was obtained in those strains by staurosporine treatment. This sensitivity was not found in VanA phenotypic resistant strains. Further characterisation will require understanding further analysis of the VanA resistance strains but is likely to be due to the lack of IreK phosphorylation of VanS in these strains.

## 6.2. Characterisation of phosphorylation targets

This thesis was an extension from work carried out by the Dworkin group at the Columbia University, New York where the auto phosphorylation of IreK and transfer of the phosphate to residue T223 on the Kinase domain of VanS<sub>B</sub> was observed *in vitro*. However, the trans-phosphorylation from phosphorylated VanS<sub>B</sub> to VanR<sub>B</sub> was not observed. In this study, experiments *in vivo* suggest that the Tn1549 cassette and IreK are interacting at a genetic level, and qPCR experiments indicate that the Tn1549 structural genes (*vanY* and *vanB*) were not upregulated in the presence of cefotaxime but were in the presence of vancomycin as perilously known (Healy *et al.*, 2000, Walsh *et al.*, 1996).

It has been highlighted in the **Introduction (Chapter 1)**, that TCS cross talk can occur and that HK and RR derived from paralogue gene families that share significant sequence structural features can cross-talk in the same organism (Fisher *et al.*, 1995;

Fisher *et al.*, 1996). In *S. pneumoniae*, it had been shown that Walk from the WalkR TCS has an aa sequence similar to that of five other HKs and that low-level crosstalk was observed between three other HKs to Walk (Wayne *et al.*, 2012).

In this study I used qPCR to demonstrate that the DdcSR TCS was unregulated in the presence of vancomycin and cefotaxime, (independent of each other) only in strains that contained the Tn1549 cassette. This strongly implicates that the Tn1549 cassette is essential in the upregulation of the DdcSR TCS in the presence of these antibiotics. A possible mechanism of action for enhanced cephalosporin resistance is via the DdcSR TCS that can lead to an altered PG profile. A direct connection between Tn1549 and DdcSR could be provided by trans-phosphorylation (cross talk) of VanS<sub>B</sub> to either DdcS or DdcR and this could be tested in future work.

### 6.3. Further characterisation of IreK domains

After the identification of an enhanced cephalosporin resistance phenotype associated with IreK in *E. faecalis*, **Chapters 4 and 5** focused on the contribution of each domain from IreK and their function in signal transduction with focus on oligomerisation. Oligomerisation of the intracellular kinase domains was characterised and further work is required that could include the identification of new inhibitors in addition to staurosporine and AZ5438 described here in both an *in vivo* and *in vitro* context. It was demonstrated in **Chapter 3** that staurosporine and the AZ5438 inhibitors could be used in conjunction of cefotaxime to restore cephalosporin sensitivity. I have demonstrated that an *in-vivo* screen could be used in this context to screen for new inhibitors in the presence of cefotaxime. Due to the pharmaceutical interest in kinase inhibitor discovery, generally for cancer therapy, there is potential that a number of existing kinase inhibitors for eukaryotic targets may be “repurposed” as an antibiotic potentiator for *Enterococcal* infection. Upon selection and identification of other inhibitors, further characterisation may include *in vitro* experiments where the binding affinities of these inhibitors are characterised using techniques such as SPR and MST.

A number of Eukaryotic kinase inhibitors have been developed but have been unsuccessful in laboratory experiments and clinical trials to treat cancer. Many of these inhibitors are synthetic analogues of staurosporine and include such drugs as Becatecarin

which has passed Phase II clinical trials (Gani and Engh, 2010). Therefore, a number of these inhibitors may be suitable as bacterial kinase targets and repurposed for treatment of infections particularly as they would need to be administered in combination with antibiotics for a relatively short period (days or weeks compared to longer term chemotherapy). A recent review at the time of this study has also highlighted the potential for these inhibitors to be used in treatment of bacterial infections (Pensinger *et al.*, 2017).

## 6.4. Structural and Functional Properties of PASTA domains

**Chapter 4** characterised the oligomerisation events of each soluble domain of IreK from *E. faecalis* and the KD from *E. faecium*. It concluded that the kinase domains were able to self oligomerize, but the PASTA domains remained monomeric. Ligand binding studies using MST and SPR identified 3 ligands that interacted with PASTA domains 1 to 5 where a  $K_d$  was determined. These included for (GlcNAc-MurNAc)<sub>4</sub> which was used as a pure PG glycan derivative. Binding of this ligand supports the model of localised concentration of eSTKs (**Figure 4.28.B**). This model is also strongly supported by fluorescence microscopy experiments in **Chapter 3**, demonstrating that removal of the PASTA domains results in delocalisation from the cell septum where PG synthesis occurs. Possible mode of action for cephalosporin resistance in Enterococcus via IreK includes changes in PG structure and crosslinking. These changes occur due to cephalosporin's targeting PBPs, causing changes in the local PG environment and structure which are detected by the IreK PASTA domains resulting in signal transduction.

The classical mechanism for upregulation of eSTKs in Gram-positive bacteria is via ligand induced dimerization **Figure 4.28.A**. In this study, I have shown that the PASTA domains in isolation do not oligomerize in the absence of ligands. However, it is possible that ligands such as vancomycin may cause dimerization and this is a potential area for further work. By contrast, I have shown that vancomycin can also upregulate *ddcY* independent of cefotaxime and removal of the *ireK* gene prevents the upregulation. Therefore, both models may have a role in the function of eSTKs in Gram-positive bacteria.

Previous studies have determined the structures from eSTKs in Gram positive bacteria including the PASTA domains from *S. aureus* (X-ray crystallography (Paracuellos

*et al.*, 2010)), the single terminal PASTA domain from *S. pneumoniae* (X-ray crystallography (Zucchini *et al.*, 2018) and the PASTA domains from *M. tuberculosis* (NMR (Barthe *et al.*, 2010) and X-ray crystallography (Prigozhin *et al.*, 2016)).

The aim of this study in **Chapter 5** was to characterise one of the ligand interactions using vancomycin with PASTA domains 4 to 5 from IreK *E. faecalis*. Although the previous structural studies used a range of techniques including NMR, SAXS and X-ray crystallography, none of them showed any interaction with potential ligands. Ligand binding experiments were characterised in the *B. subtilis* PASTA domains using STD NMR, but no structural information gained as STD NMR measures peak intensity changes of the ligand (Squeglia *et al.*, 2011).

Although high resolution structural information was not obtained using the PASTA domains from IreK from *E. faecalis*, SAXS experiments managed to demonstrate that these domains are flexible and increase in flexibility in the presence of PASTA domains. These features make crystallisation of types of proteins difficult and the dynamics and flexibility of the PASTA proteins may play an important role of its mechanism of action. The terminal PASTA domains (PASTA 4 to 5) were studied using NMR gain structural information. Full backbone assignment was not achieved in the time frame of this study due to difficulties in the resolution of overlapping resonances in the 3D experiments. Further experiments may include longer acquisition windows to enhance signal resonances.

However, in a chemical shift perturbation experiment, direct interaction of vancomycin with PASTA 4 to 5 was observed with chemical shift perturbations observed on select amino acid resonances. Backbone assignment of some of the chemical shift perturbation resonances were assigned and binding appears to be in a region of no secondary structure within the PASTA 4 to 5 domain. This region is distinctly different to that observed previously with PrkC from *B. subtilis* and the Tri-DAP peptide ligand at R500. The interaction of R500 in PrkC was with the peptide step of PG and observation here may suggest that GlcNAc and MurNAc residues may also bind in the region observed in the chemical shift perturbation experiments, but further mutagenesis experiments of residues in this region are required and experiment performed using MST to confirm the binding site.

## 6.5. Final Conclusion

This study has highlighted that cephalosporin therapy in a clinical environment may select for vancomycin resistance cassettes such as Tn1549 conferring vanB type resistance. It has been demonstrated here that the Tn1549 transposon can enhance cephalosporin resistance in *E. faecalis* and that phosphorylation from IreK to VanS<sub>B</sub> and transphosphorylation to other TCS like DdcS/R may cause the enhanced cephalosporin phenotype through TCS cross-talk. Staurosporine was shown to reverse the effect of the enhanced and intrinsic cephalosporin resistance and is thought to bind directly to IreK. This highlights the possibility of the development of using eSTKs in Gram-positive bacteria as an antibiotic target in conjunction with other antibiotic therapies like cephalosporins. Further work is now possible in identifying other inhibitors that targets eSTKs like IreK in developing novel antibiotic therapies.

## Chapter 7. Bibliography

1. **Abadía-Patiño, Lorena, Keryn Christiansen, Jan Bell, Patrice Courvalin, and Bruno Périchon.** "VanE-type vancomycin-resistant *Enterococcus faecalis* clinical isolates from Australia." *Antimicrobial agents and chemotherapy* **48**, no. 12 (2004): 4882-4885.
2. **Akamine, Pearl, Nguyen-Huu Xuong, and Susan S. Taylor.** "Crystal structure of a transition state mimic of the catalytic subunit of cAMP-dependent protein kinase." *Nature Structural and Molecular Biology* **9**, no. 4 (2002): 273.
3. **Al-Dabbagh, Bayan, Xavier Henry, Meriem El Ghachi, Geneviève Auger, Didier Blanot, Claudine Parquet, Dominique Mengin-Lecreulx, and Ahmed Bouhss.** "Active site mapping of MraY, a member of the polyprenyl-phosphate N-acetylhexosamine 1-phosphate transferase superfamily, catalyzing the first membrane step of peptidoglycan biosynthesis." *Biochemistry* **47**, no. 34 (2008): 8919-8928.
4. **Alekshun, Michael N., and Stuart B. Levy.** "Molecular mechanisms of antibacterial multidrug resistance." *Cell* **128**, no. 6 (2007): 1037-1050.
5. **Andrews, Jennifer M.** "Determination of minimum inhibitory concentrations." *Journal of antimicrobial Chemotherapy* **48**, no. suppl 1 (2001): 5-16.
6. **Arbeloa, Ana, Heidi Segal, Jean-Emmanuel Hugonnet, Nathalie Josseume, Lionnel Dubost, Jean-Paul Brouard, Laurent Gutmann, Dominique Mengin-Lecreulx, and Michel Arthur.** "Role of class A penicillin-binding proteins in PBP5-mediated  $\beta$ -lactam resistance in *Enterococcus faecalis*." *Journal of bacteriology* **186**, no. 5 (2004): 1221-1228.
7. **Arias, Cesar A., and Barbara E. Murray.** "Emergence and management of drug-resistant enterococcal infections." *Expert review of anti-infective therapy* **6**, no. 5 (2008): 637-655.
8. **Arias, Cesar A., and Barbara E. Murray.** "The rise of the Enterococcus: beyond vancomycin resistance." *Nature Reviews Microbiology* **10**, no. 4 (2012): 266.

9. **Arias, Cesar A., Diana Panesso, Danielle M. McGrath, Xiang Qin, Maria F. Mojica, Corwin Miller, Lorena Diaz et al.** "Genetic basis for *in vivo* daptomycin resistance in enterococci." *New England Journal of Medicine* **365**, no. 10 (2011): 892-900.
10. **Arias, Cesar A., German A. Contreras, and Barbara E. Murray.** "Management of multidrug-resistant enterococcal infections." *Clinical microbiology and infection* **16**, no. 6 (2010): 555-562.
11. **Arias, Cesar A., Mercedes Martín-Martinez, Tom L. Blundell, Michel Arthur, Patrice Courvalin, and Peter E. Reynolds.** "Characterization and modelling of VanT: a novel, membrane-bound, serine racemase from vancomycin-resistant *Enterococcus gallinarum* BM4174." *Molecular microbiology* **31**, no. 6 (1999): 1653-1664.
12. **Arias, Cesar A., Patrice Courvalin, and Peter E. Reynolds.** "vanC Cluster of Vancomycin-Resistant *Enterococcus gallinarum* BM4174." *Antimicrobial agents and chemotherapy* **44**, no. 6 (2000): 1660-1666.
13. **Arthur, Michel., C. Molinas, F. Depardieu, and P. Courvalin.** "Characterization of *Tn1546*, a *Tn3*-related transposon conferring glycopeptide resistance by synthesis of depsipeptide peptidoglycan precursors in *Enterococcus faecium* BM4147." *Journal of bacteriology* **175**, no. 1 (1993): 117-127.
14. **Arthur, Michel, and Richard Quintiliani.** "Regulation of VanA-and VanB-type glycopeptide resistance in enterococci." *Antimicrobial agents and chemotherapy* **45**, no. 2 (2001): 375-381.
15. **Arthur, Michel, Florence Depardieu, Guy Gerbaud, Marc Galimand, Roland Leclercq, and Patrice Courvalin.** "The VanS sensor negatively controls VanR-mediated transcriptional activation of glycopeptide resistance genes of *Tn1546* and related elements in the absence of induction." *Journal of bacteriology* **179**, no. 1 (1997): 97-106.
16. **Ator, Linda Louise, and Marvin J. Starzyk.** "Distribution of group D streptococci in rivers and streams." *Microbios* **16**, no. 64 (1976): 91-104.
17. **Baddour, Larry M., Walter R. Wilson, Arnold S. Bayer, Vance G. Fowler, Ann F. Bolger, Matthew E. Levison, Patricia Ferrieri et al.** "Infective endocarditis." *Circulation* **111**, no. 23 (2005): e394-e434.

18. **Baddour, L. M., W. R. Wilson, A. S. Bayer, V. G. Fowler Jr, I. M. Tleyjeh, M. J. Rybak, B. Barsic et al.** "on behalf of the American Heart Association Committee on Rheumatic Fever, Endocarditis, and Kawasaki Disease of the Council on Cardiovascular Disease in the Young, Council on Clinical Cardiology, Council on Cardiovascular Surgery and Anesthesia, and Stroke Council." Infective endocarditis in adults: diagnosis, antimicrobial therapy, and management of complications: a scientific statement for healthcare professionals from the *American Heart Association* [published online ahead of print September 15, 2015]. *Circulation*. doi 10 (2015).
19. **Bakal, Christopher J., and Julian E. Davies.** "No longer an exclusive club: eukaryotic signalling domains in bacteria." *Trends in cell biology* **10**, no. 1 (2000): 32-38.
20. **Ballard, Susan A., Kelly K. Pertile, M. Lim, Paul DR Johnson, and M. Lindsay Grayson.** "Molecular characterization of vanB elements in naturally occurring gut anaerobes." *Antimicrobial agents and chemotherapy* **49**, no. 5 (2005): 1688-1694.
21. **Baptista, Marina, Florence Depardieu, Patrice Courvalin, and Michel Arthur.** "Specificity of induction of glycopeptide resistance genes in *Enterococcus faecalis*." *Antimicrobial agents and chemotherapy* **40**, no. 10 (1996): 2291-2295.
22. **Baptista, Marina, Florence Depardieu, Peter Reynolds, Patrice Courvalin, and Michel Arthur.** "Mutations leading to increased levels of resistance to glycopeptide antibiotics in VanB-type enterococci." *Molecular microbiology* **25**, no. 1 (1997): 93-105.
23. **Baptista, Marina, Pierre Rodrigues, Florence Depardieu, Patrice Courvalin, and Michel Arthur.** "Single-cell analysis of glycopeptide resistance gene expression in teicoplanin-resistant mutants of a VanB-type *Enterococcus faecalis*." *Molecular microbiology* **32**, no. 1 (1999): 17-28.
24. **Barakat, Mohamed, Philippe Ortet, Cécile Jourlin-Castelli, Mireille Ansaldi, Vincent Méjean, and David E. Whitworth.** "P2CS: a two-component system resource for prokaryotic signal transduction research." *BMC genomics* **10**, no. 1 (2009): 315.

25. **Barreteau, Helene, Andreja Kovač, Audrey Boniface, Matej Sova, Stanislav Gobec, and Didier Blanot.** "Cytoplasmic steps of peptidoglycan biosynthesis." *FEMS microbiology reviews* **32**, no. 2 (2008): 168-207.
26. **Barry, Pennan M., and Jeffrey D. Klausner.** "The use of cephalosporins for gonorrhea: the impending problem of resistance." *Expert opinion on pharmacotherapy* **10**, no. 4 (2009): 555-577.
27. **Barthe, Philippe, Galina V. Mukamolova, Christian Roumestand, and Martin Cohen-Gonsaud.** "The structure of PknB extracellular PASTA domain from *Mycobacterium tuberculosis* suggests a ligand-dependent kinase activation." *Structure* **18**, no. 5 (2010): 606-615.
28. **Batchelor, Matthew, Dejian Zhou, Matthew A. Cooper, Chris Abell, and Trevor Rayment.** "Vancomycin dimer formation between analogues of bacterial peptidoglycan surfaces probed by force spectroscopy." *Organic & biomolecular chemistry* **8**, no. 5 (2010): 1142-1148.
29. **Bax, Ad, and Mitsuhiro Ikura.** "An efficient 3D NMR technique for correlating the proton and <sup>15</sup>N backbone amide resonances with the  $\alpha$ -carbon of the preceding residue in uniformly <sup>15</sup>N/<sup>13</sup>C enriched proteins." *Journal of biomolecular NMR* **1**, no. 1 (1991): 99-104.
30. **Beganovic, Maya, Megan K. Luther, Louis B. Rice, Cesar A. Arias, Michael J. Rybak, and Kerry L. LaPlante.** "A Review of Combination Antimicrobial Therapy for *Enterococcus faecalis* Bloodstream Infections and Infective Endocarditis." *Clinical Infectious Diseases* (2018).
31. **Beilharz, Katrin, Linda Nováková, Daniela Fadda, Pavel Branny, Orietta Massidda, and Jan-Willem Veening.** "Control of cell division in *Streptococcus pneumoniae* by the conserved Ser/Thr protein kinase StkP." *Proceedings of the National Academy of Sciences* **109**, no. 15 (2012): E905-E913.
32. **Bellais, Samuel, Michel Arthur, Lionnel Dubost, Jean-Emmanuel Hugonnet, Laurent Gutmann, Jean Van Heijenoort, Raymond Legrand, Jean-Paul Brouard, Louis Rice, and Jean-Luc Mainardi.** "Aslfm, the D-aspartate ligase responsible for the addition of D-aspartic acid onto the peptidoglycan precursor of *Enterococcus faecium*." *Journal of Biological Chemistry* **281**, no. 17 (2006): 11586-11594.

33. **Bender, Jennifer K., Alexander Kalmbach, Carola Fleige, Ingo Klare, Stephan Fuchs, and Guido Werner.** "Population structure and acquisition of the vanB resistance determinant in German clinical isolates of *Enterococcus faecium* ST192." *Scientific reports* **6** (2016): 21847.
34. **Berg, Rodney D.** "The indigenous gastrointestinal microflora." *Trends in microbiology* **4**, no. 11 (1996): 430-435.
35. **Bern, Marshall, Richard Beniston, and Stéphane Mesnage.** "Towards an automated analysis of bacterial peptidoglycan structure." *Analytical and bioanalytical chemistry* **409**, no. 2 (2017): 551-560.
36. **Bhate, Manasi P., Kathleen S. Molnar, Mark Goulian, and William F. DeGrado.** "Signal transduction in histidine kinases: insights from new structures." *Structure* **23**, no. 6 (2015): 981-994.
37. **Bjørkeng, Eva, Gunlög Rasmussen, Arnfinn Sundsfjord, Lennart Sjöberg, Kristin Hegstad, and Bo Söderquist.** "Clustering of polyclonal VanB-type vancomycin-resistant *Enterococcus faecium* in a low-endemic area was associated with CC17-genogroup strains harbouring transferable vanB2-*Tn5382* and pRUM-like repA containing plasmids with axe-txe plasmid addiction systems." *Apmis* **119**, no. 4-5 (2011): 247-258.
38. **Bogdanovich, Tatiana, Lois M. Ednie, Stuart Shapiro, and Peter C. Appelbaum.** "Antistaphylococcal activity of ceftobiprole, a new broad-spectrum cephalosporin." *Antimicrobial agents and chemotherapy* **49**, no. 10 (2005): 4210-4219.
39. **Bolla, Jani Reddy, Joshua B. Sauer, Di Wu, Shahid Mehmood, Timothy M. Allison, and Carol V. Robinson.** "Direct observation of the influence of cardiolipin and antibiotics on lipid II binding to MurJ." *Nature Chemistry* (2018).
40. **Boudreau, Marc A., Jed F. Fisher, and Shahriar Mobashery.** "Messenger functions of the bacterial cell wall-derived muropeptides." *Biochemistry* **51**, no. 14 (2012): 2974-2990.
41. **Bourgogne, Agathe, Danielle A. Garsin, Xiang Qin, Kavindra V. Singh, Jouko Sillanpaa, Shailaja Yerrapragada, Yan Ding et al.** "Large scale variation in *Enterococcus faecalis* illustrated by the genome analysis of strain OG1RF." *Genome biology* **9**, no. 7 (2008): R110.

42. **Bouhss, Ahmed, Nathalie Josseaume, Anatoly Severin, Keiko Tabei, Jean-Emmanuel Hugonnet, David Shlaes, Dominique Mengin-Lecreulx, Jean van Heijenoort, and Michel Arthur.** "Synthesis of the L-alanyl-L-alanine cross-bridge of *Enterococcus faecalis* peptidoglycan." *Journal of Biological Chemistry* **277**, no. 48 (2002): 45935-45941.
43. **Boyd, D. A., J. Conly, H. Dedier, G. Peters, L. Robertson, E. Slater, and M. R. Mulvey.** "Molecular Characterization of the vanD Gene Cluster and a Novel Insertion Element in a Vancomycin-Resistant *Enterococcus* Isolated in Canada." *Journal of clinical microbiology* **38**, no. 6 (2000): 2392-2394.
44. **Boyd, David A., Barbara M. Willey, Darlene Fawcett, Nazira Gillani, and Michael R. Mulvey.** "Molecular characterization of *Enterococcus faecalis* N06-0364 with low-level vancomycin resistance harboring a novel D-Ala-D-Ser gene cluster, vanL." *Antimicrobial agents and chemotherapy* **52**, no. 7 (2008): 2667-2672.
45. **Boyd, David A., Pamela Kibsey, Diane Roscoe, and Michael R. Mulvey.** "*Enterococcus faecium* N03-0072 carries a new VanD-type vancomycin resistance determinant: characterization of the VanD5 operon." *Journal of Antimicrobial Chemotherapy* **54**, no. 3 (2004): 680-683.
46. **Boyd, David A., Simon Lévesque, Anne-Claude Picard, and George R. Golding.** "Vancomycin-resistant *Enterococcus faecium* harbouring vanN in Canada: a case and complete sequence of pEfm12493 harbouring the vanN operon." *Journal of Antimicrobial Chemotherapy* **70**, no. 7 (2015): 2163-2165.
47. **Boyd, David A., Tim Du, Romeo Hizon, Brynn Kaplen, Travis Murphy, Shaun Tyler, Shirley Brown et al.** "VanG-type vancomycin-resistant *Enterococcus faecalis* strains isolated in Canada." *Antimicrobial agents and chemotherapy* **50**, no. 6 (2006): 2217-2221.
48. **Bramson, H. Neal, John Corona, Stephen T. Davis, Scott H. Dickerson, Mark Edelstein, Stephen V. Frye, Robert T. Gampe et al.** "Oxindole-based inhibitors of cyclin-dependent kinase 2 (CDK2): design, synthesis, enzymatic activities, and X-ray crystallographic analysis." *Journal of medicinal chemistry* **44**, no. 25 (2001): 4339-4358.

49. **Brown, Patrick H., and Peter Schuck.** "Macromolecular size-and-shape distributions by sedimentation velocity analytical ultracentrifugation." *Biophysical journal* **90**, no. 12 (2006): 4651-4661.
50. **Bugg, T. D. H., and C. T. Walsh.** "Intracellular steps of bacterial cell wall peptidoglycan biosynthesis: enzymology, antibiotics, and antibiotic resistance." *Natural product reports* **9**, no. 3 (1992): 199-215.
51. **Bugg, Timothy DH, Gerard D. Wright, Sylvie Dutka-Malen, Michel Arthur, Patrice Courvalin, and Christopher T. Walsh.** "Molecular basis for vancomycin resistance in *Enterococcus faecium* BM4147: biosynthesis of a depsipeptide peptidoglycan precursor by vancomycin resistance proteins VanH and VanA." *Biochemistry* **30**, no. 43 (1991): 10408-10415.
52. **Bugg, Timothy DH.** "Bacterial peptidoglycan biosynthesis and its inhibition." *Comprehensive natural products chemistry* **3** (1999): 241-294.
53. **Burger, Virginia M., Daniel J. Arenas, and Collin M. Stultz.** "A structure-free method for quantifying conformational flexibility in proteins." *Scientific reports* **6** (2016): 29040.
54. **Byappanahalli, Muruleedhara N., Meredith B. Nevers, Asja Korajkic, Zachery R. Staley, and Valerie J. Harwood.** "Enterococci in the environment." *Microbiology and Molecular Biology Reviews* **76**, no. 4 (2012): 685-706.
55. **Cai, Mengli, Ying Huang, Kazuyasu Sakaguchi, G. Marius Clore, Angela M. Gronenborn, and Robert Craigie.** "An efficient and cost-effective isotope labeling protocol for proteins expressed in shape *Escherichia coli*." *Journal of biomolecular NMR* **11**, no. 1 (1998): 97-102.
56. **Capra, Emily J., and Michael T. Laub.** "Evolution of two-component signal transduction systems." *Annual review of microbiology* **66** (2012): 325-347.
57. **Carias, Lenore L., Susan D. Rudin, Curtis J. Donskey, and Louis B. Rice.** "Genetic linkage and cotransfer of a novel, vanB-containing transposon (*Tn5382*) and a low-affinity penicillin-binding protein 5 gene in a clinical vancomycin-resistant *Enterococcus faecium* isolate." *Journal of Bacteriology* **180**, no. 17 (1998): 4426-4434.

58. **Carpenter, Christopher F., and Henry F. Chambers.** "Daptomycin: another novel agent for treating infections due to drug-resistant gram-positive pathogens." *Clinical infectious diseases* **38**, no. 7 (2004): 994-1000.
59. **Casadewall, Barbara, and Patrice Courvalin.** "Characterization of the vanD Glycopeptide Resistance Gene Cluster from *Enterococcus faecium* BM4339." *Journal of bacteriology* **181**, no. 12 (1999): 3644-3648.
60. **Casino, Patricia, Vicente Rubio, and Alberto Marina.** "Structural insight into partner specificity and phosphoryl transfer in two-component signal transduction." *Cell* **139**, no. 2 (2009): 325-336.
61. **Chakupurakal, R., M. Ahmed, D. N. Sobithadevi, S. Chinnappan, and T. Reynolds.** "Urinary tract pathogens and resistance pattern." *Journal of clinical pathology* (2010): jcp-2009.
62. **Chang, Changsoo, Christine Tesar, Minyi Gu, Gyorgy Babnigg, Andrzej Joachimiak, P. Raj Pokkuluri, Hendrik Szurmant, and Marianne Schiffer.** "Extracytoplasmic PAS-like domains are common in signal transduction proteins." *Journal of bacteriology* **192**, no. 4 (2010): 1156-1159.
63. **Chang, Soju, Dawn M. Sievert, Jeffrey C. Hageman, Matthew L. Boulton, Fred C. Tenover, Frances Pouch Downes, Sandip Shah et al.** "Infection with vancomycin-resistant *Staphylococcus aureus* containing the vanA resistance gene." *New England Journal of Medicine* **348**, no. 14 (2003): 1342-1347.
64. **Cheung, Jonah, and Wayne A. Hendrickson.** "Sensor domains of two-component regulatory systems." *Current opinion in microbiology* **13**, no. 2 (2010): 116-123.
65. **Clark, Nancye C., Linda M. Weigel, Jean B. Patel, and Fred C. Tenover.** "Comparison of *Tn1546*-like elements in vancomycin-resistant *Staphylococcus aureus* isolates from Michigan and Pennsylvania." *Antimicrobial agents and chemotherapy* **49**, no. 1 (2005): 470-472.
66. **Comenge, Yannick, Richard Quintiliani, Ling Li, Lionel Dubost, Jean-Paul Brouard, Jean-Emmanuel Hugonnet, and Michel Arthur.** "The CroRS two-component regulatory system is required for intrinsic  $\beta$ -lactam resistance in *Enterococcus faecalis*." *Journal of bacteriology* **185**, no. 24 (2003): 7184-7192.

67. **Courvalin, Patrice.** "Genetics of glycopeptide resistance in Gram-positive pathogens." *International journal of medical microbiology* **294**, no. 8 (2005): 479-486.
68. **Courvalin, Patrice.** "Vancomycin resistance in Gram-positive cocci." *Clinical Infectious Diseases* **42**, no. Supplement\_1 (2006): S25-S34.
69. **Cranfill, Paula J., Brittney R. Sell, Michelle A. Baird, John R. Allen, Zeno Lavagnino, H. Martijn de Gruiter, Gert-Jan Kremers, Michael W. Davidson, Alessandro Ustione, and David W. Piston.** "Quantitative assessment of fluorescent proteins." *Nature methods* **13**, no. 7 (2016): 557.
70. **Cui, Longzhu, Jian-Qi Lian, Hui-min Neoh, Ethel Reyes, and Keiichi Hiramatsu.** "DNA microarray-based identification of genes associated with glycopeptide resistance in *Staphylococcus aureus*." *Antimicrobial agents and chemotherapy* **49**, no. 8 (2005): 3404-3413.
71. **D'Costa, Vanessa M., Christine E. King, Lindsay Kalan, Mariya Morar, Wilson WL Sung, Carsten Schwarz, Duane Froese et al.** "Antibiotic resistance is ancient." *Nature* **477**, no. 7365 (2011): 457.
72. **Dahl, Kristin H., and Arnfinn Sundsfjord.** "Transferable *vanB2 Tn5382*-containing elements in fecal streptococcal strains from veal calves." *Antimicrobial agents and chemotherapy* **47**, no. 8 (2003): 2579-2583.
73. **Davies, Julian, and Gerard D. Wright.** "Bacterial resistance to aminoglycoside antibiotics." *Trends in microbiology* **5**, no. 6 (1997): 234-240.
74. **De Roca, Francois Reste, Caroline Duché, Shengli Dong, Alain Rincé, Lionel Dubost, David G. Pritchard, John R. Baker, Michel Arthur, and Stéphane Mesnage.** "Cleavage specificity of *Enterococcus faecalis* EnpA (EF1473), a peptidoglycan endopeptidase related to the LytM/lysostaphin family of metallopeptidases." *Journal of molecular biology* **398**, no. 4 (2010): 507-517.
75. **Degenkolb, J., M. Takahashi, G. A. Ellestad, and W. Hillen.** "Structural requirements of tetracycline-Tet repressor interaction: determination of equilibrium binding constants for tetracycline analogs with the Tet repressor." *Antimicrobial Agents and Chemotherapy* **35**, no. 8 (1991): 1591-1595.

76. **Del Papa, María Florencia, and Marta Perego.** "Enterococcus faecalis virulence regulator FsrA binding to target promoters." *Journal of bacteriology* **193**, no. 7 (2011): 1527-1532.
77. **Depardieu, Florence, Bruno Perichon, and Patrice Courvalin.** "Detection of the van alphabet and identification of enterococci and staphylococci at the species level by multiplex PCR." *Journal of Clinical Microbiology* **42**, no. 12 (2004): 5857-5860.
78. **Depardieu, F., M-L. Foucault, J. Bell, A. Dubouix, M. Guibert, J-P. Lavigne, M. Levast, and P. Courvalin.** "New combinations of mutations in VanD-Type vancomycin-resistant *Enterococcus faecium*, *Enterococcus faecalis*, and *Enterococcus avium* strains." *Antimicrobial agents and chemotherapy* **53**, no. 5 (2009): 1952-1963.
79. **Depardieu, Florence, Maria Grazia Bonora, Peter E. Reynolds, and Patrice Courvalin.** "The vanG glycopeptide resistance operon from *Enterococcus faecalis* revisited." *Molecular microbiology* **50**, no. 3 (2003): 931-948.
80. **Depardieu, Florence, Mathias Kolbert, Hendrik Pruul, Jan Bell, and Patrice Courvalin.** "VanD-type vancomycin-resistant *Enterococcus faecium* and *Enterococcus faecalis*." *Antimicrobial agents and chemotherapy* **48**, no. 10 (2004): 3892-3904.
81. **Depardieu, Florence, Patrice Courvalin, and Annie Kolb.** "Binding sites of VanRB and  $\sigma$ 70 RNA polymerase in the vanB vancomycin resistance operon of *Enterococcus faecium* BM4524." *Molecular microbiology* **57**, no. 2 (2005): 550-564.
82. **Depardieu, Florence, Patrice Courvalin, and Tarek Msadek.** "A six amino acid deletion, partially overlapping the VanSB G2 ATP-binding motif, leads to constitutive glycopeptide resistance in VanB-type *Enterococcus faecium*." *Molecular microbiology* **50**, no. 3 (2003): 1069-1083.
83. **Depardieu, Florence, Peter E. Reynolds, and Patrice Courvalin.** "VanD-type vancomycin-resistant *Enterococcus faecium* 10/96A." *Antimicrobial agents and chemotherapy* **47**, no. 1 (2003): 7-18.
84. **Desbonnet, Charlene, Amelia Tait-Kamradt, Monica Garcia-Solache, Paul Dunman, Jeffrey Coleman, Michel Arthur, and Louis B. Rice.** "Involvement of the

eukaryote-like kinase-phosphatase system and a protein that interacts with penicillin-binding protein 5 in emergence of cephalosporin resistance in cephalosporin-sensitive class A penicillin-binding protein mutants in *Enterococcus faecium*." *MBio* **7**, no. 2 (2016): e02188-15.

85. **Deshpande, Lalitagauri M., Thomas R. Fritsche, Gary J. Moet, Douglas J. Biedenbach, and Ronald N. Jones.** "Antimicrobial resistance and molecular epidemiology of vancomycin-resistant enterococci from North America and Europe: a report from the SENTRY antimicrobial surveillance program." *Diagnostic microbiology and infectious disease* **58**, no. 2 (2007): 163-170.
86. **Dhanalakshmi, T. A., S. Vijaya, and Sulaiman Sharieff.** "Spontaneous Enterococcal Meningitis: A Case Report." *Journal of Medical Sciences* **1**, no. 1 (2015): 27.
87. **Djorić, Dušanka, and Christopher J. Kristich.** "Extracellular SalB contributes to intrinsic cephalosporin resistance and cell envelope integrity in *Enterococcus faecalis*." *Journal of bacteriology* **199**, no. 23 (2017): e00392-17.
88. **Domig, Konrad J., Helmut K. Mayer, and Wolfgang Kneifel.** "Methods used for the isolation, enumeration, characterisation and identification of *Enterococcus* spp.: 2. Pheno- and genotypic criteria." *International journal of food microbiology* **88**, no. 2 (2003): 165-188.
89. **Domingo, M-C., A. Huletsky, R. Giroux, F. J. Picard, and M. G. Bergeron.** "*vanD* and *vanG*-like gene clusters in a *Ruminococcus* species isolated from human bowel flora." *Antimicrobial agents and chemotherapy* **51**, no. 11 (2007): 4111-4117.
90. **Domingo, M-C., A. Huletsky, R. Giroux, K. Boissinot, F. J. Picard, P. Lebel, M. J. Ferraro, and M. G. Bergeron.** "High prevalence of glycopeptide resistance genes *vanB*, *vanD*, and *vanG* not associated with enterococci in human fecal flora." *Antimicrobial agents and chemotherapy* **49**, no. 11 (2005): 4784-4786.
91. **Donskey, Curtis J., Marion S. Helfand, Nicole J. Pultz, and Louis B. Rice.** "Effect of parenteral fluoroquinolone administration on persistence of vancomycin-resistant *Enterococcus faecium* in the mouse gastrointestinal tract." *Antimicrobial agents and chemotherapy* **48**, no. 1 (2004): 326-328.

92. **Donskey, Curtis J., Tanvir K. Chowdhry, Michelle T. Hecker, Claudia K. Hoyen, Jennifer A. Hanrahan, Andrea M. Hujer, Rebecca A. Hutton-Thomas, Christopher C. Whalen, Robert A. Bonomo, and Louis B. Rice.** "Effect of antibiotic therapy on the density of vancomycin-resistant enterococci in the stool of colonized patients." *New England Journal of Medicine* **343**, no. 26 (2000): 1925-1932.
93. **Dubin, Krista, and Eric G. Pamer.** "Enterococci and their interactions with the intestinal microbiome." *Microbiology spectrum* **5**, no. 6 (2014).
94. **Dunny, Gary M., Byron L. Brown, and Don B. Clewell.** "Induced cell aggregation and mating in *Streptococcus faecalis*: evidence for a bacterial sex pheromone." *Proceedings of the National Academy of Sciences* **75**, no. 7 (1978): 3479-3483.
95. **Durand, Dominique, Corinne Vivès, Dominique Cannella, Javier Pérez, Eva Pebay-Peyroula, Patrice Vachette, and Franck Fieschi.** "NADPH oxidase activator p67phox behaves in solution as a multidomain protein with semi-flexible linkers." *Journal of structural biology* **169**, no. 1 (2010): 45-53.
96. **Dutta, Ireena, and Peter E. Reynolds.** "Biochemical and genetic characterization of the *vanC-2* vancomycin resistance gene cluster of *Enterococcus casseliflavus* ATCC 25788." *Antimicrobial agents and chemotherapy* **46**, no. 10 (2002): 3125-3132.
97. **Dutta, Rinku, and Masayori Inouye.** "GHKL, an emergent ATPase/kinase superfamily." *Trends in biochemical sciences* **25**, no. 1 (2000): 24-28.
98. **Dutta, Rinku, Ling Qin, and Masayori Inouye.** "Histidine kinases: diversity of domain organization." *Molecular microbiology* **34**, no. 4 (1999): 633-640.
99. **Dworkin, Jonathan.** "Ser/Thr phosphorylation as a regulatory mechanism in bacteria." *Current opinion in microbiology* **24** (2015): 47-52.
100. **Edwards, J. R.** "Meropenem: a microbiological overview." *Journal of Antimicrobial Chemotherapy* **36**, no. suppl\_A (1995): 1-17.
101. **Elliott, T. S. J., J. Foweraker, F. K. Gould, J. D. Perry, and J. A. T. Sandoe.** "Guidelines for the antibiotic treatment of endocarditis in adults: report of the Working Party of the British Society for Antimicrobial Chemotherapy." *Journal of antimicrobial chemotherapy* **54**, no. 6 (2004): 971-981.

102. **Evers, Stefan, and Patrice Courvalin.** "Regulation of VanB-type vancomycin resistance gene expression by the VanS (B)-VanR (B) two-component regulatory system in *Enterococcus faecalis* V583." *Journal of bacteriology* **178**, no. 5 (1996): 1302-1309.
103. **Fabret, Céline, and James A. Hoch.** "A two-component signal transduction system essential for growth of *Bacillus subtilis*: implications for anti-infective therapy." *Journal of bacteriology* **180**, no. 23 (1998): 6375-6383.
104. **Facklam, Richard. R.** "Comparison of several laboratory media for presumptive identification of enterococci and group D streptococci." *Applied microbiology* **26**, no. 2 (1973): 138-145.
105. **Falke, Joseph J., Randal B. Bass, Scott L. Butler, Stephen A. Chervitz, and Mark A. Danielson.** "The two-component signaling pathway of bacterial chemotaxis: a molecular view of signal transduction by receptors, kinases, and adaptation enzymes." *Annual review of cell and developmental biology* **13**, no. 1 (1997): 457-512.
106. **Fernandez, Pablo, Brigitte Saint-Joanis, Nathalie Barilone, Mary Jackson, Brigitte Gicquel, Stewart T. Cole, and Pedro M. Alzari.** "The Ser/Thr protein kinase PknB is essential for sustaining mycobacterial growth." *Journal of bacteriology* **188**, no. 22 (2006): 7778-7784.
107. **Finegold, Sydney M., Vera L. Sutter, and Glenn E. Mathisen.** "Normal indigenous intestinal flora." *Human intestinal microflora in health and disease* **1** (1983): 3-31.
108. **Fines, Marguerite, Bruno Perichon, Peter Reynolds, Daniel F. Sahm, and Patrice Courvalin.** "VanE, a new type of acquired glycopeptide resistance in *Enterococcus faecalis* BM4405." *Antimicrobial Agents and Chemotherapy* **43**, no. 9 (1999): 2161-2164.
109. **Finks, Jennie, Eden Wells, Teri Lee Dyke, Nasir Husain, Linda Plizga, Renuka Heddurshetti, Melinda Wilkins et al.** "Vancomycin-resistant *Staphylococcus aureus*, Michigan, USA, 2007." *Emerging infectious diseases* **15**, no. 6 (2009): 943.
110. **Fiser, András, Sergio R. Filipe, and Alexander Tomasz.** "Cell wall branches, penicillin resistance and the secrets of the MurM protein." *Trends in microbiology* **11**, no. 12 (2003): 547-553.

111. **Fisher, Stewart L., Weihong Jiang, Barry L. Wanner, and Christopher T. Walsh.** "Cross-talk between the histidine protein kinase VanS and the response regulator PhoB Characterization and identification of A VanS domain that inhibits activation of PhoB." *Journal of Biological Chemistry* **270**, no. 39 (1995): 23143-23149.
112. **Fitzsimmons, K., A. I. Bamber, and H. B. Smalley.** "Infective endocarditis: changing aetiology of disease." *British journal of biomedical science* **67**, no. 1 (2010): 35-41.
113. **Fleming, Alexander.** "On the antibacterial action of cultures of a penicillium, with special reference to their use in the isolation of *B. influenzae*." *British journal of experimental pathology* **10**, no. 3 (1929): 226.
114. **Flores-Mireles, Ana L., Jennifer N. Walker, Michael Caparon, and Scott J. Hultgren.** "Urinary tract infections: epidemiology, mechanisms of infection and treatment options." *Nature reviews microbiology* **13**, no. 5 (2015): 269.
115. **Fogh, Rasmus, John Ionides, Eldon Ulrich, Wayne Boucher, Wim Vranken, Jens P. Linge, Michael Habeck et al.** "The CCPN project: an interim report on a data model for the NMR community." *Nature Structural and Molecular Biology* **9**, no. 6 (2002): 416.
116. **Fontana, Roberta, Marco Aldegheri, Marco Ligozzi, Horacio Lopez, Adriana Sucari, and Giuseppe Satta.** "Overproduction of a low-affinity penicillin-binding protein and high-level ampicillin resistance in *Enterococcus faecium*." *Antimicrobial agents and chemotherapy* **38**, no. 9 (1994): 1980-1983.
117. **Foster, Patricia L.** "Adaptive mutation: the uses of adversity." *Annual Reviews in Microbiology* **47**, no. 1 (1993): 467-504.
118. **Foucault, Marie-Laure, Florence Depardieu, Patrice Courvalin, and Catherine Grillot-Courvalin.** "Inducible expression eliminates the fitness cost of vancomycin resistance in enterococci." *Proceedings of the National Academy of Sciences* **107**, no. 39 (2010): 16964-16969.
119. **Foxman, Betsy.** "The epidemiology of urinary tract infection." *Nature Reviews Urology* **7**, no. 12 (2010): 653-660.
120. **Franke, Daniel, and Dmitri I. Svergun.** "DAMMIF, a program for rapid *ab-initio* shape determination in small-angle scattering." *Journal of applied crystallography* **42**, no. 2 (2009): 342-346.

121. **Franz, Charles MAP, Melanie Huch, Hikmate Abriouel, Wilhelm Holzapfel, and Antonio Gálvez.** "Enterococci as probiotics and their implications in food safety." *International journal of food microbiology* **151**, no. 2 (2011): 125-140.
122. **Fridkin, Scott K., Jonathan R. Edwards, Jeanne M. Courval, Holly Hill, Fred C. Tenover, Rachel Lawton, Robert P. Gaynes, and John E. McGowan.** "The effect of vancomycin and third-generation cephalosporins on prevalence of vancomycin-resistant enterococci in 126 US adult intensive care units." *Annals of internal medicine* **135**, no. 3 (2001): 175-183.
123. **Galperin, Michael Y., and Eugene V. Koonin.** "A diverse superfamily of enzymes with ATP-dependent carboxylate—amine/thiol ligase activity." *Protein Science* **6**, no. 12 (1997): 2639-2643.
124. **Gani, Osman ABSM, and Richard A. Engh.** "Protein kinase inhibition of clinically important staurosporine analogues." *Natural product reports* **27**, no. 4 (2010): 489-498.
125. **Gao, Rong, and Ann M. Stock.** "Biological insights from structures of two-component proteins." *Annual review of microbiology* **63** (2009): 133-154.
126. **Garcia, Pierre Simon, Jean-Pierre Simorre, Céline Brochier-Armanet, and Christophe Grangeasse.** "Cell division of *Streptococcus pneumoniae*: think positive!" *Current opinion in microbiology* **34** (2016): 18-23.
127. **Garnier, Fabien, Sead Taourit, Philippe Glaser, Patrice Courvalin, and Marc Galimand.** "Characterization of transposon Tn1549, conferring VanB-type resistance in *Enterococcus* spp." *Microbiology* **146**, no. 6 (2000): 1481-1489.
128. **Ghuysen, Jean-Marie, Donald J. Tipper, and Jack L. Strominger.** "[118] Enzymes that degrade bacterial cell walls." *In Methods in enzymology*, vol. 8, pp. 685-699. Academic Press, 1966.
129. **Gibson, Daniel G., Lei Young, Ray-Yuan Chuang, J. Craig Venter, Clyde A. Hutchison III, and Hamilton O. Smith.** "Enzymatic assembly of DNA molecules up to several hundred kilobases." *Nature methods* **6**, no. 5 (2009): 343.
130. **Giefing, Carmen, Kira E. Jelencsics, Dieter Gelbmann, Beatrice M. Senn, and Eszter Nagy.** "The pneumococcal eukaryotic-type serine/threonine protein kinase StkP co-localizes with the cell division apparatus and interacts with FtsZ in vitro." *Microbiology* **156**, no. 6 (2010): 1697-1707.

131. **Ginsberg, Cynthia, Stephanie Brown, and Suzanne Walker.** "Bacterial cell wall components." *In Glycoscience*, pp. 1535-1600. Springer Berlin Heidelberg, 2008.
132. **Goffin, Colette, and Jean-Marie Ghuysen.** "Biochemistry and comparative genomics of SxxK superfamily acyltransferases offer a clue to the mycobacterial paradox: presence of penicillin-susceptible target proteins versus lack of efficiency of penicillin as therapeutic agent." *Microbiology and molecular biology reviews* **66**, no. 4 (2002): 702-738.
133. **Goldberg, Shalom D., Graham D. Clinthorne, Mark Goulian, and William F. DeGrado.** "Transmembrane polar interactions are required for signaling in the *Escherichia coli* sensor kinase PhoQ." *Proceedings of the National Academy of Sciences* **107**, no. 18 (2010): 8141-8146.
134. **Gordon, E., N. Mouz, E. Duee, and O. Dideberg.** "The crystal structure of the penicillin-binding protein 2x from *Streptococcus pneumoniae* and its acyl-enzyme form: implication in drug resistance 1." *Journal of molecular biology* **299**, no. 2 (2000): 477-485.
135. **Goss, Lindsey,** "Threonine Phosphorylation Regulates Two-Component Systems Involved in Cell Wall Metabolism", Columbia University, Department of Microbiology, Immunology and Infection, New York (2013)
136. **Gossen, Manfred, and Hermann Bujard.** "Anhydrotetracycline, a novel effector for tetracycline controlled gene expression systems in eukaryotic cells." *Nucleic acids research* **21**, no. 18 (1993): 4411.
137. **Gossen, Manfred, Sabine Freundlieb, Gabriele Bender, Gerhard Muller, Wolfgang Hillen, and Hermann Bujard.** "Transcriptional activation by tetracyclines in mammalian cells." *Science* **268**, no. 5218 (1995): 1766-1769.
138. **Goulian, Mark.** "Two-component signaling circuit structure and properties." *Current opinion in microbiology* **13**, no. 2 (2010): 184-189.
139. **Grant, Seth G., Joel Jessee, Fredric R. Bloom, and Douglas Hanahan.** "Differential plasmid rescue from transgenic mouse DNAs into *Escherichia coli* methylation-restriction mutants." *Proceedings of the National Academy of Sciences* **87**, no. 12 (1990): 4645-4649.
140. **Green, N. Michael.** "Avidin." *In Advances in protein chemistry*, vol. 29, pp. 85-133. Academic Press, 1975.

141. **Greenfield, Norma J.** "Using circular dichroism spectra to estimate protein secondary structure." *Nature protocols* **1**, no. 6 (2006): 2876.
142. **Grzesiek, Stephan, and Ad Bax.** "Correlating backbone amide and side chain resonances in larger proteins by multiple relayed triple resonance NMR." *Journal of the American Chemical Society* **114**, no. 16 (1992): 6291-6293.
143. **Hall, Cherisse L., Betsy L. Lytle, Davin Jensen, Jessica S. Hoff, Francis C. Peterson, Brian F. Volkman, and Christopher J. Kristich.** "Structure and Dimerization of IreB, a Negative Regulator of Cephalosporin Resistance in *Enterococcus faecalis*." *Journal of molecular biology* **429**, no. 15 (2017): 2324-2336.
144. **Hall, Cherisse L., Michael Tschannen, Elizabeth A. Worthey, and Christopher J. Kristich.** "IreB, a Ser/Thr kinase substrate, influences antimicrobial resistance in *Enterococcus faecalis*." *Antimicrobial agents and chemotherapy* **57**, no. 12 (2013): 6179-6186.
145. **Hanahan, Douglas.** "Studies on transformation of *Escherichia coli* with plasmids." *Journal of molecular biology* **166**, no. 4 (1983): 557-580.
146. **Hancock, Lynn E., and Marta Perego.** "Systematic inactivation and phenotypic characterization of two-component signal transduction systems of *Enterococcus faecalis* V583." *Journal of bacteriology* **186**, no. 23 (2004): 7951-7958.
147. **Hancock, Lynn, and Marta Perego.** "Two-component signal transduction in *Enterococcus faecalis*." *Journal of bacteriology* **184**, no. 21 (2002): 5819-5825.
148. **Handwerger, Sandra, and Antonia Kolokathis.** "Induction of vancomycin resistance in *Enterococcus faecium* by inhibition of transglycosylation." *FEMS microbiology letters* **70**, no. 2 (1990): 167-170.
149. **Hanks, Steven K., and Tony Hunter.** "Protein kinases 6. The eukaryotic protein kinase superfamily: kinase (catalytic) domain structure and classification." *The FASEB journal* **9**, no. 8 (1995): 576-596.
150. **Hanks, Steven K., Anne Marie Quinn, and Tony Hunter.** "The protein kinase family: conserved features and deduced phylogeny of the catalytic domains." *Science* **241**, no. 4861 (1988): 42-52.
151. **Hardt, Patrick, Ina Engels, Marvin Rausch, Mike Gajdiss, Hannah Ulm, Peter Sass, Knut Ohlsen et al.** "The cell wall precursor lipid II acts as a molecular signal for the

- Ser/Thr kinase PknB of *Staphylococcus aureus*." *International Journal of Medical Microbiology* **307**, no. 1 (2017): 1-10.
152. **Hayhurst, Emma J., Lekshmi Kailas, Jamie K. Hobbs, and Simon J. Foster.** "Cell wall peptidoglycan architecture in *Bacillus subtilis*." *Proceedings of the National Academy of Sciences* **105**, no. 38 (2008): 14603-14608.
  153. **Healy, Vicki L., Ivan AD Lessard, David I. Roper, James R. Knox, and Christopher T. Walsh.** "Vancomycin resistance in enterococci: reprogramming of the d-Ala–d-Ala ligases in bacterial peptidoglycan biosynthesis." *Chemistry & biology* **7**, no. 5 (2000): R109-R119.
  154. **Hegstad, K., T. Mikalsen, T. M. Coque, G. Werner, and A. Sundsfjord.** "Mobile genetic elements and their contribution to the emergence of antimicrobial resistant *Enterococcus faecalis* and *Enterococcus faecium*." *Clinical microbiology and infection* **16**, no. 6 (2010): 541-554.
  155. **Hernando-Amado, Sara, Fernando Sanz-García, Paula Blanco, and José L. Martínez.** "Fitness costs associated with the acquisition of antibiotic resistance." *Essays in biochemistry* **61**, no. 1 (2017): 37-48.
  156. **Hidron, Alicia I., Jonathan R. Edwards, Jean Patel, Teresa C. Horan, Dawn M. Sievert, Daniel A. Pollock, and Scott K. Fridkin.** "Antimicrobial-resistant pathogens associated with healthcare-associated infections: annual summary of data reported to the National Healthcare Safety Network at the Centers for Disease Control and Prevention, 2006–2007." *Infection Control & Hospital Epidemiology* **29**, no. 11 (2008): 996-1011.
  157. **Hoch, James A.** "Regulation of the phosphorelay and the initiation of sporulation in *Bacillus subtilis*." *Annual Reviews in Microbiology* **47**, no. 1 (1993): 441-465.
  158. **Hoch, James A., and Thomas J. Silhavy,** eds. Two-component signal transduction. Vol. 2. Washington, DC:: ASM press, 1995.
  159. **Hong, Hee-Jeon, Matthew I. Hutchings, and Mark J. Buttner.** "Vancomycin resistance VanS/VanR two-component systems." In *Bacterial Signal Transduction: Networks and Drug Targets*, pp. 200-213. Springer, New York, NY, 2008.
  160. **Hutchings, Matthew I., Hee-Jeon Hong, and Mark J. Buttner.** "The vancomycin resistance VanRS two-component signal transduction system of *Streptomyces coelicolor*." *Molecular microbiology* **59**, no. 3 (2006): 923-935.

161. **Huycke, Mark M., Daniel F. Sahn, and Michael S. Gilmore.** "Multiple-drug resistant enterococci: the nature of the problem and an agenda for the future." *Emerging infectious diseases* **4**, no. 2 (1998): 239.
162. **Jacob, Alan E., and Susan J. Hobbs.** "Conjugal transfer of plasmid-borne multiple antibiotic resistance in *Streptococcus faecalis* var. *zymogenes*." *Journal of bacteriology* **117**, no. 2 (1974): 360-372.
163. **Jasni, Azmiza S., Peter Mullany, Haitham Hussain, and Adam P. Roberts.** "Demonstration of conjugative transposon (*Tn5397*)-mediated horizontal gene transfer between *Clostridium difficile* and *Enterococcus faecalis*." *Antimicrobial agents and chemotherapy* **54**, no. 11 (2010): 4924-4926.
164. **Jers, Carsten, Ahasanul Kobir, Elsebeth Oline Søndergaard, Peter Ruhdal Jensen, and Ivan Mijakovic.** "*Bacillus subtilis* two-component system sensory kinase DegS is regulated by serine phosphorylation in its input domain." *PLoS One* **6**, no. 2 (2011): e14653.
165. **Jett, Bradley D., Mark M. Huycke, and Michael S. Gilmore.** "Virulence of enterococci." *Clinical microbiology reviews* **7**, no. 4 (1994): 462-478.
166. **Jones, Tiffany, Michael R. Yeaman, George Sakoulas, Soo-Jin Yang, Richard A. Proctor, Hans-Georg Sahl, Jacques Schrenzel, Yan Q. Xiong, and Arnold S. Bayer.** "Failures in clinical treatment of *Staphylococcus aureus* infection with daptomycin are associated with alterations in surface charge, membrane phospholipid asymmetry, and drug binding." *Antimicrobial agents and chemotherapy* **52**, no. 1 (2008): 269-278.
167. **Jung, Young-Hee, Eun Shim Shin, Okgene Kim, Jung Sik Yoo, Kyeong Min Lee, Jae Il Yoo, Gyung Tae Chung, and Yeong Seon Lee.** "Characterization of two newly identified genes, *vgaD* and *vatG*, conferring resistance to streptogramin A in *Enterococcus faecium*." *Antimicrobial agents and chemotherapy* **54**, no. 11 (2010): 4744-4749.
168. **Kang, Choong-Min, Derek W. Abbott, Sang Tae Park, Christopher C. Dascher, Lewis C. Cantley, and Robert N. Husson.** "The *Mycobacterium tuberculosis* serine/threonine kinases PknA and PknB: substrate identification and regulation of cell shape." *Genes & development* **19**, no. 14 (2005): 1692-1704.

169. **Kannan, Natarajan, Susan S. Taylor, Yufeng Zhai, J. Craig Venter, and Gerard Manning.** "Structural and functional diversity of the microbial kinome." *PLoS biology* **5**, no. 3 (2007): e17.
170. **Kaplan, Heidi B., and Lynda Plamann.** "A *Myxococcus xanthus* cell density-sensing system required for multicellular development." *FEMS microbiology letters* **139**, no. 2-3 (1996): 89-95.
171. **Kapust, Rachel B., József Tözsér, Jeffrey D. Fox, D. Eric Anderson, Scott Cherry, Terry D. Copeland, and David S. Waugh.** "Tobacco etch virus protease: mechanism of autolysis and rational design of stable mutants with wild-type catalytic proficiency." *Protein engineering* **14**, no. 12 (2001): 993-1000.
172. **Kawalec, M., J. Kędzierska, A. Gajda, E. Sadowy, J. Węgrzyn, S. Naser, A. B. Skotnicki, M. Gniadkowski, and W. Hryniewicz.** "Hospital outbreak of vancomycin-resistant enterococci caused by a single clone of *Enterococcus raffinosus* and several clones of *Enterococcus faecium*." *Clinical microbiology and infection* **13**, no. 9 (2007): 893-901.
173. **Kawalec, Magdalena, Marek Gniadkowski, Jolanta Ke, Aleksander Skotnicki, Janusz Fiett, and Waleria Hryniewicz.** "Selection of a teicoplanin-resistant *Enterococcus faecium* mutant during an outbreak caused by vancomycin-resistant enterococci with the VanB phenotype." *Journal of clinical microbiology* **39**, no. 12 (2001): 4274-4282.
174. **Kay, Lewis E., Mitsuhiko Ikura, Rolf Tschudin, and Ad Bax.** "Three-dimensional triple-resonance NMR spectroscopy of isotopically enriched proteins." *Journal of Magnetic Resonance* (1969) **89**, no. 3 (1990): 496-514.
175. **Kay, Lewis, Paul Keifer, and Tim Saarinen.** "Pure absorption gradient enhanced heteronuclear single quantum correlation spectroscopy with improved sensitivity." *Journal of the American Chemical Society* **114**, no. 26 (1992): 10663-10665.
176. **Kellogg, Stephanie L., Jaime L. Little, Jessica S. Hoff, and Christopher J. Kristich.** "Requirement of the CroRS two-component system for resistance to cell wall-targeting antimicrobials in *Enterococcus faecium*." *Antimicrobial agents and chemotherapy* **61**, no. 5 (2017): e02461-16.

177. **Kenner, Bernard A., Harold F. Clark, and Paul W. Kabler.** "Fecal streptococci I. Cultivation and enumeration of streptococci in surface waters." *Applied microbiology* **9**, no. 1 (1961): 15-20.
178. **Khaledi, Ariane, Monika Schniederjans, Sarah Pohl, Roman Rainer, Ulrich Bodenhofer, Boyang Xia, Frank Klawonn et al.** "Transcriptome profiling of antimicrobial resistance in *Pseudomonas aeruginosa*." *Antimicrobial agents and chemotherapy* **60**, no. 8 (2016): 4722-4733.
179. **Kikhney, Alexey G., and Dmitri I. Svergun.** "A practical guide to small angle X-ray scattering (SAXS) of flexible and intrinsically disordered proteins." *FEBS letters* **589**, no. 19 PartA (2015): 2570-2577.
180. **Kim, Dong-jin, and Steven Forst.** "Genomic analysis of the histidine kinase family in bacteria and archaea." *Microbiology* **147**, no. 5 (2001): 1197-1212.
181. **Klare, I., G. Werner, and W. Witte.** "Enterococci." In *Emerging bacterial pathogens*, vol. 8, pp. 108-122. Karger Publishers, 2001.
182. **Klare, Ingo, Carola Konstabel, Dietlinde Badstübner, Guido Werner, and Wolfgang Witte.** "Occurrence and spread of antibiotic resistances in *Enterococcus faecium*." *International journal of food microbiology* **88**, no. 2 (2003): 269-290.
183. **Knapp, Stefan, Paulo Arruda, Julian Blagg, Stephen Burley, David H. Drewry, Aled Edwards, Dorian Fabbro et al.** "A public-private partnership to unlock the untargeted kinome." *Nature chemical biology* **9**, no. 1 (2013): 3.
184. **Koeth, L. M., A. King, H. Knight, J. May, L. A. Miller, I. Phillips, and J. A. Poupard.** "Comparison of cation-adjusted Mueller–Hinton broth with Iso-Sensitest broth for the NCCLS broth microdilution method." *Journal of Antimicrobial chemotherapy* **46**, no. 3 (2000): 369-376.
185. **Köhler, Thilo, Mehri Michea-Hamzehpour, Patrick Plesiat, Anne-Lise Kahr, and Jean-Claude Pechere.** "Differential selection of multidrug efflux systems by quinolones in *Pseudomonas aeruginosa*." *Antimicrobial agents and chemotherapy* **41**, no. 11 (1997): 2540-2543.
186. **Kohler, Thomas, Christopher Weidenmaier, and Andreas Peschel.** "Wall teichoic acid protects *Staphylococcus aureus* against antimicrobial fatty acids from human skin." *Journal of bacteriology* **191**, no. 13 (2009): 4482-4484.

187. **Koteva, Kalinka, Hee-Jeon Hong, Xiao Dong Wang, Ishac Nazi, Donald Hughes, Mike J. Naldrett, Mark J. Buttner, and Gerard D. Wright.** "A vancomycin photoprobe identifies the histidine kinase VanSsc as a vancomycin receptor." *Nature chemical biology* **6**, no. 5 (2010): 327.
188. **Kristich, Christopher J., and Jaime L. Little.** "Mutations in the  $\beta$  subunit of RNA polymerase alter intrinsic cephalosporin resistance in Enterococci." *Antimicrobial agents and chemotherapy* **56**, no. 4 (2012): 2022-2027.
189. **Kristich, Christopher J., Carol L. Wells, and Gary M. Dunny.** "A eukaryotic-type Ser/Thr kinase in *Enterococcus faecalis* mediates antimicrobial resistance and intestinal persistence." *Proceedings of the National Academy of Sciences* **104**, no. 9 (2007): 3508-3513.
190. **Kristich, Christopher J., Jaime L. Little, Cherisse L. Hall, and Jessica S. Hoff.** "Reciprocal regulation of cephalosporin resistance in *Enterococcus faecalis*." *MBio* **2**, no. 6 (2011): e00199-11.
191. **Kristich, Christopher J., Louis B. Rice, and Cesar A. Arias.** "Enterococcal infection—treatment and antibiotic resistance." (2014).
192. **Kuo, J. F., and Paul Greengard.** "Cyclic nucleotide-dependent protein kinases, IV. Widespread occurrence of adenosine 3', 5'-monophosphate-dependent protein kinase in various tissues and phyla of the animal kingdom." *Proceedings of the National Academy of Sciences* **64**, no. 4 (1969): 1349-1355.
193. **Krupa, A., and N. Srinivasan.** "Diversity in domain architectures of Ser/Thr kinases and their homologues in prokaryotes." *BMC genomics* **6**, no. 1 (2005): 129.
194. **Kwong, Stephen M., Ricky Lim, Rebecca J. LeBard, Ronald A. Skurray, and Neville Firth.** "Analysis of the pSK1 replicon, a prototype from the staphylococcal multiresistance plasmid family." *Microbiology* **154**, no. 10 (2008): 3084-3094.
195. **Labbe, Benjamin D., and Christopher J. Kristich.** "Growth-and stress-induced PASTA kinase phosphorylation in *Enterococcus faecalis*." *Journal of Bacteriology* **199**, no. 21 (2017): e00363-17.
196. **Laguna, P. Del Estal, C. Zubiri García, R. Madero García, and M. Navarro Gil.** "Enterococcal meningitis in adults." *Neurologia (Barcelona, Spain)* **24**, no. 4 (2009): 245-248.

197. **Landman, David, and John M. Quale.** "Management of infections due to resistant enterococci: a review of therapeutic options." *The Journal of antimicrobial chemotherapy* **40**, no. 2 (1997): 161-170.
198. **Lang, Sue.** "Getting to the heart of the problem: serological and molecular techniques in the diagnosis of infective endocarditis." (2008): 341-349.
199. **Laub, Michael T., and Mark Goulian.** "Specificity in two-component signal transduction pathways." *Annu. Rev. Genet.* **41** (2007): 121-145.
200. **Launay, Aline, Susan A. Ballard, Paul DR Johnson, M. Lindsay Grayson, and Thierry Lambert.** "Transfer of vancomycin resistance transposon Tn1549 from *Clostridium symbiosum* to *Enterococcus* spp. in the gut of gnotobiotic mice." *Antimicrobial agents and chemotherapy* **50**, no. 3 (2006): 1054-1062.
201. **Lavollay, Marie, Michel Arthur, Martine Fourgeaud, Lionel Dubost, Arul Marie, Nicolas Veziris, Didier Blanot, Laurent Gutmann, and Jean-Luc Mainardi.** "The peptidoglycan of stationary-phase *Mycobacterium tuberculosis* predominantly contains cross-links generated by L, D-transpeptidation." *Journal of bacteriology* **190**, no. 12 (2008): 4360-4366.
202. **Lawrie, Alison M., M. E. Noble, Paul Tunnah, Nicholas R. Brown, Louise N. Johnson, and Jane A. Endicott.** "Protein kinase inhibition by staurosporine revealed in details of the molecular interaction with CDK2." *Nature structural biology* **4**, no. 10 (1997): 796-801.
203. **Lebreton, François, Florence Depardieu, Nancy Bourdon, Marguerite Fines-Guyon, Pierre Berger, Sabine Camiade, Roland Leclercq, Patrice Courvalin, and Vincent Cattoir.** "D-Ala-D-Ser VanN-type transferable vancomycin resistance in *Enterococcus faecium*." *Antimicrobial agents and chemotherapy* **55**, no. 10 (2011): 4606-4612.
204. **Leclercq, R., E. Derlot, M. Weber, J. Duval, and P. Courvalin.** "Transferable vancomycin and teicoplanin resistance in *Enterococcus faecium*." *Antimicrobial Agents and Chemotherapy* **33**, no. 1 (1989): 10-15.
205. **Leclercq, Roland, Eliane Derlot, Jean Duval, and Patrice Courvalin.** "Plasmid-mediated resistance to vancomycin and teicoplanin in *Enterococcus faecium*." *New England Journal of Medicine* **319**, no. 3 (1988): 157-161.

206. **Leclercq, Sophie, Adeline Derouaux, Samir Olatunji, Claudine Fraipont, Alexander JF Egan, Waldemar Vollmer, Eefjan Breukink, and Mohammed Terrak.** "Interplay between penicillin-binding proteins and SEDS proteins promotes bacterial cell wall synthesis." *Scientific reports* **7** (2017): 43306.
207. **Lecoq, Lauriane, Catherine Bougault, Jean-Emmanuel Hugonnet, Carole Veckerlé, Ombeline Pessey, Michel Arthur, and Jean-Pierre Simorre.** "Dynamics induced by  $\beta$ -lactam antibiotics in the active site of *Bacillus subtilis* I, d-transpeptidase." *Structure* **20**, no. 5 (2012): 850-861.
208. **Lemmin, Thomas, Cinque S. Soto, Graham Clinthorne, William F. DeGrado, and Matteo Dal Peraro.** "Assembly of the transmembrane domain of *E. coli* PhoQ histidine kinase: implications for signal transduction from molecular simulations." *PLoS computational biology* **9**, no. 1 (2013): e1002878.
209. **Letunic, Ivica, Tobias Doerks, and Peer Bork.** "SMART: recent updates, new developments and status in 2015." *Nucleic acids research* **43**, no. D1 (2014): D257-D260.
210. **Levin, Bruce R., Véronique Perrot, and Nina Walker.** "Compensatory mutations, antibiotic resistance and the population genetics of adaptive evolution in bacteria." *Genetics* **154**, no. 3 (2000): 985-997.
211. **Levy, Stuart B., and Bonnie Marshall.** "Antibacterial resistance worldwide: causes, challenges and responses." *Nature medicine* **10** (2004): S122-S129.
212. **Libby, Elizabeth A., Lindsie A. Goss, and Jonathan Dworkin.** "The eukaryotic-like Ser/Thr kinase PrkC regulates the essential WalRK two-component system in *Bacillus subtilis*." *PLoS genetics* **11**, no. 6 (2015): e1005275.
213. **Ligozzi, Marco., Fabrizia, Pittaluga, and Roberta Fontana.** "Identification of a genetic element (psr) which negatively controls expression of *Enterococcus hirae* penicillin-binding protein 5." *Journal of bacteriology* **175**, no. 7 (1993): 2046-2051.
214. **Liu, Maili, Xi-an Mao, Chaohui Ye, He Huang, Jeremy K. Nicholson, and John C. Lindon.** "Improved WATERGATE pulse sequences for solvent suppression in NMR spectroscopy." *Journal of Magnetic Resonance* **132**, no. 1 (1998): 125-129.
215. **Llano-Sotelo, Beatriz, Eduardo F. Azucena, Lakshmi P. Kotra, Shahriar Mobashery, and Christine S. Chow.** "Aminoglycosides modified by resistance

enzymes display diminished binding to the bacterial ribosomal aminoacyl-tRNA site." *Chemistry & biology* **9**, no. 4 (2002): 455-463.

216. **Lloyd, Adrian J., Andrea M. Gilbey, Anne M. Blewett, Gianfranco De Pascale, Ahmed El Zoeiby, Roger C. Levesque, Anita C. Catherwood et al.** "Characterization of tRNA-dependent peptide bond formation by MurM in the synthesis of *Streptococcus pneumoniae* peptidoglycan." *Journal of Biological Chemistry* **283**, no. 10 (2008): 6402-6417.
217. **López, María, Yolanda Sáenz, Beatriz Rojo-Bezares, Santiago Martínez, Rosa del Campo, Fernanda Ruiz-Larrea, Myriam Zarazaga, and Carmen Torres.** "Detection of *vanA* and *vanB2*-containing enterococci from food samples in Spain, including *Enterococcus faecium* strains of CC17 and the new singleton ST425." *International journal of food microbiology* **133**, no. 1 (2009): 172-178.
218. **Ludwig, Wolfgang, Karl-Heinz Schleifer, and William B. Whitman.** "Revised road map to the phylum Firmicutes." In *Bergey's Manual® of Systematic Bacteriology*, pp. 1-13. Springer New York, 2009.
219. **Lukat, Gudrun S., William R. McCleary, Ann M. Stock, and Jeffrey B. Stock.** "Phosphorylation of bacterial response regulator proteins by low molecular weight phospho-donors." *Proceedings of the National Academy of Sciences* **89**, no. 2 (1992): 718-722.
220. **Ma, Xiaolei, Nazish Sayed, Padmamalini Baskaran, Annie Beuve, and Focco Van Den Akker.** "PAS-mediated dimerization of soluble guanylyl cyclase revealed by signal transduction histidine kinase domain crystal structure." *Journal of Biological Chemistry* **283**, no. 2 (2008): 1167-1178.
221. **Madec, Edwige, Agnieszka Laszkiewicz, Adam Iwanicki, Michal Obuchowski, and Simone Séror.** "Characterization of a membrane-linked Ser/Thr protein kinase in *Bacillus subtilis*, implicated in developmental processes." *Molecular microbiology* **46**, no. 2 (2002): 571-586.
222. **Magnet, Sophie, Samuel Bellais, Lionel Dubost, Martine Fourgeaud, Jean-Luc Mainardi, Sébastien Petit-Frère, Arul Marie, Dominique Mengin-Lecreulx, Michel Arthur, and Laurent Gutmann.** "Identification of the L, D-transpeptidases responsible for attachment of the Braun lipoprotein to *Escherichia coli* peptidoglycan." *Journal of bacteriology* **189**, no. 10 (2007): 3927-3931.

223. **Maguin, Emmanuelle, Patrick Duwat, Timothee Hege, D. Ehrlich, and A. Gruss.** "New thermosensitive plasmid for gram-positive bacteria." *Journal of bacteriology* **174**, no. 17 (1992): 5633-5638.
224. **Mainardi, Jean-Luc, Martine Fourgeaud, Jean-Emmanuel Hugonnet, Lionel Dubost, Jean-Paul Brouard, Jamal Ouazzani, Louis B. Rice, Laurent Gutmann, and Michel Arthur.** "A novel peptidoglycan cross-linking enzyme for a  $\beta$ -lactam-resistant transpeptidation pathway." *Journal of Biological Chemistry* **280**, no. 46 (2005): 38146-38152.
225. **Mainardi, Jean-Luc, Raymond Legrand, Michel Arthur, Bernard Schoot, Jean van Heijenoort, and Laurent Gutmann.** "Novel mechanism of  $\beta$ -lactam resistance due to bypass of DD-transpeptidation in *Enterococcus faecium*." *Journal of Biological Chemistry* **275**, no. 22 (2000): 16490-16496.
226. **Mainardi, Jean-Luc, Regis Villet, Timothy D. Bugg, Claudine Mayer, and Michel Arthur.** "Evolution of peptidoglycan biosynthesis under the selective pressure of antibiotics in Gram-positive bacteria." *FEMS microbiology reviews* **32**, no. 2 (2008): 386-408.
227. **Manuse, Sylvie, Nicolas L. Jean, Mégane Guinot, Jean-Pierre Lavergne, Cédric Laguri, Catherine M. Bougault, Michael S. VanNieuwenhze, Christophe Grangeasse, and Jean-Pierre Simorre.** "Structure–function analysis of the extracellular domain of the pneumococcal cell division site positioning protein MapZ." *Nature communications* **7** (2016): 12071.
228. **Marion, Dominique, Mitsuhiko Ikura, Rolf Tschudin, and A. D. Bax.** "Rapid recording of 2D NMR spectra without phase cycling. Application to the study of hydrogen exchange in proteins." *Journal of Magnetic Resonance* **85** (1989): 393-399.
229. **Marion, Dominique, Paul C. Driscoll, Lewis E. Kay, Paul T. Wingfield, Ad Bax, Angela M. Gronenborn, and G. Marius Clore.** "Overcoming the overlap problem in the assignment of proton NMR spectra of larger proteins by use of three-dimensional heteronuclear proton-nitrogen-15 Hartmann-Hahn-multiple quantum coherence and nuclear Overhauser-multiple quantum coherence spectroscopy: application to interleukin 1. beta." *Biochemistry* **28**, no. 15 (1989): 6150-6156.

230. **Maris, Ann E., Maria Kaczor-Grzeskowiak, Zhongcai Ma, Mary L. Kopka, Robert P. Gunsalus, and Richard E. Dickerson.** "Primary and secondary modes of DNA recognition by the NarL two-component response regulator." *Biochemistry* **44**, no. 44 (2005): 14538-14552.
231. **Maris, Ann E., Michael R. Sawaya, Maria Kaczor-Grzeskowiak, Michael R. Jarvis, Shawn MD Bearson, Mary L. Kopka, Imke Schröder, Robert P. Gunsalus, and Richard E. Dickerson.** "Dimerization allows DNA target site recognition by the NarL response regulator." *Nature Structural and Molecular Biology* **9**, no. 10 (2002): 771.
232. **Marshall, C. G., I. A. D. Lessard, I-S. Park, and G. D. Wright.** "Glycopeptide antibiotic resistance genes in glycopeptide-producing organisms." *Antimicrobial agents and chemotherapy* **42**, no. 9 (1998): 2215-2220.
233. **Marshall, C. Gary, and Gerard D. Wright.** "The glycopeptide antibiotic producer *Streptomyces toyocaensis* NRRL 15009 has both D-alanyl-D-alanine and D-alanyl-D-lactate ligases." *FEMS microbiology letters* **157**, no. 2 (1997): 295-299.
234. **Martin, Jonathan D., and J. Orvin Mundt.** "Enterococci in insects." *Applied microbiology* **24**, no. 4 (1972): 575-580.
235. **Martinez, J. L., and F. Baquero.** "Mutation frequencies and antibiotic resistance." *Antimicrobial agents and chemotherapy* **44**, no. 7 (2000): 1771-1777.
236. **Mascher, Thorsten, John D. Helmann, and Gottfried Unden.** "Stimulus perception in bacterial signal-transducing histidine kinases." *Microbiology and Molecular Biology Reviews* **70**, no. 4 (2006): 910-938.
237. **Maslennikov, Innokentiy, Christian Klammt, Eunha Hwang, Georgia Kefala, Mizuki Okamura, Luis Esquivies, Karsten Mörs et al.** "Membrane domain structures of three classes of histidine kinase receptors by cell-free expression and rapid NMR analysis." *Proceedings of the National Academy of Sciences* **107**, no. 24 (2010): 10902-10907.
238. **McKessar, Stuart J., Anne M. Berry, Jan M. Bell, John D. Turnidge, and James C. Paton.** "Genetic characterization of *vanG*, a novel vancomycin resistance locus of *Enterococcus faecalis*." *Antimicrobial agents and chemotherapy* **44**, no. 11 (2000): 3224-3228.

239. **Meeske, Alexander J., Eammon P. Riley, William P. Robins, Tsuyoshi Uehara, John J. Mekalanos, Daniel Kahne, Suzanne Walker, Andrew C. Kruse, Thomas G. Bernhardt, and David Z. Rudner.** "SEDS proteins are a widespread family of bacterial cell wall polymerases." *Nature* **537**, no. 7622 (2016): 634.
240. **Mertens, Haydyn DT, and Dmitri I. Svergun.** "Combining NMR and small angle X-ray scattering for the study of biomolecular structure and dynamics." *Archives of biochemistry and biophysics* **628** (2017): 33-41.
241. **Mesnage, Stéphane, Mariano Dellarole, Nicola J. Baxter, Jean-Baptiste Rouget, Jordan D. Dimitrov, Ning Wang, Yukari Fujimoto et al.** "Molecular basis for bacterial peptidoglycan recognition by LysM domains." *Nature communications* **5** (2014): 4269.
242. **Miller, William R., Arnold S. Bayer, and Cesar A. Arias.** "Mechanism of action and resistance to daptomycin in *Staphylococcus aureus* and Enterococci." *Cold Spring Harbor perspectives in medicine* **6**, no. 11 (2016): a026997.
243. **Mir, Mushtaq, Jinkeng Asong, Xiuru Li, Jessica Cardot, Geert-Jan Boons, and Robert N. Husson.** "The extracytoplasmic domain of the *Mycobacterium tuberculosis* Ser/Thr kinase PknB binds specific muropeptides and is required for PknB localization." *PLoS pathogens* **7**, no. 7 (2011): e1002182.
244. **Miro, Jose M., Juan M. Pericas, and Ana del Rio.** "A new era for treating Enterococcus faecalis endocarditis: ampicillin plus short-course gentamicin or ampicillin plus ceftriaxone: that is the question!" *Am Heart Assoc* (2013): 1763-1766.
245. **Moellering, Robert C.** "Linezolid: the first oxazolidinone antimicrobial." *Annals of internal medicine* **138**, no. 2 (2003): 135-142.
246. **Mohammad, Haroon, Ahmed AbdelKhalek, Nader S. Abutaleb, and Mohamed N. Seleem.** "Repurposing niclosamide for intestinal decolonization of vancomycin-resistant enterococci." *International journal of antimicrobial agents* (2018).
247. **Mohammadi, Tamimount, Vincent Van Dam, Robert Sijbrandi, Thierry Vernet, André Zapun, Ahmed Bouhss, Marlies Diepeveen-de Bruin, Martine Nguyen-Distèche, Ben De Kruijff, and Eefjan Breukink.** "Identification of FtsW as a transporter of lipid-linked cell wall precursors across the membrane." *The EMBO journal* **30**, no. 8 (2011): 1425-1432.

248. **Montealegre, Maria Camila, Jung Hyeob Roh, Meredith Rae, Milya G. Davlieva, Kavindra V. Singh, Yousif Shamoo, and Barbara E. Murray.** "Differential penicillin-binding protein 5 (PBP5) levels in the *Enterococcus faecium* clades with different levels of ampicillin resistance." *Antimicrobial agents and chemotherapy* **61**, no. 1 (2017): e02034-16.
249. **Montelione, Gaetano T., Deyou Zheng, Yuanpeng J. Huang, Kristin C. Gunsalus, and Thomas Szyperski.** "Protein NMR spectroscopy in structural genomics." *Nature Structural and Molecular Biology* **7**, no. 11s (2000): 982.
250. **Morris, J. Glenn, David K. Shay, Joan N. Hebden, Robert J. McCarter, Beulah E. Perdue, William Jarvis, Judith A. Johnson, Thomas C. Dowling, Louis B. Polish, and Richard S. Schwalbe.** "Enterococci resistant to multiple antimicrobial agents, including vancomycin: establishment of endemicity in a university medical center." *Annals of Internal Medicine* **123**, no. 4 (1995): 250-259.
251. **Muller, Cécile, Sébastien Massier, Yoann Le Breton, and Alain Rincé.** "The role of the CroR response regulator in resistance of *Enterococcus faecalis* to D-cycloserine is defined using an inducible receiver domain." *Molecular microbiology* **107**, no. 3 (2018): 416-427.
252. **Muller, Cécile, Yoann Le Breton, Thierry Morin, Abdellah Benachour, Yanick Auffray, and Alain Rincé.** "The response regulator CroR modulates expression of the secreted stress-induced SalB protein in *Enterococcus faecalis*." *Journal of bacteriology* **188**, no. 7 (2006): 2636-2645.
253. **Mundt, J. Orvin.** "Occurrence of enterococci in animals in a wild environment." *Applied microbiology* **11**, no. 2 (1963a): 136-140.
254. **Mundt, J. Orvin.** "Occurrence of enterococci on plants in a wild environment." *Applied microbiology* **11**, no. 2 (1963b): 141-144.
255. **Muñoz-Dorado, José, Sumiko Inouye, and Masayori Inouye.** "A gene encoding a protein serine/threonine kinase is required for normal development of *M. xanthus*, a gram-negative bacterium." *Cell* **67**, no. 5 (1991): 995-1006.
256. **Murdoch, David R., G. Ralph Corey, Bruno Hoen, José M. Miró, Vance G. Fowler, Arnold S. Bayer, Adolf W. Karchmer et al.** "Clinical presentation, etiology, and outcome of infective endocarditis in the 21st century: the International

- Collaboration on Endocarditis—Prospective Cohort Study." *Archives of internal medicine* **169**, no. 5 (2009): 463-473.
257. **Murray, Barbara E.** "The life and times of the Enterococcus." *Clinical microbiology reviews* **3**, no. 1 (1990): 46-65.
258. **Mylonakis, Eleftherios, and Stephen B. Calderwood.** "Infective endocarditis in adults." *New England Journal of Medicine* **345**, no. 18 (2001): 1318-1330.
259. **Mylonakis, Eleftherios, Michael Engelbert, Xiang Qin, Costi D. Sifri, Barbara E. Murray, Frederick M. Ausubel, Michael S. Gilmore, and Stephen B. Calderwood.** "The *Enterococcus faecalis* *fsrB* gene, a key component of the *fsr* quorum-sensing system, is associated with virulence in the rabbit endophthalmitis model." *Infection and immunity* **70**, no. 8 (2002): 4678-4681.
260. **Nallapareddy, Sreedhar R., Huang Wenxiang, George M. Weinstock, and Barbara E. Murray.** "Molecular characterization of a widespread, pathogenic, and antibiotic resistance-receptive *Enterococcus faecalis* lineage and dissemination of its putative pathogenicity island." *Journal of bacteriology* **187**, no. 16 (2005): 5709-5718.
261. **Nannini, Esteban, Barbara E. Murray, and Cesar A. Arias.** "Resistance or decreased susceptibility to glycopeptides, daptomycin, and linezolid in methicillin-resistant *Staphylococcus aureus*." *Current opinion in pharmacology* **10**, no. 5 (2010): 516-521.
262. **Navarre, William Wiley, and Olaf Schneewind.** "Surface proteins of gram-positive bacteria and mechanisms of their targeting to the cell wall envelope." *Microbiology and Molecular Biology Reviews* **63**, no. 1 (1999): 174-229.
263. **Neiditch, Matthew B., Michael J. Federle, Audra J. Pompeani, Robert C. Kelly, Danielle L. Swem, Philip D. Jeffrey, Bonnie L. Bassler, and Frederick M. Hughson.** "Ligand-induced asymmetry in histidine sensor kinase complex regulates quorum sensing." *Cell* **126**, no. 6 (2006): 1095-1108.
264. **Nicolle, Lindsay E.** "Urinary catheter-associated infections." *Infectious disease clinics of North America* **26**, no. 1 (2012): 13-27.
265. **Nikaido, Hiroshi.** "Molecular basis of bacterial outer membrane permeability revisited." *Microbiology and molecular biology reviews* **67**, no. 4 (2003): 593-656.

266. **Noble, W. C., Zarina Virani, and Rosemary GA Cree.** "Co-transfer of vancomycin and other resistance genes from *Enterococcus faecalis* NCTC 12201 to *Staphylococcus aureus*." *FEMS microbiology letters* **93**, no. 2 (1992): 195-198.
267. **Nomura, Takahiro, Koichi Tanimoto, Keigo Shibayama, Yoshichika Arakawa, Shuhei Fujimoto, Yasuyoshi Ike, and Haruyoshi Tomita.** "Identification of VanN-type vancomycin resistance in an *Enterococcus faecium* isolate from chicken meat in Japan." *Antimicrobial agents and chemotherapy* **56**, no. 12 (2012): 6389-6392.
268. **Normark, B. Henriques, and S. Normark.** "Evolution and spread of antibiotic resistance." *Journal of internal medicine* **252**, no. 2 (2002): 91-106.
269. **O'Neill, J.** (2015). Tackling a Global Health Crisis: Initial Steps. Review on Antimicrobial Resistance
270. **Ochman, Howard, Jeffrey G. Lawrence, and Eduardo A. Groisman.** "Lateral gene transfer and the nature of bacterial innovation." *Nature* **405**, no. 6784 (2000): 299-304.
271. **Oliver, Daphna R., Byron L. Brown, and D. B. Clewell.** "Analysis of plasmid deoxyribonucleic acid in a cariogenic strain of *Streptococcus faecalis*: an approach to identifying genetic determinants on cryptic plasmids." *Journal of bacteriology* **130**, no. 2 (1977): 759-765.
272. **Ortiz-Lombardía, Miguel, Frédérique Pompeo, Brigitte Boitel, and Pedro M. Alzari.** "Crystal structure of the catalytic domain of the PknB serine/threonine kinase from *Mycobacterium tuberculosis*." *Journal of Biological Chemistry* **278**, no. 15 (2003): 13094-13100.
273. **Ostrowsky, Belinda E., Nancy C. Clark, Claudie Thauvin-Eliopoulos, Lata Venkataraman, Matthew H. Samore, Fred C. Tenover, George M. Eliopoulos, Robert C. Moellering Jr, and Howard S. Gold.** "A cluster of VanD vancomycin-resistant *Enterococcus faecium*: molecular characterization and clinical epidemiology." *The Journal of infectious diseases* **180**, no. 4 (1999): 1177-1185.
274. **Oyamada, Yoshihiro, Hideaki Ito, Matsuhisa Inoue, and Jun-ichi Yamagishi.** "Topoisomerase mutations and efflux are associated with fluoroquinolone resistance in *Enterococcus faecalis*." *Journal of medical microbiology* **55**, no. 10 (2006): 1395-1401.

275. **Pai, Manjunath P., Keith A. Rodvold, Paul C. Schreckenberger, Ronald D. Gonzales, Jennifer M. Petrolatti, and John P. Quinn.** "Risk factors associated with the development of infection with linezolid-and vancomycin-resistant *Enterococcus faecium*." *Clinical infectious diseases* **35**, no. 10 (2002): 1269-1272.
276. **Panesso, Diana, Lorena Abadía-Patiño, Natasha Vanegas, Peter E. Reynolds, Patrice Courvalin, and Cesar A. Arias.** "Transcriptional analysis of the *vanC* cluster from *Enterococcus gallinarum* strains with constitutive and inducible vancomycin resistance." *Antimicrobial agents and chemotherapy* **49**, no. 3 (2005): 1060-1066.
277. **Paracuellos, Patricia, Allison Ballandras, Xavier Robert, Richard Kahn, Mireille Hervé, Dominique Mengin-Lecreulx, Alain J. Cozzone, Bertrand Duclos, and Patrice Gouet.** "The extended conformation of the 2.9-Å crystal structure of the three-PASTA domain of a Ser/Thr kinase from the human pathogen *Staphylococcus aureus*." *Journal of molecular biology* **404**, no. 5 (2010): 847-858.
278. **Parte, Aidan C.** "LPSN—list of prokaryotic names with standing in nomenclature." *Nucleic acids research* **42**, no. D1 (2013): D613-D616.
279. **Patel, Robin, Mark S. Rouse, Kerryl E. Piper, and James M. Steckelberg.** "In vitro activity of GAR-936 against vancomycin-resistant enterococci, methicillin-resistant *Staphylococcus aureus* and penicillin-resistant *Streptococcus pneumoniae*." *Diagnostic microbiology and infectious disease* **38**, no. 3 (2000): 177-179.
280. **Patiño, Lorena Abadía, Patrice Courvalin, and Bruno Perichon.** "*vanE* gene cluster of vancomycin-resistant *Enterococcus faecalis* BM4405." *Journal of bacteriology* **184**, no. 23 (2002): 6457-6464.
281. **Pensinger, Daniel A., Adam J. Schaenzer, and John-Demian Sauer.** "Do shoot the messenger: PASTA kinases as virulence determinants and antibiotic targets." *Trends in microbiology* (2017).
282. **Pensinger, Daniel A., Matthew T. Aliota, Adam J. Schaenzer, Kyle M. Boldon, H. Ansari Israr-ul, William JB Vincent, Benjamin Knight, Michelle L. Reniere, Rob Striker, and John-Demian Sauer.** "Selective pharmacologic inhibition of a PASTA kinase increases *Listeria monocytogenes* susceptibility to  $\beta$ -lactam antibiotics." *Antimicrobial agents and chemotherapy* **58**, no. 8 (2014): 4486-4494.

283. **Pereira, Sandro FF, Lindsie Goss, and Jonathan Dworkin.** "Eukaryote-like serine/threonine kinases and phosphatases in bacteria." *Microbiology and Molecular Biology Reviews* **75**, no. 1 (2011): 192-212.
284. **Perichon, Bruno, Peter Reynolds, and Patrice Courvalin.** "VanD-type glycopeptide-resistant *Enterococcus faecium* BM4339." *Antimicrobial agents and chemotherapy* **41**, no. 9 (1997): 2016-2018.
285. **Philo, John S.** "A critical review of methods for size characterization of non-particulate protein aggregates." *Current pharmaceutical biotechnology* **10**, no. 4 (2009): 359-372.
286. **Podgornaia, Anna I., Patricia Casino, Alberto Marina, and Michael T. Laub.** "Structural basis of a rationally rewired protein-protein interface critical to bacterial signaling." *Structure* **21**, no. 9 (2013): 1636-1647.
287. **Polidori, M., A. Nuccorini, C. Tascini, G. Gemignani, R. Iapoco, A. Leonildi, E. Tagliaferri, and F. Menichetti.** "Vancomycin-resistant *Enterococcus faecium* (VRE) bacteremia in infective endocarditis successfully treated with combination daptomycin and tigecycline." *Journal of chemotherapy (Florence, Italy)* **23**, no. 4 (2011): 240.
288. **Prendergast, Bernard D.** "The changing face of infective endocarditis." *Heart* **92**, no. 7 (2006): 879-885.
289. **Prystowsky, Jason, Farida Siddiqui, John Chosay, Dean L. Shinabarger, John Millichap, Lance R. Peterson, and Gary A. Noskin.** "Resistance to linezolid: characterization of mutations in rRNA and comparison of their occurrences in vancomycin-resistant enterococci." *Antimicrobial agents and chemotherapy* **45**, no. 7 (2001): 2154-2156.
290. **Quale, John, David Landman, Guillermo Saurina, Elaine Atwood, Virginia DiTore, and Keval Patel.** "Manipulation of a hospital antimicrobial formulary to control an outbreak of vancomycin-resistant enterococci." *Clinical Infectious Diseases* **23**, no. 5 (1996): 1020-1025.
291. **Quintiliani Jr, Richard, and Patrice Courvalin.** "Conjugal transfer of the vancomycin resistance determinant vanB between enterococci involves the movement of large genetic elements from chromosome to chromosome." *FEMS microbiology letters* **119**, no. 3 (1994): 359-363.

292. **Rajagopal, Mithila, Melissa J. Martin, Marina Santiago, Wonsik Lee, Veronica N. Kos, Tim Meredith, Michael S. Gilmore, and Suzanne Walker.** "Multidrug intrinsic resistance factors in *Staphylococcus aureus* identified by profiling fitness within high-diversity transposon libraries." *MBio* **7**, no. 4 (2016): e00950-16.
293. **Rakette, Sonja, Stefanie Donat, Knut Ohlsen, and Thilo Stehle.** "Structural analysis of *Staphylococcus aureus* serine/threonine kinase PknB." *PLoS one* **7**, no. 6 (2012): e39136.
294. **Rasmussen, Beth, H. F. Noller, G. Daubresse, B. Oliva, Z. Misulovin, D. M. Rothstein, G. A. Ellestad, Y. Gluzman, F. P. Tally, and I. Chopra.** "Molecular basis of tetracycline action: identification of analogs whose primary target is not the bacterial ribosome." *Antimicrobial agents and chemotherapy* **35**, no. 11 (1991): 2306-2311.
295. **Raven, Kathy E., Theodore Gouliouris, Julian Parkhill, and Sharon J. Peacock.** "Genome-based analysis of *Enterococcus faecium* bacteremia associated with recurrent and mixed-strain infection." *Journal of clinical microbiology* **56**, no. 3 (2018): e01520-17.
296. **Receveur-Bréchet, Véronique, and Dominique Durand.** "How random are intrinsically disordered proteins? A small angle scattering perspective." *Current Protein and Peptide Science* **13**, no. 1 (2012): 55-75.
297. **Reith, Jan, and Christoph Mayer.** "Peptidoglycan turnover and recycling in Gram-positive bacteria." *Applied microbiology and biotechnology* **92**, no. 1 (2011): 1.
298. **Reyes, Katherine, and Marcus Zervos.** "Endocarditis caused by resistant *Enterococcus*: an overview." *Current infectious disease reports* **15**, no. 4 (2013): 320-328.
299. **Reynolds, Peter E.** "Structure, biochemistry and mechanism of action of glycopeptide antibiotics." *European Journal of Clinical Microbiology and Infectious Diseases* **8**, no. 11 (1989): 943-950.
300. **Reynolds, Peter E., and Patrice Courvalin.** "Vancomycin resistance in enterococci due to synthesis of precursors terminating in D-alanyl-D-serine." *Antimicrobial agents and chemotherapy* **49**, no. 1 (2005): 21-25.
301. **Reynolds, Peter E., Cesar A. Arias, and Patrice Courvalin.** "Gene vanXYC encodes d, d-dipeptidase (VanX) and d, d-carboxypeptidase (VanY) activities in

- vancomycin-resistant *Enterococcus gallinarum* BM4174." *Molecular microbiology* **34**, no. 2 (1999): 341-349.
302. **Rice, Louis B., Lenore L. Carias, Susan Rudin, Viera Laktičová, Aaron Wood, and Rebecca Hutton-Thomas.** "Enterococcus faecium low-affinity pbp5 is a transferable determinant." *Antimicrobial agents and chemotherapy* **49**, no. 12 (2005): 5007-5012.
303. **Richarz, René, and Kurt Wüthrich.** "Carbon-13 NMR chemical shifts of the common amino acid residues measured in aqueous solutions of the linear tetrapeptides H-Gly-Gly-X-L-Ala-OH." *Biopolymers* **17**, no. 9 (1978): 2133-2141.
304. **Roberts, Adam P., and Peter Mullany.** "Tn916-like genetic elements: a diverse group of modular mobile elements conferring antibiotic resistance." *FEMS microbiology reviews* **35**, no. 5 (2011): 856-871.
305. **Roberts, Adam P., Priscilla A. Johanesen, Dena Lyras, Peter Mullany, and Julian I. Rood.** "Comparison of Tn5397 from *Clostridium difficile*, Tn916 from *Enterococcus faecalis* and the CW459tet (M) element from *Clostridium perfringens* shows that they have similar conjugation regions but different insertion and excision modules." *Microbiology* **147**, no. 5 (2001): 1243-1251.
306. **Ruane, Karen M., Adrian J. Lloyd, Vilmos Fülöp, Christopher G. Dowson, Hélène Barreteau, Audrey Boniface, Sébastien Dementin et al.** "Specificity determinants for lysine incorporation in *Staphylococcus aureus* peptidoglycan as revealed by the structure of a MurE enzyme ternary complex." *Journal of Biological Chemistry* **288**, no. 46 (2013): 33439-33448.
307. **Ruggero, Kathleen A., Laura K. Schroeder, Paul C. Schreckenberger, Alexander S. Mankin, and John P. Quinn.** "Nosocomial superinfections due to linezolid-resistant *Enterococcus faecalis*: evidence for a gene dosage effect on linezolid MICs." *Diagnostic microbiology and infectious disease* **47**, no. 3 (2003): 511-513.
308. **Sacco, Emmanuelle, Jean-Emmanuel Hugonnet, Nathalie Josseaume, Julie Cremniter, Lionel Dubost, Arul Marie, Delphine Patin et al.** "Activation of the l, d-transpeptidation peptidoglycan cross-linking pathway by a metallo-d, d-carboxypeptidase in *Enterococcus faecium*." *Molecular microbiology* **75**, no. 4 (2010): 874-885.

309. **Sadowy, Ewa, Iwona Gawryszewska, Alicja Kuch, Dorota Żabicka, and Waleria Hryniewicz.** "The changing epidemiology of VanB *Enterococcus faecium* in Poland." *European Journal of Clinical Microbiology & Infectious Diseases* (2018): 1-10.
310. **Sahm, Daniel F., Jessica Kissinger, Michael S. Gilmore, Patrick R. Murray, Ross Mulder, Joanne Solliday, and Barbara Clarke.** "In vitro susceptibility studies of vancomycin-resistant *Enterococcus faecalis*." *Antimicrobial agents and chemotherapy* **33**, no. 9 (1989): 1588-1591.
311. **Salgado, Cassandra D., and Barry M. Farr.** "Outcomes associated with vancomycin-resistant enterococci: a meta-analysis." *Infection Control & Hospital Epidemiology* **24**, no. 9 (2003): 690-698.
312. **San Millan, Alvaro, Florence Depardieu, Sylvain Godreuil, and Patrice Courvalin.** "VanB-type *Enterococcus faecium* clinical isolate successively inducibly resistant to, dependent on, and constitutively resistant to vancomycin." *Antimicrobial agents and chemotherapy* **53**, no. 5 (2009): 1974-1982.
313. **Sasseti, Christopher M., and Eric J. Rubin.** "Genetic requirements for mycobacterial survival during infection." *Proceedings of the National Academy of Sciences* **100**, no. 22 (2003): 12989-12994.
314. **Sassi, Mohamed, François Guérin, Léonie Leseq, Christophe Isnard, Marguerite Fines-Guyon, Vincent Cattoir, and Jean-Christophe Giard.** "Genetic characterization of a VanG-type vancomycin-resistant *Enterococcus faecium* clinical isolate." *Journal of Antimicrobial Chemotherapy* (2018).
315. **Sauvage, Eric, Frédéric Kerff, Mohammed Terrak, Juan A. Ayala, and Paulette Charlier.** "The penicillin-binding proteins: structure and role in peptidoglycan biosynthesis." *FEMS microbiology reviews* **32**, no. 2 (2008): 234-258.
316. **Shankaran, Dhesingh Ravi, and Norio Miura.** "Trends in interfacial design for surface plasmon resonance based immunoassays." *Journal of Physics D: Applied Physics* **40**, no. 23 (2007): 7187.
317. **Schasfoort, Richard BM,** ed. Handbook of surface plasmon resonance. *Royal Society of Chemistry*, 2017.
318. **Schleifer, Karl H., and Renate Kilpper-Bälz.** "Transfer of *Streptococcus faecalis* and *Streptococcus faecium* to the Genus *Enterococcus* nom. rev. as *Enterococcus*

- faecalis* comb. nov. and *Enterococcus faecium* comb. nov." *International Journal of Systematic and Evolutionary Microbiology* **34**, no. 1 (1984): 31-34.
319. **Schleifer, Karl Heinz, and Otto Kandler.** "Peptidoglycan types of bacterial cell walls and their taxonomic implications." *Bacteriological reviews* **36**, no. 4 (1972): 407.
320. **Schneider, Tanja, Maria Magdalena Senn, Brigitte Berger-Bächi, Alessandro Tossi, Hans-Georg Sahl, and Imke Wiedemann.** "*In vitro* assembly of a complete, pentaglycine interpeptide bridge containing cell wall precursor (lipid II-Gly5) of *Staphylococcus aureus*." *Molecular microbiology* **53**, no. 2 (2004): 675-685.
321. **Schwan, Tom G., James M. Battisti, Stephen F. Porcella, Sandra J. Raffel, Merry E. Schrumppf, Elizabeth R. Fischer, James A. Carroll, Philip E. Stewart, Patricia Rosa, and Greg A. Somerville.** "Glycerol-3-phosphate acquisition in spirochetes: distribution and biological activity of glycerophosphodiester phosphodiesterase (GlpQ) among *Borrelia* species." *Journal of bacteriology* **185**, no. 4 (2003): 1346-1356.
322. **Schweizer, Inga, Katharina Peters, Christoph Stahlmann, Regine Hakenbeck, and Dalia Denapaite.** "Penicillin-binding protein 2x of *Streptococcus pneumoniae*: the mutation Ala707Asp within the C-terminal PASTA2 domain leads to destabilization." *Microbial Drug Resistance* **20**, no. 3 (2014): 250-257.
323. **Seedat, Jamela, Günther Zick, Ingo Klare, Carola Konstabel, Norbert Weiler, and Hany Sahly.** "Rapid emergence of resistance to linezolid during linezolid therapy of an *Enterococcus faecium* infection." *Antimicrobial agents and chemotherapy* **50**, no. 12 (2006): 4217-4219.
324. **Sghir, Abdelghani, Genevieve Gramet, Antonia Suau, Violaine Rochet, Philippe Pochart, and Joel Dore.** "Quantification of bacterial groups within human fecal flora by oligonucleotide probe hybridization." *Applied and Environmental Microbiology* **66**, no. 5 (2000): 2263-2266.
325. **Shah, Ishita M., Maria-Halima Laaberki, David L. Popham, and Jonathan Dworkin.** "A eukaryotic-like Ser/Thr kinase signals bacteria to exit dormancy in response to peptidoglycan fragments." *Cell* **135**, no. 3 (2008): 486-496.
326. **Shapiro, James A.** "Genome organization, natural genetic engineering and adaptive mutation." *Trends in Genetics* **13**, no. 3 (1997): 98-104.

327. **Shepard, Brett D., and Michael S. Gilmore.** "Antibiotic-resistant enterococci: the mechanisms and dynamics of drug introduction and resistance." *Microbes and Infection* **4**, no. 2 (2002): 215-224.
328. **Shepard, Brett D., and Michael S. Gilmore.** "Electroporation and efficient transformation of *Enterococcus faecalis* grown in high concentrations of glycine." In *Electroporation Protocols for Microorganisms*, pp. 217-226. Humana Press, 1995.
329. **Sherman, James M.** "The enterococci and related streptococci." *Journal of bacteriology* **35**, no. 2 (1938): 81.
330. **Sherman, James M.** "The streptococci." *Bacteriological reviews* **1**, no. 1 (1937): 3.
331. **Sievert, Dawn M., James T. Rudrik, Jean B. Patel, L. Clifford McDonald, Melinda J. Wilkins, and Jeffrey C. Hageman.** "Vancomycin-resistant *Staphylococcus aureus* in the United States, 2002–2006." *Clinical Infectious Diseases* **46**, no. 5 (2008): 668-674.
332. **Sifri, Costi D., Eleftherios Mylonakis, Kavindra V. Singh, Xiang Qin, Danielle A. Garsin, Barbara E. Murray, Frederick M. Ausubel, and Stephen B. Calderwood.** "Virulence effect of *Enterococcus faecalis* protease genes and the quorum-sensing locus *fsr* in *Caenorhabditis elegans* and mice." *Infection and immunity* **70**, no. 10 (2002): 5647-5650.
333. **Silhavy, Thomas J., Daniel Kahne, and Suzanne Walker.** "The bacterial cell envelope." *Cold Spring Harbor perspectives in biology* **2**, no. 5 (2010): a000414.
334. **Singh, Kavindra V., Sreedhar R. Nallapareddy, and Barbara E. Murray.** "Importance of the *ebp* (endocarditis and biofilm-associated pilus) locus in the pathogenesis of *Enterococcus faecalis* ascending urinary tract infection." *The Journal of infectious diseases* **195**, no. 11 (2007): 1671-1677.
335. **Singh, Kavindra V., Sreedhar R. Nallapareddy, Esteban C. Nannini, and Barbara E. Murray.** "Fsr-independent production of protease (s) may explain the lack of attenuation of an *Enterococcus faecalis* *fsr* mutant versus a *gelE-sprE* mutant in induction of endocarditis." *Infection and immunity* **73**, no. 8 (2005): 4888-4894.
336. **Singh, Kavindra V., Teresa M. Coque, George M. Weinstock, and Barbara E. Murray.** "In vivo testing of an *Enterococcus faecalis* *efaA* mutant and use of *efaA*

- homologs for species identification." *FEMS Immunology & Medical Microbiology* **21**, no. 4 (1998): 323-331.
337. **Sivashanmugam, Arun, Victoria Murray, Chunxian Cui, Yonghong Zhang, Jianjun Wang, and Qianqian Li.** "Practical protocols for production of very high yields of recombinant proteins using *Escherichia coli*." *Protein Science* **18**, no. 5 (2009): 936-948.
338. **Solovyova, Alexandra, Peter Schuck, Lionel Costenaro, and Christine Ebel.** "Non-ideality by sedimentation velocity of halophilic malate dehydrogenase in complex solvents." *Biophysical journal* **81**, no. 4 (2001): 1868-1880.
339. **Some, Daniel.** "Light-scattering-based analysis of biomolecular interactions." *Biophysical reviews* **5**, no. 2 (2013): 147-158.
340. **Soule, D., and M. M. Climo.** "A Clinician's Guide to the Treatment of Vancomycin Resistant Enterococci Bacteremia and Endocarditis." *Current Treatment Options in Infectious Diseases* **8**, no. 3 (2016): 194-207.
341. **Squeglia, Flavia, Roberta Marchetti, Alessia Ruggiero, Rosa Lanzetta, Daniela Marasco, Jonathan Dworkin, Maxim Petoukhov, Antonio Molinaro, Rita Berisio, and Alba Silipo.** "Chemical basis of peptidoglycan discrimination by PrkC, a key kinase involved in bacterial resuscitation from dormancy." *Journal of the American Chemical Society* **133**, no. 51 (2011): 20676-20679.
342. **Stancik, Ivan Andreas, Martin Sebastijan Šestak, Boyang Ji, Marina Axelson-Fisk, Damjan Franjevic, Carsten Jers, Tomislav Domazet-Lošo, and Ivan Mijakovic.** "Serine/Threonine protein kinases from bacteria, archaea and eukarya share a common evolutionary origin deeply rooted in the tree of life." *Journal of molecular biology* **430**, no. 1 (2018): 27-32.
343. **Steen, Anton, Girbe Buist, Kees J. Leenhouts, Mohamed El Khattabi, Froukje Grijpstra, Aldert L. Zomer, Gerard Venema, Oscar P. Kuipers, and Jan Kok.** "Cell wall attachment of a widely distributed peptidoglycan binding domain is hindered by cell wall constituents." *Journal of Biological Chemistry* **278**, no. 26 (2003): 23874-23881.
344. **Stevens, Kirk L., Michael J. Reno, Jennifer B. Alberti, Daniel J. Price, Laurie S. Kane-Carson, Victoria B. Knick, Lisa M. Shewchuk et al.** "Synthesis and evaluation of pyrazolo [1, 5-b] pyridazines as selective cyclin dependent kinase

- inhibitors." *Bioorganic & medicinal chemistry letters* **18**, no. 21 (2008): 5758-5762.
345. **Stinear, Timothy P., Dianne C. Olden, Paul DR Johnson, John K. Davies, and M. Lindsay Grayson.** "Enterococcal *vanB* resistance locus in anaerobic bacteria in human faeces." *The Lancet* **357**, no. 9259 (2001): 855-856.
346. **Stock, Ann M., Victoria L. Robinson, and Paul N. Goudreau.** "Two-component signal transduction." *Annual review of biochemistry* **69**, no. 1 (2000): 183-215.
347. **Stokes, Jonathan M., Shawn French, Olga G. Ovchinnikova, Catrien Bouwman, Chris Whitfield, and Eric D. Brown.** "Cold stress makes *Escherichia coli* susceptible to glycopeptide antibiotics by altering outer membrane integrity." *Cell chemical biology* **23**, no. 2 (2016): 267-277.
348. **Štrancar, Katja, Audrey Boniface, Didier Blanot, and Stanislav Gobec.** "Phosphinate Inhibitors of UDP-N-Acetylmuramoyl-L-Alanyl-D-Glutamate: L-Lysine Ligase (MurE)." *Archiv der Pharmazie* **340**, no. 3 (2007): 127-134.
349. **Studier, F. William, and Barbara A. Moffatt.** "Use of bacteriophage T7 RNA polymerase to direct selective high-level expression of cloned genes." *Journal of molecular biology* **189**, no. 1 (1986): 113-130.
350. **Svergun, Dmitri I.** "Restoring low resolution structure of biological macromolecules from solution scattering using simulated annealing." *Biophysical journal* **76**, no. 6 (1999): 2879-2886.
351. **Tacconelli, E., N. Magrini, G. Kahlmeter, and N. Singh.** "Global priority list of antibiotic-resistant bacteria to guide research." *Discovery, and development of new antibiotics*, Geneva: WHO (2017).
352. **Tacconelli, Evelina, Elena Carrara, Alessia Savoldi, Stephan Harbarth, Marc Mendelson, Dominique L. Monnet, Céline Pulcini et al.** "Discovery, research, and development of new antibiotics: the WHO priority list of antibiotic-resistant bacteria and tuberculosis." *The Lancet Infectious Diseases* (2017).
353. **Tally, Francis P., and Michael F. DeBruin.** "Development of daptomycin for gram-positive infections." *Journal of Antimicrobial Chemotherapy* **46**, no. 4 (2000): 523-526.
354. **Tally, Francis P., Michael Zeckel, Margaret M. Wasilewski, Claudio Carini, Cindy L. Berman, George L. Drusano, and Frederick B. Oleson Jr.** "Daptomycin: a novel

- agent for Gram-positive infections." *Expert opinion on investigational drugs* **8**, no. 8 (1999): 1223-1238.
355. **Tamber, Sandeep, Joseph Schwartzman, and Ambrose L. Cheung.** "Role of PknB kinase in antibiotic resistance and virulence in community-acquired methicillin-resistant *Staphylococcus aureus* strain USA300." *Infection and immunity* **78**, no. 8 (2010): 3637-3646.
356. **Tang, Jun, Lisa M. Shewchuk, Hideyuki Sato, Masaichi Hasegawa, Yoshiaki Washio, and Naohiko Nishigaki.** "Anilinopyrazole as selective CDK2 inhibitors: design, synthesis, biological evaluation, and X-ray crystallographic analysis." *Bioorganic & medicinal chemistry letters* **13**, no. 18 (2003): 2985-2988.
357. **Taylor, R. K., M. N. Hall, L. Enquist, and T. J. Silhavy.** "Identification of OmpR: a positive regulatory protein controlling expression of the major outer membrane matrix porin proteins of *Escherichia coli* K-12." *Journal of bacteriology* **147**, no. 1 (1981): 255-258.
358. **Telenti, Amalio, Paul Imboden, Francine Marchesi, L. Matter, K. Schopfer, T. Bodmer, D. Lowrie, M. J. Colston, and S. Cole.** "Detection of rifampicin-resistance mutations in *Mycobacterium tuberculosis*." *The Lancet* **341**, no. 8846 (1993): 647-651.
359. **Terzaghi, Betty E., and W. E. Sandine.** "Improved medium for lactic streptococci and their bacteriophages." *Applied microbiology* **29**, no. 6 (1975): 807-813.
360. **Timmers, Gert Jan, Wil C. Van Der Zwet, Ina M. Simoons-Smit, Paul HM Savelkoul, Helena HM Meester, Christina MJE Vandenbroucke-Grauls, and Peter C. Huijgens.** "Outbreak of vancomycin-resistant *Enterococcus faecium* in a haematology unit: risk factor assessment and successful control of the epidemic." *British journal of haematology* **116**, no. 4 (2002): 826-833.
361. **Trinh, C-H., Yang Liu, Simon EV Phillips, and Mary K. Phillips-Jones.** "Structure of the response regulator VicR DNA-binding domain." *Acta Crystallographica Section D: Biological Crystallography* **63**, no. 2 (2007): 266-269.
362. **Tsvetkova, Krassimira, Jean-Christophe Marvaud, and Thierry Lambert.** "Analysis of the mobilization functions of the vancomycin resistance transposon Tn1549, a member of a new family of conjugative elements." *Journal of bacteriology* **192**, no. 3 (2010): 702-713.

363. **Ubeda, Carles, Ying Taur, Robert R. Jenq, Michele J. Equinda, Tammy Son, Miriam Samstein, Agnes Viale et al.** "Vancomycin-resistant *Enterococcus* domination of intestinal microbiota is enabled by antibiotic treatment in mice and precedes bloodstream invasion in humans." *The Journal of clinical investigation* **120**, no. 12 (2010): 4332.
364. **Uttinger, M. J., J. Walter, T. Thajudeen, S. E. Wawra, and W. Peukert.** "Brownian dynamics simulations of analytical ultracentrifugation experiments exhibiting hydrodynamic and thermodynamic non-ideality." *Nanoscale* **9**, no. 45 (2017): 17770-17780.
365. **Uversky, Vladimir N., and A. Keith Dunker.** "Understanding protein non-folding." *Biochimica et Biophysica Acta (BBA)-Proteins and Proteomics* **1804**, no. 6 (2010): 1231-1264.
366. **Vakulenko, Sergei B., and Shahriar Mobashery.** "Versatility of aminoglycosides and prospects for their future." *Clinical microbiology reviews* **16**, no. 3 (2003): 430-450.
367. **Van Schaik, Willem, and Rob JL Willems.** "Genome-based insights into the evolution of enterococci." *Clinical Microbiology and Infection* **16**, no. 6 (2010): 527-532.
368. **Van Tyne, Daria, and Michael S. Gilmore.** "Raising the Alarmone: Within-Host Evolution of Antibiotic-Tolerant *Enterococcus faecium*." *mBio* **8**, no. 1 (2017): e00066-17.
369. **Venkitakrishnan, Rani Parvathy, Outhiriaradjou Benard, Marianna Max, John L. Markley, and Fariba M. Assadi-Porter.** "Use of NMR saturation transfer difference spectroscopy to study ligand binding to membrane proteins." *In Membrane Protein Structure and Dynamics*, pp. 47-63. Humana Press, Totowa, NJ, 2012.
370. **Vesić, Dušanka, and Christopher J. Kristich.** "MurAA is required for intrinsic cephalosporin resistance of *Enterococcus faecalis*." *Antimicrobial agents and chemotherapy* **56**, no. 5 (2012): 2443-2451.
371. **Vickerman, M. Margaret, Jillian M. Mansfield, Min Zhu, Katherine S. Walters, and Jeffrey A. Banas.** "Codon-optimized fluorescent mTFP and mCherry for

- microscopic visualization and genetic counterselection of streptococci and enterococci." *Journal of microbiological methods* **116** (2015): 15-22.
372. **Volkov, Vladimir V., and Dmitri I. Svergun.** "Uniqueness of *ab initio* shape determination in small-angle scattering." *Journal of applied crystallography* **36**, no. 3 (2003): 860-864.
373. **Vollmer, Waldemar, Bernard Joris, Paulette Charlier, and Simon Foster.** "Bacterial peptidoglycan (murein) hydrolases." *FEMS microbiology reviews* **32**, no. 2 (2008b): 259-286.
374. **Vollmer, Waldemar, Didier Blanot, and Miguel A. De Pedro.** "Peptidoglycan structure and architecture." *FEMS microbiology reviews* **32**, no. 2 (2008a): 149-167.
375. **von Nussbaum, Franz, Michael Brands, Berthold Hinzen, Stefan Weigand, and Dieter Häbich.** "Antibacterial natural products in medicinal chemistry—exodus or revival?." *Angewandte Chemie International Edition* **45**, no. 31 (2006): 5072-5129.
376. **Vranken, Wim F., Wayne Boucher, Tim J. Stevens, Rasmus H. Fogh, Anne Pajon, Miguel Llinas, Eldon L. Ulrich, John L. Markley, John Ionides, and Ernest D. Laue.** "The CCPN data model for NMR spectroscopy: development of a software pipeline." *Proteins: Structure, Function, and Bioinformatics* **59**, no. 4 (2005): 687-696.
377. **Walsh, Christopher T., Stewart L. Fisher, I-S. Park, M. Prahalad, and Z. Wu.** "Bacterial resistance to vancomycin: five genes and one missing hydrogen bond tell the story." *Chemistry & biology* **3**, no. 1 (1996): 21-28.
378. **Walsh, Christopher, and Gerard Wright.** "Introduction: antibiotic resistance." (2005): 391-394.
379. **Wang, Hongxia, Julio C. Ayala, Jorge A. Benitez, and Anisia J. Silva.** "Interaction of the histone-like nucleoid structuring protein and the general stress response regulator RpoS at *Vibrio cholerae* promoters that regulate motility and hemagglutinin/protease expression." *Journal of bacteriology* **194**, no. 5 (2012): 1205-1215.
380. **Wang, Qianqian, Roberta Marchetti, Sladjana Prusic, Kentaro Ishii, Yohei Arai, Ippei Ohta, Shinsuke Inuki et al.** "A Comprehensive Study of the Interaction between Peptidoglycan Fragments and the Extracellular Domain of

- Mycobacterium tuberculosis* Ser/Thr Kinase PknB." *ChemBioChem* 18, no. 21 (2017): 2094-2098.
381. **Watkin, Richard, and Jonathan Sandoe.** "British Society of Antimicrobial Chemotherapy (BSAC) guidelines for the diagnosis and treatment of endocarditis: what the cardiologist needs to know." (2012): 757-759.
382. **Wayne, Kyle J., Shuo Li, Krystyna M. Kazmierczak, Ho-Ching T. Tsui, and Malcolm E. Winkler.** "Involvement of WalK (VicK) phosphatase activity in setting WalR (VicR) response regulator phosphorylation level and limiting cross-talk in *Streptococcus pneumoniae* D39 cells." *Molecular microbiology* 86, no. 3 (2012): 645-660.
383. **Weber, Patrick, Djalal Meziane-Cherif, Ahmed Haouz, Frederick A. Saul, and Patrice Courvalin.** "Crystallization and preliminary X-ray analysis of a D-Ala: D-Ser ligase associated with VanG-type vancomycin resistance." *Acta Crystallographica Section F: Structural Biology and Crystallization Communications* 65, no. 10 (2009): 1024-1026.
384. **Wehenkel, Annemarie, Pablo Fernandez, Marco Bellinzoni, Vincent Catherinot, Nathalie Barilone, Gilles Labesse, Mary Jackson, and Pedro M. Alzari.** "The structure of PknB in complex with mitoxantrone, an ATP-competitive inhibitor, suggests a mode of protein kinase regulation in mycobacteria." *FEBS letters* 580, no. 13 (2006): 3018-3022.
385. **Weigel, Linda M., Don B. Clewell, Steven R. Gill, Nancye C. Clark, Linda K. McDougal, Susan E. Flannagan, James F. Kolonay, Jyoti Shetty, George E. Killgore, and Fred C. Tenover.** "Genetic analysis of a high-level vancomycin-resistant isolate of *Staphylococcus aureus*." *Science* 302, no. 5650 (2003): 1569-1571.
386. **Wen, Bin, Junhui Peng, Xiaobing Zuo, Qingguo Gong, and Zhiyong Zhang.** "Characterization of protein flexibility using small-angle X-ray scattering and amplified collective motion simulations." *Biophysical journal* 107, no. 4 (2014): 956-964.
387. **Werner, Guido, Birgit Strommenger, and Wolfgang Witte.** "Acquired vancomycin resistance in clinically relevant pathogens." (2008): 547-562.

388. **Werner, Guido, Carola Fleige, Birgit Ewert, Jenny A. Laverde-Gomez, Ingo Klare, and Wolfgang Witte.** "High-level ciprofloxacin resistance among hospital-adapted *Enterococcus faecium* (CC17)." *International journal of antimicrobial agents* **35**, no. 2 (2010): 119-125.
389. **Werner, Guido, T. M. Coque, A. M. Hammerum, R. Hope, W. Hryniewicz, A. Johnson, Ingo Klare et al.** "Emergence and spread of vancomycin resistance among enterococci in Europe." (2008).
390. **West, Ann H., and Ann M. Stock.** "Histidine kinases and response regulator proteins in two-component signaling systems." *Trends in biochemical sciences* **26**, no. 6 (2001): 369-376.
391. **Whitmore, Lee, and B. A. Wallace.** "DICHROWEB, an online server for protein secondary structure analyses from circular dichroism spectroscopic data." *Nucleic acids research* **32**, no. suppl\_2 (2004): W668-W673.
392. **Willett, Jonathan W., and John R. Kirby.** "Genetic and biochemical dissection of a HisKA domain identifies residues required exclusively for kinase and phosphatase activities." *PLoS genetics* **8**, no. 11 (2012): e1003084.
393. **Williamson, Mike P.** "Using chemical shift perturbation to characterise ligand binding." *Progress in nuclear magnetic resonance spectroscopy* **73** (2013): 1-16.
394. **Wishart, David S., Colin G. Bigam, Jian Yao, Frits Abildgaard, H. Jane Dyson, Eric Oldfield, John L. Markley, and Brian D. Sykes.** "<sup>1</sup>H, <sup>13</sup>C and <sup>15</sup>N chemical shift referencing in biomolecular NMR." *Journal of biomolecular NMR* **6**, no. 2 (1995): 135-140.
395. **Wittekind, Micheal., and Luciano Mueller.** "HNCACB, a high-sensitivity 3D NMR experiment to correlate amide-proton and nitrogen resonances with the alpha- and beta-carbon resonances in proteins." (1993): 201-205.
396. **Woegerbauer, Markus, Josef Zeinzinger, Burkhard Springer, Peter Hufnagl, Alexander Indra, Irina Korschineck, Johannes Hofrichter et al.** "Prevalence of the aminoglycoside phosphotransferase genes aph (3')-IIIa and aph (3')-IIa in *Escherichia coli*, *Enterococcus faecalis*, *Enterococcus faecium*, *Pseudomonas aeruginosa*, *Salmonella enterica* subsp. *enterica* and *Staphylococcus aureus* isolates in Austria." *Journal of medical microbiology* **63**, no. 2 (2014): 210-217.

397. **World Health Organization.** "20th WHO Model List of Essential Medicines. 2017." World Health Organization. Online. Accessed (2018).
398. **Wright, Gerard D., Theodore R. Holman, and Christopher T. Walsh.** "Purification and characterization of VanR and the cytosolic domain of VanS: a two-component regulatory system required for vancomycin resistance in *Enterococcus faecium* BM4147." *Biochemistry* **32**, no. 19 (1993): 5057-5063.
399. **Xu, Xiaogang, Dongfang Lin, Guoquan Yan, Xinyu Ye, Shi Wu, Yan Guo, Demei Zhu et al.** "*vanM*, a new glycopeptide resistance gene cluster found in *Enterococcus faecium*." *Antimicrobial agents and chemotherapy* **54**, no. 11 (2010): 4643-4647.
400. **Yeats, Corin, Robert D. Finn, and Alex Bateman.** "The PASTA domain: a  $\beta$ -lactam-binding domain." *Trends in biochemical sciences* **27**, no. 9 (2002): 438-440.
401. **Young, K. D.** Bacterial Cell Wall. In *Encyclopedia of Life Sciences*; John Wiley & Sons, Ltd: Chichester, UK, 2010.
402. **Young, Tracy A., Benedicte Delagoutte, James A. Endrizzi, Arnold M. Falick, and Tom Alber.** "Structure of *Mycobacterium tuberculosis* PknB supports a universal activation mechanism for Ser/Thr protein kinases." *Nature Structural and Molecular Biology* **10**, no. 3 (2003): 168.
403. **Yunck, Rachel, Hongbaek Cho, and Thomas G. Bernhardt.** "Identification of MltG as a potential terminase for peptidoglycan polymerization in bacteria." *Molecular microbiology* **99**, no. 4 (2016): 700-718.
404. **Zeng, Ximin, and Jun Lin.** "Beta-lactamase induction and cell wall metabolism in Gram-negative bacteria." *Frontiers in microbiology* **4** (2013).
405. **Zhanel, George G., Divna Calic, Frank Schweizer, Sheryl Zelenitsky, Heather Adam, Philippe RS Lagacé-Wiens, Ethan Rubinstein, Alfred S. Gin, Daryl J. Hoban, and James A. Karlowsky.** "New lipoglycopeptides." *Drugs* **70**, no. 7 (2010): 859-886.
406. **Zhang, TianHua, Jawad K. Muraih, Nasim Tishbi, Jennifer Herskowitz, Rachel L. Victor, Jared Silverman, Stephanie Uwumarenogie, Scott D. Taylor, Michael Palmer, and Evan Mintzer.** "Cardiolipin prevents membrane translocation and permeabilization by daptomycin." *Journal of Biological Chemistry* **289**, no. 17 (2014): 11584-11591.

407. **Zhang, Xinglin, Vincent de Maat, Ana M. Guzmán Prieto, Tomasz K. Praisnar, Jumamurat R. Bayjanov, Mark de Been, Malbert RC Rogers et al.** "RNA-seq and Tn-seq reveal fitness determinants of vancomycin-resistant *Enterococcus faecium* during growth in human serum." *BMC genomics* **18**, no. 1 (2017): 893.
408. **Zheng, B., Tomita, H., Inoue, T., & Ike, Y.** (2009). Isolation of VanB-type *Enterococcus faecalis* strains from nosocomial infections: first report of the isolation and identification of the pheromone-responsive plasmids pMG2200, encoding VanB-type vancomycin resistance and a Bac41-type bacteriocin, and pMG2201, encoding erythromycin resistance and cytolysin (Hly/Bac). *Antimicrobial agents and chemotherapy*, **53**(2), 735-747.
409. **Zhu, Wenming, Nancye C. Clark, Linda K. McDougal, Jeffery Hageman, L. Clifford McDonald, and Jean B. Patel.** "Vancomycin-resistant *Staphylococcus aureus* isolates associated with Inc18-like *vanA* plasmids in Michigan." *Antimicrobial agents and chemotherapy* **52**, no. 2 (2008): 452-457.
410. **Zhu, Xi, B. Zheng, S. Wang, R. J. L. Willems, F. Xue, X. Cao, Y. Li, S. Bo, and J. Liu.** "Molecular characterisation of outbreak-related strains of vancomycin-resistant *Enterococcus faecium* from an intensive care unit in Beijing, China." *Journal of Hospital Infection* **72**, no. 2 (2009): 147-154.
411. **Zirakzadeh, Ali, and Robin Patel.** "Epidemiology and mechanisms of glycopeptide resistance in enterococci." *Current opinion in infectious diseases* **18**, no. 6 (2005): 507-512.
412. **Zucchini, Laure, Chryslène Mercy, Pierre Simon Garcia, Caroline Cluzel, Virginie Gueguen-Chaignon, Frédéric Galisson, Céline Freton et al.** "PASTA repeats of the protein kinase StkP interconnect cell constriction and separation of *Streptococcus pneumoniae*." *Nature microbiology* **3**, no. 2 (2018): 197.
413. **Zurenko, Gary E., Betty H. Yagi, Ronda D. Schaadt, John W. Allison, James O. Kilburn, Suzanne E. Glickman, Douglas K. Hutchinson, Michael R. Barbachyn, and Steven J. Brickner.** "*In vitro* activities of U-100592 and U-100766, novel oxazolidinone antibacterial agents." *Antimicrobial Agents and Chemotherapy* **40**, no. 4 (1996): 839-845.

## Chapter 8. Appendix

### 8.1. DNA gBlock Sequences

**Table 8.1: gBlock sequences.** gBlock identifiers and associated sequences as described in **Table 2.12**.

gBlocks were ordered from IDT.

<b>gCWT001</b>
ATGGTGAGCAAGGGCGAGGAGCTGTTACCGGGGTGGTGCCCATCCTGGTTCGAGCTGGACGGCGACGTA AACGGCCACAAGTTCAGCGTGTCCGGCGAGGGCGAGGGCGATGCCACCTACGGCAAGCTGACCCTGAAGT TCATCTGCACCACCGGCAAGCTGCCCGTGCCTGGCCACCTCGTGACCACCTGACCTACGGCGTGCAGT GCTTCAGCCGCTACCCCGACCACATGAAGCAGCAGACTTCTTCAAGTCCGCCATGCCCGAAGGCTACGTCC AGGAGCGCACCATCTTCTTCAAGGACGACGGCAACTACAAGACCCGCGCCGAGGTGAAGTTTCGAGGGCGA CACCTGGTGAACCGCATCGAGCTGAAGGGCATCGACTTCAAGGAGGACGGCAACATCCTGGGGCACAAG CTGGAGTACAACATAACAGCCACAACGTCTATATCATGGCCGACAAGCAGAAGAACGGCATCAAGGTGA ACTTCAAGATCCGCCACAACATCGAGGACGGCAGCGTGCAGCTCGCCGACCACTACCAGCAGAACACCCCC ATCGGCGACGGCCCGTGCTGCTGCCGACAACCACTACCTGAGCACCCAGTCCAAGCTGAGCAAAGACCC CAACGAGAAGCGCGATCACATGGTCTGCTGGAGTTCGTGACCGCCGCGGGATCACTCTCGGCATGGAC GAGCTGTACAAGTAA
<b>gCWT002</b>
ATGGTGAGCAAGGGCGAGGAGGATAACATGGCCATCATCAAGGAGTTCATGCGCTTCAAGGTGCACATGG AGGGTCCGTGAACGGCCACGAGTTCGAGATCGAGGGCGAGGGCGAGGGCCGCCCTACGAGGGCACCC AGACCGCCAAGCTGAAGGTGACCAAGGGTGGCCCCCTGCCCTTCGCTGGGACATCCTGTCCCCTCAGTTC ATGTACGGTCCAAGGCCTACGTGAAGCACCCCGGACATCCCCGACTACTTGAAGCTGTCTTCCCCGAG GGCTTCAAGTGGGAGCGCGTGATGAACTTCGAGGACGGCGGCGTGGTGACCGTGACCCAGGACTCCTCCC TGCAGGACGGCGAGTTCATCTACAAGGTGAAGTGCAGCGGCACCAACTTCCCCTCCGACGGCCCCGTAATG CAGAAGAAGACCATGGGCTGGGAGGCCTCCTCCGAGCGGATGTACCCCGAGGACGGCGCCCTGAAGGGC GAGATCAAGCAGAGGCTGAAGTGAAGGACGGCGGCCACTACGACGCTGAGGTCAAGACCACCTACAAG GCCAAGAAGCCCGTGCAGCTGCCCGGCGCTACAACGTCAACATCAAGTTGGACATCACCTCCCACAACGA GGACTACCCATCGTGGAACAGTACGAACGCGCGAGGGCCGCACTCCACCGCGGCATGGACGAGCTG TACAAGTAA
<b>gCWT003</b>
ATGGTGAGCAAGGGCGAGGAGACCACAATGGGCGTAATCAAGCCCGACATGAAGATCAAGCTGAAGATG GAGGGCAACGTGAATGGCCACGCCTTCGTGATCGAGGGCGAGGGCGAGGGCAAGCCCTACGACGGCACC AACACCATCAACCTGGAGGTGAAGGAGGGAGCCCCCTGCCCTTCTCCTACGACATTCTGACCACCGCGTTC GCCTACGGCAACAGGGCCTTACCAAGTACCCCGACGACATCCCCAACTACTTCAAGCAGTCTTCCCCGAG GGTACTCTTGGGAGCGCACCATGACCTTCGAGGACAAGGGCATCGTGAAGGTGAAGTCCGACATCTCCAT GGAGGAGGACTCCTTCATCTACGAGATACACCTCAAGGGCGAGAATTCCCCCAACGGCCCCGTGATGC

---

AGAAGAAGACCACCGGCTGGGACGCCTCCACCGAGAGGATGTACGTGCGCGACGGCGTGCTGAAGGGCG  
ACGTCAAGCACAAGCTGCTGCTGGAGGGCGGCGGCCACCACCGGTTGACTTCAAGACCATCTACAGGGC  
CAAGAAGGCGGTGAAGCTGCCGACTATCACTTTGTGGACCACCGCATCGAGATCTGAACCACGACAAGG  
ACTACAACAAGGTGACCGTTTACGAGAGCGCCGTGGCCCGCAACTCCACCGACGGCATGGACGAGC  
TGTACAAGTAA

---

**gCWT004**

---

ATGGTTTCTAAAGGAGAAGAATTGTTTACTGGGGTCGTCCCTATTCTGTGGAACCTTGACGGCGATGTAAC  
GGGCATAAATTCTCTGTATCTGGGAAGGTGAGGGAGATGCGACGTATGGAAAGCTTACCCTTAAATTCAT  
CTGCACGACCGGCAAATTGCCTGTACCGTGGCCGACTTTGGTACGACGTTAACATATGGAGTACAGTGTTT  
CTCTAGATACCCAGACCACATGAAACAACATGACTTTTTCAAAGTGCAATGCCTGAGGGGTATGTCCAAGA  
GCGAACCATCTTCTTTAAAGATGACGGAACTACAAGACTAGAGCGGAAGTTAAGTTTGAGGGCGACACAT  
TGGTCAACCGCATTGAACTAAAGGGGATTGACTTTAAGAAGACGGCAACATTCTAGGGCACAAGTTAGAG  
TATAACTACAACAGTCATAATGTGTATATCATGGCGGATAAGCAAAAAGAACGGCATTAAAGTCAATTTCAA  
GATCCGCCATAACATAGAAGATGGAAGTGTGCAATTAGCAGATCATTATCAGCAAAATACCCCGATAGGGG  
ATGGTCCAGTGCTACTTCCGGATAATCACTACTTGAGCACTCAGTCTAAGTTGAGCAAAGATCCTAACGAAA  
AGCGCGACCACATGGTTTTGTTGGAATTTGCTACTGCCGCTGGAATAACCCCTTGGCATGGACGAGCTTTACA  
AG

---

**gCWT005**

---

GGTAATAAATACGAAGAGACACCTGATGTAATCGGGAAAACTGTAAAAGAAGCAGAGCAAATATTCAATA  
AAAATAACCTGAAATTGGGTAAAATTTCTAGAAGTTATAGTGATAAATATCCTGAAAATGAAATTATTAAGA  
CAACTCCTAATACAGGTGAACGTGTTGAACGTGGTGACAGCGTTGATGTTGTTATATCAAAGGCCCTGAA  
AAGGTTAAAAATGCCAAATGTCATTGGTTTACCTAAGGAGGAAGCCTTGAGAAATTAATCGTTAGGTCTT  
AAAGATGTTACGATTGAAAAAGTATATAATAATCAAGCACAAAAGGATACATTGCAAATCAAAGTGTAAC  
CGCAAATACTGAAATCGCTATTCATGATTCTAATATTAACCTATATGAATCTTTAGGCATTAAGCAAGTTTAT  
GTAGAAGACTTTGAACATAAATCCTTTAGCAAAGCTAAAAAGCCTTAGAAGAAAAGGATTTAAAGTTGA  
AAGTAAAGAAGAGTATAGTGACGATATTGATGAGGGTGATGTAATTTCTCAATCTCCTAAAGGAAATCAG  
TAGATGAGGGGTCAACGATTTCAATTTGTTGTTTCTAAAGGTAAAAAAGCGACTCATCAGATGTCAAAACG  
ACAACTGAATCGGTAGATGTACCATACACTGGTAAAAATGATAAGTCACAAAAAGTTAAAGTTTATATTTAA  
GATAAAGATAATGACGGTTCAACTGAAAAAGGTAGTTTCGACATTACTAGTGATCAACGTATAGACATTCCT  
TTAAGAATTGAAAAAGGAAAAACAGCAAGTTATATTGTTAAAGTTGACGGTAAAACTGTAGCTGAAAAAGA  
AGTCAGTTATGATGATATTTAA

---

**gCWT006**

---

ATGCCTAAGGATGTCAAATACCTGATGTCTCCGGAATGGAATACGAAAAAGCCGAGGGCTCTTGAAAA  
AGAAGGTTTACAGGTTGATTCCGAGGTGTTGGAAATCTCAGATGAAAAAATTGAAGAGGGCCTGATGGTA  
AAAACGGATCCTAAAGCGGATACCACAGTCAAAGAAGGCGCCACGGTCACCTTTATAAGAGCACCGGAA  
AAGCAAAAACGGAGATCGGTGATGTGACAGGCCAAACGGTCGACCAAGCAAAAAAAGCGTTGAAGGACC  
AAGGGTTAATCATGTAACAGTAAATGAAGTGAATGACGAGAAAAATGCGGGCACTGTCAATGACCAAAAT

---

---

CCTTCAGCAGGGACTGAGCTGGTCCCGAGTGAAGATCAAGTCAAACCTTACAGTCAGTATCGGACCCGAAGA  
CATTACGCTTAGAGACTTGAAAACCTACAGTAAAGAAGCAGCGTCTGGATATCTGGAAGACAACGGATTGA  
AGCTTGTAGAAAAAGAAGCATACTCAGATGATGTTCCAGAAGGACAGGTTGTCAAACAAAAACCAGCAGC  
AGGTACGGCAGTAAAGCCGGGAAACGAAGTTGAAGTGACATTCTCTCTCGGACCAGAGAAAAACCTGCG  
AAAACAGTGAAGAAAAGGTCAAGATCCCCTACGAACCAGAAAATGAAGGGGACGAGCTTCAAGTGCAAA  
TCGCGGTTGACGATGCGGATCACAGCATCTCTGACACTTACGAAGAATTAAGATAAAAAGAGCCGACTGAA  
CGAACGATCGAACTAAAGATTGAACCAGGCCAAAAAGGGTACTATCAAGTAATGGTAAACAATAAAGTTGT  
CAGCTACAAAACCATTGAGTATCCGAAAGATGAA

---

**gCWT007**

---

AAGCCAACATCAGTCAAGGTTCCCTAACGTCGCGGGTACGAGCCTTAAGGTTGCCAAACAGGAGCTATACGA  
CGTTGGGCTAAAGGTAGGCAAATACGACAGATAGAAAGTGACACAGTTGCGGAGGGTAACGTGGTCCGT  
ACTGATCCGAAGGCAGGTACTGCAAAGCGCCAGGGGAGCTCTATTACTCTTTATGTTAGTATCGGTAATAA  
GGGGTTCGACATGGAGAACTACAAGGGACTTGATTACCAGGAAGCGATGAACTCTAATAGAGACGTAT  
GGTGTCCCTAAAAGTAAGATCAAGATCGAGCGTATTGTGACTAATGAGTATCCTGAGAATACTGTCATCTCA  
CAAAGTCTAGCGCAGGAGACAAGTTCAATCCGAATGGGAAATCAAAGATAACACTAAGTGTAGCTGTTAG  
TGATACCATCACAATGCCGATGGTAACTGAGTATAGCTATGCCGATGCTGTGAATACTTTAACCGCTTTGGG  
CATAGACGCATCTCGAATTAAGCATATGTGCCGTCATCATCAGCTACCGGATTTGTCCAATACATAG  
TCCGAGCAGTAAAGCCATAGTGAGCGGGCAGAGTCCATATTACGGGACAAGTCTTAGCCTTAGCGACAAA  
GGAGAGATCAGCTTGTATTTGTACCCAGAAGAACTCACTCATCTAGCAGTTCTAGCTCTAGCACTAGTTCA  
AGCAACAGCAGTTCAACGAACGATTCTACTGCTCCAGGTAGCAACACCGAATTGTCTCCGTCTGAAACCACC  
GCTCAGACTCCT

---

**gCWT008**

---

TCACCAGATGAGGTAGCTGTTCCAGACGTATCAGGGAAGACGGAGGACCAAGCAGTTGCGCTATTGCAAA  
AGGAGGGGTTTCGTAATTGGCAAGACGGCGGAAAAGAACTCTGATGAAGTGGACGAAGGCAAAGTCATAA  
ATACTGATCCGGAAGCGGGTGAGATGAAGGAGAAAAGGGACGAAAATAAACCTTTTCGTCTCAATAGGTTT  
AAAGAAGATAACAATGGACGATTACACAGGTCGTAGTTATACTGACACCAAGGCATTGTTGGAGGAGCAG  
GGATTCAAGAATATTTCAAGCGAAGAGGCATATTCTAGTGAGATAGAAAAGGATTGATTATCAGCCAGAC  
TCCTACGCAAGGCACTGAGGTGGTCGCTAAATCAACTGACGTGAAGTTTGTAGTGAGTAAGGGCGCTGAAC  
CGATAACATTGAAGGACTTACGAGGGTATACAAAACCTGCCGTGGAGGATTACGCGAGCCATTAGGACTT  
AAAGTATCATCTAAGGAGGAGAATAGTAGTACAGTGAAAAAGGTCAGGTGATTTCTCAATCTCCTTCAGC  
CGGAACTGCTATGAATAGTGGAGACACTATTGAAATCGTAATTAGTGCTGGGCCAAAGGAAAAACAGGTA  
AAGGAGGTTACGAAGACATTTAACATACCGTACACCCCTAGTGATGAAGAAAACCTCAGCCACAAAAGAT  
CCAGATATATATCCAGGATAAAGATCACAGCATGACGAGCGCATACAGAGAAATGAGTATCACTCAGAACA  
CCTCTGTGGAGATTACGTTTCAAATCGAAGAGGGGAAGCTCTGCCGGCTATAAAATCATTAGTGACGACAAA  
GTGATTGATGAAGGAACGGTGCCATATCCGAAT

---

---

**gCWT009**

---

GGAAATGACAAGGTCCTGTCCCAGCCTTCATTGGATTATCTAAGGCAGACGCCCAACAACAAGCGGATAA  
TATCGACTTGGTCTTGACGTTCAAGCAGCAAGAATGCGAAGATCAGCCTAAGGGCAATATATGCGCACAGG  
ATCCAAAACAGGGTACTGACGTAGACAAAGAGTCTACAGTAAACCTAGTCGTGTCTACCGGTGCCCGAAA  
GTCGCGGTCCCAAATGTAATTGACAAAAATATAGACGAGGCTAAGAAGCAGCTTGAGGACAAAGGCTTCG  
AGGTTGAAACGAAGCAAACCGAATCATCTCAGGATGAAGGGACCATTTTAAGCCAGAATCCGGACCCAGG  
CAAAGAATTAGAGAAAGGCTCTACGGTGACACTTGAAGTTGCAAAGCTGAGGAGAAAGCCACGGTGCCA  
GATGTTGTAGGACGTACCTGCGACGAAGCTAAAGCACAGTTGAGAGCGGGGTGATCTTACTGCGGTCT  
GCACGGACCAGCCTACTAATGACCCGAACCAGGTAGGCAAAGTAATTTCTACGACACCTCAATCTAGCACCC  
AAGTGGACCCGGAAGCAAAGTTACTATCGTAGTCGGAAGGCAGTCGAAAAAACAAGGTGCCGGAGG  
TGCGTGGTAAGACCTTGGCAGAGGCGCGACAAATCCTTCAGCAGTCTGTTTTACGAACGTACAGGTGCC  
CAAGGGTCACCAGGGGACGATAACGCAAAAGTGTTGCAAGCAACCCGACCCGGGGAGCGAAGTAGAC  
GATCCTGCTGCTACTCCGATAACTTTAATGACCGTCCCGGGGGATGGTGGTAACGTAATGGAGGGAATGG  
CAATGGGGGCGCTATCGCTGGCTTGCCGGGCTTCGGCGAT

---

**gCWT010**

---

ATCACCGAGATGTACAAGTCCCTGACGTCCGCGGCCAAAGCTCTGCCGATGCCATCGCAACACTTCAAAT  
CGTGGGTTTAAGATACGAACCTTACAGAAGCCAGATAGTACAATTCGCCGGATCACGTAATTGGAACGGA  
CCCTGCGGCGAATACTAGTGTGAGCGCAGGAGATGAGATTACGGTCAATGTAAGTACTGGGCCGGAGCAA  
CGAGAAATCCCTGACGTGAGCACACTTACCTATGCTGAGGCGGTTAAAAAATTACTGCGGCTGGCTTTGG  
GCTATTCAAGCAGGCTAATAGTCCGTCAACCCAGAACTAGTCGAAAAGTCATTGGGACTAACCCGCTG  
CTAATCAAACAAGCGCAATTACAAACGTGGTGATAATAATTGTTGGGTAGTGGTCTGCCACTAAGGACATT  
CCTGATGTAGCAGGCCAAACAGTGGATGTTGCCAGAAGAATCTAACGTATATGGTTTTACGAAGTTTAG  
CCAGGCTAGTGTGATTCTCCTAGACCTGCTGGAGAAGTTACGGGAACCAACCCGCTGCCGGAACACTG  
TACCTGTGGATAGCGTCATAGAACTTCAAGTATCAAAGGGTAACCAGTTTGTGATGCCAGACCTTAGTGG  
ATGTTTTGGGTAGATGCCGAGCCTAGACTTCGAGCCTTAGGCTGGACCGGGATGCTAGATAAGGGTGACG  
ACGTTGATGCAGGCGGTAGCCAGCACAATCGCGTCGTCTATCAGAATCCACCAGCGGGTACAGGTGTAAT  
AGAGATGGGATAATTACCCTACGCTTTGGGCAG

---

**gCWT011**

---

AGTCCTAAAAAGATAGCTGTTCCAGATGTCGCGAACATGACCGTTGAAGAAGCAAAGAAGGAATTGGAAA  
AGCAGGGATTATAGTCGGCGAACACAAGAAGCGTCATTCTGAGGACATCGAAAAGGATAAAGTGATTGA  
GACAGATCCAGCTGAGGGCACGTTACGTGTGAAGGACACCGAAGTAGACCTTATTGTAAGTCTTGGGGTG  
GAAAAGTCACCTATGGACAACATATAGGGCAGAAAATCGACCAGGTCCAAAGCGTTCTAAAAGACAAGTT  
CATGGGCGATGTCGTGTAACCTACGTCCATAGCAGTGAGGAGGCAGGCTCTATAATAGATCAGGACCCG  
GCTCCGAATACAGAGATCGTGCCGAAGGAAACCAATGTCGTATTTACAGTCTCACAGGGCAAGAAGCCAAT  
ATCAGTAAGAAACGTAGTGGGGTATAGCAAGACAGACCTTGATAATTATGTCAACTCTGAAGGTTTGAAGT  
GGCGAGTCGAAAGAGAAGATTACAGTCTACCATCGCTAAAGGATTGGTGTCTCACAGAAGCCAGCGGC  
AGGAACTAATTTGGTTGAGGGCGACACCATAGCGTGGTGCTTTCTAAGGGCCAGAGGAAAAACCGGTA

---

---

AAAACTTTCGTTAAGACTATGTTGATTCCGTATGAGCCAACGGAGGAGGGCATGGAGCAGTTAATTCGCAT  
TGAAATCCAGGACAAGAATCACAGTATGGCGAAGCCGCTTGAAGAATTTTTATCAACAGCGACCGAGAAT  
ACAAAATCCAGCTTGTTATTGAAGAAGGCGAAGAAGCCGCTACAAGATATTACGCGATTCTGCTATTATAG  
CAGAGGAGAAGTTCAGTTACGATGATGTAAAC

---

**gCWT012**

---

TTAGGAATGGGGACAACCGTGGTTGGTGCCATCCTTTTACCAGATTCATTTGTCTTAGCAAATGTGGGGGAC  
AGTCGTGCTTATTTAGTTCGTGACCAACACATGTTACAATTAACAGAAGATCATTCTTTAGTGAATGAACTA  
GTAAAATCAGGGGAGATTACTCGTGAGATGGCTGCAAATCATCCACGAAAAAATGTCCTAACCGTTCTTT  
GGGAATGCCTGGCACTGTGGAAGTCGATGTAACCAATCATGAATGGCTGCCTAATGACTATTTACTGTTATG  
TTCGGACGGTTAAACCAATATGGTTCCTGAGACAAAAATTTAGAAAATTTAGAGACGTCAGATCCCTTAGA  
ATCCAAATTAAGCCAACCTCGTTGCCAAGCAAATGAAGCGGGTGGTTTAGATAACATTACCGTGTTAGTGAT  
ACACTTTGACGAACAGAAGGAGGAAAACCAATGATAGAAATCGGCAAGAAGCTGAATGGTCGATATCACG  
AAAGTAGTACGAGTAATTAAGACAAGAGGTTGGGACAGGAGTGTTTAGCTTCAAGAACCAAGTAGGTACT  
GTTAACATCTATTTGCTTTTCAAATAGTGTCTCAGCAATAAGAAGAAGCTGCTCCTGTCCCGCGTTTAT  
CTTAAGGTTAAGTCTAGGAAGGTAAGTCATTTGACTTATGTCCTAGGCTCTTTTAAATTAAGAATCGAG  
AGGCTCCCTTGATTTCTGCACTATCCTGTATATTGAAAGTAGTTAGGAGTGGTTTATCTGAAAGGTCAA  
ATCAGAAAAGCGTTAAGCGGTTTTTATTATGTATACGCAGATGGAGAAACATATCAAACAAGAGCGCGAGG  
GAATTTTCGTAATCGAAAAATTACGCCACTCGTGGGAGATGAAGTACTTTTTGAAAGCGATAATTTAACAGA  
TGGTTATGTGTTGAAATTTTACCAAGACGAAATGAATTAGTGCGCCCGCCTGTTGCAAATGTGGAT

---

**gCWT013**

---

AGTTGATGCGCCATGTTCAAGGCTTAGGGCTAATGCGCCGTAAACCAGACATTAATACCATAAAACGGCCA  
ATGATTTTCAAATTTACCTAAAATTCAGTTAGAAATCTTAGAAAAGTGTGCCCAACACTAAAACAATGGG  
GTATAATGGTCTATAGCACTTGTACTATTACGCCAGAAGAAAATCAGGAAGTGGTGGCAGCCTTTTTAGCCA  
AACACCCTGAATTTGAAAAAATTGAAATTGTTGCAAATGAAAACGTCCAAGCAGTAGTAAAAGAGCAAGAA  
CTGGTTCTGTATCCCATCAATACATGACAGATGGCTTCTTTATTTGCTGTATGCGGAAAAGTTAGTTCAAATG  
AGGTGAAATAATTTGAAATCAACGTTCAATCAGATGTCGGTCGCAAAAAGAAATACGAACCAAGATTATGC  
CAACGTTTTTGAACAACAACACATAACCTTTGCTGTTTTAGCAGATGGCATGGGTGGTCACCAAGCACA  
GAAGGAGGAAAACCAATGATAGAAATCGGCAAGAAGCTGAATGGTCGATATCACATTATTGGCAGCATCG  
GAAGCGGCGGCATGGCCAACGTTTATTTAGCACACGATTTAATTTTAGACCGAGACGTTGCAGTAAAAGTC  
TTGCGCTTTGACTTCCAAAACGATCAAGCCGCCATCCGACGTTTTCAGCGTGAAGCACTAGCCGCAACTGAG  
CTGGTTCACCCGAATATCGTCAGTGTGTACGATGTAGGCGAAGAAGATGGACTACAATATTTAGTCATGGA  
ATATGTGAAAGGAATGGACTTAAAACGTTACATCAAACGCATTTCCAATTCCTTATCCACAGTTGTGGA  
CATTACGCAACAAATTTTATCTGCTGTCGCAATGGCACATGAACATAGAATTATTCACCGGGATTTAAAACC  
GCAAAACATTCTGATTGACGAACACGGCACAGTCAAATTAAGTACTTTGGGATTGCGATTGCCTGTCA

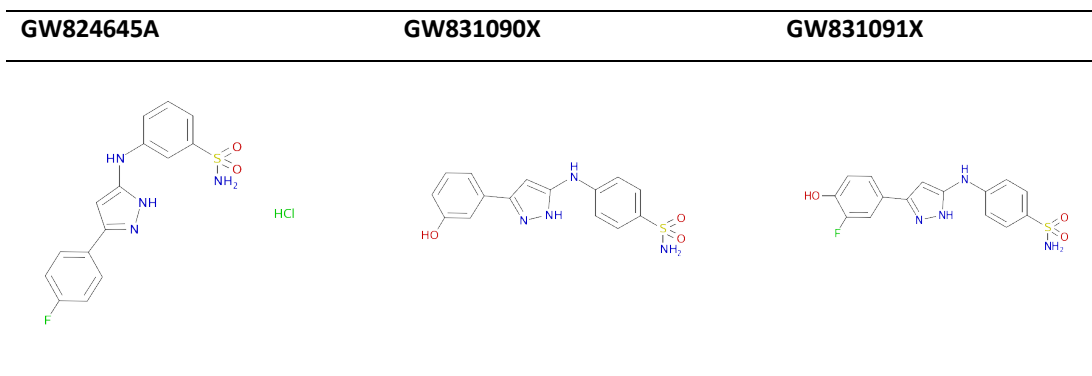
---

## 8.2. MIC of Enterococcal isogenic series and CSLI controls for each antibiotic

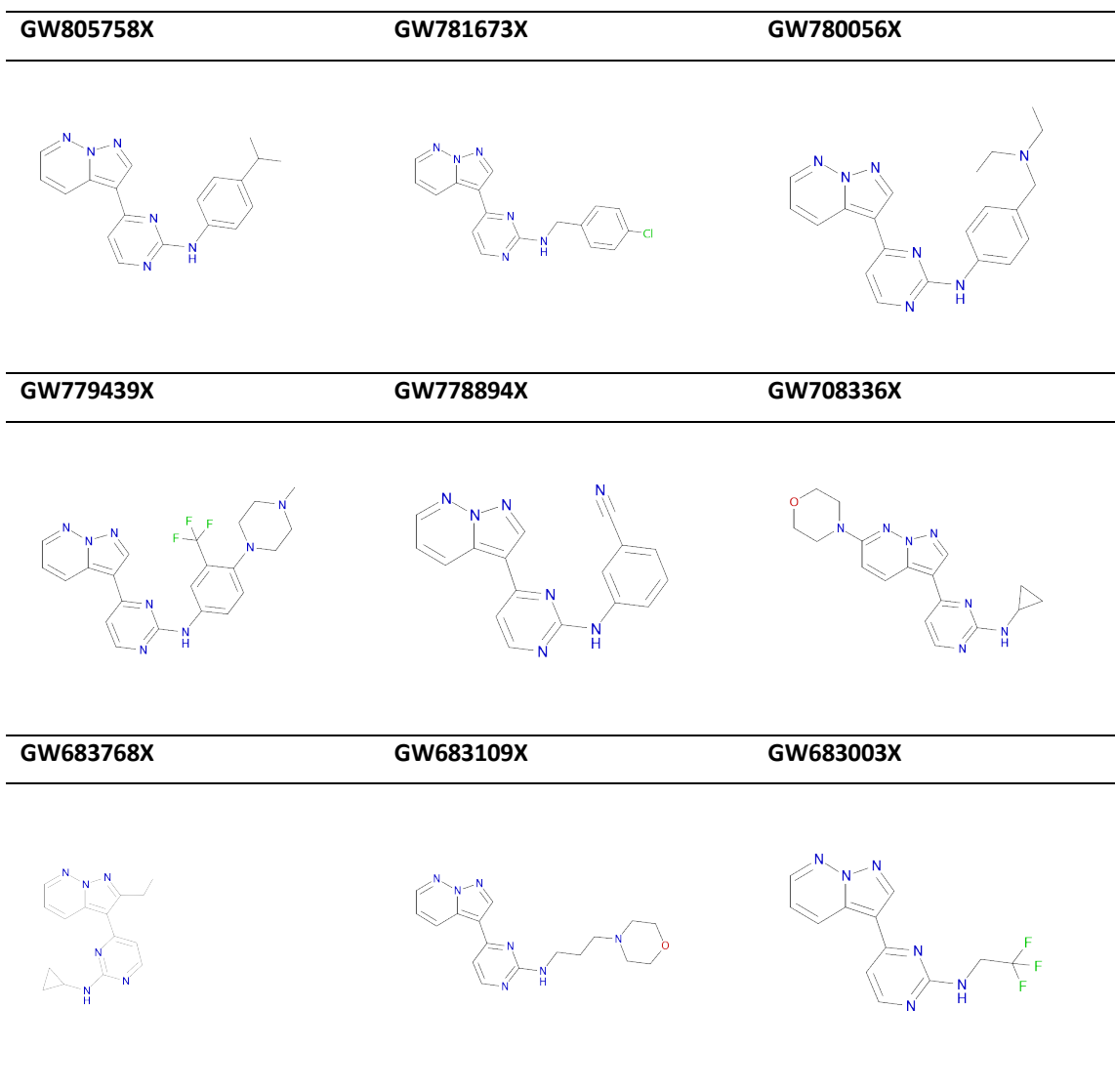
**Table 8.2: MIC of OG1RF isogenic series with CSLI control strains.** Experiments were in accordance to CSLI protocols and performed in duplicates. MIC reported in  $\mu\text{g mL}^{-1}$ .

Antibiotic	<i>E. faecalis</i> OG1RF WT	<i>E. faecalis</i> OG1RF <i>ΔireK</i>	<i>E. faecalis</i> OG1RF Tn1549	<i>E. faecalis</i> OG1RF Tn1549 <i>ΔireK</i>	<i>S. aureus</i> ATCC 29213	<i>E. coli</i> ATCC 25922	<i>K. pneumoniae</i> ATCC 700603
Ampicillin	0.03125	0.015625	0.0625	0.015625	0.0625	0.25	256
Cefazolin	32	8	32	32	0.5	1	256
Cephalothin	16	4	64	64	0.0625	8	<256
Cephalexin	32	16	128	32	2	8	64
Cefoxitin	<256	128	<256	<256	2	4	128
Ceftriaxone	16	0.5	256	8	4	0.0625	8
Cefotaxime	2	0.0625	256	1	1	0.0625	8
Ceftazidime	128	8	<256	64	8	0.25	64
Cefepime	8	2	32	8	2	0.01563	2
Ceftabiprole	0.03125	>0.00781	0.03125	0.03125	0.125	<256	8
Meropenam	1	0.5	2	2	0.0625	>0.00781	>0.00781
Vancomycin	4	1	64	32	0.5	<256	<256
Fosfomicin	16	16	128	64	16	<256	<256
Bacitracin	128	16	128	128	128	<256	<256
D-Cyclo serine	128	64	128	64	32	32	64
Daptomycin	64	8	32	16	4	<256	<256
Kanamycin	256	256	256	128	1	0.5	16
Linezolid	2	2	2	2	0.0625	<256	<256
Rifampicin	<256	<256	<256	<256	<256	4	8

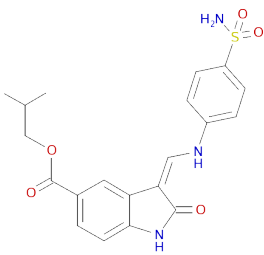
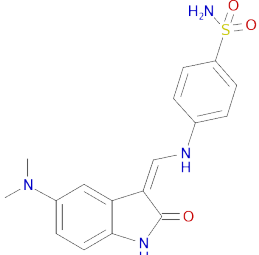
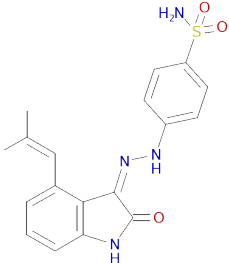
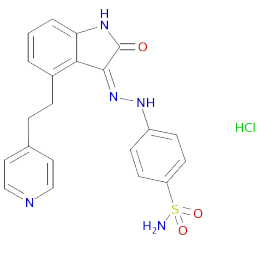
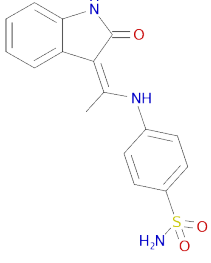
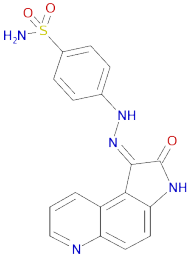
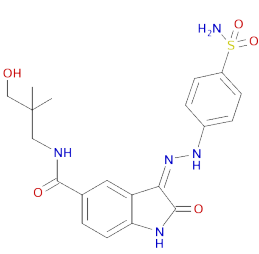
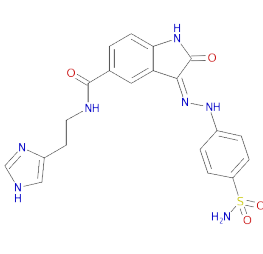
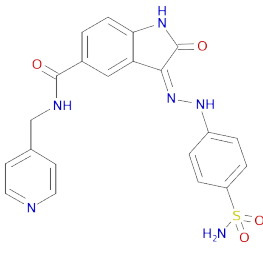
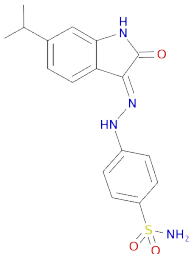
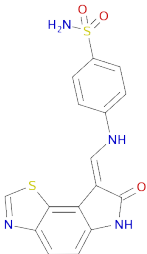
**Table 8.3: GSK protein kinase inhibitor set 1.** Includes inhibitors from Tang *et al.*, (2003) tested in MIC experiment against *E. faecalis* OG1RF Tn1549



**Table 8.4: GSK protein kinase inhibitor set 2.** Includes inhibitors from Stevens *et al.*, (2008) tested in MIC experiment against *E. faecalis* OG1RF Tn1549



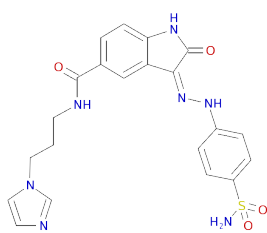
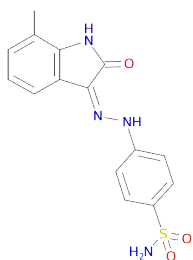
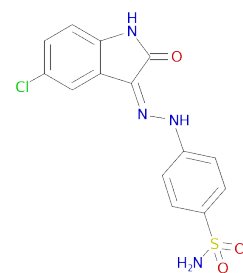
**Table 8.5: GSK protein kinase inhibitor set 3.** Includes inhibitors from Bramson *et al.*, (2001) tested in MIC experiment against *E. faecalis* OG1RF Tn1549

<p><b>GW589933X</b></p>	<p><b>GW416981X</b></p>	<p><b>GW416469X</b></p>
		
<p><b>GW396574X</b></p>	<p><b>GW352430A</b></p>	<p><b>GW335962X</b></p>
		
<p><b>GW305178X</b></p>	<p><b>GW301784X</b></p>	<p><b>GW300660X</b></p>
		
<p><b>GW300657X</b></p>	<p><b>GW300653X</b></p>	<p><b>GW297361X</b></p>
		

---

**GW290597X**

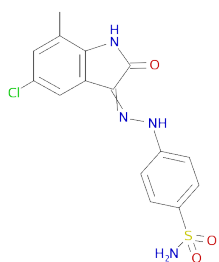
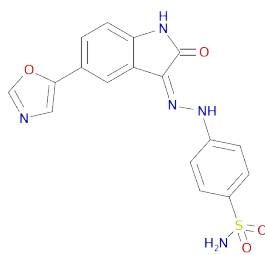
---

**GW282536X****GW280670X**

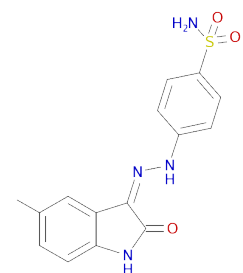
---

**GW279320X**

---

**GW276655X****GW275944X**

---



## 8.4. Extended AUC data

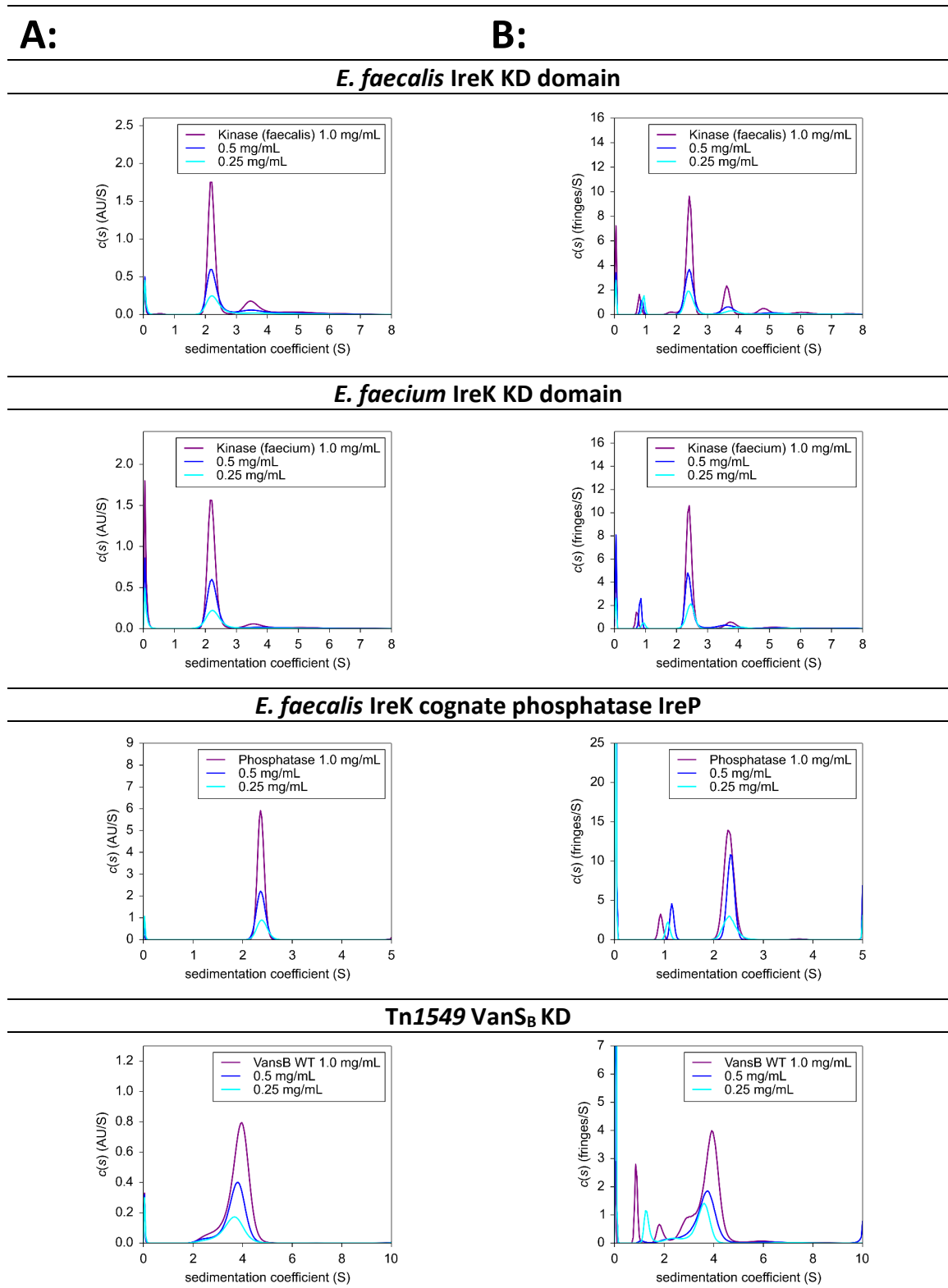


**Figure 8.1: Sedimentation coefficient distributions of Kinase and Phosphatase domains used in this study. (A) Absorbance data and (B) Interference data.**

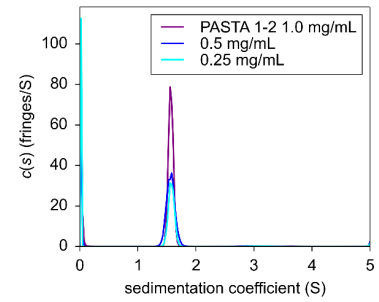
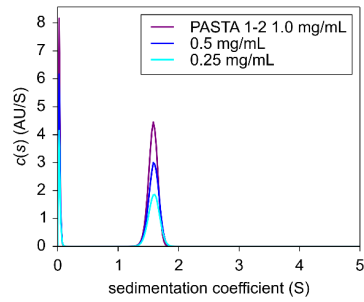
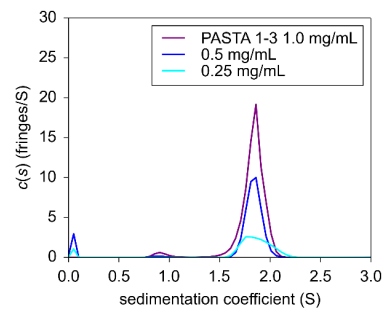
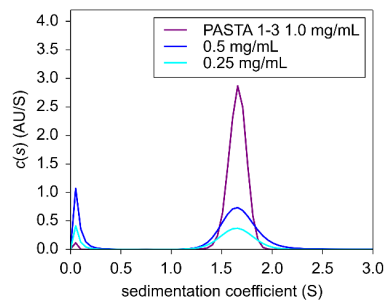
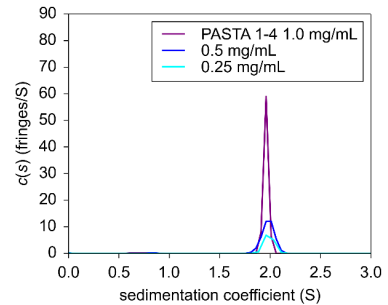
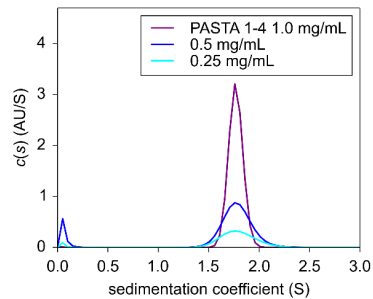
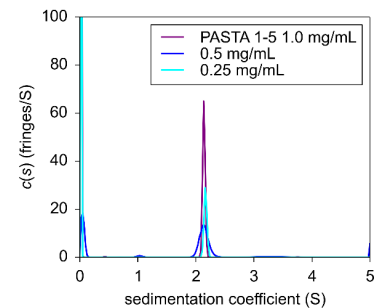
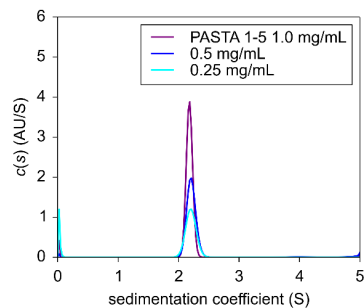
**Table 8.6: Species estimated molecular weights from the c(s) analysis of IreP.** For each sample concentration the signal-weighted sedimentation coefficient and the estimated MW of each species is shown together with the best-fit frictional ratio ( $f/f_0$ ) for the distribution. IreP Phosphatase domain all appear as predominantly one species with a best-fit molecular weight consistent with that of a monomer.

Monomer MW (kDa)	Detection method	Concentration (mg mL <sup>-1</sup> )	Peak 1		Peak 2		$f/f_0$
			MW (kDa)	Sed. Co (S)	MW (kDa)	Sed. Co (S)	
<b>IreP Phosphatase</b>							
28.3	Absorbance	1.0	-	-	28.9	2.37	1.35
		0.5	-	-	28.6	2.37	1.34
		0.25	-	-	28.7	2.40	1.33
	Interference	1.0 <sup>#</sup>	7.4	0.93	28.9	2.31	1.39
		0.5 <sup>#</sup>	8.7	1.16	24.8	2.34	1.24
		0.25 <sup>#</sup>	8.5	1.08	26.9	2.33	1.31

**Table 8.7: Species estimated molecular weights from the c(s) analysis of Vans<sub>B</sub>.** For each sample concentration the signal-weighted sedimentation coefficient and the estimated MW of each species is shown together with the best-fit frictional ratio ( $f/f_0$ ) for the distribution. The Vans<sub>B</sub> constructs all appear to be in an equilibrium between two different species. This is most likely a monomer/dimer equilibrium, but it is difficult to be certain from these calculated molecular weights as the  $f/f_0$  varies.

(Determining the  $K_D$  of the self-association would require a broader concentration range).

Monomer MW (kDa)	Detection method	Concentration (mg mL <sup>-1</sup> )	Peak 1		Peak 2		Peak 3		$f/f_0$
			MW (kDa)	Sed. Co (S)	MW (kDa)	Sed. Co (S)	MW (kDa)		
<b>IreP Phosphatase</b>									
32.4	Absorbance	1.0	-	-	-	-	65.0*	3.80*	1.36
		0.5	-	-	-	-	53.1*	3.67*	1.24
		0.25	-	-	-	-	56.6*	3.56*	1.33
	Interference	1.0 <sup>#</sup>	8.8	0.88	27.6	1.88	81.4*	3.85*	1.56
		0.5 <sup>#</sup>	10.9	1.14	-	-	60.4*	3.56*	1.39
		0.25 <sup>#</sup>	10.2	1.33	22.8	2.26	44.4*	3.53*	1.14

**A:****B:****PASTA 1-2****PASTA 1 to 3****PASTA 1 to 4****PASTA 1 to 5**

**Figure 8.2: Sedimentation coefficient distributions of PASTA domains from *E. faecalis* IreK used in this study. (A) Absorbance data and (B) Interference data.**

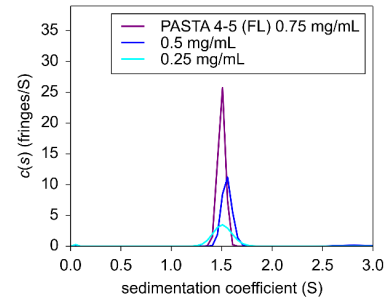
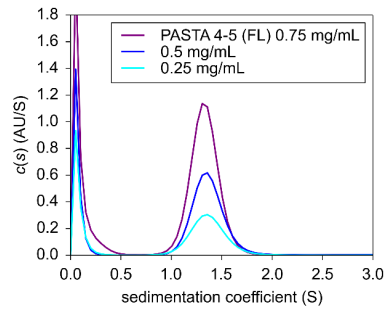
---

**A:****B:**

---

**PASTA 4 to 5**

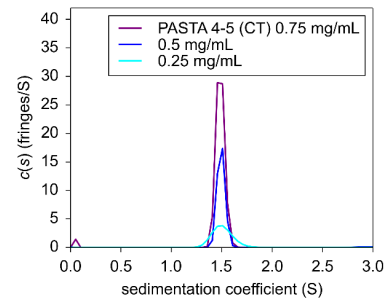
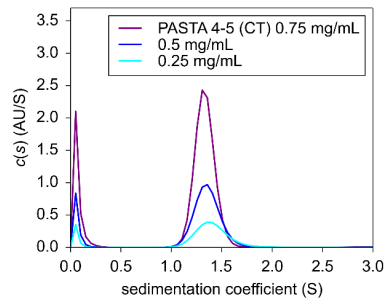
---



---

**PASTA 4 to 5 C-terminal truncation**

---

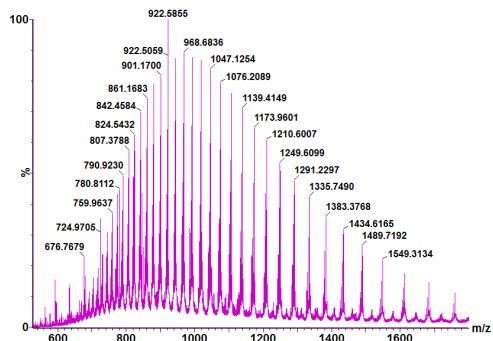


---

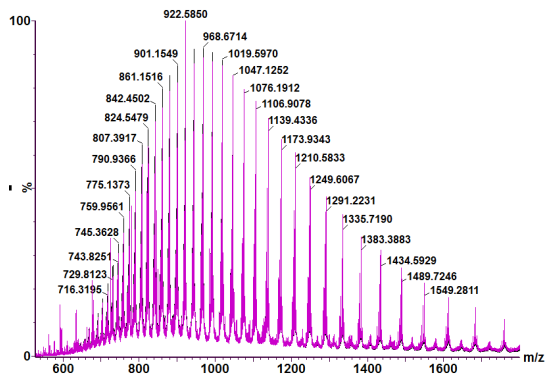
**Figure 8.3: Sedimentation coefficient distributions of the terminal PASTA domains from *E. faecalis* IreK used in this study. (A) Absorbance data and (B) Interference data.**

## 8.5. Mass Spectrometry

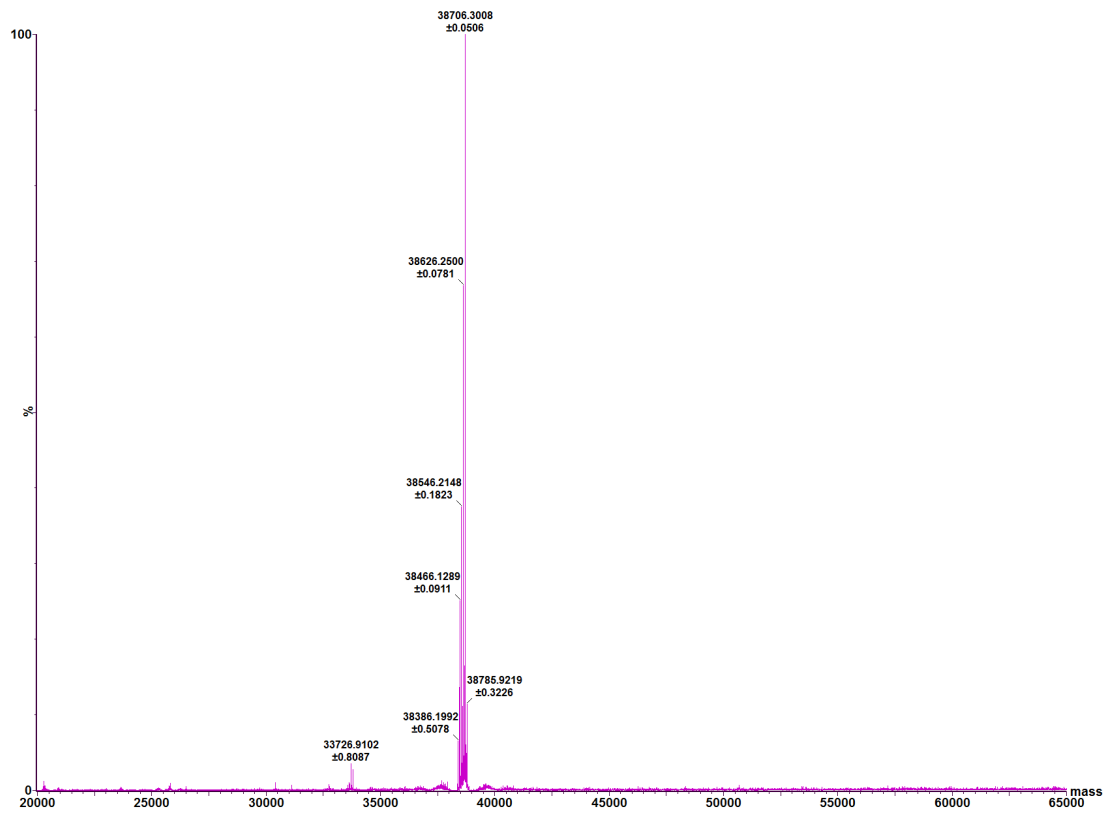
**A:**



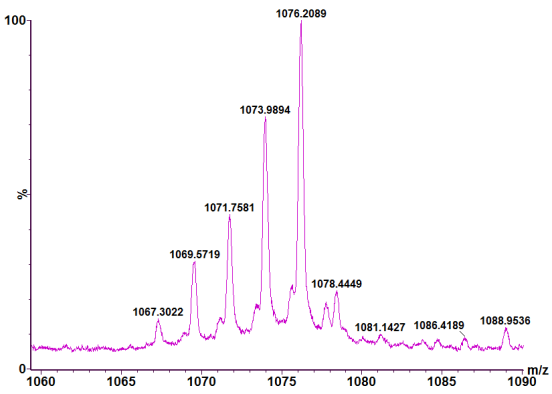
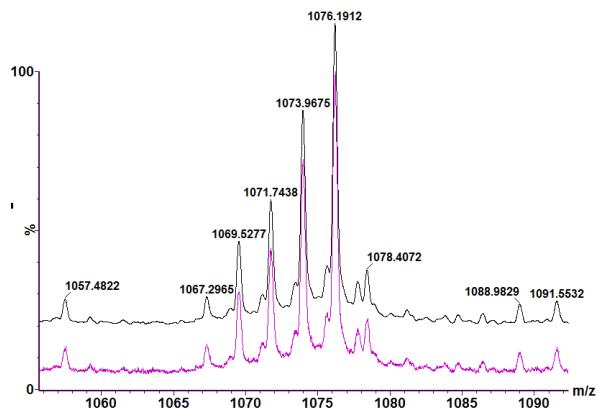
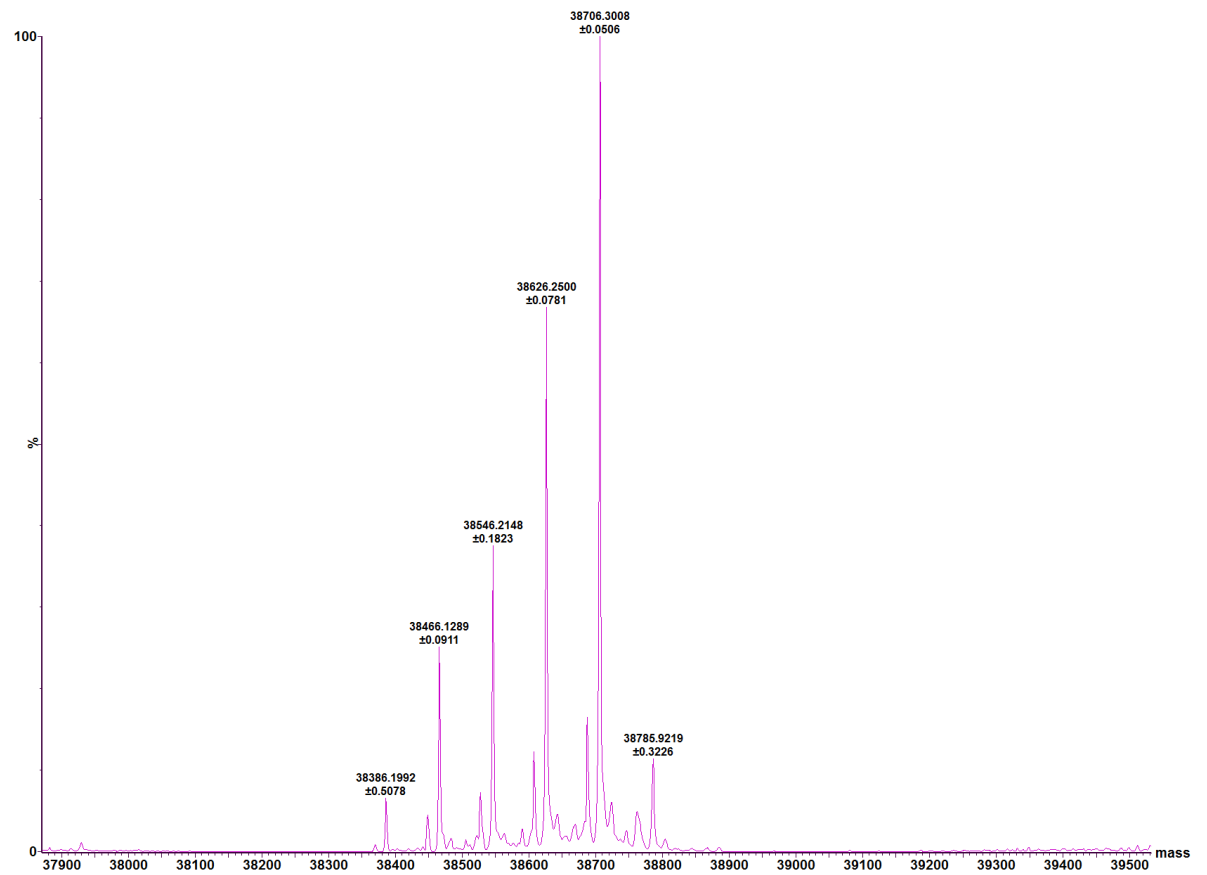
**B:**



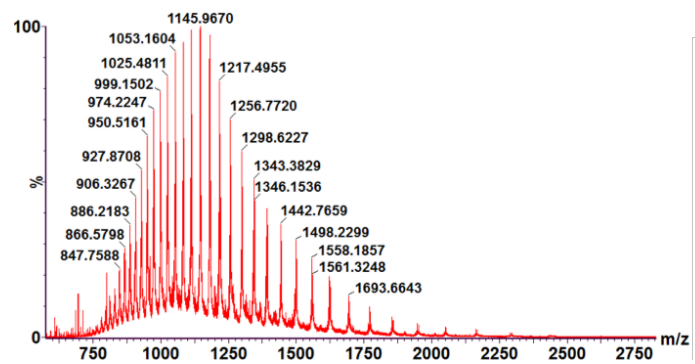
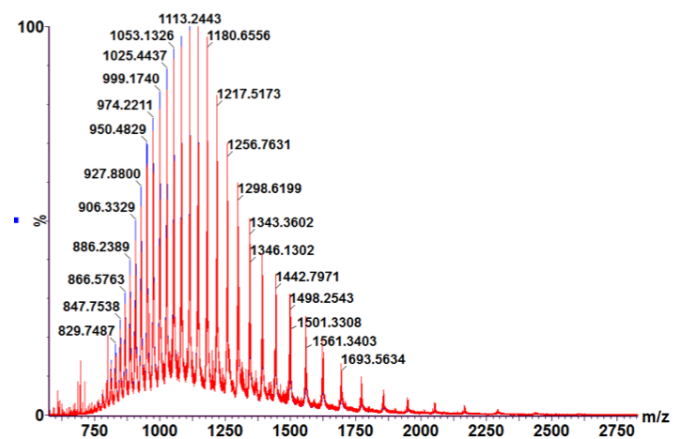
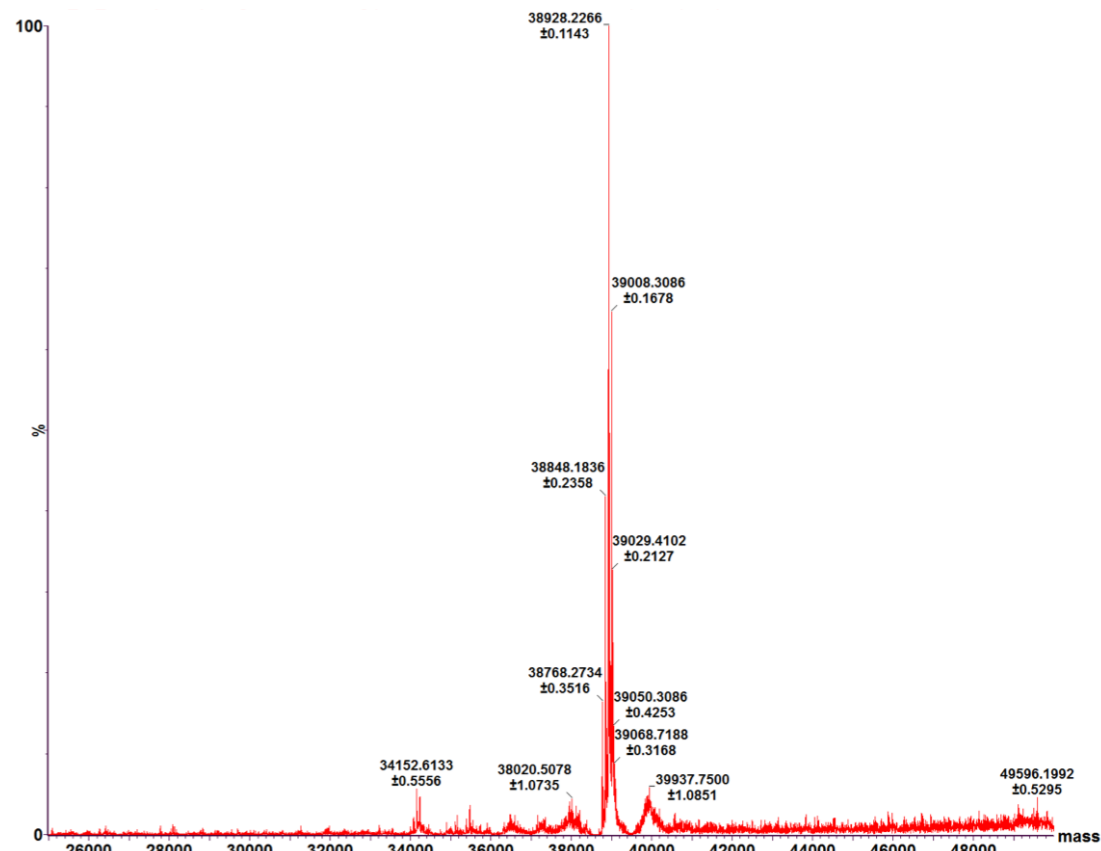
**C:**



**Figure 8.4: ESI-MS of *E. faecalis* KD. (A) Raw Mass Spectrum, (B) Superimposition of Raw data and mock mass data from maximum entropy algorithm (C) mock mass spectrum from maximum entropy algorithm.**

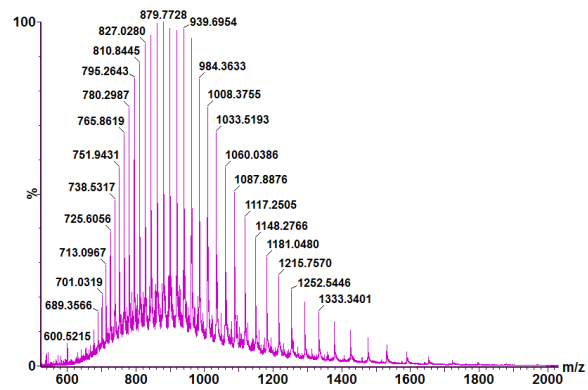
**A:****B:****C:**

**Figure 8.5: Highlighted ESI-MS of *E. faecalis* KD to show post translational modifications. (A) Raw Mass Spectrum, (B) Superimposition of Raw data and mock mass data from maximum entropy algorithm (C) mock mass spectrum from maximum entropy algorithm.**

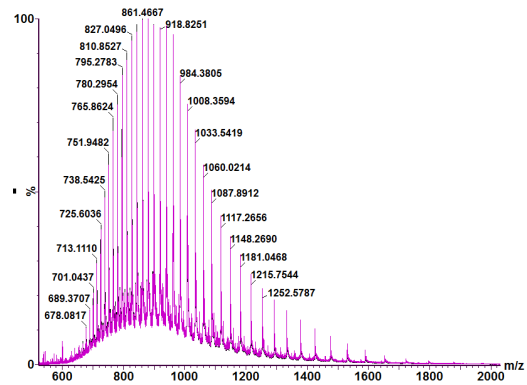
**A:****B:****C:**

**Figure 8.6: Highlighted ESI-MS of *E. faecium*.** (A) Raw Mass Spectrum, (B) Superimposition of Raw data and mock mass data from maximum entropy algorithm (C) mock mass spectrum from maximum entropy algorithm.

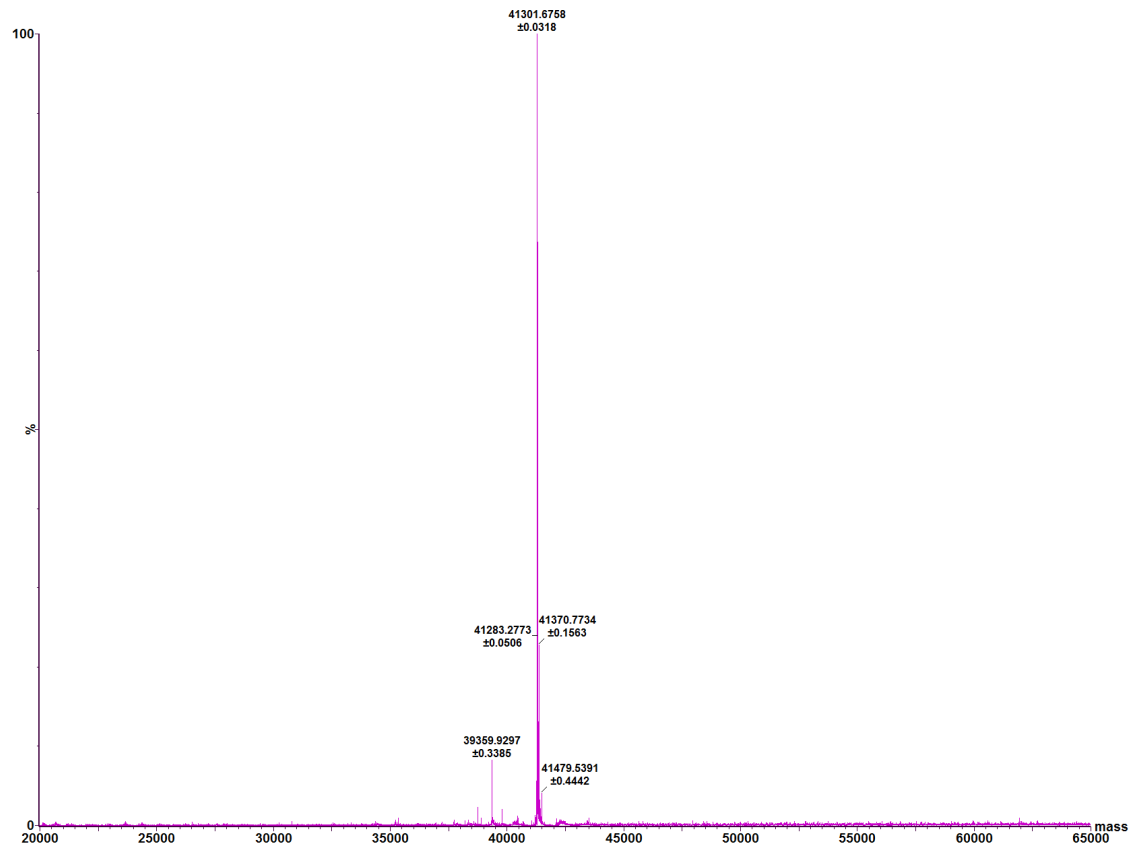
**A:**



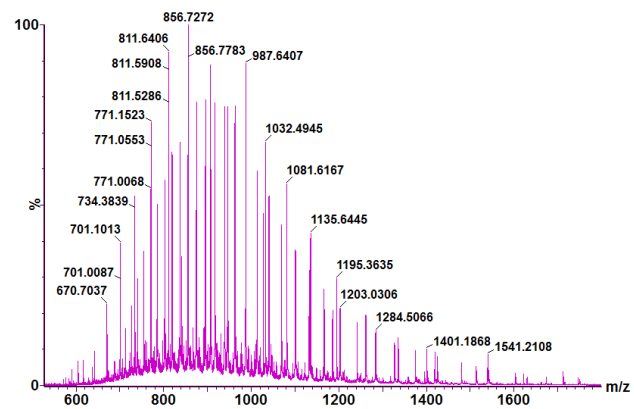
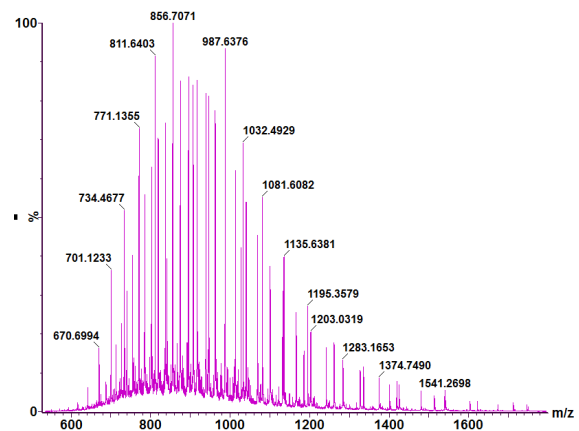
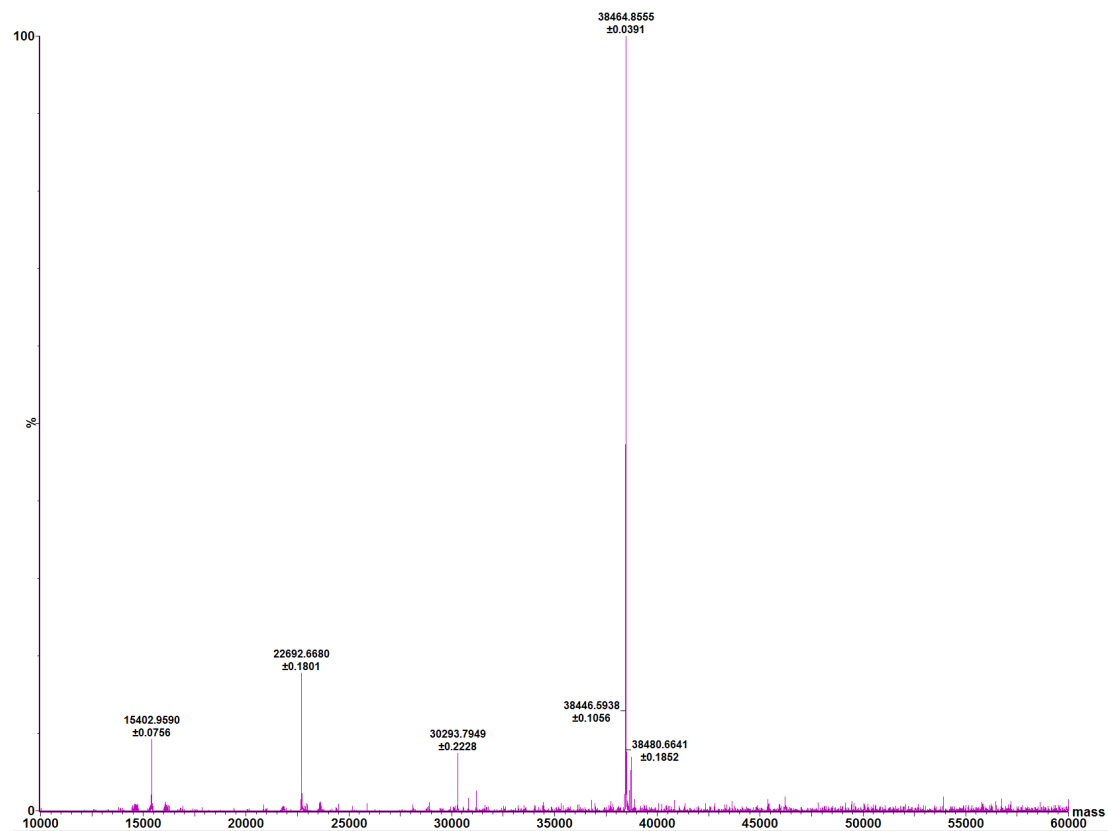
**B:**



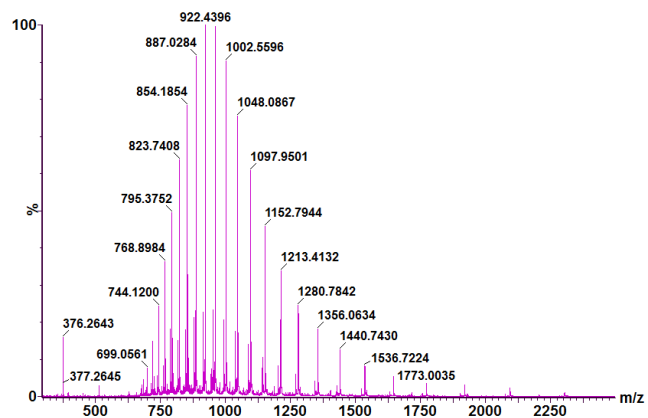
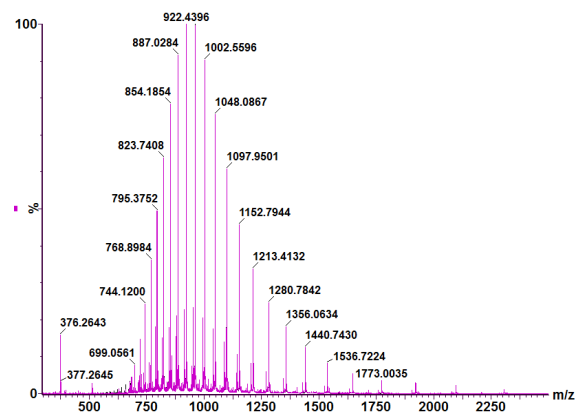
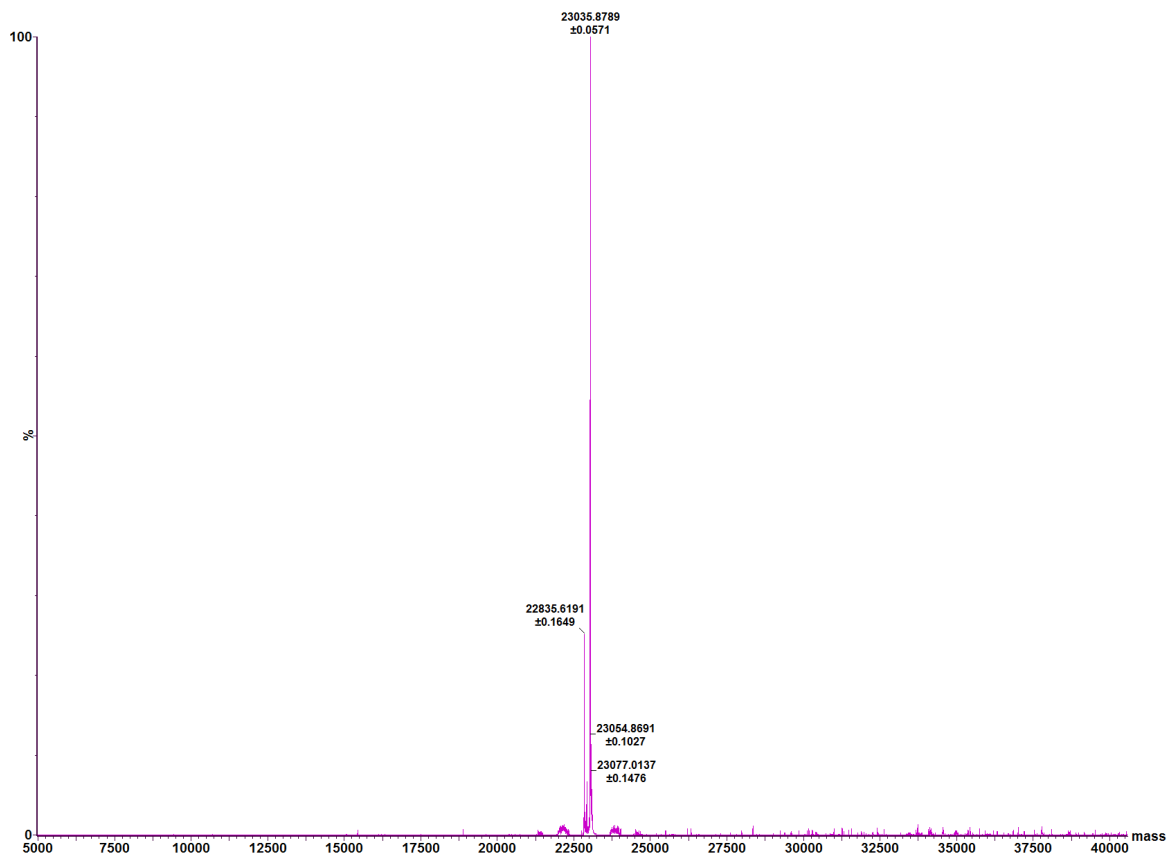
**C:**



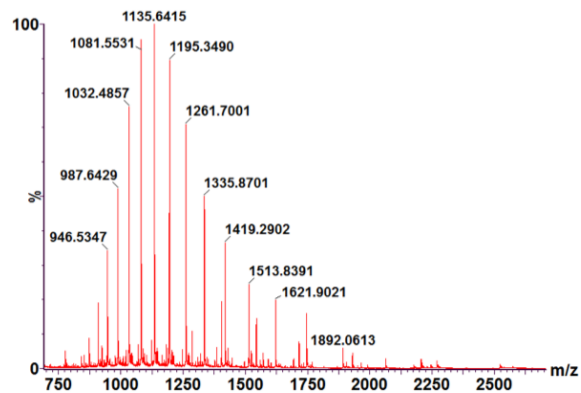
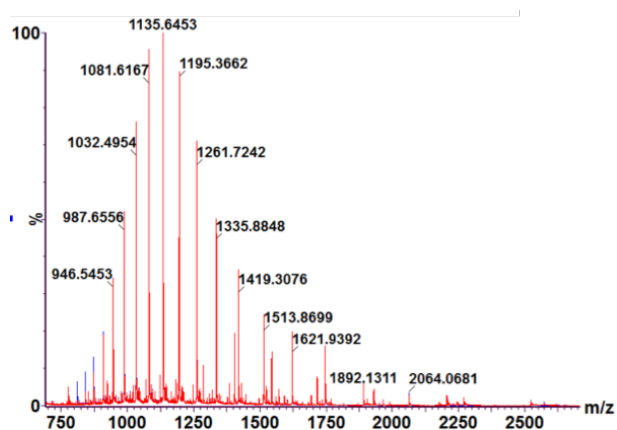
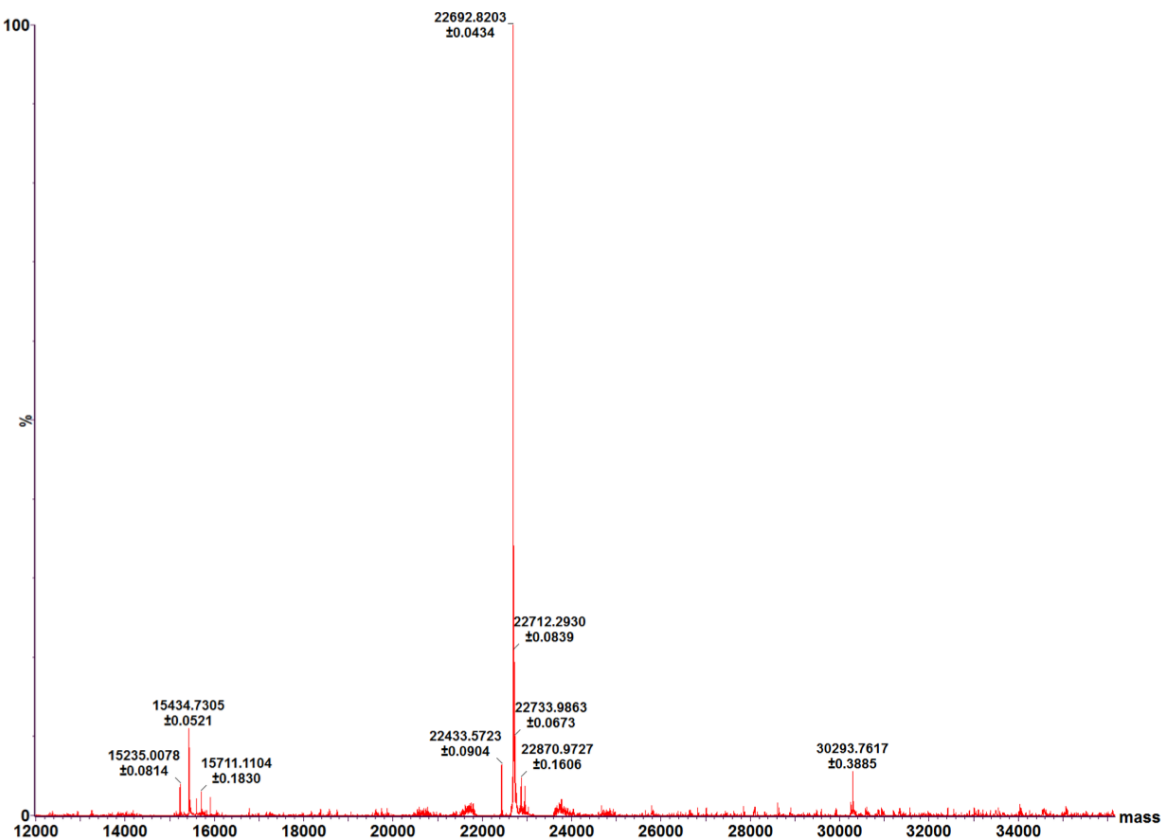
**Figure 8.7: Highlighted ESI-MS of PASTA 1 to 5 (His).** (A) Raw Mass Spectrum, (B) Superimposition of Raw data and mock mass data from maximum entropy algorithm (C) mock mass spectrum from maximum entropy algorithm.

**A:****B:****C:**

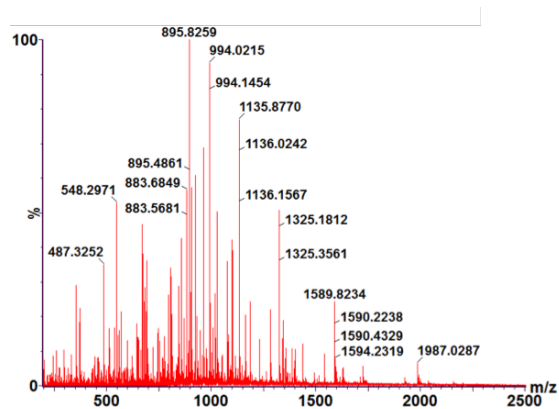
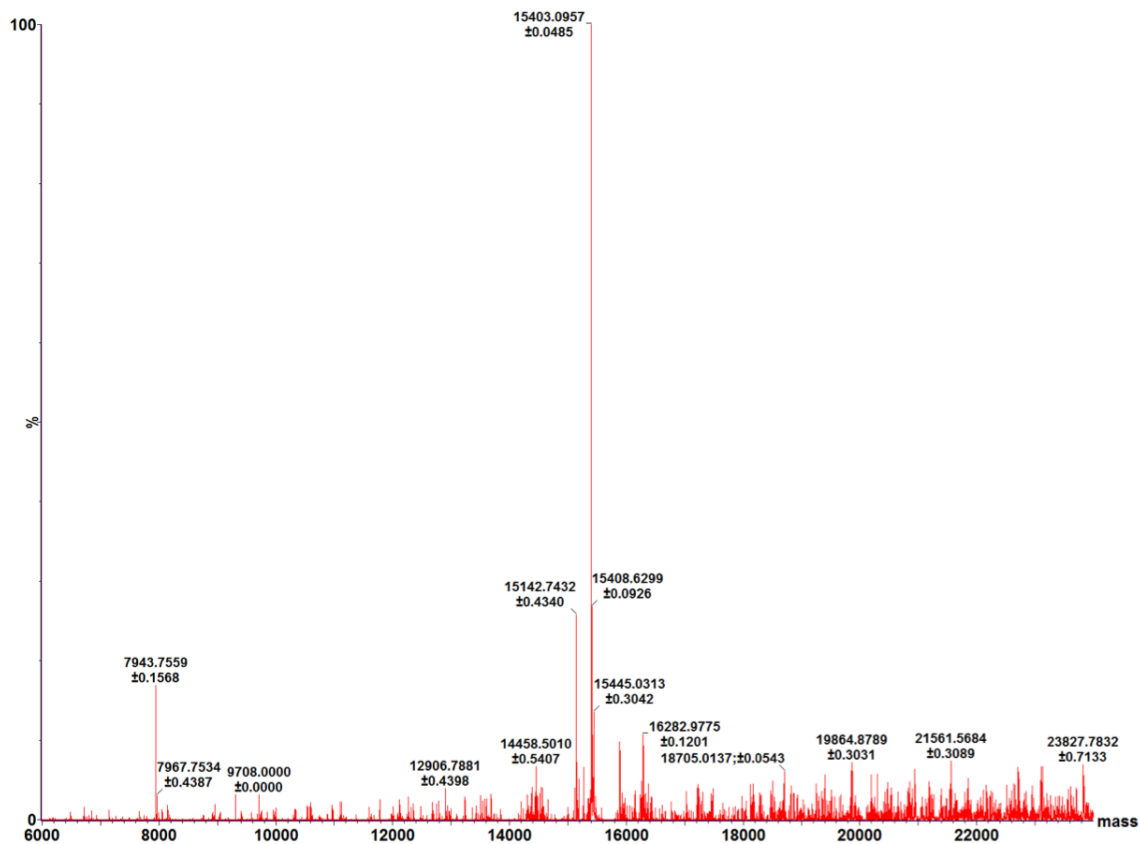
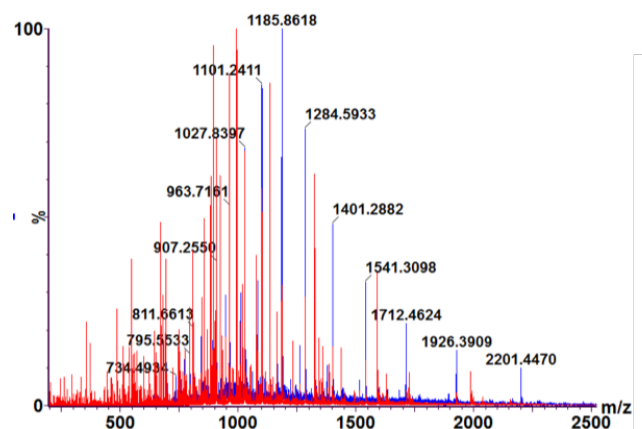
**Figure 8.8: Highlighted ESI-MS of PASTA 1 to 5 (TEV).** (A) Raw Mass Spectrum, (B) Superimposition of Raw data and mock mass data from maximum entropy algorithm (C) mock mass spectrum from maximum entropy algorithm.

**A:****B:****C:**

**Figure 8.9: Highlighted ESI-MS of PASTA 1 to 4 (TEV).** (A) Raw Mass Spectrum, (B) Superimposition of Raw data and mock mass data from maximum entropy algorithm (C) mock mass spectrum from maximum entropy algorithm.

**A:****B:****C:**

**Figure 8.10: Highlighted ESI-MS of PASTA 1 to 3 (TEV).** (A) Raw Mass Spectrum, (B) Superimposition of Raw data and mock mass data from maximum entropy algorithm (C) mock mass spectrum from maximum entropy algorithm.

**A:****C:****B:**

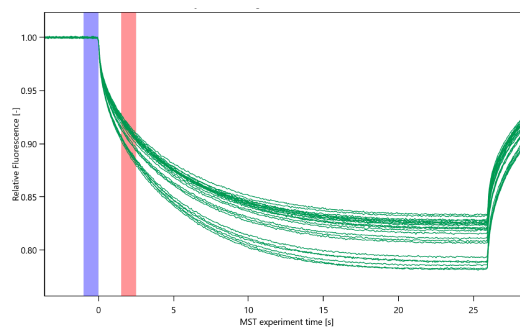
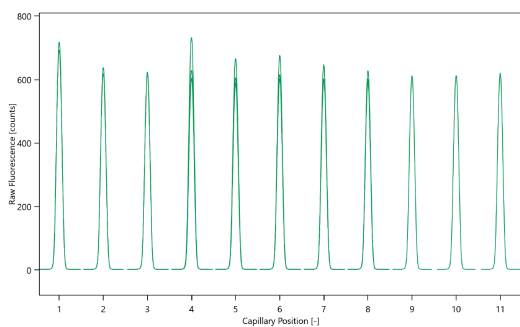
**Figure 8.11: Highlighted ESI-MS of PASTA 1 to 2 (TEV).** (A) Raw Mass Spectrum, (B) Superimposition of Raw data and mock mass data from maximum entropy algorithm (C) mock mass spectrum from maximum entropy algorithm.

## 8.6. Nanotemper MST controls

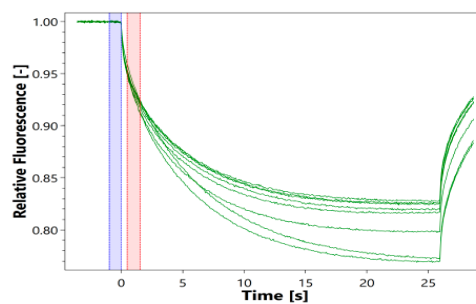
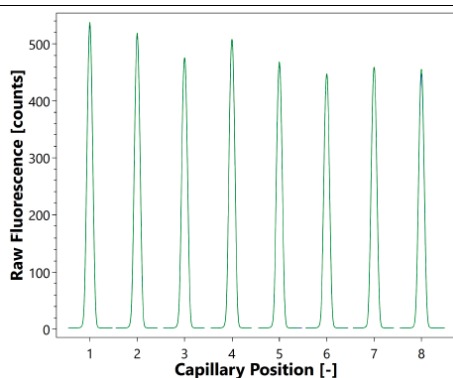
**A:**

**B:**

**Vancomycin**



**Teicoplanin**



**(GlcNAc-MurNAc)<sub>4</sub>**

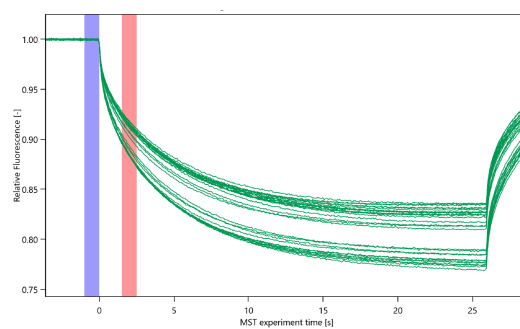
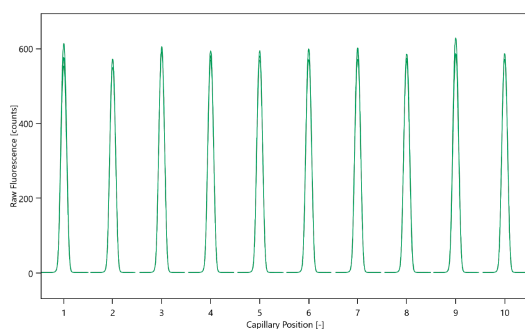
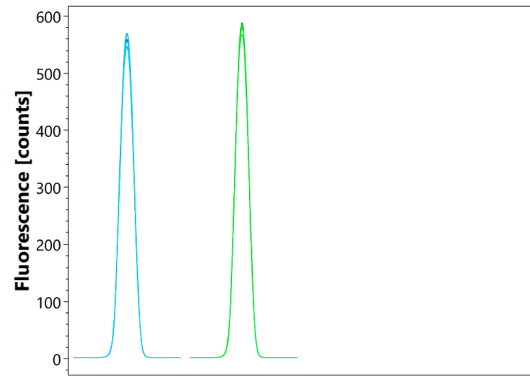
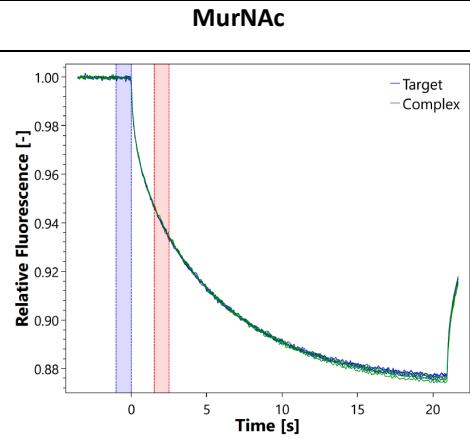
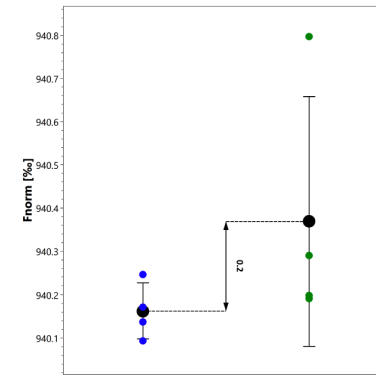


Figure 8.12: Nanotemper experiment controls with ligand that produced a  $K_D$ .

**A:****B:****C:**

**GlcNAc**

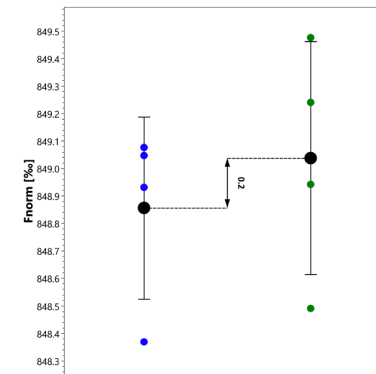
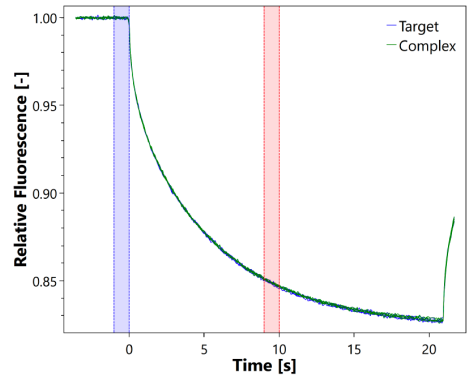
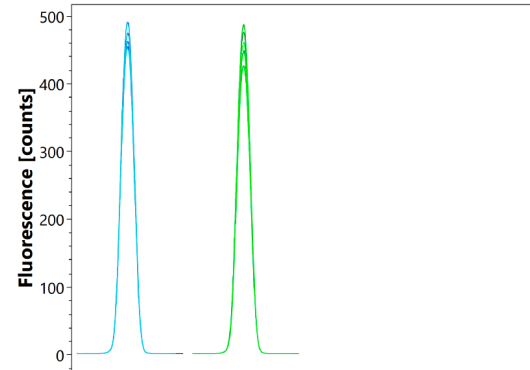


Figure 8.13: Nanotemper experiment controls with PG glycan monomers.

**A:**

**B:**

**C:**

Lys-Pentapeptide

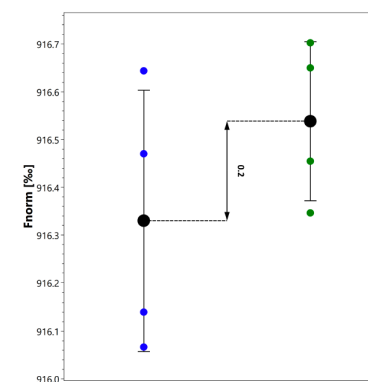
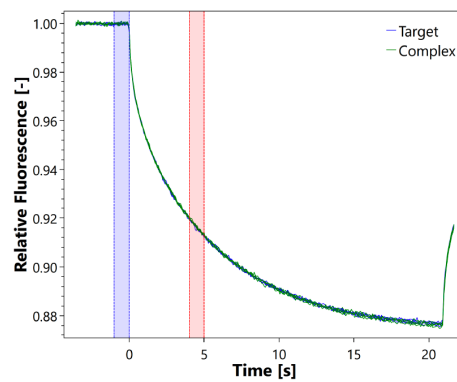
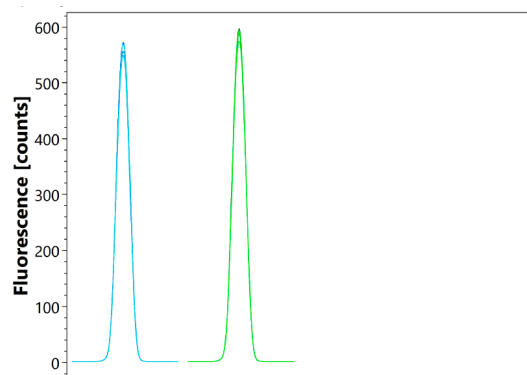
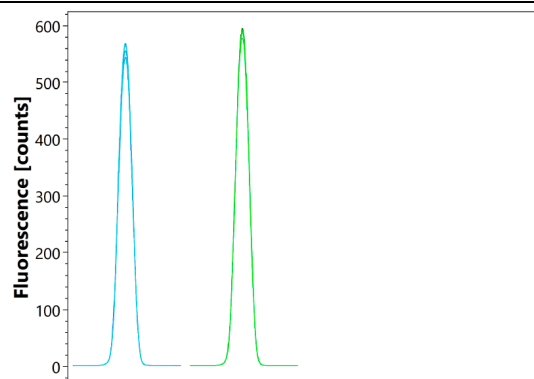
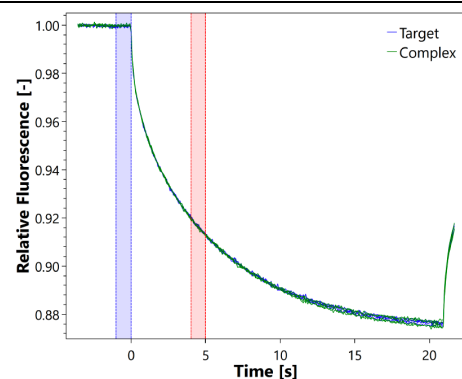
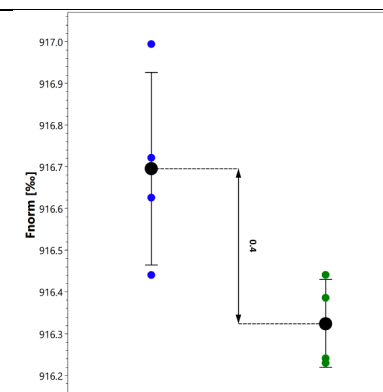
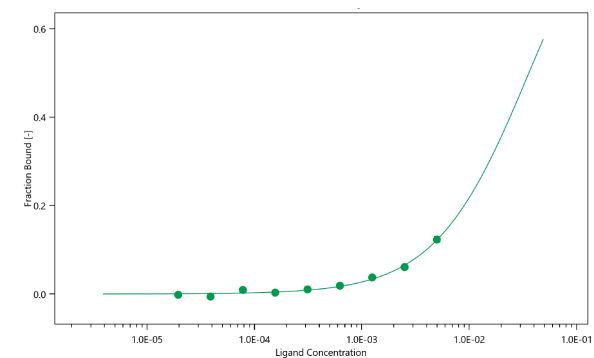
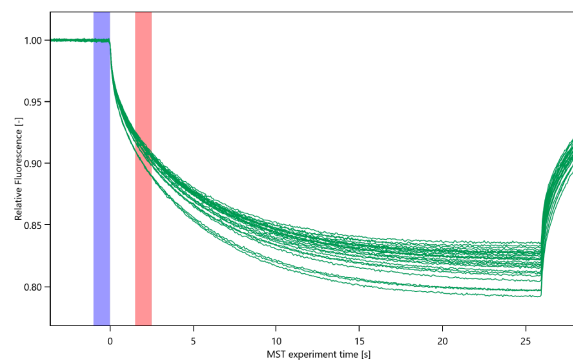
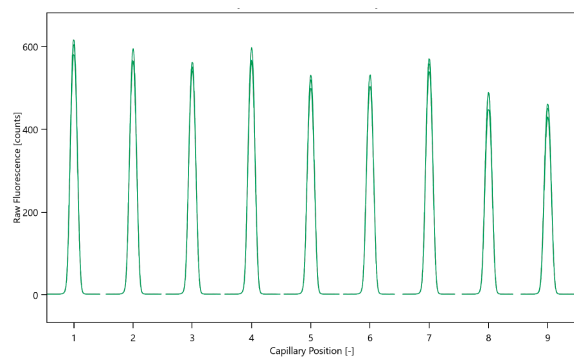


Figure 8.14: Nanotemper experiments with PG pentapeptide stem.

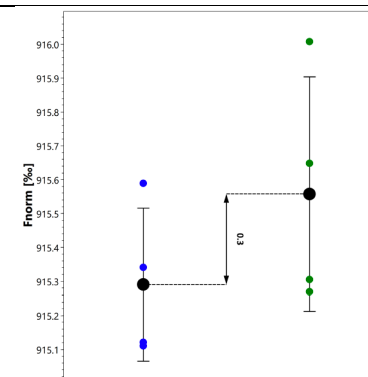
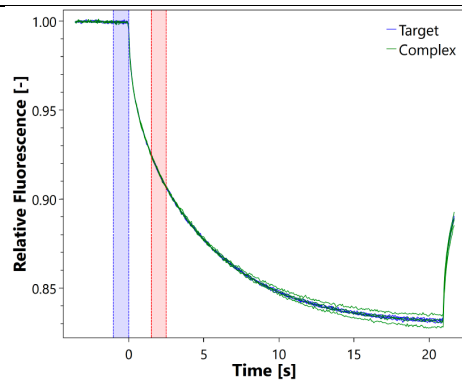
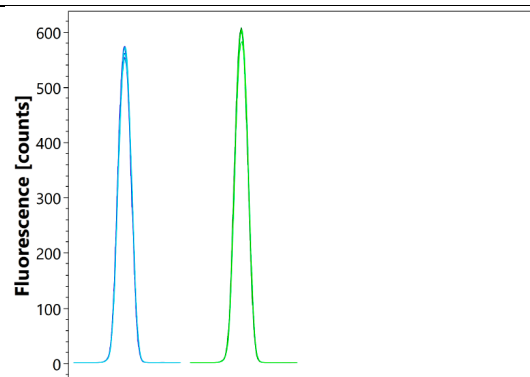
**A:****B:****C:****Chitobiose****Chitotose****Figure 8.15: Nanotemper experiment controls with GlcNAc polymers**

**A:**

**B:**

**C:**

**MDP Control**



**MDP**

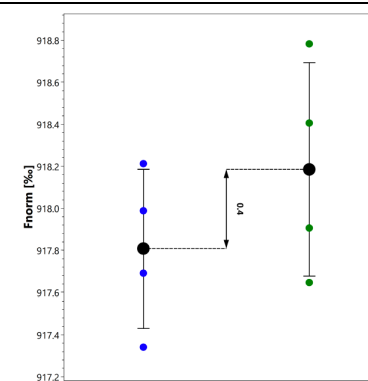
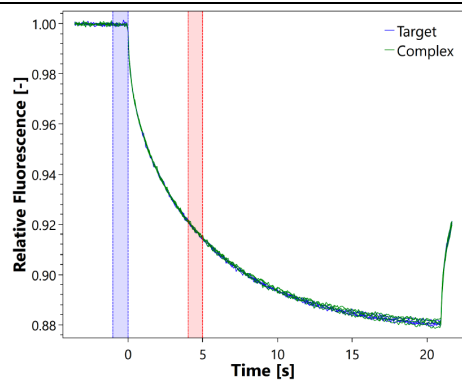
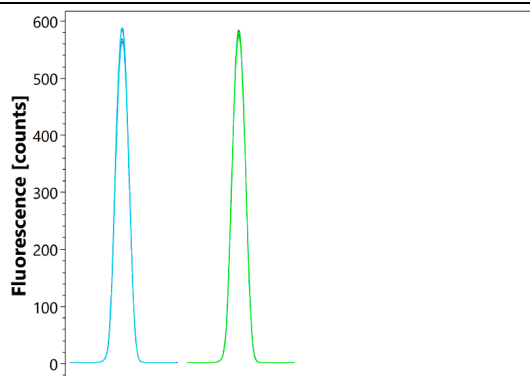


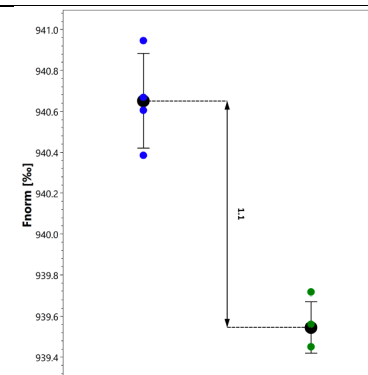
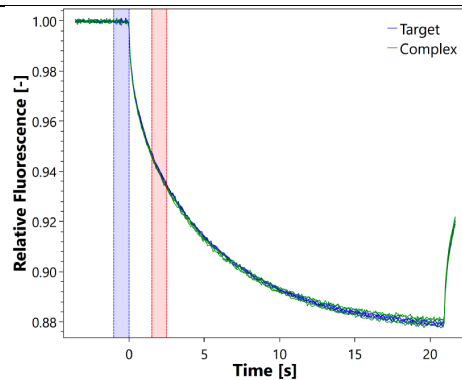
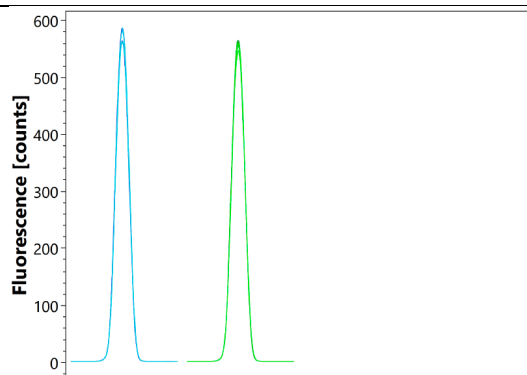
**Figure 8.16: Nanotemper experiment controls with PG peptide stem (Dipeptide)**

**A:**

**B:**

**C:**

**Lys Tri Peptide**



**Dap Tri Peptide**

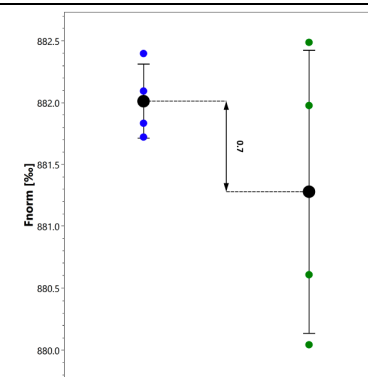
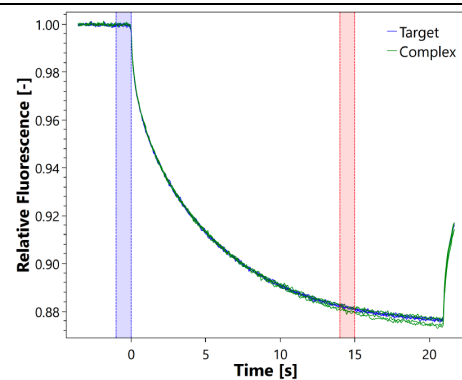
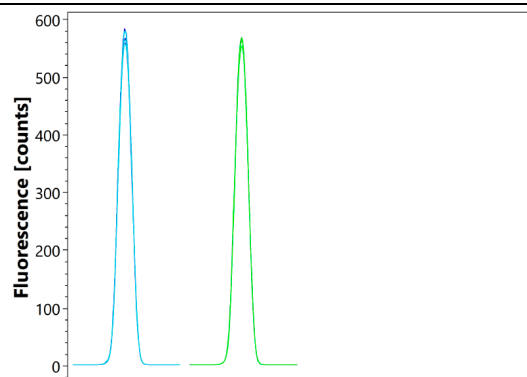
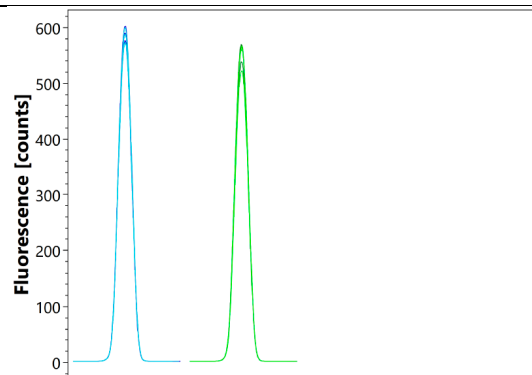
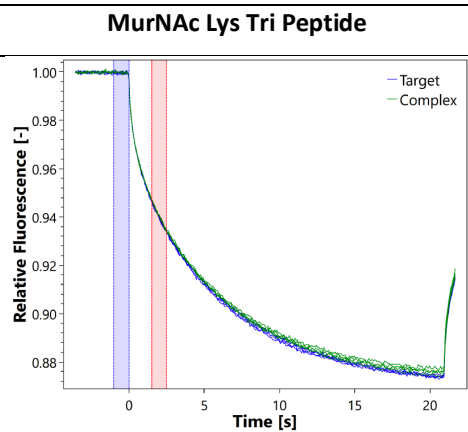
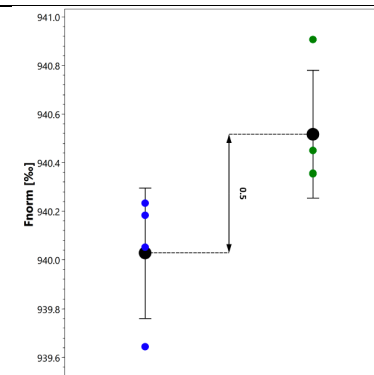


Figure 8.17: Nanotemper experiment controls with PG peptide stem (Unamidated Tripeptide).

**A:****B:****C:**

MurNAC Dap Tri Peptide

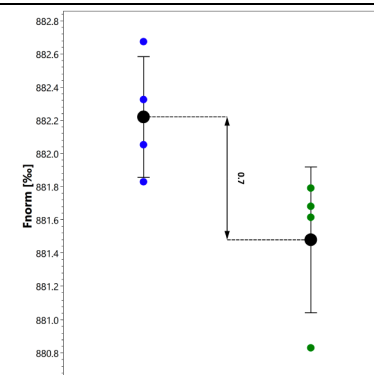
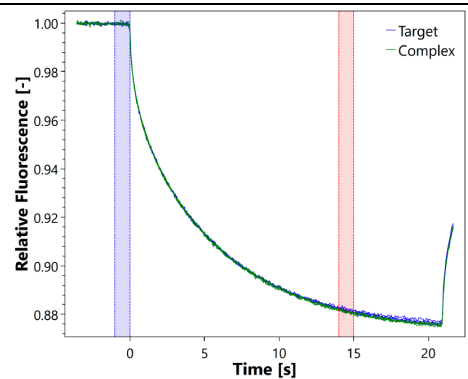
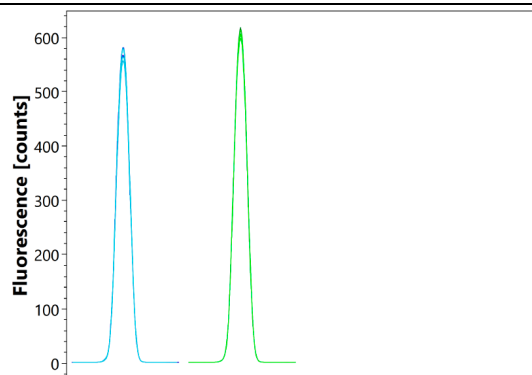
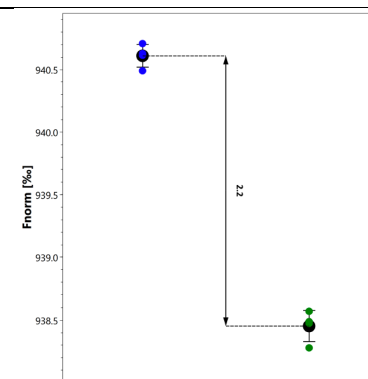
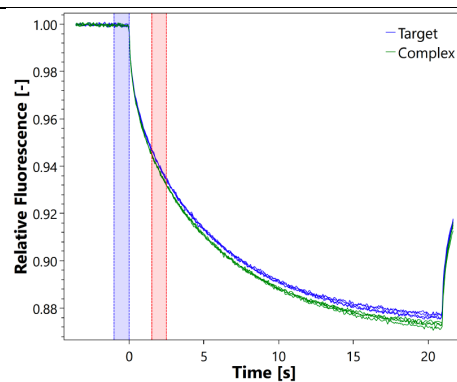
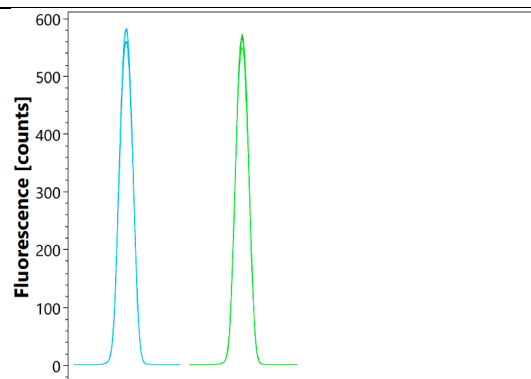
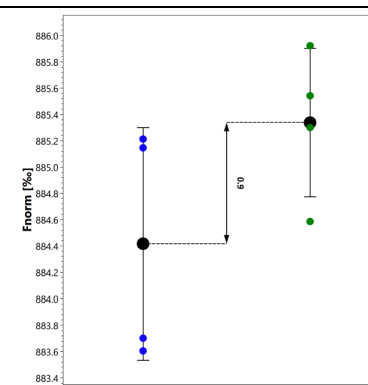
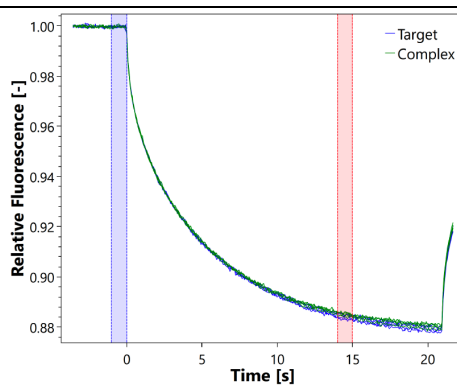
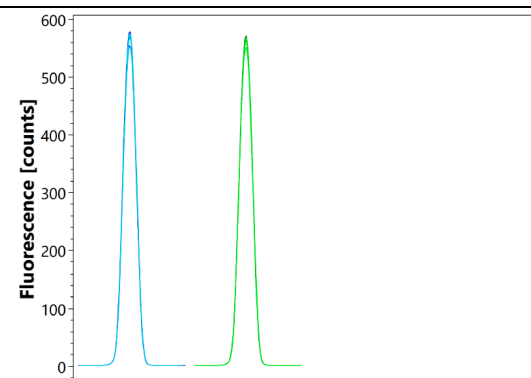


Figure 8.18: Nanotemper experiment controls with PG peptide stem (Unamidated MurNAC Tripeptide).

**A:****B:****C:****Amidated Lys Tri Peptide****MurNAC Dap Tri Peptide****Figure 8.19: Nanotemper experiment controls with PG peptide stem (Amidated Tripeptide)**